

ENCLOSURE 2

M170037

NEDO-33005-A, Revision 1

Non-Proprietary Information– Class I (Public)

IMPORTANT NOTICE

This is a non-proprietary version of NEDE-33005P-A, Revision 1, from which the proprietary information has been removed. Portions of the enclosure that have been removed are indicated by an open and closed bracket as shown here [[]].

Note the NRC's Final Safety Evaluation is enclosed in NEDO-33005-A, Revision 1. Portions of the Safety Evaluation that have been removed are indicated with a double square bracket as shown here. [[]].



HITACHI

GE Hitachi Nuclear Energy

NEDO-33005-A
Revision 1
February 2017

Non-Proprietary Information – Class I (Public)

Licensing Topical Report

TRACG Application for Emergency Core Cooling Systems / Loss-of-Coolant-Accident Analyses for BWR/2-6

*Copyright 2011-2017 GE-Hitachi Nuclear Energy Americas, LLC
All Rights Reserved*

INFORMATION NOTICE

This is a non-proprietary version of NEDE-33005P-A Revision 1 which has the proprietary information removed. Portions of the document that have been removed are indicated by an open and closed double square bracket as shown here [[]].

Within the US NRC Safety Evaluation, the proprietary portions of the document that have been removed are indicated with a double square bracket as shown here [[]].

IMPORTANT NOTICE REGARDING CONTENTS OF THIS REPORT

Please Read Carefully

The design, engineering, and other information contained in this document is furnished for the purpose of obtaining NRC approval of the GEH Licensing Topical Report, NEDE-33005P, *“TRACG Application for Emergency Core Cooling Systems / Loss-of-Coolant-Accident Analyses for BWR/2-6.”* The only undertakings of GEH with respect to information in this document are contained in contracts between GEH and participating utilities, and nothing contained in this document shall be construed as changing those contracts. The use of this information by anyone for any purposes other than that for which it is intended is not authorized; and with respect to any unauthorized use, GEH makes no representation or warranty, and assumes no liability as to the completeness, accuracy, or usefulness of the information contained in this document.

February 22, 2017

Mr. Jerald G. Head
Senior Vice President, Regulatory Affairs
General Electric-Hitachi
Nuclear Energy Americas, LLC
P.O. Box 780, M/C A-18
Wilmington, NC 28401-0780

SUBJECT: FINAL SAFETY EVALUATION FOR GE HITACHI NUCLEAR ENERGY - AMERICAS, LLC TOPICAL REPORT NEDE-33005P AND NEDO-33005, REVISION 0, "LICENSING TOPICAL REPORT TRACG APPLICATION FOR EMERGENCY CORE COOLING SYSTEMS / LOSS-OF-COOLANT-ACCIDENT ANALYSES FOR BWR/2-6" (CAC NO. ME5405)

Dear Mr. Head:

By letter dated January 27, 2011 (Agencywide Documents Access and Management System (ADAMS) Accession No. ML110280323), GE Hitachi Nuclear Energy Americas LLC (GE-H) submitted Topical Report (TR) NEDE-33005P/NEDO-33005, Revision 0, "Licensing Topical Report TRACG Application for Emergency Core Cooling Systems / Loss-of-Coolant-Accident Analyses for BWR/2-6," to the U.S. Nuclear Regulatory Commission (NRC) staff for review.

By letter dated January 18, 2017, an NRC draft safety evaluation (SE) regarding our approval of TR NEDE-33005P, Revision 0, "Licensing Topical Report TRACG Application for Emergency Core Cooling Systems / Loss-of-Coolant-Accident Analyses for BWR/2-6," was provided for your review and comment (ADAMS Accession No. ML17012A287). By letter dated January 27, 2017, you provided comments on the draft SE (ADAMS Accession No. ML17027A094). The NRC staff's disposition of the GE-H comments on the draft SE are discussed in the attachment to the final SE enclosed with this letter.

The NRC staff has found that TR NEDE-33005P, Revision 0, is acceptable for referencing in licensing applications for nuclear power plants to the extent specified and under the limitations delineated in the TR and in the enclosed final SE. The enclosed final SE is a publicly available version with GE-H proprietary material redacted. The final SE defines the basis for our acceptance of the TR.

Our acceptance applies only to material provided in the subject TR. We do not intend to repeat our review of the acceptable material described in the TR. When the TR appears as a reference in licensing applications, our review will ensure that the material presented applies to the specific plant involved. License amendment requests that deviate from this TR will be subject to a plant-specific review in accordance with applicable review standards.

J. Head

- 2 -

In accordance with the guidance provided on the NRC website, we request that GE-H publish approved proprietary and non-proprietary versions of TR NEDE-33005P, Revision 0, within three months of receipt of this letter. The approved versions shall incorporate this letter and the enclosed final SE after the title page. Also, they must contain historical review information, including NRC requests for additional information (RAIs) and your responses. The approved versions shall include a "-A" (designating approved) following the TR identification symbol.

As an alternative to including the RAIs and RAI responses behind the title page, if changes to the TR were provided to the NRC staff to support the resolution of RAI responses, and the NRC staff reviewed and approved those changes as described in the RAI responses, there are two ways that the accepted version can capture the RAIs:

1. The RAIs and RAI responses can be included as an Appendix to the accepted version.
2. The RAIs and RAI responses can be captured in the form of a table (inserted after the final SE) which summarizes the changes as shown in the approved version of the TR. The table should reference the specific RAIs and RAI responses which resulted in any changes, as shown in the accepted version of the TR.

If future changes to the NRC's regulatory requirements affect the acceptability of this TR, GE-H will be expected to revise the TR appropriately or justify its continued applicability for subsequent referencing. Licensees referencing this TR would be expected to justify its continued applicability or evaluate their plant using the revised TR.

Sincerely,

/RA/

Kevin Hsueh, Chief
Licensing Processes Branch
Division of Policy and Rulemaking
Office of Nuclear Reactor Regulation

Project No. 710

Enclosure:
Final SE (Non-Proprietary)

J. Head

SUBJECT: FINAL SAFETY EVALUATION FOR GE HITACHI NUCLEAR ENERGY - AMERICAS, LLC TOPICAL REPORT NEDE-33005P AND NEDO-33005, REVISION 0, "LICENSING TOPICAL REPORT TRACG APPLICATION FOR EMERGENCY CORE COOLING SYSTEMS / LOSS-OF-COOLANT-ACCIDENT ANALYSES FOR BWR/2-6" (CAC NO. ME5405) DATED: February 22, 2017

DISTRIBUTION:

PUBLIC	RidsNrrDprPlpb	RidsNrrDss	RLukes, NRR
RidsNrrLADHarrison	RidsNrrDssSnpb	RidsNroOd	JDean, NRR
RidsOgcMailCenter	RidsNrrDpr	KHsueh, NRR	BParks, NRR
RidsACRS_MailCTR	RidsResOd	JGolla, NRR	

ADAMS Accession No.: ML17046A301; *concurred via email

NRR-106

OFFICE	NRR/DPR/PLPB/PM	NRR/DPRPLPB/LA*	NRR/DSS/SNPB/BC	NRR/DPR/PLPB/BC
NAME	JGolla	DHarrison	RLukes	KHsueh
DATE	2/21/17	2/17/17	2/14/17	2/22/17

OFFICIAL RECORD COPY

GE-Hitachi Nuclear Energy Americas

Project No. 710

cc:

Mr. James F. Harrison
GE-Hitachi Nuclear Energy Americas LLC
Vice President - Fuel Licensing
P.O. Box 780, M/C A-55
Wilmington, NC 28401-0780
james.harrison@ge.com

Ms. Patricia L. Campbell
Vice President, Washington Regulatory Affairs
GE-Hitachi Nuclear Energy Americas LLC
1299 Pennsylvania Avenue, NW
9th Floor
Washington, DC 20004
patriciaL.campbell@ge.com

Mr. Brian R. Moore
Vice President, Fuel Engineering, Acting
Global Nuclear Fuel-Americas, LLC
P.O. Box 780, M/C A-55
Wilmington, NC 28401-0780
Brian.Moore@gnf.com

SAFETY EVALUATION BY THE OFFICE OF NUCLEAR REACTOR REGULATION

RELATED TO

GENERAL ELECTRIC-HITACHI LICENSING TOPICAL REPORT NEDE-33005P AND
NEDO-33005, "TRACG APPLICATION FOR EMERGENCY CORE COOLING SYSTEMS/
LOSS-OF-COOLANT ACCIDENT ANALYSES FOR BWR/2-6"

EXECUTIVE SUMMARY

Licensing Topical Report (LTR) NEDE-33005P, Revision 0, "TRACG Application for Emergency Core Cooling Systems/Loss-of-Coolant-Accident Analyses for BWR/2-6" was submitted to the U.S. Nuclear Regulatory (NRC) by General Electric-Hitachi Nuclear Energy (GEH, or the vendor) by letter dated January 27, 2011, for NRC staff review and approval. The LTR describes an emergency core cooling system (ECCS) evaluation model (EM) that GEH developed to analyze boiling water reactor (BWR) loss-of-coolant accidents (LOCAs). The EM is referred to as TRACG-LOCA. The NRC staff review and basis for approving TRACG-LOCA is provided in this safety evaluation (SE). This SE is also intended to provide guidance to NRC staff for reviewing plant-specific requests for licensing action that are based on, or supported by, TRACG-LOCA.

This SE is organized into eleven successive chapters. The first two chapters provide background and regulatory basis for the NRC staff review. Chapter 3 discusses the accident scenario specification and delineates the applicability of the TRACG-LOCA approval. Chapter 4 presents a review of the TRACG code and its execution.

Chapters 5 through 8 focus on the application of TRACG to ECCS evaluation; while Chapter 5 is focused on the analytic methodology, Chapter 6 addresses the LOCA-relevant key models that were reviewed by the NRC staff. Chapter 7 provides a review of the overall combination of uncertainty associated with TRACG-LOCA. Although Chapter 6 reviews the key models in consideration of their respective qualification, Chapter 8 additionally provides a review of the analysis of qualification events (i.e., large-scale LOCA tests) and a demonstration analysis for the BWR/2 event, which is expected to be the most challenging application of the EM within its plant design applicability.

Finally, Chapters 9 through 11 discuss licensing aspects of the NRC staff review. Chapter 9 discusses licensing considerations of TRACG-LOCA, including its relationship to other GEH LTRs and expectations regarding plant-specific submittals based on TRACG-LOCA. Chapter 10 provides the limitations associated with the TRACG-LOCA approval, and Chapter 11 presents the overall review conclusion.

Based on its detailed review, the NRC staff determined that NEDE-33005P is acceptable for referencing in licensing actions. For the purpose of compliance with Title 10 of the *Code of Federal Regulations* 50.46 requirements, TRACG-LOCA, as documented in NEDE-33005P, may be considered an acceptable evaluation model. With regard to referencing in licensing actions, NEDE-33005P may be considered approved for use.

Contents

1.0	Introduction	- 1 -
1.1.	Correspondence Summary.....	- 1 -
1.2.	Review Approach	- 1 -
2.0	Regulatory Basis	- 2 -
2.1.	Applicable Regulatory Requirements	- 2 -
2.2.	Standard Review Plan Guidance.....	- 4 -
2.3.	NRC Regulatory Guides	- 5 -
2.4.	Additional Literature.....	- 5 -
2.4.1.	Code Scaling, Applicability, and Uncertainty.....	- 5 -
2.4.2.	Compendium of ECCS Research.....	- 5 -
2.4.3.	Additional Sources	- 5 -
3.0	Accident Scenario Identification	- 6 -
3.1.	Nuclear Power Plant Selection	- 6 -
3.1.1.	Fuel Design-Specific Considerations	- 6 -
3.2.	Scenario Specification	- 7 -
3.3.	Phenomena Identification and Ranking.....	- 8 -
3.3.1.	PIRT Process – NRC Staff Evaluation	- 8 -
3.4.	Accident Scenario Identification – Conclusion.....	- 11 -
4.0	TRACG Background and Execution.....	- 11 -
4.1.	TRACG Overview	- 11 -
4.1.1.	Frozen Code Version Selection.....	- 11 -
4.1.2.	Provision of Complete Code Documentation	- 11 -
4.2.	Summary of Previous Review Findings.....	- 13 -
4.3.	Numerical Methods.....	- 14 -
4.3.1.	Nodalization.....	- 14 -
4.3.2.	Time Discretization.....	- 16 -
4.3.3.	Initialization.....	- 17 -
5.0	TRACG-LOCA Methodology	- 18 -
5.1.	Time in Cycle.....	- 20 -
5.2.	Operating Statepoints.....	- 20 -
5.3.	Power Distribution and Channel Groupings	- 22 -
5.4.	Break Spectrum Analysis	- 23 -
5.5.	Adherence to TS LCOs and Equipment Performance Requirements	- 25 -
5.5.1.	Initial Conditions	- 25 -

5.5.2.	Plant Parameters.....	- 26 -
5.6.	General Design Criterion 35 Compliance	- 27 -
6.0	Review of Key Models.....	- 28 -
6.1.	Sources of Heat During a Loss-of-Coolant Accident	- 28 -
6.1.1.	Initial Stored Energy of the Fuel	- 29 -
6.1.2.	Fission Heat	- 31 -
6.1.3.	Decay of Actinides and Fission Product Decay Heat	- 31 -
6.1.4.	Metal-Water Reaction Rate	- 33 -
6.1.5.	Thermal Parameters for Swelling and Rupture of the Cladding and Fuel Rods.....	- 36 -
6.2.	Blowdown Phenomena	- 37 -
6.2.1.	Break Characteristics and Flow.....	- 38 -
6.2.2.	Noding Near the Break and ECCS Injection Point	- 40 -
6.2.3.	Critical Heat Flux	- 41 -
6.3.	Post-CHF Phenomena	- 42 -
6.3.1.	Flow Regime Map	- 43 -
6.3.2.	Entrainment, Interfacial Shear, and Wall Shear Models.....	- 43 -
6.3.3.	Heat Transfer	- 45 -
6.4.	Spray Cooling Phenomena.....	- 47 -
6.4.1.	CCFL	- 47 -
6.4.2.	Core Spray Flow Distribution.....	- 48 -
6.4.3.	Rewet and Quench Behavior	- 50 -
7.0	Estimation of Overall Computational Uncertainty	- 53 -
7.1.	General.....	- 54 -
7.2.	Code Uncertainty.....	- 55 -
7.3.	Statistical Treatment of Overall Computational Uncertainty.....	- 56 -
7.3.1.	Introduction: Precedential Perspective on the Use of Order Statistics	- 56 -
7.3.2.	Summary of GEH Approach	- 57 -
7.3.3.	NRC Staff Evaluation of GEH Approach	- 57 -
7.4.	PCT Analysis Resolution and Core Detail	- 60 -
8.0	Evaluation Model Qualification and Demonstration	- 61 -
8.1.	Statistical Analysis for Qualification Events.....	- 61 -
8.2.	Review of Studies for BWR/2 Plant	- 62 -
9.0	Licensing Considerations	- 65 -
9.1.	TRACG-LOCA Application	- 65 -
9.2.	Evaluating Changes	- 65 -
9.3.	Concurrent GEH LTRs and Related Licensing.....	- 66 -

9.3.1.	Extended Power Uprates	- 66 -
9.3.2.	Interim Methods.....	- 68 -
9.3.3.	Maximum Extended Load Line Limit Analysis Plus.....	- 69 -
10.0	Limitations.....	- 72 -
10.1.	Applicability.....	- 72 -
10.1.1.	Limitation 1.1: Nuclear Power Plant Specification	- 73 -
10.1.2.	Limitation 1.2: Fuel System Design Applicability	- 73 -
10.1.3.	Limitation 1.3: Competitor and Co-Resident Fuel System Applicability	- 73 -
10.1.4.	Limitation 1.4: First-of-Kind Applications	- 73 -
10.1.5.	Limitation 1.5: Regulatory Compliance	- 73 -
10.1.6.	Limitation 1.6: Promulgation of 10 CFR 50.46c	- 74 -
10.2.	Deterministic Analysis and Models	- 74 -
10.2.1.	Limitation 2.1: Core Detail	- 74 -
10.2.2.	Limitation 2.2: Hot Channels.....	- 74 -
10.2.3.	Limitation 2.3: Break Spectrum Analysis	- 74 -
10.2.4.	Limitation 2.4: Initial Conditions and Plant Parameters	- 74 -
10.2.5.	Limitation 2.5: General Design Criterion 35 Compliance	- 75 -
10.2.6.	Limitation 2.6: Calorimetric Power Uncertainty.....	- 75 -
10.2.7.	Limitation 2.7: Use of the Shumway Correlation.....	- 75 -
10.3.	Upstream and Concurrent Methods.....	- 75 -
10.3.1.	Reporting Requirements to Upstream/Concurrent Methods.....	- 75 -
10.3.2.	Limitations on the Use of Upstream/Concurrent Methods	- 76 -
10.4.	Statistical Analysis	- 76 -
10.4.1.	Limitation 4.1: Limiting Break Sizes	- 76 -
10.4.2.	Limitation 4.2: Sample Size	- 76 -
10.4.3.	Limitation 4.3: Rejection of Results	- 76 -
10.4.4.	Limitation 4.4: Successive Elimination.....	- 76 -
10.4.5.	Limitation 4.5: Dispositioning Unacceptable Results	- 76 -
10.4.6.	Limitation 4.6: Resampling	- 77 -
10.5.	Interim Limitation on Cathcart-Pawel Results	- 77 -
10.6.	Applicability of TRACG-LOCA to Expanded Operating Domains	- 77 -
10.7.	BWR/3-6 First-of-a-kind Application.....	- 77 -
11.0	Conclusion	- 78 -
12.0	References.....	- 78 -

LIST OF ACRONYMS

ABB	Allmänna Svenska Elektriska Aktiebolaget Brown Boveri
ADAMS	Agencywide Documents Access and Management System
AEC	Atomic Energy Commission
ANS	American Nuclear Society
AOO	Anticipated Operational Occurrence
ASEA	Allmänna Svenska Elektriska Aktiebolaget
ASME	American Society of Mechanical Engineers
ATWS	Anticipated Transients Without Scram
BEPU	Best-Estimate Plus Uncertainty
B-J	Baker-Just
BWR	Boiling Water Reactor
CHF	Critical Heat Flux
CCFL	Counter-Current Flow Limitation
CLTR	Constant Pressure Power Uprate Licensing Topical Report
C-P	Cathcart-Pawel
CPPU	Constant Pressure Power Update
CSAU	Code Scaling, Applicability, and Uncertainty
CSHT	Core Spray Heat Transfer
CWO	Core-Wide Oxidation
DEGB	Double-Ended Guillotine Break
ECC	Emergency Core Cooling
ECCS	Emergency Core Cooling System
ECR	Equivalent Cladding Reacted
ELTR	Extended Power Uprate Licensing Topical Report
EM	Evaluation Model
EPU	Extended Power Uprate
EOOS	Equipment Out-of-Service
ESBWR	Economic, Simplified Boiling Water Reactor
FIST	Full Integral Scale Test
FIX-II	<i>Series of integral effects tests simulating a Swedish-designed BWR</i>
FSAR	Final Safety Analysis Report
GE	General Electric
GEH	GE Hitachi Nuclear Energy Americas
GESTAR-II	General Electric Standard Application for Reactor Fuel
GEXL	General Electric Critical Quality Boiling Length
GIRAFFE	<i>Gravity-driven integral full-height test for passive heat removal</i>
GNF	Global Nuclear Fuel
ICF	Increased Core Flow
IET	Integral Effect Test
IMLTR	Interim Methods Licensing Topical Report
LCO	Limiting Condition for Operation
LHGR	Linear Heat Generation Rate
LOCA	Loss of Coolant Accident
LOOP	Loss of Offsite Power
LTR	Licensing Topical Report
MAPLHGR	Maximum Average Planar Linear Heat Generation Rate
MCPR	Minimum Critical Power Ratio
MELLLA+	Maximum Extended Load Line Limit Analysis Plus
MLO	Maximum Local Oxidation

NEDO-33005-A Revision 1
Non-Proprietary Information - Class I (Public)

M+SAR	Maximum Extended Load Line Limit Analysis Plus Safety Analysis Report
NRR	Office of Nuclear Reactor Regulation
OLMCPR	Operating Limit Minimum Critical Power Ratio
OLTP	Original Licensed Thermal Power
OPA	Offsite Power Available
ORNL	Oak Ridge National Laboratory
PCT	Peak Cladding Temperature
PIRT	Phenomena Identification and Ranking Table
PLHGR	Peak Linear Heat Generation Rate
PSTF	Pressure Suppression Test Facility
PWR	Pressurized Water Reactor
RAI	Request for Additional Information
RIL	Research Information Letter
RLA	Request for Licensing Action
RG	Regulatory Guide
ROSA	Rig of Safety Assessment
SBWR	Simplified Boiling Water Reactor
SE	Safety Evaluation
SGT	Sun-Gonzalez-Tien
SIT	Systems Interaction Test
SRP	Standard Review Plan
SSTF	Steam Sector Test Facility
THTF	Thermal Hydraulic Test Facility
TLTA	Two-Loop Test Apparatus
TMOL	Thermal-Mechanical Operating Limit
TR	Topical Report
TRAC	Transient Reactor Analysis Code
TRACG	GEH-proprietary version of the Transient Reactor Analysis Code
TS	Technical Specification
UFM	Ultrasonic Flow Meter

SAFETY EVALUATION BY THE OFFICE OF NUCLEAR REACTOR REGULATION
RELATED TO
GENERAL ELECTRIC-HITACHI LICENSING TOPICAL REPORT NEDE-33005P, AND
NEDO-33005, "TRACG APPLICATION FOR EMERGENCY CORE COOLING SYSTEMS/
LOSS-OF-COOLANT ACCIDENT ANALYSES FOR BWR/2-6"

1.0 INTRODUCTION

By letter dated January 27, 2011, General Electric (GE)-Hitachi Nuclear Energy (GEH, or the vendor) submitted for US Nuclear Regulatory Commission (NRC) staff review Topical Report (TR) NEDE-33005P, Revision 0, and NEDO-33005, Revision 0, "TRACG Application for Emergency Core Cooling Systems/Loss-of-Coolant-Accident Analyses for BWR/2-6" (Reference 1). The TR describes an emergency core cooling system (ECCS) evaluation model (EM) that GEH developed to analyze boiling water reactor (BWR) loss of coolant accidents (LOCAs). For the sake of brevity, this safety evaluation (SE) will hereafter refer to the TR as NEDE-33005P, and to the EM itself as TRACG-LOCA.

1.1. CORRESPONDENCE SUMMARY

During the NRC staff review, GEH supplemented the TR with six submittals. The vendor provided supporting information related to TRACG and its post-processing tools by letter March 30, 2012 (Reference 2). The vendor supplemented the TR with responses to NRC staff requests for additional information (RAIs) in five batches, as shown in Table 1, below (References 3 - 7). Table 1 also provides the GEH letter number and the Agencywide Documents Access and Management System (ADAMS) Accession Number for each RAI response transmittal, for convenient reference.

Batch	Date	RAIs	Letter No.	Accession No.
1	October 7, 2014	1 - 66	MFN 14-064	ML14281A014
2	February 19, 2016	67 - 98	MFN 16-008	ML16050A138
3	June 13, 2016	33*, 99, 100	MFN 16-020	ML16165A348
4	June 21, 2016	101, 102	MFN 16-039	ML16173A330
5	October 21, 2016	33*, 65*, 103, 104	MFN 16-072	ML16295A253

*The responses to RAIs 33 and 65 were revised.

Table 1. Index of RAI Responses.

1.2. REVIEW APPROACH

As discussed in Chapter 2 of this SE, there are numerous sources of regulatory guidance for performing the review of an ECCS evaluation model. Some of these sources were published concurrent with efforts to revise the ECCS performance requirements to permit realistic ECCS evaluation in 1988, and others were developed more recently. The 1988 vintage guidance pertains most specifically to ECCS evaluation, and despite that the state of the art has evolved significantly since the publication of this guidance, it remains most applicable to the review of an ECCS EM. However, more recent guidance, which is more generalized to the review of

accident and transient analysis methods, provides a reasonable framework to perform the review, including the concept of a graded approach to reviewing the evaluation model. Unfortunately, using a single element of the available guidance leads to an incomplete review, while using all of the guidance would lead to significant amounts of repetition of effort. Therefore, the NRC staff review was accomplished by hybridizing the available guidance to construct an evaluation model review that balances the more general aspects of the EM review with recognition of the fact that TRACG is a mature code that has been accepted by the NRC staff in previous applications. This SE focuses on the detailed code features that are somewhat unique and important to ECCS evaluation among other applications.

2.0 REGULATORY BASIS

The TRACG-LOCA EM was developed in accordance with the regulatory requirements established in Title 10, "Energy," of the *U.S. Code of Federal Regulations* (10 CFR), Part 50, "Domestic Licensing of Production and Utilization Facilities," Section 46, "Acceptance criteria for ECCSs for light-water nuclear power reactors" (10 CFR 50.46). In developing TRACG-LOCA, GEH considered guidance contained in two NRC Regulatory Guides (RGs). These include: (1) RG 1.157, "Best-Estimate Calculations of Emergency Core Cooling System Performance," and (2) RG 1.203, "Transient and Accident Analysis Methods" (References 8 and 9).

The NRC staff reviewed NEDE-33005P to determine whether TRACG-LOCA is an acceptable evaluation model as set forth in 10 CFR 50.46. In its review, the NRC staff relied on the regulatory guidance described above, as well as applicable chapters contained in NUREG-0800, "Standard Review Plan for the Review of Safety Analysis Reports for Nuclear Power Plants, Light Water Reactor Edition." Principally, the NRC staff relied on Standard Review Plan (SRP), Chapter 15.0.2, "Review of Transient and Accident Analysis Methods" (Reference 10).

As described in Section 2.1, below, the TRACG-LOCA EM is required to provide an estimated uncertainty associated with its results, and comparisons must be made to experimental data to show that its results realistically describe reactor behavior under hypothetical LOCA conditions. The NRC provides an acceptable approach to determining uncertainty associated with safety analysis methods in NUREG/CR-5249, "Quantifying Reactor Safety Margins: Application of Code Scaling, Applicability, and Uncertainty Evaluation Methodology to a Large-Break, Loss-of-Coolant Accident" (Reference 11). In addition, the NRC provides a compendium of experimental data pertinent to ECCS evaluation model in NUREG-1230, "Compendium of ECCS Research for Realistic LOCA Analysis" (Reference 12). These documents provide additional, supporting guidance for the documentation contained in NEDE-33005P and the related NRC review.

2.1. APPLICABLE REGULATORY REQUIREMENTS

Holders of operating licenses under 10 CFR Part 50 are required, pursuant to subsection 50.34, to submit final safety analysis reports (FSARs) to the NRC. In part, 50.34(b)(4) states:

...Analysis and evaluation of ECCS cooling performance following postulated loss-of-coolant accidents shall be performed in accordance with the requirements of §50.46...

GEH developed TRACG-LOCA as a realistic, best-estimate, or best-estimate plus uncertainty (BEPU) evaluation model,^A to be used to evaluate ECCS performance at BWRs. The enabling regulatory framework is established in Paragraph 50.46(a)(1)(i) which states, in part:

Each boiling or pressurized light-water nuclear power reactor fueled with uranium oxide pellets within cylindrical zircaloy or ZIRLO cladding must be provided with an emergency core cooling system (ECCS) that must be designed so that its calculated cooling performance following postulated loss-of-coolant accidents conforms to the criteria set forth in paragraph (b) of this section. ECCS cooling performance must be calculated in accordance with an acceptable evaluation model and must be calculated for a number of postulated loss-of-coolant accidents of different sizes, locations, and other properties sufficient to provide assurance that the most severe postulated loss-of-coolant accidents are calculated... [T]he evaluation model must include sufficient supporting justification to show that the analytical technique realistically describes the behavior of the reactor system during a loss-of-coolant accident. Comparisons to applicable experimental data must be made and uncertainties in the analysis method and inputs must be identified and assessed so that the uncertainty in the calculated results can be estimated. This uncertainty must be accounted for, so that, when the calculated ECCS cooling performance is compared to the criteria set forth in paragraph (b) of this section, there is a high level of probability that the criteria would not be exceeded. Appendix K, Part II Required Documentation, sets forth the documentation requirements for each evaluation model...

Paragraph (b) of 50.46, as referenced in the above excerpt, provides the acceptance criteria for ECCS evaluation. The acceptance criteria are as follows:

(b)(1) *Peak cladding temperature.* The calculated maximum fuel element cladding temperature shall not exceed 2200°F.^B

(2) *Maximum cladding oxidation.* The calculated total oxidation of the cladding shall nowhere exceed 0.17 times the total cladding thickness before oxidation...

(3) *Maximum hydrogen generation.* The calculated total amount of hydrogen generated from the chemical reaction of the cladding with water or steam shall not exceed 0.01 times the hypothetical amount that would be generated if all of the metal in the cladding cylinders surrounding the fuel, excluding the cladding surrounding the plenum volume, were to react.

(4) *Coolable Geometry.* Calculated changes in core geometry shall be such that the core remains amenable to cooling.

^A In addition to the term, "realistic," the terms, "best-estimate," and, "BEPU," are also frequently used in a similar context. It should be understood that, in order for the analytic results to be considered acceptable for the purposes of demonstrating compliance with § 50.46 requirements, the realistic, or so-called best-estimate, results must be expressed at some upper level that includes an allowance for estimated uncertainty. The distinction among these terms is discussed in further detail in Enclosure C, "ACRS Comments on Code Scaling, Applicability and Uncertainty Associated with the use of Realistic ECCS Evaluation Models," to SECY-88-162, "Revision of the ECCS Rule Contained in Appendix K and Section 50.46 of 10 CFR Part 50."

^B Note that Reference 1 documents results and compares peak cladding temperatures using Kelvin, as opposed to degrees Fahrenheit. Expressed in Kelvin, 2200 °F is approximately 1478 K.

(5) *Long-Term Cooling*. After any calculated successful initial operation of the ECCS, the calculated core temperature shall be maintained at an acceptably low value and decay heat shall be removed for the extended period of time required by the long-lived radioactivity remaining in the core.

The evaluation model addresses Criteria (b)(1) through (b)(3) by providing analytic results to compare directly to the acceptance criteria. The evaluation model provides the peak cladding temperature (PCT), the maximum local oxidation (MLO), which is also known as equivalent cladding reacted (ECR), and core-wide oxidation (CWO). Additional discussion pertaining to Criteria (b)(4) and (b)(5) are located in Section 3.2, "Scenario Specification," of this SE.

Additional requirements, which govern assumptions that must be employed in the ECCS evaluation, are contained in 10 CFR Part 50 Appendix A, "General Design Criteria for Nuclear Power Plants," General Design Criterion (GDC) 35, "Emergency core cooling," which states:

A system to provide abundant emergency core cooling shall be provided. The system safety function shall be to transfer heat from the reactor core following any loss of reactor coolant at a rate such that (1) fuel and clad damage that could interfere with continued effective core cooling is prevented and (2) clad metal-water reaction is limited to negligible amounts.

Suitable redundancy in components and features, and suitable interconnections, leak detection, isolation, and containment capabilities shall be provided to assure that for onsite electric power system operation (assuming offsite power is not available) and for offsite electric power system operation (assuming onsite power is not available) the system safety function can be accomplished, assuming a single failure.

These requirements – § 50.34, § 50.46, and GDC 35 – form the regulatory basis for the NRC staff review.

2.2. STANDARD REVIEW PLAN GUIDANCE

As discussed in Section 2.0, the NRC staff performed its review using the SRP.

The NRC staff relied principally on the over-arching guidance in SRP Chapter 15.0.2. This SRP chapter documents the areas of an evaluation model to be reviewed, including: (1) Documentation; (2) Evaluation Model; (3) Accident Scenario Identification Process; (4) Code Assessment; (5) Uncertainty Analysis; and (6) Quality Assurance Plan. The SRP chapter provides guidance intended to focus review resources, primarily, on ensuring (1) that the scenario to be analyzed is appropriately specified, (2) that previously un-reviewed aspects of the evaluation model that are pertinent to the scenario under consideration are appropriately reviewed, and (3) that the application of the model evaluates uncertainties appropriately. Accomplishing these review objectives provides assurance that the results obtained from TRACG-LOCA, with uncertainty accounted for, demonstrate with high probability that the criteria of § 50.46(b)(1-3) are not exceeded, consistent with § 50.46(a)(1)(i) requirements.

Chapter 15.0.2 of the SRP provides guidance to the NRC staff in performing the safety review of NEDE-33005P. It describes methods or approaches that the NRC staff has found acceptable for meeting NRC requirements. For the purposes of reviewing an ECCS EM, however, the SRP

is not considered a complete, standalone reference to provide all the required review guidance. Additional documents, discussed in Sections 2.3 and 2.4 of this SE, also apply.

2.3. NRC REGULATORY GUIDES

Regulatory Guides provide guidance to licensees, applicants, and vendors on implementing specific parts of the NRC's regulations, techniques used by the NRC staff in evaluating specific problems or postulated accidents, and data needed by the staff in its review of applications for permits or licenses. The particular guides applicable to ECCS evaluation model development include RG 1.203 and RG 1.157.

Regulatory Guide 1.203 is the analog to SRP 15.0.2. It describes a process that the NRC staff considers acceptable for use in developing and assessing evaluation models that may be used to analyze transient and accident behavior that is within the design basis of a nuclear power plant.

RG 1.157 was developed in concert with the revision to § 50.46 that permitted the use of realistic ECCS EMs. This RG describes models, correlations, data, model evaluation procedures, and methods that are acceptable to the NRC staff for meeting the requirements for a realistic or best-estimate calculation of ECCS performance during a LOCA and for estimating the uncertainty of that calculation.

2.4. ADDITIONAL LITERATURE

2.4.1. Code Scaling, Applicability, and Uncertainty

The NRC staff review was based, in part, on NUREG/CR-5249, "Quantifying Reactor Safety Margins: Application of Code Scaling, Applicability, and Uncertainty Evaluation to a Large-Break, Loss-of-Coolant Accident" (Reference 11). This NUREG/CR report describes an uncertainty evaluation methodology called code scaling, applicability, and uncertainty (CSAU). The NRC staff considered the information contained in NUREG/CR-5249 in its review.

2.4.2. Compendium of ECCS Research

The requirements contained in § 50.46(a)(1)(i) state, in part, that "comparisons to applicable experimental data must be made..." Accordingly, the guidance in RG 1.203 and RG 1.157 frequently indicate that models, correlations, formulas, etc., will be considered acceptable, provided they are checked against or compared to relevant data sets. The NRC provides a set of such relevant data sets in NUREG-1230, "Compendium of ECCS Research for Realistic LOCA Analysis" (Reference 12).

2.4.3. Additional Sources

The NRC-published regulatory guidance and technical reference materials specifically pertinent to ECCS EMs were all published prior to 1990. The state of the art for LOCA research and EM development has evolved since then. Hence, additional sources of relevant research, which are not necessarily included in the literature reviewed above, were considered as appropriate.

3.0 ACCIDENT SCENARIO IDENTIFICATION

3.1. NUCLEAR POWER PLANT SELECTION

The EM is applicable to GEH-designed nuclear steam supply systems of the BWR/2 through BWR/6 product lines. This applicability is identified in Chapter 2 of Reference 1, and the qualification and demonstration analyses focus on BWR/2 through BWR/6 analyses. Based on these two considerations, the NRC staff determined that GEH is consistent with this element of the accident scenario identification process as set forth in SRP 15.0.2.

The applicability is considered a limitation to the NRC staff approval of TRACG-LOCA. The applicability of the EM to other BWR designs, such as ASEA Brown Boveri (ABB)-designed BWRs, was not considered. The applicability to evolutionary designs, such as the Economic Simplified Boiling Water Reactor (ESBWR), is addressed in separate applications. The model is not considered applicable to pressurized water reactor designs. Refer to Limitation 1.1, "Nuclear Power Plant Specification," in Chapter 10 of this SE for additional discussion.

3.1.1. Fuel Design-Specific Considerations

In addition to the BWR plant category designation, it is important also to recognize that TRACG-LOCA was reviewed considering the GE14 and GNF2 fuel product lines. Although minor upgrades to these fuel designs can probably be readily accommodated by the evaluation model, the introduction of new fuel design features that require substantial revision to the evaluation model or methodology would require additional review. This is Limitation 1.2, "Fuel System Design Applicability," in Chapter 10 of this SE.

It should be noted also that GEH has established means to account for the characteristics of other fuel designs. These include limiting power shapes, cladding material properties, and critical quality-boiling length correlations. Limitation 1.3, "Competitor and Co-Resident Fuel System Applicability," permits modeling of competitor or co-resident fuel to the extent that TRACG-LOCA can accommodate the design features of such fuel, but requires that operating constraints on such fuel remain supported by, or more conservative than, the analytic methods furnished by the vendor(s) of that fuel.

In this sense, operating constraints include applicable fuel design operating limits, but also fuel and core parameters that are initial conditions to the ECCS evaluation. As this limitation applies to operating characteristics of what would be legacy fuel, the practical implication is that the legacy fuel must be operated within the constraints specified in the legacy ECCS evaluation. If, as an initial condition in the legacy evaluation, a MAPLHGR of 12.5 kW/ft is assumed, then the fuel is expected to be operated at or below this value, regardless of whether the TRACG-LOCA analysis supports a higher value. This limitation is necessary because the TRACG-LOCA application, and approval basis, considers thermal-hydraulic modeling features that are confirmed to be applicable to GNF fuel designs. Other ECCS evaluation models reflect similar, proprietary characteristics of specific fuel designs.

Limitation 1.3 specifies that, if TRACG-LOCA is used to establish less limiting operating characteristics for legacy fuel than those established within the design and licensing basis for that fuel, then the implementing licensee would be required to submit a request for licensing

action (RLA)^c for prior NRC staff review and approval. This is because the NRC staff review did not consider any demonstration analyses, nor evaluate specific modeling techniques or experimental basis, that justify application of TRACG-LOCA analytic results to other vendor fuel designs.

3.2. SCENARIO SPECIFICATION

In Section 2.5.2 of Reference 1, GEH states:

The LOCA scenarios include the full range of pipe breaks for the distinct BWR product lines (BWR/2; BWR/3,4; and BWR/5,6). The scenarios are differentiated by break size and location. Typical BWR LOCA scenarios are described in Section 3.2 [of NEDE-33005]. The LOCA transient is divided into Blowdown and Refill/Reflood phases so that the application methodology can be focused on the processes and components that are important to each phase.

The scenarios described above are evaluated with respect to the critical safety parameters, PCT, ECR, and CWO. These critical safety parameters tie directly to the § 50.46(b)(1) through (b)(3) acceptance criteria. GEH also states, in Section 2.5 of Reference 1, that by satisfying the PCT and ECR acceptance criteria, the TRACG-LOCA results also demonstrate that Criterion (b)(4), related to coolable geometry, is satisfied.

This assertion is acceptable relative to TRACG-LOCA, because separate GEH fuel assembly design criteria require fuel assembly structural integrity and control blade insertability under seismic and LOCA conditions. Specifically, the thermal-mechanical design criteria provided in Section 1.1.2.B of the General Electric Standard Application for Reactor Fuel (GESTAR II) establish these requirements (Reference 13). When the PCT and ECR remain below regulatory limits, the fuel cladding remains sufficiently ductile that the thermal-mechanical design criteria assure that the fuel will remain in a coolable configuration. Thus, the NRC staff accepts GEH's disposition for Criterion (b)(4) of § 50.46.

GEH states further that existing analyses demonstrate that Criterion (b)(5), regarding long-term core cooling, is satisfied, and that the criterion need not be evaluated as part of the TRACG ECCS/LOCA analysis. This position is reflected in Limitation 1.5, "Regulatory Compliance," of the TRACG-LOCA approval. Refer to Chapter 10 of this SE for additional detail.

Because the vendor has identified the scenario under consideration – a BWR hypothetical LOCA – the NRC staff concluded that GEH has addressed this element of the accident scenario identification process as set forth in SRP 15.0.2. Based on these considerations, the NRC staff determined that TRACG-LOCA is acceptable with respect to scenario specification.

^c The term *requested licensing action* is adopted within Office of Nuclear Reactor Regulation (NRR) Office Instruction LIC-109, "Acceptance Review Procedures," to include, more broadly than license amendment requests, activities that require NRC approval prior to implementation. Such activities include license amendments, relief requests, exemptions, security and emergency plan changes, etc. Refer to ADAMS Accession ML091810088 for additional discussion.

3.3. PHENOMENA IDENTIFICATION AND RANKING

The ranking and identification of phenomena relevant to a specified accident scenario is a structured process described in Reference 11. As described in SRP 15.0.2, it is an acceptable means to approach the accident scenario identification process (Reference 10).

GEH presents its phenomena identification and ranking table (PIRT) in Chapter 3 of Reference 1. As discussed above, the PIRT identifies critical safety parameters, which tie directly to the § 50.46(b)(1) through (b)(3) acceptance criteria. The PIRT also identifies downcomer level and core water level as “intermediate safety parameters,” because, according to GEH, “These safety parameters are the criteria used to judge the performance of the safety systems and the margins in the design” (Reference 1, Page 3-1).

The NRC staff review was based on the regulatory guidance contained in References 10 and 11. The RAIs listed in Table 2, below, are relevant to the NRC staff review.^D

Batch	RAI	Topic	Ref.
1	14	Treatment of Medium-Ranked PIRT Parameters	3
1	22	Treatment of Jet Pump Critical Flow	3
1	37	Statement in PIRT Table Entry F3	3
1	38	Air/Two-Phase CCFL in BWR/2	3
1	58	Emergency Core Cooling in Upper Plenum	3

Table 2. RAI Responses Related to Phenomena Identification and Ranking.

GEH initiates Chapter 3 of the Licensing Topical Report (LTR) by presenting several demonstration analyses for the variety of reactor designs and for various break locations and sizes. Building on these analyses, the PIRT offers the GEH interpretation of the overall significance of the various phenomena on the critical safety parameters for both small breaks and large breaks for the three main product groupings, i.e., BWR/2, BWR/3-4, and BWR/5-6. GEH assigns importance values of high, medium, and low. Section 3.4 indicates that those phenomena assigned high importance have a significant effect on the primary safety parameters, while medium-ranked phenomena have a small effect on the primary safety parameters. Although Revision 0 of the LTR indicated that medium-ranked parameters “may be excluded in the overall uncertainty evaluation” (Reference 1, Page 3-16), GEH clarified, in response to RAI 14.a, that all medium-ranked PIRT parameters would be included in the statistical analysis, along with the high-ranked phenomena (Reference 3). Further, the response to RAI 14.b indicated analyses would generically be performed in accordance with the highest rank assigned to a particular phenomenon, regardless of the specific plant class. Low-importance phenomena have insignificant or no effect on the primary safety parameters and “need not be considered in the overall uncertainty evaluation,” states GEH (Reference 1, Page 3-16).

3.3.1. PIRT Process – NRC Staff Evaluation

As per Chapter 15.0.2 of the SRP, Section III, “Review Procedures,” Sub-section C, “Accident Scenario Identification Process,” the NRC staff review of the PIRT process confirms that the

^D These RAIs address other issues besides the PIRT importance of one particular phenomenon or another. This section of the SE, however, considers only those portions of the RAI responses that address the PIRT importance of phenomena. Additional aspects of the RAI response are evaluated, as appropriate, in other sections of the SE.

dominant physical phenomena influencing the outcome of the accident are correctly identified and ranked. A structured process for this effort is described in CSAU. The staff review included an evaluation of the PIRT process relative to that described in CSAU, comparison to other relevant PIRTs (References 14 and 15), and additional input from the vendor through the RAI process.

In its review, the NRC staff determined that the GEH PIRT was generally consistent with the analogous PIRTs. The RAIs were generated to address discrepancies between the analogous PIRTs, and to address demonstration analysis results that suggested higher importance was attributable to specific phenomena than GEH assigned. Specifically, the vendor responses to RAIs 22, 37, 38, and 58 were considered in the PIRT review (Reference 3).

The NRC staff review approach was simplified, somewhat, by GEH's treatment of medium-ranked PIRT parameters. Since the medium-ranked phenomena are included in the statistical analysis, they are treated effectively the same as the high-ranked phenomena. Thus, the distinction between medium- and high-ranked phenomena is insignificant. For example, the issue discussed in RAI 22, related to the medium ranking assigned to a phenomenon in the jet pumps, was resolved in part because the particular phenomenon is treated the same as a highly ranked phenomenon.

The issue addressed in RAI 22 is the PIRT treatment of jet pump reverse flow. While GEH characterizes this phenomenon as having medium importance, two other sources rank the phenomenon highly. In particular, Reference 15 observed that jet pump reverse flow was important during blowdown, because it helps to determine the total core flow. In its response, GEH acknowledged that the jet pump reverse flow phenomenon may have a higher importance than many other medium-ranked parameters, but that the use of a three-tiered (i.e., high, medium, and low) ranking process does not allow for distinguishing such importance. GEH also stated that the PIRT process is somewhat subjective, and added that the assignment of a medium rank to the jet pump reverse flow importance ensures that it is treated consistently with high-rank parameters, in that the calculations include the biases and uncertainties associated with the phenomenon. Since the calculations include the phenomenon along with its biases and uncertainties, the NRC staff determined that the distinction between medium and high importance for the jet pump reverse flow is insignificant for the purposes of LOCA analysis, and thus accepted the RAI response provided by the vendor.

In RAI 37, the NRC staff noted that the PIRT entry for Item F3, "Noncondensable Return at Low Pressures," included a statement that the PCT transient is over before the vessel is depressurized to containment pressure. However, the statement was inconsistent with demonstration calculations in Chapter 3 of Reference 1, as well as NRC staff audit calculations. In response to the RAI, GEH agreed to remove the statement. The statement had no effect on the PIRT treatment, as the highest ranking for the phenomenon was high, specifically for the BWR/2 event. Since the statement in the table had no effect on GEH's treatment of the parameter, the NRC staff accepted the vendor's deletion of the statement.

The response to RAI 38 discusses PIRT Entry M3, counter-current flow limitation (CCFL): Air In/Two-Phase Flow Out (Reference 3). In the RAI, the NRC staff questioned the assignment of medium importance to the phenomenon, even in consideration of the fact that the BWR/2 demonstration calculations appear to indicate that the phenomenon has a more direct impact on the PCT, suggesting a higher ranking would be more appropriate. The response notes that [[

]] Thus, the vendor stated, uncertainty regarding the total amount of ingested air has a lower effect on PCT than the simpler consideration of whether or not air is ingested into the reactor coolant system. Sensitivity studies performed in response to RAI 13.b corroborate this assertion: [[

]] Moreover, the phenomenon is assigned a medium value, meaning its uncertainty is addressed in the analysis.^E The response to RAI 13 is discussed in greater detail in Section 8.2 of this SE.

The response to RAI 58 addresses the importance of PIRT Item F2, which is ECC Interaction/Mixing/Subcooling in the Upper Plenum. The phenomenon has a high ranking, but GEH states, in Section 5.1.6.2 of Reference 1, that its uncertainty is addressed by other parameters, [[

]]. In the RAI, the NRC staff noted the upper plenum spray model as discussed in Section 7.8.2 of Reference 16 provides some discussion that appears to contradict. In particular, the calculated upper plenum spray trajectories could affect mixing in the upper plenum.

The vendor begins its response to RAI 58 by stating, "The premise of the question is that item F2 is important. This is not the case." Even so, Reference 1 assigns a high importance to the phenomenon. The discussion in the PIRT table provides the basis: [[

]] (Reference 1, Table 4.2-1, Entry F3). In the RAI response, however, GEH explains that emergency core cooling interaction and mixing in the upper plenum is addressed by several other phenomena in addition to those listed in Section 5.1.6.2 of Reference 1 (i.e., [[]]). This includes the upper plenum spray distribution and CCFL. The vendor makes this observation from the standpoint that the importance is assessed relative to the phenomenon's impact on the critical safety parameters, which relate to the core. The key impact of upper plenum mixing is the availability of liquid to flow into a hot channel. [[

]] Based on the consideration of these additional phenomena in play relative to the influence of upper plenum mixing on the critical safety parameters, the NRC staff determined that the GEH assessment of the importance of upper plenum mixing and ECC interaction is acceptable.

In conclusion, the NRC staff review determined that there was generally acceptable agreement between the GEH PIRT for TRACG-LOCA, and other, contemporary PIRTs. In cases where GEH assigned a lower-rank importance to a particular phenomenon as compared to other PIRTs, the NRC review determined that (1) GEH provided an adequate basis for its particular ranking, and (2) despite a lower ranking, the phenomenon is either treated statistically (if ranked

^E The uncertainty attributed to PIRT Item M3 defers to PIRT Item F3. The results shown in response to RAI 13 indicate that [[

medium), or the uncertainty associated with the phenomenon is addressed by other relevant phenomena that are also considered in the PIRT. Based on these considerations, the NRC staff determined that GEH's PIRT for TRACG-LOCA was acceptable.

3.4. ACCIDENT SCENARIO IDENTIFICATION – CONCLUSION

Based on the considerations discussed in the preceding sections, the NRC staff determined that GEH is consistent with the guidance associated with specifying an accident scenario. The review established that TRACG-LOCA is to be used for analyzing ECCS performance in the BWR/2-6 product line, for GNF fuel. Specific considerations for other fuel designs are reflected in Section 3.1 of this SE. The EM will be used to determine compliance with the acceptance criteria contained in paragraphs (b)(1) through (b)(3) of § 50.46, with additional consideration of the remaining criteria as discussed in Section 3.2 of this SE. Finally, GEH has applied the PIRT process in an acceptable way to ensure that the important phenomena relative to the critical safety parameters are appropriately treated in the evaluation model.

4.0 TRACG BACKGROUND AND EXECUTION

This section provides a brief background on the origin and development of TRACG for an unfamiliar reader. Sections 4.1.1 and 4.1.2 are included as a confirmation that the vendor identified the "frozen version" of the computer code that will be used for ECCS evaluation, and the appropriate, supporting documentation. This content is provided in accordance with the review procedures outlined in SRP 15.0.2 (Reference 10, Page 3). Section 4.2 identifies the prior applications to operating BWR analysis, for which TRACG has been approved for use. Finally, Section 4.3 reviews topics related to the TRACG numerical methods used in ECCS evaluation, consistent with guidance provided in RG 1.157 (Reference 8).

4.1. TRACG OVERVIEW

The Transient Reactor Analysis Code (TRAC) family of codes began as a pressurized water reactor analysis code developed for the NRC at Los Alamos National Laboratory. A BWR version of the code was developed jointly by the NRC and GEH at the Idaho National Engineering Laboratory as TRAC-BD1/MOD1; the primary objective of this effort was to develop the capability to simulate BWR LOCAs.

In the mid-1980s, GEH developed a proprietary version of the code designated as TRACG. The objective of the proprietary code development was to have a code capable of realistic analyses of transients, stability, and anticipated transients without scram (ATWS) events. Further developments for the TRACG code have included the implementation of a three-dimensional kinetics model and an implicit integration scheme. The basic thermal-hydraulic model is a two-fluid model explicitly represented in the code with six conservation equations and appropriate closure relationships.

4.1.1. Frozen Code Version Selection

TRACG04P is selected as the computer code used in the analysis.

4.1.2. Provision of Complete Code Documentation

TRACG is described in GEH LTR NEDE-32176P, "TRACG Model Description" (Reference 16). Its general purpose qualification is provided in NEDE-32177P, "TRACG Qualification"

(Reference 17). Specific applications of the TRACG code are documented in NRC-approved LTRs (References 18 - 22). Table 3 summarizes the TRACG AOO applications for US operating BWRs.

4.2. SUMMARY OF PREVIOUS REVIEW FINDINGS RELATED TO TRACG FOR AOO APPLICATIONS

LTR Number	Title	Notes	Accession No.
NEDE-32906P-A, Rev. 1 (Reference 18)	TRACG Application for Anticipated Operational Occurrences (AOO) Transient Analysis	Approved TRACG02A for realistic analysis of AOOs	ML060390557
NEDE-32906P-A, Rev. 3 (Reference 19)	TRACG Application for Anticipated Operational Occurrences (AOO) Transient Analysis	Corrected a small error in the quantification of the accuracy of the void coefficient	ML062720163
NEDE-32906P-A, Supplement 1 (Reference 20)	TRACG Application for Anticipated Transient Without Scram Analyses	Extended TRACG02A acceptance for modeling anticipated transients without scram	ML033381073
NEDE-32906P-A, Supplement 2 (Reference 21)	TRACG Application for Anticipated Operational Occurrences Transient Analysis	Modified approach for calculating critical power ratio during transient analysis	ML060800312
NEDE-32906P-A, Supplement 3 (Reference 22)	Migration to TRACG04/PANAC11 from TRACG02/PANAC10 for TRACG AOO and ATWS Overpressure Transients	Implemented TRACG04P and PANAC11 for use in AOO, ASME Overpressure, and ATWS Overpressure analyses	ML110970401

Table 3. Summary of Previous Review Findings Related to TRACG for AOO Applications.

4.3. NUMERICAL METHODS

In the course of its review, the NRC staff evaluated the TRACG numerical methods with regard to their adequacy for ECCS evaluation. This aspect of the evaluation considered the TRACG nodalization, time discretization, and steady-state initialization. The NRC staff generated four RAIs related to the execution of TRACG for ECCS evaluation. These RAIs, summarized in Table 4, are addressed in this section of the SE.

Batch	RAI	Topic	Ref.
1	41	6-Sector VSSL Nodalization Sensitivity	3
2	71	Changes to Nodalization	4
1	10	Time Step Sensitivity	3
2	77	Steady-State Initialization	4

Table 4. RAI Responses Related to Numerical Methods.

This portion of the review evaluated GEH's consistency with Regulatory Position 2.1.1, "Numerical Methods," of RG 1.157 (Reference 8).

4.3.1. Nodalization

Regulatory Position 2.1.1, "Numerical Methods," of RG 1.157 states, "*Numerical simulations of complex problems such as those considered here, treat the geometry of the reactor in an approximate manner, making use of discrete volumes or nodes to represent the system. Sensitivity studies and evaluations of the uncertainty introduced by noding should be performed.*"

The basic nodalization philosophy used in TRACG-LOCA is provided in Chapter 6 of Reference 17. The general approach is to apply nodalization detail to the plant model that is consistent with the models used in the integral effects test (IET) comparisons. As applied to a plant, the axial levels and node boundaries in the vessel are selected so as to resolve important geometric features such as the recirculation pump suction, the top of the jet pump, and the location of important core features such as the core support plate and the lower tie plate.

Nodalization sensitivity is discussed in Section 5.2 of Reference 1, and is also addressed, with respect to ECCS-LOCA analysis, in Section 6.9.2 of Reference 17. The vendor addressed nodalization sensitivity by increasing the noding detail in regions of the system model, using separate studies for each region in which detail was increased. Generally, the studies showed that [[

]] which is discussed in

Section 4.3.2 of this SE. These studies show that increasing the noding detail in various regions of the model can cause variations in PCT, but that [[

]].

[[

]]

It should be noted, however, that GEH attributed a significant amount of variability associated with its results to the parallel channel effect, which is defined and discussed in Section 7.4 of this SE. In short, the parallel channel effect introduced additional variability when attempts were made to quantify code or computational (i.e., non-parametric) uncertainty. As such, the variability associated with the timestep sensitivity study, or with other such measures like small perturbation analyses, tended to be inflated. The same variability was observed in the BWR/3-6 nodalization sensitivity study results, making it difficult to discern the true adequacy of the nodalization.

During the review process, GEH added significantly more detail to the core model, which had the effect of reducing the model sensitivity to the parallel channel effect. Because of this, the variability associated with both time step sensitivity and small parametric perturbations was reduced. Given this reduced variability, GEH incorporated additional nodalization sensitivity studies specifically for the detailed, BWR/2 model. The more detailed, BWR/2 model exhibited significantly less PCT sensitivity to changes in the level of detail in the vessel nodalization. For example, increasing detail in the vessel component, as well as in selected regions within the vessel, such as the upper plenum, bypass, and lower plenum, showed less than [[]] fluctuation in PCT, in each case. For comparison, the BWR/2 timestep sensitivity study indicated that the standard deviation associated with time step variation was [[]], and the small perturbation analyses performed in response to RAI 9 showed a variation (min to max for a sample of 59 cases) of [[]].

The NRC staff issued RAI 41 to query the existence of a [[]] azimuthal sensitivity study, which is referenced in Section 5.1.1.9 of the LTR. This section discusses the uncertainty associated with 3-dimensional effects in the lower plenum, and GEH referenced the [[]]

]] sensitivity study. In the response to RAI 41, GEH clarified that this study had been performed in 2002, but was not included in the qualification LTR. The vendor provided further information quantifying that the increased detail caused the PCT to [[]]

]]. GEH used this information to conclude that the vessel azimuthal detail in the standard nodalization was adequate. Based on the minor change in PCT, the NRC staff agrees with GEH's conclusion.

Based on the NRC staff review of the information contained in LTR Section 5.2, as discussed above, the NRC staff determined that GEH has investigated the effect of nodalization and concluded that the default nodalization is adequate for ECCS-LOCA analysis. Specifically, the BWR/2, detailed core model nodalization sensitivity studies showed acceptably small fluctuation in PCT when compared to more detailed nodalization schemes. On this basis, the NRC staff determined that GEH's approach to nodalization is consistent with the guidance in RG 1.157 and hence acceptable. The following paragraphs address a generic process for increasing nodalization detail, and also provide a limitation requiring that the nodalization sensitivity studies for the BWR/4 plant be updated, and results reported to the NRC staff, prior to plant-specific implementation of TRACG-LOCA for BWR/3-6s.

In LTR Section 5.2, GEH provides a process to modify the default nodalization for LOCA analysis, stating, "Additional details may be added or changed from the standard nodalization provided the changes are shown not to invalidate the qualification bases and the effect on modeling biases and uncertainties are assessed." In RAI 71, the NRC staff requested additional information concerning this process. In the response to RAI 71, GEH stated that the LTR

specifies the least-detailed nodalization that is acceptable, meaning that such changes would only serve to increase the level of detail. GEH provided an example, wherein [[

]] The process requires confirming that the added detail does not cause results to differ in a statistically significant way.

In considering this information, the NRC staff determined that this process, if implemented administratively, would be subject to the requirements contained in 10 CFR 50.59, "Changes, Tests, and Experiments." Specifically, an update to the nodalization would be considered a change to an element of TRACG-LOCA, and would need to satisfy the *conservative or essentially the same* clause that excludes such a change from requiring prior NRC review and approval in facility-specific implementation.^F

In addition to the above considerations, the NRC staff recognizes that the initial nodalization sensitivity studies were performed for the BWR/4 demonstration plant, but not subsequently updated using the more detailed core model, as the BWR/2 demonstration plant was used instead. Thus, the NRC staff will require GEH to perform updated nodalization sensitivity analyses and report the results to the NRC staff for each of a BWR/4 and BWR/6 demonstration plant prior to allowing BWR/3-6 implementation. This is Limitation 7, "BWR/3-6 First-of-a-Kind Application," as discussed in Section 10.7 of this SE.

4.3.2. Time Discretization

Regulatory Position 2, "Considerations for Thermal-Hydraulic Best-Estimate Codes," of RG 1.157, reflects the NRC staff guidance applicable to the discretization of transient time. Regulatory Position 2.1.1, "Numerical Methods," states, in part, "*Numerical methods treat time in a discrete manner, and the effect of time-step size should also be investigated.*"

This topic is addressed by the vendor in Section 6.9.2 of Reference 17. Reference 17 provides a sensitivity study that varies the maximum time step between [[

]] for a BWR-4 large-break LOCA. In RAI 10, the NRC staff requested that the vendor expand this sensitivity study to small- and intermediate-break events for the BWR/4, and to a BWR/2 large-break.

In the response, GEH updated the time step sensitivity study to include the requested plants and break sizes, and also to use the updated, more detailed core model (see SE Section 5.3). The studies included [[]] cases with increasing time step sizes. The results associated with the more detailed core model, which will be used in production safety analysis, showed very little variation in PCT as a function of the time step size. The standard deviation in PCT of the [[]] cases associated with each sensitivity study ranged from [[]]. Shown in Figure 1 is an example of the sensitivity study result, which applies to a BWR/4 intermediate break using the detailed core model (Reference 3, Figure R10-5).

^F Although 10 CFR 50.59 requirements do not apply when a more specific regulation such as 10 CFR 50.46 provides more explicit requirements for accomplishing a change, both requirements must be considered individually, each on its own merits. Additional discussion on the interplay between these requirements is available in RIS 2016-04, "Clarification of 10 CFR 50.46 Reporting Requirements and Recent Issues with Related Guidance Not Approved for Use" (Reference 23). In short, to be implemented administratively, the nodalization change would not be permitted to constitute a *departure from a method*... and reporting the effects of such a change would fall under the requirements of 10 CFR 50.46(a)(3).

[[

Figure 1. Time Step Sensitivity for BWR/4 Intermediate Break with Detailed Core Model.

]]

Based on this result, the NRC staff determined that GEH has investigated the effect of time-step size and concluded that, in the range of the TRACG default maximum time step size of [[

]]. On this basis, the NRC staff determined that the time discretization used in TRACG-LOCA is consistent with the guidance in RG 1.157 and hence acceptable.

4.3.3. Initialization

Although not addressed explicitly in the applicable regulatory guidance, it is important, when analyzing a thermal-hydraulic transient system response, to ensure that the system model can achieve a converged, steady-state initial condition. This is an indication that the code performs in a stable manner, and a confirmation that the initial system parameters have been represented correctly.

In the response to RAI 77, GEH explained its process for ensuring that a steady-state calculation has adequately converged prior to performing transient calculations. The process includes checking a limited set of heat balance parameters, to ensure that any fluctuations are within a specified tolerance. GEH stated that the tolerances are approximately [[

]]. The steady-state case is typically run [[]] after reaching the specified tolerances to ensure that the parameters continue to remain within tolerance.

The approach described above will ensure that the steady-state condition is properly modeled prior to initiating a transient analysis. Based on this consideration, the NRC staff determined that the GEH process for ensuring steady-state convergence is acceptable.

5.0 TRACG-LOCA METHODOLOGY

The TRACG-LOCA methodology relies on a combination of extensive system analysis and simplifying assumptions to identify appropriately limiting conditions prior to performing a statistical uncertainty analysis. Most variability in initial and boundary conditions is addressed through detailed, deterministic system analysis that identifies several sets of plant-specific limiting conditions to evaluate using the statistical analysis. The EM also addresses some aspects of initial and boundary condition variability through the use of simplifying conservative or bounding assumptions. Detailed core modeling, including the use of multiple limiting channels located in two separate rings of the core, addresses the variability of cycle design-dependent parameters, such as power distribution, peaking factors, and exposure.

The NRC staff review of the analytic methodology is based on Regulatory Position 3.1, "Initial and Boundary Conditions and Equipment Availability," of RG 1.157, which states as follows (Reference 8):

The heat generated by the fuel during a loss-of-coolant accident depends on the power level of the reactor at the time of the loss-of-coolant accident and on the history of operation. [...] Given the assumed initial conditions, relevant factors such as the actual total power, actual peaking factors, and actual fuel conditions should be calculated in a best-estimate manner.

The calculations performed should be representative of the spectrum of possible break sizes from the full double-ended break of the largest pipe to a size small enough that it can be shown that smaller breaks are of less consequence than those already considered. The analysis should also include the effects of longitudinal splits in the largest pipes, with the split area equal to twice the cross-sectional area of the pipe. The range of break sizes considered should be sufficiently broad that the system response as a function of break size is well enough defined so that interpolations between calculations, without considering unexpected behavior between the break sizes, may be made confidently.

Other boundary and initial conditions and equipment availability should be based on plant technical specification limits. These other conditions include, but may not be limited to, availability and performance of equipment, automatic controls, and operator actions. Appendix A to 10 CFR Part 50 requires that a single failure be considered when analyzing safety system performance and that the analysis consider the effect of using only onsite power and only offsite power.

Based on the above guidance, the NRC staff review of the initial and boundary conditions and equipment availability addressed the following:

- (1) Time in cycle
- (2) Operating statepoints
- (3) Power distribution and channel groupings
- (4) Break spectrum analysis
- (5) Adherence to TS LCOs and equipment performance
- (6) General Design Criterion 35 compliance

A complete description of the way that GEH treats initial and boundary conditions requires review of both Chapters 6 and 8 of Reference 1, as well as consideration of additional

commitments made in response to RAIs. Such discussion is provided in detail in the succeeding subsections of this SE. Generally, GEH distinguishes between initial conditions and plant parameters, and the items identified in the list above fall within these two categories. Section 6.2 of Reference 1 addresses initial conditions, and Section 6.3 addresses plant parameters.

The RAI responses relevant to this review are listed in Table 5, below. They are listed in the order in which they are discussed.

Batch	RAI	Topic	Ref.
1	27	Operating Domain Applicability	3
2	84	Disposition for Increased Core Folow	4
1	3	Channel Grouping	3
1	6	Channel Grouping	3
1	7	Channel Grouping and Analysis Resolution	3
1	9	Channel Grouping	3
2	72	Hot Channel Power Distribution Initial Conditions	4
2	73	Hot Channel Power Distribution Initial Conditions	4
2	74	Hot Channel Power Distribution Initial Conditions	4
4	102	Hot Channel Power Distribution Initial Conditions	6
1	4	Single Parameter Sensitivity Studies	3
1	31	Use of De-biased Simulations for Analysis	3
1	57	Discharge Flow Uncertainty	3
2	89	Break Spectrum Analysis	4
2	86	Treatment of TS-Controlled Parameters	4
2	87	Applicability of Generic Scram Time Curve	4
2	75	Control Blade Interference/Scram Time	4
1	12	Treatment of GDC 35	3
2	76	Treatment of GDC 35	4

Table 5. RAI Responses Related to TRACG-LOCA Methodology.

5.1. TIME IN CYCLE

Fuel rod exposure is addressed in Section 6.2.7 of the LTR. The LTR provides a general description of the cycle-dependent burnup characteristics of GE14 fuel. The LTR states, “fuel rod power is restricted based on the fuel rod exposure (i.e., PLHGR limit). The thermal mechanical design envelope for allowable PLHGR versus exposure provides the limiting conditions for the rod exposure.” GEH considers a range of fuel rod exposures, including for both UO₂ and Gadolinia rods. Limiting channels are included in the core model to represent the life of the fuel. While the minimum number of hot channels associated with a core model is [[]], the vendor will include additional hot channel components to represent additional burnup points in the plant MAPLHGR curve. This topic is addressed in more detail in Section 5.3 of the SE.

Many exposure-dependent effects correlate to the time-in-cycle, but are addressed by other aspects of the model. For example, Section 6.2.5 of the LTR describes the exposure-dependent characteristics of the radial and axial power peaking. In addition, the stored energy and decay heat models require either explicit or bounding treatment of time-in-cycle. Fuel rod design characteristics, such as fuel thermal conductivity and pellet-cladding gap thermal conductivity, are also exposure-dependent.

5.2. OPERATING STATEPOINTS

Permissible operating statepoints for a BWR are defined by the power-to-flow operating domain. The power-to-flow operating domain governs important initial conditions such as the axial void profile and the total core power. At the time of the review of NEDE-33005P, the maximum operating domain for BWRs extended to 120-percent of the original licensed thermal power level (OLTP), and at that power level, the permissible flow range extended from a minimum of

80-percent of recirculation flow, up to 108-percent. This is known as the Maximum Extended Load Line Limit Analysis Plus (MELLLA+) operating domain.

A typical MELLLA+ operating domain is illustrated in Figure 2, which is a reproduction of Figure 6.2-1 of NEDE-33005P.

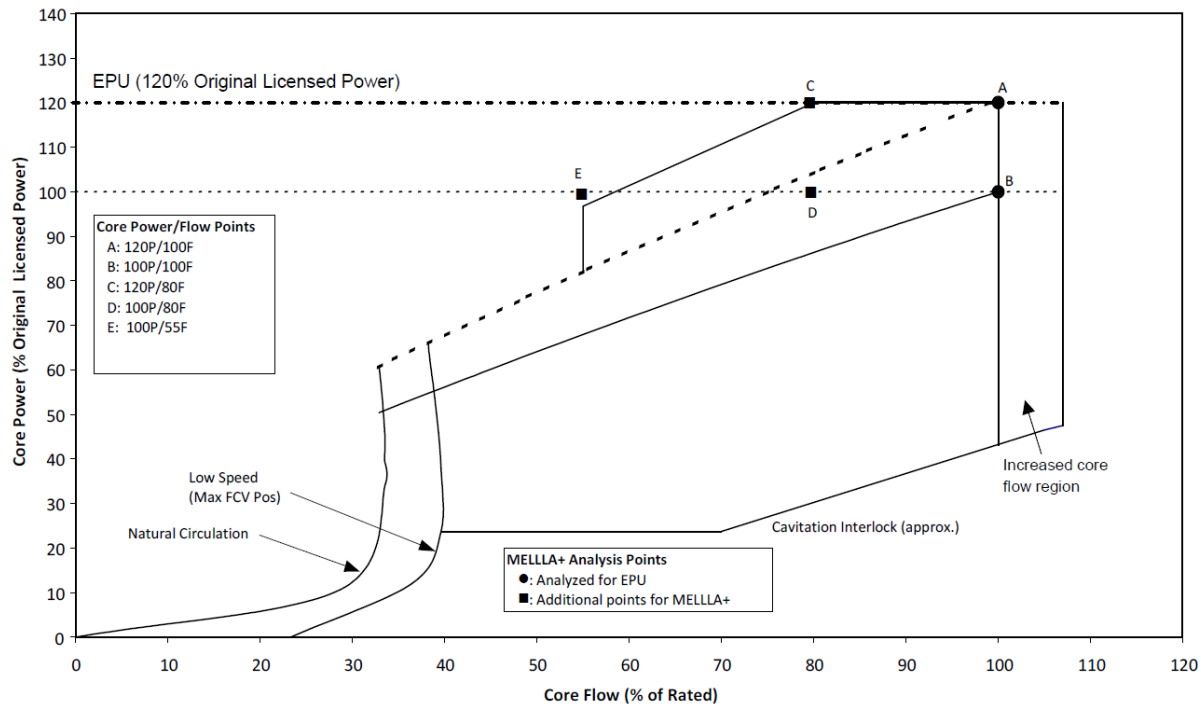


Figure 2. MELLLA+ Power-to-Flow Operating Domain.

The system response is studied for a variety of statepoints, to envelope the operating domain. For MELLLA+ plants, this means that small- and large-break LOCAs are analyzed to cover points A, C, and E in Figure 2. As noted in the response to RAI 27, the power-to-flow operating domain is plant specific in that not all plants are licensed to operate in the MELLLA+ operating domain, and not all plants have received license amendments to implement EPU.⁶ Thus, as noted in the response to RAI 27, “Each application will use the plant-specific power-flow map and determine the power-flow condition that leads to the highest PCT.”

The Increased Core Flow (ICF) region may not always be analyzed. As noted in the response to RAI 84, [[

]] Thus, GEH states that the ICF region will be evaluated on an application-specific basis to determine if analysis is required.

GEH will deterministically increase core power by two-percent to account for calorimetric uncertainty. In some cases, NRC licensees have installed ultrasonic flow meters to improve this

⁶ In addition, not all BWRs that implement EPU's uprate to the full 120%-original licensed thermal power (OLTP) value. An EPU is considered an uprate that increases the licensed thermal power output anywhere between 7- and 20-percent of OLTP.

value, and have reduced the calorimetric uncertainty. If this is the case, licensees implementing TRACG-LOCA may use an appropriately justified thermal power uncertainty. This does not apply, however, to any reduced calorimetric uncertainty associated with a UFM for which the NRC has withdrawn its approval. Such licensees must revert to the generic, 2-percent uncertainty. This is Limitation 2.6, as discussed in Chapter 10 of this SE. Refer also to Reference 24 for additional details.

5.3. POWER DISTRIBUTION AND CHANNEL GROUPINGS

The treatment of the power distribution is described in Section 6.2.5 of the LTR. The treatment was revised significantly during the NRC staff review. While the original LTR specified the use of [[]] channel groupings in a typical core model, the response to RAIs 3, 6, 7, and 9 indicated that GEH would instead use a more detailed core model, comprised of at least [[]] channel groups; [[]]. In addition, the treatment of power peaking factors in the hot bundle was revised by the response to RAIs 72-74. As noted in the response to RAI 102, the revision requires [[]]

]]. The NRC staff evaluation pertains to the revised model, and is supplemented with additional approval conditions that ensure that relevant factors such as the actual total power, actual peaking factors, and actual fuel conditions are calculated in a best-estimate manner, as recommended by RG 1.157.

The peak bundle power at a given plant has several constraints that are important in the ECCS evaluation. These include the axial power distribution, the peak linear heat generation rate, and the critical power ratio. The axial power distribution tends to be tightly correlated with cycle burnup, with bottom-peaked power shapes more likely for fresh fuel bundles, and top-peaked power shapes becoming more dominant as the exposure increases. GEH stated that, for a given bundle power, and axial and local power shapes, the maximum LHGR or the minimum MCPR will yield the highest PCT. The demonstration analyses indicate that a basis for a limiting power shape can be identified, and the BWR/4 demonstration analyses, in particular, include sensitivity studies of the limiting axial node.

The following excerpt from LTR Section 6.2.5 provides a detailed description of the constraints on bundle peaking:

Three limits constrain the design and operation of fuel bundles: Thermal Mechanical Operating Limit (TMOL), which is the limiting Peak Linear Heat Generation Rate (PLHGR), MAPLHGR [Maximum Average Planar Linear Heat Generation Rate] and Operating Limit Minimum Critical Power Ratio (OLMCPR).
[[]]

]]

The LTR includes several figures, Figures 6.2-2 to 6.2-6, which illustrate cycle performance with respect to margin to LHGR and MCPR operating limits for a variety of plant vintages and fuel bundle designs. The response to RAI 73 also includes similar data for more recent bundle designs, including GE11, GE12, and GNF2 fuel. The figures in the response to RAI 73 confirm

that modern fuel bundle designs perform consistently with the designs considered in the LTR. All of these figures illustrate the general trend in cycle performance described above, namely that [[

]]

In the response to RAI 102, GEH summarized its revised approach to modeling the hot channel groupings in the core. Based on the RAI response, GEH will ensure that each core is modeled [[]. As described in the RAI response, the channels capture the variations in axial peaking [[]. The vendor also captures variations in limiting fuel and thermal-hydraulic conditions [[

]] Variability in core spray flow availability is addressed [[

]]

Sensitivities to the axial location of the peak node are addressed in the demonstration analyses. An explicit sensitivity study is provided in Section 8.1.4.2 for the BWR/4 analysis. A similar study is provided for a BWR/2 in response to RAI 29, which is addressed in Section 8.2 of this SE. Regarding the axial power distribution, GEH notes that the results for the critical safety parameters are sensitive to the initial conditions and a basis for the limiting initial condition can be established. For the demonstration analyses, the limiting heated nodes are [[] for the bottom-peak, and [[] for the top-peak.^H Sensitivity studies confirm that this is the case; for the BWR/4, the study results are provided in Table 8.1-5 of Reference 1.

The NRC staff determined that this analytic approach provides an acceptably detailed core model to capture the effects of variation in power distribution, time-in-cycle, and steady-state thermal-hydraulic performance, as recommended by RG 1.157. Since the model and sensitivity studies account for all of these effects, the NRC staff determined that TRACG-LOCA is acceptable in this regard. Noting the processes described in response to RAI 6 and RAI 102, Limitations 2.1, "Core Detail," and 2.2, "Hot Channels," apply as described in Chapter 10 of this SE.

5.4. BREAK SPECTRUM ANALYSIS

The break spectrum analysis is performed for the limiting statepoint. The spectrum includes both recirculation discharge and suction line breaks, breaks in the main steam lines, and ancillary line breaks like the core spray line. The response to RAI 4 discusses the use of sensitivity studies to identify limiting conditions. The response to RAI 31 discusses the use of de-biased code runs to complete the spectral analysis. The response to RAI 89 follows on to RAI 31. The response to RAI 57 discusses uncertainty in the critical flow model. The response is tangentially related to the break spectrum, since the effective break area is the product of the break area and the discharge flow uncertainty; however, the response to RAI 57 is more appropriately evaluated in Section 6.2 of this SE.

^H Note that the standard channel nodalization includes [[]] axial nodes, of which 25 are heated.

The deterministic break spectrum includes a variety of split break sizes, as well as a double-ended guillotine break (DEGB). The split breaks are analyzed at a resolution that is sufficient to permit overlap, in terms of effective break area, between successive break sizes when considering the discharge flow uncertainty. The statistical analysis includes consideration of the discharge flow uncertainty, and is performed for the limiting break size. If a conclusively limiting break size is not identified, the potentially limiting breaks are treated as sensitivity studies. These modeling approaches are revisited in Chapter 7, "Estimation of Overall Computational Uncertainty," of this SE. Limitation 4.1 in Chapter 10 of the SE requires GEH to adhere to this analytic approach.

As described in the demonstration analyses in LTR Chapter 8, the analytic method is not prescriptive with regard to whether model biases should be removed from, or compensated in, the computer code prior to analyzing the break spectrum to determine the limiting break size (i.e., "de-biased").¹ The NRC staff questioned this approach in RAI 31, seeking justification for analyzing the break spectrum without first de-biasing TRACG. Similar considerations would also apply in performing system analyses to identify the limiting initial conditions. Namely, performing a series of analyses without first correcting the code for biases could result in the erroneous identification of the limiting break size or other initial conditions. In the response to RAI 31, GEH provided several comparisons to illustrate that implementing the more detailed core model had a more significant effect on the break spectrum than did the compensation for model bias in the code. For the limiting intermediate break size region, this behavior is apparent in Figure R31-1 of the RAI response. When comparing the detailed core model using both biased and de-biased TRACG models, it is clear that the break spectrum performs, for the limiting break size region, very similarly. Nonetheless, GEH pointed out that the break spectrum is traditionally determined from best-estimate nominal results, from which the NRC staff understands that GEH will analyze plant-specific break spectra using de-biased code runs.

The NRC staff continued its evaluation of this issue with follow-on RAI 89. While RAI 31 and its response focused on the use of biased or de-biased results relative to the evaluation of the break spectrum, RAI 89 focused on whether the nominal break spectrum appropriately identified the break characteristics that would be limiting when the statistical analysis was performed and the corresponding upper tolerance limits were determined. In the response to RAI 89, GEH executed statistical analysis for $[[\quad]]$ break sizes clustered around the limiting break size. The results showed that, among the $[[\quad]]$ cases, the one-sided upper tolerance limit PCT varied within a range of $[[\quad]]$. GEH compared this to the estimated analysis resolution^j associated with the detailed channel grouping model, which is on the order of $[[\quad]]$, and concluded that the variation was insignificant. Moreover, the limiting one-sided upper tolerance limit was $[[\quad]]$ than that associated with the one-sided upper tolerance limit determined for the nominally limiting break size.

Based on its review of the sensitivity studies provided in the LTR, as supplemented with analyses provided in the RAI responses, the NRC staff determined that GEH appropriately analyzes the break spectrum to determine the limiting breaks. Thus, the NRC staff concluded

¹ GEH introduces the term "de-biased" in the response to RAI 89, stating, "The biased results in the response to... RAI-31 refer to the TRACG calculation results in which those TRACG model biases determined in Section 5 of the LTR are not removed. On the contrary, the non-biased results in the response to... RAI-31 refers to the results in which the TRACG model biases are removed. The non-biased results are actually, more precisely, de-biased results, which will be called hereafter."

^j Refer to Section 7.4 for discussion of the analysis resolution.

that GEH is consistent with the portion of Regulatory Position 3.1 of RG 1.157, which recommends that calculations be representative of the full spectrum of possible break sizes. The GEH approach also conforms to the passage in 10 CFR 50.46(a)(1)(i), requiring postulated LOCAs of different sizes, locations, and other properties be calculated, sufficient to provide assurance that the effects of the most severe hypothetical LOCAs are calculated. Based on these considerations, the NRC staff determined that TRACG-LOCA is acceptable with respect to the break spectrum analysis. Limitation 2.3, "Break Spectrum Analysis," specifies the appropriate approach to identify the limiting break for statistical analysis.

5.5. ADHERENCE TO TS LCOS AND EQUIPMENT PERFORMANCE REQUIREMENTS

Chapter 6 of the LTR describes the EM approach with regard to initial conditions and plant parameters. Many parameters that fall into either category are controlled by facility TS or related, design-basis requirements. The LTR makes a distinction between plant parameters and initial conditions as follows:

A distinction is made in [NEDE-33005] between *initial conditions* and *plant parameters*. The initial rated conditions for a nuclear power plant, specified in absolute units, are considered as plant parameters in certain contexts. In [NEDE-33005], however, those key plant inputs that determine the overall steady-state nuclear and hydraulic conditions prior to the transient are considered to be *initial conditions*...

The term *plant parameter* is reserved for quantities such as protection system setpoints, valve capacities and stroke times, and scram characteristics that influence the characteristics of the transient response but do not have an effect on steady-state operation.

5.5.1. Initial Conditions

A number of initial conditions, including total core power and flow, limiting bundle power distribution, average bundle power distribution, and fuel rod exposure, are addressed in the preceding sections of this chapter. Remaining initial conditions include feedwater temperature, steam dome pressure, and downcomer water level.

The treatment of feedwater temperature is described in Section 6.2.2; [[

]]

The treatment of steam dome pressure is described in 6.2.3 of the LTR. Steam dome pressure is a TS-controlled parameter. The vendor stated that [[]]] is expected to be limiting, but evaluated the sensitivity of the results to the dome pressure in the demonstration analyses. The sensitivity studies documented in Section 8 of the LTR indicate that the [[]]]. This is an item subject to plant-specific confirmation as a part of preparation of a qualified base deck and break spectrum analysis.

The downcomer water level is controlled between two alarm setpoints: the low level (L4) and the high level (L7). In a typical BWR/4, this may correspond to a level control range of

approximately 0.2 meters. Similar to feedwater temperature and steam dome pressure, sensitivity studies demonstrated [[

]] The studies discussed in Section 8.1 of the LTR indicated that varying the initial level by [[

]] In practice, GEH will confirm on a plant-by-plant basis that the downcomer water level does not significantly affect the TRACG-LOCA results, or will use a limiting initial condition. With regard to feedwater level control, this disposition is appropriate in consideration of the fact that the level control system has no safety basis, and the reactor trip and ECCS actuation signals associated with reactor vessel water level are not received until inventory is depleted below L4.

In summary, the analytic sensitivity to initial conditions is evaluated in the TRACG-LOCA analysis. [[

]] The approach is presented in Chapter 6 of the LTR, and its application is demonstrated in Chapter 8. If the results of the sensitivity studies indicate that the critical safety parameters are sensitive to a particular initial condition, the uncertainty associated with that initial condition will be considered in the analysis, either by using a bounding input, or by applying the uncertainty in the uncertainty analysis. The GEH approach is acceptable, subject to Limitation 2.4, "Initial Conditions and Plant Parameters," as discussed in Chapter 10 of this SE.

5.5.2. Plant Parameters

Regarding the ECCS performance evaluation, GEH states that the plant FSAR provides a list of significant inputs. These inputs are generally analyzed at TS analytic limits, as indicated in Table 6.3-1 of the LTR. The use of TS analytic limits for plant parameters is generally acceptable, because it introduces conservatism into the analysis relative to a given plant's actual, permissible, operating state.

In the LTR, GEH states that realistic uncertainty distributions for TS-controlled parameters may be used. In response to RAI 86, GEH clarified that the use of analytic limits precludes the need to develop and implement realistic uncertainty distributions; however, plants using an NRC-approved instrument setpoint methodology may replace analytic limits with realistic uncertainty distributions. The vendor further stated that NRC licensees seeking to implement such realistic distributions, but without having previously implemented an NRC-approved instrument setpoint methodology, would need to seek prior NRC review and approval. Since the licensees would be using uncertainties associated with an NRC-approved methodology, the NRC staff determined that the adoption of this more realistic approach would be acceptable. Limitation 2.4, "Initial Conditions and Plant Parameters," establishes the requirement for treatment of plant-specific initial conditions, and allows for the approach whereby initial condition uncertainty may be treated more realistically using an NRC-approved instrument setpoint methodology.

Chapter 6 of the LTR introduces and justifies [[

]] Section 6.3.1 describes the methods [[

]] and the response to RAI 87 provided additional information supporting the use [[

]].^K It was determined by modeling steamline breaks for a variety of reactor and containment designs, [[

]] In the response to RAI 87, GEH provided a comparison of the scram times [[

]]

The scram time is set either by the high drywell pressure scram signal, as described above, or by the L3 signal, which is determined mechanistically from the TRACG trip logic. Then, the scram speed is modeled using the TS scram speed applicable to the plant. RAI 75 sought clarification whether scram speed could be affected by equipment degradation, such as shadow corrosion-induced channel bow, or by the attendant effects of a seismic event. In response, GE stated that TS LCOs, Surveillance Requirements, and seismic analysis requirements ensure that such mechanisms do not adversely affect the scram performance relative to the TS requirement. Based on this explanation, the NRC staff agrees that the TS scram speed is an appropriately bounding approach to modeling the scram.

The review described above established that GEH treats initial conditions and plant operating parameters in an appropriate fashion. However, the NRC staff determined that a limitation is necessary to ensure that this practice is carried forward into plant-specific analysis. Excluding uncertainty as determined using an NRC-approved instrument setpoint methodology, variability in initial conditions and plant parameters not specifically addressed in Chapter 6 of the LTR, as supplemented by RAI responses, shall not be analyzed using the statistical analysis, but rather shall be treated deterministically as set forth in revised Chapter 6 of the LTR. Significant plant parameters must be assumed to be in their most pessimistic condition with regard to the results; Technical Specification Analytic Limits for which the ECCS evaluation is an Applicable Safety Analysis shall be used; and parameters shown to have an insignificant effect on the results may be assumed to be in a nominal condition. This is Limitation 2.4, as discussed in Chapter 10 of this SE.

5.6. GENERAL DESIGN CRITERION 35 COMPLIANCE

The analyzed break spectrum is required to address compliance with GDC 35, which requires:

A system to provide abundant emergency core cooling shall be provided. The system safety function shall be to transfer heat from the reactor core following any loss of reactor coolant at a rate such that (1) fuel and clad damage that could interfere with continued effective core cooling is prevented and (2) clad metal-water reaction is limited to negligible amounts.

Suitable redundancy in components and features, and suitable interconnections, leak detection, isolation, and containment capabilities shall be provided to assure that for onsite electric power system operation (assuming offsite power is not available) and for offsite power system operation (assuming onsite power is not

^K Plant scram can be initiated by low downcomer water level (L3), or by high drywell pressure. [[

]]

available) the system safety function can be accomplished, assuming a single failure.

Based on the above, the NRC staff review of GDC 35 compliance assesses limiting single failures and the treatment of offsite power availability.

Limiting single failures are addressed within the deterministic break spectrum analysis. Consideration of the limiting single failures specific to a break size range is provided, which includes both a system-level evaluation of hardware availability, and analysis of the consequences of the equipment failure. Examples of this evaluation are provided in the demonstration analyses provided in Chapter 8.

The demonstration analyses presented in Chapter 8 of the LTR use a conservative approach to modeling power system availability. Attributes of offsite power availability, such as a delayed scram in comparison to a loss-of-offsite power, which exacerbate the consequences of the event, are modeled. Otherwise, a loss-of-offsite power is assumed. Using this hybrid approach leads to a conservative modeling approach. Additional information clarifying the modeling approach is provided in the response to RAI 12. The response to RAI 12 also indicates []

]]

In response to RAI 76, GEH clarified further that realistic assumptions, to be consistent with either OPA or LOOP, will be used to show compliance with GDC 35. The vendor also revised text in Table 2.5-1 of the LTR to state, "Consistent with the requirement of General Design Criteri[on] 35, both loss of onsite power and loss of offsite power are assumed individually. System availability to loss of either onsite or offsite power is modeled consistently with realistic plant configurations." The revised table entry indicates that the deterministic analysis will evaluate both scenarios to identify the limiting, which assures that GDC 35 is satisfied.

The response to RAI 12 also indicated that, in the TRACG LOCA application methodology, there is no consideration of any credit gained from non-safety grade systems. This approach is consistent with NRC staff expectations regarding the use of safety-grade systems to mitigate design basis events. The use of only safety-grade systems ensures that there is a high probability that the systems will function as assumed in the analysis.

Based on the review described above, the NRC staff determined that GEH has addressed the requirements of GDC 35 within TRACG-LOCA, and from this perspective, the EM is acceptable. Limitation 2.5, "General Design Criterion 35 Compliance," requires each application of TRACG-LOCA to evaluate whether loss-of-offsite power or offsite power available conditions are limiting.

6.0 REVIEW OF KEY MODELS

Chapter 6 presents the NRC staff review of key TRACG models with regard to ECCS evaluation. This chapter follows the guidance set forth in Regulatory Positions 3.2 through 3.14 of RG 1.157, to the extent that such guidance applies to modeling BWR LOCAs.

6.1. SOURCES OF HEAT DURING A LOSS-OF-COOLANT ACCIDENT

Sources of energy during a postulated LOCA include mainly the initial stored energy in the fuel and the decay heat. The use of the Cathcart-Pawel (C-P) oxidation correlation is also reviewed,

as are thermal parameters for swelling and rupture of the fuel rods. Table 6 provides a list of RAIs relevant to this portion of the review, in the order first discussed.

Batch	RAI	Topic	Ref.
1	24	Use of PRIME as opposed to GESTR-LOCA	3
1	42	Dynamic gap conductance uncertainty	3
5	33	Rod internal pressure and fuel pin rupture	7
4	101	Decay heat modeling	6
1	54	Request for correction of Figure 5.1-18	3
3	100	Cathcart-Pawel oxidation limit	5
2	97	Cladding plastic deformation	4

Table 6. RAI Responses Related to Sources of Heat During a LOCA.

6.1.1. Initial Stored Energy of the Fuel

Regulatory Position 3.2.1 of RG 1.157 states, in part (Reference 8):

The steady-state temperature distribution and stored energy in the fuel before the postulated accident should be calculated in a best-estimate manner for the assumed initial conditions, fuel conditions, and operating history. To accomplish this, the thermal conductivity of the fuel pellets and the thermal conductance of the gap between the fuel pellet and the cladding should be evaluated. Thermal conductivity of the fuel is a function of temperature and is degraded by the presence of gases in crack voids between fuel fragments.^L An acceptable model for thermal conductivity should be developed from the in-pile test results for fuel centerline and off-center temperatures, taking into account the conductivity of gases in crack voids.

Thermal conductance of the fuel-cladding gap is a strong function of hot gap size and of the composition and pressure of the gases in the fuel rod. The calculation of hot gap size should take into account UO₂ or mixed-oxide fuel swelling, densification, creep, thermal expansion and fragment relocation, and cladding creep. [...] An acceptable model for the above fuel parameters should be based on in-pile and out-of-pile test data...

Best-estimate fuel models will be considered acceptable provided the models include essential phenomena identified above and provided their technical basis is demonstrated with appropriate data and analyses.

The TRACG-LOCA EM uses fuel parameter inputs supplied by the NRC-approved PRIME code (Reference 25). These PRIME inputs are used by TRACG to calculate the steady-state temperature distribution and stored energy in the fuel. The PRIME inputs also include the composition and pressure of the fuel rod gases, which are used to calculate the gap gas

^L Since publication of RG 1.157, additional mechanisms affecting nuclear fuel thermal conductivity as a function of fuel pellet exposure have been identified, which have been shown to affect ECCS performance, as predicted using a realistic evaluation model, significantly. Refer to NRC Information Notice (IN) 2009-23, "Nuclear Fuel Thermal Conductivity Degradation," and IN 2011-21, "Realistic Emergency Core Cooling System Evaluation Model Effects Resulting From Nuclear Fuel Thermal Conductivity Degradation," for further discussion (References 26 and 27).

conductivity. The inputs are generated assuming a realistic operating power history. The PRIME code has been found acceptable for use in simulating BWR fuel performance. During the course of the NRC staff review, GEH updated its analytic platform to replace GESTR-M-based fuel performance analysis with PRIME-based analysis. Thus, the TR as submitted indicated that either of these methods would be used, but this approach has since been modified to phase out the use of GESTR. This is a difference both in the TR as originally submitted, and in the TRACG-AOO application as documented in Reference 22.^M

In the response to RAI 24, GEH stated that only PRIME would be used for modeling in accordance with the TRACG-LOCA EM (Reference 3). Since the code is NRC-approved and accounts for the phenomena described above, the NRC staff determined that this approach is acceptable. Note, however, that the limitations applicable to the PRIME code, delineated in Section 4.0 of the NRC staff approving SE, are also applicable to TRACG-LOCA analysis. This is Limitation 3.2, "Limitations on the Use of Upstream/Concurrent Methods," as discussed in Chapter 10 of this SE. Additional justification must be reviewed and approved by the NRC staff in order to apply TRACG-LOCA using a different set of limitations or a different fuel performance model.

Uncertainties associated with the fuel rod stored energy and gap gas conductivity are derived in accordance with the PRIME methods qualification and ported to the TRACG-LOCA evaluation model accordingly (Reference 1, Section 5.1.3.6). Relative to previous TRACG applications, which used GESTR-based uncertainties, the TRACG-LOCA uncertainties include not only pellet heat transfer uncertainty, but also chamfer stored energy and additional power uncertainty. The response to RAI 42 provides additional discussion regarding the inclusion of these terms, explaining that combining them produces a root mean square value of []. This uncertainty value is evaluated in Section 8.5 of the technical evaluation report enclosed in Reference 25 and found to be acceptable.

The uncertainty in dynamic gap conductance is lumped with the pellet stored energy uncertainty. Thus, the NRC staff reviewed the basis for this [] value to confirm that it included sufficient margin to account for uncertainty associated with the ability of TRACG to model pellet contraction following reactor scram. In the response to RAI 42, the vendor noted that one of the uncertainty parameters combined to reach the [] value was a [] "additional power uncertainty." A review of Reference 25 (specifically, Page 3-7 of NEDC-33258P-A) indicates that this value is provided for monitoring uncertainty and future concerns, confirming that it is a margin term. This is an acceptable treatment; however, the NRC staff notes that the Limitations provided in Chapter 10.3 of this SE apply; the allocation of this margin term to other items (i.e., "future concerns" as noted in NEDC-33258P-A) within the PRIME approval basis would require revisiting the treatment of pellet stored energy within the TRACG-LOCA approval basis. Sensitivity studies associated with the PRIME implementation into downstream safety analyses demonstrated that the effect of changing the gap gas conductance []. In a revision to the response to RAI 33, GEH used this []

[] Refer to Section 6.1.5 of this SE for additional discussion.

Based on its review, the NRC staff determined that GEH obtains the initial stored energy using an NRC-approved fuel performance code, and the incorporation of the PRIME-based inputs is

^M TRACG-AOO has been updated to eliminate the reliance on GESTR-based models and inputs in production safety analysis.

consistent with other NRC-approved applications of TRACG. In addition, the PRIME-based fuel performance model incorporates models for the phenomena listed in Regulatory Position 3.2.1 of RG 1.157. Based on these considerations, the NRC staff determined that TRACG-LOCA is acceptable with respect to initial stored energy in the fuel.

6.1.2. Fission Heat

Regulatory Position 3.2.2 of RG 1.157 states:

Fission heat should be included in the calculation and should be calculated using best-estimate reactivity and reactor kinetics calculations. Shutdown reactivities resulting from temperatures and voids should also be calculated in a best-estimate manner. The point kinetics formulation is considered an acceptable best-estimate method for determining fission heat in safety calculations for loss-of-coolant accidents. Other best-estimate models will be considered acceptable provided their technical basis is demonstrated with appropriate data and analyses. Control rod assembly insertion may be assumed if it is expected to occur.

Fission heat is calculated using a point kinetics model, which has been validated against a more detailed, three-dimensional, nodal kinetics model. The 3D model has been approved by the NRC staff. In addition, fission heat contributes a negligible amount of energy following scram. Void reactivity feedback contributes a significant amount of negative reactivity prior to that point. GEH presents its basis for the void coefficient in Section 5.1.3.1 of Reference 1. ||

||

Section 5.1.3.2 of Reference 1 provides the basis for the point kinetics model. A figure compares the point kinetics model to the 3-D kinetics model in TRACG-AOO for a small-break LOCA event, showing reasonable agreement for the power transient.

The vendor uses a point kinetics model, which is consistent with RG 1.157 recommendations. Comparisons of the void reactivity curve and a small-break LOCA power transient between the point kinetics model and the TRACG-AOO-based 3-D nodal kinetics model show reasonable agreement. Based on these considerations, and in light of the fact that kinetics and void reactivity have a highest PIRT ranking of medium, the NRC staff determined the GEH approach for fission heat is acceptable.

6.1.3. Decay of Actinides and Fission Product Decay Heat

Regulatory Position 3.2.3 of RG 1.157 states:

The heat from radioactive decay of actinides, including neptunium and plutonium generated during operation as well as isotopes of uranium, should be calculated in accordance with fuel cycle history and known radioactive properties. The actinide decay heat chosen should be appropriate for the facility's operating

history. Best-estimate models will be considered acceptable provided their technical basis is demonstrated with appropriate data and analyses.

Regulatory Position 3.2.4 of RG 1.157 states:

The heat generation rates from radioactive decay of fission products, including the effects of neutron capture, should be included in the calculation and should be calculated in a best-estimate manner. The energy release per fission (Q value) should also be calculated in a best-estimate manner. Best-estimate methods will be considered acceptable provided their technical basis is demonstrated with appropriate data and analyses. The [1979 ANSI/ANS-5.1 Decay Heat Standard] is considered acceptable for calculating fission product decay heat.

The decay heat model included in TRACG04 is enhanced over what was previously provided in TRACG02. Whereas the TRACG02 code included the May-Witt decay heat model, TRACG04 adds both the 1979 and 1994 ANS decay heat models (Reference 22). The SE approving Reference 22 notes that the 1979 or 1994 standards are used in AOO, ATWS, and ASME overpressure analysis; however, Reference 1 indicates that the 1979 ANS decay heat model is used for ECCS evaluation. The NRC staff notes that this approach is in line with the guidance contained in RG 1.157.

The original LTR contained discrepancies and typographical errors in the description of the TRACG-LOCA decay heat model (Reference 1). The NRC staff review is based on the corrected information, which was provided in response to RAI 101 (Reference 6). The review also considers information provided in response to RAI 54 (Reference 3).

The TRACG decay heat model is carried forward from SAFER/GESTR-LOCA, as described in Appendix B to NEDE-30996P-A (References 28 and 29). TRACG implements decay heat models based on both the 1979 and 1994 ANS standards, like an auxiliary code, DECAY. According to the response to RAI 101, the DECAY computer code was developed to address issues identified in IN 96-39, "Estimates of Decay Heat Using ANS 5.1 Decay Heat Standard May Vary Significantly" (Reference 30).

The TRACG decay heat model is simplified in that it assumes []

[]) As time from shutdown increases, this assumption drives the TRACG decay heat conservatively higher than the DECAY code which calculates these contributions to the decay heat in a realistic manner.

Additional assumptions in the TRACG decay heat model also contribute conservatism, or enable its use in a bounding manner, when compared to DECAY and the SAFER model. []

[])

Figures R101-1 and R101-2 of the RAI response show that these conservatisms cause the TRACG04 decay power curve to sit slightly above the SAFER and DECAY curves. []

]] Since the SAFER model, from which the TRACG model was derived, is based on the ANS/ANSI 5.1 1979 standard, the NRC staff determined that it is consistent with the recommendations in RG 1.157. The model has already been accepted by the NRC staff, and the DECAY model was implemented to address concerns in IN 96-39. The TRACG model also introduces conservative, simplifying assumptions relative to the previous, legacy models. Based on these considerations, the NRC staff determined that the TRACG04 decay heat model is acceptable for ECCS evaluation.

[[

]] The NRC staff confirmed that the irradiation time is slightly conservative based on conventional uranium loadings in the GNF2 bundle design and typical BWR/4 power levels and core inventory. However, GEH must confirm that this conversion is bounding, based on plant-specific attributes for each application of TRACG-LOCA.

The uncertainty for the model is also based on the standard. In the uncertainty analysis, a value is randomly sampled from the uncertainty distribution, and applied to the decay heat curve [[

]] The time-variation in uncertainty for a bundle average exposure of [[]] is shown in Figure 5.1-16 of the LTR, which was updated in response to RAI 54. The uncertainty in decay heat is applied independently of core power; initial core power uncertainty is treated deterministically [[]]. Since the decay heat uncertainty approach prevents reducing the uncertainty by averaging effects, and accounts for the time-dependent changes in the decay heat uncertainty in accordance with the ANS 1979 decay heat standard, the NRC staff determined that the treatment of decay heat uncertainty is acceptable for TRACG-LOCA.

6.1.4. Metal-Water Reaction Rate

Regulatory Position 3.2.5 of RG 1.157 states:

The rate of energy release, hydrogen generation, and cladding oxidation from the reaction of the zircaloy cladding with steam should be calculated in a best-estimate manner. Best-estimate models will be considered acceptable provided their technical basis is demonstrated with appropriate data and analyses. For rods calculated to rupture their cladding during the loss-of-coolant accident, the oxidation of the inside of the cladding should be calculated in a best estimate manner.

Further, RG 1.157 indicates that use of the Cathcart-Pawel oxidation kinetics correlation is considered acceptable for calculating the effect of metal-water reaction.

The requirements in § 50.46(b) impose a limit on cladding oxidation of 0.17 times the total cladding thickness before oxidation, or, as stated previously in this SE, 17-percent ECR. The Atomic Energy Commission (AEC) deliberation over the 17-percent ECR acceptance criterion is discussed in detail in the 1973 Opinion of the Commission regarding ECCS acceptance criteria for light-water-cooled nuclear power reactors (Reference 31, pp. 1085 - 1138).

In its proceedings, the AEC noted that the “limits specified in these criteria will assure that some ductility would remain in the zircaloy cladding as it goes through the quenching process” (Reference 31, Page 1096). The values were selected because experimental data indicated that cladding ductility is influenced not only by oxidation alone, but also by the temperature at which the oxidation occurs. The AEC received recommendations from fuel vendors, the AEC staff, and the public regarding the selection of an appropriate oxidation limit. The AEC’s consideration included not only the total oxidation but also the thickness of brittle oxidation and zirconium layers in the cladding and the ratio of the thickness of the brittle layers to the remaining ductile layers. Noting wide agreement on the value of 17 percent ECR as a threshold above which cladding generally exhibited brittle behavior, the AEC settled on this value as the cladding oxidation limit.

The experimental studies supporting this limit evaluated cladding ductile performance and correlated it to the thicknesses of the differing layers (i.e., oxide, brittle zirconium, ductile zirconium) rather than to a measured ECR. The percentage values were calculated, based on the test conditions, using the Baker-Just (B-J) correlation. Thus, the AEC also noted that “the Regulatory Staff in their concluding statement compared various measures of oxidation (page 90) and concluded that a 17 percent total oxidation limit is satisfactory, [emphasis added] *if calculated by the Baker-Just equation*” (Reference 31, Page 1097).

Upon revision to § 50.46 in 1988 to allow more realistic emergency core cooling performance calculations, the state of the art for cladding oxidation calculations had evolved. In addition to Baker-Just, Chapter 6.13 of NUREG-1230 reviews Cathcart-Pawel alongside two additional oxidation rate equations (Reference 12). The NUREG-1230, as well as RG 1.157, recommend the use of Cathcart-Pawel based on its superior accuracy when compared to Baker-Just.

However, as noted in Research Information Letter (RIL) 02-02, Attachment 2, the original and confirmatory ring compression tests on which the 17 percent ECR criterion was based relied on an ECR value calculated using Baker-Just (Reference 32). As noted on Page 9 of Reference 32, Attachment 2, “had the Cathcart-Pawel correlation – which did not exist at that time – been used, the cladding oxidation limit would have been about 13%. Therefore, the Baker-Just correlation must be used when comparing results with the old 17% limit.”

The use of a 17 percent limit on ECR when applied to cladding oxidation values calculated using the Cathcart-Pawel correlation does not provide the same level of assurance of cladding ductility as the same limit when applied to a result calculated using the Baker-Just correlation. In its present reviews of ECCS evaluation models, the NRC staff is imposing a limitation specifying that the ECR results calculated using the Cathcart-Pawel correlation are considered acceptable in conformance with § 50.46(b)(2) if the ECR value is less than 13 percent. If the ECR value is determined to be less than 13-percent, then there is reasonable assurance that an analogous value, if calculated using the Baker-Just correlation, would remain below 17-percent and still in compliance with the 10 CFR 50.46(b)(2) acceptance criterion.

In response to RAI 100, GEH indicated that several approaches to adhere to this interim limitation would be possible. First, calculations could be performed, using the Cathcart-Pawel correlation, to compare to the 13-percent limit. Second, GEH indicated the Baker-Just correlation could be used for comparison to the 17-percent limit. A third approach would incorporate a more performance-based limit that recognizes the role of various embrittlement mechanisms in establishing acceptance criteria that ensure that the cladding remains ductile, consistent with the intent of § 50.46(b)(2).

The NRC staff determined that a 13 percent limit on the ECR predicted using Cathcart-Pawel is appropriate; this determination is based on a comparison of the test conditions used in the ring compression tests that were used to support the original basis for the 1973 rulemaking. These tests involved oxidizing the cladding at temperatures near the regulatory limit of 2200 °F. At lower oxidation temperatures, the difference between Cathcart-Pawel and Baker-Just diminishes, i.e., a higher, Cathcart-Pawel-calculated ECR value would equate to 17 percent Baker-Just. Therefore, if GEH pursues Approach 1, limiting the Cathcart-Pawel calculated ECR below 13 percent, then there is reasonable assurance that the analogous ECR, calculated using Baker-Just, would remain below 17 percent, provided that the calculated PCT remains below 2200 °F. On this basis, the NRC staff determined that the GEH-proposed Option 1 is acceptable because it would comply with the regulatory acceptance criterion of 17 percent, established in 10 CFR 50.46(b)(2), using the Baker-Just kinetics equation. Since this approach relies on the Cathcart-Pawel equation to determine the ECR critical safety parameter, the NRC staff determined that Limitation 5, "Interim Limitation on Cathcart-Pawel Results," as discussed in Section 10.5 of this SE.

The use of the Baker-Just correlation, as GEH proposed in Option 2, would also be acceptable. This determination is based on the fact that the acceptance criterion, as originally established, was based on the use of the Baker-Just equation. A Baker-Just equivalent to the Cathcart-Pawel-calculated value would need to be determined for a sufficient number of limiting analytic cases, and nodal locations, to provide assurance that the limiting Baker-Just oxidation ECR for the plant being analyzed has been calculated. Since this approach would use a Baker-Just equivalent of the ECR based on the transient time at temperature from the ECCS evaluation, the NRC staff also determined that this approach would be acceptable. As this approach uses the Baker-Just equation to determine a critical safety parameter to compare against the 17 percent acceptance criterion, the NRC staff did not determine that a limitation applies to this approach.

If GEH were to implement Option 3, i.e., apply a more performance based alternative to the existing, 17 percent, B-J-based acceptance criterion, the licensing process required to implement such an approach in a plant-specific analysis has not been established. Thus, the NRC staff makes no determination whether (1) such an approach would be acceptable on a plant-specific basis, or (2) such an approach would require a specific exemption to the acceptance criterion published in § 50.46(b)(2), pursuant to the requirements of § 50.12. Thus, the NRC agrees with GEH that, "The licensing process needed for an early adoption of the third approach has not been completely defined by the NRC so some risk by the licensee is encountered should they choose this third option" (Reference 5, Enclosure 1, Page 16).

In view of the interim 13-percent acceptance criterion when using the C-P reaction model, should the NRC staff position in this matter change, the NRC will notify GEH with a letter providing a basis for the change and revising the limitation as necessary. This is Limitation 5, discussed in Chapter 10 of this SE.

6.1.5. Thermal Parameters for Swelling and Rupture of the Cladding and Fuel Rods

Regulatory Position 3.3.1 of RG 1.157 states:

A calculation of the swelling and rupture of the cladding resulting from the temperature distribution in the cladding and from the pressure difference between the inside and outside of the cladding, both as a function of time, should be included in the analysis and should be performed in a best-estimate manner. The degree of swelling and rupture should be taken into account in the calculation of gap conductance, cladding oxidation and embrittlement, hydrogen generation, and heat transfer and fluid flow outside of the cladding. The calculation of fuel and cladding temperatures as a functions of time should use values of gap conductance and other thermal parameters as functions of temperature and time. Best-estimate methods to calculate the swelling of the cladding should take into account spatially varying cladding temperatures, heating rates, anisotropic material properties, asymmetric deformation of cladding, and fuel rod thermal and mechanical parameters. Best-estimate methods will be considered acceptable provided their technical basis is demonstrated with appropriate data and analyses.

The TRACG gap conductance model is evaluated with regard to ECCS-LOCA evaluation in Section 6.1.1 of this SE. The TRACG fuel rod swelling and rupture models are “based on an empirical fit to experimental data for BWR size fuel rods. The cladding strain is a function of the cladding temperature and the hoop stress” (Reference 1, Table 2.5-1). The gap conductance calculations include allowance for fuel rod and pellet geometry, as well as for transient variations in fuel rod parameters such as plenum temperature and rod internal pressure. Some heat transfer effects outside the cladding, such as droplet shattering upon impingement on ruptured fuel rod segments, are neglected.

The models important for predicting fuel rod rupture include the rod internal pressure and a cladding perforation model.

The reference initial rod pressure is passed into TRACG from the power- and exposure-dependent fuel files obtained from PRIME. In the revised response to RAI 33, GEH provided a plot of PRIME predictions of rod internal pressure as compared to data (a reprint of a figure that was included in Reference 25) [[

]] The NRC staff reviewed the referenced RAI response, RAI 46, as contained in Reference 25, i.e., NEDE-33256P-A, Revision 1, and agrees with GEH’s assessment [[

]] The study varied the gap gas pressure, [[

]] On this basis, the staff accepts GEH’s [[

]]

The cladding rupture model correlates the rupture hoop stress to the postulated rupture temperature. This is consistent with the practice established in NUREG-0630; however, [[

]] In the revised response to RAI 33, GEH provided curves showing the model, and comparing it to rupture stress and temperature data, including proprietary GEH data and data from NUREG-0630. The upper and lower bounds reasonably envelope the data. [[

]] This approach not only covers the data set, but, based on the way GEH established the upper and lower bounds for the curve, the approach also introduces more spread toward lower rupture temperatures. This, in turn, results in a tendency for early rupture to be predicted. This is somewhat conservative, because an earlier rupture drives higher two-sided cladding oxidation.

In RAI 97, the NRC staff requested that GEH provide additional detail regarding models used to calculate cladding plastic deformation, and the attendant effects that would result from potential in-stack fuel relocation. For example, pellet relocation with a sufficiently high rubble packing factor could increase the heat load to the cladding in the balloon region. In response, the vendor clarified [[

]] The vendor also described the model for plastic deformation. It reflects the cladding strain behavior that is described in NUREG-0630. Furthermore, GEH clarified that the model has been implemented in the SAFER evaluation model and accepted by the NRC. Finally, [[

]] Based on this study, and on the prior approval of the cladding plastic deformation model and its consistency with NUREG-0630, the NRC staff determined that the GEH disposition for cladding plastic deformation is acceptable.

6.2. BLOWDOWN PHENOMENA

The NRC staff review of blowdown phenomena, including break characteristics and flow, nodding near the break, and critical heat flux (CHF) is reviewed in the following sub-sections. The NRC staff review resulted in issuance of 3 RAIs, which are listed in Table 7, below.

Batch	RAI	Topic	Ref.
1	57	Critical Flow Uncertainty	3
1	3	Nodalization Sensitivity	3
1	44	Treatment of GEXL Correlation Uncertainty	3

Table 7. RAI Responses Related to Blowdown Phenomena.

6.2.1. Break Characteristics and Flow

Regulatory Position 3.4.1 of RG 1.157 states:

In analyses of hypothetical loss-of-coolant accidents, a spectrum of possible break sizes should be considered, as indicated in Regulatory Position 3.1. The discharge flow rate should be calculated with a critical flow rate model that considers the fluid conditions at the break location, upstream and downstream pressures, and break geometry. The critical flow model should be justified by comparison to applicable experimental data over a range of conditions for which the model is applied. The model should be a best-estimate calculation, with uncertainty in the critical flow rate included as part of the uncertainty evaluation. Best-estimate models will be considered acceptable provided their technical basis is demonstrated with appropriate data and analyses.

The TRACG critical flow model is described in Section 6.3 of Reference 16. It uses separate models for each of liquid-only, two-phase, and vapor-only conditions. For transitions between these conditions, TRACG interpolates between the two applicable correlations.

The discharge model is qualified as documented in both Reference 17, Section 3.4, and in NEDC-32725P, Revision 1, "TRACG Qualification for SBWR [Simplified Boiling Water Reactor]" (Reference 33, Section 3.3.4). The qualification is based on Marviken tests, as well as to data from the Pressure Suppression Test Facility (PSTF),^N Edwards blowdown experiments, and the GIRAFFE systems interactions test (SIT). In Reference 16, GEH noted that the critical flow model was evaluated also using comparisons to the blowdowns from PSTF, the Two-Loop Test Apparatus (TLTA), Full Integral Scale Test (FIST), and FIX tests. []

[]

In its review, the NRC staff identified concerns with the model treatment of critical flow uncertainty, as documented in RAI 57. The RAI addressed the following topics:

- a) The uncertainty assessment is based on nine tests used to define critical flow behavior over a span of liquid to vapor flow regimes
- b) The selection of nine tests to the exclusion of other possible, relevant tests
- c) The method used to compare TRACG model performance to test data to define an uncertainty distribution
- d) The selection of critical flow discharge coefficients for the statistical evaluation
- e) The influence of non-condensibles on the predicted behavior

^N PSTF is described in Section 3.1.5 of Reference 17. The test rig was a vessel with a blowdown pipe at the bottom. To replicate top-break scenarios, the rig could be equipped with a vertical standpipe inside the vessel. The test provided data for comparison to both pressure and level predictions.

In response to Portion a), GEH reviewed open literature for several contemporary realistic ECCS evaluation models and concluded that the uncertainty used in the GEH critical flow model is quantitatively consistent with other methods. The vendor noted that [[

]] While the NRC staff accepts that the model uncertainty ranges appear consistent, this argument alone is not particularly compelling. Such a consideration also warrants considering the sampled probability density functions, and the underlying density functions are generally proprietary and thus incomparable.

Notwithstanding the above, GEH also noted that the uncertainty database largely includes similar assessment tests among the methods (i.e., Marviken). In addition, GEH stated that the break spectrum analysis includes analysis of break sizes with such granularity as to overlap the critical flow uncertainty, a feature of the analytic method that reduces the significance of the critical flow model relative to the results.

To demonstrate the combined effect of critical flow uncertainty, or discharge coefficient, and break area^o, GEH simulated a BWR/4 break spectrum. At each break area, GEH performed [[]]

sensitivity studies by ranging the [[]]. These results were plotted alongside a nominal break spectrum analysis, with PCT illustrated as a function of the effective break area (Reference 3, Figure R57-1). [[

]]

The above reasoning works for an intermediate-break-limited plant. However, if the double-ended guillotine, or the maximum split break, is limiting, the rationale is invalid. As can be seen in Figure R57-1, the trend of increasing PCT with effective break area continues for both the double-ended guillotine break and the maximum split break. In other words, there is a shallow increase in PCT associated with increases in the critical flow multiplier. However, in the case of the BWR/4, the consequences of these breaks are eclipsed by the limiting intermediate break. Moreover, the uncertainty evaluation at the limiting large break size will explicitly incorporate the effects of critical flow uncertainty via the critical flow multiplier.

The BWR/2 spectrum is generally limited by the double-ended guillotine break. Thus, in Figure R57-2, GEH provided a similar effective break area study for the BWR/2 break spectrum. As noted in the RAI response, [[

]] Thus, in a fashion similar to the large break region for the BWR/4 spectrum, the uncertainty analysis will account acceptably for the minor effect caused by critical flow uncertainty for the double-ended break.

^o In LOCA simulation, the discharge coefficient or critical flow multiplier has a scaling effect on the break area. The product of break area and discharge coefficient is commonly known as the effective break area.

In response to Portions b) and c) of RAI 57, GEH deferred to the relative insensitivity of the PCT to the critical flow uncertainty. In response to Portion d), GEH stated that discharge coefficients are not used, and that the critical flow uncertainty is sampled from its uncertainty distribution.

In response to Portion e) of the RAI, GEH stated that, in BWR LOCA analysis, the ingress and generation of a significant amount of non-condensibles does not occur until the later phases of the event, at which time the flow through the break is no longer choked.

In consideration of all of the above information, the NRC staff accepts the GEH disposition for critical flow uncertainty. Primarily, GEH has provided sensitivity studies [[

] The range studied by GEH exceeds the uncertainty range permitted by its sampling, but that uncertainty range is based on a variety of tests that span conditions in the multiple flow regimes considered in the critical flow model. The sensitivity studies indicated that further widening of the sampling distribution, to values that testing showed were unlikely, would not reasonably be expected to drive a significant increase in the predicted PCT.

Based on the review described above, the NRC staff determined that GEH is consistent with the guidance provided in Regulatory Position 3.4.1 of RG 1.157. The vendor has justified its critical flow model by comparison to relevant experimental data, and considers the uncertainty in the uncertainty analysis. The deterministic break spectrum is performed with sufficient resolution as to permit overlap, in terms of effective break area, with the discharge coefficient uncertainty. GEH has also studied the sensitivity of its analyses to critical flow multiplier, as described above. While the overall transient is somewhat insensitive to the multiplier, the uncertainty treatment ensures that, even in consideration of the double-ended guillotine break event, the effects of critical flow uncertainty are accounted for in the analysis with bounds representative of the experimental database. Based on these considerations, the NRC staff determined that the discharge flow model in TRACG-LOCA is acceptable; the resolution of the break spectrum is addressed as Limitation 2.3 in Chapter 10 of this SE.

6.2.2. Noding near the Break and ECCS Injection Point

Regulatory Position 3.5 of RG 1.157 states:

The break location and ECCS injection point are areas of high fluid velocity and complex fluid flow and contain phenomena that are often difficult to calculate. The results of these calculations are often highly dependent on the noding. Sufficient sensitivity studies should be performed on the noding and other important parameters to ensure that the calculations provide realistic results.

GEH assessed nodalization as discussed in Section 5.2 of the LTR. Nodalization sensitivity studies included increasing the noding detail at the break location for a BWR/4. For the limiting intermediate break, Table 5.2-1 of the LTR indicates that increasing the break resolution effects a PCT reduction slightly less than [[]]

Although this may seem like a significant amount, an additional consideration explains the magnitude, which GEH discussed in the response to RAI 3. The sensitivity studies were

performed using the LTR Revision 0, less-detailed, core model. The statistical trials associated with this model introduced a significant amount of non-phenomenological variability (about [[]]) that was subsequently reduced (to about [[]]) by using a more detailed core model. GEH estimates that the use of the more detailed core model would reduce the PCT variation associated with break nodding [[]]. In any case, the [[]] difference in PCT associated with the change in break nodding is within the analytic resolution of the model used to perform the evaluation. Since GEH studied the break nodalization and determined that associated changes in PCT were within the analysis resolution of the model, the NRC determined that GEH was consistent with this element of RG 1.157. GEH will update its nodalization sensitivity studies based on the revised modeling approaches, consistent with Limitation 7, "BWR/3-6 First-of-a-Kind Application," as discussed in Section 10.7 of this SE.

With specific regard to nodding near the break point, it should also be noted that discharge flow tests simulated as part of the TRACG qualification, such as the Marviken tests (Reference 17, Section 3.4.1.6) and the PSTF blowdown experiments (Section 3.1.5.4), also included sensitivity studies of the TRACG nodalization of those tests. These tests are significantly simpler than a reactor analysis; however, these nodalization sensitivity studies indicated that the chosen TRACG nodalization was adequate, as varying nodding detail did not significantly affect the predicted outcomes of the tests, in terms of predicted break flow rates and system pressures. These sensitivity studies provide additional evidence regarding the sufficient predictive capability of TRACG at the chosen level of break nodding detail.^P

6.2.3. Critical Heat Flux

Regulatory Position 3.8 of RG 1.157 states:

Best-estimate models developed from appropriate steady-state or transient experimental data should be used in calculating critical heat flux (CHF) during loss-of-coolant accidents. The codes in which these models are used should contain suitable checks to ensure that the range of conditions over which these correlations are used are within those intended. Research has shown that CHF is highly dependent on the fuel rod geometry, local heat flux, and fluid conditions. After CHF is predicted at an axial fuel rod location, the calculation may use nucleate boiling heat transfer correlations if the calculated local fluid and surface conditions justify the reestablishment of nucleate boiling. Best-estimate models will be considered acceptable provided their technical basis is demonstrated with appropriate data and analyses.

The determination of CHF is used to transition TRACG from using nucleate boiling heat transfer correlations to using transition and film boiling, and vapor convection correlations. Within its range of applicability, the General Electric Critical Quality Boiling Length (GEXL) correlation is used. Outside this range, either the modified Zuber or modified Biasi correlations are used. GEXL is NRC-approved, and the modified Zuber and Biasi correlations are commonly used in Appendix K-conformant and realistic ECCS evaluation models.

^P This additional consideration is presented after the conclusions for two reasons. First, it is not apparent that either of the referenced sensitivity studies was intended to investigate, specifically, the effect of nodding near the break relative to predicted discharge flow and system pressure. Second, these tests are significantly simpler than the system analysis, and the comparison is directly to system pressure and flowrate, rather than to a critical safety parameter (as in the system analysis).

Critical power uncertainty is incorporated into the uncertainty analysis. In the response to RAI 44, GEH stated that fuel-type specific values for the GEXL bias and uncertainty will be applied, or a more conservative GEXL bias and bounding uncertainty that bounds all fuel types in the core will be applied. The bounding approach would be used, according to GEH, for competitor fuel designs where determining the precise values is difficult.

Since GEH is using an NRC-approved, fuel design-specific correlation to determine the transition to film boiling, the NRC staff determined that the vendor is consistent with Regulatory Position 3.8, as the correlation reflects the fuel-design specific considerations discussed therein. The more general CHF correlations are acceptable when GEXL does not apply. The bounding uncertainty approach is acceptable for average channels in the core, but hot channel modeling of competitor fuel is restricted by Limitation 1.3. Co-resident fuel in the core would be addressed by the evaluation model furnished by that fuel's vendor. Limitations 3.1 and 3.2, regarding upstream methods, also apply.

6.3. POST-CHF PHENOMENA

Accurate prediction of post-CHF heat transfer over a range of thermal-hydraulic conditions is of particular importance in ECCS evaluation. Acceptable estimation of the PCT requires that the EM can predict both the cooling phenomena present once the core uncovers, and the rate at which liquid coolant in the core recovers. In a BWR, which depends heavily on core spray flow injected above the core, this also requires the code to simulate counter-current flow and predict the core spray distribution. All of these items must be simulated accurately so that both the magnitude and duration of the PCT transient can be predicted. The cladding oxidation phenomena are highly dependent on both the duration and magnitude of the cladding temperature transient.

Like many other system analysis codes, TRACG models the core using a system of one-dimensional channels. The field equations average the state parameters over the cross section of the channel. Additional constitutive correlations are needed to simulate and accurately represent the more detailed, sub-channel flow variations, including wall-to-fluid interactions and phasic interactions in the fluid.

Such correlations are typically empirically derived using separate effects tests.^Q With particular regard to TRACG04, the relations have been reviewed and accepted for use in simulating AOOs and the ATWS and ASME overpressure transients. Thus, while the models have been previously reviewed, their extension to post-CHF flow regimes requires consideration within the TRACG-LOCA review. This includes extending void fraction predictions to low pressures associated with LOCA, considering dispersed droplet flow and heat transfer, liquid droplet or film rewet of heated surfaces. The review also necessitates consideration of CCFL and core spray flow distribution.

Regulatory Position 3.9 of RG 1.157 states:

Models of heat transfer from the fuel to the surrounding fluid in the post-CHF regimes of transition and film boiling should be best-estimate models based on comparison to applicable steady-state or transient data. Any model should be evaluated to demonstrate that it provides acceptable results over the applicable

^Q As will be discussed later in this SE, the Sun-Gonzalez-Tien correlation, used in TRACG for dispersed flow film boiling heat transfer, is theoretically derived.

ranges. Best-estimate models will be considered acceptable provided their technical basis is demonstrate with appropriate data and analyses.

The evaluation presented below establishes that GEH is consistent with Regulatory Position 3.9, but also follows the graded approach suggested by SRP 15.0.2, acknowledging TRACG’s prior approval precedent. RAIs associated with this review segment are listed in Table 8, below.

Batch	RAI	Topic	Ref.
2	78	Flow Regime Uncertainties	4
2	98	Disperse Droplet Flow Modeling	4
2	69	Adherence to Correlation Limitations	4
1	45	Sun-Gonzalez-Tien Uncertainty Treatment	3
1	47	Interior Rod Heat Transfer Coefficient Bias	3

Table 8. RAI Responses Related to Post-CHF Phenomena.

6.3.1. Flow Regime Map

The TRACG flow regime map is presented in Chapter 5 of Reference 16. The flow regime map is fairly simple, based primarily on void fraction. Flow regime boundaries are provided to define the transition between bubbly/churn and annular flow. In the higher void regime, the entrainment model is used to assist in identifying the transition between annular flow and dispersed droplet flow. In its review, the NRC staff requested that GEH explain how uncertainty in the flow regime map is addressed in TRACG-LOCA. In the response to RAI 78, the vendor stated that, because the flow regime selection logic is dependent on void fraction, and the void fraction includes an explicit uncertainty treatment, there is no explicit treatment of uncertainty associated with the flow regime selection. The NRC staff also notes that the flow regime is used to transition among heat transfer correlations, and each heat transfer correlation is accompanied by an uncertainty range. In consideration of the supplemental information furnished by GEH, and the NRC staff observation, the NRC staff determined that the vendor addressed the issue regarding flow regime uncertainty acceptably.

6.3.2. Entrainment, Interfacial Shear, and Wall Shear Models

These models, which govern the prediction of phasic interactions, are considered together in the evaluation of TRACG, primarily because their qualification is based on a similar set of data. The models are indirectly qualified using void fraction, pressure drop, and two-phase level data in various geometries, system pressures, hydraulic diameters, and mass fluxes. Model applicability is then confirmed using integral effects tests.

As noted above, the TRACG entrainment model is used to identify the transition from purely annular flow to annular flow with dispersed droplets. It is based on a correlation developed by Mishima and Ishii, and is described in Section 5.1.2 of Reference 16. GEH modified the implementation of the Mishima and Ishii correlation in TRACG in order to provide a more accurate prediction of conditions in which the entrainment fraction approaches unity. The original correlation, its modified form, and two-sigma uncertainty bands of the modified form are shown in Figure 5-3 of Reference 16. The figure also shows the data used to define the correlation, indicating that the modified correlation agrees well with the data. It should be noted that the data represent low pressures, i.e., 0.1 – 0.4 MPa. However, the model is indirectly qualified, alongside the interfacial shear model, using void fraction data that extend from

0.5 MPa to the full BWR operating pressure. The response to RAI 69 indicated that qualification of the entrainment and interfacial shear models at intermediate pressures has been added by comparisons to Toshiba void fraction data.

The development of these TRAC models is described in earlier references, e.g., NUREG/CR-2573, "BWR Refill-Reflood Program Task 4.7 – Model Development Basic Models for the BWR Version of TRAC" (Reference 34). In Reference 34, it was noted that a model for interfacial drag for inverted annular flow had not yet been developed; this capability was added later. At that time, the models were developed based on void fraction data. The original assessment included comparisons to level predictions of FRIGG 36-rod bundle tests, the PSTF 5801-15 level swell test, and the Oak Ridge National Laboratory (ORNL) Thermal Hydraulic Test Facility (THTF) Film Boiling Test, Run 3.06.6B. The THTF test was representative of PWR conditions, and hence used PWR-representative rod bundle geometry and higher pressure conditions. The early assessment showed that the initial TRACB models performed well when assessed against these data sets.

The modern TRACG interfacial shear model is assessed by evaluating how well TRACG can predict void fraction, in Section 3.1 of Reference 17. The separate effects qualification includes the following steady-state experiments:

- A full-size 8x8 BWR fuel bundle from the FRIGG facility
- Single heated tube and adiabatic tests
- Large hydraulic diameter facilities
- Toshiba 16-rod bundle tests at low pressure
- PSTF level swell tests

In each of the steady-state tests listed above, GEH compared TRACG predictions of void fraction to those measured, and concluded that TRACG was capable of predicting the measured void fraction to within [[]]. The tests used various means to infer void fraction; some used gamma or x ray densitometry, while others used pressure drop.

The applicability of the interfacial shear model for modern, i.e., 10x10 fuel designs was confirmed by comparison to pressure drop measurements from critical heat flux tests (Reference 21, SE Section 3.20.1). It should be noted, however, that this evaluation was limited to pre-CHF conditions, and found acceptable, in part, because that application did not require modeling of post-CHF conditions. Of the tests listed above, only one of the tube tests, from the CISE facility in Italy, produced data that indicated void fractions approaching a value of 1.

The two-phase flow wall friction factors are qualified using rod bundle data from the ATLAS test facility, as described in Section 3.5 of Reference 16. However, Section 3.5 of Reference 16 also notes that the extension of the qualification to LOCA conditions is provided by LOCA tests, such as TLTA and FIST data comparisons, that feature thermal-hydraulic conditions that exceed dryout conditions.

In response to RAI 98, GEH provided additional justification for the applicability of its entrainment, interfacial shear, and wall shear models to high-void, low-pressure conditions (Reference 4). In the RAI response, GEH stated that such conditions are "observed in the late phase of a typical BWR LOCA, where the RPV has been depressurized, fuel heatup is close to the end and ECCS is cooling the bundle from the top of the bundle for non-jet pump plants (BWR/2s) or from both the top and the bottom of the bundle for jet pump BWRs (BWR/3-6s)."

This condition includes counter-current flow at the top of the bundle, and because the bundle power is decaying, CCFL is unlikely. Thus, the liquid downflow rate is calculated by the wall shear and interfacial shear acting on the liquid.

In order to justify the applicability of these models to LOCA conditions, GEH relies on comparisons to tests more specifically tailored to those conditions. Specifically, the response to RAI 98 lists the Core Spray Heat Transfer (CSHT), FIST, TLTA, and Rig of Safety Assessment (ROSA)-III tests as the testing that provides confirmation of adequate inter-working of the entrainment, interfacial shear, and wall shear models, in addition to the post-CHF heat transfer models.

For the uncertainty treatment associated with interfacial shear, [[

]] Specifically with regard to LOCA applications, the uncertainty is assessed using the Toshiba data. Figure 5.1-8 of Reference 1 shows the effect on mean void deviation when a multiplier is applied to the interfacial shear parameter. [[

]] Since the void deviation is more sensitive to multipliers that are less than one than it is to multipliers that are greater than one, the NRC staff determined that this approach is acceptable. The multiplier is also shown to produce a range of void deviations that are consistent with the [[
]] agreement shown in the body of void fraction comparisons.

In its review, the NRC staff requested that GEH provide additional, clarifying information regarding the statistical treatment of uncertainty associated with PIRT Item A3, the lower plenum two-phase level and side entry orifice uncover time. In the response to RAI 23, GEH stated that this PIRT phenomenon is affected by other physical phenomena that are explicitly addressed in the uncertainty analysis, [[

]]

Based on its review, the NRC staff determined that TRACG employs correlations for entrainment, wall shear, and interfacial shear that are specific and appropriate to span the two-phase fluid conditions anticipated in a BWR LOCA. The models are assessed using a variety of data sets that include multiple void conditions, geometries, and system pressures applicable to BWR LOCA conditions. The uncertainty treatment for core interfacial shear is consistent with the broader range of GEH void fraction comparisons, but is based more specifically on comparison to Toshiba void fraction tests at the lower system pressures expected in a LOCA. Finally, reasonable agreement to separate effects and integral LOCA tests indicates that the TRACG two-phase fluid flow models perform acceptably. Based on these considerations, the NRC staff determined that the TRACG interfacial shear, wall shear and entrainment models are acceptable for ECCS evaluation.

6.3.3. Heat Transfer

The heat transfer selection logic for TRACG is discussed in Section 6.6.2 of Reference 16. The response to RAI 69 also includes a succinct table of the heat transfer correlations used by

TRACG, along with the flow conditions that cause the code to invoke each correlation (Reference 4).

In film boiling conditions, the modified Bromley correlation is used for inverted annular, low void, conditions. The correlations are described briefly in Section 6.6.9 of Reference 16. The Bromley correlation has been previously applied in the SAFER evaluation model. As noted in Section 5.1.3.20 of Reference 1, its uncertainty treatment is based on an assessment of quench tests. Since the correlation was approved for use in SAFER, the NRC staff determined that its application in TRACG was acceptable.

The Sun-Gonzalez-Tien (SGT) correlation (Reference 35) is used for dispersed flow, high void conditions, and is described in Section 6.6.10 of Reference 16. SGT has been used in the CORECOOL code to justify the application of spray heat transfer coefficients, rather than to calculate them directly.

The SGT correlation is theoretically derived (Reference 345). As such, it technically has no defining data set. However, it is assessed against both THTF and CSHT separate effects tests,^R as discussed in Section 3.2 of the TRACG Qualification Report. The detailed assessment includes [[

]]

It should be noted that, in order to compensate for the channel-averaging effect discussed in the introduction to Section 6.3 of this SE, TRACG [[

]] is defined in Figure 7-21 of Reference 16. This approach was devised based on comparisons of a 4x4 test bundle, modeled using the Dittus-Boelter correlation, using both an extended, sub-channel model and a channel average model. The comparisons showed that the channel average model [[

]]. Thus, when simulating the CSHT experiments, GEH used the modeling approach described above. The qualification of SGT against [[]] CSHT experiments shows similar agreement to the extended, sub-channel model.

In the uncertainty analysis, GEH applies the same uncertainty to SGT as for the Dittus-Boelter correlation, which is used for single-phase convection for both liquid and vapor. In the response to RAI 45, GEH stated [[

^R These tests examined the two-phase heating behavior in rod bundle configurations. In certain contexts, they would more appropriately be considered as integral tests. For example, Chapter 7 of NEDE-33005 refers to them as such. However, in the qualification report, these are located in the section describing separate effects tests, presumably because they are being used to qualify heat transfer correlations that account for multiple heat transfer mechanisms and are applied to rod bundle geometries. Note also that the SGT model "accounts for radiation and convection to the vapor-droplet medium" individually (See Page 2 of the SGT paper).

]] (Reference 3). In the RAI response, GEH also indicated that the demonstration statistical analyses provided in Chapter 7 of Reference 1, wherein the experimental data generally fall within the TRACG-calculated statistical results, provide an indication that the uncertainty range is appropriate.

Single-phase steam cooling is modeled using the Dittus-Boelter correlation, which is modified to account the impact of variations in fluid physical properties due to high temperature difference between the wall and vapor, as stated in the GEH response to RAI 47 (Reference 3). [[
]] Although the uncertainty parameters are derived from 4x4 bundle tests, GEH indicated in the response to RAI 47 that favorable comparisons to full-bundle test data indicate that the correlation performs reasonably well at multiple geometries.

These heat transfer models are qualified using a number of separate effects and integral effects tests. In addition to the THTF and CSHT tests discussed above, GEH used TRACG to simulate three FIST tests, and several ROSA-III tests. The tests generally showed that TRACG predicted the data well. In addition, as discussed in Section 8.1 of this SE, GEH repeated several CSHT, FIST, and SSTF tests using its statistical methods. The results of these analyses – in particular, good agreement regarding the slope of the heatup transient – showed that the TRACG statistical analysis enveloped the experimental data, providing confirmation that the statistical analysis produces reasonable results.

Based on the review summarized above, the NRC staff determined that GEH has adopted realistic models for post-CHF heat transfer for use in TRACG-LOCA. The models have been compared against relevant experimental data, in both steady-state (i.e., CSHT) and transient tests. Thus, GEH is consistent with the guidance in RG 1.157, and on that basis, the NRC staff determined that the TRACG-LOCA post-CHF heat transfer models are acceptable.

6.4. SPRAY COOLING PHENOMENA

The NRC staff review of spray cooling phenomena is described in the following subsections. These phenomena include counter-current flow limitation (CCFL), the distribution of the core spray flow, the minimum temperature for stable film boiling (T_{min}), and the quench front model. RAIs associated with this segment of the review are listed in Table 9, below.

Batch	RAI	Topic	Ref.
1	16	Guide Tube-Bypass CCFL Parameters	3
1	64	CCFL Constant Uncertainty Bands and Data	3
1	20	VSSL Ring 1/Ring 2 PCT Characteristics	3
2	94	Adequacy of Core Spray Flow Distribution Model	4
2	70	LPCS Performance Benchmarking	4
1	50	T_{min} Uncertainty Treatment	3
5	104	Applicability of Rewet Models to ECCS Analysis	7

Table 9. RAI Responses Related to Spray Cooling Phenomena.

6.4.1. CCFL

The Kutateladze correlation is used in TRACG to compute the onset of CCFL. At various places, TRACG checks the flow rates to determine whether CCFL exists. For the core, this includes the upper tie plate and the side entry orifice. The derivation of the CCFL correlation, along with testing data to support its application to the side entry orifice and upper tie plate is

provided in Reference 36. Noting the 1975 vintage of this report, GEH also confirms the validity and uncertainty of the correlation for newer fuel designs, and investigates whether other locations in the assembly can exhibit CCFL behavior. Such exercises were undertaken, for example, in the development of Reference 19, and more recently for GNF-2 fuel in Reference 37. Based on the experimental data, specific biases and uncertainties are applied for each individual CCFL location.

[[
]] In the response
to RAI 16, [[
]] to the one specified in Section 5.1.2.4 of Reference 1. The
sensitivity study showed [[

]] In addition to this sensitivity study, a further verification of the TRACG CCFL modeling capability is provided in the comparison to SSTF test EA3-1, which is discussed in Chapter 7 of the LTR. In particular, Figure 7.4-16 indicated that TRACG generally [[
]] This
comparison is relevant to the guide tube-bypass CCFL behavior, because the behavior affects the ability to establish or retain liquid in the bypass region of the core. Based on the study and the SSTF comparison, the NRC staff concluded that the [[
]] and
determined that the CCFL model used at this location was acceptable.

The response to RAI 64 provided additional clarification regarding how the uncertainty distribution for the CCFL parameters are determined. The response indicated that the uncertainty characterization for the side entry orifice was based on the distribution of differences between the TRACG CCFL constant, and the values measured from the tests. GEH also stated that the upper tie plate CCFL constant is a function of the fuel product line. [[

]] The RAI response indicates that GEH bases its uncertainty characterization for CCFL on experimental data obtained for the specific geometry of the CCFL location in question.

Since GEH bases its uncertainty treatment for CCFL on empirical data that are representative of the component designs at the CCFL locations of interest, the NRC staff determined that TRACG-LOCA is acceptable with respect to CCFL modeling.

6.4.2. Core Spray Flow Distribution

The modeling of the core spray flow distribution is addressed in Section 5.1.6.4 of Reference 1. For BWR/3-6 applications, [[
]] This approach provides a conservative lower bound on spray cooling to reach channels in the core. [[
]] For the BWR/2 plant design, [[
]], but still conservatively biased low.

The core spray modeling approach is supported by a series of experiments that reflect different plant classes and nozzle designs. The testing was also performed in varying scales using both air-water and steam-water environments. The testing basis is concisely summarized in Reference 38.

In reviewing the analyses based on this approach, the NRC staff observed that [[
]] in a number of demonstration analyses did not exhibit limiting PCTs.
In the response to RAI 20, GEH explained [[

]]

In the response to RAI 94, [[

]]

In the response to RAI 70, GEH provided information to address variations in core spray nozzle designs, and testing applicability to various reactor and fuel bundle designs. GEH stated that testing from SSTF, among other facilities, was used to confirm the predictive capability of spray distribution in a steam environment. Specific testing included a range of system pressures and spray flow rates, various nozzle designs, and different steam updraft flow rates. Also, GEH indicated that SSTF tests were initially performed for a BWR/6 design, but later included nozzle and sparger designs representative of BWR/4 and 5 designs as well. Additional analysis and testing of specific BWR/2 nozzle design was also performed in order to confirm the applicability of the methodology to Nine Mile Point Unit 1. GEH also noted that the purpose of these tests was to estimate the amount of spray flow that would reach specific bundles, but that the facility did not include detailed fuel assembly components.

For the BWR/2 application, however, the core spray distribution requires a plant-specific hardware capability analysis. Core spray distribution data are analyzed to determine a minimum value of core spray flow that could reach an interior bundle. This evaluation considers variability in reactor pressure, and in the availability of a core spray topping pump. An example of the core spray flow application is shown in Figure 5.1-23 of Reference 1, [[

]] As is the case with the BWR/3-6 application, hot bundles in an interior ring of the core receive the flow minimum, and an analogous set of hot bundles in a separate ring receive core spray flow based on upper plenum availability and counter-current flow limitations.

In evaluating the core spray flow distribution, the NRC staff confirmed that the distribution assumptions employed in the BWR/3-6 analyses are conservative by comparing the results of two sensitivity studies employing alternative core spray flow distribution assumptions. The NRC staff also obtained additional information describing the extensive experimental basis supporting GEH's core spray flow modeling, which particularly supports the modeling approach used for the BWR/2. Since the core spray flow distribution is modeled conservatively for BWR/3-6, and since the BWR/2 modeling approach retains conservatism, but is based on numerous core

spray flow distribution experiments, the NRC staff determined that the core spray flow distribution modeling for TRACG-LOCA is acceptable.

6.4.3. Rewet and Quench Behavior

At the time that the second-peak heatup begins to slow and transition to cooldown, the PCT location tends to be in a vapor-cooled or dispersed flow condition (Reference 39). Droplets may be in the channel, but are unable to contact the heated rods. Eventually, a quench front can rise, or in the case of spray cooling from above, a liquid film can fall along the surface of the fuel rod. A significant number of parameters influence the point at which disperse droplets in the core may contact the fuel rod, or at which point the liquid film may contact the rod at the point of the PCT location. These include fuel rod material properties, and thermal-hydraulic properties of the coolant in the channel.

The phenomena discussed above are addressed in TRACG by models that calculate the minimum temperature for stable film boiling (T_{min}), and for the axial advancement of a liquid quench front on a fuel rod or channel surface. The TRACG code uses the Shumway correlation (Reference 40) to predict the minimum temperature below which the code will calculate transition boiling, thereby increasing the heat flux from the fuel rod (Reference 41). The quench front model is a simplified correlation that approximates the solution employed in the SAFER method (References 28 and 29). It is described in Section 6.6.13 of Reference 16.

Minimum Temperature for Stable Film Boiling

In the response to RAI 50, GEH provided a clarification that, for LOCA applications, TRACG uses the Shumway correlation to predict T_{min} . The vendor also provided justification for the associated uncertainty treatment in this RAI response.

The Shumway report provides a succinct summary of the challenge associated with predicting the minimum temperature for stable film boiling accurately (Reference 40, Page 10):

The reason there are so many correlations seems to be that the shape of the boiling curve is influenced by many phenomena which change dominance with experimental conditions. The minimum heat flux or temperature is not exclusively dependent on hydrodynamic or thermodynamic properties of the fluid. It varies with surface conditions such as roughness and surface thermodynamic properties. Factors such as velocity, pressure, subcooling, drop size, liquid contact angle, wetting agents, and gravitational field all influence minimum conditions.

The Shumway correlation includes "some effect of flowrate, pressure, void fraction, fluid properties and wall properties" (Reference 40, Page 39). In its implementation, GEH eliminates the void correction, because it has a tendency to increase the predicted rewet temperature, but as Shumway noted, "the accuracy of the void effect [was] untested" (Reference 40, Page 39; Reference 41, Page 7). GEH also assumes that the fuel rods are comprised of unoxidized zircaloy; formation of an oxide layer has been shown to increase the rewet temperature significantly due to the reduced heat capacity and increased surface roughness of zirconium oxide as compared to unoxidized zircaloy (Reference 41, Page 7). With these modifications, the vendor claims that the implementation of the correlation is conservative, as it predicts a lower value of T_{min} than would be expected for oxidizing fuel rods in a steam environment.

The Shumway correlation is based on data collected for stainless steel. The author included a dimensionless term for wall and fluid material properties based on other, contemporary correlations (e.g., Reference 42); however, Shumway did not provide a validation of the dimensionless term.

In Reference 41, GEH provides an evaluation of the Shumway correlation, comparing it to other, similar correlations and various sources of quench data. Perhaps most notably, GEH provides a comparison of Shumway for various materials, including zirconium, zirconium oxide, and the Groeneveld-Stewart correlation that is implemented in the NRC's TRACE code. The data sources include fresh and oxidized zircaloy, as well as Inconel 600. From Figure 6 of Reference 41, it can be seen that the Shumway correlation trends well with Peterson and Bajorek data (Reference 43) for unoxidized zircaloy, and that the data for oxidized zircaloy fall significantly above the Shumway correlation prediction for unoxidized zircaloy.

These data extend to 0.4 MPa, however, and the correlation is used in demonstration LOCA analyses, in Chapter 8 of the LTR, to predict quenching up to about 3 MPa. While Peterson and Bajorek did not obtain data for unoxidized zircaloy quench behavior above 0.4 MPa, they noted that the predicted rewet temperature becomes asymptotic with increasing pressure (Reference 43). They were also able to show this behavior for stainless and carbon steel, for pressures up to 3 MPa. Other authors corroborate these findings. The Shumway correlation, which GEH illustrated as a function of pressure in Figures 5 and 6 of Reference 41, indicates similar behavior for unoxidized zircaloy.^S This is expected, because as Peterson and Bajorek note, "Gas properties, such as heat capacity and thermal conductivity, have a strong correlation with pressure at low pressure." In other words, the phenomenology is associated with the coolant properties, rather than the material.

In Reference 1, Section 5.1.3.26, GEH indicates that the correlation is applied with a [[]] uncertainty value about the calculated difference between T_{min} and T_{sat} . The vendor further notes that the upper end of this uncertainty range approximates the uncertainty applied in SAFER applications.

In the response to RAI 104, GEH documented the results of sensitivity studies that were performed using the BWR/2 large break LOCA event, in which a base case of the EM, using 181 cases, was compared to a run with the same sample, but with the Shumway correlation T_{min} biased to a low value. The BWR/2 event is studied because it exhibits the most severe results, in terms of both degree and duration of cladding heatup. In the biased evaluation, the licensing parameter for PCT [[]], while the licensing parameter for ECR [[]]. The information provided in this study indicates that significant changes to the predicted T_{min} value do not have a significant effect on the overall results, as they may in other applications like anticipated transients without scram (ATWS) with instability, which apply the correlation at higher pressures and potentially over multiple dryout and rewet cycles. Furthermore, the apparent insensitivity of the model to changes in the predicted T_{min} can be attributed to the general behavior of the transient exhibited in both testing and in plant analytic results, in which the PCT is achieved, and the cladding begins a modest cooldown, prior to T_{min} being reached.

^S This comparison was made by evaluating the data shown in Figure 6 of MFN 13-073, and the data shown in Figure 7 of the Peterson and Bajorek paper. When corrected for units and saturation conditions at the given pressure, it can readily be seen that the Shumway correlation exhibits asymptotic behavior, with the pressure effect leveling off at approximately 1 MPa, just as the data for stainless and carbon steel suggest.

The NRC staff review led to several determinations. First, at the pressures postulated for LOCA conditions, more zirconium-specific data exists to justify the application of the modified Shumway correlation. Second, disabling the void term and neglecting the thermal effect of the zirconium oxide layer that forms during the transient results in a conservative application of the correlation. Finally, the predicted rewet temperature is not a significant contributor to the overall results, as evidenced by sensitivity studies provided in the response to RAI 104. Based on these considerations, the NRC staff determined that the use of the Shumway correlation is acceptable for TRACG-LOCA.

The NRC staff review findings are based on consideration of LOCA-specific phenomenology and sensitivity studies using operating BWRs. Therefore, the conclusions are limited specifically to LOCA applications. This limitation is reflected as Limitation 2.7, "Use of the Shumway Correlation," in Chapter 10 of this SE.

Quench Model

The updated TRACG quench front model is described in Reference 44. The second half of Reference 44 evaluates the quench front model against several LOCA tests, which include test runs from THTF, TLTA, and ROSA-III. These comparisons cover a range of pressures at time of quench from [] [], and the tests are simulated using TRACG runs with the quench front model on and off. Because of the extended heatup and precursory cooling associated with LOCA cladding heatup events, the comparison between TRACG runs reveals little difference in PCT. For the run with the greatest difference, for ROSA-III test 912, []

]]

In the response to RAI 104, the vendor provided additional information to justify the TRACG models with respect to application in ECCS evaluation. The response included a review of the information described above, in addition to some additional IETs relevant to BWR/2 (i.e., CSHT tests that reflected falling film quench fronts) and sensitivity studies using a BWR/2, which involves extended heatups and falling film quench behavior. In the BWR/2 transient particularly, these models are significantly more important in predicting the overall sequence of events than in other classes of BWR designs.

The evaluation of the IET comparisons provided by GEH in response to RAI 104 indicated that, although in some cases the peak rod temperatures were slightly under-predicted by TRACG, quench times tended to be delayed relative to test data that included a quench. This tendency results in a longer duration of cladding heatup, preventing a non-conservative under-estimation of the ECR.

A sensitivity study, similar to that performed for the Shumway correlation, was performed for the quench front model. The BWR/2 base case was re-executed, biasing the quench model with a constant, low multiplier. The results showed that the biased quench front model produced significantly higher ECR values, as would be expected. Because the PCT occurs at different

elevations, and in different cases, than the maximum ECR, an opposite effect on PCT was observed. The RAI response explained this behavior.

The NRC staff acknowledges that applying a bias to the quench model causes the predicted ECR to increase. However, based on the qualification studies using the LOCA IETs and on the competing influence of the quench model on the BWR/2 PCT and ECR, the NRC staff determined that GEH’s quench model was acceptable. The proposed uncertainty treatment for the quench front model includes sampling to the biased value used in the sensitivity study, but also samples other values so that the competing effects shown in the studies are included in the analysis.

7.0 ESTIMATION OF OVERALL CALCULATIONAL UNCERTAINTY

The following section of the evaluation is based on Regulatory Position 4, “Estimation of Overall Calculational Uncertainty,” of RG 1.157. It should be noted that RG 1.157 was written contemporarily with CSAU (Reference 11), and the guidance for estimating overall calculational uncertainty was based on a CSAU-like approach, in which uncertainties are estimated through the construction of a response surface, and thousands of perturbations of key uncertainty parameters were analyzed using the response surface. Since publication of RG 1.157, realistic ECCS evaluation models used for domestic licensing purposes have evolved. Appendix B of RG 1.203 recognizes this evolution, and in particular, its Reference A-7 discusses the development of more novel approaches (References 9, 45)

Newer methods, like TRACG-LOCA, rely on direct simulation of a more limited sample of cases. The sample size is determined using order statistics theory. In order to show conformance to the “high probability” language contained in § 50.46(a)(1)(i), upper tolerance limits for each of the critical safety parameters are obtained from the sample. Provided those upper tolerance limits remain below the acceptance criteria contained in § 50.46(b)(1) through (b)(3), the “high probability” requirements are satisfied.

The NRC staff review regarding the estimation of overall calculational uncertainty is discussed in this chapter. This review distinguishes between, and evaluates, the types of uncertainty that GEH chooses to analyze explicitly in the uncertainty analysis, and those types that are addressed via other means. The review also considers the statistical process, and underlying theory, used to evaluate the overall uncertainty and derive the “high probability” results for the critical safety parameters.

Table 10 summarizes the RAIs related to this portion of the review.

Batch	RAI	Topic	Ref.
1	1	General Justification for Uncertainty Treatment	3
2	92	CSHT Qualification Analyses	4
1	66	Sample Size and Joint Upper Tolerance Limits	3
2	89	Deterministic Break Spectrum Analysis	4
5	65	Continuity of Sample Characteristics	7
3	99	Statistical Meaning of Limiting Results	5
5	103	Application of Joint Upper Tolerance Limits	7
1	7	Analysis Resolution	3
1	6	Phenomenological Uncertainty, etc.	3
1	9	BWR/2 Noise-Driven Bifurcation	3

1	4	Core Detail	3
---	---	-------------	---

Table 10. RAI Responses Related to Estimation of Overall Uncertainty.

During the review process, GEH made two major modifications to its uncertainty approach. The final approach, which was accepted by the NRC staff, is summarized in the response to RAI 103. This review is primarily based on this ultimate approach.

7.1. GENERAL

Regulatory Position 4.1 of RG 1.157 distinguishes between code uncertainty and other sources, including uncertainty associated with the experimental data used in the code assessment process, input boundary and initial conditions, and fuel behavior.

To an extent, the TRACG code assessment accounts for both uncertainty associated with the individual models, and with the experimental data used in the code assessment process, as discussed in Section 5.0 of the LTR. GEH clarified its position on this matter in the response to RAI 1.d, stating "...the measurement uncertainty in the data is intrinsically accounted for when code comparison to experimental results is made."

The effects of scaling the models to BWR plant simulation are discussed in LTR Chapter 5.3. Scalability is demonstrated by comparing TRACG predictive capabilities at various levels, including component-specific tests, scaled integral system tests, and relevant plant data.

The vendor employs simplifying assumptions in a generally conservative fashion. For example, core spray flow variability is addressed in a simplifying assumption [[

]] In other cases, GEH provides sensitivity studies to demonstrate that a particular simplifying assumption is conservative. This is demonstrated in the review of the scram time logic discussed in Section 5.5 of this SE. Given the above, it is clear that GEH has evaluated its simplifying assumptions to determine that either the assumption is conservative, or that it has an insignificant effect on the figures of merit.

Many sources of uncertainty with importance relative to the figures of merit are addressed in the deterministic analysis, or are bounded by the use of conservative, simplifying assumptions. Thus, the deterministic break spectrum is already a conservative estimation of plant performance with regard to sources of uncertainty such as initial and boundary conditions, break locations and sizes, single failures, fuel behavior, and the like. When model uncertainty is analyzed for the limiting break of a given spectrum, it is evaluated using properties that bound such sources of uncertainty. Since this uncertainty is bounded, the NRC staff determined that the GEH approach is acceptable.

Regulatory Position 4.1 of RG 1.157 concludes as follows:

[...] Regulatory Position 3 provides a description of the features that should be included in the overall code uncertainty evaluation that is called for in paragraph 50.46(a)(1). This uncertainty evaluation should make use of probabilistic and statistical methods to determine the code uncertainty. For a calculation of this complexity, a completely rigorous mathematical treatment is neither practical nor

required. In many cases, approximations and assumptions may be made to make the overall calculational uncertainty evaluation possible. A careful statement of these assumptions and approximations should be made so that the NRC staff may make a judgment as to the validity of the uncertainty evaluation. The purpose of the uncertainty evaluation is to provide assurance that for postulated loss-of-coolant accidents a given plant will not, with a probability of 95% or more, exceed the applicable limits specified in paragraph 50.46(b).

The uncertainty evaluation furnished by GEH uses statistical methods to evaluate individual sources of model uncertainty. Probabilistic methods are then used to determine upper tolerance limits for each of the critical safety parameters, considering the PIRT-important sources of model uncertainty. In TRACG-LOCA, simplifying assumptions, supported by deterministic analysis and system evaluation, are used to address other important sources of uncertainty, such as for plant inputs and initial conditions. The simplifying assumptions tend to drive the plant operating state to a pessimistic condition, which yields conservative results. When the uncertainty analysis is applied to the conservative plant operating state, the NRC staff agrees that the results show, with probability 95-percent or more, that the acceptance criteria would not be exceeded, given that the results of the uncertainty analysis conform to the acceptance criteria. Thus, the NRC staff determined that GEH is consistent with the guidance in this Regulatory Position.

7.2. CODE UNCERTAINTY

Regulatory Position 4.2 of RG 1.157 states, in part:

Code uncertainty should be evaluated through direct data comparison with relevant integral systems and separate-effects experiments at different scales. In this manner, an estimate of the uncertainty attributable to the combined effect of the models and correlations within the code can be obtained for all scales and for different phenomena.

The vendor addresses code uncertainty by assessing the uncertainty associated with individual models, correlations, and closure relations by evaluating model capabilities against relevant separate effects tests. The testing is described, largely, in Reference 17, and summarized with regard to ECCS/LOCA analysis in Chapter 5.1 of the LTR. The NRC staff evaluation considered the individual uncertainty applied to specific models as part of the review of those models. These considerations are addressed in Chapter 6 of this SE.

These comparisons should be performed for important key parameters to demonstrate the overall best-estimate capability of the code... In addition, a code uncertainty evaluation should be performed for other important parameters for the transient of interest to evaluate compensating errors.

The qualification analysis presented in LTR Section 7.4 addresses this element of RG 1.157 guidance. In addition to making comparisons to peak rod temperatures for FIST large- and small-break LOCA tests, system pressure and temperature comparisons are provided for SSTF tests, and rod temperature comparisons are again provided for CSHT. These comparisons are made using the statistical methods, and they show that the TRACG-predicted results are

generally consistent with the test data with no readily discernible bias or nonconservative tendencies.^T

The experimental information used to determine code uncertainty will usually be obtained from facilities that are much smaller than nuclear power reactors. Applicability of these results should be justified for larger scales. The effects of scale can be assessed through comparisons to available large-scale separate effects tests and through comparison to integral tests from various sized facilities. If there are scaling problems, particularly if predictions are nonconservative, the code should be improved for large-scale plants (i.e., nuclear reactors). Codes not having scaling capability will not be acceptable if their predictions are non-conservative.

The vendor assessed the effects of scale using integral effects tests from several facilities, as discussed in Chapter 5.3 of the LTR. These facilities varied in scale from small (1:624) to SSTF, which is a full-scale mockup of a sector of a BWR/6 core. Favorable comparisons to experimental data at all scaling levels demonstrates the scalability of the evaluation model. Based on its review of LTR Chapter 5.3 and supporting information contained in Reference 17, the NRC staff determined that GEH is consistent with this element of RG 1.157.

7.3. STATISTICAL TREATMENT OF OVERALL CALCULATIONAL UNCERTAINTY

7.3.1. Introduction: Precedential Perspective on the Use of Order Statistics

Initially, GEH proposed to determine the requisite upper quantile by applying a similar approach to that used in TRACG for AOO analysis. In this approach, GEH would select from two possible ways to obtain the desired statistical coverage, which are described in Section 7.1 of the LTR. A sample of 59 statistical trials is analyzed. Based on this sample size, GEH would examine the results for each figure of merit to determine whether the results conform to a normal distribution. If so, the uncertainty would be estimated as 2.024 times the standard deviation of the result.

If the results were not normally distributed, order statistics theory would be applied. Based on non-parametric order statistics, the highest-ranked result in a sample of 59 provides an estimator for the 95/95 one-sided upper tolerance limit with regard to a single figure of merit. This approach was employed in the demonstration analyses provided in Chapter 8 of the LTR.

While this approach was consistent with TRACG for AOO analysis,^U it was not consistent with the NRC's long-standing practice of accepting order statistics-based ECCS evaluations on the basis that they provide tri-variate upper tolerance limits. That is, the NRC staff has accepted

^T It should be noted that, in some cases, the CSHT comparison using the uncertainty methodology, which is presented in LTR Chapter 7.4, indicated that TRACG nominally under-predicted the PCT associated with the particular CSHT run, and with uncertainty analysis included, the TRACG-predicted highest PCT came into the range of the CSHT-observed PCTs. This particular test was chosen because it produced the worst comparison. In response to RAIs 82 and 92, GEH produced additional CSHT test comparisons, including those with higher PCTs, which indicated much better agreement between TRACG and observed test results. GEH also pointed out that the nominal TRACG model in four other CSHT tests over-predicted the PCTs for all rod groups.

^U Note, also, that this approach is consistent with the TRACG-LOCA application for the ESBWR; however, the ESBWR has a reactor and ECCS design that leads to a much more benign, and less phenomenologically complex, LOCA transient.

evaluations that use order statistics, provided that simultaneous upper tolerance limits are established for each of the critical safety parameters.

The first order statistics-based ECCS evaluation model was approved by the NRC in 2003 (Reference 46). In that method, the NRC staff accepted a univariate tolerance limit based on that vendor's successful demonstration that PCT was the most limiting of the three critical safety parameters. GEH has not attempted to make a similar assertion. Additionally, that method has been revised and now produces trivariate tolerance limits (Reference 47, Page 33). Aside from this example, contemporary, realistic ECCS evaluation models that have been approved by the NRC for operating plants and rely on order statistics produce trivariate, 95/95 tolerance limits for the critical safety parameters. See, for example, Page 7 of the NRC staff safety evaluation approving WCAP-16009-NP-A, "Realistic LOCA Evaluation Methodology Using the Automated Statistical Treatment of Uncertainty Method" (Reference 48).

7.3.2. Summary of GEH Approach

In its response to RAI 103, GEH devised an approach that produces tri-variate, 95/95 upper tolerance limits for each of the critical safety parameters. The approach draws on the theory of Reference 49 to establish two sampling schemes. In the first scheme, Scheme A, GEH will use a sample size intended to provide tri-variate, 95/95 upper tolerance limits. These limits will be approximated by choosing the highest-ranked order statistics for each of the three critical safety parameters, i.e., the highest PCT, and the greatest amount of ECR and core-wide hydrogen generation. In the second approach, Scheme B, GEH will use a sample size that provides the requisite coverage, but allows for the rejection of two cases from within the sample set. For Scheme A, the sample size is 124; for Scheme B, the sample size is 181.

GEH indicated, in its response to RAI 99, and confirmed in its response to RAI 103, that the sampling scheme will be determined at the onset of the analysis. This precludes reducing the overall statistical confidence in the results by increasing sample size *a posteriori*. This concept of reduction in statistical confidence is discussed in further detail in Section 24.11, "What's Wrong With This Picture," of Reference 50.

Scheme B, with two rejected sample constituents, will be selected if GEH or a supported NRC licensee determines that one or more of the critical safety parameters will be challenged in a particular application. The example provided in the RAI response is for BWR/2 applications, wherein the extended transient results in oxidation levels that approach the 17-percent B-J oxidation criterion.

The vendor uses the theory developed in References 50 and 51 to establish the method of elimination in application of Scheme B. The strategy is illustrated in Figure R103-2 of the response to RAI 103. The vendor will determine the tolerance region by eliminating two cases that contribute the highest-ranked statistics for any of the critical safety parameters. The upper tolerance limits will then be chosen, independently, from the remaining 179 cases within the sample. The contributors for each of PCT, ECR, and hydrogen generation may come from different cases, provided each is the highest-ranked from the cases remaining in the sample.

7.3.3. NRC Staff Evaluation of GEH Approach

The NRC staff evaluation for the overall combination of uncertainty is based on Regulatory Position 4.4 of RG 1.157.

Regulatory Position 4.4 of RG 1.157 states as follows:

The methodology used to obtain an estimate of the overall calculational uncertainty at the 95% probability limit should be provided and justified. If linear independence is assumed, suitable justification should be provided. The influence of the individual parameters on code uncertainty should be examined by making comparisons to relevant experimental data. Justification should be provided for the assumed distribution of the parameter and the range considered.

For the statistical analysis, GEH devises a sample of sufficient size to determine 95/95 upper tolerance limits for each of the three critical safety parameters. The theory used in determining the sample sizes assumes that the distributions for each of the critical safety parameters is dependent, without any underlying assumption as to their correlation. This assumption results in reliance on a larger sample size from which to obtain the upper tolerance limits (References 49 through 53), and hence the NRC staff determined that the approach is acceptable.^v

In reality, the true statistical distribution for the key parameters (e.g., peak cladding temperature) is unknown. The choice of a statistical distribution should be verified using applicable engineering data and information. The statistical parameters appropriate for that distribution should be estimated using available data and results of engineering analyses. Supporting documentation should be provided for this selection process. These estimated values are assumed to be the true values of the statistical parameters of the distribution. With these assumptions, an upper one-sided probability limit can be calculated at the 95% level...

Since GEH revised its approach to remove the ability to use normally-distributed, one-sided upper tolerance limits, and instead exclusively uses non-parametric statistics to determine the upper tolerance limits for the critical safety parameters, this element of guidance does not apply.

... As the probability limit approaches 2200 °F, more care must be taken in the selection and justification of the statistical distribution and in the estimation of its statistical parameters. If a normal distribution is selected and justified, the probability limit can be conservatively calculated using two standard deviations. The added conservatism of the two standard deviations compared to the 95th percentile is used to account for the uncertainty in the probability distribution...

Certainly, the guidance provided above is relevant if an approach like that envisioned in CSAU is used, wherein a response surface is constructed, and thousands of statistical trials are simulated using the response surface. The upper quantile of such a large sample size can be inferred using far less than two times the standard deviation. However, contemporary approaches have abandoned the response surface approach in lieu of performing direct simulation. As is the case with TRACG-LOCA, the approach relies on distribution-free statistics, and the upper tolerance limits are set by the worst-case results from the sample, rather than by adding a multiple of the standard deviation to the mean.

^v The general idea being, that under-estimation of the sample size leads to excessive variability in the estimation of the tolerance region, and as such, can lead to its under-prediction. This would be non-conservative.

... Other techniques that account for the uncertainty in a more detailed manner may be used. These techniques may require the use of confidence levels, which are not required by the above approach.

Ultimately, this element of the RG 1.157 Regulatory Position drove the successive revisions to the GEH sampling approach.

GEH initially proposed characterizing its results at a quantified upper tolerance level. The response to RAI 66 documented a shift in the methodology. The NRC staff acknowledges that the responses to RAIs 66 and 89 indicated that GEH's initially proposed approach was reproducible, with statistically insignificant differences among different samples applied to the same transient. In the response to RAI 66, GEH further studied the issue by running a 124-case sample, and comparing limiting results from the first 59 cases to the entire population. The difference in sample sizes did not yield statistically different results. However, this information was only provided using a single, two-part sample, and applied to a single plant analysis. It was not possible to infer that similar results should be more generally expected. The response to RAI 89 included a statistical analysis of several different breaks, and, in the region where the break sizes produced similar results because of overlap in the randomly sampled discharge coefficient, the limiting results, again, were not statistically different.

Drawing on the published work of Guba, Makai, and Pal (Reference 49), one might infer that a random sample of size 124 is required to provide a 95/95 joint upper tolerance region for a trivariate set of attributes (PCT, MLO, CWO). The tolerance region would be defined by the worst-ranked result for each figure of merit. The NRC staff issued RAI 66, in part, to address GEH's inconsistency with this approach. In response, however, the vendor merely eliminated its statement of confidence in the results. The topic was revisited in RAI 99, and in response, GEH proposed instead to use three independent, random samples of size 59 to evaluate each of three limiting break configurations. The NRC staff also did not accept this approach, because in the demonstration analyses, the deterministic break spectra for all product lines appear to show a conclusively limiting break size, meaning that the information obtained from analyzing the other break sizes does not contribute meaningfully to the overall limiting results.

In order to address the NRC staff concerns, GEH ultimately agreed to perform the two-scheme statistical analysis using a sample of either 124 cases with zero rejections, or 181 cases with two rejections, and estimating the upper tolerance limits by selecting the highest remaining order statistic for each of the three critical safety parameters. The NRC staff accepts this approach because it provides tri-variate, 95/95 upper tolerance limits for each of the critical safety parameters.

The evaluation of the peak cladding temperature at the 95% probability level need only be performed for the worst-case break identified by the break spectrum analysis in order to demonstrate conformance with paragraph 50.46(b). However, in order to use this approach, justification must be provided that demonstrates that the overall calculational uncertainty for the worst case bounds the uncertainty for other breaks within the spectrum. It may be necessary to perform separate uncertainty evaluations for large- and small-break loss-of-coolant accidents because of the substantial difference in system thermal-hydraulic behavior.

The vendor conforms to this element of guidance by evaluating a plant-specific break spectrum to identify the limiting break characteristics, and performing distinct uncertainty analyses for the limiting breaks. If the spectrum does not conclusively identify a single limiting break, then the

multiple, possibly limiting breaks will be treated as sensitivity studies, meaning the statistical analysis is repeated for the different, possibly limiting, break characteristics.

The revised paragraph 50.46(a)(1)(i) requires that it be shown with a high probability that none of the criteria of paragraph 50.46(b) will be exceeded, and is not limited to the peak cladding temperature criterion. However, since the other criteria are strongly dependent on peak cladding temperature, explicit consideration of the probability of exceeding the other criteria may not be required if it can be demonstrated that meeting the temperature criterion at the 95% probability level ensures with equal or greater probability that the other criteria will not be exceeded.

GEH considers each of PCT, ECR, and core-wide oxidation explicitly.

Based on the review and evaluation described above, the NRC staff determined that the TRACG-LOCA approach for estimating the overall uncertainty associated with the analytic results, incorporated by expressing the upper tolerance limits associated with such results, is acceptable. Several limitations to the approach apply, as set forth in Chapter 10.

7.4. PCT ANALYSIS RESOLUTION AND CORE DETAIL

The concept of PCT analysis resolution is introduced in Chapter 6.4 of the LTR. It characterizes “an inherent uncertainty that is common to analyses using system codes, which is not separately identified by physical phenomena” (LTR, Page 6-28). Small changes in the input cause variability in the results, and this effect is sometimes called computational noise. The analysis resolution quantifies this uncertainty. It can be estimated by running statistical analyses that perturb parameters by small fractions of their ordinary statistical distributions, and examining the spread of the results.

GEH attributed the magnitude of the analysis resolution to two key contributors: numerical techniques and channel plugging, or the parallel channel effect. The channel plugging effect arises because subtle changes in lower plenum behavior, or in bypass behavior, can cause the orifices at the channel bottom to either remain open with a vapor flow path, or to ‘plug’ with liquid. Whether or not the plugging occurs can be affected by minute changes in other system parameters, but the effect can drastically change the behavior of the hot channel heatup. Effectively, the plugging phenomenon can cause a bifurcation in PCT results over a statistical trial, with one grouping of curves reflecting the PCT transient of a plugged hot channel, and the other reflecting the transient of an unplugged hot channel. The plugged channel does not benefit from the vapor cooling associated with the steam updraft that occurs in a channel with a more open flow path at the bottom.

In its review, the NRC staff did not accept GEH’s position that channel plugging should be considered a dominant contributor to the analysis resolution without further evaluation. Rather, the NRC staff determined that the plugging behavior, and resulting PCT bifurcation, suggested that the core model did not contain sufficient detail as to permit a realistic representation of the effects of the channel plugging phenomenon. The staff position was documented in RAI 7, among others including RAIs 6, 9 and 4.

As noted in the response to RAI 4, GEH implemented a TRACG core model with significantly greater detail, which minimized the effects of non-phenomenological variability on the code

output. The responses to RAIs 6, 7, and 9 demonstrated that the non-phenomenological variability was significantly reduced, once the detailed core model was implemented.

[[

]] Based on these results, the NRC staff determined that the improved core detail adequately addressed the stochastic behavior associated with channel plugging.

In addition to the studies described above, GEH [[]] its small perturbation analysis to sample, [[]], rather than the originally proposed [[]]. These changes significantly reduced the PCT bifurcation associated with channel plugging, and provided a significantly reduced estimate of the analysis resolution. Additional studies using a [[]] provided results that were consistent with the [[]], suggesting that [[]] was a sufficient constraint upon which to determine the analysis resolution. As noted in the response to RAI 7.d, the use of [[]] also reduced the analysis resolution to a value that was “much less than the total uncertainty used in determining the upper tolerance limits” (MFN 14-064 (Reference 3), Page 27).

Based on the review described above, the NRC staff determined that GEH devised an acceptable means to estimate the numerical resolution associated with its analysis. The method relies on a model that uses increased core detail in order to reduce the heightened model sensitivity to the parallel channel effect, and the use of a small parameter perturbation analysis. Using the improved model, the vendor demonstrated that the analysis resolution was on the order of [[]].

8.0 EVALUATION MODEL QUALIFICATION AND DEMONSTRATION

8.1. STATISTICAL ANALYSIS FOR QUALIFICATION EVENTS

In Section 7.4 of Reference 1, GEH provided a series of statistical analyses for qualification events, with the stated purpose of validating the values used for the model uncertainties by showing that the test data fall within the resulting uncertainty band of the calculations. The vendor selected the large and small breaks from the FIST series, specifically, Tests 6DBA1B and 6SB2C. GEH also exercised its statistical analysis for two Core Spray Heat Transfer tests, as well as for Steam Sector Test Facility Test EA3-1.

Comparisons of pressures and rod temperatures to the FIST tests indicated excellent agreement, with most data points falling within the minimum and maximum results from the TRACG analyses. In particular, the limiting rod temperature transients were generally over-predicted, with maximum cladding temperature transients predicted by TRACG that tended to extend for longer than those exhibited by the tests.

GEH provided comparisons of system pressure, temperatures at the pool periphery, and fill fractions for the lower plenum, bypass, and upper plenum for the SSTF comparison. The

system pressure trend shows that the test data generally fall within the bounds of the calculation. The pool temperature predictions follow general trending of the data, but GEH explained that the TRACG predictions, like the test data, fluctuated once the lower plenum filled. The mass fraction in the lower plenum showed that the lower plenum refill time fell within the bounds of the TRACG calculations. The trending for the bypass and upper plenum fill fractions suggests an element of conservatism with regard to the TRACG predictive capabilities for upper plenum mixing and CCFL; [[

]]

In selecting the CSHT tests to simulate, GEH chose those tests where the TRACG nominal analysis tended to under-predict the rod temperature trends. These tests were Tests 111 and 112. The application of the statistical methods to these CSHT tests brought the TRACG limiting predicted peak temperatures either very close to, or within the uncertainty bounds of the experimentally measured temperatures. In the responses to RAIs 92 and 104, GEH explained that TRACG's nominal models tended to over-predict the PCTs for four other CSHT tests, and that increasing the sample sizes associated with these simulations to 124 (instead of 59), would add to the spread in temperature distribution associated with these tests.

8.2. REVIEW OF STUDIES FOR BWR/2 PLANT

The NRC staff reviewed the BWR/2 demonstration analysis in detail, in particular because the BWR/2 results have both high PCT and ECR values. The NRC staff review generated numerous RAIs that were specific to modeling approaches and phenomena of particular import to the BWR/2 analysis, as summarized in Table 11, below.

Batch	RAI	Topic	Ref.
1	13	BWR/2 Air Ingress and Break Location	3
1	38	Air and Two-Phase CCFL in BWR/2	3
1	59	PIRT Item F3 – Non-Condensibles	3
1	29	BWR/2 Axial Peaking	3
1	35	Significance of BWR/2 Doppler/Void Coefficients	3
1	32	BWR/2 Isolation Condenser	3
1	62	BWR/2 Isolation Condenser	3
2	96	Uncertainty Estimate for BWR/2 Results	4

Table 11. RAI Responses Related to BWR/2 Analyses.

The BWR/2 break spectrum is shown in Figure 8.3-23 of Reference 1. For the BWR/2, the limiting PCTs are produced by the larger breaks. In particular, the limiting PCT is produced by a double-ended guillotine break on the recirculation discharge. The results of the uncertainty analysis for this break are shown in Figures 8.3-33 and 8.3-34. [[

]]

The spectrum analysis [[

]] This behavior is the general subject of RAI 13, the focus of which is the effect that air ingress has on the PCT response.

In RAI 13.a, the NRC staff requested that GEH explain why opposite impacts from break geometry are obtained between the suction and discharge spectra. []

]]

The studies that GEH performed confirmed that the limiting break geometry in the BWR/2 spectrum is []

]]

Since the vendor provided a reasonable, phenomenological explanation for the break spectrum behavior, supported its findings with sensitivity studies, and ensures that model sensitivities attributable to break configuration are bounded by conservative modeling, the NRC staff accepted the vendor's explanation of the behavior. In the remainder of the response to RAI 13, GEH discussed additional sensitivity studies to evaluate the effect of varying amounts of air ingress due to different break locations, sizes, and geometries. These studies confirmed that, in consideration of varying levels of air infiltration for different break locations, sizes, and geometries, that the [] remained the limiting break in terms of PCT.

The studies described above provided information to inform GEH's response to RAI 38, which is evaluated in Section 3.3.1 of this SE. The NRC staff requested GEH reconsider its assignment of a medium rank for PIRT items M3, and in response, GEH indicated [] PCTs shown in the response to RAI 13, and in the larger breaks of the BWR/2 spectrum.

The NRC staff review of the effect of noncondensibles continued with RAI 59, in which the NRC staff requested that GEH provide normality test descriptive statistics for the uncertainty treatment associated with PIRT Item F3, "Noncondensibile Return at Low Pressure." In its response, GEH indicated that the phenomenon itself is addressed []

]] such that it is not a significant factor in PCT performance in BWR/2 accident scenarios.

The BWR/2 analyses presented in the LTR did not include a description of sensitivity studies to identify limiting axial power shapes. By comparison, the BWR/4 analysis provides this information, which ultimately supports the conclusion that an appropriately limiting axial power shape was modeled. This information, for the BWR/2 analysis, was provided in the response to RAI 29. To study the model sensitivity to axial peaking factor, GEH performed a two-step analysis. The first step evaluated the PCT and ECR for the different hot channels in the reference core. In the second step, GEH varied the elevation of the peak node in full-range uncertainty analyses, and then performed mean-to-mean comparisons among the different axial shapes. From this study, GEH concluded [[

]] This conclusion is supported by the results of the sensitivity studies, [[

]] The vendor further observed [[

]] The NRC staff accepted GEH's analysis, since it indicated that the analytic approach identified a reasonably limiting axial power shape; however, tables included for initial conditions for both the BWR/4 analysis and the BWR/2 analysis indicate that [[

]] While the NRC staff agrees, based on the studies provided for both BWR/4 and BWR/2, [[
]] sensitivity studies will be performed for each TRACG-LOCA application to provide the basis for a limiting initial condition.

In its review of the limiting transient for the BWR/2, the NRC staff observed that the boiling transition peak for the limiting channel is not fully quenched. In RAI 35, the NRC staff requested that GEH justify that parameters affecting the boiling transition temperature increase, such as void and Doppler coefficient, do not appreciably influence the PCT. In its response, GEH stated that the prompt voiding in the core due to rapid pressure reduction associated with a large break is sufficient to reduce fission power to almost zero even before the scram becomes effective. The NRC staff agrees with GEH's account of the large break event and concluded that the concerns discussed in the RAI are addressed.

The BWR/2 design includes an isolation condenser. The NRC staff requested additional information relative to modeling, or not modeling, the isolation condenser relative to the single failure analysis, and relative to the relevant model uncertainty. In the response to RAI 32, GEH stated that any isolation condenser single failures are bounded by never crediting the isolation condenser. GEH also explained the logic used to determine the limiting single failure, which relates to failure of other hardware, including diesel generators and the core spray system. In the response to RAI 62, GEH reiterated that the isolation condensers are not credited. Not crediting the isolation condenser in the break spectrum analysis produces a conservative effect in the range of small- and intermediate-break events, because the system provides additional cooling inventory, and helps to reduce the RCS pressure, thus enhancing the core spray effectiveness. GEH further committed to validate the isolation condenser heat transfer uncertainty treatment on a plant-specific basis. Based on the RAI responses, and in consideration of the fact that the large-break event is limiting for the BWR/2 plant design, the NRC staff did not review the models pertinent to isolation condenser heat transfer, and use of these models would require NRC review prior to implementation in a plant-specific analysis.

Finally, in its review of the BWR/2 statistical analysis, the NRC staff observed that the PCT distribution for the [[
]] and questioned the accuracy of the uncertainty assessment. [[

]] Since the NRC staff is basing its approval on GEH's agreement to use order statistics, and to use a larger sample size than employed in the demonstration analysis, the NRC staff confirmed that the questionable parametric statistics associated with the small break will be addressed by the switch to order statistic. Since the small break is non-limiting, the NRC staff concluded that the concern conveyed in the RAI was addressed.

Based on the NRC staff review of the BWR/2 analysis, the NRC staff determined that specific considerations and unique considerations for this plant design are adequately addressed in the TRACG-LOCA methodology.

9.0 LICENSING CONSIDERATIONS

GEH describes the methodology application in Chapter 9 of the LTR. The chapter summarizes the processes for initial TRACG-LOCA plant analysis, and for evaluating changes to the plant configuration, the analytic method, or the introduction of new fuel. The chapter also addresses limitations to other GEH LTRs, such as the Interim Methods Licensing Topical Report (IMLTR) and MELLA+.

9.1. TRACG-LOCA APPLICATION

TRACG-LOCA is being incorporated into the GESTAR-II process via Amendment 37. As such, licensees using GESTAR-II may administratively implement TRACG-LOCA, provided that such implementation is consistent with the limitations delineated in this SE, and that implementing licensees determine that TRACG-LOCA is applicable to the facility design. It should be noted that reporting requirements of 10 CFR 50.46(a)(3) apply to TRACG-LOCA implementations.

From time to time, NRC licensees may seek license amendments that are based, at least in part, on evaluations of ECCS performance using TRACG-LOCA. For example, Section 9.3 of this SE reviews power uprates and operating domain expansions. Other amendments may seek changes to equipment out-of-service (EOOS) options. When such license amendments are submitted, the NRC staff expects that the requesting licensees will provide a summary of the ECCS performance evaluation on a level of detail consistent with the demonstration analyses discussed in LTR Chapter 8.

9.2. EVALUATING CHANGES

The LTR includes several sections on evaluating changes, which discuss the way that GEH may use TRACG-LOCA to assess items like code changes, plant configuration changes, and new fuel introductions.

Such changes are typically evaluated, and if the change is determined to have an effect on the predicted PCT, then the change must be treated in accordance with 10 CFR 50.46(a)(3) requirements. However, the regulations in 10 CFR 50.46(a)(3) simply require licensees to estimate the effect of each change to, or error in, an acceptable evaluation model, or in its application. The estimated effect then must be reported to the NRC. The regulations are not specific with regard to how the effect of such a change or error is estimated. As such, the NRC

did not make any regulatory determinations with regard to the process used to evaluate changes.

9.3. CONCURRENT GEH LTRS AND RELATED LICENSING

In Section 9.9 of the LTR, GEH discusses compliance with the requirements of IMLTR and the MELLLA+ LTR. While the main purposes of TRACG-LOCA are to demonstrate compliance with 10 CFR 50.46 requirements and to support corresponding core operating limits, TRACG-LOCA analyses may also be used to support licensing requests, such as those associated with expanded operating domains like Maximum Extended Load Line Limit Analysis Plus (MELLLA+) and extended power uprate (EPU). Although GEH chose to address IMLTR and MELLLA+ in this respect, the NRC staff review considered a broader array of GEH LTRs.

This section of the SE discusses several licensing topical reports whose considerations regarding ECCS performance were based on the SAFER/GESTR-LOCA analytic method (References 28, 29). The SAFER/GESTR-LOCA method included several elements that influenced the wording contained in the passages that are excerpted below.

- [[

]]

- [[

]]

- Results: SAFER/GESTR-LOCA produced several different PCT results. These included a nominal PCT, in addition to: (1) an Appendix K PCT result, which was obtained using Appendix K-conformant model features, (2) an upper bound PCT, which was determined by adding an allowance for uncertainty to the nominal PCT, and (3) a licensing basis PCT, which was determined by including additional margin to the nominal PCT to account for differences between the nominal and the Appendix K PCT, and to account for plant-specific uncertainties not addressed specifically within Appendix K requirements.

9.3.1. Extended Power Uprates

GEH maintains a suite of licensing topical reports that are referenced by licensees in requests to implement extended power uprates (EPUs). These include:

- NEDC-32424P-A, "Generic Guidelines for General Electric Boiling Water Reactor Extended Power Uprates," commonly referred to as EPU Licensing Topical Report (ELTR) 1 (Reference 54).
- NEDE-32525P-A, "Generic Evaluations for General Electric Boiling Water Reactor Extended Power Uprates," commonly referred to as ELTR 2 (Reference 55).

- NEDE-33004P-A, "Licensing Topical Report: Constant Pressure Power Uprate," commonly referred to as the Constant Pressure Power Uprate (CPPU) LTR, or CLTR (Reference 56).

ELTR1

The NRC staff safety evaluation approving ELTR 1 noted the following with regard to ECCS performance:

- (a) Reanalysis of the LOCA response utilizing the SAFER/GESTR computer model will improve the apparent safety margins, especially the margin between the calculated peak cladding temperature and the 2200-degree Fahrenheit limit contained in 10 CFR 50.46. ELTR 1 implies that this margin can be used in the relaxation of inputs to the ECCS codes, which corresponds to changes in operational requirements of ECCS equipment. It is the staff's position that this "additional" margin must be used judiciously. Therefore, the staff will not support changes that would relax equipment requirements, such as emergency diesel generator start times, pump flow requirements, and so on, as part of an amendment request for extended power uprate. The staff suggests that the relaxation of these parameters might be pursued as a BWR Owners Group initiative, but in any case must be treated separately from the generic BWR power uprate program.
- (b) If a licensee updates a plant from a previous ECCS computer code to the SAFER/GESTR code, a baseline run using SAFER/GESTR at the present power level must be included so that the true effect of the power uprate can be assessed. Inclusion of SAFER/GESTR results obtained using relaxed input parameters (as previously discussed) may be included in the power uprate amendment request, but must be accompanied by corresponding results obtained by using the present input parameters and uprated power.

Appendix D to ELTR 1 provides the basis for EPU ECCS evaluations performed in accordance with this LTR. While the content of Appendix D is generally based on the use of SAFER methods, it is more broadly constrained by a requirement to use an NRC-approved evaluation model, and a requirement to evaluate the entire break spectrum and limiting single failure for uprated operating conditions. A TRACG-LOCA-based ECCS evaluation would be considered an acceptable evaluation model for such an analysis, on a plant-specific basis.

ELTR2

The NRC staff safety evaluation of ELTR2 states the following with regard to design basis accidents:

Plant-specific analyses will continue to demonstrate the ability of each plant to cope with the full spectrum of hypothetical pipe break sizes from breaks as small as instrument lines to breaks in the largest recirculation, steam, feedwater and ECCS lines... Challenges to the fuel and containment, as well as potential radiological releases to the environment, will be assessed on a plant-specific basis using NRC-approved methods.

The evaluations presented in ELTR2, including those discussed in ELTR2, Supplement 1, Volume 1, conclude that the ECCS equipment performs acceptably relative to EPU operation, given acceptable results from an NRC-approved ECCS evaluation model like SAFER/GESTR-

LOCA. In performing plant-specific evaluations, TRACG-LOCA-based analyses would be considered similarly acceptable.

CLTR

The CLTR builds on the guidelines and evaluations provided in ELTR 1 and 2, and on the experience from EPU applications that had been reviewed and approved between the approval of ELTR 1 and 2 and the approval of the CLTR in 2003. Based on this experience, the NRC staff approved a limited set of analyses that would be used to support conclusions about ECCS performance at EPU plants.

Key considerations included that (1) the implementation of an EPU tended not to affect the LOCA break spectrum and limiting single failure, and (2) the implementation of an EPU tended to increase the predicted PCT on the order of 20 °F or less. Based on these considerations, the NRC staff approved a disposition requiring the evaluation of the limiting break and a sub-set of smaller break sizes for the ECCS performance evaluation at uprated conditions.

The CLTR is also limited, to some extent, to GE14 fuel designs. The NRC understands that some recent NRC licensees using more advanced fuel designs have used a hybrid of CLTR and ELTR1/ELTR2 dispositions. The TRACG-LOCA evaluation model specifically delineates its applicability to the EPU operating domains, such that an EPU application could be supported by a TRACG-LOCA break spectrum ECCS evaluation. However, it should be noted that the generic disposition discussed above is based on (1) SAFER/GESTR-LOCA analyses, and (2) a conclusion that the limiting break does not change for EPU operation.

Years of NRC staff experience reviewing BWR EPUs has revealed that, in fact, an EPU can change a plant-specific break spectrum, making a smaller break event more limiting. In addition, the difference in analytic assumptions employed between SAFER/GESTR-LOCA and TRACG-LOCA can, itself, introduce changes in a plant-specific break spectrum. Therefore, the NRC staff concluded that the ECCS-LOCA analytic dispositions set forth in the CLTR should not be used in justifying a plant-specific BWR EPU when the plant licensing basis method is TRACG-LOCA. Rather, the analytic summary discussed in Section 9.1 of this SE should be furnished with the EPU application. This determination is reasonably consistent with the practice discussed regarding Interim Methods and MELLLA+, in the following sections of this SE, and is reflected in Limitation 6, discussed in Chapter 10 of this SE.

9.3.2. Interim Methods

Some plants incorporate NEDC-33173P, "Applicability of GE Methods to Expanded Operating Domains," or the so-called IMLTR in the licensing bases (Reference 57). The IMLTR imposes limitations based on the database against which GEH methods are qualified. Several of the limitations, identified below, warrant additional discussion within the framework of TRACG-LOCA.

ECCS Evaluations

For applications requesting implementation of EPU or expanded operating domains, including MELLLA+, the small and large break ECCS-LOCA analyses will include top-peaked and mid-peaked power shape in establishing the MAPLHGR and determining the PCT. This limitation is applicable to both the licensing bases PCT and the upper bound PCT. The plant-specific applications will report the limiting small and large break licensing basis and upper bound PCTs.

The ECCS-LOCA will be performed for all statepoints in the upper boundary of the expanded operating domain, including the minimum core flow statepoints, the transition statepoint as defined in Reference 2 and the 55 percent core flow statepoint. The plant-specific application will report the limiting ECCS-LOCA results as well as the rated power and flow results. The SRLR will include both the limiting statepoint ECCS-LOCA results and the rated conditions ECCS-LOCA results.

This limitation is based on the SAFER/GESTR-LOCA analytic methods, reflecting both the SAFER/GESTR-LOCA power shapes and the licensing basis and upper bound PCTs. Plant-specific TRACG-LOCA analysis will evaluate all necessary statepoints in the power-to-flow operating domain. In addition, the method considers both bottom-/mid- and top-peaked power shapes. Plant-specific analyses also include a spectrum of break sizes to identify limiting break sizes for each of a small-, intermediate- and large-break. Once the uncertainty analysis is complete, TRACG provides upper quantile results for the limiting initial condition, such that there is no longer a distinction between licensing basis and upper bound PCT. Noting these differences, a TRACG-LOCA analysis can be used to satisfy this limitation. As discussed in Section 9.1 of this SE, the submittal of a TRACG-LOCA analytic summary will permit sufficient NRC staff review to determine whether this IMLTR limitation is satisfied. This review determination is reflected in Limitation 6, in Chapter 10 of this SE.

9.3.3. Maximum Extended Load Line Limit Analysis Plus

Several limitations related to concurrent changes, set forth in Section 12.4 of the staff SE approving MELLLA+, require ECCS performance evaluation (Reference 58). TRACG-LOCA is an acceptable method for performing such evaluations, provided that the conditions being evaluated remain within the TRACG-LOCA qualification range.

Several limitations are specific to ECCS-LOCA evaluations, specifically those discussed in Sections 12.10 through 12.14 of the staff SE approving MELLLA+. These include limitations related to the ECCS-LOCA off-rated multiplier (Section 12.10), the axial power distributions required for analysis in the MELLLA+ operating domain (Section 12.11), reporting of ECCS performance evaluation results (Section 12.12), requirements for small break LOCA analysis (Section 12.13), and requirements for break spectrum analysis (Section 12.14).

ECCS-LOCA Off-Rated Multiplier Limitations

The following indented paragraphs refer to applications of the SAFER/GESTR-LOCA methods:

The plant-specific application will provide the 10 CFR Part 50, Appendix K, and the nominal PCTs calculated at the rated EPU power/rated CF, rated EPU power/minimum CF, and the low-flow MELLLA+ boundary (Transition Statepoint). For the limiting statepoint, both the upper bound and the licensing PCT will be reported. The M+SAR will justify why the transition statepoint ECCS-LOCA response bounds the 55 percent CF statepoint. The M+SAR will provide discussion on what power/flow combination scoping calculations were performed to identify the limiting statepoints in terms of DBA-LOCA PCT response for the operation within the MELLLA+ boundary. The M+ SAR will justify that the upper bound and licensing basis PCT provided is in fact the limiting PCT considering uncertainty applications to the non-limiting statepoints.

LOCA analysis is not performed on cycle-specific basis; therefore, the thermal limits applied in the M+SAR LOCA analysis for the 55 percent CF MELLLA+ statepoint and/or the transition statepoint must be either bounding or consistent with cycle-specific off-rated limits. The COLR and the SRLR will contain confirmation that the off-rated limits assumed in the ECCS-LOCA analyses bound the cycle-specific off-rated limits calculated for the MELLLA+ operation. Every future cycle reload shall confirm that the cycle-specific off-rated thermal limits applied at the 55 percent CF and/or the transition statepoints are consistent with those assumed in the plant-specific ECCS-LOCA analyses.

Off-rated limits will not be applied to the minimum CF statepoint.

If credit is taken for these off-rated limits, the plant will be required to apply these limits during core monitoring.

Each statepoint identified above is analyzed in the TRACG-LOCA analysis for MELLLA+ plants. However, TRACG-LOCA does not produce Appendix K, licensing basis, or upper bound results. Instead, the TRACG-LOCA analysis will produce nominal results from the system analysis, and upper quantile results from applying the uncertainty analysis at each state point. Noting these differences, the inclusion of a detailed description of the TRACG-LOCA analysis and its results will provide sufficient information for the staff reviewing a plant-specific MELLLA+ application to determine whether this condition is satisfied. This conclusion is reflected in Limitation 6, discussed in Chapter 10 of this SE.

Axial Power Distribution

For MELLLA+ applications, the small and large break ECCS-LOCA analyses will include top peaked and mid-peaked power shape in establishing the MAPLHGR and determining the PCT. This limitation is applicable to both the licensing bases PCT and the upper bound PCT. The plant-specific applications will report the limiting small and large break licensing basis and upper bound PCTs.

This limitation was written with regard to elements of the SAFER/GESTR-LOCA methodology, which relied on a mid-peaked axial power shape, and produced a number of different kinds of results, including licensing basis, Appendix K, and upper limit PCTs. The TRACG-LOCA methodology includes various power shapes, and evaluates a spectrum of break sizes to determine limiting small-, intermediate- and large-break results. Thus, in the application of the TRACG-LOCA methodology, a specific licensee can analyze various power shapes and determine nominal and upper quantile PCTs for the limiting break sizes. This information will satisfy the MELLLA+ limitation regarding axial power distribution.

ECCS Reporting

For SAFER/GESTR-LOCA applications:

Both the nominal and Appendix K PCTs should be reported for all of the calculated statepoints, and

The plant-variable and uncertainties currently applied will be used, unless the NRC staff specifically approves a different plant variable uncertainty method for application to the non-rated statepoints.

When relying on TRACG-LOCA results, NRC licensees will instead report nominal and upper quantile PCT results. Uncertainties and plant variables will be determined in accordance with the methodology.

Small Break LOCA Analysis

For SAFER/GESTR-LOCA applications:

Small break LOCA analysis will be performed at the MELLLA+ minimum CF and the transition statepoints for those plants that: (1) are small break LOCA limited based on small break LOCA analysis performed at the rated EPU conditions; or (2) have margins of less than or equal to [[]] relative to the Appendix K or the licensing basis PCT.

Since TRACG-LOCA analyses require consideration of the entire spectrum of break sizes, this limitation is inherently satisfied by any application of the TRACG-LOCA methodology.

LOCA Break Spectrum

The scope of small break LOCA analysis for MELLLA+ operation relies upon the EPU small break LOCA analysis results. Therefore, the NRC staff concludes that for plants that will implement MELLLA+, sufficient small break sizes should be analyzed at the rated EPU power level to ensure that the peak PCT break size is identified.

Since TRACG-LOCA analyses require consideration of the entire spectrum of break sizes, this limitation is inherently satisfied by any application of the TRACG-LOCA methodology.

10.0 LIMITATIONS

This section of the SE summarizes the limitations^W that apply to the NRC staff review of NEDE-33005. The limitations are organized into seven categories, and are summarized in the table below. A brief discussion of each limitation follows the table, including cross-references to SE sections and RAI responses.

Limitation	Description
1	Applicability
	1.1 <i>Nuclear Power Plant Specification</i>
	1.2 <i>Native Fuel System Design Applicability</i>
	1.3 <i>Competitor and Co-Resident Fuel System Applicability</i>
	1.4 <i>First-of-Kind Applications</i>
	1.5 <i>Regulatory Compliance</i>
	1.6 <i>Promulgation of 10 CFR 50.46c</i>
2	Deterministic Analysis
	2.1 <i>Core Detail</i>
	2.2 <i>Hot Channels</i>
	2.3 <i>Break Spectrum Analysis</i>
	2.4 <i>Initial Conditions and Plant Parameters</i>
	2.5 <i>General Design Criterion 35 Compliance</i>
	2.6 <i>Calorimetric Power Uncertainty</i>
	2.7 <i>Use of the Shumway Correlation</i>
3	Upstream and Concurrent Methods
	3.1 <i>Reporting Requirements for Upstream/Concurrent Methods</i>
	3.2 <i>Limitations on the Use of Upstream/Concurrent Methods</i>
4	Statistical Analysis
	4.1 <i>Limiting Break Sizes</i>
	4.2 <i>Sample Size</i>
	4.3 <i>Rejection of Results</i>
	4.4 <i>Successive Elimination</i>
	4.5 <i>Dispositioning Unacceptable Statistical Results</i>
	4.6 <i>Resampling</i>
5	Interim Limitation on Cathcart-Pawel
6	Applicability of TRACG-LOCA to Expanded Operating Domains
7	BWR/3-6 First-of-a-Kind Application

Table 12. Summary of TRACG-LOCA Limitations.

10.1. APPLICABILITY

The following limitations delineate the applicability of TRACG-LOCA.

^W This SE has favored the term “limitations,” however, no distinction is made between “limitations” and “conditions” as used in Office of Nuclear Reactor Regulation Office Instruction LIC-500, “Topical Report Process.”

10.1.1. Limitation 1.1: Nuclear Power Plant Specification

The methods described in NEDE-33005 are considered applicable to General Electric-designed nuclear steam supply systems of the BWR/2 through BWR/6 vintage. The model is not considered applicable for any other classes of plant designs. An extension of such applicability would require the submittal, review, and approval of a separate LTR. Refer to SE Section 3.1.

10.1.2. Limitation 1.2: Fuel System Design Applicability

The review considered Global Nuclear Fuel (GNF) fuel designs through GNF-2. Extension to evolutionary GNF fuel product lines may be completed in accordance with the NRC-approved General Electric Standard Application for Reactor Fuel (GESTAR-II). If a new fuel design feature cannot be readily accommodated via the TRACG-LOCA methodology, or is not supported by its qualification, GEH shall submit the modeling or methodology changes, or updated qualification, needed to accommodate the design to the NRC for review and approval prior to implementing such changes in licensing applications of the TRACG-LOCA methodology. Refer to SE Section 3.1.

10.1.3. Limitation 1.3: Competitor and Co-Resident Fuel System Applicability

Passages within the LTR and the RAI responses discuss modeling approaches and uncertainty treatments that are fuel-design-specific. Such items include limiting power shapes, cladding material properties, and critical quality-boiling length correlations. The analytic treatment of competitor and co-resident fuel is acceptable to the extent that it is supported by modeling approaches appropriate for the fuel design. However, the co-resident fuel must be operated within constraints that are at least as restrictive, jointly and severally, as those established by, or employed in, the ECCS evaluation furnished by the competitor. Alternatively, a licensee may propose an RLA justifying the applicability and acceptability of using TRACG-LOCA to set less limiting operating characteristics. Refer to SE Section 3.1.

10.1.4. Limitation 1.4: First-of-Kind Applications

If an NRC licensee chooses to apply this method in a fashion inconsistent with the existing TRACG-LOCA approval basis and requiring prior NRC staff approval, it is recommended that such a request be submitted as a standalone request. Embedding such a request in a separate requested licensing action (RLA), such as a request for an expanded operating domain, could result in the rejection of the RLA for use of unapproved methods, or in complicating or delaying the review of the RLA.

10.1.5. Limitation 1.5: Regulatory Compliance

This model is considered approved for use by the NRC staff for the purpose of evaluating emergency core cooling system performance under the requirements of § 50.46(a)(1)(i). More specifically, the model is considered acceptable for demonstrating compliance with the acceptance criteria set forth in §50.46(b), paragraphs (1) through (3). GEH addresses compliance with criteria (b)(4) and (b)(5) in Section 2.5 of the LTR. Compliance with Criterion (b)(4) is addressed by compliance with Criteria (b)(1) and (b)(2). GEH stated that the “bases and demonstration of compliance with Criterion [(b)(5), long-term cooling]... do not need to be evaluated as part of the TRACG ECCS/LOCA analysis.”

Based on the statements by GEH, the NRC staff did not consider the application of TRACG-LOCA for evaluating long-term core cooling scenarios pursuant to Criterion (b)(5) of § 50.46. This limitation should not be construed to preclude the use of TRACG for compliance with § 50.46, Criterion (b)(5), but rather to clarify that such use has not been considered in the present review effort, and would require a separate application review, should a licensee wish to apply long-term cooling licensing calculations using the TRACG-LOCA methodology. Refer to SE Section 3.2.

10.1.6. Limitation 1.6: Promulgation of 10 CFR 50.46c

The approval of TRACG-LOCA applies to the revision of 10 CFR § 50.46 appearing in the January 1, 2016, version of Title 10 of the Code of Federal Regulations. A subsequent revision to the emergency core cooling requirements is presently under consideration by the Commission, which may result in the promulgation of new, performance-based requirements under § 50.46c. A revision or supplement to NEDE-33005 would be required to obtain NRC approval to use TRACG-LOCA for the purposes of compliance with § 50.46c.

10.2. DETERMINISTIC ANALYSIS AND MODELS

The following limitations apply to the use of TRACG-LOCA to evaluate a plant-specific break spectrum and determine the limiting breaks, upon which to perform the statistical analysis.

10.2.1. Limitation 2.1: Core Detail

Use of the detailed channel grouping described in the response to request for additional information (RAI) 6 constitutes a minimum required for analysis. Each core analyzed shall [[

]] Refer to SE

Section 5.3 for additional detail.

10.2.2. Limitation 2.2: Hot Channels

As discussed in the response to RAI 102, [[

]] The RAI response provides additional detail regarding the initial conditions for these hot channels, their location in the core, and the process for adding additional, hot channels. GEH shall adhere to this process in performing plant-specific evaluations. Refer to SE Section 5.3 for additional detail.

10.2.3. Limitation 2.3: Break Spectrum Analysis

The break spectrum analysis shall be performed at the limiting location and ECCS configuration to identify the most severe event(s). In regions of limiting break sizes, the break spectrum analysis shall be performed at sufficient resolution as to permit overlap, in terms of effective break area, when the critical flow uncertainty is applied in the subsequent statistical analysis. Refer to SE Sections 6.2 and 5.4 for additional detail.

10.2.4. Limitation 2.4: Initial Conditions and Plant Parameters

Excluding uncertainty as determined using an NRC-approved instrument setpoint methodology, variability in initial conditions and plant parameters not specifically addressed in Chapter 6 of the LTR, as supplemented by the RAI responses, shall not be analyzed using the statistical

analysis, but rather shall be treated deterministically as set forth in revised Chapter 6 of the LTR. If the deterministic approach is applied, significant plant parameters must be assumed to be in their most pessimistic condition with regard to the results; Technical Specification Analytic Limits for which the ECCS evaluation is an Applicable Safety Analysis shall be used; and parameters shown to have an insignificant effect on the results may be assumed to be in a nominal condition. Refer to SE Section 5.5 for additional detail.

10.2.5. Limitation 2.5: General Design Criterion 35 Compliance

The approach for plant-specific compliance with GDC 35 is provided in response to RAIs 12 and 76. Each plant implementing TRACG-LOCA shall evaluate whether the loss-of-offsite-power (LOOP) or offsite power available (OPA) condition is more limiting for each break scenario to establish that the GDC 35 requirement is met. An explicit analysis of both conditions for every scenario is not required if sufficient evidence exists to conclude whether OPA or LOOP is limiting otherwise. Refer to SE Section 5.6 for additional detail.

10.2.6. Limitation 2.6: Calorimetric Power Uncertainty

The vendor shall apply a 2-percent increase to thermal power to account for calorimetric power uncertainty. An alternative value may be used if appropriately justified. However, if an implementing licensee uses an ultrasonic flow meter for which the NRC has withdrawn its approval of the supporting licensing topical report, such licensee must revert to the generic, 2-percent value. Refer to NRC Regulatory Issue Summary 2007-24, "NRC Staff Position on use of the Westinghouse Crossflow Ultrasonic Flow Meter for Power Uprate or Power Recovery," for additional details. Refer to SE Section 5.2 for additional discussion.

10.2.7. Limitation 2.7: Use of the Shumway Correlation

The basis set forth for acceptance of the Shumway Correlation, as described in Section 6.4.3 of this SE, is specific to ECCS evaluations, including consideration of the conservatism associated with application of the correlation, its significance in ECCS evaluation, and the thermal-hydraulic conditions associated with a BWR LOCA. Therefore, the Shumway Correlation shall not be construed as accepted by the NRC staff for any other application unless specifically determined in separate correspondence.

10.3. UPSTREAM AND CONCURRENT METHODS

Upstream methods include any evaluation model or computational device that provides input to the TRACG-LOCA evaluation model. Concurrent methods are codes, relations, or subroutines that are implemented within TRACG, but the approval basis is documented elsewhere, such as TGBLA06/PANAC11, or the GEXL correlation. Concurrent methods are technically considered part of the emergency core cooling system evaluation model, but their approval basis is documented in separate LTRs.

10.3.1. Limitation 3.1: Reporting Requirements to Upstream/Concurrent Methods

Errors in, and changes to, concurrent or upstream methods, and in their applications, are subject to the reporting requirements of 10 CFR § 50.46(a)(3), to the extent that they impact TRACG-LOCA evaluations. If errors in, or changes to, concurrent or upstream methods, or in their applications, are identified, they must be dispositioned in accordance with § 50.46(a)(3)

and other applicable regulatory requirements. However, optional changes to concurrent or upstream methods, need only be dispositioned when adopted within a plant-specific application.

10.3.2. Limitation 3.2: Limitations on the Use of Upstream/Concurrent Methods

All upstream and concurrent methods must be used in TRACG-LOCA within their existing approval bases. Such methods must be applied in adherence to all conditions and limitations applied thereto. Refer, for example, to Section 6.1.1, for additional discussion.

10.4. STATISTICAL ANALYSIS

The following limitations apply to the statistical combination of uncertainty. Each of these limitations follows the discussion provided in Section 7.3 of this SE.

10.4.1. Limitation 4.1: Limiting Break Sizes

GEH shall perform a statistical analysis for the limiting hypothetical LOCA in each plant application. Each analysis shall rely on a random sample of 124 cases to provide tri-variate, 95/95 tolerance limits for the three critical safety parameters, without any rejected cases. Alternatively, 181 cases may be analyzed for the purpose of rejecting two analytic cases. Limiting results for each of peak cladding temperature, equivalent cladding reacted, and core-wide oxidation shall be obtained by identifying the most limiting result for each figure of merit from the sample, once the rejected cases have been eliminated. If the deterministic break spectrum identifies more than one potentially limiting LOCA scenario, then each potentially limiting scenario shall be statistically analyzed as a sensitivity.

10.4.2. Limitation 4.2: Sample Size

The methodology is approved under the consideration that GEH will perform one sample, consisting of either 124 or 181 cases. The sample size must be determined in advance of the statistical analysis, and no changes to the sample size are permitted.

10.4.3. Limitation 4.3: Rejection of Results

If a sample of 124 cases is selected, no statistical trials may be rejected from the sample. If a sample of 181 cases is selected, two statistical trials may be rejected from the sample.

10.4.4. Limitation 4.4: Successive Elimination

If using the sampling scheme with 181 cases and two rejections, GEH must determine the elimination strategy at the time the sample size is chosen. For example, the vendor must choose whether to eliminate the two cases with the highest ECR, or the two cases with the highest PCT, or one of each, prior to initiating the statistical analysis.

10.4.5. Limitation 4.5: Dispositioning Unacceptable Results

Once the limiting plant configuration is determined and the licensing statistical analysis is applied, GEH must document, in auditable format, the characteristics of any licensing statistical analyses that produced unacceptable results, and what changes were subsequently made to produce acceptable results. If a TRACG-LOCA analysis is used to support a RLA submitted to the NRC, such information shall be included in the request.

This limitation applies to the licensing statistical analysis only, and should not be construed to require such documentation of normal engineering and design analysis that would not otherwise be included in the documentation associated with a particular TRACG-LOCA analysis.

10.4.6. Limitation 4.6: Resampling

Unless a plant makes a major design change, such as the implementation of a power uprate or introduction of a new fuel type that would be expected to change predicted ECCS performance significantly, resampling is not permitted in concert with re-analysis.

10.5. INTERIM LIMITATION ON CATHCART-PAWEL RESULTS

The use of the Cathcart-Pawel oxidation correlation requires consideration of the fact that the 17 percent limit was based on the use of the Baker-Just equation. Local cladding oxidation results obtained using the Cathcart-Pawel equation will be considered acceptable, provided they are below 13 percent. If Cathcart-Pawel ECR remains below 13 percent and the PCT is below 2200 °F, there is reasonable assurance that the ECR would also remain below 17 percent, if calculated using Baker-Just. This limitation is an interim measure pending Commission adoption of a revision to the 10 CFR 50.46(b) acceptance criteria; should the staff position on this matter change, the NRC will notify GEH via a letter providing the revised position. This is discussed in Section 6.1.4 of this SE.

10.6. APPLICABILITY OF TRACG-LOCA TO EXPANDED OPERATING DOMAINS

In license amendment requests to implement expanded operating domains, for which the ECCS-LOCA analysis is based on TRACG-LOCA, the requesting licensee shall include documentation of the supporting ECCS-LOCA analysis in the license amendment request. Such inclusion will address the relevant conditions and limitations applicable to both NEDC-33173P-A, "Applicability of GE Methods to Expanded Operating Domains" (also known as the Interim Methods Licensing Topical Report, IMLTR), and NEDC-33006P-A, "Maximum Extended Load Line Limit Analysis Plus."

Additional discussion addressing the prior limitations and conditions, specifically, is included in Chapter 9, "Licensing Considerations," of this SE.

10.7. BWR/3-6 FIRST-OF-A-KIND APPLICATION

The NRC staff review effort included a detailed review of TRACG-LOCA as applied to a BWR/2, and as such, the application of TRACG-LOCA to Nine Mile Point Nuclear Station, Unit 1, is acceptable without further limitation. However, the NRC staff notes that the demonstration analyses and nodalization sensitivity studies supporting application of TRACG-LOCA to BWR/3-6 plants, were not updated to reflect the increased core detail and revised statistical approach that were revised as a result of the NRC staff review. As such, the NRC staff requires that GEH perform updated demonstration analyses for each of a BWR/4 and BWR/6, and an update to the BWR/4 nodalization sensitivity studies, and provide them for NRC staff review and acceptance, prior to first-of-a-kind application of TRACG-LOCA to a BWR/3-6. Specifically, the jet pump plant nodalization studies should be updated/reviewed/accepted prior to application to a jet pump plant. The BWR/4 demonstration studies should be updated/reviewed/accepted prior to application to a BWR/3-4, and similarly, the BWR/6 demonstration studies should be updated/reviewed/accepted prior to application to a BWR/5-6. This limitation can be satisfied by

revising the jet pump plant nodalization studies documented in LTR Section 5.2, Table 5.2-1 and Figures 5.2-1 through 5.3-9 and the key summary demonstration analyses documented in LTR Chapter 8, Figure 8.1-29 for the BWR/4 and Figure 8.2-18 for the BWR/6.

11.0 CONCLUSION

Based on the review described in the preceding sections, and subject to the limitations delineated in Chapter 10 of this SE, the NRC staff determined that NEDE-33005P is acceptable for referencing in licensing actions. For the purpose of compliance with 10 CFR 50.46 requirements, TRACG-LOCA, as documented in Reference 1 and revised by the RAI responses, may be considered an acceptable evaluation model. With regard to referencing in licensing actions, Reference 1 as revised by the RAI responses may be considered approved for use.

12.0 REFERENCES

1. General Electric (GE)-Hitachi Nuclear Energy Americas (GEH), "TRACG Application for Emergency Core Cooling Systems/Loss-of-Coolant-Accident Analyses for BWR/2-6," Reports NEDE-33005P (Proprietary) and NEDO-33005 (Publicly Available), and Cover Letter MFN 11-001, Project No. 710, January 27, 2011, Agencywide Document Access and Management System (ADAMS) Package No. ML110280321.
2. Harrison, James F., GEH, letter to U.S. NRC, "Supporting Information for the Review of GE-Hitachi Nuclear Energy Americas Topical Report NEDE-33005P, 'TRACG Application for Emergency Core Cooling Systems/Loss-of-Coolant Accident Analyses for BWR/2-6' (TAC No. ME5405)," MFN 12-026, Project No. 710, March 30, 2012, ADAMS Accession No. ML12096A115.
3. Harrison, James F., GEH, letter to U.S. NRC, "Response to Request for Additional Information Re: GE-Hitachi Nuclear Energy Americas Topical Report NEDE-33005P, Revision 0, 'TRACG Application for Emergency Core Cooling Systems/Loss-of-Coolant-Accident Analyses for BWR/2-6,' (TAC No. ME5405)," MFN 14-064, Project No. 710, October 7, 2014, ADAMS Package No. ML14281A014.
4. Harrison, James F., GEH, letter to U.S. NRC, "Response to Request for Additional Information Regarding Review of Licensing Topical Reports NEDE-33005P and NEDO-33005, 'Licensing Topical Report TRACG Application for Emergency Core Cooling Systems/Loss-of-Coolant-Accident Analyses for BWR/2-6,' (TAC No. ME5405)," MFN 16-008, Project No. 710, February 19, 2016, ADAMS Package No. ML16050A138.
5. Harrison, James F., GEH, letter to U.S. NRC, "Response to Request for Additional Information Regarding Review of Licensing Topical Reports NEDE-33005P and NEDO-33005, 'Licensing Topical Report TRACG Application for Emergency Core Cooling Systems/Loss-of-Coolant-Accident Analyses for BWR/2-6,' (TAC No. ME5405)," MFN 16-020, Project No. 710, June 13, 2016, ADAMS Package No. ML16165A348.
6. Harrison, James F., GEH, letter to U.S. NRC, "Response to Requests for Additional Information 101 and 102 Regarding Review of Licensing Topical Reports NEDE-33005P and NEDO-33005, 'Licensing Topical Report TRACG Application for Emergency Core Cooling Systems/Loss-of-Coolant-Accident Analyses for BWR/2-6,' (TAC No. ME5405)," MFN 16-039, Project No. 710, June 21, 2016, ADAMS Package No. ML16173A330.
7. Harrison, James F., GEH, letter to U.S. NRC, "Response to Requests for Additional Information 103 and 104, 65 (Revised) and 33 (Revised), Regarding Review of Licensing Topical Reports NEDE-33005P and NEDO-33005, 'TRACG Application for Emergency Core Cooling Systems/Loss-of-Coolant-Accident Analyses for BWR/2-6' (TAC No. ME5405)," MFN 16-072, Project No. 710, October 21, 2016, ADAMS Package No. ML16295A253.

8. U.S. NRC, "Best-Estimate Calculations of Emergency Core Cooling System Performance," Regulatory Guide 1.157, ADAMS Accession No. ML003739584.
9. U.S. NRC, "Transient and Accident Analysis Methods," Regulatory Guide 1.203, ADAMS Accession No. ML053500170.
10. U.S. NRC, "Standard Review Plan for the Review of Safety Analysis Reports for Nuclear Power Plants: Light Water Reactor Edition," NUREG-0800, Chapter 15.0.2, "Review of Transient and Accident Analysis Methods," Revision 0, March 2007, ADAMS Accession No. ML070820123.
11. U.S. NRC, "Quantifying Reactor Safety Margins: Application of Code Scaling, Applicability, and Uncertainty Evaluation Methodology to a Large-Break Loss-of-Coolant Accident," NUREG/CR-5249, December 1989, ADAMS Accession No. ML030380503.
12. U.S. NRC, "Compendium of ECCS Research for Realistic LOCA Analysis," NUREG-1230, Revision 4, December 1988, ADAMS Accession Nos. ML053490333 (Cover – Page 8-37) and ML053620415 (Appendix A – End).
13. Global Nuclear Fuel (GNF), "General Electric Standard Application for Reactor Fuel (GESTAR II), Main and United States Supplement," Reports NEDE-24011-P-A, Revision 22 (Proprietary) and NEDO-24011-A, Revision 22 (Non-Proprietary), and Cover Letter MFN 15-089, Project No. 712, November 20, 2015, ADAMS Package No. ML15324A145. Note: This document is frequently updated. Revision 22 was the latest approved revision available at the time of publication of this SE.
14. Straka, M., and Ward, L. W., "BWR PIRT and Assessment Matrices for BWR LOCA and Non-LOCA Events," SCIE-NRC-393-99, Scientech, Rockville, MD: 1999.
15. Ratnayake, Ruwan K., et al., "Identification and Ranking of Phenomena Leading to Peak Cladding Temperatures in Boiling Water Reactors During Large Break Loss of Coolant Accident Transients," Proceedings of ICONE10: 10th International Conference on Nuclear Engineering, Arlington, VA, April 14-18, 2002.
16. GEH, "TRACG Model Description," Reports NEDE-32176P, Revision 4 (Proprietary) and NEDO-32176, Revision 4 (Publicly Available), and Cover Letter MFN 08-072, Project No. 710, January 31, 2008, ADAMS Package No. ML080370259.
17. GEH, "TRACG Qualification," Reports NEDE-32177P, Revision 3 (Proprietary) and NEDO-32177, Revision 3 (Publicly Available), and Cover Letter MFN 07-452, Project No. 710, August 29, 2007, ADAMS Package No. ML072480007.
18. GE, "TRACG Application for Anticipated Operational Occurrences (AOO) Transient Analyses," Reports NEDE-32906P-A, Revision 1 (Proprietary) and NEDO-32906, Revision 1 (Publicly Available), and Cover Letter MFN 06-042, Project No. 710, February 6, 2006, ADAMS Package No. ML060390557.
19. GE, "TRACG Application for Anticipated Operational Occurrences Transient Analyses," Reports NEDE-32906P-A, Revision 3 (Proprietary) and NEDO-32906, Revision 3 (Publicly Available), and Cover Letter MFN 06-327, Project No. 710, September 25, 2006, ADAMS Package No. ML062720163.
20. GE, "TRACG Application for Anticipated Transient Without Scram Analyses," Reports NEDE-32906P, Supplement 1-A (Proprietary) and NEDO-32906, Supplement 1-A (Publicly Available), and Cover Letter MFN 03-148, Project No. 710, November 26, 2003, ADAMS Package No. ML033381073.
21. GE, "TRACG Application for Anticipated Operational Occurrences Transient Analyses," Reports NEDE-32906P, Supplement 2-A (Proprietary) and NEDO-32906, Supplement 2-A (Publicly Available), and Cover Letter MFN 06-079, Project No. 710, March 16, 2006, ADAMS Package No. ML060800312.
22. GEH, "Migration to TRACG04/PANAC11 from TRACG02/PANAC10 for TRACG AOO and ATWS Overpressure Transient," Reports NEDE-32906P, Supplement 3-A, Revision 1

- (Proprietary) and NEDO-32906, Supplement 3-A, Revision 1 (Publicly Available), and Cover Letter MFN 10-140, April 16, 2010, ADAMS Package No. ML110970401.
23. U.S. NRC, "Clarification of 10 CFR 50.46 Reporting Requirements and Recent Issues with Related Guidance Not Approved For Use," Regulatory Issue Summary 2016-04, April 19, 2016, ADAMS Accession No. ML15324A296.
 24. U.S. NRC, "NRC Staff Position on use of the Westinghouse Crossflow Ultrasonic Flow Meter for Power Uprate or Power Recovery," Regulatory Issue Summary 2007-24, September 27, 2007, ADAMS Accession No. ML063450261.
 25. GNF, "The PRIME Model for Analysis of Fuel Rod Thermal – Mechanical Performance," Part 1, "Technical Bases," NEDC-33256P-A (Proprietary) and NEDO-33256-A (Publicly Available); Part 2, "Qualification," NEDC-33257P-A (Proprietary) and NEDO-33257-A (Publicly Available); Part 3, "Application Methodology," NEDC-33258P-A (Proprietary) and NEDO-33258-A (Publicly Available); and Cover Letter MFN 10-046, Project No. 712, September 15, 2010, ADAMS Package No. ML102600259.
 26. U.S. NRC, "Nuclear Fuel Thermal Conductivity Degradation," Information Notice (IN) 2009-23, October 8, 2009, ADAMS Accession No. ML091550527.
 27. U.S. NRC, "Realistic Emergency Core Cooling System Evaluation Model Effects Resulting From Nuclear Fuel Thermal Conductivity Degradation," IN 2011-21, December 13, 2011, ADAMS Accession No. ML113430785.
 28. GE, "SAFER Model for Evaluation of Loss-of-Coolant Accidents for Jet Pump and Non-Jet Pump Plants," NEDE-30996P-A, Volume I, "SAFER – Long Term Inventory Model for BWR Loss-of-Coolant Analysis," October 1987, ADAMS Package No. ML091210245 (Proprietary report; no publicly available copy located).
 29. GE, "SAFER Model for Evaluation of Loss-of-Coolant Accidents for Jet Pump and Non-Jet Pump Plants," NEDE-20996P-A, Volume II, "SAFER Application Methodology," October 1987, ADAMS Accession No. ML102350281 (Proprietary report; no publicly available copy located).
 30. U.S. NRC, "Estimates of Decay Heat Using ANS 5.1 Decay Heat Standard May Vary Significantly," IN 1996-39, July 5, 1996, ADAMS Accession No. ML031060021.
 31. U.S. Atomic Energy Commission, "Acceptance Criteria for Emergency Core Cooling Systems for Light-Water-Cooled Nuclear Power Reactors," CLI-73-39, Opinions and Decisions of the Atomic Energy Commission with Selected Orders, Docket RM-50-1, December 28, 1973.
 32. Travers, W.P., U.S. NRC, memorandum to Chairman Meserve et al., "Research Information Letter 0202 Issued on June 20, 2002, to Support Changes in § 50.46 and Appendix K Update," July 23, 2002, ADAMS Accession No. ML021120159.
 33. GE, "TRACG Qualification for SBWR," Report NEDC-32575P (Proprietary report; no publicly available copy located) and Cover Letter MFN 02-053, Project No. 717, August 30, 2002, ADAMS Package No. ML022560081.
 34. U.S. NRC, "BWR Refill-Reflood Program Task 4.7 – Model Development Basic Models for the BWR Version of TRAC," NUREG/CR-2573 (also Electric Power Research Institute Report No. EPRI NP-2375 and GE Report No. GEAP-22051), September 1983.
 35. Sun, K. H., Gonzalez, J. M., and Tien, C. L., "Calculations of Combined Radiation and Convection Heat Transfer in Rod Bundles Under Emergency Core Cooling Conditions," 75-HT-64, American Society of Mechanical Engineers, New York, NY, August 1975.
 36. GE, "Calculation of Counter-Current Flow Limiting Conditions in BWR Geometry," NEDE-13430, Project No. 710, September 1975, ADAMS Accession No. ML14281A513 (Proprietary report; no publicly available copy located).
 37. Diller, P. R., Abdollahian, D., and Andersen, J. G. M., "GNF2 Counter-Current Flow Limitation Testing," *Proceedings of the International Congress on Advances in Nuclear Power Plants, 8–12 June, 2008*, American Nuclear Society, La Grange Park, IL, 2008.

38. U.S. NRC, "BWR Refill-Reflood Program Task 4.2 – Core Spray Distribution Final Report," NUREG/CR-1707, March 1981.
39. Carbajo, Juan J., "A Study on the Rewetting Temperature," Nuclear Engineering and Design 84 (1985) 21-52.
40. Shumway, R.W., Idaho National Engineering Laboratory, "TRAC-BWR Heat Transfer: Assessment of TMIN," EGG-RST-6781, Idaho Falls, Idaho, January 1985.
41. Harrison, J. F., GEH, letter to U.S. NRC, "Use of the Shumway Tmin Correlation with Zircaloy for TRACG Analyses," MFN 13-073, Project No. 710, September 9, 2013, ADAMS Package No. ML13253A105.
42. Henry, R. E., "A Correlation for the Minimum Film Boiling Temperature," *Heat Transfer Research and Design*, AIChE [American Institute of Chemical Engineering] Symposium, Seris 70, No. 138, 1974, 81-90.
43. Peterson, L. J., and Bajorek, S. M., "Experimental Investigation of Minimum Film Boiling Temperature for Vertical Cylinders at Elevated Pressure," *Proceedings of the 10th International Conference on Nuclear Engineering, 14–18 April, 2002*, American Society of Mechanical Engineers, New York, NY, 2002.
44. Harrison, J. F., GEH, letter to U.S. NRC, "Updated TRACG Quench Front Model Description and Qualification," MFN 13-085, Project No. 710, October 15, 2013, ADAMS Package No. ML13289A211.
45. Holmstrom, H., et al., "Status of Code Uncertainty Evaluation Methodologies," *Proceedings of the International Conference on New Trends in Nuclear System Thermohydraulics*, Dipartimento di Costruzioni Meccaniche Nucleari, Pisa, Italy, 1994, ADAMS Accession No. ML003769914.
46. Framatome ANP, "Realistic Large Break LOCA Methodology for Pressurized Water Reactors," EMF-2103(P/NP)(A), Revision 0, Project No. 728, September 15, 2003, ADAMS Package No. ML032691410.
47. U.S. NRC, "Final Safety Evaluation of Topical Report EMF-2103, Revision 3, 'Realistic Large Break LOCA Methodology for Pressurized Water Reactors,'" Project No. 728, June 29, 2016, ADAMS Package No. ML16172A329.
48. Westinghouse Electric Company, "Realistic Large Break LOCA Evaluation Methodology Using Automated Statistical Treatment of Uncertainty Method," WCAP-16009-P/NP-A, and Cover Letter LTR-NRC-05-13, Project No. 700, March 11, 2005, ADAMS Package No. ML050910156.
49. Guba, A., Makai, M., and Pal, L., "Statistical Aspects of Best Estimate Method – I," *Reliability Engineering and System Safety*, 80 (2003) 217-232.
50. U.S. NRC, "Applying Statistics," NUREG-1475, Revision 1, March 2011, ADAMS Accession No. ML11102A076.
51. Tukey, J. W., "Nonparametric Estimation II: Statistically Equivalent Blocks and Tolerance Regions – The Continuous Case," *Annals of Mathematical Statistics*, Volume 18 (1947) 529-539.
52. Fraser, D. A. S., "Sequentially Determined Statistically Equivalent Blocks," *Annals of Mathematical Statistics*, Volume 22 (1951) 372-381.
53. Nutt, W. T., and Wallis, G. B., "Evaluation of Nuclear Safety from the Outputs of Computer Codes in the Presence of Uncertainties," *Reliability Engineering and System Safety*, 83 (2004) 57-77.
54. GE, "Generic Guidelines for General Electric Boiling Water Reactor Extended Power Uprate," Reports NEDC-32424P-A (Proprietary) and NEDO-32424-A (Publicly Available), Project No. 710, January 2000. Official record copies not located in ADAMS.
55. GE, "Generic Evaluations of General Electric Boiling Water Reactor Extended Power Update," Reports NEDC-32523P-A (Proprietary) and NEDO-32523-A (Publicly Available),

Project No. 710, February 2000, ADAMS Package No. ML003712834 (Proprietary report only; publicly available version of report not located).

56. GE, "Constant Pressure Power Uprate," Reports NEDC-33004P-A (Proprietary) and NEDO-33004-A (Publicly Available), and Cover Letter MFN 03-058, Project N. 710, July 2003, ADAMS Package No. ML032170315.
57. GEH, "Applicability of GE Methods to Expanded Operating Domains," Reports NEDC-33173P-A, Revision 4 (Proprietary) and NEDO-33173-A, Revision 4 (Publicly Available), and Cover Letter MFN 12-124, Project No. 710, November 2012, ADAMS Package No. ML123130130.
58. GEH, "Maximum Extended Load Line Limit Analysis Plus," Reports NEDC-33006P-A, Revision 3 (Proprietary) and NEDO-33006-A, Revision 3 (Publicly Available), and Cover Letter MFN 09-362, Project No. 710, June 2009, ADAMS Package No. ML091800530.

Attachment: Resolution of Comments

Principal Contributor: Ben Parks, SNPB/DSS

Date: February 22, 2017

**Comment Summary for Draft Safety Evaluation for
 NEDE-33005P Revision 0, “TRACG Application for Emergency Core Cooling Systems/
 Loss-of-Coolant-Accident Analyses for BWR/2-6”**

Location	GE Comment	NRC Disposition
Executive Summary	<p>GEH suggests the following change (Line 46):</p> <p>NEDE-33005P</p> <p><i>Suggested change shown in the markup.</i></p>	The NRC finds the change acceptable. Change incorporated in final SE.
List of Acronyms	<p>Four acronyms are in the SER but are not in the List of Acronyms.</p> <p>GEH suggests the following changes:</p> <ol style="list-style-type: none"> 1. Add the following acronyms: B-J (Baker Just), C-P (Cathcart-Pawel), IET (Integral Effect Test, and TR (Topical Report) 2. CSAU: Delete ‘Analysis’ 3. GEH: Change “General Electric-Hitachi” to “GE Hitachi” 4. GNF: Change “Fuels” to “Fuel” 5. SRP: Change “Plant” to “Plan” <p><i>Suggested changes shown in the markup.</i></p>	The changes are editorial; however, the acronym “GE” embedded within “GEH” does not appear in the list of acronyms. Change accepted and incorporated in final SE; in addition, add to the list of acronyms, “GE General Electric”
Section 3.3.1 PIRT Process – NRC Staff Evaluation	<p>Page 10:</p> <p>GEH recommends expanding the text. GEH suggests the following change to Footnote E:</p> <p>[[</p> <p style="text-align: center;">]]</p> <p><i>Suggested changes shown in the markup.</i></p>	The change provides a more detailed description of the contributors to the effect described in the footnote, but does not change its meaning. NRC finds the change acceptable. Change incorporated in final SE.

Location	GE Comment	NRC Disposition
Section 4.1.2 Provision of Complete Code Documentation	Page 12: The text incorrectly implies that Table 3 lists all recently approved TRACG applications. Those listed are only TRACG AOO applications. GEH suggests the following change (Lines 8-9): Table 3 summarizes the <u>TRACG AOO applications for US</u> more recent, application-specific approvals received for TRACG for currently licensed and operating BWRs. <i>Suggested changes shown in the markup.</i>	The NRC staff intent in the discussion is consistent with the vendor-proposed revision. The NRC finds the change acceptable. Change incorporated in final SE.
Section 4.2 Summary of Previous Review Findings	Page 13: To be consistent with the changes suggested in Section 4.1.2. GEH suggests the following change (Line 1): 4.2. SUMMARY OF PREVIOUS REVIEW FINDINGS <u>RELATED TO TRACG FOR AOO APPLICATIONS</u> <i>Suggested changes shown in the markup.</i>	The NRC staff intent in the discussion is consistent with the vendor-proposed revision. The NRC finds the change acceptable. Change incorporated in final SE.
Section 4.2 Summary of Previous Review Findings	Page 13: To be consistent with the changes suggested in Section 4.1.2. GEH suggests the following change (Line 2): Table 3. Summary of Previous Review Findings Related to TRACG <u>for AOO Applications</u> . <i>Suggested changes shown in the markup.</i>	The NRC staff intent in the discussion is consistent with the vendor proposed revision. The NRC finds the change acceptable. Change incorporated in final SE.

Location	GE Comment	NRC Disposition
<p>Section 4.3.1 Nodalization</p> <p>Section 6.2.2 Noding near the Break and ECCS Injection Point</p> <p>Section 10.0 Limitations</p>	<p>GEH suggests that the use of the terminology 'later vintage' be revised to reflect the 'first-of-a-kind' terminology, consistent with the GEH suggested change to the title of Section 10.7.</p> <p><i>The following suggested changes are shown in the markup:</i></p> <ol style="list-style-type: none"> 1. Section 4.3.1: Nodalization: <ul style="list-style-type: none"> • Page 15 (Line 44): TRACG-LOCA for in later vintage <u>BWR/3-6s</u>. • Page 16 (Lines 20-21): Limitation 7, "Later Vintage <u>BWR/3-6 First-of-a-Kind Application</u>," as 2. Section 6.2.2: Noding near the Break and ECCS Injection Point <ul style="list-style-type: none"> • Page 41 (Line 24): Limitation 7, "Later Vintage <u>BWR/3-6 First-of-a-Kind Application</u>," as 3. Section 10.0: Limitations <ul style="list-style-type: none"> • Page 74 (Line 7): Table 12: Later Vintage <u>BWR/3-6 First-of-a-Kind Application</u> 	<p>The change is editorial. The NRC finds the change acceptable. Change incorporated in final SE.</p>
<p>Section 5.2 Operating Statepoints</p>	<p>Page 21: The figure should be cited from the MELLLA+ LTR and referred to as typical since some plant-specific maps are different.</p> <p>GEH suggests the following change (Line 5): <u>A typical</u> The MELLLA+ operating domain is illustrated <u>in Figure 1-1 of Reference 58</u> Figure 2.</p> <p><i>Suggested change shown in the markup.</i></p>	<p>The figure in question is a reproduction of Figure 6.2-1 of NEDE-33005P. Since the figure was obtained from the LTR that is the subject of the SE, the NRC staff retained the figure as-is.</p> <p>The proposed change is modified as follows: A typical The MELLLA+ operating domain is illustrated in Figure 2, which is a reproduction of Figure 6.2-1 of NEDE-33005P.</p>

Location	GE Comment	NRC Disposition
Section 5.2 Operating Statepoints	<p>Page 21: The figure should be cited from the MELLLA+ LTR and referred to as typical since some plant-specific maps are different. If the figure is retained, then a better figure is needed since the figure in the SE has Points D and E misaligned.</p> <p>GEH suggests the following change (Line 7): Replace Figure 2 with Figure 1-1 from Reference 58.</p>	<p>The figure in question is a reproduction of Figure 6.2-1 of NEDE-33005P. Since the figure was obtained from the LTR that is the subject of the SE, the NRC staff retained the figure as-is. Change not accepted.</p>
Section 5.2 Operating Statepoints	<p>Page 21: If Figure 1-1 from Reference 58 replaces the existing Figure 2, then the points analyzed for MELLLA+ plants needs to be revised.</p> <p>GEH suggests the following change (Line 11): points <u>A</u>, <u>B</u>, <u>D</u>, and <u>E</u> in Figure 2. <i>Suggested change shown in the markup.</i></p> <p>Note that if the existing Figure 2 is not replaced, then the points should be A, C, and E.</p>	<p>The figure contained in NEDE-33005P was retained in the SE (i.e., existing Figure 2 was not replaced); therefore, the GEH suggestion to identify Points A, C, and E was considered by the staff. As noted on Page 71 of the SE, the applicable requirement for MELLLA+ is to analyze, “the rated EPU [extended power uprate] power/rated CF [core flow], rated EPU power/minimum CF, and the low-flow MELLLA+ boundary (Transition Statepoint). These correspond to Points A, C, and E, on the figure. Therefore, the NRC staff agrees with this suggested change because it is consistent with the MELLLA+ analytic requirements. The proposed change is modified as follows: points A, C, and E in Figure 2.</p>
Section 5.3 Power Distribution and Channel Groupings	<p>Page 23: GEH suggests the following change (Line 29) the limiting <u>heated</u> nodes are <i>Suggested changes shown in the markup.</i></p>	<p>The NRC staff agrees with the clarification. The NRC finds the change acceptable. Change incorporated in final SE.</p>
Section 5.3 Power Distribution and Channel Groupings	<p>Page 23: Standard and hot channel are the same. Clarify the footnote.</p> <p>GEH suggests the following change to Footnote H: Note that the standard <u>channel nodalization</u>, hot channel includes [[]] axial nodes, <u>of which 25 are heated</u>. <i>Suggested changes shown in the markup.</i></p>	<p>The NRC staff intent in the discussion is consistent with the vendor-proposed revision. The NRC finds the change acceptable. Change incorporated in final SE.</p>

Location	GE Comment	NRC Disposition
Section 5.4 Break Spectrum Analysis	Page 25: Typographical error. GEH suggests the following change (Line 9): receommends <i>Suggested change shown in the markup.</i>	The change is editorial. The NRC finds the change acceptable. Change incorporated in final SE.
Section 5.5.1 Initial Conditions	Page 26: Limitation 2.5 should be Limitation 2.4. GEH suggests the following change (Line 27): Limitation 2. 5 <u>4</u> <i>Suggested change shown in the markup.</i>	The change is editorial. The NRC finds the change acceptable. Change incorporated in final SE.
Section 5.5.2 Plant Parameters	Page 26: Limitation 2.5 should be Limitation 2.4. GEH suggests the following change (Line 46): Limitation 2. 5 <u>4</u> <i>Suggested change shown in the markup.</i>	The change is editorial. The NRC finds the change acceptable. Change incorporated in final SE.
Section 6.1 Sources of Heat During a Loss-of- Coolant Accident	Page 29: GEH suggests the following change (Line 8): Cathcart-Pawel (<u>C-P</u>). <i>Suggested change shown in the markup.</i>	The NRC finds the change acceptable. Change incorporated in final SE..
Section 6.1.1 Initial Stored Energy of the Fuel	Page 30: The current statement is inaccurate. GEH suggests the following changes (Lines 9-10): These <u>PRIME</u> inputs include <u>are used by TRACG to calculate</u> the steady-state temperature distribution and stored energy in the fuel. The <u>PRIME</u> inputs also include the composition and pressure of the fuel rod gases, which are used to calculate the gap gas conductivity. <i>Suggested changes shown in the markup.</i>	The NRC staff intent in the discussion is consistent with the vendor-proposed revision. The NRC finds the change acceptable. Change incorporated in final SE.

Location	GE Comment	NRC Disposition
Section 6.1.1 Initial Stored Energy of the Fuel	Page 30: GEH suggests the following changes (Line 25): H Limitation 3.2, "Limitations on <u>the Use of Upstream/Concurrent Methods,</u> " <i>Suggested changes shown in the markup.</i>	The change is editorial. The NRC finds the change acceptable. Change incorporated in final SE.
Section 6.1.3 Decay of Actinides and Fission Product Decay Heat	Page 32: The current statement is inaccurate. GEH suggests the following changes (Line 44): TRACG implements decay heat curves <u>models</u> based on both the 1979 and 1994 ANS standards, via <u>like</u> an auxiliary code, DECAF. <i>Suggested changes shown in the markup.</i>	The NRC staff understands that specific curves are generated as output of the TRACG decay heat models, and the review was accomplished using some such curves as representations of decay heat modeling approaches. Furthermore, the response to RAI 101 makes the distinction that the TRACG decay heat models are based on DECAF. The NRC staff intent in the discussion is consistent with the vendor proposed revision, and with the RAI response as submitted. The NRC finds the change acceptable. Change incorporated in final SE.
Section 6.1.3 Decay of Actinides and Fission Product Decay Heat	Page 33: Clarify the sentence. GEH suggests the following change (Line 4): higher than a comparable model <u>the DECAF code</u> that calculates <i>Suggested change shown in the markup.</i>	The change is editorial in that it adds specificity; however, the NRC staff identified an additional change to the sentence structure that would be needed to accept the proposed change. The proposed change is modified and incorporated as follows: Higher than a comparable model the DECAF code that , which calculates
Section 6.1.3 Decay of Actinides and Fission Product Decay Heat	Page 33: The current sentence is inaccurate. GEH suggests the following change (Line 39): The same uncertainty <u>multiplicative factor</u> is applied to each channel in the core, <i>Suggested change shown in the markup.</i>	The NRC staff intent in the discussion is consistent with the vendor proposed revision. The NRC finds the change acceptable. Change incorporated in final SE.
Section 6.1.4 Metal-Water Reaction Rate	Page 34: GEH suggests the following change (Line 37): Baker-Just (B-I) <i>Suggested change shown in the markup.</i>	The change is editorial. The NRC finds the change acceptable. Change incorporated in final SE.

Location	GE Comment	NRC Disposition
Section 6.1.4 Metal-Water Reaction Rate	Page 36: The SE language is confusing when compared to Limitation 5. The interim limitation is the 13% acceptance criterion for Cathcart-Pawel. GEH suggests the following changes (Lines 14-15): In view of the fact that the use of a 17-percent <u>interim 13-percent</u> acceptance criterion solely using the B-J reaction 48 kinetics equation is an interim limitation when using the C-P reaction model, should the NRC <i>Suggested changes shown in the markup.</i>	The NRC staff intent in the discussion is consistent with the vendor proposed revision. The NRC finds the change acceptable. Change incorporated in final SE.
Section 6.1.5 Thermal Parameters for Swelling and Rupture of the Cladding and Fuel Rods	Page 36: The sentence incorrectly implies that most or all heat transfer effects outside the cladding are neglected, whereas the opposite is true. GEH suggests the following change (Lines 44-45): Some h <u>Heat</u> transfer effects outside the cladding, such as droplet shattering upon impingement on ruptured fuel rod segments, are neglected. <i>Suggested change shown in the markup.</i>	The NRC staff intent in the discussion is consistent with the vendor-proposed revision. The NRC finds the change acceptable. Change incorporated in final SE.
Section 6.1.5 Thermal Parameters for Swelling and Rupture of the Cladding and Fuel Rods	Page 37: The sentence is incorrect. TRACG calculates the internal rod pressure to account for local power. GEH suggests the following changes (Line 2): The <u>reference initial</u> rod internal pressure is passed <i>Suggested changes shown in the markup.</i>	As written, the sentence may have implied that coupled calculations are performed using both PRIME and TRACG, when in fact PRIME supplies initial conditions for the TRACG calculation. The NRC staff intent in the discussion is consistent with the vendor-proposed revision. The NRC finds the change acceptable. Change incorporated in final SE.
Section 6.1.5 Thermal Parameters for Swelling and Rupture of the Cladding and Fuel Rods	Page 37: GEH suggests the following change (Line 20): <i>Suggested change shown in the markup</i>	The staff evaluation determined that data reflected ramp rates expected for BWR LOCA events. Such a model would only be viewed as conservative if the events typically exhibited higher ramp rates, contrary to the following sentence in the SE. Change not accepted.

Location	GE Comment	NRC Disposition
Section 6.2.1 Break Characteristics and Flow	Page 40: GEH suggests the following change (Line 44): Limitation 2.42.3 <i>Suggested change shown in the markup</i>	The change is editorial. The NRC finds the change acceptable. Change incorporated in final SE.
Section 6.2.3 Critical Heat Flux	Page 42: Limitation 1.2 is different than Limitation 1.3. Revise the text to be consistent with Limitation 1.3. GEH suggests the following change (Lines 27-30): The bounding uncertainty approach is acceptable for average channels in the core, but as per Limitation 1.2, TRACG-LOCA is restricted to analysis of GNF fuel designs, meaning that the analyzed hot channels must be designed by GNF <u>hot channel modeling of competitor fuel is restricted by Limitation 1.3.</u> <i>Suggested change shown in the markup</i>	The NRC staff intent in the discussion is consistent with the vendor proposed revision. The NRC finds the change acceptable. Change incorporated in final SE.
Section 6.3 Post-CHF Phenomena	Page 42: GEH suggests the following change (Line 36): Particular import <u>importance</u> <i>Suggested change shown in the markup</i>	The change is editorial. The NRC finds the change acceptable. Change incorporated in final SE.
Section 6.3.3 Heat Transfer	Page 46: Reference 35 is not explicitly cited in the SER. GEH suggests the following change (Line 33): correlation (<u>Reference 35</u>) is used <i>Suggested change shown in the markup.</i>	The NRC staff intent in the discussion is consistent with the vendor proposed revision. Furthermore, the citation of Reference 34 in the following paragraph is erroneous. The NRC finds the change acceptable. Change incorporated in final SE. Also, the citation to Reference 34 in the following paragraph is corrected to Reference 35.

Location	GE Comment	NRC Disposition
Section 6.4.3 Rewet and Quench Behavior	Page 51: The word “correction” is misleading because it implies modifying, after the fact, what the author understood (as did others in his day) the importance of material properties. The term was designed into the correlation from the beginning. GEH suggests the following change (Lines 30 and 32): correction <u>dimensionless</u> term <i>Suggested change shown in the markup</i>	The NRC staff was unable to confirm whether the author would agree with such inference, and therefore makes no conclusion regarding whether “correction” or “dimensionless” is more appropriate; however, adoption of the proposed revision does not alter the meaning of the text. The NRC finds the change acceptable. Change incorporated in final SE.
Section 7.3.2 Summary of GEH Approach	Page 58: It is unclear what GEH assertion in RAI 103 was not accepted by the NRC since SE Section 7.3.3 contains the NRC staff evaluation accepting the GEH approaches identified in RAI 103. GEH suggests the following change (Lines 35-38): GEH asserted, in its response to RAI 103, that the order of selective elimination is unimportant, because the resulting, estimated tolerance region will still remain bounding of the true 95/95 joint tolerance region that would exist in reality. As discussed in the following section, the NRC staff did not accept this portion of the proposed approach. <i>Suggested change shown in the markup.</i>	The staff concern discussed in this paragraph is addressed by Limitation 4.4. Based on this consideration, and on the vendor feedback, the NRC staff determined that this paragraph is moot, and hence agrees that it can be deleted. The NRC finds the change acceptable. Change incorporated in final SE.
Section 7.3.3 NRC Staff Evaluation of GEH Approach	Page 59: GEH suggests the following change (Line 11): References 49 and <u>through</u> 53 <i>Suggested change shown in the markup.</i>	The change is editorial. The NRC finds the change acceptable. Change incorporated in final SE.
Section 7.3.3 NRC Staff Evaluation of GEH Approach	Page 60: GEH suggests the following change (Line 21): Guba, Makai, and Pal (<u>Reference 49</u>). <i>Suggested change shown in the markup.</i>	The change is editorial. The NRC finds the change acceptable. Change incorporated in final SE.

Location	GE Comment	NRC Disposition
Section 7.4 PCT Analysis Resolution and Core Detail	Page 62: GEH suggests the following change (Line 26): (MFN 14-064 (Reference 3), Page 27). <i>Suggested change shown in the markup.</i>	The change is editorial. The NRC finds the change acceptable. Change incorporated in final SE.
Section 8.2 Review of Studies for BWR/2 Plant	Page 65: GEH suggests the following change (Line 31): generated <u>indicated</u> <i>Suggested change shown in the markup.</i>	The change is editorial. The NRC finds the change acceptable. Change incorporated in final SE.
Section 8.2 Review of Studies for BWR/2 Plant	Page 66: Statement pertaining to GEH commitment is misleading. There is no need to validate the isolation condenser heat transfer if the isolation condenser is not being credited or even modeled. GEH suggests the following change (Lines 11-12): GEH further committed to validate the isolation condenser heat transfer uncertainty treatment on a plant specific basis. <i>Suggested change shown in the markup.</i>	The NRC staff disagrees with this remark. Particularly, the final sentence of the vendor response to RAI 62 states, "If the isolation condenser is to be credited, we commit to validate the distributions that are appropriate on a plant- specific basis." This paragraph of the SE concludes by stating these models would require review prior to plant specific implementation. Change not accepted.
Section 9.1 TRACG-LOCA Application	Page 66: GEH suggests the following change (Line 39): Amendment XX <u>37</u> . <i>Suggested change shown in the markup.</i>	The change is editorial. The NRC finds the change acceptable. Change incorporated in final SE.
Section 9.3.1 Extended Power Uprates	Page 68: When the PDF was created from the word file, the link to the reference for ELTR 1 was broken. GEH suggests the following change (Line 12): Fix the broken link to the reference for ELTR 1.	No link was intended. Appropriate correction has been made in the final SE.

Location	GE Comment	NRC Disposition
Section 9.3.1 Extended Power Uprates	Page 68: When the PDF was created from the word file, the link to the reference for ELTR 2 was broken. GEH suggests the following change (Line 15): Fix the broken link to the reference for ELTR 2.	No link was intended. Appropriate correction has been made in the final SE.
Section 9.3.2 Interim Methods	Page 70: GEH suggests the following change (Line 15): will included <i>Suggested change shown in the markup.</i>	The change is editorial. The NRC finds the change acceptable. Change incorporated in final SE.
Section 9.3.2 Interim Methods	Page 70: GEH suggests the following change (Lines 38-39): Add a blank line to separate '9.3.3 Maximum Extended Load Line Limit Analysis Plus' from the paragraph immediately above it. <i>Suggested change shown in the markup.</i>	The change is editorial. The NRC finds the change acceptable. Change incorporated in final SE.
Section 9.3.3 Maximum Extended Load Line Limit Analysis Plus	Page 71: Enhance readability and clarity. GEH suggests the following change (Line 9): Add an un-indented sentence before the indented paragraphs that states: <u>The following indented paragraphs refer to applications of the SAFER/GESTR-LOCA methods:</u> <i>Suggested change shown in the markup.</i>	The change is editorial. The NRC finds the change acceptable. Change incorporated in final SE.
Section 9.3.3 Maximum Extended Load Line Limit Analysis Plus	Page 72: Enhance readability and clarity. GEH suggests the following change (Line 18): Add an un-indented sentence before the indented paragraphs that states: <u>For SAFER/GESTR-LOCA applications:</u> <i>Suggested change shown in the markup.</i>	The change is editorial. The NRC finds the change acceptable. Change incorporated in final SE.

Location	GE Comment	NRC Disposition
Section 9.3.3 Maximum Extended Load Line Limit Analysis Plus	<p>Page 72: Enhance readability and clarity.</p> <p>GEH suggests the following change (Line 32): Add an un-indented sentence before the indented paragraphs that states: <u>For SAFER/GESTR-LOCA applications:</u> <i>Suggested change shown in the markup.</i></p>	The change is editorial. The NRC finds the change acceptable. Change incorporated in final SE.
Section 9.3.3 Maximum Extended Load Line Limit Analysis Plus	<p>Page 73: GEH suggests the following change (Line 3): Add a blank line to separate the LOCA Break Spectrum limitation from the paragraph immediately following it. <i>Suggested change shown in the markup.</i></p>	The change is editorial. The NRC finds the change acceptable. Change incorporated in final SE.
Section 10.0 Limitations	<p>Page 74: GEH suggests the following change (Line 3): organized into six <u>seven</u> categories <i>Suggested change shown in the markup.</i></p>	The change is editorial. The NRC finds the change acceptable. Change incorporated in final SE.
Section 10.1.2 Limitation 1.2: Fuel System Design Applicability	<p>Page 75: GEH suggests the following change (Line 11): Global Nuclear Fuels (GNF) fuel <i>Suggested change shown in the markup.</i></p>	The change is editorial. The NRC finds the change acceptable. Change incorporated in final SE.
Section 10.2.3 Limitation 2.3: Break Spectrum Analysis	<p>Page 76: GEH suggests the following change (Line 44): Sections 6.2 and 7.45.4 <i>Suggested change shown in the markup.</i></p>	The change is editorial. The NRC finds the change acceptable. Change incorporated in final SE.
Section 10.2.6 Limitation 2.6: Calorimetric Power Uncertainty	<p>Page 77: Delete a comma. With the comma, the sentence reads as if the NRC has withdrawn approval of all ultrasonic flow meters.</p> <p>GEH suggests the following change (Line 23): licensee uses an ultrasonic flow meter; for which the NRC has <i>Suggested change shown in the markup.</i></p>	The change is editorial. The NRC finds the change acceptable. Change incorporated in final SE.

Location	GE Comment	NRC Disposition
Section 10.3.1 Reporting Requirements to Upstream/Concurrent Methods	Page 78: GEH suggests the following change (Line 1): <u>Limitation 3.1:</u> Reporting Requirements to Upstream/Concurrent Methods <i>Suggested change shown in the markup.</i>	The change is editorial. The NRC finds the change acceptable. Change incorporated in final SE.
Section 10.3.2 Limitations on the Use of Upstream/Concurrent Methods	Page 78: GEH suggests the following change (Line 9): <u>Limitation 3.2:</u> Limitations on the Use of Upstream/Concurrent Methods <i>Suggested change shown in the markup.</i>	The change is editorial. The NRC finds the change acceptable. Change incorporated in final SE.
Section 10.4.6 Limitation 4.6: Resampling	Page 79: Please clarify whether changing the fuel to a new product is a “major design change”. GEH suggests the following change (Lines 13-14): power uprate <u>or introduction of a new fuel type</u> , <i>Suggested change shown in the markup.</i>	The NRC staff intent in the discussion is consistent with the vendor proposed revision, subject to clarification. The proposed change is modified and incorporated as follows: power uprate or introduction of a new fuel type that would be expected to change predicted ECCS performance significantly,

<p>Section 10.7 Later-Vintage BWR Application</p>	<p>Pages 79-80: Suggest that the NRC staff consider the more precise wording suggested below to clarify the requirements for removing this limitation.</p> <p>GEH suggests the following change (Page 79 Line 39 through Page 80 Line 13):</p> <p>10.7. LATER-VINTAGE BWR/3-6 FIRST-OF-A-KIND APPLICATION</p> <p>The NRC staff review effort included a detailed review of TRACG-LOCA as applied to a BWR/2, and as such, the application of TRACG-LOCA to Nine Mile Point Nuclear Station, Unit 1, is acceptable without further limitation. However, the NRC staff notes that the demonstration analyses and nodalization sensitivity studies supporting application of TRACG-LOCA to later-vintage BWRs, specifically BWR/3-6 product lines plants, were not updated to reflect the increased core detail and revised statistical approach that were devised revised as a result of the NRC staff review. As such, the NRC staff requires that GEH perform updated demonstration analyses for each of a BWR/4 and BWR/6, and an update to the BWR/4 nodalization sensitivity studies, and provide them for NRC staff review and acceptance, prior to implementation-first-of-a-kind application of TRACG-LOCA at later-vintage to a BWR/3-6 product lines. <u>Specifically, the jet pump plant nodalization studies should be updated/reviewed/accepted prior to application to a jet pump plant. The BWR/4 demonstration studies should be updated/reviewed/accepted prior to application to a BWR/3-4, and similarly, the BWR/6 demonstration studies should be updated/reviewed/accepted prior to application to a BWR/5-6.</u> This limitation can be satisfied either by revising the <u>jet pump plant nodalization studies documented in LTR Section 5.2 Table 5.2-1 and Figures 5.2-1 through 5.3-9 and the key summary demonstration analyses documented provided in LTR Chapter 8</u></p>	<p>The NRC staff intent in the discussion is consistent with the vendor proposed revision. The NRC finds the change acceptable. Change incorporated in final SE.</p>
--	---	--

Location	GE Comment	NRC Disposition
	<p>Figure 8.1-29 for the BWR/4 and Figure 8.2-18 for the BWR/6 of the LTR, or by performing analyses of specific plants.</p> <p><i>Suggested change shown in the markup.</i></p>	
<p>Section 11.0 Conclusion</p>	<p>Page 80: GEH suggests the following change (Lines 19-21): For the purpose of compliance with 10 CFR 50.46 requirements, TRACG-LOCA, as documented in Reference 1 <u>and revised by the RAI responses</u>, may be considered an acceptable evaluation model. With regard to referencing in licensing actions, Reference 1 <u>as revised by the RAI responses</u> may be considered approved for use.</p> <p><i>Suggested change shown in the markup.</i></p>	<p>The NRC staff intent in the discussion is consistent with the vendor proposed revision. The NRC finds the change acceptable. Change incorporated in final SE.</p>
<p>Section 12.0 References</p>	<p>Pages 81-82: GEH suggests the following changes:</p> <ul style="list-style-type: none"> • Page 81, Line 43: Reference 17: MFN 07-457452 • Page 82, Line 47: Reference 31: December 20<u>8</u> <p><i>Suggested change shown in the markup.</i></p>	<p>The change is editorial. The NRC finds the change acceptable. Change incorporated in final SE.</p>

ACKNOWLEDGMENTS

The TRACG Emergency Core Cooling Systems / Loss-of-Coolant-Accident Analysis (ECCS/LOCA) Application Report is the result of technical contributions from many individuals. The following individuals contributed to the preparation of the current report:

J. G. M. Andersen
A. Barrett
F. T. Bolger
J. R. Fitch
J. Fricano
J. Hagaman
R. Harrington
J. F. Harrison
J. M. Healzer
C. L. Heck
M. Holmes
L. A. Klebanov
N. Kurul
K. Muftuoglu
S. LaFountain
G. Li
J. D. Rambo
D. T. Rock
B. Sarikaya
L. K. Schichlein
P. Sharpe
J. C. Shaug
F. D. Shum
B. S. Shiralkar
A. Trofimova

In addition to the direct contributors, D. Abdollahian, W. Marquino, S. P. Congdon, and J. Stewart at the GE-Hitachi Nuclear Energy Americas (GEH), supported by J. Haces, J. Garcia, L. Prieto and M. Trueba at ENUSA, have made significant contributions to the development of the TRACG ECCS/LOCA Application. The advice and careful review from D. C. Pappone, J. L. Casillas, E. C. Eckert, R. B. Linford, and F. M. Paradiso is also acknowledged and greatly appreciated.

CONTENTS

	Page
1.0 Introduction	1-1
1.1 Background	1-1
1.2 Summary	1-2
1.3 Scope of Review	1-3
2.0 Licensing Requirements and Scope of Application.....	2-1
2.1 General Requirements	2-1
2.2 Specific 10 CFR 50.46 Licensing Acceptance Criteria for ECCS Performance.....	2-1
2.3 Analysis Requirements.....	2-1
2.4 Standard Review Plan Guidelines (NUREG-0800)	2-2
2.5 Proposed Application Methodology.....	2-2
2.5.1 Conformance with Regulatory Guide 1.157	2-2
2.5.2 Conformance with CSAU Methodology	2-20
2.6 Implementation Requirements	2-24
2.7 Range of Application.....	2-25
3.0 Phenomena Identification and Ranking.....	3-1
3.1 Organization of PIRTs for ECCS/LOCA	3-1
3.2 BWR LOCA Transient Response.....	3-2
3.2.1 Large Liquid Break LOCA Scenario for Jet Pump Plants.....	3-2
3.2.2 Steam Line Break LOCA Scenario.....	3-4
3.2.3 Small Break LOCA Scenario.....	3-4
3.2.4 Large Liquid Break LOCA Scenario for BWR/2	3-5
3.3 Top-Down Rationale for Choice of PIRT Parameters	3-12
3.4 Phenomena Identification and Ranking Table	3-15
4.0 Applicability of TRACG to ECCS/LOCA	4-1
4.1 Model Capability.....	4-1
4.2 Model Assessment Matrix.....	4-11
5.0 Model Uncertainties and Biases	5-1
5.1 Model Parameters and Uncertainties.....	5-1

NEDO-33005-A Revision 1
Non-Proprietary Information – Class I (Public)

5.1.1	Lower Plenum Region	5-1
5.1.2	Bypass Region	5-5
5.1.3	Core Region	5-8
5.1.4	Guide Tube	5-30
5.1.5	Downcomer.....	5-30
5.1.6	Upper Plenum Region.....	5-31
5.1.7	Jet Pump.....	5-37
5.1.8	Recirculation Pump.....	5-39
5.1.9	Steam Separator	5-39
5.1.10	Steam Dryer	5-39
5.1.11	Steam Line	5-40
5.1.12	Recirculation Line.....	5-41
5.1.13	Isolation Condenser	5-41
5.1.14	Feedwater System	5-42
5.1.15	Containment.....	5-42
5.1.16	Summary	5-43
5.2	Effects of Nodalization.....	5-48
5.3	Effects of Scale.....	5-57
5.3.1	Full Scale Test Coverage	5-57
5.3.2	Scaled Integral LOCA Simulation Tests for Jet Pump Plants	5-62
5.3.3	Scaled Integral LOCA Simulation Tests for Non-Jet Pump Plants.....	5-81
5.3.4	Summary – Effects of Scale.....	5-81
6.0	Application Uncertainties and Biases	6-1
6.1	Input.....	6-1
6.2	Initial Conditions.....	6-2
6.2.1	Total Core Power and Flow	6-3
6.2.2	Feedwater Temperature	6-3
6.2.3	Steam Dome Pressure	6-3
6.2.4	Downcomer Water Level.....	6-4
6.2.5	Limiting Bundle Power Distribution	6-4

NEDO-33005-A Revision 1
Non-Proprietary Information – Class I (Public)

6.2.6	Average Bundle Power Distribution.....	6-7
6.2.7	Fuel Rod Exposure.....	6-7
6.2.8	PLHGR, MCPR and MAPLHGR Uncertainty	6-8
6.3	Plant Parameters	6-16
6.3.1	Scram Time.....	6-17
6.3.2	Scram Speed	6-17
6.4	PCT Analysis Resolution	6-24
7.0	Combination of Uncertainties	7-1
7.1	Approaches for combining uncertainties.....	7-1
7.1.1	Order Statistics (OS) Method	7-1
7.1.2	Normal Distribution One-Sided Upper Tolerance Limit.....	7-3
7.2	Process for Combining Uncertainties.....	7-4
7.3	Implementation of Statistical Methodology	7-5
7.3.1	Conformance with Design Limits.....	7-5
7.4	Statistical Analysis for Qualification Events.....	7-6
7.4.1	FIST Large Break LOCA	7-6
7.4.2	FIST Small Break Test 6SB2C.....	7-7
7.4.3	Conclusions from the FIST Test Simulations.....	7-8
7.4.4	SSTF Test EA3-1.....	7-8
7.4.5	Core Spray Heat Transfer Tests.....	7-11
8.0	Demonstration Analysis	8-1
8.1	TRACG LOCA Analysis and Sensitivity Studies for a Typical BWR/4 Plant.....	8-2
8.1.1	TRACG Nodalization for ECCS/LOCA Calculations for a BWR/4 Plant.....	8-2
8.1.2	Nominal ECCS/LOCA Results for Large and Small Breaks for BWR/4.....	8-6
8.1.3	Sensitivity to Model (PIRT) Parameters for BWR/4.....	8-13
8.1.4	Sensitivity to Initial Conditions and Plant Parameters for BWR/4	8-19
8.1.5	Break Spectrum Results for BWR/4.....	8-34
8.1.6	Statistical Results for BWR/4 LOCA	8-49
8.2	TRACG LOCA Analysis Results and Sensitivity Studies for a Typical BWR/6 Plant.....	8-60

NEDO-33005-A Revision 1
 Non-Proprietary Information – Class I (Public)

8.2.1	TRACG Nodalization for ECCS/LOCA Calculations for a BWR/6 Plant....	8-60
8.2.2	Nominal ECCS/LOCA Results for Large and Small Breaks for BWR/6.....	8-65
8.2.3	Sensitivity to Initial Conditions and Plant Parameters for BWR/6	8-70
8.2.4	Break Spectrum Results for BWR/6.....	8-83
8.2.5	Statistical Results for BWR/6 LOCA	8-91
8.3	TRACG LOCA Analysis Results and Sensitivity Studies for a Typical BWR/2 (non-jet pump) Plant.....	8-100
8.3.1	TRACG Nodalization for ECCS/LOCA Calculations for a BWR/2 Plant..	8-100
8.3.2	Nominal ECCS/LOCA Results for Large and Small Breaks for BWR/2....	8-104
8.3.3	Sensitivity to Model (PIRT) Parameters for BWR/2.....	8-113
8.3.4	Sensitivity to Initial Conditions and Plant Parameters for BWR/2	8-120
8.3.5	Break Spectrum Results for BWR/2.....	8-131
8.3.6	Statistical Results for BWR/2 LOCA	8-140
9.0	Methodology Application.....	9-1
9.1	Analysis Process Summary	9-1
9.2	Applicability of Statistical Analysis.....	9-3
9.3	Break Spectrum	9-6
9.4	Reloads	9-6
9.5	Mixed Cores, Variations in Batch Sizes.....	9-6
9.6	LOCA Analysis of Non-GNF Fuel	9-7
9.7	Equipment Out of Service Flexibility Options.....	9-7
9.8	Operating Domain	9-7
9.9	Compliance with the Requirements of Methods LTR NEDC-33173P-A and MELLLA+ LTR NEDC-33006P-A	9-7
9.10	Exposure-dependent MAPLHGR limits	9-11
10.0	Summary	10-1
11.0	References	11-1
	Appendix A GEH Responses to NRC RAIs on NEDE-33005P Revision 0.....	A-1

LIST OF FIGURES

Figure		Page
Figure 3.2-1	Reactor Vessel Pressure Transient for Various Breaks.....	3-6
Figure 3.2-2	Downcomer Water Level Transient for Various Breaks.....	3-6
Figure 3.2-3	Core Flow Transient for Various Breaks	3-7
Figure 3.2-4	Peak Cladding Temperature Transient for Various Breaks	3-7
Figure 3.2-5	Core Power Transient Following Scram	3-8
Figure 3.2-6	RPV Pressure Transient for Large Liquid Line Break.....	3-8
Figure 3.2-7	Downcomer Water Level Transient for a Large Liquid Line Break.....	3-9
Figure 3.2-8	Major Phenomena during Large Break LOCA Refill/Reflood	3-9
Figure 3.2-9	PCT Transient for Large Liquid Break LOCA	3-10
Figure 3.2-10	RPV Pressure Transient for a BWR/2 Large Break.....	3-10
Figure 3.2-11	Core Flow Transient for BWR/2 Large Break.....	3-11
Figure 3.2-12	PCT Transient for BWR/2 Large Break.....	3-11
Figure 5.1-1	Void Fraction Deviations for Tests Applicable to Regions with Large Hydraulic Diameter.....	5-3
Figure 5.1-2	Sensitivity of TRACG Prediction of Average Void Fraction in Large Hydraulic Diameter Test Facilities to PIRT Multiplier	5-4
Figure 5.1-3	Fractional Error in CCFL Constant at Top of Bypass.....	5-7
Figure 5.1-4	Void Coefficient Fit at Different Exposures (Gwd/ST).....	5-8
Figure 5.1-5	Point Kinetics Void Coefficient Model for LOCA Applications.....	5-9
Figure 5.1-6	Comparison of Small Break Initial Power Response for Point Kinetics and 3D Neutronics Models.....	5-10
Figure 5.1-7	Void Fraction Deviations for Toshiba Tests	5-12
Figure 5.1-8	Sensitivity of TRACG Prediction of Toshiba Void Fraction to PIRT Multiplier on (C_o-1)	5-12
Figure 5.1-9	Lognormal Probability Distribution for PIRT22	5-13
Figure 5.1-10	Fractional Error in CCFL Constant at the Side Entry Orifice.....	5-16
Figure 5.1-11	Fractional Error in Modified Zuber Critical Heat Flux Correlation	5-19
Figure 5.1-12	Fractional Error in Modified Bromley Heat Transfer Coefficient.....	5-20
Figure 5.1-13	Fractional Error in Wall Temperature Calculated with the Dittus-Boelter Heat Transfer Coefficient.....	5-23
Figure 5.1-14	Clad Rupture Stress as a Function of Clad Temperature	5-24
Figure 5.1-15	Fractional Deviations in Quench Front Velocity	5-26

NEDO-33005-A Revision 1
 Non-Proprietary Information – Class I (Public)

Figure 5.1-16	Decay Heat Uncertainty at an Exposure of 11 GWD/MTU	5-28
Figure 5.1-17	Initial Oxide Thickness Model.....	5-29
Figure 5.1-18	Void Fraction Deviations for Tests Applicable to Regions with Large Hydraulic Diameter.....	5-32
Figure 5.1-19	Sensitivity of TRACG Prediction of Average Void Fraction in EBWR Test Facility to PIRT Multiplier on Interfacial Drag Coefficient	5-33
Figure 5.1-20	Probability Distribution for Multiplier on Interfacial Drag Coefficient	5-33
Figure 5.1-21	Minimum Channel Spray Flow vs. Spray Header Flow Example.....	5-36
Figure 5.1-22	Core Spray Flow Rates Example	5-36
Figure 5.1-23	Core Spray to the Minimum Flow Bundle vs. Pressure Example	5-37
Figure 5.2-1	Vessel Axial Nodalization Sensitivity for Large-Break LOCA.....	5-52
Figure 5.2-2	Vessel Axial Nodalization Sensitivity for Intermediate-Break LOCA.....	5-52
Figure 5.2-3	Vessel Axial Nodalization Sensitivity for Small-Break LOCA.....	5-53
Figure 5.2-4	Vessel Radial and Azimuthal Nodalization Sensitivity for Large-Break LOCA.....	5-53
Figure 5.2-5	Vessel Radial and Azimuthal Nodalization Sensitivity for Intermediate Break	5-54
Figure 5.2-6	Vessel Radial and Azimuthal Nodalization Sensitivity for Small-Break LOCA.....	5-54
Figure 5.2-7	Channel Axial Nodalization Sensitivity for Large-Break LOCA	5-55
Figure 5.2-8	Channel Axial Nodalization Sensitivity for Intermediate-Break LOCA	5-55
Figure 5.2-9	Channel Axial Nodalization Sensitivity for Small-Break LOCA	5-56
Figure 5.3-1	Vessel Pressure vs. Time Comparison	5-66
Figure 5.3-2	Vessel Mass vs. Time Comparison	5-66
Figure 5.3-3	Comparison of Average Channel ΔP (Inventory) vs. Nondimensional Time	5-67
Figure 5.3-4	Vessel Liquid Mass PI-Group Comparison - Blowdown Period.....	5-72
Figure 5.3-5	Vessel Liquid Mass PI-Group Comparison - Reflood Period.....	5-72
Figure 5.3-6	Vessel Pressure PI-Group Comparison - Blowdown Period	5-73
Figure 5.3-7	Vessel Pressure PI-Group Comparison - Reflood Period	5-73
Figure 5.3-8	Peak Cladding Temperatures vs. Time	5-78
Figure 5.3-9	Local Convection Energy.....	5-79
Figure 5.3-10	Mixture Densities for FIST	5-79
Figure 5.3-11	Mixture Densities for ROSA.....	5-80
Figure 5.3-12	Mixture Densities for BWR/6	5-80

NEDO-33005-A Revision 1
 Non-Proprietary Information – Class I (Public)

Figure 6.2-1	Typical MELLLA+ Power/Flow Map	6-12
Figure 6.2-2	Data for Bundles Close to LHGR Limits	6-13
Figure 6.2-3	Data for Bundles Close to MCPR Limits	6-14
Figure 6.2-4	Core Average Axial Shape	6-15
Figure 6.2-5	Maximum Nodal Peaking Channel Power Distribution	6-15
Figure 6.2-6	Maximum CPRRAT Channel Power Distribution	6-15
Figure 6.3-1	Time for Drywell Pressure to Reach High Drywell Pressure Following LOCA	6-21
Figure 6.3-2	Control Reactivity Insertion for Various Scram Speeds	6-21
Figure 6.3-3	Reactor Power Transient following DBA for Various Scram Speeds	6-22
Figure 6.3-4	Effect of Scram Speed on BWR/4 PCT (PLHGR Channel) for DBA	6-22
Figure 6.3-5	Reactor Power Transient following Small Break for Various Scram Speeds	6-23
Figure 6.3-6	Effect of Scram Speed on BWR/4 PCT for Small Break	6-23
Figure 6.4-1	PCT Range for BWR/4 Limiting Break	6-27
Figure 6.4-2	PCT Distribution for BWR/4 Limiting Break	6-27
Figure 6.4-3	Individual PCT Traces for BWR/4 Limiting Break	6-28
Figure 6.4-4	Hot Channel PCT Traces for BWR/4 Limiting Break	6-28
Figure 6.4-5	Model PIRTs Rank Correlations	6-29
Figure 6.4-6	Plant-Specific PIRTs Rank Correlations	6-30
Figure 6.4-7	Hot Channel PCT Traces for [[]]	6-31
Figure 6.4-8	Hot Channel PCT Traces for [[]]	6-31
Figure 6.4-9	PCT Range for BWR/4 0.67 ft ² Break with [[]]	6-32
Figure 6.4-10	PCT Distribution for BWR/4 0.67 ft ² Break with [[]]	6-32
Figure 7.1-1	Schematic Process for Combining Uncertainties	7-2
Figure 7.4-1	Comparison of System Pressure for FIST Test 6DBA1B	7-14
Figure 7.4-2	Comparison of Rod Temperatures (Elevation 1.96 m) for FIST Test 6DBA1B	7-14
Figure 7.4-3	Comparison of Rod Temperatures (Elevation 1.22 m) for FIST Test 6DBA1B	7-15
Figure 7.4-4	Correlation of Rod Temperatures (Elevation 1.96 m) with PIRTs for FIST Test 6DBA1B	7-16
Figure 7.4-5	Comparison of System Pressure for FIST Test 6SB2C	7-17

NEDO-33005-A Revision 1
 Non-Proprietary Information – Class I (Public)

Figure 7.4-6	Comparison of Rod Temperatures (Elevation 2.97 m) for FIST Test 6SB2C	7-17
Figure 7.4-7	Comparison of Rod Temperatures (Elevation 1.96 m) for FIST Test 6SB2	7-18
Figure 7.4-8	Comparison of Rod Temperatures (Elevation 1.22 m) for FIST Test 6SB2C	7-18
Figure 7.4-9	Correlation of Rod Temperatures (Elevation 1.96 m) with PIRTs for FIST Test 6SB2C	7-19
Figure 7.4-10	Comparison of System Pressure for SSTF Test EA3-1	7-20
Figure 7.4-11	Comparison of Temperature at Pool Periphery at the Bottom for SSTF Test EA3-1	7-21
Figure 7.4-12	Comparison of Temperature at Pool Periphery at Mid-Depth for SSTF Test EA3-1	7-22
Figure 7.4-13	Comparison of Temperature at Pool Periphery at the Surface for SSTF Test EA3-1	7-23
Figure 7.4-14	Comparison of Lower Plenum Fill Fraction for SSTF Test EA3-1	7-24
Figure 7.4-15	Correlation of Lower Plenum Refill Time with PIRTs for SSTF Test EA3-1	7-25
Figure 7.4-16	Comparison of Bypass Fill Fraction for SSTF Test EA3-1	7-26
Figure 7.4-17	Comparison of Upper Plenum Fill Fraction for SSTF Test EA3-1	7-27
Figure 7.4-18	Comparison of Temperature at Bottom of Pool Periphery Including Variations in Test Conditions for SSTF Test EA3-1	7-28
Figure 7.4-19	Comparison of Lower Plenum Fill Fraction Including Variations in Test Conditions for SSTF Test EA3-1	7-29
Figure 7.4-20	Results of Monte Carlo Analysis vs. Test Data for Rod Group 2.....	7-30
Figure 7.4-21	Results of Monte Carlo Analysis vs. Test Data for Rod Group 3.....	7-30
Figure 7.4-22	Results of Monte Carlo Analysis vs. Test Data for Rod Group 4.....	7-31
Figure 7.4-23	Results of Monte Carlo Analysis vs. Test Data for Rod Group 6.....	7-31
Figure 7.4-24	Results of Monte Carlo Analysis vs. Test Data for Rod Group 9.....	7-32
Figure 7.4-25	Results of Monte Carlo Analysis vs. Test Data for Rod Group 2.....	7-32
Figure 7.4-26	Results of Monte Carlo Analysis vs. Test Data for Rod Group 3.....	7-33
Figure 7.4-27	Results of Monte Carlo Analysis vs. Test Data for Rod Group 4.....	7-33
Figure 7.4-28	Results of Monte Carlo Analysis vs. Test Data for Rod Group 6.....	7-34
Figure 7.4-29	Results of Monte Carlo Analysis vs. Test Data for Rod Group 2.....	7-34
Figure 7.4-30	Results of Monte Carlo Analysis vs. Test Data for Rod Group 3.....	7-35
Figure 7.4-31	Results of Monte Carlo Analysis vs. Test Data for Rod Group 4.....	7-35

NEDO-33005-A Revision 1
 Non-Proprietary Information – Class I (Public)

Figure 7.4-32	Results of Monte Carlo Analysis vs. Test Data for Rod Group 6.....	7-36
Figure 8.1-1	TRACG Vessel Nodalization for Typical BWR/4 Model	8-4
Figure 8.1-2	TRACG Component Nodalization for Typical BWR/4 Model	8-5
Figure 8.1-3	TRACG Modeling of Guillotine and Split Breaks.....	8-6
Figure 8.1-4	System Pressure and ECC Flows for BWR/4 Suction DBA	8-9
Figure 8.1-5	PCT for Various Channels for BWR/4 Suction DBA.....	8-9
Figure 8.1-6	System Pressure and ECC Flows for BWR/4 Small Break	8-12
Figure 8.1-7	PCT for Various Channels for BWR/4 Small Break	8-12
Figure 8.1-8	BWR/4 DBA PCT Sensitivity to PIRT Uncertainties	8-15
Figure 8.1-9	BWR/4 0.1 ft ² LOCA PCT Sensitivity to PIRT Uncertainties	8-17
Figure 8.1-10	Rod Axial Peaking Variations.....	8-28
Figure 8.1-11	Channel Average Axial Peaking Variations	8-28
Figure 8.1-12	BWR/4 ECCS Configuration.....	8-40
Figure 8.1-13	Scram Time vs. Break Size for BWR/4 Suction Breaks.....	8-41
Figure 8.1-14	Pressure Response for BWR/4 Small Breaks.....	8-41
Figure 8.1-15	PCT Response for BWR/4 Small Breaks.....	8-42
Figure 8.1-16	Pressure Response for BWR/4 Intermediate Breaks.....	8-42
Figure 8.1-17	PCT Response for BWR/4 Intermediate Breaks.....	8-43
Figure 8.1-18	Pressure Response for BWR/4 Intermediate to Large Breaks	8-43
Figure 8.1-19	PCT Response for BWR/4 Intermediate to Large Breaks	8-44
Figure 8.1-20	Pressure Response for BWR/4 Large Breaks.....	8-44
Figure 8.1-21	PCT Response for BWR/4 Large Breaks.....	8-45
Figure 8.1-22	Start of BWR/4 Heatup Relative to ADS and ECCS Activation.....	8-45
Figure 8.1-23	BWR/4 Break Spectrum for Recirculation Line Suction Breaks with Battery Failure.....	8-46
Figure 8.1-24	BWR/4 Break Spectrum for Recirculation Line Discharge Breaks with Battery Failure.....	8-46
Figure 8.1-25	BWR/4 Break Spectrum for Recirculation Line Discharge Breaks with LPCI Injection Valve Failure.....	8-47
Figure 8.1-26	Pressure Response for BWR/4 Non-Recirculation Line Breaks.....	8-47
Figure 8.1-27	PCT Response for BWR/4 Non-Recirculation Line Breaks	8-48
Figure 8.1-28	BWR/4 Feedwater Line Break Spectrum for Hot Channels	8-48
Figure 8.1-29	Summary of BWR/4 Statistical Analyses at Various Break Sizes.....	8-54
Figure 8.1-30	Range of Trials for PCT Transient for BWR/4 DBA	8-54

NEDO-33005-A Revision 1
 Non-Proprietary Information – Class I (Public)

Figure 8.1-31	Overall PCT Distribution for BWR/4 Suction DBA.....	8-55
Figure 8.1-32	Overall PCT Trials for BWR/4 Suction DBA.....	8-55
Figure 8.1-33	Range of Trials for PCT Transient for BWR/4 Intermediate Break	8-56
Figure 8.1-34	Overall PCT Distribution for BWR/4 Intermediate Break	8-56
Figure 8.1-35	Overall PCT Trials for BWR/4 Intermediate Break	8-57
Figure 8.1-36	Range of Trials for PCT Transient for BWR/4 Small Break.....	8-57
Figure 8.1-37	Overall PCT Distribution for BWR/4 Small Break	8-58
Figure 8.1-38	Overall PCT Trials for BWR/4 Small Break	8-58
Figure 8.1-39	BWR/4 Feedwater Line Break Statistical Analysis Results	8-59
Figure 8.1-40	Range of Trials for PCT Transient for BWR/4 Limiting Feedwater Line Break	8-59
Figure 8.2-1	TRACG Vessel Nodalization for Typical BWR/6 Model	8-62
Figure 8.2-2	TRACG Nodalization of Feedwater and Steam Lines for Typical BWR/6..	8-63
Figure 8.2-3	TRACG Nodalization of Recirculation Lines for Typical BWR/6 Model ...	8-64
Figure 8.2-4	System Pressure and ECC Flows for BWR/6 Discharge DBA	8-68
Figure 8.2-5	PCT for Various Channels for BWR/6 Discharge DBA.....	8-68
Figure 8.2-6	System Pressure and ECC Flows for BWR/6 Small Break	8-69
Figure 8.2-7	PCT for Various Channels for BWR/6 Small Break	8-69
Figure 8.2-8	Typical BWR/6 ECCS Configuration.....	8-86
Figure 8.2-9	Pressure Response for BWR/6 Small Breaks.....	8-87
Figure 8.2-10	PCT Response for BWR/6 Small Breaks.....	8-87
Figure 8.2-11	Pressure Response for BWR/6 Intermediate Breaks.....	8-88
Figure 8.2-12	PCT Response for BWR/6 Intermediate Breaks.....	8-88
Figure 8.2-13	Pressure Response for BWR/6 Large Breaks.....	8-89
Figure 8.2-14	PCT Response for BWR/6 Large Breaks.....	8-89
Figure 8.2-15	Start of BWR/6 Heatup Relative to ADS and ECCS Activation	8-90
Figure 8.2-16	Break Spectrum for BWR/6 Recirculation Line Discharge Breaks.....	8-90
Figure 8.2-17	Break Spectrum for BWR/6 Recirculation Line Suction Breaks.....	8-91
Figure 8.2-18	Summary of BWR/6 Statistical Analyses at Various Break Sizes.....	8-95
Figure 8.2-19	Range of Trials for PCT Transient for BWR/6 DBA	8-95
Figure 8.2-20	Overall PCT Trials for BWR/6 Discharge DBA.....	8-96
Figure 8.2-21	Overall PCT Distribution for BWR/6 Discharge DBA.....	8-96
Figure 8.2-22	Range of Trials for PCT Transient for BWR/6 Intermediate Break	8-97

NEDO-33005-A Revision 1
 Non-Proprietary Information – Class I (Public)

Figure 8.2-23	Overall PCT Trials for BWR/6 Intermediate Break	8-97
Figure 8.2-24	Overall PCT Distribution for BWR/6 Intermediate Break	8-98
Figure 8.2-25	Range of Trials for PCT Transient for BWR/6 Small Break.....	8-98
Figure 8.2-26	Overall PCT Trials for BWR/6 Small Break	8-99
Figure 8.2-27	Overall PCT Distribution for BWR/6 Small Break	8-99
Figure 8.3-1	TRACG Vessel Nodalization for Typical BWR/2 Model	8-102
Figure 8.3-2	TRACG Component Nodalization for Typical BWR/2.....	8-103
Figure 8.3-3	System Pressure and Void Fraction in Central Cell of Core for Discharge DBA	8-109
Figure 8.3-4	Break Flow and CS Flow for BWR/2 Discharge DBA	8-109
Figure 8.3-5	Lower Plenum Level for BWR/2 Discharge DBA	8-110
Figure 8.3-6	PCT for Various Channels for BWR/2 Discharge DBA.....	8-110
Figure 8.3-7	Pressure and Void Fraction in Central Cell for BWR/2 Small Break.....	8-111
Figure 8.3-8	Break Flow and CS Flow for BWR/2 Small Break	8-111
Figure 8.3-9	Lower Plenum Level for BWR/2 Small Break	8-112
Figure 8.3-10	PCT for Various Channels for BWR/2 Small Break	8-112
Figure 8.3-11	BWR/2 Small Break PCT Sensitivity to Individual Uncertainties	8-114
Figure 8.3-12	BWR/2 Intermediate Break PCT Sensitivity to Individual Uncertainties ..	8-116
Figure 8.3-13	BWR/2 Large Break PCT Sensitivity to Individual Uncertainties	8-118
Figure 8.3-14	Effect of BWR/2 Containment Boundary Conditions	8-130
Figure 8.3-15	Effect of BWR/2 ECCS Temperature	8-130
Figure 8.3-16	BWR/2 Scram Time vs. Break Size.....	8-134
Figure 8.3-17	Pressure and DC Level Response for BWR/2 Small Breaks.....	8-135
Figure 8.3-18	PCT and Bypass Level Response for BWR/2 Small Breaks	8-135
Figure 8.3-19	Pressure and DC Level Response for BWR/2 Intermediate Breaks	8-136
Figure 8.3-20	PCT and Bypass Level Response for BWR/2 Intermediate Breaks	8-136
Figure 8.3-21	Pressure and DC Level Response for BWR/2 Large Breaks	8-137
Figure 8.3-22	PCT and Bypass Level Response for BWR/2 Large Breaks	8-137
Figure 8.3-23	Break Spectrum for BWR/2 Discharge and Suction Side Breaks	8-138
Figure 8.3-24	Pressure Response for BWR/2 Non-Recirculation Line Breaks.....	8-138
Figure 8.3-25	PCT Response for BWR/2 Non-Recirculation Line Breaks.....	8-139
Figure 8.3-26	Oxidation for BWR/2 Limiting LOCA (DBA).....	8-139
Figure 8.3-27	PCT Distribution for BWR/2 Discharge DBA.....	8-144

NEDO-33005-A Revision 1
 Non-Proprietary Information – Class I (Public)

Figure 8.3-28	Individual PCT Trials for BWR/2 Discharge DBA	8-144
Figure 8.3-29	Peak Oxidation Thickness Distribution for BWR/2 Discharge DBA	8-145
Figure 8.3-30	Peak Oxidation Thickness Trials for BWR/2 Discharge DBA	8-145
Figure 8.3-31	Core Average Oxidation Volume Distribution for BWR/2 Discharge DBA	8-146
Figure 8.3-32	Core Average Oxidation Volume Trials for BWR/2 Discharge DBA	8-146
Figure 8.3-33	Range of Trials for PCT Transient for BWR/2 Discharge DBA	8-147
Figure 8.3-34	Range of Trials for Peak Oxidation Thickness Transient for BWR/2 Discharge DBA	8-147
Figure 8.3-35	PCT Distribution for BWR/2 Discharge Small Break	8-148
Figure 8.3-36	Individual PCT Trials for BWR/2 Small Break	8-148
Figure 8.3-37	Peak Oxide Thickness Distribution for BWR/2 Small Break	8-149
Figure 8.3-38	Individual Peak Oxide Thickness Trials for BWR/2 Small Break	8-149
Figure 8.3-39	Range of Trials for PCT Transient for BWR/2 Small Break	8-150
Figure 8.3-40	Range of Trials for Peak Oxide Thickness Transient for BWR/2 Small Break	8-150
Figure 8.3-41	BWR/2 Break Spectrum with Uncertainties – PCT Results	8-151
Figure 8.3-42	BWR/2 Break Spectrum with Uncertainties – MLO Results	8-151
Figure 9.1-1	LOCA Analysis Process Flowchart	9-2
Figure 9.2-1	Analysis Change Evaluation Process Flowchart	9-5

LIST OF TABLES

Table		Page
Table 2.5-1	Key RG 1.157 Elements and Evaluation of TRACG Process	2-4
Table 2.5-2	Code Scaling, Applicability and Uncertainty Evaluation Methodology.....	2-24
Table 3.3-1	Top Down Rationale for Identification of PIRT Parameters	3-13
Table 3.4-1	Phenomena that Govern BWR/2-6 LOCA Responses.....	3-17
Table 4.1-1	BWR LOCA Phenomena and TRACG Model Capability Matrix.....	4-2
Table 4.2-1	Qualification Matrix for BWR/2-6 LOCA Phenomena.....	4-12
Table 5.1-1	Error Measures for Wall Temperature and Dittus-Boelter Heat Transfer Coefficient (Estimated)	5-21
Table 5.1-2	Parameters Governing High and Medium Ranked PIRT Phenomena	5-44
Table 5.2-1	Summary of Nodalization Sensitivity Studies for Jetpump Plants	5-50
Table 5.2-2	Summary of Nodalization Sensitivity Studies for BWR/2	5-51
Table 5.3-1	Full Scale Test Data Coverage for LOCA Phenomena.....	5-59
Table 5.3-2	Comparison of BWR/6 with FIST and ROSA Test Facilities	5-64
Table 6.2-1	Key Plant Initial Conditions.....	6-9
Table 6.2-2	Summary of LHGR and MCPR Targets	6-11
Table 6.3-1	System Unique Plant Parameters	6-19
Table 6.3-2	Parameters Common to Multiple Safety Systems.....	6-20
Table 7.4-1	Test Parameters Varied for Monte Carlo Simulation of SSTF Test EA3-1..	7-13
Table 8.1-1	TRACG Channel Grouping for Typical BWR/4 Model.....	8-3
Table 8.1-2	BWR/4 Suction DBA Key Transient Parameters	8-8
Table 8.1-3	BWR/4 0.0093 m ² Suction Break Key Transient Parameters.....	8-11
Table 8.1-4	Allowable Operating Range Specification Basis for BWR/4 LOCA	8-20
Table 8.1-5	BWR/4 Sensitivity to Location of Axial Peak	8-25
Table 8.1-6	BWR/4 Sensitivity to Power/Flow Conditions	8-26
Table 8.1-7	BWR/4 Effect of Radial Peaking Distribution on PCT for DBA	8-26
Table 8.1-8	Allowable Operating Range Categorization for BWR/4 LOCA.....	8-27
Table 8.1-9	Bases for Initial Conditions Uncertainty Characterizations for BWR/4 LOCA.....	8-30
Table 8.1-10	BWR/4 LOCA MCPR and PLHGR Initial Condition Uncertainty Results .	8-31

NEDO-33005-A Revision 1
 Non-Proprietary Information – Class I (Public)

Table 8.1-11	Results of Initial Condition Uncertainty Characterizations for BWR/4 LOCA.....	8-32
Table 8.1-12	BWR/4 Sensitivity to Containment Boundary Conditions	8-33
Table 8.1-13	BWR/4 Single Failures and Available ECCS	8-38
Table 8.1-14	BWR/4 PCT Summary.....	8-39
Table 8.1-15	Plant Initial Conditions for BWR/4 Monte Carlo Analysis	8-51
Table 8.1-16	Plant Parameters varied in BWR/4 Monte Carlo Trials.....	8-52
Table 8.1-17	Overall Statistical Trial Summary for BWR/4 Suction Line Break.....	8-53
Table 8.2-1	TRACG Channel Grouping for Typical BWR/6 Model	8-61
Table 8.2-2	BWR/6 Plant-specific Steady Operating and ECCS Parameters	8-67
Table 8.2-3	Allowable Operating Range Specification Basis	8-71
Table 8.2-4	Allowable Operating Range Characterization for BWR/6 LOCA.....	8-76
Table 8.2-5	Bases for Initial Conditions Uncertainty Characterizations for BWR/6 LOCA.....	8-78
Table 8.2-6	Initial Condition Uncertainty Characterizations for BWR/6 LOCA.....	8-80
Table 8.2-7	Single Failures and Available ECCS for BWR/6	8-86
Table 8.2-8	Plant Parameters varied in BWR/6 Monte Carlo Trials.....	8-93
Table 8.2-9	Overall Statistical Trial Summary for BWR/6 Discharge Line Break.....	8-94
Table 8.3-1	TRACG Channel Grouping for Typical BWR/2 Model	8-101
Table 8.3-2	BWR/2 Discharge DBA Key Transient Parameters	8-107
Table 8.3-3	BWR/2 0.0186 m ² Discharge Break Key Transient Parameters.....	8-108
Table 8.3-4	Allowable Operating Range Specification Basis for BWR/2 LOCA	8-121
Table 8.3-5	Allowable Operating Range Characterization for BWR/2 LOCA.....	8-125
Table 8.3-6	Basis for Initial Condition Uncertainty Characterizations for BWR/2 LOCA.....	8-127
Table 8.3-7	Initial Condition Uncertainty Characterizations for BWR/2 LOCA.....	8-128
Table 8.3-8	BWR/2 Single Failures and Available ECCS	8-133
Table 8.3-9	BWR/2 PCT Summary.....	8-134
Table 8.3-10	Plant Parameters varied in BWR/2 Monte Carlo Trials.....	8-143
Table 9.9-1	Compliance with Methods LTR NEDC-33173P-A Limitations.....	9-8
Table 9.9-2	Compliance with MELLLA+ NEDC-33006P-A Limitations.....	9-9

ABSTRACT

This report discusses the application of TRACG, the GE-Hitachi Nuclear Energy Americas (GEH) proprietary version of the Transient Reactor Analysis Code (TRAC), to analyses of Loss-of-Coolant Accidents (LOCAs) for Boiling Water Reactors (BWRs) types 2 through 6. These analyses include the evaluation of core heatup and oxidation and reactor vessel parameters, including pressure, inventory and flows (emergency core coolant system (ECCS)/LOCA analyses). Evaluation of the containment is not included in this application. The report describes how realistic calculations can be used together with statistical quantification of uncertainties to support licensing evaluations for LOCA events.

Realistic analyses performed with TRACG have been used previously to support applications of the SAFER code for ECCS/LOCA licensing calculations. TRACG applications are expected to offer benefits in terms of more accurate and realistic simulations of BWR events and improved operating margins. The NRC has approved the use of TRACG as an acceptable methodology for performing licensing analyses of Anticipated Operational Occurrences (AOOs) for BWR/2-6s [3] [4] and for LOCA analysis of the ESBWR [39].

REVISION SUMMARY

Revision	Description of Change
0	Initial Issue
1	<p>Created the “-A” version by adding the NRC’s Final Safety Evaluation (Reference 81) and GEH’s responses to the NRC's Requests for Additional Information (RAIs) (References 82 through 86).</p> <p>Revised the LTR consistent with the GEH responses to the NRC’s RAIs (References 82 through 86).</p> <p>Added References 81 through 86.</p>

ACRONYMS AND ABBREVIATIONS

2D	Two-Dimensional
3D	Three-Dimensional
ACRS	Advisory Committee on Reactor Safeguards
ADS	Automatic Depressurization System
AL	Analytical Limit
ANS	American Nuclear Society
ANSI	American National Standards Institute
AOO	Anticipated Operational Occurrence
APLHGR	Average Planar Linear Heat Generation Rate
ATWS	Anticipated Transient Without Scram
AV	Allowable Value
BD	Blowdown
BT	Boiling Transition
BWR	Boiling Water Reactor
CCFL	Counter-Current Flow Limitation
CHF	Critical Heat Flux
CFR	Code of Federal Regulations
CPR	Critical Power Ratio
CS	Core Spray
CSAU	Code Scaling Applicability and Uncertainty
CSHT	Core Spray Heat Transfer
CWO	Core-Wide Oxidation
D/G	Diesel Generator
DBA	Design Basis Accident
DW	Drywell
EBWR	Experimental Boiling Water Reactor
ECC	Emergency Core Coolant
ECCS	Emergency Core Coolant System
EMDAP	Evaluation Model Development and Assessment Process
EOC	End of Cycle
EPU	Extended Power Uprate
ESBWR	Economical Simplified Boiling Water Reactor
FFWTR	Final Feedwater Temperature Reduction
FIST	Full Integral Simulation Test
FSAR	Final Safety Analysis Report
GDC	General Design Criteria
GE	General Electric
GEH	GE-Hitachi Nuclear Energy Americas
GESTAR	GE Standard Application for Reactor Fuel
GEXL	GE critical quality (X) – boiling length (L) correlation
GRS	Gesellschaft für Anlagen-und Reaktorsicherheit
GT	Guide Tube
HPCI	High Pressure Core Injection

NEDO-33005-A Revision 1
Non-Proprietary Information – Class I (Public)

HPCS	High Pressure Core Spray
HT	Heat Transfer
HTC	Heat Transfer Coefficient
ICPR	Initial Critical Power Ratio
INEL	Idaho National Engineering Laboratory (now known as INL)
INL	Idaho National Laboratory
IST	Integral Systems Test
JP	Jet Pump
KWU	Kraftwerk Union Aktiengesellschaft
LHGR	Linear Heat Generation Rate
LOCA	Loss-of-Coolant Accident
LP	Lower Plenum
LPCI	Low Pressure Core Injection
LPCS	Low Pressure Core Spray
LPF	Local (Pin Power) Peaking Factor
LTC	Long-Term Cooling
LTP	Lower Tie Plate
LTR	Licensing Topical Report
LWR	Light Water Reactor
MAPLHGR	Maximum Average Planar Linear Heat Generation Rate
MCPR	Minimum Critical Power Ratio
MELLLA+	Maximum Extended Load Limit Line Analysis Plus
MLO	Maximum Local Oxidation
MSIV	Main Steam Isolation Valve
MSLB	Main Steam Line Break
ND-OSUTL	Normal Distribution One-Sided Upper Tolerance Limits
NMP1	Nine Mile Point Unit 1
NPSH	Net Positive Suction Head
NRC	Nuclear Regulatory Commission
NTSP	Nominal Trip Setpoint
OPL	Operating Parameters for Licensing
ORNL	Oak Ridge National Laboratory
OSUTL	One-Sided Upper Tolerance Limits
PANACEA	GE BWR Core Simulator
PCT	Peak Cladding Temperature
PDF	Probability Density Function
PIRT	Phenomena Identification and Ranking Table
PLHGR	Peak Linear Heat Generation Rate
PSTF	Pressure Suppression Test Facility
PWR	Pressurized Water Reactor
RG	Regulatory Guide
RHR	Residual Heat Removal
RMS	Root Mean Square
ROSA	Rig of Safety Assessment
RPF	Radial Peaking Factor

NEDO-33005-A Revision 1
Non-Proprietary Information – Class I (Public)

RPV	Reactor Pressure Vessel
RR	Refill/Reflood
SBA	Small Break Accident
SEO	Side Entry Orifice
SLO	Single Loop Operation
SRP	Standard Review Plan
SRV	Safety/Relief Valve
SSTF	Steam Sector Test Facility
TBV	Turbine Block Valve
TGBLA	GE Bundle Lattice Analysis
T/H	Thermal-Hydraulic
TLTA	Two-Loop Test Apparatus
TPO	Thermal Power Optimization
TRAC	Transient Reactor Analysis Code
TRACG	GE proprietary version of TRAC
UP	Upper Plenum

1.0 INTRODUCTION

1.1 BACKGROUND

TRACG is the GE-Hitachi Nuclear Energy Americas (GEH) proprietary version of the Transient Reactor Analysis Code (TRAC). TRACG uses realistic one-dimensional and three-dimensional (3D) models and numerical methods to simulate the phenomena that govern the operation of boiling water reactors (BWRs). GEH currently performs Emergency Core Coolant System/Loss-of-Coolant Accident (ECCS/LOCA) licensing calculations for operating plants using an Nuclear Regulatory Commission (NRC)-approved set of computer codes and methods (the “SAFER/GESTR” methodology [21]) that does not include TRACG. However, TRACG analyses have been used historically to support ECCS/LOCA licensing applications by comparing TRACG and SAFER calculations for both jet pump (JP) and non-jet pump plant LOCAs [22] [25]. The existing TRACG code documentation, consisting of a model description licensing topical report (LTR) [1], a qualification LTR [2] and a user’s manual [29], is fully supportive of application to ECCS/LOCA. The TRACG Qualification LTR [2] includes comparisons of TRACG calculations with data from separate effects, component performance and integral system effects tests that are directly supportive of its use for BWR LOCA analyses. The NRC has approved the application of TRACG for ECCS/LOCA analyses of the Economical Simplified Boiling Water Reactor (ESBWR) reactor pressure vessel (RPV) and containment [39]. In non-LOCA analysis categories, NRC approvals have been granted for the generic (BWR/2-6) application of TRACG for analyses of anticipated operational occurrences (AOOs) [3] [4] and anticipated transient without scram (ATWS) overpressure transients [65], for ESBWR stability analysis [66] and for specific BWR/2-6 stability calculations ([67] and [68]).

TRAC was originally developed for pressurized water reactor (PWR) analysis by Los Alamos National Laboratory and the initial PWR version was named TRAC-P1A [5]. The development of the BWR version of TRAC started in 1979 as a cooperative effort between General Electric (GE) and the Idaho National Engineering Laboratory (INEL). The primary objective of this activity was the development of a version of TRAC for simulation of BWR LOCAs. The main tasks were refinement of the basic TRAC models for BWR applications and the development of models for specific BWR phenomena and components. This work culminated in the mid-1980s with the parallel development of TRACB04 at GE ([7], [8], [9], [10], [11], [12], [13]) and the very similar TRACG-BD1/MOD1 at INEL. In the earlier stages, GE, the NRC and the Electric Power Research Institute (EPRI) jointly funded the development of the code. A detailed description of these earlier versions of TRAC for BWRs is contained in References [14] and [15].

GE, along with its technical associates, continued to develop TRACG with the objective of expanding the capabilities of the code to include transient, stability and ATWS applications. Major developments included the implementation of the three-dimensional kinetics model and an implicit integration scheme. Modeling of the BWR fuel bundle was also improved. The current TRACG is based on a multi-dimensional two-fluid model for the reactor thermal hydraulics and a three-dimensional reactor kinetics model. The TRACG models, described in detail in the

TRACG Model Description Licensing Topical Report [1], allow for detailed and realistic simulation of a wide range of BWR phenomena and provide code capability for the simulation of a large variety of test and reactor configurations. TRACG has been extensively qualified against separate effects tests, component performance tests, integral system effects tests and operating BWR transient plant data. The details of the qualification studies are presented in the TRACG Qualification Licensing Topical Report [2].

1.2 SUMMARY

This document demonstrates the acceptability of TRACG LOCA analysis results for licensing BWR/2-6 power plants within the applicable licensing bases. LOCA events are analyzed to evaluate the reactor system response including, specifically, the peak cladding temperature (PCT), local cladding oxidation and core-wide cladding oxidation. This application report addresses the capability of TRACG to demonstrate compliance with the acceptance criteria for ECCS performance during a postulated LOCA as stated in 10 CFR 50.46 and to thereby show that TRACG analyses can be used as an alternate to the currently approved ECCS/LOCA analysis process for licensing calculations. The document describes the quantification of uncertainties and their effect on the realistic nominal results of TRACG analyses to provide a “licensing calculation.” By definition, this licensing calculation bounds the true mean of the key LOCA parameters (e.g., PCT) with a 95% probability at a 95% confidence level. The LOCA parameters so derived are shown to comply with the corresponding licensing requirements (e.g., $PCT_{95/95} < 2200$ F) for the most severe LOCA.

The transient analysis of LOCA events addresses the uncertainties and biases in the models and plant parameters by means of a statistical method described in Section 7. Conservative values may be used for some plant parameters for convenience. The uncertainties (and/or biases) considered include the following:

- Model uncertainties
- Experimental uncertainties
- Uncertainties related to effects of scale
- Plant uncertainties

In general, uncertainties may be dependent on the plant, the fuel type, and the LOCA event so that changes in the statistical analysis may be required as these factors change. Demonstration of the statistical analysis and the criteria for modification of the analysis are provided in this report.

The overall analysis approach described herein is consistent with the Code Scaling Applicability and Uncertainty (CSAU) analysis methodology [16] and Regulatory Guide (RG) 1.157 [17]. Conformance with both the CSAU methodology and the Regulatory Guide is demonstrated in subsequent sections.

1.3 SCOPE OF REVIEW

GEH requests that the NRC approve TRACG for use as an alternative to previously approved methods for analyzing and demonstrating compliance with licensing limits for ECCS/LOCA in BWR/2-6 plants. The currently approved process using SAFER/GESTR would be retained. Upon approval, the new process using TRACG becomes available as an optional approved method.

The scope includes all LOCA transients for which the SAFER methodology has been approved, including inventory loss events such as breaks in all piping connected to the reactor vessel or inadvertent actuation of safety/relief valves. Analysis of containment response to LOCAs is not included in this application; however, mass and energy release from the reactor system can be calculated using TRACG for downstream analyses using other applications. In the TRACG application, the containment conditions will be treated as boundary conditions for the LOCA analysis.

2.0 LICENSING REQUIREMENTS AND SCOPE OF APPLICATION

2.1 GENERAL REQUIREMENTS

The *General Design Criteria (GDC) for Nuclear Power Plants* are stipulated in Appendix A to 10 CFR 50. The applicable GDC is GDC 35, which requires each BWR to be equipped with an emergency core cooling system (ECCS) that refills the vessel in a timely manner to satisfy the requirements of the regulations for ECCS performance given in 10 CFR Part 50, §50.46 and Appendix K to 10 CFR 50 [18]. GDC 35 also requires redundant ECCS components to adequately cool the core during a LOCA.

2.2 SPECIFIC 10 CFR 50.46 LICENSING ACCEPTANCE CRITERIA FOR ECCS PERFORMANCE

The specific 10 CFR 50.46 licensing acceptance criteria for ECCS performance are as follows:

- The calculated maximum fuel element cladding temperature shall not exceed 2,200°F.
- The calculated local oxidation of the cladding shall nowhere exceed 17% of the total cladding thickness before oxidation.
- The calculated amount of hydrogen generated from the chemical reaction of the cladding with water or steam shall not exceed 1% of the hypothetical amount that would be generated if all the metal in the cladding cylinders surrounding the fuel, excluding the cladding surrounding the plenum volume, were to react.
- Calculated changes in core geometry shall be such that the core remains coolable.
- After any calculated successful initial operation of the ECCS, the calculated core temperature shall be maintained at an acceptably low value, and decay heat shall be removed for the extended period of time required by the long-lived radioactivity.

2.3 ANALYSIS REQUIREMENTS

The calculational framework for assessment of ECCS performance in terms of core behavior is called an “evaluation model.” The evaluation model includes: one or more computer programs; the mathematical models, assumptions and correlations included in the programs; the procedure for selecting and processing each program’s input and output information; the specification of analysis elements not included in the computer programs; and the values of parameters and all other information necessary to specify the calculation procedure.

On September 16, 1988, the NRC staff amended the requirements of §50.46 and Appendix K to reflect the improved understanding of ECCS performance obtained through the extensive research performed since the promulgation of the original requirements in January 1974. Paragraph 50.46 (a)(1) permits the use of a realistic evaluation model. It also requires that the uncertainty in the realistic evaluation model be quantified and considered with the applicable limits in Paragraph 50.46 (b) listed above to ensure that there is a high probability that the criteria will not be exceeded. Regulatory Guide 1.157 [17] describes models, correlations, data,

model evaluation procedures and methods that are acceptable to the NRC staff for a realistic or best-estimate calculation of ECCS performance during a LOCA and for estimating the uncertainty in the calculation. Both the NRC and the Advisory Committee on Reactor Safeguards (ACRS) have stated that the CSAU methodology [16] is in full compliance with Regulatory Guide 1.157. Compliance of the GEH methodology for ECCS/LOCA analysis with Regulatory Guide 1.157 is demonstrated in Section 2.5.1. Conformance with the CSAU process is shown in Section 2.5.2.

RG 1.203 "Transient and Accident Analysis Methods" was issued by the Office of Regulatory Research in December 2005 [77]. The primary focus of this regulatory guide is the Evaluation Model Development and Assessment Process (EMDAP). The guide builds on the first 10 steps of the CSAU process covering code development, assessment and acceptance. Many features of RG 1.203 are similar to those in the CSAU methodology.

2.4 STANDARD REVIEW PLAN GUIDELINES (NUREG-0800)

NRC Standard Review Plan (SRP) guidelines covering the EMDAP are given in Reference [19]. The guidelines for review of ECCS/LOCA safety analysis are identified in Section 15.6.5, *Loss-of-Coolant Accidents Resulting from Spectrum of Postulated Piping Breaks Within the Reactor Coolant Pressure Boundary*. Section 15.0.2 *Review of Transient and Accident Analysis Methods* was issued by the Office of Nuclear Reactor Regulation in December 2005. This is complementary to RG 1.203 and covers the review process for the evaluation models. It provides review guidance on the acceptability of the elements of the evaluation model with respect to its implementation. It also provides for exceptions for minor modifications to existing approved codes, where all the elements of the review process are not required.

2.5 PROPOSED APPLICATION METHODOLOGY

TRACG is a complete transient thermal-hydraulic model and, as such, it will be used to calculate the entire LOCA transient. TRACG calculates the PCT, local oxidation and core-wide oxidation. Thus, conformance with Criteria 1 through 3 of 10 CFR 50.46 is demonstrated by the TRACG analysis results. As discussed in Reference [23], conformance with Criterion 4 (coolable geometry) is demonstrated by conformance to Criteria 1 and 2. The bases and demonstration of compliance with Criterion 5 (long-term cooling) are also documented in Reference [23] and do not need to be evaluated as part of the TRACG ECCS/LOCA analysis.

2.5.1 Conformance with Regulatory Guide 1.157

The proposed application methodology using TRACG for BWR ECCS/LOCA analyses conforms to the guidance provided in Regulatory Guide 1.157, "Best-Estimate Calculations of Emergency Cooling System Performance" [17]. This section shows how the proposed application methodology aligns point-by-point with RG 1.157.

Regulatory Guide 1.157 describes models, correlations, data, model evaluation procedures and methods that are acceptable to the NRC staff for meeting the requirements for a realistic or

best-estimate calculation of ECCS performance during a LOCA and for estimating the uncertainty in that calculation. It also describes the acceptable features of best-estimate computer codes and acceptable methods for determining the uncertainty in the calculations. The guide lists TRAC-BWR as an acceptable code for best-estimate calculations of ECCS performance. Table 2.5-1 compares specific features of the GEH methodology with the requirements described in Regulatory Guide 1.157.

Table 2.5-1 Key RG 1.157 Elements and Evaluation of TRACG Process

Regulatory Position 1: Best-Estimate Calculations		
Staff Position	GEH Process	Evaluation
Licensees may use TRAC-PWR, TRAC-BWR, RELAP5, COBRA and FRAP codes	TRACG, a derivative of TRAC-BWR, is used.	TRACG uses the same structure and field equations as TRAC-BF1. The bulk of the constitutive relations are the same [1]. Differences are listed in Appendix A of Reference [1]. TRACG is in the family of acceptable codes.
Licensee must demonstrate that the code and models used are acceptable and applicable to the specific facility over the intended operating range.	Description of models [1] and qualification against test data [2] demonstrate applicability.	Range of models and correlations (TRACG Model Report [1]) and model acceptability by qualification against test data (TRACG Qualification Report [2]) reviewed by NRC.
Licensee must quantify uncertainty for the specific application.	Uncertainty is quantified in this report for ECCS/LOCA application.	Uncertainty quantified by propagation of individual model uncertainties through a Monte-Carlo process. Process conforms with CSAU and Regulatory Guide guidelines.
The model should be compared with applicable experimental data and should predict the mean of the data.	TRACG evaluations against a wide range of applicable test data generally predict the mean of the data [2].	Bias and uncertainty in the TRACG predictions are quantified in the Qualification Report [2].
Effects of all important variables should be considered.	TRACG capability to treat important phenomena is addressed in Section 3.0 of this report.	TRACG considers all important LOCA parameters.
Best-estimate code should be compared with applicable experimental data (e.g., separate effects tests and integral simulations of LOCAs) to determine overall uncertainty and bias.	Comparisons are made in the Model Report [1] and Qualification Report [2] for separate effects and integral tests.	This report provides a comparison of key integral tests with the TRACG calculations. Statistical bands on TRACG calculations, generated using the TRACG individual uncertainties, demonstrate data coverage by the overall calculational uncertainty and bias.

Table 2.5-1 (Cont'd) Key RG 1.157 Elements and Evaluation of TRACG Process

Regulatory Position 3: Best-Estimate Code Features		
3.1 Initial and Boundary Conditions and Equipment Availability		
Staff Position	GEH Process	Evaluation
Most limiting initial conditions expected over the life of the plant should be used.	Most limiting operating conditions (e.g., power/flow, pressure, exposure) have been determined.	Limiting operating conditions are used in the analyses as explained in Section 8.0.
Given the assumed initial conditions, relevant factors such as the actual total power, actual peaking factors, and actual fuel conditions should be used.	Rated power and Technical Specification thermal limits are used. [[]]	Limiting, but possible, conditions are employed.
The calculations should be performed over the spectrum of possible break sizes up to a full double-ended break of the largest pipe. Effects of longitudinal splits with the split area equal to twice the cross-sectional area of the pipe should be included.	The full spectrum of breaks is analyzed. The split break evaluation has no specific consideration of break geometry; the conditions upstream of the break are determined by flow from both sides of the break location.	The break spectrum is analyzed to identify the case leading to the highest PCT.

Table 2.5-1 (Cont'd) Key RG 1.157 Elements and Evaluation of TRACG Process

3.1 Initial and Boundary Conditions and Equipment Availability		
Staff Position	GEH Process	Evaluation
Other boundary and initial conditions (equipment availability, control systems and operator actions) should be based on plant technical specification limits.	Trips such as scram, MSIV closure, and ADS opening are based on technical specification limits. Instrument setpoints and equipment performance are set to their analytical limits. The LOCA analysis takes no credit for non-safety systems to mitigate the accident. When the expected operation of a non-safety system can cause the results to be more severe (e.g., bypass valve pressure regulation), it is considered.	Analytical values corresponding to the technical specification limits are used with account taken for their uncertainties. No credit is taken for non-safety systems or for mitigating operator actions.
Single failure and loss of onsite and offsite power should be considered.	Consistent with the requirement of General Design Criteria 35, both loss of onsite power and loss of offsite power are assumed individually. System availability and system responses to loss of either onsite or offsite power is modeled [[]] Sensitivities to single failures are considered.	Process conforms to Regulatory Guide and Appendix A of 10 CFR 50.
3.2 Sources of Heat During a LOCA		
3.2.1 Initial Stored Energy of the Fuel		
Staff Position	GEH Process	Evaluation
The steady-state temperature distribution and stored energy in the fuel should be calculated on a best-estimate basis.	Because the stored energy is dependent on the plant operating history at the time of LOCA, a realistic operating trajectory is used to calculate this parameter.	Reasonable approach, considering operating states.
An acceptable model should recognize the effects of fuel burnup, fuel pellet cracking and relocation, cladding creep, and gas mixture conductivity.	The PRIME [76] model includes all of these effects. The TRACG dynamic gap conductance model (Section 7.5.2 of Reference 1) is initialized by using inputs provided by PRIME.	PRIME [76] has been separately reviewed and accepted for use by the NRC staff.
The model must be checked against several sets of relevant data.	The PRIME [76] model has been extensively compared with irradiated BWR fuel data.	PRIME [76] has been separately reviewed and accepted for use by the NRC staff.

Table 2.5-1 (Cont'd) Key RG 1.157 Elements and Evaluation of TRACG Process

3.2.2 Fission Heat, 3.2.3 Decay of Actinides, 3.2.4 Fission Product Decay Heat		
Staff Position	GEH Process	Evaluation
Fission heat should be based on best-estimate reactor kinetics calculations. The point kinetics formulation is acceptable.	[[]]	The void reactivity effect plays a dominant role in the fission power magnitude during the initial transient following a break. [[]]
The heat from radioactive decay of actinides, including neptunium and plutonium generated during operation, as well as isotopes of uranium, should be calculated in accordance with fuel cycle history.	Heat from radioactive decay of actinides, including neptunium, plutonium and isotopes of uranium, is included in the calculation.	The model used is in compliance with Regulatory Guide guidelines.
The heat generation from radioactive decay of fission products should be calculated in accordance with the 1979 American Nuclear Society (ANS) standard.	The heat generation from radioactive decay of fission products is calculated in accordance with the 1979 ANS standard. [[]]	Calculations are made in accordance with the 1979 ANS Standard. Sensitivities to variations in voids, enrichment and operating history are shown in Appendix B of Reference [21].

NEDO-33005-A Revision 1
Non-Proprietary Information – Class I (Public)

3.2.5 Metal-Water Reaction Rate		
Staff Position	GEH Process	Evaluation
The metal-water reaction rate should be calculated with a best-estimate model. For rods calculated to rupture, oxidation of the inside of the cladding should be calculated.	The Cathcart correlation (Equation 6.6-136 of Reference [1]) is used at all temperatures. The model is also used on the inside surface of the cladding if the fuel rod perforates.	Acceptable model is used. Metal-water reaction is not important for most BWRs, as PCTs are below 1200 K (1700°F). It is only significant for BWR/2 large breaks.
Below 1900°F, model should be checked against appropriate data. It should recognize the effects of steam pressure, pre-oxidation of cladding, deformation during oxidation and internal oxidation from both steam and UO ₂ fuel.	The Cathcart correlation is used. This will tend to be conservative at temperatures below 1310 K (1900°F). Effects of internal oxidation from UO ₂ and steam pressure effects are not included.	Conservative, but acceptable model is used.
Above 1900°F, Cathcart’s data is acceptable.	The Cathcart correlation is used.	In conformance with the Regulatory Guide position.
3.2.6 Heat Transfer from Reactor Internals		
Staff Position	GEH Process	Evaluation
Heat transfer (HT) from piping, vessel walls and internal hardware should be calculated in a best-estimate manner.	TRACG models pipe and vessel walls and internal hardware as “heat slabs.” Conduction through the slabs is modeled with 1-D nodalization (Section 4 of Reference [1]). Geometrical details (e.g., penetrations) are not simulated but mass and surface area of structures are preserved. Heat transfer coefficients (HTCs) to the fluid in contact with the heat slabs include Single-phase convection, subcooled and nucleate boiling and condensation as appropriate (Section 6.6 of Reference [1]).	Heat transfer from reactor internals is modeled in a best-estimate manner to ensure that heat release to the adjoining fluid is calculated accurately. TRACG simulations of integral experiments (e.g., Two-Loop Test Apparatus (TLTA) & Full Integral Simulation Test (FIST)) show good comparisons for vessel pressure and lower plenum voiding. Heat slab nodalization and heat transfer coefficient sensitivity studies have been performed [2]. Uncertainties are primarily associated with the heat transfer coefficients.
3.3 Reactor Core Thermal/Physical Parameters		
3.3.1 Thermal Parameters for Swelling and Rupture of the Cladding and Fuel Rods		
Staff Position	GEH Process	Evaluation
The model should calculate fuel cladding swelling and rupture resulting from the temperature distribution in the cladding and from the pressure difference between the inside and outside of the cladding, both as a function of time.	TRACG calculates swelling and rupture based on an empirical fit to experimental data for BWR size fuel rods. The cladding strain is a function of the cladding temperature and the hoop stress (Section 7.5.3.3 of Reference [1]).	TRACG model for cladding swelling is empirically based and conforms with the guidance in the Regulatory Guide.

NEDO-33005-A Revision 1
Non-Proprietary Information – Class I (Public)

<p>The degree of swelling and rupture should be taken into account in the calculation of gap conductance, cladding oxidation and embrittlement, hydrogen generation, and heat transfer and fluid flow outside of the cladding.</p>	<p>The change in gap size affects the gap conductance calculation (Section 7.5.2.5 of Reference [1]). Cladding oxidation and hydrogen generation are functions of the cladding surface area. Changes in cladding embrittlement are not calculated by TRACG. While the effects of the area change on the flow outside the rod can be handled by TRACG, the design process does not account for this effect. Experimental data have shown insensitivity to this effect.</p>	<p>Cladding embrittlement is not calculated in TRACG. Requirements for coolable geometry are met by meeting criteria on PCT and oxidation.</p>
<p>The calculation of fuel and cladding temperatures as a function of time should use values of gap conductance and other thermal parameters as functions of temperature and time.</p>	<p>TRACG has a dynamic gap conductance model (Section 7.5.2 of Reference [1]) which accounts for changes in gap conductance, plenum temperature, rod internal pressure and thermal properties with time.</p>	<p>The TRACG gap conductance model meets the requirements of the Regulatory Guide.</p>
<p>The calculation of the swelling of cladding should take into account spatially varying cladding temperatures, heating rates, anisotropic material properties, asymmetric deformation of cladding, and fuel rod thermal and mechanical parameters.</p>	<p>TRACG simulates the fuel rod with axial and radial nodes. The calculation of cladding swelling accounts for spatial variations in temperatures and heating rates. Asymmetric effects are accounted for through the use of test data.</p>	<p>TRACG model for cladding swelling is empirically based and meets Regulatory Guide requirements.</p>
3.3.2 Other Core Thermal Parameters		
Staff Position	GEH Process	Evaluation
<p>Physical and chemical changes in in-core materials (e.g., eutectic formation, phase change.) should be included as necessary.</p>	<p>Material properties for zircaloy account for the alpha and beta phases. The Zr-H₂O reaction to produce ZrO₂ is modeled. Melting of UO₂ is precluded by the GE SAFDL applied for AOO transients and this bounds all LOCA calculations provided the 2,200°F limit on PCT is satisfied. Eutectic formations are not significant provided the 2,200°F limit on PCT is satisfied.</p>	<p>The phenomena necessary for BWR LOCA are modeled.</p>

NEDO-33005-A Revision 1
Non-Proprietary Information – Class I (Public)

3.4.1 Break Characteristics and Flow		
Staff Position	GEH Process	Evaluation
The critical flow model should consider the fluid conditions at the break location, upstream and downstream pressures, and break geometry.	The TRACG critical flow model (Section 6.3 of Reference [1]) accounts for break conditions (subcooled, two-phase or steam) and upstream and downstream pressures. Break geometry can be treated with the use of discharge coefficients.	Split and double-ended breaks can be analyzed. The TRACG model is empirically based but accounts for all relevant parameters and has been qualified by extensive comparisons to data.
Critical flow model should be checked against an acceptable set of relevant data; recognize thermal nonequilibrium conditions when the fluid is subcooled; provide a means of transition from nonequilibrium to equilibrium conditions.	The TRACG critical flow model (which is also used in TRACBD1 and RELAP5) has been extensively checked against data [26]. Assessment studies with TRACG [2] include data from the Marviken, PSTF, Edwards, TLTA, FIST, and FIX facilities.	TRACG model conforms with Regulatory Guide guidance.
The uncertainties and bias of the model should be stated, as well as the range of applicability.	The uncertainty and bias of the TRACG critical flow model have been quantified (Section 6.3.6 of Reference [1]).	TRACG model conforms with Regulatory Guide guidance.
3.4.2 ECC Bypass		
Staff Position	GEH Process	Evaluation
Emergency Core Coolant (ECC) bypass during the blowdown (BD) phase of a LOCA should be calculated in a best estimate manner. One-dimensional models justified through analysis and data are acceptable.	TRACG models “flooding” or CCFL-like phenomena through a Kutateladze type of correlation (Section 6.1.7.2 of Reference [1]). The correlation used in TRACG is conservative for predicting ECC bypass (Section 6.1.7.4 of Reference 1).	The ECC bypass phenomenon is important for PWRs but is not significant for BWRs (Section 6.1.7.4 of Reference [1]). Therefore, a conservative model is acceptable for BWR analysis.
3.5 Noding Near the Break and ECCS Injection Point		
Staff Position	GEH Process	Evaluation
Sufficient sensitivity studies should be performed on the noding and other important parameters to ensure calculations provide realistic results.	Sensitivities to nodalization near the break and ECC injection point have been addressed in the TRACG Qualification LTR [2]. Nodalization is consistent between test facility and BWR models in these regions. Uncertainties in other parameters are addressed as Phenomena Identification and Ranking Table (PIRT) parameter uncertainties.	Process conforms with Regulatory Guide guidance.

NEDO-33005-A Revision 1
Non-Proprietary Information – Class I (Public)

3.6 Frictional Pressure Drop		
Staff Position	GEH Process	Evaluation
The frictional pressure drop in pipes and other components should be calculated using models that include variation of friction factor with Reynolds number and effects of two-phase flow effects on friction.	Wall friction is calculated with a fit to the Moody curves as a function of Reynolds number and surface roughness (Section 6.2.1.3 of Reference [1]). A modified two-phase Chisholm multiplier is used (Section 6.2.1.4 of Reference [1]).	Models conform with Regulatory Guide guidance.
The gravitational, friction and acceleration components of pressure drop should be consistently calculated.	The terms in the two-phase momentum equations are consistently formulated and calculated (Section 3 of Reference [1]).	Most data comparisons are for total pressure drop. Because the void fraction is independently qualified, these comparisons validate the consistency of the pressure drop components.
Model should be checked against experimental data and the bias and uncertainty should be stated.	The frictional pressure drop models in TRACG have been extensively compared with experimental data for tubes and bundles and estimates of the mean bias and uncertainty have been determined (Section 6.2.1.6 of Reference [1]).	Models conform with Regulatory Guide guidance.
3.7 Momentum Equation		
Staff Position	GEH Process	Evaluation
The momentum equation should include terms for: 1) temporal change in momentum, 2) momentum convection, 3) area change momentum flux, 4) momentum change due to compressibility, 5) pressure loss resulting from wall friction, 6) pressure loss resulting from area change, and 7) gravitational acceleration.	The momentum equations are formulated for each phase and contain all the relevant terms (Section 3.1.2 of Reference [1] for the differential form; Sections 3.2.1.1 and 3.2.2.1 of Reference [1] for the difference form).	Equations for individual phase flows are used with the appropriate interfacial terms.
Technical basis should be demonstrated with data and analysis.	The validity of the momentum equations is demonstrated by comparisons with pressure drop, void fraction and critical flow data (Sections 3.5, 3.1 and 3.4 of Reference [2]).	The momentum equations represent best-estimate models and are adequately qualified against test data.

NEDO-33005-A Revision 1
Non-Proprietary Information – Class I (Public)

3.8 Critical Heat Flux		
Staff Position	GEH Process	Evaluation
Best-estimate models developed from appropriate steady-state or transient experimental data should be used for calculating critical heat flux (CHF).	TRACG uses the best-estimate GEXL correlation for calculation of CHF (Section 6.6.6.1 of Reference [1]). The GEXL correlation is based on an extensive data base for steady-state CHF in BWR rod bundles. At low flow conditions, a modified Zuber correlation is used (Section 6.6.6.1 of Reference [1]).	The correlations cover the range of LOCA conditions. The correlations have been validated for time varying conditions characteristic of operational transients and LOCAs (Sections 3.2.1 and 5.1.2 of Reference [2]).
Return to nucleate boiling is allowed if justified by local fluid and surface conditions.	TRACG allows a return to transition boiling if the wall temperature is below T_{min} and the local quality is less than the critical quality. Nucleate boiling is restored when the wall temperature is less than T_{CHF} .	The TRACG model has been validated against experimental data from BWR rod bundles (Sections 5.1.2, 5.2.3 and 3.6.2 of Reference[2]).
Technical basis should be demonstrated with data and analysis.	The TRACG CHF model has been extensively qualified for transient conditions simulating LOCAs [2].	The TRACG model conforms with the guidance in the Regulatory Guide.
3.9 Post-CHF Heat Transfer		
Staff Position	GEH Process	Evaluation
A model for post-CHF heat transfer should: <ul style="list-style-type: none"> a. Be checked against an acceptable set of relevant data. b. Recognize effects of liquid entrainment, thermal radiation, thermal nonequilibrium, low and high mass flow rates, low and high power densities and saturated and subcooled inlet conditions. 	TRACG calculates post-dryout heat transfer in two regimes: (1) dispersed droplet flow at high flow and quality; and (2) inverted annular flow at low flow and quality. These heat transfer regimes are described in Sections 6.6.9 and 6.6.10 of Reference [1]. Liquid entrainment is considered. The TRACG model allows for different temperatures for the two phases. The radiation model is described in Section 6.6.12 of Reference [1]. The Bromley correlation for low quality film boiling has been compared against a range of bundle reflooding data (Section 6.6.9.3 of Reference [1]). Comparisons against data at high qualities are shown in Section 6.6.10.3 of Reference [1]. Comparisons have also been made against Oak Ridge National Laboratory (ORNL) tests (Section 3.2.1 of Reference [2]).	The correlations cover the range of expected LOCA conditions and have been validated against appropriate data sets.

NEDO-33005-A Revision 1
Non-Proprietary Information – Class I (Public)

Correlations for heat transfer from uncovered fuel bundles should: a. Be checked against an acceptable set of relevant data. b. Recognize the effects of radiation and of laminar, turbulent and transition flows.	The correlations used in the uncovered portion of the bundle are described in Section 6.6.10 of Reference 1. The single-phase steam correlation includes the laminar, turbulent and transition regimes. Additionally, the effects of droplets are accounted for through the Sun-Tien-Gonzalez correlation (Equation 6.6-49). The radiation heat transfer model is described in Section 6.6.12 of Reference 1.	The models are in conformance with the requirements of the Regulatory Guide. Comparisons with core spray (CS) data are shown in Section 6.6.10.3 of Reference 1.
Uncertainties and bias in the models for post-CHF heat transfer should be stated.	Model uncertainty and bias in the low and high void fraction film boiling regimes are provided in Sections 6.6.9.3 and 6.6.10.3 of Reference 1.	The TRACG model conforms with the guidance in the Regulatory Guide.
3.10 Pump Modeling		
Staff Position	GEH Process	Evaluation
The characteristics of rotating primary system pumps should be derived from a best-estimate dynamic model that includes momentum transfer between the fluid and the rotating member, with variable speed as a function of time. The model for two-phase flow should be verified by comparison to applicable data.	The governing equations for the pump are given in Section 7.2.1 of Reference 1. The momentum equation for the pump component includes a term for the momentum transfer from the rotating member to the fluid. Homologous curves are used to characterize the pump head and torque as a function of the fluid volumetric flow and pump speed. Degradation factors based on test data are applied to account for two-phase effects on pump performance.	The TRACG model conforms with the guidance in the Regulatory Guide.
3.11 Core Flow Distribution During Blowdown		
Staff Position	GEH Process	Evaluation
The core flow through the hottest region (no larger than one fuel bundle) should be calculated as function of time. Calculations should account for any crossflow between regions.	The high power bundle is modeled as a separate region in TRACG.	In the BWR configuration, the channels surrounding each fuel bundle preclude crossflow between bundles.

NEDO-33005-A Revision 1
Non-Proprietary Information – Class I (Public)

3.12 Post-Blowdown Phenomena		
3.12.1 Containment Pressure		
Staff Position	GEH Process	Evaluation
The containment pressure used for evaluating effectiveness during the post-blowdown phase of a LOCA should be best- estimate and include the effects of containment heat sinks.	The containment is not explicitly modeled for TRACG LOCA analysis. A sensitivity analysis is performed to define the limiting pressure boundary condition for the flow paths between the reactor vessel and the containment.	A TRACG containment model is not required for the present application as licensing approval is not sought for containment modeling. LOCA analysis uses conservative containment boundary conditions and this conforms to the regulation.
3.12.2 Calculation of Post-Blowdown Thermal Hydraulics for Pressurized Water Reactors		
Not Applicable		
3.12.3 Steam Interaction With ECC Water in Pressurized Water Reactors		
Not Applicable		
3.12.4 Post-Blowdown Heat Transfer for Pressurized Water Reactors		
Not Applicable		
3.13 Convective Heat Transfer Coefficients for BWR Rods Under Spray Cooling		
Staff Position	GEH Process	Evaluation
Following the blowdown period, convective heat transfer coefficients should be determined based on the calculated fluid conditions and heat transfer modes.	Following blowdown, TRACG uses convective heat transfer coefficients appropriate to the heat transfer regime. The heat transfer selection logic is shown in Section 6.6.2 of Reference 1.	The TRACG models have been extensively qualified by tests simulating jet pump and external pump BWRs [2].
During the period following lower plenum flashing, but prior to ECC initiation, heat transfer models should include steam cooling or two-phase flow convection.	Following lower plenum flashing, TRACG applies convective heat transfer coefficients appropriate to the heat transfer regime. The heat transfer selection logic is shown in Section 6.6.2 of Reference 1. Steam cooling, nucleate boiling and film boiling are considered.	TRACG models for post lower plenum flashing heat transfer phenomena are best-estimate and conform with the guidance in the Regulatory Guide.

NEDO-33005-A Revision 1
Non-Proprietary Information – Class I (Public)

Following ECC initiation, but prior to reflooding, heat transfer models should account for rod-to-rod variations in heat transfer.	Best-estimate correlations are used for steam/droplet cooling (Section 6.6.10 of Reference 1), and rod-to-rod and rod-to-channel radiative heat transfer in an absorbing medium (Section 6.6.12 of Reference 1). The steam/droplet heat transfer coefficients distinguish between interior and peripheral rods based on data. TRACG spray heat transfer models have been validated against spray cooling tests (Section 6.6.10.3 of Reference 1).	TRACG has the required models. These effects are more important for BWR/2 plants, which rely solely on core spray heat transfer (CSHT) for termination of cladding heatup, than for jet pump plants.
After the two-phase level reaches the level under consideration, a best-estimate heat transfer model should be used. This model should include the effects of any flow blockage.	TRACG applies convective heat transfer coefficients appropriate to the heat transfer regime. The heat transfer selection logic is shown in Section 6.6.2 of [1]. Typically, the modified Bromley correlation (Section 6.6.9 of Reference 1) is used at low void fractions.	Effects of flow blockage due to clad swelling are not considered in TRACG other than by possible adjustments in the user inputs. Experimental data [27] have shown minor sensitivity to even large amounts of flow blockage.
Thermal hydraulic models that do not consider multiple channels should be compared with experimental data or more detailed calculations to ensure that all important phenomena are adequately calculated.	Multiple channels are modeled in TRACG.	Comparisons with data from the 30° Steam Sector Test Facility (Section 5.4 of Reference 2) have shown the capability of TRACG to model the multi-channel phenomena seen in the refill/reflood (RR) phase of a BWR LOCA.
3.14 BWR Channel Box Under Spray Cooling		
Staff Position	GEH Process	Evaluation
Following the blowdown period, heat transfer from the channel box and wetting of the channel box should be determined based on the calculated fluid conditions on both sides of the channel box and should make use of best-estimate rewetting models that have been compared with applicable experimental data.	Following blowdown, TRACG applies convective heat transfer coefficients appropriate to the heat transfer regime on both sides of the channel box. The heat transfer selection logic is shown in Section 6.6.2 of [1]. TRACG employs a quench front propagation correlation (Section 6.6.13 of [1]) that is a fit to a two-dimensional conduction solution. These models have been extensively validated against core spray cooling data ([25], [2]).	The TRACG model conforms with the guidance in the Regulatory Guide.
3.15 Special Considerations for a Small-Break LOCA in Pressurized Water Reactors		
Not Applicable		

NEDO-33005-A Revision 1
 Non-Proprietary Information – Class I (Public)

3.16 Other Features of Best-Estimate Codes		
Staff Position	GEH Process	Evaluation
Completeness: Comparisons of the overall calculations to integral experiments should be performed to ensure that important phenomena can be predicted.	Comparisons of TRACG predictions to integral experiments are shown in Section 5 of Reference 2. An overall assessment of TRACG capabilities to predict these data is shown elsewhere in this report.	The integral test comparisons show that all major LOCA phenomena are adequately represented by TRACG.
Data Comparisons: Individual models should be compared against data. Uncertainty and bias in models should be evaluated.	Comparisons of TRACG against separate effects data are shown in Sections 3.1 through 3.9 of Reference 2. An integral evaluation of model bias and uncertainty is made elsewhere in this report.	The separate-effects test comparisons show that the individual models in TRACG are in good agreement with the test data..
Regulatory Position 4: Estimation of Overall Computational Uncertainty		
4.1 General		
Staff Position	GEH Process	Evaluation
The calculational uncertainty should include the uncertainty due to individual models (“code uncertainty”), experimental data, boundary and initial conditions, fuel behavior and simplifying assumptions.	Uncertainties due to individual models, boundary and initial conditions and fuel behavior are accounted for explicitly. Some boundary and initial conditions are chosen conservatively. The selection of experimental data for model validations was based on adequate accuracy in the experiments. Deviations between test data and TRACG calculations implicitly include experimental uncertainties. Effects of simplifying assumptions are implicit in comparisons with integral tests.	The required uncertainty components are included in the calculational uncertainties used for TRACG BWR LOCA analyses.
A 95% probability level is acceptable for comparing best-estimate predictions to the applicable limits of Paragraph 50.46(b) of 10 CFR 50.	Calculations are expected to bound the 95th percentile value of PCT and cladding oxidation.	The TRACG model conforms with the guidance in the Regulatory Guide.

NEDO-33005-A Revision 1
Non-Proprietary Information – Class I (Public)

Justification should be provided for the assumed parameter distributions and ranges.	Justification for the assumed parameter distributions and ranges is provided in Section 5 of this report.	This corresponds to CSAU Step 4 on ranging of the parameters.
The evaluation of PCT at the 95% level need only be performed for the limiting break. Justification must be provided that the overall calculational uncertainty at the limiting condition bounds that at the other conditions.	Calculations are performed for the limiting break. Justification that the overall calculational uncertainty at the limiting condition bounds that at the other conditions is provided elsewhere in this report.	The TRACG model conforms with the guidance in the Regulatory Guide.

2.5.2 Conformance with CSAU Methodology

The TRACG LOCA application methodology also addresses all the elements of the NRC-developed CSAU evaluation methodology as documented in the report *Quantifying Reactor Safety Margins, Application of Code Scaling, Applicability, and Uncertainty Evaluation Methodology to a Large-Break Loss-of-Coolant Accident* [16]. The CSAU report describes a rigorous process for evaluating the total model and plant parameter uncertainty for a nuclear power plant calculation. Further details on the CSAU methodology are contained in the NRC Regulatory Guide 1.157. The CSAU methodology incorporates the elements of phenomena identification and ranking, documentation of models, model assessment against Systems Effects Tests (SETs) and Integral System Tests (ISTs) for the key phenomena, and quantification of uncertainties due to the models, scaling and plant parameters. In the currently approved SAFER/GESTR process, a statistically based Upper Bound PCT is derived but not used directly. As stated in the previous section, it is utilized to demonstrate the conservatism in the licensing approach, which incorporates the models and correlations required by Appendix K. In the CSAU process, the overall model uncertainty is derived from the propagation of individual model uncertainties through code calculations; IST experimental comparisons are used as a check on the derived uncertainty. The CSAU approach provides the framework by which uncertainty analyses are performed; however, it is flexible in that many of the details required to fully describe its application to particular analyses are not defined. Sections 4 through 7 of this report provide additional details to augment the CSAU framework and define the statistical methodology for application of TRACG to the BWR/2-6 LOCA analyses. Section 8 of the report documents representative results from a large number of demonstration calculations in order to further define and illustrate the LOCA applications.

The CSAU methodology consists of 14 steps, as summarized below and outlined in Table 2.5-2. The summary indicates the manner in which each step is addressed in this report.

1. Specify scenario.

The LOCA scenarios include the full range of pipe breaks for the distinct BWR product lines (BWR/2; BWR/3,4; and BWR/5,6). The scenarios are differentiated by break size and location. Typical BWR LOCA scenarios are described in Section 3.2. The LOCA transient is divided into Blowdown and Refill/Reflood phases so that the application

methodology can be focused on the processes and components that are important during each phase.

2. Select nuclear plant(s).

The included plant types are BWR/2s, BWR/3s, BWR/4s, BWR/5s, and BWR/6s. Both jet pump and non-jet pump BWR designs are included. For the jet pump designs, the recirculation flow control systems include motor-generator designs, flow-control valve designs and variable-speed pump designs. The ESBWR was analyzed using TRACG and that application has been separately reviewed and approved by the NRC [39].

3. Identify and rank phenomena.

All processes and phenomena that occur during an event do not equally influence plant behavior. The candidate phenomena are reduced to a manageable set by identifying and ranking the phenomena with respect to their influence on the primary safety criteria. The phases of the events and the important components are investigated. The processes and phenomena associated with each component are examined. Cause and effect are differentiated. After the processes and phenomena have been identified, they are ranked with respect to their effect on the primary safety criteria for the event. A phenomena identification and ranking table (PIRT) is established to guide the subsequent uncertainty quantification. The PIRTs for ECCS/LOCA are developed in Section 3.0.

4. Select frozen code.

TRACG04P is the frozen code selected for the analysis. TRACG04P has also been used for AOO analysis [4]. All aspects of management, control, maintenance, testing and documentation of the code are governed by GEH internal procedures (see Section 6.1).

5. Document code.

The details of the models are contained in the TRACG Model Description LTR [1]. A summary description of the TRACG assessment is provided in Section 4.2 and the details are contained in the TRACG Qualification LTR [2]. This report describes the application process. The User' Manual [29] provides guidance on the use of the code.

6. Determine code applicability.

To demonstrate applicability, one must begin with capability. Capability to calculate an event for a nuclear power plant rests on four elements: (1) conservation equations, which provide the code capability to address global processes; (2) constitutive correlations and models, which provide code capability to model and scale particular processes; (3) numerics, which provide code capability to perform efficient and reliable calculations; and (4) structure and nodalization, which address code capability to model plant geometry and perform efficient and accurate plant calculations. All four elements must be considered when evaluating the code capability for a specific application. Code capability is only one aspect needed to demonstrate that the code is applicable. Applicability also implies that the capability of the code has been demonstrated by

actually applying the code in the intended manner and then assessing the results. The capability of TRACG to model phenomena that are important to BWR simulations has been addressed generically in Table 4.1-1 in Section 4.1. Assessment aspects have also been addressed generically by Table 4.2-1 in Section 4.2.

7. Establish assessment matrix.

The determination of uncertainty for a computer code must be based on a sufficient data set, which necessarily will include both separate and integral effects tests and available plant data. All phenomena and components that were identified and ranked important in the PIRT for the selected events for the nuclear power plant must be covered by the assessment matrix. The approach is to start generically at a high level and work down to the detailed levels. At the more detailed level where the specific scenario has been characterized, some PIRT rankings may be reduced because the phenomena are not important for that particular application scenario. For those highly ranked phenomena that remain, it is necessary to identify the model quantities associated with the phenomena so that the uncertainties, biases and probability distribution functions for these quantities can be determined. The LOCA PIRTs are documented in Section 3.0. The assessment coverage of the PIRTs is summarized in Table 4.2-1.

8. Define nodalization for plant calculations.

The plant model must be nodalized finely enough to represent both the important phenomena and design characteristics of the nuclear power plant but coarsely enough to remain economical. In principle, nodalization can be treated as an individual contributor to code uncertainty; however, quantification of nodalization uncertainty can be very costly. Thus, the preferred path is to establish a standard nodalization based on the assessment against separate and integral effects tests. Nodalization studies have been performed in assessing this test data in order to determine the level of detail necessary to represent the important phenomena and then consistent levels of detail have been applied to establish standard noding schemes for the BWR. The standard BWR nodalization for TRACG for ECCS/LOCA applications is defined based on the qualification and is described in the TRACG Qualification LTR [2]. The standard nodalization shown in the Qualification LTR is a representative and typical of the least-detailed nodalization that is considered acceptable. Minor details may be added or changed from the standard nodalization provided the changes are shown not to invalidate the qualification bases and the effect on modeling biases and uncertainties are assessed.

9. Determine code and experiment uncertainty.

Simulations of experiments are used to determine the code accuracy. Comparisons to separate effects test data are used to quantify the uncertainty in the individual models and correlations. Typically, experimental uncertainty is inherent in these comparisons and is not separated out. Quantification of the uncertainties in the model parameters is discussed in Section 5.1. The effect on the primary safety parameters for the nuclear

power plant can be determined by varying the inputs to the individual models by a specified amount (e.g., $+1\sigma$). The uncertainties of the code in simulating the important phenomena for LOCA are addressed in Section 8.0.

10. Determine effects of scale.

The differences for similar physical processes, at scales up to and including full scale, should be evaluated to establish a statement of potential scaling effects. For TRACG, this has been done by evaluating the experimental basis for the individual models and correlations against plant conditions, by performing qualification against separate-effects tests, integral effects tests at different scales and full-scale plant data (where plant data exist), and by using a plant nodalization based on the qualification studies. Specific needs for LOCA are addressed in Section 5.3.

11. Determine effects of plant operating conditions.

Uncertainties in the nuclear power plant simulations may result from uncertainties in plant operating state at the initiation of the transient event or in plant process parameters. For example, the plant power distribution is a function of burnup history and control rod pattern prior to the transient. Realistic variations in input and process parameters are determined with experimental data and/or analytical studies. The uncertainties are best quantified as biases and distributions, but can be treated as separate bounding biases if necessary. Specific needs for LOCA are addressed in Section 6.0.

12. Perform plant sensitivity calculations.

Nuclear power plant calculations for a given event are used to determine the code's output sensitivity (in the primary safety criteria parameters) to various plant operating conditions that arise from uncertainties in the reactor state at the initiation of the transient event or in plant process parameters. Similarly, nuclear power plant calculations are used to address the uncertainties introduced by the code models and correlations. In this manner, the sensitivities of the safety-related quantities to these parameters are evaluated individually or collectively. The nominal calculation and the sensitivity studies for LOCAs are documented in Section 8.0.

13. Combine biases and uncertainties.

In this step, all the biases and uncertainties are combined in an overall bias and uncertainty. There are different techniques that can be used, as discussed in Section 7.0. The combined bias and uncertainty for the particular safety parameters for ECCS/LOCA are determined in Section 8.0.

14. Determine total uncertainty.

The statement of total uncertainty for the code is given as an error band or a statement of probability for the limiting value of the primary safety criteria parameter. How these total uncertainties are applied in the evaluation of specified acceptable ECCS/LOCA design limits is documented in Section 9.0.

Table 2.5-2 summarizes where each step of CSAU steps are addressed for TRACG LOCA methodology.

Table 2.5-2 Code Scaling, Applicability and Uncertainty Evaluation Methodology

CSAU Step	Topic	Addressed In
1	Scenario Specification	Section 2.5.2
2	Nuclear Power Plant Selection	Section 2.5.2
3	Phenomena Identification and Ranking	Section 3.0
4	Frozen Code Version Selection	Reference [1]
5	Code Documentation	References [1], [2], [29]
6	Determination of Code Applicability	Section 4.0
7	Establishment of Assessment Matrix	Section 4.2
8	Nuclear Power Plant Nodalization Definition	Sections 8.1.1, 8.2.1, 8.3.1
9	Definition of Code and Experimental Accuracy	References [1], [2]
10	Determination of Effects of Scale	Section 5.3
11	Determination of the Effect of Reactor Input Parameters and State	Section 6.0
12	Performance of Nuclear Power Plant Sensitivity Calculations	Section 8.0
13	Determination of Combined Bias and Uncertainty	Section 7.0, 8.0
14	Determination of Total Uncertainty	Section 7.0, 8.0

2.6 IMPLEMENTATION REQUIREMENTS

The implementation of TRACG for licensing requires:

- Review and approval by the NRC of:
 1. The uncertainties documented in Section 5.0.
 2. The statistical process for analyzing ECCS/LOCA described in Section 7.0.
- A generic analysis for each BWR plant type and for a representative fuel.

The analyses performed in this report cover the LOCA break spectrum and include results for the overall biases and uncertainties to be applied to the limiting LOCAs. Specific comparisons with acceptance criteria (PCT, local oxidation and core-wide oxidation) are based on application of the statistical application processes described in

Section 7.0. These results, documented in Section 8.0 demonstrate compliance with the acceptance criteria for BWR/2 and BWR/3-6.

- Plant-specific implementation following the methodology documented in this report including the use of the generically applicable values for the uncertainties and the approved statistical process.
- Updating of the overall bias and uncertainty for subsequent plant cycles as required by criteria discussed in Section 9.0.

2.7 RANGE OF APPLICATION

The intended application is ECCS/LOCA analysis as required by 10 CFR 50.46 for BWR/2-6. This covers the entire spectrum of break sizes and locations. The break could be initiated anywhere in the operating domain for a BWR operating at or below the technical specification limits. Equipment out of service or performance relaxations can also be analyzed. The application range includes, but is not restricted to:

- Extended Power Uprate and Maximum Extended Load Line Limit Analysis Plus (MELLLA+) operating domain
- Transition and equilibrium cores
- Single loop operation (SLO)
- Automatic depressurization system (ADS) valve out of service
- Feedwater heater out of service
- Feedwater temperature reduction

3.0 PHENOMENA IDENTIFICATION AND RANKING

The critical safety parameters specified by 10 CFR 50.46 for ECCS/LOCA are PCT, maximum cladding oxidation and maximum hydrogen generation. (The requirement for a coolable geometry is implicitly satisfied when these safety parameters meet the prescribed limits. Long-term cooling (LTC) is addressed as part of the current design analysis and is not being re-evaluated as part of the TRACG analysis.) Intermediate safety parameters include the downcomer level and two-phase mixture level inside the core shroud. These safety parameters are the criteria used to judge the performance of the safety systems and the margins in the design. The values of the critical safety parameters are determined by the governing physical phenomena. Phenomena Identification and Ranking Tables (PIRTs) are used to delineate the important physical phenomena. PIRT entries (hereafter referred to simply as “PIRTs”) are ranked with respect to their effect on the critical safety parameters. For example, the PCT is determined by the reactor vessel inventory and its distribution between the various vessel regions, core power generation, core flow and core heat transfer.

The processes and phenomena that occur during a LOCA do not have an equal influence on plant behavior and, specifically, on the critical safety parameters. Accordingly, the processes and phenomena are ranked with respect to their effect on the critical safety parameters for a prescribed LOCA event. The ranking procedure differentiates the phases of the event and the system components that are important to the plant behavior during each of the phases with due consideration of cause and effect. The final ranking results from an evaluation of the relative importance of the processes and phenomena associated with each of the system components that govern the plant behavior during one or more of the event phases.

3.1 ORGANIZATION OF PIRTS FOR ECCS/LOCA

The transient response of a BWR following a Loss-of-Coolant Accident differs for the various BWR product lines and varies with break location and size. Figure 3.2-1 through Figure 3.2-4 show the typical system response to large and small breaks for a jet pump BWR. Large liquid breaks (break area greater than 0.1 m^2) are characterized by core flow coastdown, a rapid loss of inventory and relatively rapid depressurization (Figure 3.2-1 through Figure 3.2-3). There is an early boiling transition and temperature excursion in the high power fuel bundles (Figure 3.2-4) because of the power/flow mismatch. Large steam line breaks depressurize the reactor vessel rapidly but do not result in core heatup because the flashing-induced level swell keeps the core cooled by a two-phase mixture throughout the transient (Figure 3.2-1 through Figure 3.2-4).

Small breaks (break area less than 0.01 m^2) are characterized by a slow loss of inventory that can be offset by the available high pressure ECC systems. The pressure initially remains close to operating pressure, then increases in response to the closure of the main steam line isolation valves, and is subsequently controlled by safety/relief valve (SRV) actuations. When high pressure makeup is not available, the reactor vessel downcomer water level drops until it actuates the ADS. The depressurization allows the low pressure ECC systems to activate and thereby ends the heatup transient. The milder flow coastdown precludes an early boiling transition and

the fuel remains well cooled until the vessel depressurizes (Figure 3.2-4). The ADS actuation for small breaks causes them to have more or less the same transient characteristics as the larger breaks. To address the differing importance of some of the governing phenomena, however, the LOCA PIRT has been segregated into separate large and small break PIRTs.

From a LOCA perspective, the BWR reactors with jet pumps (BWR/3 to BWR/6) differ primarily in the capacity of their ECC systems and the vessel location where the ECC water is injected. The similarity of the ECC systems for the BWR/3 and BWR/4 on the one hand and for the BWR/5 and BWR/6 on the other means that they can be grouped together. In subsequent sections of this report, these two groups will be referred to generically as the “BWR/4” and “BWR/6” product lines.

The large break LOCA for a non-jet pump (BWR/2) plant has unique characteristics. For these plants, a large recirculation line break is effectively a “bottom break” for the vessel inventory and the core cannot be reflooded. Control of core heatup relies exclusively on the core spray systems. Figure 3.2-10 through Figure 3.2-12 illustrate the response of a non-jet pump plant to a large break LOCA. The governing phenomena differ from the jet pump plants whose LOCA response is characterized by rapid vessel refill. Accordingly, a separate PIRT has been developed for the BWR/2 large break. The response to small breaks is qualitatively similar for all BWR product lines and is examined within the context of a single small-break PIRT.

3.2 BWR LOCA TRANSIENT RESPONSE

Figure 3.2-1 through Figure 3.2-4 show the transient LOCA response of the vessel pressure, downcomer water level, core flow and PCT for a large liquid break, a large steam break and a small break. Figure 3.2-5 shows the core power following the scram. Depressurization begins as the break starts to discharge to the drywell (DW). A scram on high drywell pressure occurs almost immediately for all breaks with the possible exception of very small breaks where it may result from low downcomer water level. The core power transient response is similar for all breaks.

3.2.1 Large Liquid Break LOCA Scenario for Jet Pump Plants

The pressure response to a large liquid break is shown in more detail in Figure 3.2-6. For the liquid break, the initial depressurization is mild. As the downcomer level falls from loss of inventory, the Main Steam Isolation Valves (MSIVs) isolate the vessel and the depressurization rate slows for a few seconds. Shortly thereafter (~10 s for a break in the recirculation line), the downcomer water level drops to the recirculation suction line elevation (“break uncover”) and steam is discharged through the break. The depressurization increases rapidly following the transition to steam discharge. The depressurization proceeds until the containment pressure is reached in 200 – 300 s.

Figure 3.2-3 shows that the net core flow drops sharply in the first few seconds and coasts down to a small natural circulation flow within 10 s following a large break in a recirculation line. The flow reverses through the jet pumps attached to the broken loop. Loss of offsite power results in

the coastdown of the other recirculation pump. The rapid core flow reduction leads to a boiling transition and cladding heatup in parts of the core. With the increasing vessel depressurization rate following break uncover, the initially subcooled water inventory in the lower plenum flashes to produce an upsurge in core flow at about 12 s into the transient. The flow upsurge quenches the early boiling transition and restores nucleate boiling throughout the core. Inventory loss continues as the blowdown proceeds but a significant amount of inventory is held up in the core throughout the blowdown period because of the updrafting steam from the lower plenum. As the depressurization rate subsides, there is a corresponding drop in the flashing rate. The reduced flashing rate causes a reduction in core inventory that leads to core dryout and heatup.

As the downcomer level (Figure 3.2-7) drops below Level 2, the ECC systems are triggered (ECCS is also triggered by high pressure in the drywell but LOCA analysis may not take credit for this trip). High pressure systems inject water following a delay associated with valve lineup and the startup of the diesel motors. Low pressure systems start to inject water when the vessel pressure drops below the pressure permissive. The ECC systems restore the core inventory and terminate the heatup.

Figure 3.2-8 summarizes the key characteristics of the refill phase of the LOCA transient. To some extent, inventory is held up in the core by continued flashing of liquid in the lower plenum. In BWR/5s and BWR/6s, low pressure coolant injection (LPCI) enters inside the shroud in the peripheral bypass region surrounding the fuel bundles. This is supplemented by the core spray systems, which inject into the upper plenum (UP). The upper plenum fills to the level of the core spray spargers.

As steam is updrafting through the high power bundles, the ECC water drains preferentially through the low power peripheral bundles to the lower plenum. The remaining bundles are fed by leakage from the bypass region. Thus, various bundle flow regimes can exist in different regions of the core during the refill period. The two dominant flow regimes are: (1) cocurrent upflow with a high quality dispersed droplet flow throughout the bundle; and (2) countercurrent flow in the lower part of the bundle with an upper region that is primarily steam. Bundles in the latter flow regime will usually experience the higher heatup with the PCT occurring in the upper part of the bundle.

In BWR/3s and BWR/4s, the LPCI enters the lower plenum through the jet pumps as the core spray systems inject to the upper plenum. Consequently, condensation of steam voids in the lower plenum and refill of the lower plenum are key phenomena for these plants. For all jet pump plants, the heatup transient is over in less than 200 s following the LOCA. Figure 3.2-9 shows a typical PCT trace for a large liquid break. The response is characterized by two temperature peaks. The early peak results from a power /flow mismatch and is terminated by lower plenum flashing. The second peak results from a sustained loss of inventory in the core and is terminated by the addition of water from the ECC systems and the refill process described above. Liquid breaks in the recirculation lines result in the highest PCT.

For the preparation of the LOCA PIRTs, the LOCA transient has been divided into two time segments. The “Blowdown Phase” covers the early part of the transient up to the point where the

low pressure ECC systems start injecting water into the reactor vessel. The “Refill/Reflood Phase” covers the remaining part of the transient subsequent to low pressure ECC system actuation. High pressure ECC injection may be available early in the blowdown segment in some scenarios but it does not materially change the blowdown characteristics and is included in the “Blowdown Phase.”

3.2.2 Steam Line Break LOCA Scenario

As shown in Figure 3.2-1, large steam breaks lead to an immediate and rapid reactor vessel depressurization and earlier flashing of the lower plenum in comparison to liquid line breaks. The core flow coastdown (Figure 3.2-3) is not as rapid because there is no jet pump flow reversal as in the case of a recirculation line break. The sustained depressurization causes the downcomer level to swell and remain elevated (Figure 3.2-2). Liquid entrainment in the break flow is expected. Despite an increase in steam quality and voids, a boiling transition (BT) in the core is not expected because cooling of the core by a two-phase mixture throughout the transient prevents sustained dryout and heatup. As the steam line break is not a PCT limiting event for the BWR, it has not been explicitly covered in the PIRT. However, comments pertaining to the steam line break have been included where appropriate. This LOCA transient shares many of the characteristic phenomena of small liquid breaks following ADS (e.g., level swell due to depressurization and core coverage by a two-phase mixture).

3.2.3 Small Break LOCA Scenario

Figure 3.2-1 through Figure 3.2-4 show the response of key system parameters to a small break. The small-break LOCA scenario assumes that high pressure ECC makeup is not available. As a result, inventory is slowly lost through the break and the downcomer level drops steadily. The vessel is isolated by the closure of the MSIVs when the level reaches Level 2. The pressure is maintained close to operating pressure by cycling of the SRVs. Eventually, as the level reaches Level 1, the ADS timer is actuated and depressurization starts after the prescribed timer delay. This occurs at several hundred seconds into the transient with the exact time depending on the size of the break. The subsequent rapid vessel depressurization allows the low-pressure ECC systems to be activated.

The recirculation pumps coast down on loss of offsite power. The natural circulation flow from the downcomer to the core is sufficient to maintain the core in a well-cooled state. The core inventory flashes and the void fraction increases once the vessel begins to depressurize following the activation of the ADS. Towards the end of the depressurization, heatup in the upper part of the core may occur. The low-pressure ECC systems add inventory to the vessel (upper plenum, core bypass and lower plenum) and restore the heat transfer. The refill phase phenomena referred to in the discussion of the large break scenario are also relevant for small breaks. A typical PCT response of a BWR to small break is shown in Figure 3.2-4.

For a small break, the BWR/2 behavior is similar to the jet pump plants. The BWR/2s have two core sprays but no lower plenum injection from ECC systems. They also have an emergency condenser that condenses steam from the steam dome and returns the condensate to the

downcomer. This system helps to depressurize the system and reduces the inventory loss during the ADS depressurization.

The small break LOCA transient can also be divided into the “Blowdown” and “Refill/Reflood” phases with the two phases demarcated by the start of the low pressure ECCS. The PIRT ranks the importance of phenomena separately for each phase.

3.2.4 Large Liquid Break LOCA Scenario for BWR/2

The BWR/2s have five external recirculation loops with a recirculation pump in each loop. There are no jet pumps in the downcomer. A large break in one of the loops will result in almost immediate stagnation of the core flow, followed by flow reversal (Figure 3.2-11) as the pumps in the unbroken loops coast down. The power/flow mismatch results in a boiling transition in the high power portion of the core.

The level in the downcomer drops rapidly as the downcomer and recirculation lines are drained. The vessel pressure response is shown in Figure 3.2-10. The vessel depressurizes faster than for the jet pump plants because the downcomer side of the break becomes a steam discharge. Lower plenum flashing occurs early in the transient and causes a momentary increase in the core flow (Figure 3.2-11). This effect is smaller than for jet pump plants because of the reduced inventory in the lower plenum and the blowdown path through the lower plenum to the break. Consequently, lower plenum flashing may not be sufficient to quench the core. Because of liquid downflow in the core, the upper plenum and core regions do not retain significant inventory as the blowdown from the lower plenum proceeds. The downflow through the core does, however, provide core cooling that limits the initial cladding temperature rise (Figure 3.2-12).

The ECC systems available in the BWR/2 consist of two low pressure core sprays (CSs). The emergency condensers and ADS systems are of little significance in a large bottom break scenario. The core continues to heat up from the decay heat under the mitigating influence of spray cooling and steam cooling (Figure 3.2-12). The amount of core spray water reaching the high power bundles is a key parameter. The fuel channels rewet because of the spray water descending into the fuel channel and forming a film on the channel wall. This film progresses downwards by precursory cooling at the quench front and axial conduction. The combined effects of radiative heat transfer to the channel walls and spray heat transfer turn the fuel rod cladding temperature over as the decay heat reduces with time. Because of the relatively high temperatures reached, metal-water reaction can become significant. Fuel rod ballooning and perforation due to fission gas pressurization are likely.

The PIRT for BWR/2 large breaks has been divided into the “Blowdown” and “ECC” phases. The ECC phase corresponds to the refill/reflood phase for the jet pump plants. Refilling of the vessel is not possible for non-jet pump plants for a large break in the recirculation line attached to the lower plenum.

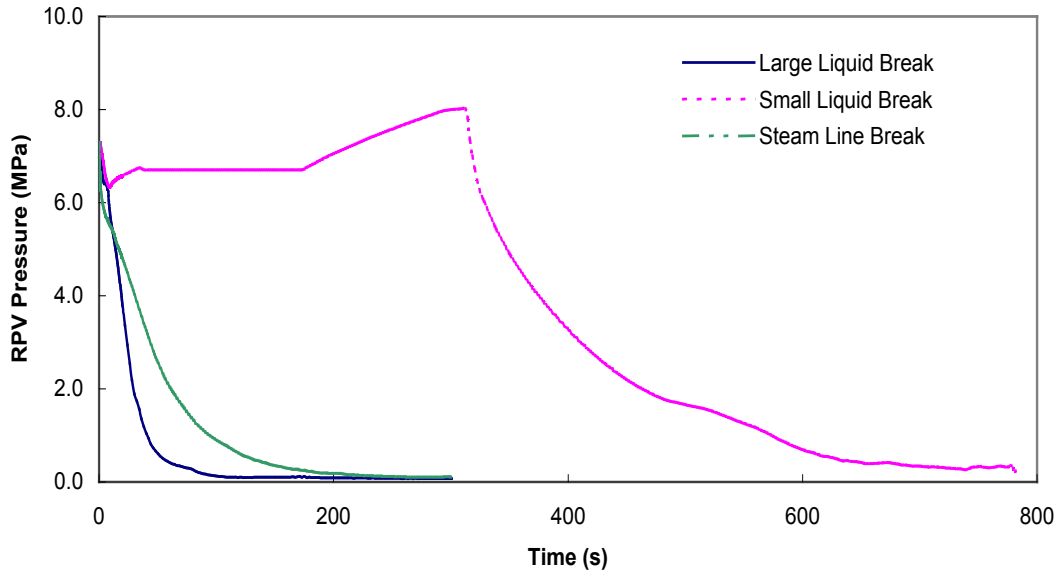


Figure 3.2-1 Reactor Vessel Pressure Transient for Various Breaks

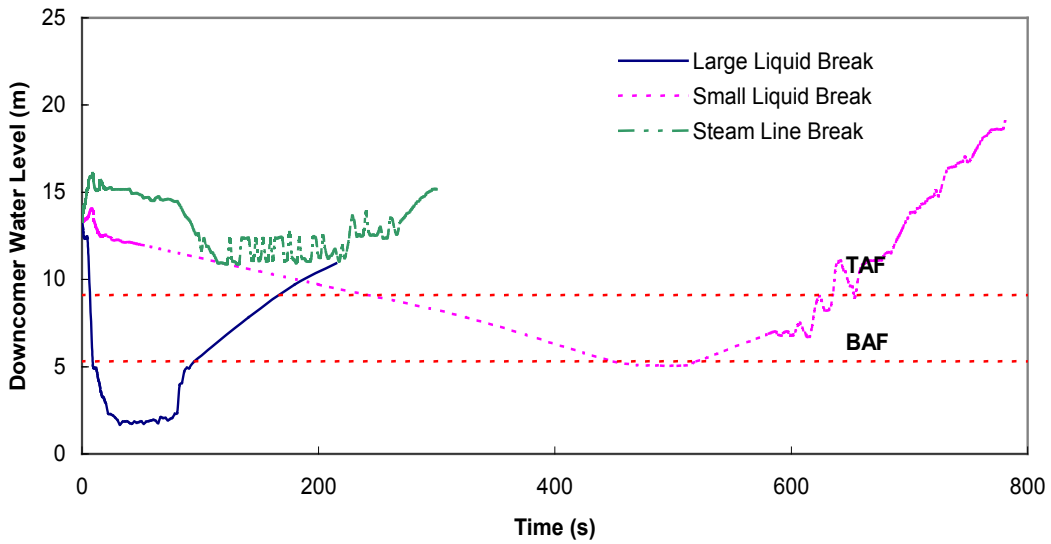


Figure 3.2-2 Downcomer Water Level Transient for Various Breaks

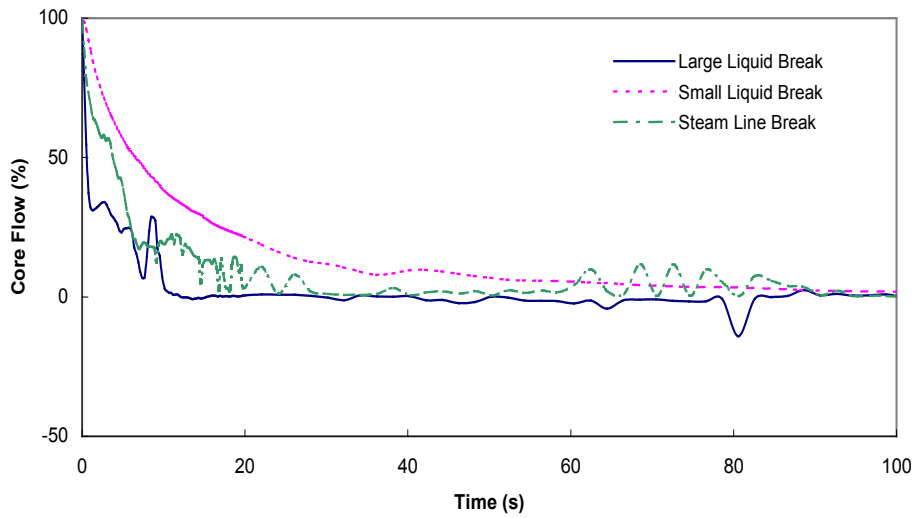


Figure 3.2-3 Core Flow Transient for Various Breaks

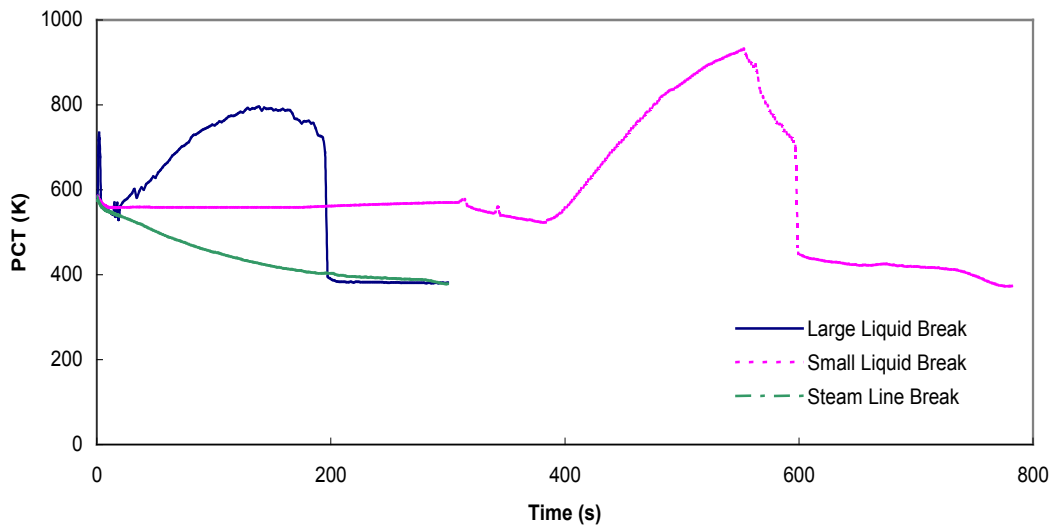


Figure 3.2-4 Peak Cladding Temperature Transient for Various Breaks

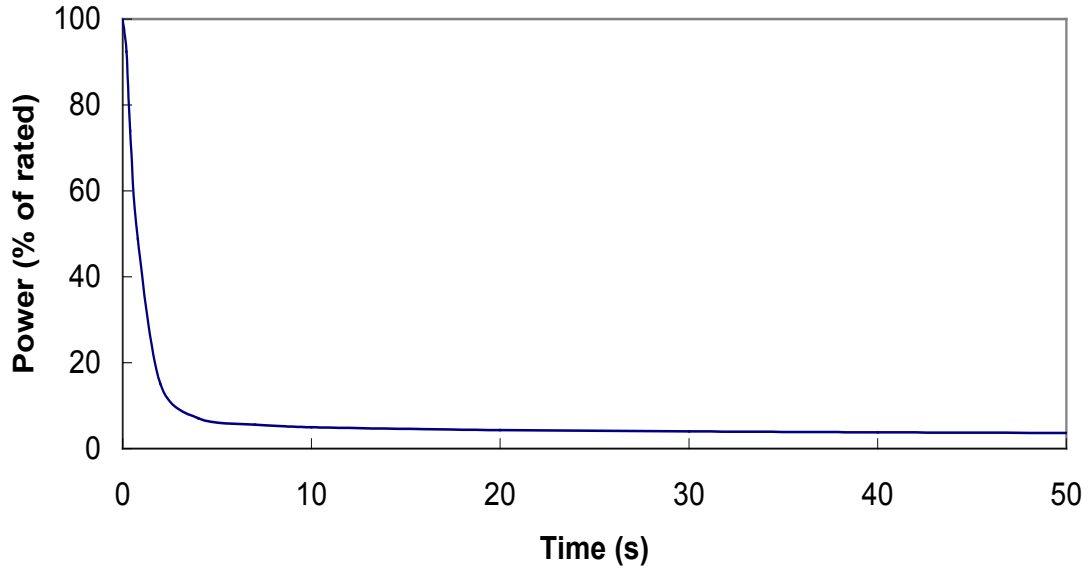


Figure 3.2-5 Core Power Transient Following Scram

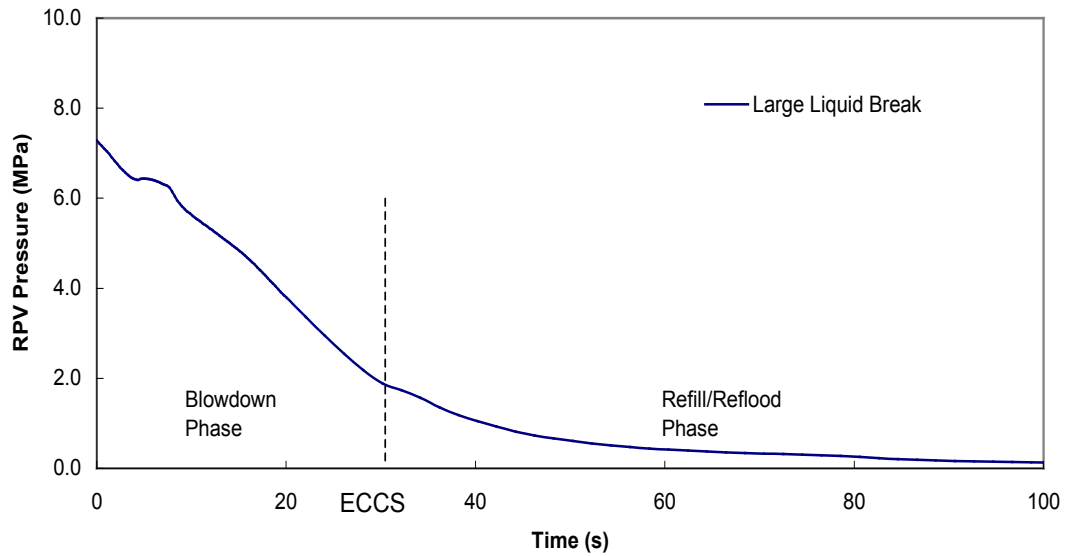


Figure 3.2-6 RPV Pressure Transient for Large Liquid Line Break

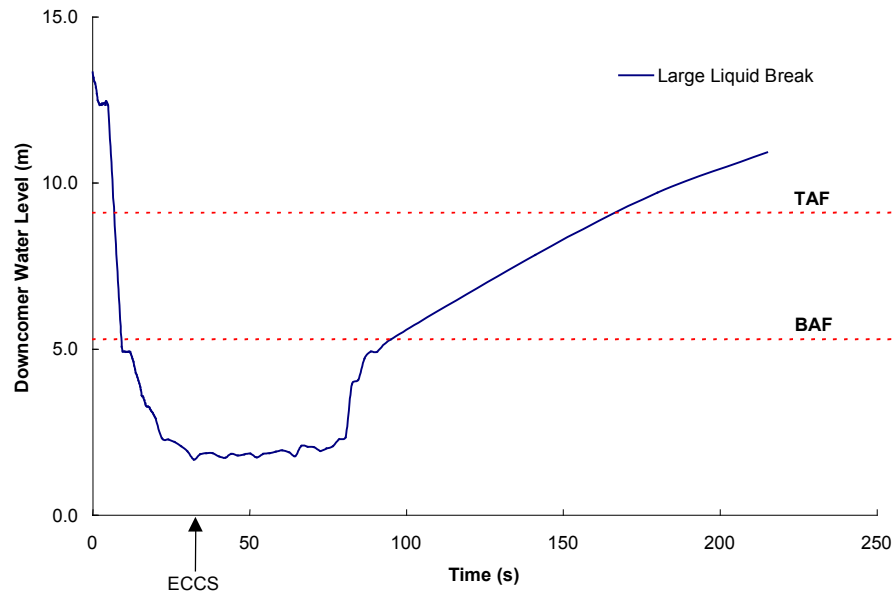
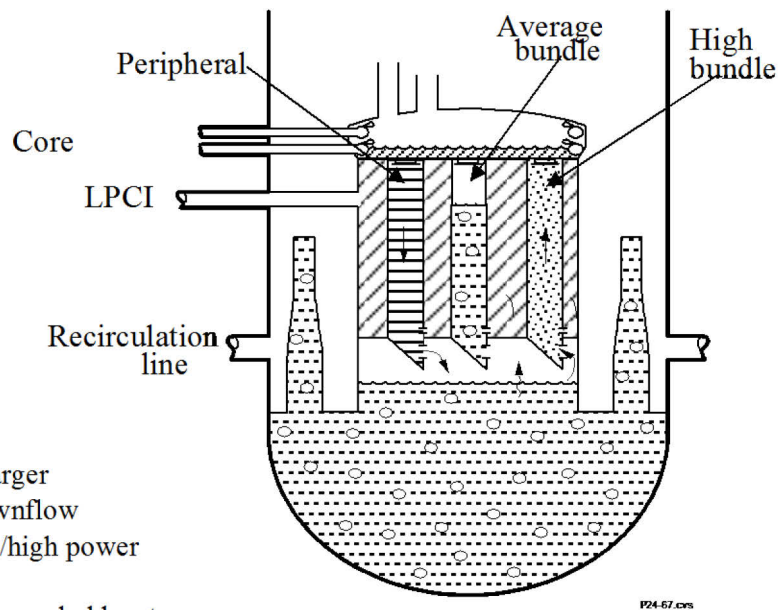


Figure 3.2-7 Downcomer Water Level Transient for a Large Liquid Line Break



Major Phenomena

- Upper plenum fills to sparger
- Peripheral bundles in downflow
- Liquid holdup in average/high power bundles
- Some high power bundles cooled by steam upflow

Figure 3.2-8 Major Phenomena during Large Break LOCA Refill/Reflood

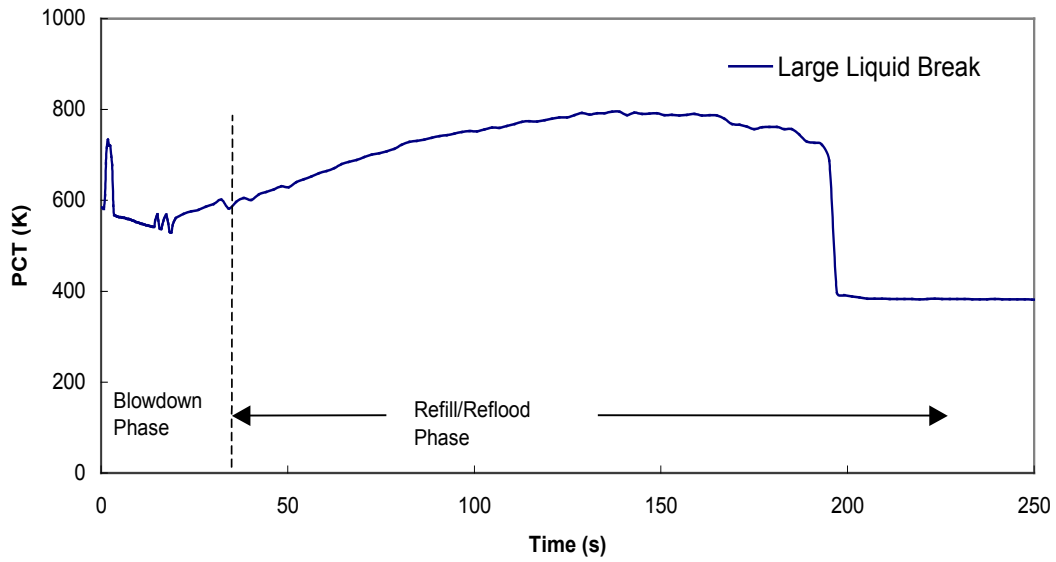


Figure 3.2-9 PCT Transient for Large Liquid Break LOCA

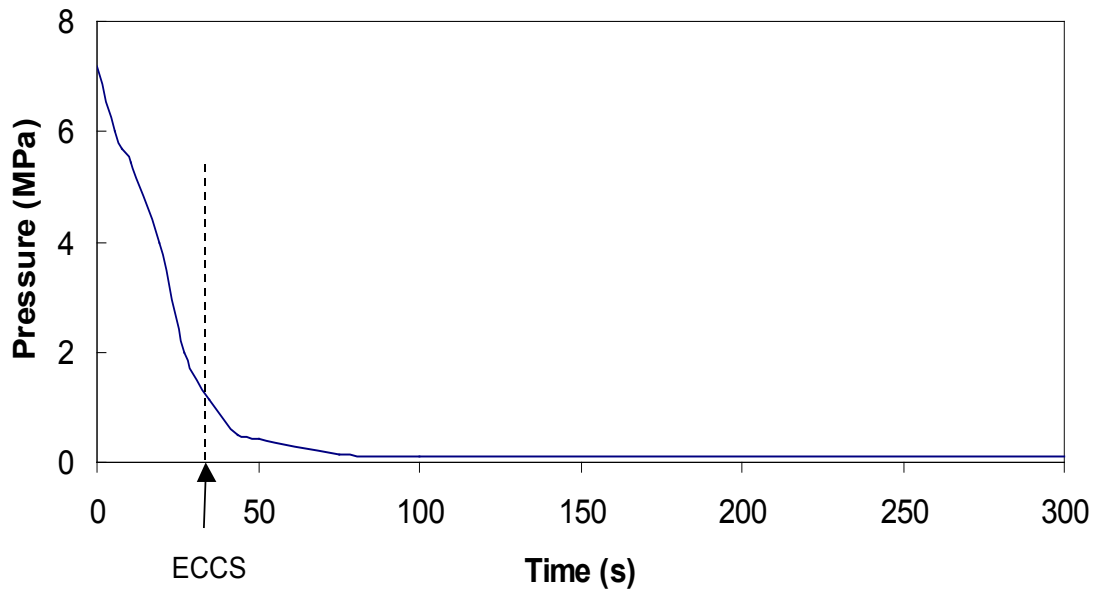


Figure 3.2-10 RPV Pressure Transient for a BWR/2 Large Break

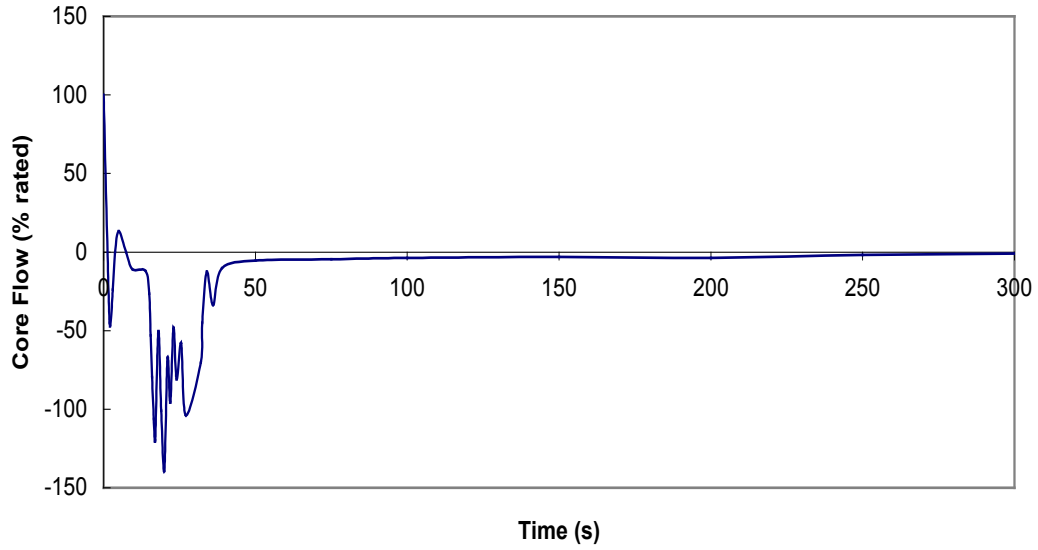


Figure 3.2-11 Core Flow Transient for BWR/2 Large Break

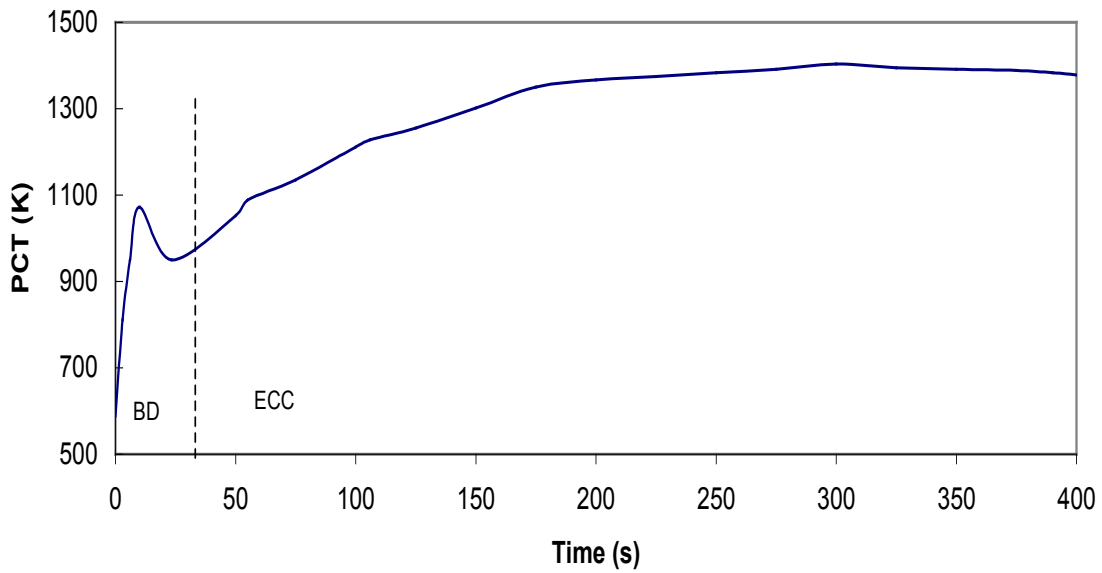


Figure 3.2-12 PCT Transient for BWR/2 Large Break

3.3 TOP-DOWN RATIONALE FOR CHOICE OF PIRT PARAMETERS

Table 3.3-1 shows the top-down rationale for the choice of the LOCA PIRT parameters. The top down analysis starts with the safety parameters for LOCA listed in the first row, namely, the PCT, water levels in the core and downcomer, and cladding oxidation. The first column shows the parameters that are of primary importance for LOCAs because they directly affect the safety parameters. These top level or “global” parameters include the vessel inventory and its regional distribution, and the core flow, heat transfer and refill characteristics. The second column lists the parameters that determine the behavior of the primary (Column 1) parameters during the transient. For example, the reactor vessel inventory is determined by the flows leaving and entering the vessel. The third column lists the actual phenomena that influence the parameters in the second column. The parameters in the third column, together with some from the second column, are identified as “PIRT phenomena” and are evaluated for their relative influence on the LOCA response of the plant. This evaluation is performed from a bottom-up perspective in the Phenomena Identification and Ranking Tables (PIRTs) that follow. Some parameters (e.g., ECC pump capacity and setpoints (asterisked in Column 4 of Table 3.3-1)) are identified as “plant parameters” rather than PIRT phenomena and are included at a later stage in the sensitivity studies and statistical evaluations that address the overall uncertainty in the TRACG calculation of the plant LOCA response.

Table 3.3-1 Top Down Rationale for Identification of PIRT Parameters

Safety Parameters: Downcomer Level, Core Water Level, PCT and Cladding Oxidation		
Primary Parameter	Contributing Parameters	Determining Phenomena
Reactor Vessel Inventory	Break Flow	Critical flow; friction; break uncover; liquid entrainment
	ADS Flow	Valve capacity*; critical flow
	ECCS flow	ECC setpoints*; timer delays*; diesel startup time*; ECC pump capacity*
Blowdown Inventory Distribution (core, core bypass, lower plenum, upper plenum, downcomer, recirculation line)	Flashing/inventory redistribution	Depressurization rate; energy release from vessel walls and internal structures
	Two-phase levels	Void fraction; countercurrent flow; CCFL; CCFL breakdown
Core Power Generation	Fission Power	Scram reactivity; void reactivity
	Decay Heat	Core exposure*; core design*
	Fuel rod stored energy	Gap conductance; fuel rod thermal properties
	Metal-water reaction	Reaction rate; rod ballooning and perforation
Core Flow	Flow coastdown	Recirculation pump coastdown characteristics; two-phase flow degradation; jet pump two-phase flow and flow reversal
	Natural circulation flow	Core pressure drop; core, upper plenum and separator void fractions; separator pressure drop
Core Heat Transfer	Wall heat transfer – blowdown	Core flow distribution; boiling transition; post dryout heat transfer; cladding rewet
	Wall heat transfer – refill/reflood	Fuel bundle flow regime; low void fraction film boiling and rewetting; channel-to-bypass heat transfer
	Spray cooling heat transfer	Dispersed droplet heat transfer; radiative heat transfer; axial conduction quenching

Table 3.3-1 (cont'd) Top Down Rationale for Identification of PIRT Parameters

Safety Parameters: Downcomer Level, Core Water Level, PCT and Cladding Oxidation		
Inventory Distribution during Refill	Cold water injection	Void quenching in lower plenum, upper plenum, bypass, downcomer and jet pumps
	Core spray distribution - ECC flow to individual bundles	Spray nozzle characteristics*; steam quenching above and below two-phase level; interaction between spray and upper plenum flows; noncondensable return at low pressure
	Bypass to core leakage	Leakage path characteristics*
	Bundle flow regime	Steam generation in lower plenum (depressurization); leakage flow from bypass; bundle power generation
	Upper plenum inventory	CCFL at top of bypass; CCFL breakdown; peripheral bundle downflow

Note: * Plant parameter

3.4 PHENOMENA IDENTIFICATION AND RANKING TABLE

Table 3.4-1 was developed to rank the phenomena that govern BWR/2-6 LOCA responses. The PIRT phenomena have been ranked within three categories: (1) large break LOCA for jet pump plants; (2) large break LOCA for non-jet pump plants; and (3) small break LOCA. For each event type, the transient is divided into two phases – *Blowdown* and *Refill/Reflood* (or *ECC*) for evaluation of the importance of the listed phenomena. The ranking is performed for each major region/component in the reactor system. The PIRT rankings represent a consensus of GEH expert opinions based on long experience in BWR thermal-hydraulics and LOCA analyses. The rankings are independent of TRACG model capability to represent the phenomena or model sensitivity to the phenomena. The ranking of the phenomena ranges from “not applicable” to “high importance” as described below:

High importance (H): These phenomena have a significant effect on the primary safety parameters and must be included in the overall uncertainty evaluation. An example of such a phenomenon would be the *film boiling heat transfer* for a large break LOCA (C15 in Table 3.4-1). The film boiling heat transfer coefficient determines the heatup of the fuel rods following loss of core inventory.

Medium importance (M): These phenomena have a smaller effect on the primary safety parameters. They are not considered the most dominant phenomena, but they are not deemed negligible either. An example of such a parameter would be the *stored heat in the core plate and control blades* for a large break LOCA (B3 in Table 3.4-1). The energy added to the core bypass region from this source is much smaller than that due to the effects of flashing due to depressurization.

Low importance (L) or not applicable (N/A): These phenomena have insignificant or no effect on the primary safety parameters and need not be considered in the overall uncertainty evaluation. An example of such a phenomenon would be *nucleate boiling heat transfer* during a large break LOCA (C1 in Table 3.4-1). Nucleate boiling heat transfer keeps the fuel well cooled with a margin that is sufficiently large to preclude its affecting the subsequent transient and PCT.

The PIRT serves two purposes in addition to its role in determining the extent of the statistical process that is used to arrive at the total uncertainty in the calculation of the LOCA safety parameters. The first is to identify the code models that must be assessed with respect to their capability to simulate the important phenomena. The second is to cross-reference the important phenomena to the code qualification basis to identify the qualification data that are applicable to validation of those models. As part of this assessment, the range of the PIRT phenomena covered by the applicable test data is compared with the range of the intended application to confirm that the code has been qualified for the important phenomena, highly and medium ranked parameters, over the appropriate range.

In its ultimate role, the PIRT identifies the important phenomena, including highly and medium ranked parameters, whose uncertainties are to be carefully evaluated and combined through a statistical process to arrive at the total uncertainty in the code’s prediction of the safety

parameters. The development of the uncertainties for the highly and medium ranked phenomena is described in Section 5.0 and their combined effect on the critical safety parameters is quantified for each of the LOCA scenarios in Section 8.0.

Table 3.4-1 Phenomena that Govern BWR/2-6 LOCA Responses

II														0000000000 0000000000	00000000000000 00000000000000		
		000000 000000															
00 00		00 00	000 000	00 00	00 00	00 00	00 00	00 00	000 000	00 00	00 00	00 00	00 00	00 00	00 00		
00 00																	
																	II

NEDO-33005-A Revision 1
 Non-Proprietary Information – Class I (Public)

Table 3.4-1 (cont'd) Phenomena that Govern BWR/2-6 LOCA Responses

II	0000000000 -----	000 ----			00000 -----								00000000000000000000 -----		
		000000 -----	00000000 -----	00000000 -----	000000 -----	00000000 -----	00000000 -----	00000000 -----	00000000 -----	0000000000 -----	00000000000000 -----			00000000000000000000 -----	00000000000000000000 -----
00 --	00000000000000000000000000000000 -----	00 --	00 --	00 --	00 --	00 --	00 --	00 --	00 --	00 --	00 --	00 --	00 --	000000000000 -----	00000000000000000000 -----
0	0000 -----														

}}

NEDO-33005-A Revision 1
 Non-Proprietary Information – Class I (Public)

Table 3.4-1 (cont'd) Phenomena that Govern BWR/2-6 LOCA Responses

II	0000000000 -----	000 ----			00000 -----								00000000000000000000 -----	
		000000 -----	00000000 -----	00000000 -----	000000 -----	00000000 -----	00000000 -----	00000000 -----	00000000 -----	00000000 -----	000000000000 -----	0000000000000000 -----	00000000000000000000 -----	00000000000000000000 -----
00 --	00000000000000000000000000000000 -----	00 --	000 ---	00 --	00 --	00 --	00 --	00 --	00 --	00 --	00 --	00 --	00000000000000 -----	00000000000000000000 -----
]]

NEDO-33005-A Revision 1
 Non-Proprietary Information – Class I (Public)

Table 3.4-1 (cont'd) Phenomena that Govern BWR/2-6 LOCA Responses

[[0000000000 -----	000 ----			00000 -----								00000000000000000000 -----		
		000000 -----	00000000 -----	00000000 -----	000000 -----	00000000 -----	00000000 -----	00000000 -----	00000000 -----	00000000 -----	000000000000 -----	0000000000000000 -----	00000000000000000000 -----	00000000000000000000 -----	
00 --	00000000000000000000000000000000 -----	00 --	00 --	00 --	00 --	00 --	00 --	00 --	00 --	00 --	00 --	00 --	000000000000 -----	00000000000000000000 -----	
0 -	00000000 -----													00000000000000000000 -----	00000000000000000000 -----
]]	

NEDO-33005-A Revision 1
 Non-Proprietary Information – Class I (Public)

Table 3.4-1 (cont'd) Phenomena that Govern BWR/2-6 LOCA Responses

II	0000000000 -----	000 ----			00000 -----							00000000000000000000 -----		
		000000 -----	00000000 -----	00000000 -----	000000 -----	00000000 -----	00000000 -----	00000000 -----	00000000 -----	00000000 -----	000000000000 -----	00000000000000000000 -----	00000000000000000000 -----	
00 --	00000000000000000000000000000000 -----	00 --	000 ---	00 --	00 --	00 --	00 --	00 --	00 --	00 --	00 --	00 --	000000000000 -----	00000000000000000000 -----
0 -	00000000 -----													
0 -	0000000000 -----													
														II

NEDO-33005-A Revision 1
 Non-Proprietary Information – Class I (Public)

Table 3.4-1 (cont'd) Phenomena that Govern BWR/2-6 LOCA Responses

II	0000000000 -----	000 ----			00000 -----								00000000000000000000 -----	
		000000 -----	00000000 -----	00000000 -----	000000 -----	00000000 -----	00000000 -----	00000000 -----	00000000 -----	00000000 -----	000000000000 -----	0000000000000000 -----	00000000000000000000 -----	00000000000000000000 -----
00 --	00000000000000000000000000000000 -----	00 --	00 --	00 --	00 --	00 --	00 --	00 --	00 --	00 --	00 --	00 --	0000000000000000 -----	000000000000000000000000 -----
0	00000000000000000000000000000000 -----													
														II

NEDO-33005-A Revision 1
 Non-Proprietary Information – Class I (Public)

Table 3.4-1 (cont'd) Phenomena that Govern BWR/2-6 LOCA Responses

II	0000000000 -----	000 ----			00000 -----								00000000000000000000 -----		
		000000 -----	00000000 -----	00000000 -----	000000 -----	00000000 -----	00000000 -----	00000000 -----	00000000 -----	0000000000 -----	00000000000000 -----	00000000000000000000 -----			
00 --	00000000000000000000 -----	00 --	000 --	00 --	00 --	00 --	00 --	00 --	00 --	00 --	00 --	00 --	000000000000 -----	00000000000000000000 -----	
0 -	00000000000000000000 -----														
														II	

4.0 APPLICABILITY OF TRACG TO ECCS/LOCA

The objective of this section is to demonstrate the applicability of TRACG for the analysis of LOCA transients in BWR plants. The code's capability for ECCS/LOCA applications is assessed by examining the adequacy of the individual TRACG models for the highly ranked and medium ranked phenomena identified in Section 3.0.

4.1 MODEL CAPABILITY

The capability of a code to calculate a nuclear power plant event depends on four elements:

- Conservation equations that enable the code to model the global physical processes associated with the event;
- Correlations and models that enable the code to simulate and scale specific physical processes associated with the event;
- A numerical formulation that enables the code to reliably perform accurate and efficient calculations of the event history;
- A structure that enables the code to accurately nodalize the plant geometry.

These four elements must be considered when evaluating the applicability of a code to a nuclear power plant calculation for a specific event or class of events. The key phenomena for the event class are identified by generating the PIRTs for the intended application as described in Section 3.0. The capability of TRACG to simulate these key phenomena is specifically addressed and documented by the qualification studies documented in Reference [2]. A matrix relating important BWR LOCA (PIRT) phenomena to the TRACG models that address the phenomena is shown in Table 4.1-1. The numbers in the second row of the table are the section numbers in the TRACG model report [1] where the models are described. A bold X denotes the primary model associated with the PIRT phenomenon and non-bold Xs denote secondary models associated with the phenomenon.

Table 4.1-1 BWR LOCA Phenomena and TRACG Model Capability Matrix

[[

Table 4.1-1 (cont'd) BWR LOCA Phenomena and TRACG Model Capability Matrix

Table 4.1-1 (cont'd) BWR LOCA Phenomena and TRACG Model Capability Matrix

Table 4.1-1 (cont'd) BWR LOCA Phenomena and TRACG Model Capability Matrix

Table 4.1-1 (cont'd) BWR LOCA Phenomena and TRACG Model Capability Matrix

Table 4.1-1 (cont'd) BWR LOCA Phenomena and TRACG Model Capability Matrix

Table 4.1-1 (cont'd) BWR LOCA Phenomena and TRACG Model Capability Matrix

Table 4.1-1 (cont'd) BWR LOCA Phenomena and TRACG Model Capability Matrix

Table 4.1-1 (cont'd) BWR LOCA Phenomena and TRACG Model Capability Matrix

]]

4.2 MODEL ASSESSMENT MATRIX

The assessment of TRACG models is summarized in Table 4.2-1. The models are identified so that they may be easily correlated to the model description and qualification reports. For each model, the relevant elements from the Model Description LTR [1] and the Qualification LTR [2] are identified.

For each of the governing BWR phenomena, TRACG qualification has been performed against a wide range of data. In this section, the qualification basis is related to the phenomena that are important for the intended application. This is a necessary step to confirm that the code has been adequately qualified for the intended application.

The complete list of phenomena is cross-referenced to the model capabilities in Table 4.1-1. Similarly, as shown in Table 4.2-1, the complete list of phenomena is cross-referenced to the qualification assessment basis. Data from separate effects tests, component tests, integral system tests and plant tests as well as plant data have been used to qualify the capability of TRACG to model the phenomena.

Table 4.2-1 Qualification Matrix for BWR/2-6 LOCA Phenomena

[[.....			
		
..
o														
]]

NEDO-33005-A Revision 1
 Non-Proprietary Information – Class I (Public)

Table 4.2-1 (cont'd) Qualification Matrix for BWR/2-6 LOCA Phenomena

[[..... -----	... ----		 -----						 ----- -----			
	 ----- ----- ----- -----										
.. -- ----- -----	.. --	.. --	.. --	.. --										
]]

NEDO-33005-A Revision 1
 Non-Proprietary Information – Class I (Public)

Table 4.2-1 (cont'd) Qualification Matrix for BWR/2-6 LOCA Phenomena

[[..... -----	... ----					 -----					 -----			
	 ----- ----- ----- -----												
.. -- ----- --	.. --	.. --	.. --												
. - -----																
]]

NEDO-33005-A Revision 1
 Non-Proprietary Information – Class I (Public)

Table 4.2-1 (cont'd) Qualification Matrix for BWR/2-6 LOCA Phenomena

[[..... -----	... ----		 -----		 ----- -----					
	 ----- ----- ----- ----- ----- -----						
.. -- ----- -----	.. --	.. --	.. --	.. --	.. -- ----- -----						
]]

NEDO-33005-A Revision 1
 Non-Proprietary Information – Class I (Public)

Table 4.2-1 (cont'd) Qualification Matrix for BWR/2-6 LOCA Phenomena

[[..... -----	... ----		 -----		 ----- -----						
	 ----- ----- ----- ----- ----- ----- -----						
.. -- ----- -----	.. --	.. --	.. --	.. --	.. --	.. --	.. --						
]]

NEDO-33005-A Revision 1
 Non-Proprietary Information – Class I (Public)

Table 4.2-1 (cont'd) Qualification Matrix for BWR/2-6 LOCA Phenomena

[[..... -----	... ----		 -----				 ----- -----			
	 ----- ----- ----- -----								
.. -- ----- -----	.. --	.. --	.. --	.. --								
]]

NEDO-33005-A Revision 1
 Non-Proprietary Information – Class I (Public)

Table 4.2-1 (cont'd) Qualification Matrix for BWR/2-6 LOCA Phenomena

[[..... -----	... ----		 -----		 ----- -----						
	 ----- ----- ----- ----- ----- ----- -----						
.. -- ----- -----	.. --	.. --	.. --	.. --	.. --	.. --	.. --						
 -----													
]]

NEDO-33005-A Revision 1
 Non-Proprietary Information – Class I (Public)

Table 4.2-1 (cont'd) Qualification Matrix for BWR/2-6 LOCA Phenomena

[[..... -----	... ----		 -----							 ----- -----			
	 ----- ----- ----- -----											
.. -- ----- -----	.. --	.. --	.. --	.. --											
. -----															
]]

NEDO-33005-A Revision 1
 Non-Proprietary Information – Class I (Public)

Table 4.2-1 (cont'd) Qualification Matrix for BWR/2-6 LOCA Phenomena

[[.....					
				
..
															
]]

NEDO-33005-A Revision 1
 Non-Proprietary Information – Class I (Public)

Table 4.2-1 (cont'd) Qualification Matrix for BWR/2-6 LOCA Phenomena

[[..... -----	... ----		 -----		 ----- -----					
	 ----- ----- ----- ----- ----- -----						
.. -- ----- -----	.. --	.. --	.. --	.. --	.. --	.. --						
.												
]]

NEDO-33005-A Revision 1
 Non-Proprietary Information – Class I (Public)

Table 4.2-1 (cont'd) Qualification Matrix for BWR/2-6 LOCA Phenomena

[[.....			
	
..
..												
..												
]]

NEDO-33005-A Revision 1
 Non-Proprietary Information – Class I (Public)

Table 4.2-1 (cont'd) Qualification Matrix for BWR/2-6 LOCA Phenomena

[[..... -----	... ----		 -----		 -----					
	 ----- ----- ----- ----- ----- -----						
.. -- ----- --	.. --	.. --	.. --	.. --	.. --						
.. -- -----												
.. -- -----												
.. -- -----												
]]

NEDO-33005-A Revision 1
 Non-Proprietary Information – Class I (Public)

Table 4.2-1 (cont'd) Qualification Matrix for BWR/2-6 LOCA Phenomena

[[..... -----	... ----		 -----			 -----					
	 ----- ----- ----- ----- ----- -----							
.. -- ----- --	.. --	.. --	.. --	.. --	.. --							
.. -- -----													
]]

5.0 MODEL UNCERTAINTIES AND BIASES

Model biases and uncertainties for LOCA application of TRACG are assessed as described below for each of the high and medium-ranked phenomena identified in Section 3.0. The assessments are typically performed on the basis of comparisons between separate effects test data and best-estimate TRACG calculations. The biases and uncertainties derived from the data comparisons are used to establish probability density functions (PDFs) for PIRT multipliers on the TRACG parameters and correlations that govern the code's simulation of the high and medium-ranked phenomena. Biases are compensated by appropriate choice of the mean value of the PIRT multiplier, and uncertainties are addressed by choosing PDFs to represent the standard deviation of the data comparisons. In general, no attempt is made to separate out the uncertainty in the data comparisons from the possible effect of measurement errors (i.e., measurement uncertainties are implicitly included in the standard deviation of the TRACG/test data comparisons). There are some TRACG parameters affecting the high and medium-ranked phenomena for which no applicable test data are available. For these cases, bounding PIRT PDF is chosen on the basis of engineering judgment and comparisons with similar parameters for which data are available. In some instances, the parameter was found to have little effect on the figure of merit for the LOCA calculation (peak cladding temperature or oxidation) and it was possible to use a conservative estimate of the uncertainty. The results of the evaluation are summarized in Table 5.1-2 at the end of Section 5.1.

5.1 MODEL PARAMETERS AND UNCERTAINTIES

This section discusses the biases and uncertainties in the TRACG parameters and correlations that have a potential effect on each of the high and medium-ranked phenomena listed in Table 3.4-1. As in Table 3.4-1, the presentation is organized by plant region, starting with the lower plenum and ending with the containment. Under the heading of each phenomenon, the applicable TRACG parameters and correlations are identified, the sources of the test data and the statistical characteristics of the deviations between TRACG calculations and the test data are described and the choice of the PDF is explained.

5.1.1 Lower Plenum Region

5.1.1.1 A1 – Flashing/Redistribution (H)

Flashing and the associated redistribution of liquid inventory in the lower plenum of the TRACG model are controlled by liquid-side interfacial heat transfer. The bubbly flow regime is the dominant flow regime for this behavior. TRACG uses the Lee-Ryley correlation in conjunction with a bubble diameter based on a critical Weber number for liquid-side heat transfer in the bubbly flow regime [1]. The Lee-Ryley correlation applies to heat transfer to spherical particles under forced circulation conditions. It predicts the water droplet evaporation data from which it was originally developed with an error less than 10%. Following the procedure previously adopted for the AOO application [3], the uncertainty in the PIRT multiplier on the interfacial heat transfer at the bubble surface is specified as a [[

]]

5.1.1.2 A2 – Heat Slab Stored Energy Release (H)

The release of stored energy from heat slabs in the lower plenum is controlled by either wall-to-liquid heat transfer or heat conduction. Wall heat transfer under subcooled or nucleate boiling conditions is calculated in TRACG with the Chen correlation [1], [35], [36]. As stated in the AOO application report [3], comparison with a large database supports the use of a normal distribution with zero bias and an 11% standard deviation for the Chen correlation. For single-phase heat transfer, the operative TRACG heat transfer correlation is Dittus-Boelter. Comparison with a large data base supports the use of a [[]] uncertainty for the Dittus-Boelter correlation [1]. To cover both modes of heat transfer, a [[]] uncertainty range is used. For thick heat slabs, such as the reactor pressure vessel walls, heat conduction rather than the wall surface heat transfer may limit stored energy release. Nodalization studies [2] were performed to ensure an adequate representation of thick heat slabs in the TRACG plant models. The effect of doubling the nodalization in the RPV cylindrical wall and the top and bottom heads was less than [[]] on PCT. On this basis, it was concluded that the present heat slab modeling is adequate for TRACG LOCA calculations.

5.1.1.3 A3 – Two-Phase Level (SEO Uncovery Time) (H)

The two-phase level in the lower plenum is controlled by vapor generation and the relative velocity between phases. Vapor generation is controlled by flashing (A1) and wall heat transfer (A2). [[

]] was obtained on the basis of TRACG predictions of relevant void fraction data as described below under A5.

5.1.1.4 A3X – Break Uncovery Time (non-jet pump plants) (H)

Break uncovery time in the lower plenum is controlled by the same phenomena as the two-phase level (A3).

5.1.1.5 A4 – Two-Phase Level (JP Uncovery Time) (H)

Jet pump uncovery time in the lower plenum is controlled by the same phenomena as the two-phase level (A3).

5.1.1.6 A5 – Void Distribution (H)

[[

]] A statistical summary of the comparisons of TRACG predictions with measurements from these data sets, combined as a single set of deviations, is shown in Figure 5.1-1. The absolute mean bias is [[]] void and the absolute standard deviation is [[]] void. [[]]

[[

]] (A comparable evaluation for the core and bypass is described below under C2AX.)

[[

]]

[[

]]

Figure 5.1-1 Void Fraction Deviations for Tests Applicable to Regions with Large Hydraulic Diameter

[[

]]

Figure 5.1-2 Sensitivity of TRACG Prediction of Average Void Fraction in Large Hydraulic Diameter Test Facilities to PIRT Multiplier

5.1.1.7 A6 – Condensation/Void Collapse (H)

Condensation and void collapse in the lower plenum are controlled by liquid-side interfacial heat transfer (A1).

5.1.1.8 A10 – Lower Plenum Stratification (H)

Lower plenum stratification can occur when water injected into the lower plenum is colder than the water in the plenum. In addition to liquid-side interfacial heat transfer (A1), stratification can be affected by the nodalization employed to represent the lower plenum in the TRACG plant models. A nodalization study [2] was performed to ensure that the effect of thermal stratification in the lower plenum was adequately simulated in the plant models. Increasing the number of axial levels used to represent the lower plenum from [[]]] changed the calculated PCT by less than [[]]]. On this basis, the existing [[]]] nodalization of the lower plenum was judged to be adequate for TRACG LOCA calculations.

5.1.1.9 A11 – 3-D Effects (M)

Modeling of the lower plenum must also address possible azimuthal variations in the thermodynamic variables that may influence the plant response to a LOCA. A nodalization study was performed to ensure that the effects of azimuthal variations were adequately represented in the TRACG plant models. Increasing the number of azimuthal sectors from one

(standard model) to [[]] for the BWR/4 design basis accident (DBA). The one-sector model can be used for the TRACG LOCA calculations because the modeling simplicity thereby realized [[]] that would result from the use of a more refined model.

5.1.2 Bypass Region

5.1.2.1 B1 – Flashing (M)

Bypass flashing is controlled by liquid-side interfacial heat transfer in the TRACG model. The uncertainty in liquid-side interfacial heat transfer in the bypass was addressed in the same manner as for the lower plenum (A1).

5.1.2.2 B2 – Two-Phase Level (H)

The bypass two-phase level is controlled by vapor generation and the relative velocity between the phases. Vapor generation is determined by liquid-side interfacial heat transfer (B1) and wall heat transfer. Wall heat transfer is addressed under [[]]

[[]] The relative phase velocity in the TRACG model is calculated from a balance between buoyancy and interfacial shear. The uncertainty in the bypass interfacial shear was addressed in the same manner as for the core region, as described below under C2AX.

5.1.2.3 B3 – Stored Heat (Core Plate/Control Blades/Shroud) (M)

The release of stored energy from metal masses in contact with the bypass is primarily controlled by wall heat transfer (A2). This phenomenon may also be affected by heat conduction in the structures. A sensitivity study [2] was performed to ensure an adequate simulation of the internal heat slabs in the TRACG plant models. The study was performed by varying the heat capacity of the internal heat slabs. The results showed less than a [[]] effect on PCT when the heat capacity of the reactor internal heat slabs was reduced to zero.

5.1.2.4 B4 – CCFL/CCFL Breakdown (Guide Tube-Bypass) (H)

CCFL may occur at a geometrically restricted area where the downward liquid flow is limited by the upward vapor flow. A Kutateladze-type correlation is used in TRACG to predict CCFL [1]. When CCFL breakdown occurs, the downflow of liquid is limited only by the hydraulic resistance of the flow path. The control rod is fully inserted during a LOCA and the most restricted flow area between the guide tube and the bypass is at the velocity limiter. The flow area at this location is of the same order as that of the side entry orifice (SEO). [[]]

]]

5.1.2.5 B5 – CCFL/CCFL Breakdown (Top of Bypass) (H)

CCFL test data for the flow restriction at the top of the bypass were obtained from Reference [46]. The test facility was an 18° sector, full-height simulation of a BWR from the bottom of the jet pumps to the top of the separator standpipes. The tests were run by injecting steam into the bypass while supplying saturated water to the upper plenum. The core was filled with saturated water. A statistical summary of the differences between the CCFL coefficients inferred from the 29 tests reported in Reference [46] and the TRACG CCFL coefficient at the top of the bypass is shown in Figure 5.1-3. The TRACG coefficient predicts the data with a bias of [[]] and a standard deviation of [[]]. On the basis of these results, the PIRT multiplier on the CCFL constant at the top of the bypass was conservatively specified to have a [[]]

5.1.2.6 B6 – Channel-Bypass Leakage Flow (H)

This phenomenon is addressed below under C11.

5.1.2.7 B7 – Refill (H)

The bypass refill flow path is from the upper plenum to the bypass via the top guide. It is expected that refill will be controlled by CCFL (B5). [[]] Sensitivity calculations were performed in which the [[]]. The results showed a negligible effect on both the large and small break PCTs. This confirms that refill uncertainty will be governed by the uncertainty in the CCFL correlation.

5.1.2.8 B8 – LPCI Interaction/Condensation (M)

LPCI interaction with the bypass is governed by liquid-side interfacial heat transfer. The uncertainty treatment of liquid interfacial heat transfer is discussed in Section 5.1.1.1 (A1).

[[

]]

Figure 5.1-3 Fractional Error in CCFL Constant at Top of Bypass

5.1.2.9 B9 – 3-D Effects (LPCI) (M)

A nodalization study [2] was performed to ensure adequate simulation of azimuthal variations in the bypass region in the TRACG plant models. The results of this study are described above in Section 5.1.1.9, under A11.

5.1.2.10 B9-2d – 2D Effects (M)

A nodalization study [2] was performed to ensure adequate simulation of radial variations in the bypass region in the TRACG plant models. [[

]] change in the PCT. On this basis, it was concluded that [[
]] was adequate for TRACG LOCA calculations.

5.1.2.11 B12 – Pressure Drop (M)

The uncertainty in the bypass pressure drop is governed by the uncertainties in the static head (B2) and in the local loss at the top guide (B7).

5.1.3 Core Region

5.1.3.1 C1AX – Void Coefficient (M)

A detailed discussion of the treatment of uncertainty in the TRACG void coefficient model for 3-D kinetics was presented in the AOO application report [4]. For LOCA analysis, the void reactivity effects are confined to just the first few seconds of the transient prior to the scram so the fission power is calculated from a simpler point kinetics model instead of the 3-D kinetics model. The void coefficients from Reference [4] are shown in Figure 5.1-4 as a function of core average void fraction at several exposures. The core exposure range of interest is from 15 GWd/ST to 30 GWd/ST for any reload core. This range of exposures is modeled nominally by the solid curve shown in Figure 5.1-5. Over this same exposure range, the maximum standard deviation in the absolute value of the void coefficient due to the lattices is [[

]] These are representative numbers that are generically applicable for the fuel-to-moderator ratios that are characteristic of modern BWR lattices.

The colored dashed lines in Figure 5.1-5 that pass through the ends of the 1-sigma error bars (determined as described above) are obtained by multiplying just the constant coefficient in the nominal void coefficient fit by a factor. The other coefficients in the functional fit are not changed. The ± 1 sigma variation in the void coefficient prediction is simulated by using a factor of [[

[[

]]

Figure 5.1-4 Void Coefficient Fit at Different Exposures (GWd/ST)

[[

]]

Figure 5.1-5 Point Kinetics Void Coefficient Model for LOCA Applications

5.1.3.2 C1DX – Kinetics (M)

[[

]]

[[

]]

Figure 5.1-6 Comparison of Small Break Initial Power Response for Point Kinetics and 3D Neutronics Models

5.1.3.3 C2AX – Interfacial Shear (H)

Although this PIRT phenomenon is entitled “Interfacial Shear,” it more generally concerns representation of the uncertainties of TRACG model parameters that affect the prediction of void fraction in the core and bypass. The core and bypass are distinguished from the regions of the vessel discussed above under A5 by their comparatively small hydraulic diameters. Two sets of TRACG comparisons with test data were used to define the bias and uncertainty of parameters influencing core and bypass void fraction for LOCA calculations. As described in the AOO application report [3], data from the FRIGG test facility [33], which form the basis for the GEH design void correlation, are the most relevant data for pressures within or near the normal operating range. TRACG02 predictions of the FRIGG void fraction data for fully developed nucleate boiling showed a small positive bias in absolute void fraction of [[]] and a standard deviation of [[]] [3][6]. The uncertainty observed in these data comparisons was reflected in the TRACG02 model through a PIRT multiplier (PIRT22) on the interfacial shear parameter (C_{o-1}). The relatively small bias in the predictions, especially in comparison with the experimental uncertainty of [[]] in the void fraction measurement, was used to justify the choice of an [[]] for PIRT22. From an examination of the dependence of void fraction predictions on PIRT22, it was concluded that a PIRT22 standard deviation of [[]] would appropriately represent the prediction standard deviation of [[]]. (As described in the AOO application report [3], the error in the TRACG

predictions is somewhat larger for subcooled boiling. This is attributed to uncertainty in the onset of net vapor generation, which is covered under C2BX.)

For LOCA application, the predictions of the FRIGG data were repeated with TRACG04. The results gave a bias of [[]] and a standard deviation of [[]], differing only slightly from the results obtained using TRACG02. The database for specifying the void uncertainty for LOCA calculations was augmented by comparisons of TRACG predictions with a series of low-pressure void fraction tests performed by Toshiba [47], [48]. These tests were conducted with a 16-rod bundle at pressures of 0.50 and 1.00 MPa. A total of 15 tests were run over a range of bundle powers at two mass fluxes. A statistical summary of the deviations between the TRACG predictions and the Toshiba void fraction measurements is shown in Figure 5.1-7. TRACG predicted the Toshiba data with a negligible bias and a standard deviation of [[]]. Figure 5.1-7 indicates that it is reasonable to assume that the void fraction deviations are normally distributed.

[[

]]

[[

]]

Figure 5.1-7 Void Fraction Deviations for Toshiba Tests

[[

]]

Figure 5.1-8 Sensitivity of TRACG Prediction of Toshiba Void Fraction to PIRT Multiplier on (C_o-1)

[[

]]

Figure 5.1-9 Lognormal Probability Distribution for PIRT22

5.1.3.4 C2BX – Subcooled Void Fraction (M)

In Table 3.4-1, the highest ranking for C2BX is L. It has been raised to M for the present analysis because the uncertainty associated with TRACG’s prediction of the FRIGG void data was obtained by partitioning the FRIGG data set into subcooled and nucleate boiling regimes. (See above under C2AX.) As described in Reference [3], the optimum parameter for implementing void fraction uncertainty in the subcooled boiling regime is [[

]] Reference [37] shows that the scatter in the prediction of the subcooling at the net vapor generation point, $h_f - h_{fd}$, can be bounded by a [[

]] variation. Comparisons to 8x8 bundle void fraction data show that the larger scatter in the void fraction deviations in the subcooled boiling region [[

]] for the fully developed nucleate boiling region) is covered when a [[

]] perturbation is applied to the [[

]]. The mean error is also slightly larger for subcooled boiling [[

]] A [[

]] in the void fraction for the subcooled boiling region. On this basis, a 1σ uncertainty of [[

5.1.3.5 C3AX – Pellet Heat Distribution (H)

The pellet radial power distribution is calculated by lattice physics methods and is provided as an input to TRACG [1]. [[

]]

5.1.3.6 C3BX – Pellet Heat Transfer Parameters (H)

The TRACG fuel rod model based originally on the GESTR model [21] has been updated to incorporate the thermal conductivity model from PRIME [76]. The overall uncertainty in pellet heat transfer parameters is handled as described in Reference [3] by [[

]] In Reference [3], the uncertainty in the calculation of the fuel centerline to coolant temperature difference has been determined to be [[as discussed in Reference [66]. Following the specification developed for AOO applications, the desired uncertainty in centerline to coolant temperature difference for LOCA applications is represented by [[

]]

5.1.3.7 C3CX – Gap Conductance / Stored Energy (H)

The uncertainty in initial gap conductance and the corresponding pellet stored energy is covered by the uncertainty in pellet conductivity as described under C3BX.

5.1.3.8 C3 – Variable Gap Conductance (M)

The variation in the dynamic gap conductance is primarily due to the change in the gap size as the fuel pellet contracts following the scram. The uncertainty in the pellet contraction is primarily associated with the TRACG relocation model [1] that governs the transient interaction of the segments of the fractured fuel pellets. [[

]]

5.1.3.9 C4 – Flashing (M)

The uncertainty in flashing in the core region is taken into account through the uncertainty in liquid-side interfacial heat transfer. The magnitude of the interfacial heat transfer at the vapor bubble surface is varied through a [[as described above under A1.

5.1.3.10 C5 – SEO Inlet Uncovery/Vapor Flow Split (H)

Uncovery of the side entry orifice (SEO) and the subsequent vapor flow split are dependent on the interfacial drag coefficient C_1 and the hydraulic losses. The treatment of uncertainty in the interfacial drag coefficient is described above under A5. For a highly voided bundle, the hydraulic losses at the lower tie plate (LTP) and the SEO are of primary importance. For the AOO application [3], the LTP and SEO uncertainties were not considered explicitly, but were bounded through the spacer loss uncertainty. For the LOCA application, the flow regimes vary greatly through the transient and an explicit allowance is made for the uncertainty in the flow losses at the SEO. Available data can be bounded by applying an uncertainty of $[[\quad]]$ to the SEO loss coefficient, with a $[[\quad]]$

5.1.3.11 C6 – CCFL/CCFL Breakdown at the SEO (H)

The side entry orifice (SEO) is the most restrictive flow area between the lower plenum and the bundle. Steam entering the bundle from the lower plenum must pass through the SEO in the lower fuel support casting. The size of the orifice varies from approximately 2.2 inches to 1.4 inches in diameter depending on plant design and position of the bundle in the core. Because of the relatively small size of this orifice, CCFL can be expected to occur at low steam flows. CCFL at the SEO can allow the bundle to be reflooded prior to the filling of the lower plenum.

Tests were conducted at GE to investigate CCFL with the prototype BWR SEO geometry [49], [50]. Figure 5.1-10 summarizes the statistics obtained from a comparison of these data to the CCFL correlation employed in TRACG. The results show that the TRACG CCFL constant is $[[\quad]]$ and has a standard deviation of $[[\quad]]$. The results also show that it is reasonable to use a $[[\quad]]$ to describe the uncertainty in the CCFL constant at the SEO.

[[

]]

Figure 5.1-10 Fractional Error in CCFL Constant at the Side Entry Orifice

5.1.3.12 C7 – CCFL/CCFL Breakdown at the UTP/Spacer (H)

The uncertainty in the TRACG CCFL constant at the upper tie plate was addressed in the AOO application [3]. Comparisons were made on the basis of tests performed for a range of fuel types and it was concluded that the uncertainty could be described by a [[
]]. These data include GE11 bundles with part length rods and are also applicable to the most restrictive area in the GE14 bundle at the top spacer in the fully rodded section.

5.1.3.13 C8 – Multiple Channel Effects - Refill (H)

The uncertainty in the flow distribution between the fuel channels was addressed in the AOO application [3]. The uncertainty in the flow distribution is covered by the uncertainty in the interfacial shear and the hydraulic loss factors. The uncertainty in the interfacial shear has been discussed above under C2AX and the uncertainty in the loss factors is discussed below under C24. Additional discussion on parallel channel effect is provided in Section 6.4 which explains how this uncertainty is included in the calculations.

5.1.3.14 C8X – Void Collapse (M)

The uncertainty in void collapse is controlled by the uncertainty in liquid-side interfacial heat transfer, which is addressed above under C4.

5.1.3.15 C9 – Parallel Channel Flow Distribution-Blowdown (H)

The uncertainty in the parallel channel flow distribution is controlled by the uncertainty in the interfacial shear (C2AX) and the uncertainty in the hydraulic loss factors (C24).

5.1.3.16 C10 – Void Distribution, Axial and between Channels (H)

The uncertainty in the axial and radial void distribution is controlled by the uncertainties in the interfacial shear (C2AX).

5.1.3.17 C11 – Bundle-Bypass Leakage Flow (H)

The uncertainty in the channel to bypass leakage flow was addressed in the AOO application [3]. Combining the uncertainties in the flow through the leakage holes and the flow through the finger springs, it was shown that the total uncertainty in the leakage flow is [[]]. For LOCA applications, it is necessary to also consider the uncertainty in backflow leakage from the bypass to the bundle. Test data for backflow leakage at temperatures ranging from 150 to 400°F are compared with the leakage flow correlation used in TRACG in Reference [51]. The data are correlated with a bias of [[]] and a standard deviation of [[]]. Thus, the use of the AOO uncertainty for LOCA calculations will cover the uncertainty in both forward and backflow leakage. The uncertainty is imposed by using a [[]] for the leakage path loss coefficient.

5.1.3.18 C12 – Natural Circulation Flow (M)

Natural circulation is controlled by a balance between buoyancy and friction. Therefore, the uncertainty in this phenomenon is covered by the uncertainties in interfacial shear/drag and the hydraulic loss factors. The uncertainty in interfacial shear for the core and bypass is described under C2AX and the uncertainty in interfacial drag, applicable to the plenums and downcomer, is described under A5. The relevant hydraulic loss factor uncertainties are covered under C24 and I3.

5.1.3.19 C13 – Dryout/BT (Steady-State and Transient Effects) (H)

Dryout is calculated to occur when the critical power/quality is exceeded; rewet will occur if the critical power/quality is no longer exceeded and the wall temperature is below the minimum film boiling temperature, T_{\min} (C20). Critical power/quality is calculated with the GE critical quality boiling length correction (GEXL) or either the modified Zuber or Biasi CHF correlations, depending on the flow conditions. The manner in which these correlations are employed depends on the direction of the liquid and vapor flows. For cocurrent upflow, the GEXL correlation is used for critical power. For countercurrent flow and cocurrent downflow, CHF is calculated with either the modified Zuber or Biasi correlation, depending on mass flux. In practical terms, the Biasi correlation is used in very limited circumstances involving high flow conditions.

The GEXL correlation was derived from full-scale critical power test data covering the expected range of plant operation. The correlation typically has a small bias and a standard deviation between $[-0.05, 0.05]$ depending on fuel type. For LOCA demonstration calculations in Section 8.0, a bias of $[-0.05, 0.05]$ are used. This bias and uncertainty is a generic uncertainty that covers all fuel products up through GE14 design. For product-specific applications, it is equally acceptable to use values appropriate to the known fuel design (e.g., GNF2). The bias and uncertainty are applied with a $[-0.05, 0.05]$. TRACG has been compared to transient tests simulating typical BWR transients [2]. For the transient tests including 8x8 and 9x9 fuel, TRACG predicted the transient $\Delta\text{CPR}/\text{ICPR}$ with an average error of 0.002 and a variance of 0.01. Because the error in predicting the transient ΔCPR is small compared to the uncertainty in the GEXL correlation, it is not necessary to include an extra uncertainty for this term.

An uncertainty for the modified Zuber correlation was derived by comparisons with the CHF data of Walkush [52]. Walkush obtained CHF data for flow through a vertical annulus with a heated inner ring. The measurements included tests with countercurrent flow and cocurrent upflow and downflow. The CHF data were correlated vs. exit void fraction for void fractions ranging from 10 to 70%. The distribution of the fractional deviations between the modified Zuber correlation and the Walkush measurements is shown in Figure 5.1-11. The deviations are well represented by a $[-0.1, 0.1]$. The conservative bias was intentionally built into the modified Zuber correlation employed in TRACG and will be retained for the LOCA calculations. An uncertainty of $[-0.1, 0.1]$

Reference [1] presents information from a number of sources on comparisons between the Biasi CHF correlation and experimental data. The RMS error in the correlation with respect to the database from which it was originally derived was reported to be 7.3% [35]. Comparison of the Biasi correlation with 1928 data points from a Harwell round-tube data bank [53] gave a bias of -8% and a standard deviation of 17%. Comparison of the correlation with experimental points from a number of other data banks [54] showed that 73% and 99% of the data were within 30% of the correlation for constant dryout quality and constant inlet subcooling, respectively. On the basis of this collection of data comparisons, a $[-0.1, 0.1]$ was specified for the Biasi correlation.

[[

]]

Figure 5.1-11 Fractional Error in Modified Zuber Critical Heat Flux Correlation |

5.1.3.20 C14 – Film Boiling - Low Void (H)

TRACG uses the modified Bromley correlation for convective heat transfer for low void (<0.4) conditions and low fluid velocities. An uncertainty for the modified Bromley correlation was derived on the basis of comparisons with test data reported in Reference [55]. The test data used for the uncertainty determination included quench tests, in which a heated rod was immersed in a pool of saturated or subcooled water at atmospheric pressure, and full-scale bundle reflooding experiments conducted at Kraftwerk Union Aktiengesellschaft (KWU). The quench tests included data over a range of subcooling up to 30 °F. A statistical summary of the results of the comparisons is shown in Figure 5.1-12. The mean bias is [[

[[

]]

]]

Figure 5.1-12 Fractional Error in Modified Bromley Heat Transfer Coefficient

5.1.3.21 C15 – Film Boiling -Dispersed Flow (H)

Heat transfer for film boiling under dispersed flow conditions is calculated in TRACG with the Sun-Gonzalez-Tien heat transfer coefficient. The uncertainty in the Sun-Gonzalez-Tien heat transfer coefficient is [[

]] A second parameter influencing heat transfer under dispersed flow conditions is vapor side interfacial heat transfer. As in the case of liquid-side interfacial heat transfer (A1), TRACG uses the Lee-Ryley correlation in conjunction with a droplet diameter based on a critical Weber number to calculate vapor-side interfacial heat transfer in the dispersed flow regime [1]. In the absence of separate effects data that can be used to directly define the uncertainty in the vapor-side interfacial heat transfer correlation, an uncertainty range of [[

]] is used.

5.1.3.22 C16 – Thermal Radiation (H)

The uncertainty in the TRACG radiation model was addressed by assigning an uncertainty range to the emissivity. An appropriate range for the uncertainty was derived by making a series of TRACG predictions for a stagnant-air test in the GE Core Spray Heat Transfer Facility. The central feature of this facility was an electrically heated full-scale 8x8 fuel bundle. The test matrix included steady-state tests in which no liquid was injected and the bundle contained essentially stagnant air. The channel box was externally cooled and maintained at 311 K. Under these conditions, convective heat transfer is minimized and radiation is the dominant mode of heat transfer. The TRACG results showed that the peak cladding temperature was bounded above and below by calculations with [] This indicates that the uncertainty in the thermal radiation model can be covered by a []

5.1.3.23 C17 – Steam Cooling (H)

TRACG calculates heat transfer to superheated steam with the Dittus-Boelter heat transfer coefficient [1]. An extensive investigation of heat transfer to superheated steam in a rod bundle is presented in Reference [56]. Reference [56] describes a series of steady-state tests over a pressure range from 13.1 to 40.7 bar and a mass flux range from 33.9 to 169.6 kg/m²-s. The tests were conducted in an interior-peaked rod bundle with an outlet-peaked axial heat flux profile. Measured rod temperatures were compared with predictions based on several heat transfer coefficients including Dittus-Boelter. Two approaches were used to calculate the local steam temperature for the predictions - a bundle average approach and an extended rod-centered subchannel approach. The bundle average approach resulted in [] in the predicted wall temperatures. The extended rod-centered subchannel approach resulted in [] The RMS error in the predictions was [] Combining the RMS error with the mean bias gives a standard deviation of about [] for both approaches. These results are summarized in the “Wall Temperature” columns of Table 5.1-1.

Table 5.1-1 Error Measures for Wall Temperature and Dittus-Boelter Heat Transfer Coefficient (Estimated)

[]	[]		[]	
[]	[]	[]	[]	[]
[]	[]	[]	[]	[]
[]	[]	[]	[]	[]
[]	[]	[]	[]	[]

The wall temperature error on which the statistical evaluation in Reference [56] is based was defined as

$$Error(T) = \frac{T_{w,m} - T_{w,p}}{T_{w,m}}$$

where

$T_{w,m}$ = measured wall temperature

$T_{w,p}$ = predicted wall temperature

For purposes of TRACG analysis, the focus is on the corresponding error in the heat transfer coefficient, defined as

$$Error(h) = \frac{h_p - h_m}{h_p}$$

It is easily shown that

$$Error(h) = \frac{Error(T)}{1 - \frac{T_s}{T_{w,m}}} \quad \text{where } T_s = \text{steam temperature.}$$

It is obvious from this expression that the fractional error in the predicted heat transfer coefficient can be several times as large as that in the predicted wall temperature.

The data described in Reference [56] include 1935 measurement points. Of these, 60 points from four runs are shown graphically in the report along with the steam temperature calculated by both the bundle average and extended rod-centered subchannel approaches. It is worthwhile to note that those 60 points from four runs in Reference [56] are for internal rods only. On the basis of these 60 points, it was determined that

[[]]

The average values of the multipliers, determined on the basis of the 60 points for which the data are available, were used to estimate the mean bias and standard deviation for the Dittus-Boelter heat transfer coefficient as shown in the “Dittus-Boelter HTC” columns of Table 5.1-1.

On the basis of these results, it was concluded that if the TRACG model for calculating the steam temperature is similar to the bundle average approach, it would be necessary to take a [[]] on the Dittus-Boelter heat transfer coefficient for steam cooling conditions. If the TRACG model is similar to the extended rod-centered subchannel approach, a [[]]

]] would be appropriate. The TRACG model used for LOCA application is based on a bundle average approach. [[

]]

The wall temperature data were further processed for distributional characteristics and to see if the statistics for the subset of 60 points were similar to those tabulated in Reference [56] for the entire data set. The statistical summary plot (Figure 5.1-13) indicates that it would be acceptable to assume the deviations are [[]]. The mean and standard deviation of the wall temperature deviations (based on bundle average approach) of the 60 points are [[]]. These compare with [[]], respectively, for the entire data set (Table 5.1-1). From this it may be concluded that the 60 points constitute a representative sample of the full data set and, hence, that the statistics for the heat transfer coefficient inferred from the 60 points are representative of the entire data set.

[[

]]

Figure 5.1-13 Fractional Error in Wall Temperature Calculated with the Dittus-Boelter Heat Transfer Coefficient

5.1.3.24 C18 – Fuel Cladding Strain /Perforation (H)

The key drivers governing strain-induced fuel rod perforation are the temperature-dependent clad rupture stress and the rod internal pressure. Based on material properties, the rupture stress and its associated uncertainty is modeled in TRACG as three curves corresponding to nominal, lower bound, and upper bound rupture stress curves as functions of cladding temperature (Figure

5.1-14). At each temperature, the upper and lower bounds are used to define uniformly-distributed samples above and below the nominal rupture stress, respectively.

The instantaneous clad hoop stress is directly related to the fuel rod internal pressure. Nominal fuel rod internal pressures are calculated in TRACG as described in Section 7.5.3.1 of Reference [1] using parameters calculated by PRIME [76] and passed to TRACG [[

]]

[[

]]

Figure 5.1-14 Rupture Stress Model Compared to Data

5.1.3.25 C19 – Spray Cooling (H)

The uncertainty in spray cooling heat transfer is covered by the uncertainties in the parameters described under C15, C16, C17 and C21.

5.1.3.26 C20 – T_{min} (Minimum Stable Film Boiling Temperature) (H)

TRACG calculates the minimum film boiling temperature (T_{min}) using the Shumway correlation which is described mathematically by Equation (6.6-52) of Reference [1]. Comparisons of the Shumway correlation to data for a wide range of pressures are available in Section 6.6.7.3 of Reference [1] and in Reference [80]. For the Shumway correlation, a [[
]] applied to the calculated difference between T_{min} and the saturation temperature (T_{sat}) sufficiently covers the correlation standard deviation of 55 K indicated in Reference [80]. [[

]] Although the Shumway correlation was developed using stainless steel data, it accounts for the material properties and is generally applicable for other materials (including zircaloy) as is shown in Reference [80]. A key conclusion from Reference [80] is that the Shumway correlation applied for zircaloy provides a value of T_{min} that is lower than most of the zircaloy data. Lower values of T_{min} are more conservative because they delay the return to nucleate boiling and thus result in higher and more conservative calculated values for the local cladding surface temperatures (T_{clad}).

[[

]]

5.1.3.27 C21 – Axial Conduction Controlled Quenching (H)

The motion of a quench front along a heated surface is a function of axial conduction, radial convection and internal heat generation. The uncertainty in the model can be represented in terms of the correlation used to calculate the quench front velocity. In TRACG this correlation expresses a modified Peclet Number as a function of a modified Biot Number with the heat transfer coefficient behind the quench front and the Leidenfrost temperature as parameters. The form of the correlation in TRACG was derived on the basis of data from Bennett, et al. [57] and Duffey and Porthouse [58]. A statistical summary of the fractional deviations between the TRACG correlation and these data is shown in Figure 5.1-15. [[

]]

[[

]]

Figure 5.1-15 Fractional Deviations in Quench Front Velocity

5.1.3.28 C22 – Channel-Bypass HT (H)

The uncertainty in channel to bypass heat transfer is covered by an [[]]] which governs heat transfer for subcooled and nucleate boiling to the inside channel wall and a [[]]] uncertainty on wall heat transfer to the bypass which covers either nucleate boiling or single phase heat transfer (A2).

5.1.3.29 C23 – Water Rod Hydraulics (M)

The parameters controlling the uncertainty in water rod hydraulics are liquid-side interfacial heat transfer, interfacial shear and the orifice loss coefficient. The first three control the flashing of the inventory in the water rod, while the third controls the flow through the water rod. The treatment of the uncertainty in liquid-side interfacial heat transfer and interfacial shear are described under C4 and C2AX. The water rod flow path is through a ring of entrance holes at the bottom, past the orifice and out through a ring of exit holes at the top. There are no separate effects data that can be used to directly derive an uncertainty for the orifice loss coefficient but the orifice loss is precisely calibrated to control the water rod leakage. Accordingly, it is reasonable to impose a [[]]] uncertainty with a uniform distribution for the orifice loss.

5.1.3.30 C24 – Core Pressure Drop (M)

A detailed discussion of the uncertainty in the frictional components of the core pressure drop was provided in the AOO application report [3]. The uncertainties in the core pressure drop include the uncertainties in SEO/LTP, spacers, and UTP, which are presented in Tables 5-2, 5-3 and 5-4 of Reference [3]. The spacer frictional pressure drop is based on full-scale measurement

for conditions covering the range of expected reactor conditions. The uncertainty in the pressure drop for the spacers is determined from full-scale ATLAS data and is presented in Table 5-3 of Reference [3] for different fuel types. It is concluded in [3] that [[

]] can be used for all bundle types. For the LOCA application, the uncertainty in the SEO/LTP pressure drop is considered separately and is bounded by an uncertainty of [[]]] (For additional discussion of the SEO/LTP pressure drop uncertainty see Section 5.1.3.10.) It was shown that the uncertainty in all components of the core pressure drop could be bounded by imposing a [[]]]

The LOCA application uses a [[

]]

5.1.3.31 C25 – Decay Heat (H)

TRACG calculates the decay heat as a function of time in a way that conservatively approximates the American National Standards Institute (ANSI)/ANS-5.1-1979 standard entitled “American National Standard for Decay Heat Power in Light Water Reactors” [59]. In this standard, values are provided for decay heat power from fissioning of the major fissionable nuclides present in light water reactors (LWRs) (i.e., U235 and Pu239 (thermal) and U238 (fast)) and methods are prescribed for evaluating the total fission product decay heat power from the data given for these specific fuel nuclides. By way of this methodology, the decay heat curve becomes a function of the fuel design, depletion environment and power history. Thus, in theory, each point in the reactor has a unique decay heat curve. Fortunately, the variations in decay heat due to the above effects are small and curves can be defined [[

]] with little loss in accuracy. The details of the derivation as well as the calculation of the uncertainties are described in References [59] and [38]. TRACG implementation details are provided in Section 9.3 of Reference [1]. For the purpose of illustration, the nominal decay heat curve and the $\pm 1\sigma$ curves are shown in Figure 5.1-16 for an exposure of 11 GWd/MTU. [[

]],

as determined from the uncertainty specified as part of the ANS decay heat standard.

[[

]]

Figure 5.1-16 Decay Heat Uncertainty at an Exposure of 11 GWD/MTU

5.1.3.32 C26 – Metal-Water Reaction (H)

TRACG uses the Cathcart-Pawel correlation [60] to calculate the reaction rate of Zircaloy cladding with water. Reference [60] includes a statistical evaluation of the reaction rate correlation. The coefficients in the correlation were derived by a linear regression analysis of the logarithm of the reaction rate data as a function of temperature. This ensured a zero bias in the correlation. Ten data points were available to determine the coefficients in the regression equation. The deviations of these ten points from the correlation were processed to obtain a statistical estimate of [[]] for the standard deviation. Reference [60] states that the application of Bowman and Shenton’s normality test did not invalidate the assumption that the differences between the observations and the correlation are normally distributed.

5.1.3.33 C26I – Initial Oxide Thickness

The initial, or pre-transient, oxide thickness is not an element of the PIRT presented in Table 3.4-1. Compared to the metal-water reaction uncertainties, it has less direct effect on critical parameters. However, it is considered in the methodology for completeness as part of the metal-water reaction model, regardless of its ranking. The pre-transient oxide model has the general form

$$\tau_{ox} = Ae^{(B \cdot x)}$$

or, equivalently

$$\ln(\tau_{ox}) = \ln(A) + B \cdot x$$

where τ_{ox} is the oxide thickness in microns, x is the local burnup in GWd/MTU, and A and B are fitting parameters. The best estimate fit to the metallographic data yielded [[

]].

Figure 5.1-17 shows the comparison of the model to the actual database for oxide thickness. The model is developed from a dataset with 128 points. In the LOCA methodology, the initial oxide thickness for a given exposure is sampled from a normal distribution with its mean value at the nominal thickness.

[[

Figure 5.1-17 Initial Oxide Thickness Model

]]

5.1.4 Guide Tube

5.1.4.1 D1 – Flashing/Redistribution (M)

Flashing in the guide tube is controlled by liquid-side interfacial heat transfer, which is addressed in the same manner as described above under A1.

5.1.4.2 D2 – CCFL/CCFL Breakdown: Top of GT (H)

This is the same parameter as discussed above under B4.

5.1.4.3 D3 – Condensation (H)

Condensation is controlled by liquid-side interfacial heat transfer (D1).

5.1.4.4 D4 – Refill (H)

The refill flow path is from the bypass to the control rod guide tube with the major source of hydraulic loss being the expansion to a large volume. The TRACG variables that can affect the flow are liquid-side interfacial heat transfer (D1), the interfacial drag coefficient and the expansion loss coefficient. The uncertainty in the guide tube interfacial drag coefficient was addressed as described under A5. There are no separate effects data available for determination of an uncertainty for the expansion loss coefficient. A [[
]] was imposed for the LOCA calculations.

5.1.5 Downcomer

5.1.5.1 E1 – Break Uncovery (Two-Phase Break Flow) (H)

Break uncovery in the downcomer is controlled by the break flow and the interfacial drag coefficient. Uncertainties in the break flow are covered under L1, M1 and R3. The uncertainty in the downcomer interfacial drag coefficient was addressed in the same manner as described under A5 in Section 5.1.1.6.

5.1.5.2 E2 – Void Profile/Two-Phase Level (H)

The void profile and two-phase level in the downcomer are controlled by the interfacial drag coefficient (E1).

5.1.5.3 E3 – ECCS Interaction/ Condensation (M)

Condensation in the downcomer is controlled by liquid-side interfacial heat transfer, which is addressed in the same manner as described under A1.

5.1.5.4 E4 – 3-D Effects (M)

Potential three-dimensional effects in the downcomer were addressed by a nodalization study [2], the results of which are described above under A11.

5.1.5.5 E6 – Flashing (M)

Flashing in the downcomer is controlled by liquid-side interfacial heat transfer (A1).

5.1.6 Upper Plenum Region

5.1.6.1 F1 – Void Distribution/Two-Phase Level (H)

[[

]] These data are characterized by their applicability to the prediction of void fraction in regions with relatively large hydraulic diameter. Accordingly, selections from this data set, taking into consideration other aspects of the test conditions, will be used as the basis for defining the [[

]] A statistical summary of the comparisons of TRACG predictions with measurements from these four data sets, combined as a single set of deviations, is shown in Figure 5.1-18. The absolute mean bias is [[]] void and the absolute standard deviation is [[]] void.

[[

]] (A comparable evaluation for lower plenum is described under A5 in Section 5.1.1.6 and for the core and bypass is described below under C2AX in Section 5.1.3.3.)

[[

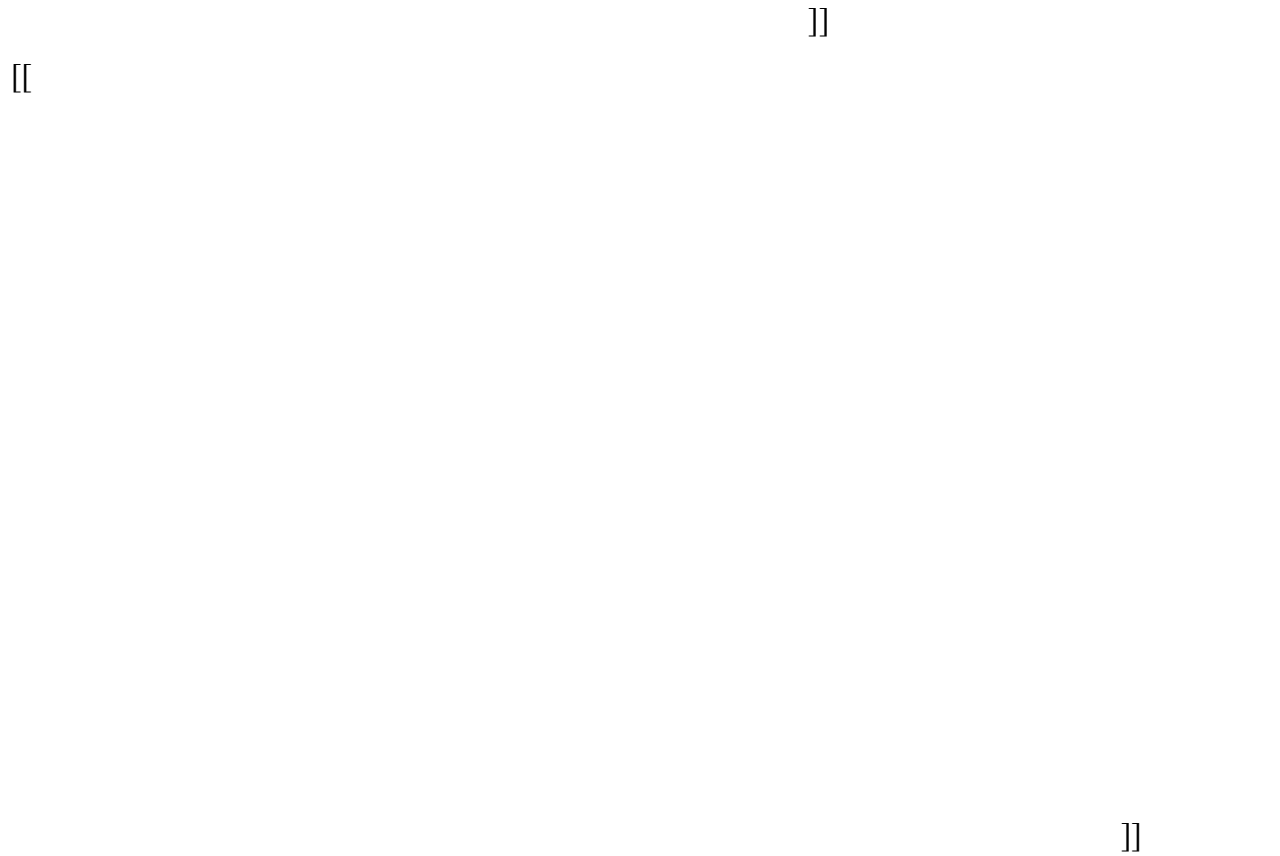


Figure 5.1-18 Void Fraction Deviations for Tests Applicable to Regions with Large Hydraulic Diameter

[[

]]

Figure 5.1-19 Sensitivity of TRACG Prediction of Average Void Fraction in EBWR Test Facility to PIRT Multiplier on Interfacial Drag Coefficient

[[

]]

Figure 5.1-20 Probability Distribution for Multiplier on Interfacial Drag Coefficient

5.1.6.2 F2 – ECC Interaction/Mixing/Subcooling Distribution (H)

ECC interaction with the upper plenum fluid is controlled by liquid-side interfacial heat transfer (A1) and the interfacial drag coefficient (F1).

5.1.6.3 F3 – Noncondensable Return At Low Pressures (H)

The primary effect of this parameter is the reduction of condensation heat transfer in the upper plenum due to the presence of noncondensable gases. TRACG applies a degradation factor to the liquid-side interfacial heat transfer to account for this effect. An uncertainty estimate for this factor can be obtained from the database used for the development of the Kuhn-Schrock-Peterson (K-S-P) correlation for the degradation of condensation heat transfer due to noncondensibles. This correlation was developed specifically for film condensation in vertical tubes but the degradation mechanism is essentially the same as that in the upper plenum. The uncertainty in the K-S-P correlation derived from 70 steam-air tests is [[]]. On this basis, the uncertainty in the degradation factor applied to liquid-side interfacial heat transfer is specified as [[]]

5.1.6.4 F4 – Spray Distribution (Uncovered Upper Plenum) (H)

[[]]

|

|

|

|

]]

[[

Figure 5.1-21 Minimum Channel Spray Flow vs. Spray Header Flow Example

[[

]]

|

Figure 5.1-22 Core Spray Flow Rates Example

]]

|

[[

]]

Figure 5.1-23 Core Spray to the Minimum Flow Bundle vs. Pressure Example

5.1.7 Jet Pump

5.1.7.1 G2 – JP Characteristics – Coastdown (M)

The coastdown of the jet pump flow following a recirculation pump trip is controlled by the coastdown of the recirculation pumps and the jet pump characteristics described below. The coastdown of the recirculation pumps is described under H2. The jet pump characteristics are addressed via the M-N curve. The AOO application report [3] includes a detailed description of the treatment of uncertainties in the jet pump characteristics. Additional details are provided in RAI responses for Supplement 3 of the same report [4]. Comparisons to a full-scale one-nozzle jet pump for drive flows from 42% to 119% of rated flow show essentially no bias for the TRACG N-ratio and a standard deviation of [[]]. Comparisons to a full-scale five-nozzle jet pump for drive flows from 77% to 94% of rated flow show no bias for the TRACG N-ratio and a standard deviation of [[]]. In addition to the comparisons to full-scale test data, TRACG calculations were compared to 1/6-scale jet pump performance data for drive flows of 1.4, 2.8 and 4.2 liters/s, covering M-ratios from –2 to 4. The results showed that there was no apparent trend with scale and, consequently, that the 1/6-scale data could be used to characterize jet pump performance outside the range of normal operation [3]. The jet pump characteristics can be perturbed by varying the jet pump inlet loss. For the one-nozzle pump, a [[]]

pump, a [[]]

]] For the five-nozzle jet

5.1.7.2 G3 – JP Characteristic - Reverse Flow (M)

There are no full-scale jet pump data for reverse drive flow but, as stated above under G2, the jet pump performance is not scale sensitive and therefore the 1/6-scale jet pump data can be used to determine the uncertainty in the jet pump model for reverse drive flow. [[

]] indicating that the TRACG model is a very good fit to most of the data.

The jet pump characteristics for reverse flow can be perturbed by varying the jet pump [[

]]

5.1.7.3 G4 – Flow Coastdown following Recirculation Pump Trip (H)

The uncertainty in flow coastdown following a recirculation pump trip is controlled by the uncertainty in jet pump performance (G2) and the uncertainty in recirculation pump inertia (H2).

5.1.7.4 G5 – LPCI Condensation in Jet Pump (H)

The uncertainty in LPCI condensation in the jet pump is controlled by the uncertainty in liquid-side interfacial heat transfer. Following the procedure previously adopted for the lower plenum (A1), the magnitude of the interfacial heat transfer is varied using a [[

]]

5.1.7.5 G6 – Two-Phase Flow Combinations/ Level In Jet Pumps (M)

The uncertainty in two-phase flow and level in the jet pumps is controlled by the uncertainties in liquid-side interfacial heat transfer (G5) and the interfacial drag coefficient (A5).

5.1.7.6 G7 – Pressure Drop (M)

The uncertainty in jet pump pressure drop is controlled by the uncertainties in the suction and nozzle losses described under G2 and G3.

5.1.8 Recirculation Pump

5.1.8.1 H2 – Pump Characteristics/Coastdown (M)

The uncertainty in the mechanical inertia of the recirculation pump is controlled by the tolerances of the pump components and is expected to be quite small. For the TRACG LOCA evaluations, a bounding uncertainty of [[]] in the pump inertia was imposed.

5.1.8.2 H3 – Pump Two-Phase Degradation (M)

[[]]

]]

5.1.8.3 H4 – Pump Pressure Drop (M)

[[]]

]]

5.1.9 Steam Separator

5.1.9.1 I3 – Pressure Drop (M)

The uncertainties in the loss correlations for steam separator pressure drop are addressed in the AOO application report [3]. On the basis of the deviation of the TRACG correlations from two and three-stage separator pressure drop data, it was shown that an uncertainty of [[]] in the separator loss coefficients would adequately cover the uncertainty in the predictions of data. This uncertainty is used with a [[]]

5.1.10 Steam Dryer

5.1.10.1 J2 – Pressure Drop (M)

References [62] and [63] present steam dryer pressure drop test data for BWR/4,5 and BWR/6 dryer designs, respectively. The BWR/4,5 data include 26 measurements of dryer pressure drop as a function of steam velocity normal to the dryer face. The ratio of the dryer pressure drop to the square of the steam velocity shows no significant trend with velocity over the tested range of 1 to 5 ft/s. [[]]

]]

5.1.11 Steam Line

5.1.11.1 L1 – Critical Flow through Break or ADS (H)

Critical flow data were obtained from the Pressure Suppression Test Facility (PSTF) Vessel Blowdown, Marviken and GIRAFFE SIT Tests [34]. Section 3.3.4 of Reference [34] presents a summary comparison between TRACG calculations and critical flow measurements for liquid, two-phase and steam blowdown from two Marviken and three PSTF Vessel Blowdown Tests. The bias and standard deviation of the combined data set have been calculated in accordance with the statistical weighting procedure described in Reference [34]. TRACG calculates the combined PSTF/Marviken data set with a [[

]] A smaller uncertainty could be justified for the blowdown from the steam line but, for simplicity, the common (larger) uncertainty has been applied for all break locations.

A quantitative evaluation of TRACG accuracy was also made on the basis of the break flow at 20 minutes from test initiation and the maximum break flow for each of the four GIRAFFE SIT tests [34]. TRACG calculates the break flow at 20 minutes after test initiation with a [[

]] The maximum break flow in these simulations is in the critical flow regime. Based on the composite results of these evaluations, a [[

]]

5.1.11.2 L2 – Droplet Entrainment (M)

The uncertainty in steam line droplet entrainment is covered by the use of a bounding input value for the steam dryer efficiency (Section 8).

5.1.11.3 L3 – Pressure Drop (M)

The uncertainty in steamline pressure drop was addressed in the AOO application [3]. A [[]] uncertainty was specified on the basis of comparisons between TRACG predictions and pressure drop data. This uncertainty is applied to the local losses that dominate the pressure drop. It is large enough to also cover the uncertainty in the correlations used to calculate wall friction.

5.1.12 Recirculation Line

5.1.12.1 M1 – Critical Flow Through Break (H)

[[]] The basis for these values is described under L1.

5.1.12.2 M2 – Flashing (H)

The uncertainty in recirculation line flashing is controlled by the uncertainty in liquid-side interfacial heat transfer. The treatment of this uncertainty in the recirculation line is the same as that described above for the lower plenum (A1).

5.1.12.3 M3 – CCFL: Air In/Two-Phase Flow Out (M)

The effect of the uncertainty in long-term air ingress via the recirculation line break is covered by the uncertainty in the degradation of condensation heat transfer in the upper plenum (F3).

5.1.12.4 M8 – Pressure Drop (M)

The uncertainty in recirculation line pressure drop was addressed in the AOO application [3]. A [[]] uncertainty was specified on the basis of comparisons between TRACG predictions and pressure drop data. This uncertainty is applied to the local losses that dominate the pressure drop. It is large enough to also cover the uncertainty in the correlations used to calculate wall friction.

5.1.12.5 M9 – LPCI/Break Flow Interaction (M)

Interfacial heat transfer of cooler LPCI water injected into the recirculation line with steam in the line influences the calculated pressure gradient in the line which in turn influences the break flow. [[]]

5.1.13 Isolation Condenser

5.1.13.1 Q2 – Isolation Condenser (IC) Capacity (M)

Isolation condenser capacity refers to the volume of condensate held up initially in the condenser. The initial level in the condenser tubes is normally at the top of the heat transfer surface. The uncertainty in this parameter is small and is taken to be of the order of [[]]

5.1.13.2 Q5 – Secondary Side Heat Transfer (M)

Data from operating plants with isolation condensers shows that the heat transfer capacity averages a factor of 2 larger than the design value. [[]]

]]

5.1.14 Feedwater System

5.1.14.1 R1 – Flow Dynamics Feedwater/Attached Piping Line Volume (M)

The volume of the feedwater piping that participates in the LOCA transient is accurately known. A nominal tolerance of [[]] was used for sensitivity studies to set a bounding input value (Section 8).

5.1.14.2 R2 – Feedwater/Attached Piping Temperature Dynamics (M)

Sensitivity studies were performed to set a bounding input value for the water temperature in the feedwater attached piping (Section 8). The sensitivity studies considered a range of feedwater temperatures from the normal operating value to the value with Final Feedwater Temperature Reduction (FFWTR).

5.1.14.3 R3 – Critical Flow Through FW Break (H)

As for other break locations (L1, M1) a [[]].

5.1.15 Containment

5.1.15.1 DW0 and SP1 – Drywell Pressure (H) and Suppression Pool Temperature (M)

The containment is not modeled with TRACG for ECCS/LOCA application. Instead, boundary conditions are prescribed on the basis of independent containment calculations. Feedback from containment pressure is limited to the latter stages of the transient because the break flow is choked until the reactor vessel depressurizes to near the containment pressure. The ECC water for the LPCS and LPCI is drawn from the suppression pool in the wetwell and its temperature is determined by the suppression pool heatup.

[[

]] PCT sensitivity to the choice of containment boundary conditions is described in Section 8.

5.1.16 Summary

This section provided the assessment of model biases and uncertainties for LOCA application for each of the high and medium-ranked phenomena identified in Section 3.0. Table 5.1-2 provides the complete list of the uncertainty parameters treated as part of the methodology. The table also highlights the parameters that were reviewed and approved as part of other applications, namely TRACG AOO [3] and ESBWR TRACG [39] applications. The green shading is used to indicate the uncertainty is the same as previously reviewed and approved. A partial shading of a row is used to indicate that the uncertainty has not changed but has a different ranking for LOCA, therefore applies here.

Table 5.1-2 Parameters Governing High and Medium Ranked PIRT Phenomena

[[

|
|

|
|

|

|
|

5.2 EFFECTS OF NODALIZATION

The nodalization strategy for the various reactor components was developed from the qualification of TRACG against test data for these components. The same consistent nodalization strategy was then applied for full-scale plant calculations. The adequacy of the nodalization has been demonstrated and supported by sensitivity studies. This section summarizes the conclusions from these sensitivity studies. Standard nodalizations for modeling of BWR reactor vessels and other components have been presented in the *TRACG Qualification Report* [2].

The effects of nodalization on the LOCA model are primarily studied by comparing the PCT results. In order to conclude that the standard nodalization is adequate, sensitivity studies must indicate that the overall trends of the transient analysis is the same and the differences in the PCT results are insignificantly small. The nodalization sensitivity studies covered a wide range of nodes in the input model including various regions in the vessel and the broken recirculation line. The vessel component of TRACG has axial, radial, and azimuthal noding capability. The nodes are levels, rings, and sectors for axial, radial, and azimuthal discretization, respectively.

For the nodes representing the [[

]]

Table 5.2-1 and Table 5.2-2 summarize the added detail of the noding sensitivity [[

]]

In all of the sensitivity cases, [[

Figure 5.2-11 provide a visual comparison of [[]]

] Figure 5.2-1 through

]]

In conclusion, the standard nodalization shown in the *TRACG Qualification Report* [2] as employed in the LOCA analysis is adequate. A more detailed nodalization does not significantly change the computed results as the overall trends are the same and the PCT values are [[

] The standard nodalization is a representative and typical of the least-detailed nodalization that is considered acceptable. Additional details may be added or changed from the standard nodalization provided the changes are shown not to invalidate the qualification bases and the effect on modeling biases and uncertainties are assessed.

[[

Figure 5.2-1 Vessel Axial Nodalization Sensitivity for Large-Break LOCA

]]

[[

Figure 5.2-2 Vessel Axial Nodalization Sensitivity for Intermediate-Break LOCA

]]

[[

Figure 5.2-3 Vessel Axial Nodalization Sensitivity for Small-Break LOCA

[[

**Figure 5.2-4 Vessel Radial and Azimuthal Nodalization Sensitivity for Large-Break
LOCA**

[[

]]

Figure 5.2-5 Vessel Radial and Azimuthal Nodalization Sensitivity for Intermediate Break

[[

]]

Figure 5.2-6 Vessel Radial and Azimuthal Nodalization Sensitivity for Small-Break LOCA

[[

Figure 5.2-7 Channel Axial Nodalization Sensitivity for Large-Break LOCA

]]

[[

Figure 5.2-8 Channel Axial Nodalization Sensitivity for Intermediate-Break LOCA

]]

[[

Figure 5.2-9 Channel Axial Nodalization Sensitivity for Small-Break LOCA

[[

]]

Figure 5.2-10 Vessel Axial Nodalization Sensitivity for BWR/2

]]

[[

]]

Figure 5.2-11 Channel Axial Nodalization Sensitivity for BWR/2

5.3 EFFECTS OF SCALE

The TRACG model description report [1] shows that the ranges of applicability of the basic models and correlations used by the code cover the geometric scales and operating conditions of BWR plants [1; Table 6-1]. This is a necessary condition for valid application of TRACG calculations for the full-scale BWR. The TRACG qualification report [2] shows that TRACG is capable of predicting the results of a large number of separate effects, component performance, scaled integral system and BWR plant tests. From these results, it can be concluded that there is no apparent effect of scale in TRACG's predictive capability. This constitutes a sufficient condition for valid application of TRACG calculations for full-scale plants. The results presented below substantiate the conclusion that there is no effect of scale in TRACG's predictive capability for phenomena of importance to BWR LOCA events.

5.3.1 Full Scale Test Coverage

5.3.1.1 Full Scale Component and Integral Systems Tests

A number of BWR components have been tested at full scale. Table 5.3-1 shows a summary of the highly ranked PIRTs and the extent of coverage by full-scale component tests. Of these, the most important is the fuel channel, which consists of a rod bundle inside a channel box. Void fraction and heat transfer data have been obtained in fuel channels at normal and accident

conditions. These data have been used as separate effects data to validate the basic TRACG interfacial shear, wall shear, interfacial heat transfer and wall heat transfer models.

Jet pumps, separators and dryers have also been tested at full scale. The performance data from these tests are directly applicable to BWR plant calculations. The Marviken critical flow tests provide data at a sufficiently large scale to qualify the capability of TRACG for critical flow calculations.

A large number of BWR fuel rods have been tested to characterize the gap conductance, stored energy, fission gas release and fission gas pressure as functions of the fuel rod operating parameters of pellet power generation and exposure. The models used for calculation of fuel rod behavior in TRACG are based on these data.

Table 5.3-1 also shows a column for the Steam Sector Test Facility (SSTF) Integral System Tests. This facility represented a 30-degree full-scale sector of a BWR/6. Tests of the refilling phase of a LOCA were performed in this facility and the test data provide a basis for TRACG qualification for the prediction of such phenomena as parallel channel behavior and regional inventory distribution.

Table 5.3-1 Full Scale Test Data Coverage for LOCA Phenomena

[[
○	○○○○○○○○○○○○○○			
○	○○○○○○			
○	○○○○○○○○○○○○○○			
]]

Table 5.3-1 (cont'd) Full Scale Test Data Coverage for LOCA Phenomena

[[
o	oooooooooooooooooooo			
o	oooooooooooo			
o	oooooooo			
o	oooooooooooooooooooo			
o	oooooooooooo			
o	oooooooooooooooooooo			
o	oooooooooooooooooooo			
]]

5.3.1.2 Operating Plant Tests

Tests performed at BWR plants provide qualification data for a number of phenomena that are highly ranked for LOCA (Table 4.2-1). These include power distribution measurements during normal operation and measurements of power changes during transients that provide a precise qualification basis for TRACG's void fraction and void coefficient models. Measurements are also available for the flow/power transient following a pump trip and for changes in the reactor pressure and downcomer level during loss of feedwater, pump trip and isolation transients.

5.3.2 Scaled Integral LOCA Simulation Tests for Jet Pump Plants

Scaled integral LOCA simulation tests provide important demonstrations of the performance of a BWR plant subjected to a LOCA and, in the context of the present document, serve to qualify the application of the TRACG computer code to the prediction of the outcomes of postulated BWR LOCAs. Scaling considerations related to integral-system test facilities can be divided into what are known as 'top-down' and 'bottom-up' scaling criteria [69]. An important bottom-up feature of the integral tests considered herein was their use of one or more full-scale fuel bundles with simulated BWR fuel rods in a prototypical array with BWR spacers, upper and lower tieplates and channel box. The choice of the number of fuel bundles was dictated primarily by the requirement for sufficient test facility power to produce prototypical rod heatup transients during a LOCA simulation. The basis for the top-down scaling of the regional volumes and flows was the ratio of the number of full-size test facility bundles to the total number of bundles in the prototype. Prototypical thermodynamic conditions were preserved by starting the tests from BWR operational reactor vessel pressure.

Test facility scaling for LOCA application is evaluated herein by considering three integral-system test facilities simulating a jet pump BWR.

- The FIST facility [70] was an integral system test facility designed to simulate the post-LOCA response of a 2895 MWt BWR/6-218 system with 624 8x8 fuel bundles. It had a nominal volumetric scaling of 1:624 with one full-height electrically heated rod bundle and proportionally distributed regional volumes. The initial power and the core, recirculation, feedwater and ECCS flows were scaled at 1:624. The vessel pressure and feedwater temperature were scaled at 1:1. The power decay was designed to match the bundle average heat flux of the BWR/6-218 core. FIST Test 6DBA1B simulated a recirculation suction line guillotine break with an LPCI failure (two out of three LPCI loops unavailable). The test covered the blowdown and refill/reflood phases of the LOCA transient. Test measurements included pressure, break flow, vessel inventory distribution and heater rod temperatures.
- The ROSA-III facility [71] was an integral system test facility designed to simulate the post-LOCA response of a 3800-MWt BWR/6-251 system with 848 8x8 fuel bundles. It had a nominal volumetric scaling of 1:424 with four half-length electrically heated rod bundles. The four half-length bundle concept was designed to study thermal-hydraulic interaction between neighboring bundles having different power levels. The relative

elevations of the system components, including the two recirculation loops, were simulated within the constraints imposed by the half-height facility. The core, recirculation, feedwater and ECCS flows were scaled at 1:424 and the vessel pressure and feedwater temperature were scaled at 1:1. The power decay was designed to match the bundle average heat flux of the BWR/6-251 core. Test 926 simulated a recirculation suction line guillotine break with a high pressure core spray (HPCS) failure. The test covered the blowdown and refill/reflood phases of the LOCA transient. Test measurements included pressure, break flow, vessel inventory distribution and heater rod temperatures.

- The Steam Sector Test Facility (SSTF) [72] was a full-scale representation of a 30-degree sector of a BWR/6-218 vessel from the lower plenum to the separator standpipes with 42 full-size and 16 partial-size simulated fuel bundles. The lower plenum and guide tubes were also represented, but not scaled geometrically to the sector. The test covered the reflood phase of the LOCA transient. Steam was injected in the core, bypass and lower plenum to simulate vapor generation. Test measurements included flows and inventories in the fuel channels, upper plenum, lower plenum, bypass and guide tubes.

Table 5.3-2 presents a comparison of key parameters from the FIST and Rig of Safety Assessment (ROSA) scaled test facilities and the simulated BWR/6 plant.

The BWR/6 data for the scaling evaluation are taken from the results of a TRACG analysis of a guillotine rupture in the recirculation suction line with the same two out of three LPCI failure simulated in FIST Test 6DBA1B. The input model for the BWR/6 analysis was based on a BWR/6-238 plant with 748 fuel bundles and is the same model used for the TRACG LOCA demonstration cases in Section 8. The suction line break, although not the current BWR/6 DBA, was selected for the scaling study because it was the only large recirculation line break tested in FIST and ROSA-III. A primary purpose of the scaling study is to show, by means of present-day scaling methodology, that the fact that FIST and ROSA were scaled to different versions of the BWR/6 design than the one for which the demonstration calculations in Section 8 are performed does not compromise the applicability of the test data to the evaluation of TRACG's predictive capability for a LOCA transient.

Two distinct phases of the large-break LOCA transient are identified for scaling purposes: (1) blowdown (including the start of high-pressure ECCS injection); and (2) reflood. The blowdown phase starts at event initiation and ends when the first low-pressure ECCS system initiates. During the early part of the blowdown phase, the vessel liquid inventory and pressure transients are dominated by break flow, decay power and inventory flashing. During the latter part of the blowdown phase, the dominant phenomena are high-pressure ECCS injection, feedwater flashing and, in the test facilities, the release of stored energy from the fuel and vessel structures. The reflood phase is dominated by the low-pressure subcooled ECCS injection flows and the continued release of stored energy in the scaled test facilities.

Table 5.3-2 Comparison of BWR/6 with FIST and ROSA Test Facilities

	BWR/6	FIST	ROSA
Plant represented	BWR/6-238	BWR/6-218	BWR/6-251
Plant rated (OLTP) power (MWt)	3579	2895	3800
Test number	N/A	6DBA1B	926
Nominal volumetric Scaling	1:1	1:624	1:424
Vessel free volume (m ³)	499	0.684	1.246
Vessel height (m)	20.6	19.4	6.0
Number of bundles	748	1	4 ⁽⁴⁾
Active fuel/heated length (m)	3.81	3.81	1.88
Rod assembly	10x10	8x8	8x8
Initial power (MW)	4295 ⁽¹⁾	5.05	3.97
Power to vessel volume ratio (MW/m ³)	8.61	7.38	3.19 ⁽²⁾
Initial pressure (MPa)	7.18	7.19	7.37
Feedwater temperature (K)	501	486	489
Break	Recirculation Line Suction DBA		
Break area (m ²)	0.203	0.000280	0.000539
Single failure assumption	2 of 3 LPCI ⁽³⁾	2 of 3 LPCI ⁽³⁾	1 of 1 HPCS
ECCS temperature (K)	321	322	313
HPCS initiation pressure (MPa)	3.12	5.03	N/A
LPCS initiation pressure (MPa)	1.50	1.97	2.13
LPCI initiation pressure (MPa)	1.50	1.68	1.45

Notes:

- ⁽¹⁾ 120% of OLTP.
- ⁽²⁾ Compensated by 9 s of constant power operation at start of test.
- ⁽³⁾ Failure of one diesel generator can result in loss of 2 of the 3 LPCI loops
- ⁽⁴⁾ Bundles were half of full-scale height

5.3.2.1 Comparison of LOCA Transient Response for BWR/6 and Scaled Test Facilities

The TRACG qualification report [2] includes an extensive set of comparisons of FIST, ROSA and SSTF test data to the predictions of TRACG models simulating the test facilities. The qualification report comparisons show that TRACG is capable of predicting the important features of the test data. The present assessment compares the FIST, ROSA and BWR/6 vessel pressure and mass transients to demonstrate that these major features of the test facility responses are comparable to the plant response. The vessel pressure controls the rate of liquid inventory flashing and the timing of ECCS actuation. The vessel inventory sets the conditions for the heatup and subsequent cooldown of the fuel rods. In addition, the measured FIST and SSTF

bundle inventory transients are compared with the BWR/6 bundle inventory transient to show that the conditions leading to the rod heatup transients are similar.

Figure 5.3-1 shows measured and calculated FIST and ROSA vessel pressures and the calculated BWR/6 pressure, normalized to their initial values. The comparison demonstrates that the depressurization transients are similar for FIST, ROSA and BWR/6. Differences associated with details of the initial power decay and break flow transients and the timing of the closure of the feedwater and steamline isolation valves occur at the start of the transient but, once established, the downward trajectories of the pressures for the first 45 s are in very close agreement. At about 45 s, the rate of the BWR/6 pressure decrease changes in response to the onset of flashing of the residual inventory in the feedwater lines adjacent to the reactor vessel. A similar effect occurs in ROSA at about 70 s.

Figure 5.3-2 shows that the overall vessel mass transients for FIST, ROSA and BWR/6 are similar and reinforces the conclusion that the test facilities are representative of the BWR. The decrease in mass during the blowdown phase is due to inventory loss through the break. The faster initial decrease of the FIST inventory is attributed to a combination of larger initial subcooling upstream of the break location and lower frictional resistance between the downcomer and the break relative to the other two facilities [73]. Slope changes in the 8 to 13 s range occur when the liquid level in the downcomer reaches the break elevation. The combined effects of HPCS initiation at 40 s and the start of feedwater flashing at 44 s causes a distinct leveling of the BWR/6 vessel mass transient in the vicinity of 50 s. The ROSA test did not have HPCS and feedwater flashing in ROSA was delayed until about 70 s. The FIST HPCS initiated at 27 s and caused some reduction in the rate of decrease of the vessel mass.

Figure 5.3-3 compares the bundle pressure drops from FIST and average bundles from SSTF and BWR/6 normalized to the initial BWR/6 average bundle pressure drop. The bundle pressure drop is dominated by gravitational head after the initial blowdown and, as such, is directly correlated with bundle inventory. The figures show that the transient trends are similar in the test facilities and the BWR/6 plant.

The comparisons presented above show that measurements of the transient behavior of key LOCA variables from tests conducted in facilities scaled to one bundle (FIST), four half-length bundles (ROSA) and a 30-degree, 58-bundle sector of a full-scale BWR/6 plant (SSTF) are in good agreement with TRACG calculations of these same variables using the standard BWR/6 LOCA model. In addition, TRACG calculations using models of the scaled test facilities documented in the TRACG qualification report [2], are shown to be in good agreement with the test measurements. These results support the following conclusions:

- The test facilities were appropriately scaled for simulation of the important LOCA phenomena expected in the full-scale plant.
- TRACG is capable of simulating the phenomena that govern the transient response of a BWR plant during a LOCA.
- TRACG has no significant calculational bias for scale effects.

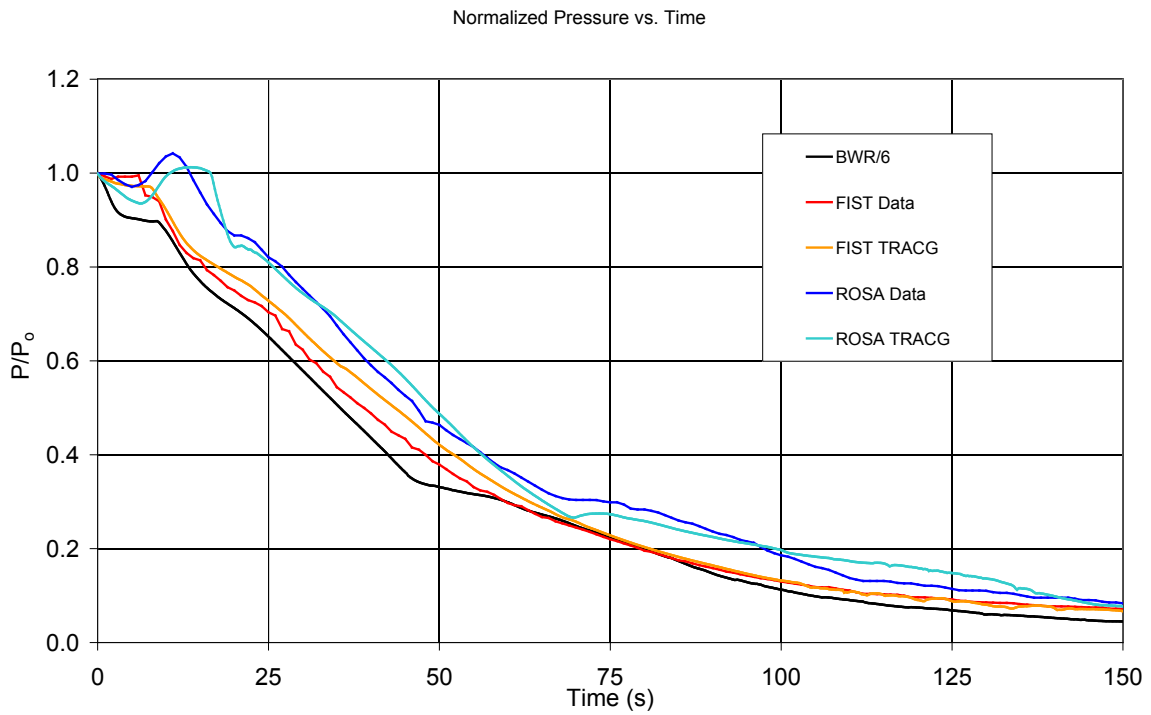


Figure 5.3-1 Vessel Pressure vs. Time Comparison

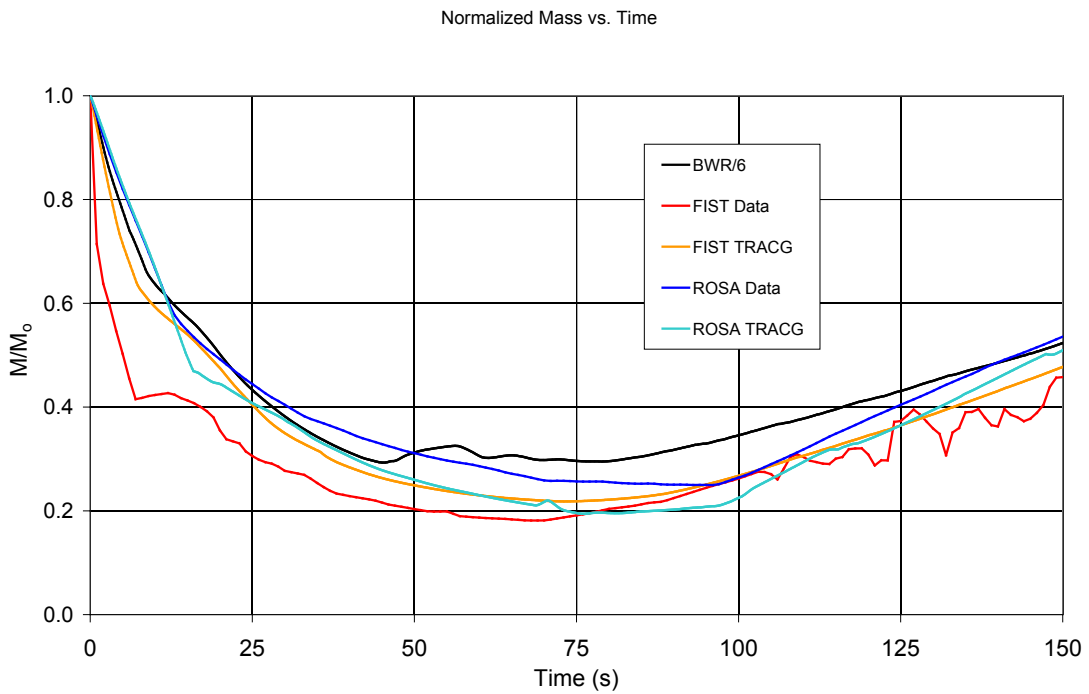


Figure 5.3-2 Vessel Mass vs. Time Comparison

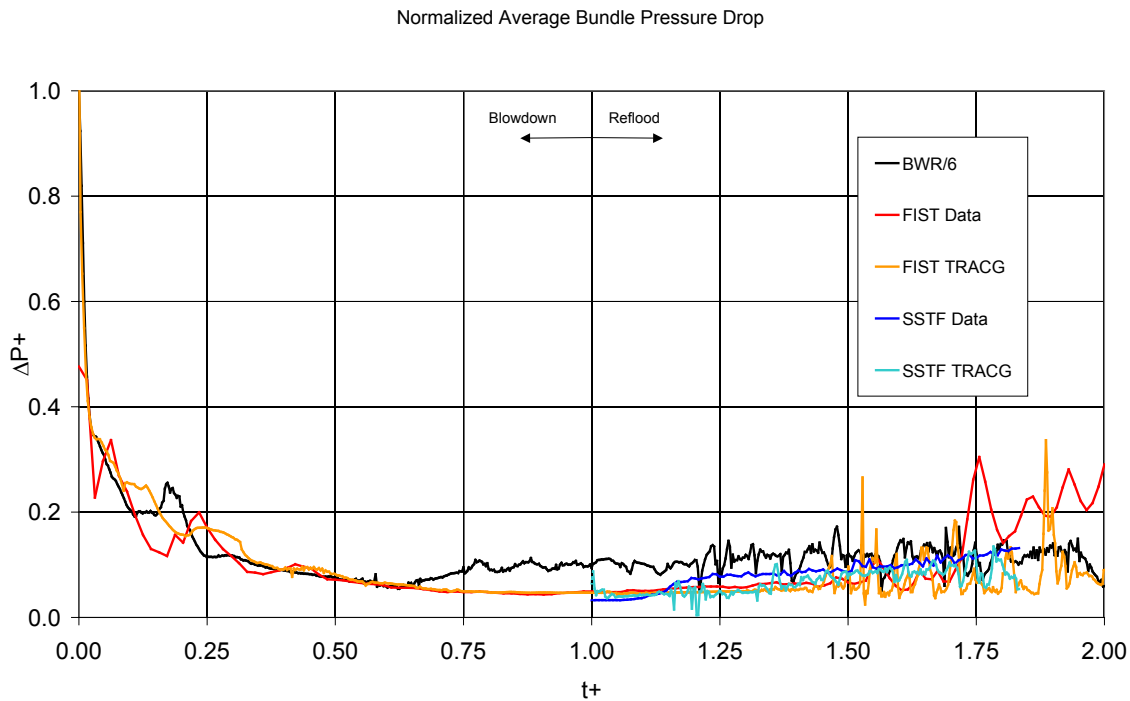


Figure 5.3-3 Comparison of Average Channel ΔP (Inventory) vs. Nondimensional Time

5.3.2.2 Detailed Phenomena Scaling

The comparisons described above show that the scaling, along with other design considerations, of the FIST and ROSA integrated system test facilities, provided a satisfactory representation of a BWR/6 in terms of overall transient behavior. This section presents a procedure for evaluating the test facility scaling in more detail by considering the individual contributions to the transient behavior of the vessel liquid mass and pressure. The basis for this procedure is the scaling methodology developed by an NRC Technical Program Group as documented in Reference [69]. This scaling methodology, called Hierarchical Two-Tiered Scaling (H2TS), addresses both integrated system behavior (top-down scaling) and specific sub-system processes (bottom-up scaling). The focus of this section is the top-down scaling of vessel pressure and liquid mass.

The application of the H2TS procedure starts with the writing of equations that govern the behavior of the variables of interest within a particular region. Each term in the governing equations is multiplied and divided by a suitably chosen non-dimensional parameter grouping (a “PI-group”) that renders the original term as the product of the PI-group and a variable of order unity over the transient time period of interest (in the case of LOCA, blowdown and reflood). The PI-groups then provide the basis for identifying the important phenomena in the prototype and for assessing the adequacy of the scaling of those phenomena in the test facilities. Details of the derivation of simplified equations governing the reactor vessel liquid mass and pressure

during a LOCA can be found in Reference [74]. The equations are based on the approximation that the contents of the vessel remain saturated at a spatially invariant pressure, $P(t)$.

Liquid Mass

The equation for the rate of change of vessel liquid mass is:

$$\dot{M}_\ell = -\sum_k \frac{\dot{Q}_k}{h_{fg}} + \sum_i W_{\ell,i} + \sum_i \frac{h_{sub} W_{\ell,i}}{h_{fg}} - \frac{1}{h_{fg}} [V_o f_3 + M_\ell f_4] \dot{P} \quad (5.3-1)$$

The first term on the right-hand side of Equation 5.3-1 represents evaporation by energy release from the reactor core (or heated rod bundle) and the vessel wall and internal structures. The second term represents liquid removal through the break and steam/ADS lines and liquid addition by the feedwater and ECCS systems. The third term represents vapor condensation on the ECCS inflows. The last term represents conversion of liquid to steam by flashing. The subscripts “k” and “i” in these expressions identify, respectively, the various elements of the system contributing to energy addition and liquid addition or removal (e.g., the different systems providing ECCS inflow). The following notation has been used:

M_ℓ = vessel liquid mass

V_o = vessel fluid volume (a constant)

P = vessel pressure

\dot{Q} = heat release rate to vessel liquid

W_ℓ = liquid flow

h_{sub} = difference between inflow enthalpy and liquid saturation enthalpy at pressure, P

$f_3 = 1 - \rho_g h'_g$

$f_4 = \frac{\rho_g}{\rho_l} h'_g - h'_f$

The “prime” superscript in the last two relations denotes differentiation of the saturation enthalpy with respect to pressure.

A non-dimensional form of Equation 5.3-1 is generated by dividing and multiplying each of the variables by a reference value and then combining the reference values into nondimensional coefficients called PI-groups:

$$h_{fg}^+ \dot{M}_\ell^+ = -\sum_k \Pi_{M,\dot{Q},k} \dot{Q}_k^+ + h_{fg}^+ \sum_i \Pi_{M,W,i} W_{\ell,i}^+ + \sum_i \Pi_{M,sub,i} h_{sub,i}^+ W_{\ell,i}^+ - (\Pi_{M,P1} V_o^+ f_3^+ + \Pi_{M,P2} M_\ell^+ f_4^+) \dot{P}^+ \quad (5.3-2)$$

The “+” superscript denotes the original variable divided by its reference value. The PI parameters are non-dimensional coefficients defined, as shown below, in terms of the reference values (denoted by the subscript “r”).

$$\begin{aligned}\Pi_{M,\dot{Q},k} &= \frac{\dot{Q}_{k,r}}{h_{fg,r}\dot{M}_{\ell,r}} \\ \Pi_{M,W,i} &= \frac{W_{\ell,i,r}}{\dot{M}_{\ell,r}} \\ \Pi_{M,sub,i} &= \frac{h_{sub,i,r}}{h_{fg,r}} \frac{W_{\ell,i,r}}{\dot{M}_{\ell,r}} \\ \Pi_{M,PI} &= \frac{V_o f_{3,r} \dot{P}_r}{h_{fg,r} \dot{M}_{\ell,r}} \\ \Pi_{M,P2} &= \frac{M_{\ell,r} f_{4,r} \dot{P}_r}{h_{fg,r} \dot{M}_{\ell,r}}\end{aligned}$$

Vessel Pressure

The equation governing the rate of change of vessel pressure with the simplifications permitted by the constant volume and absence of noncondensable gases in the present application is:

$$V_o f_2 \dot{P} = \sum_k \dot{Q}_k + \sum_i [W_i (h_i - h)] + \sum_i W_i P^* / \rho \quad (5.3-3)$$

where, in addition to the variables defined above,

$$\begin{aligned}P^* &= P + \left. \frac{\partial e}{\partial v} \right|_P = \frac{h_{fg}}{v_{fg}} \\ f_2 &= \frac{1}{v} \left. \frac{\partial e}{\partial P} \right|_v = \frac{1}{v} [h'_f + x h'_{fg} - \frac{h_{fg}}{v_{fg}} (v'_f + x v'_{fg})] - 1\end{aligned}$$

v = vessel mixture specific volume (= $1/\rho$)

e = vessel mixture specific internal energy

W = mass flow rate

h = vessel mixture specific enthalpy

h_i = specific enthalpy of mass in/outflow

x = vessel mixture quality

The right side of this equation contains terms representing heat release, enthalpy added or removed from the vessel mixture by in and outflows, and mechanical energy associated with the flow terms. A non-dimensional form of the pressure equation is:

$$f_2^+ \dot{P}^+ = \sum_k \Pi_{P,\dot{Q}k} \dot{Q}_k^+ + \sum_i \Pi_{P,W_h,i} W_i^+ \Delta h_i^+ + \frac{P^{*+}}{\rho^+} \sum_i \Pi_{P,mech,i} W_i^+ \quad (5.3-4)$$

where, in the same manner as for the mass equation, the PI parameters are defined as:

$$\begin{aligned} \Pi_{P,\dot{Q}k} &= \frac{\dot{Q}_{k,r}}{\dot{P}_r V_o f_{2,r}} \\ \Pi_{P,W_h,i} &= \frac{W_{i,r} (h_i - h)_r}{\dot{P}_r V_o f_{2,r}} \\ \Pi_{P,mech,i} &= \frac{W_{i,r} P_r^*}{\dot{P}_r V_o f_{2,r} \rho_r} \end{aligned}$$

Reference Parameters

The reference values constituting the PI-groups in Equations 5.3-2 and 5.3-4 were specified on the basis of test inputs and parameters, test data and, for the BWR/6 and where test data were insufficient for the purpose, TRACG simulation results. As described in the introduction to this section, the purpose of converting the mass and pressure equations to nondimensional form is to make each of the variable terms of order unity over the phase of the LOCA transient (blowdown or reflood) being examined. By choosing the reference values to make the variable terms in the equations of order unity over a given LOCA phase, the (constant) PI-groups can be used to assess the relative importance of the individual terms in the equation and to compare the test facility and BWR/6 PI-group magnitudes for the important terms. A comparison of PI-group magnitudes between the BWR/6 and the LOCA test facilities gives an indication of how well the individual phenomena were scaled in the tests.

The reference liquid mass and pressure time derivatives are defined as:

$$\begin{aligned} \dot{M}_{\ell,r} &= \frac{\Delta M_{\ell}}{\Delta t} \\ \dot{P}_r &= \frac{\Delta P}{\Delta t} \end{aligned} \quad (5.3-5)$$

where Δ denotes the change in the associated variable over the LOCA phase of interest. With this choice of reference values, the average values of the non-dimensional time derivatives over the LOCA phase will equal unity.

To make the other variable terms in Equations 5.3-2 and 5.3-4 of order unity, the reference values of the rate of energy input and the flows into and out of the vessel are chosen as the average values of these variables over the LOCA phase. The reference values of the saturation properties are evaluated at the average of the beginning and endpoint pressures for the LOCA phase and the reference value of the liquid mass is evaluated as the average of its beginning and endpoint values.

5.3.2.3 Results and Discussion for Detailed Phenomena Scaling

The PI-groups associated with the vessel liquid mass and pressure equations for BWR/6, FIST and ROSA are compared in for the blowdown and reflood phases in Figures 5.3-4 through 5.3-7. For phenomena that originate from several sources (i.e., heat release from the core/heated rods and vessel structures), both the individual values and the total are shown. The sign convention adopted for the plotting of the results is that a positive bar indicates that the phenomenon is acting so as to increase the variable (liquid mass or pressure) and vice versa. Thus, in Figures 5.3-4 and 5.3-5, core and structure heating, break flow and flashing are all negative because they act to decrease the liquid mass in the vessel.

For the blowdown phase (Figure 5.3-4), liquid inventory loss through the break is the dominant phenomenon affecting vessel liquid mass. Secondary effects are the conversion of liquid to vapor by boiloff from fuel and structure energy release and by flashing due to depressurization. The similar magnitudes of the PI-groups indicate that the test facilities are scaled well for the important phenomena during the blowdown phase of the LOCA transient.

The liquid mass during the reflood phase (Figure 5.3-5) is dominated by subcooled ECCS injection. The ROSA test differed from both the BWR/6 and FIST in that it had a postulated failure of the HPCS. This is largely compensated by its having the equivalent of two additional LPCI loops so that the total ECCS flow is scaled well. Secondary effects are condensation on the subcooled ECCS flow and, in the test facilities, structural heat release. The higher magnitude for structural heat release in the test facilities, particularly in FIST, is a result of the surface-to-volume distortion in the scaled vessels, which is a common characteristic of sub-scale test facility designs.

The PI-groups associated with the vessel pressure equation for BWR/6, FIST and ROSA are compared in Figure 5.3-6 for the blowdown phase and Figure 5.3-7 for the reflood phase. For the blowdown phase, the rate of change of vessel pressure is determined by the competing effects of enthalpy convection, heat input from the fuel and structure and work done on the vessel surroundings. In terms of the overall strength of these three major phenomena, as shown in the “Total Heat,” “Net Convection” and “Total Flow Work” categories, the facilities are scaled well. The scaled heat input contribution is somewhat larger in the test facilities. The vessel pressure during the reflood phase (Figure 5.3-7) is determined by the competing effects of heat input and enthalpy convection.

The results presented in Figure 5.3-4 to Figure 5.3-7 support the conclusion that, in general, the FIST and ROSA test facilities were well-scaled to the BWR plant whose LOCA response they were intended to simulate. If the ratio of the prototype PI-group value to the corresponding test facility value is in the range of 1/3 to 3 then that particular phenomenon is typically characterized as “well-scaled.” This criterion is the same as the one proposed and used in Reference [74]. With the exceptions noted in the above discussion, this criterion is satisfied and, in fact, generally exceeded by the results presented here.

NEDO-33005-A Revision 1
 Non-Proprietary Information – Class I (Public)

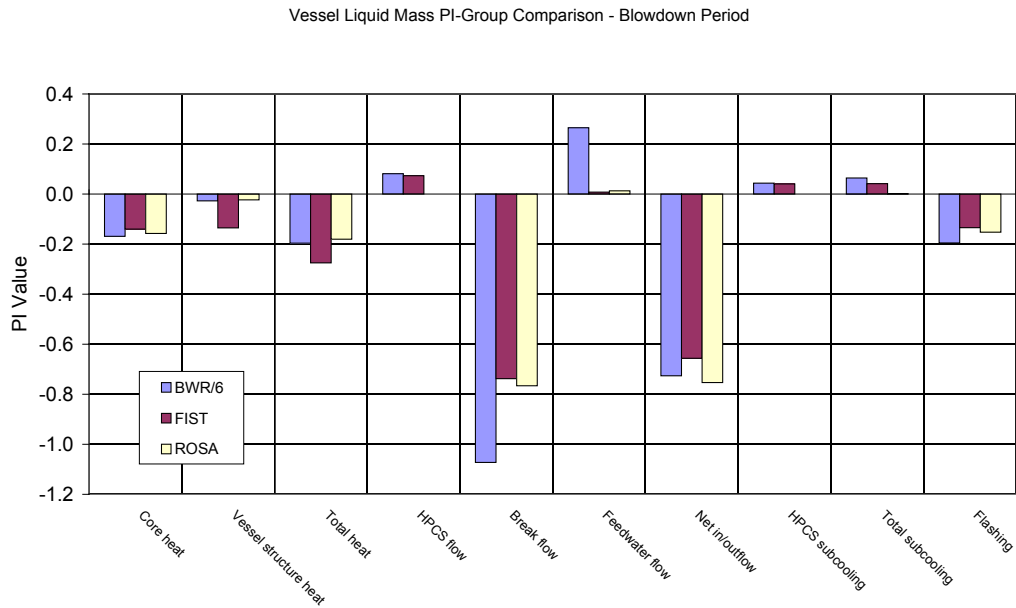


Figure 5.3-4 Vessel Liquid Mass PI-Group Comparison - Blowdown Period

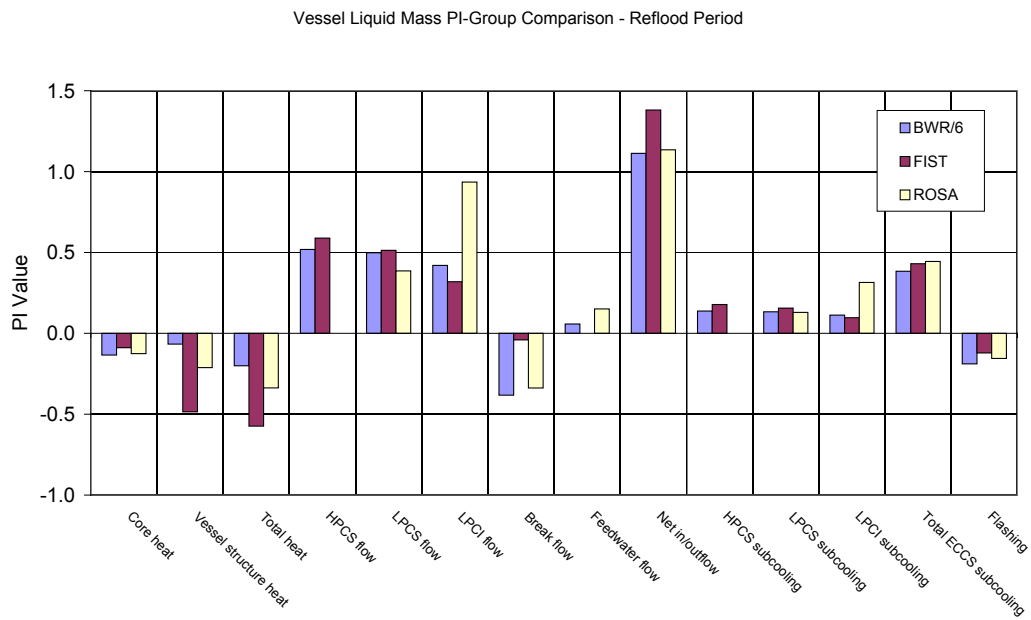


Figure 5.3-5 Vessel Liquid Mass PI-Group Comparison - Reflood Period

NEDO-33005-A Revision 1
 Non-Proprietary Information – Class I (Public)

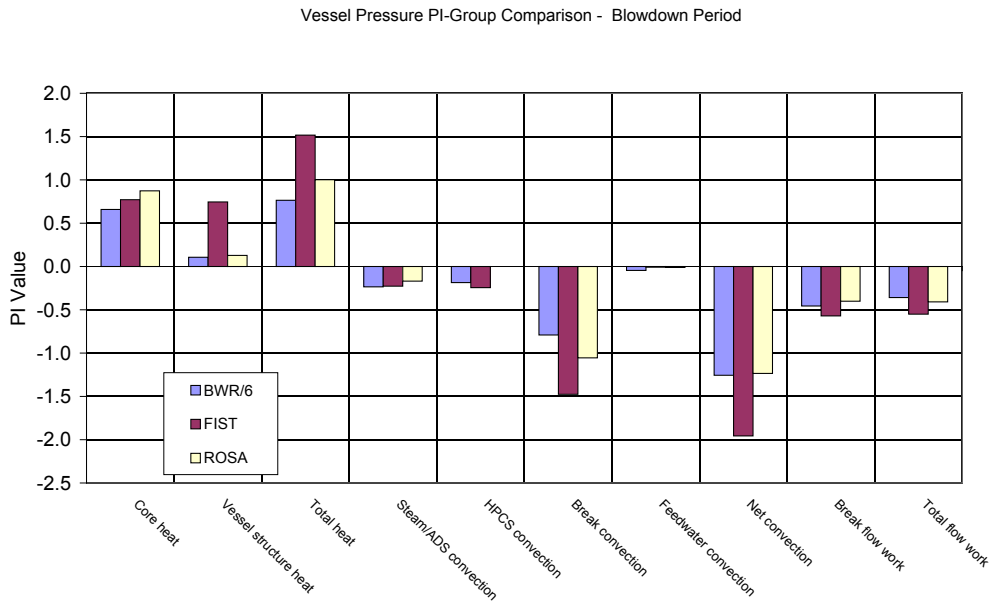


Figure 5.3-6 Vessel Pressure PI-Group Comparison - Blowdown Period

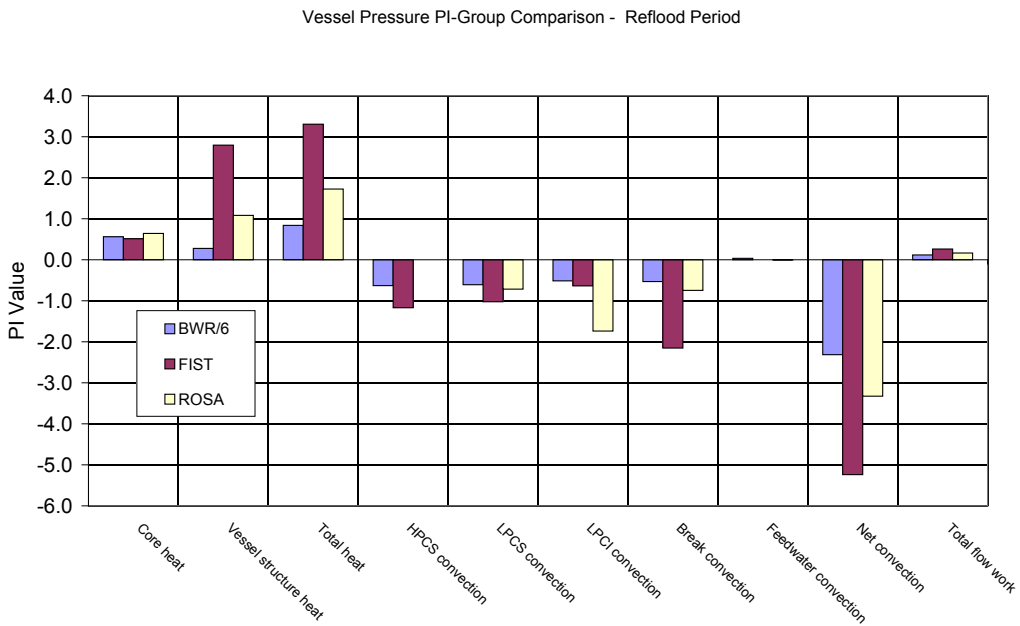


Figure 5.3-7 Vessel Pressure PI-Group Comparison - Reflood Period

5.3.2.4 Peak Cladding Temperature

The major design consideration in a BWR LOCA analysis is the PCT over the course of the transient. Scaling considerations related to PCT have been implicitly addressed in the sections above by noting that the FIST, ROSA and SSTF rod bundles were designed to be prototypical of BWR fuel and by including comparisons of the variables that effectively set the boundary conditions for fuel rod heat transfer - vessel pressure, vessel inventory and bundle inventory (equivalent to bundle void fraction). Reference [2] has shown that TRACG is capable of predicting the PCT transients observed in the test facilities. In this section, the factors governing PCT are examined in more detail to develop a basis for comparing PCT behavior between the test facilities and the BWR and to demonstrate that TRACG's ability to predict PCT behavior in FIST and ROSA supports the conclusion that it would do equally well predicting the PCT in a BWR subjected to a postulated LOCA.

Governing Equations

The magnitude of the local temperature excursion that results in the PCT is dictated by the decay power, the convective heat removal at the fuel rod surface and the rod heat capacity at the PCT location. Significant rod temperature excursions occur when the convective heat removal is reduced relative to the decay power by the onset of boiling transition. The rate of temperature increase depends on the ratio of the excess of decay power over surface convection to the rod heat capacity. The magnitude of the PCT depends on the temperature rise rate and the length of time that the convective heat removal remains suppressed. Following the notation introduced in Reference [75], and neglecting the effect of radiative heat transfer, the fundamental equation governing the rod temperature excursion over a given time interval is:

$$\Delta E' = \int_{t_1}^{t_2} q' dt - \int_{t_1}^{t_2} \xi h (T_w - T_s) dt \quad (5.3-6)$$

with the notation

- $\Delta E'$ = rod energy per unit length
- q' = decay power per unit length
- ξ = rod circumference
- h = surface heat transfer coefficient
- T_w = clad surface temperature
- T_s = fluid temperature

The first and second terms on the right hand side of (5.3-6) represent, respectively, the added decay energy over the time interval and the heat transfer from the rod surface. The rod energy change per unit length can also be expressed in terms of the rod temperature and material properties as:

$$\Delta E' = 2\pi \int_0^R r dr \int_{T_1}^{T_2} \rho c dT = 2\pi \int_0^R (\rho c)^* \Delta T r dr \quad (5.3-7)$$

with the notation

R = rod outer radius

ρ = rod density

c = rod specific heat

T = rod temperature

$(\rho c)^* = \rho c$ evaluated at a suitably chosen T^* between T_1 and T_2

A spatially averaged rod temperature change can be defined as

$$\Delta T \equiv \frac{2\pi \int_0^R (\rho c)^* \Delta T r dr}{2\pi \int_0^R (\rho c)^* r dr} = \frac{\Delta E'}{2\pi \int_0^R (\rho c)^* r dr} \equiv \frac{\Delta E'}{C'} \quad (5.3-8)$$

where, by definition, C' is the rod heat capacity per unit length. Combining (5.3-6) and (5.3-8) gives

$$\Delta T = \frac{\int_{t_1}^{t_2} q' dt - \int_{t_1}^{t_2} \xi h (T_w - T_s) dt}{C'} \quad (5.3-9)$$

As a final step, the change in the rod surface temperature, ΔT_w , can be related to the rod temperature change by an expression of the form

$$\Delta T_w = (1 + \lambda) \Delta T \quad (5.3-10)$$

where λ is a parameter that accounts for the redistribution of rod stored energy. In the electrically heated rods, λ is small in comparison with unity but it can have a significant effect in a fuel rod, which begins the LOCA transient with a large temperature gradient from the center of the pellet to the cladding surface.

Results and Discussion

Figure 5.3-8 shows the FIST, ROSA and BWR/6 temperature histories at the location where the PCT occurs. Both the test measurement and the TRACG calculation are shown for FIST and ROSA. The time at which the temperature excursion leading to the PCT begins (boiling transition) is comparable in the test facilities and the BWR/6 and is bracketed between 38 and 55 s from the start of the LOCA. The BWR/6 PCT is 654 K - compared with measurements of 641 K in FIST and 782 K in ROSA. The rate of temperature increase is higher in the BWR/6 but the duration of the temperature excursion (time between start and peak value) is considerably

shorter - about 23 s - compared with 72 s and 65 s for the FIST and ROSA measurements, respectively.

It can be seen from Figure 5.3-8 that the TRACG PCT predictions for both FIST and ROSA are in good agreement with the test measurements in terms of both the rate of the temperature rise and the PCT magnitude. The good agreement between TRACG and the test measurements over the time interval from the initiation to the peak of the PCT temperature excursions provides confidence that the TRACG convective heat removal over the same time period is a good representation of what occurred in the tests where independent measurements of local convective heat flux are not available.

Figure 5.3-9 shows the TRACG calculations of convection energy per unit length (MJ/m) at the PCT location versus time. The quantity plotted in these figures is

$$\int_0^t \xi h(T_w - T_s) d\tau$$

The figures also show the actuation times for the ECCS systems – HPCS, LPCS and LPCI for FIST and the BWR/6 and LPCS and LPCI for ROSA. It can be seen that the overall convective heat removal is comparable for the two test facilities and the BWR/6, indicating that the basic objective of the test facility rod heat transfer scaling was satisfied. Closer examination shows a distinct flattening of each of the convection energy integrals, indicating an abrupt reduction in the convective heat flux, at the start of the PCT temperature excursion. The major distinction between the three curves is the duration of the period of suppressed convection - about 57 s for FIST (46 s, 103 s), 74 s for ROSA (51 s, 125 s) and 23 s for the BWR/6 (38 s, 61 s).

Some insight into the differences in convective heat removal between the two test facilities and the BWR/6 is gained by examining the vessel inventory history in Figure 5.3-2. It can be seen that the HPCS flow is sufficient to arrest the vessel inventory loss in the BWR/6 at very nearly the time that the PCT excursion begins and well before the start of the reflood phase. In contrast, there is no liquid inventory restoration in ROSA because it had no HPCS. The FIST facility had HPCS flow at a scaled magnitude comparable to the BWR/6 but it was more than offset by the boiloff from structural energy release. Liquid inventory recovery sufficient to turn over the PCT excursion in FIST and ROSA is delayed until after the LPCS and LPCI systems have been actuated.

The effects of the differences in the external sources of vessel inventory on the vessel, the PCT bundle and the PCT cell within the bundle are shown in terms of mixture density versus time for the three facilities in Figures 5.3-10 through 5.3-12. The figures also show the timing of the ECCS flows and the time interval over which the PCT temperature excursion occurs. Mixture density is defined as the mass of the region divided by the region volume. In all three cases, the temperature excursion begins when the local density drops to approximately 100 kg/m³. Under these conditions, the liquid film on the wall of the hottest rod location has dried up and the heat transfer rate is reduced to near zero as the transition to film boiling and vapor convection takes place. These heat transfer modes are unable to keep the rod temperature from rising but, in

combination with the continually decreasing decay heat rate, they result in a decreasing rate of temperature increase. The temperature excursion continues until sufficient liquid has been restored to the hot location environment to allow a liquid film to be reestablished on the rod surface. This quenches the hot spot and terminates the temperature excursion.

In the case of FIST, Figure 5.3-10, the activation of the HPCS at 27 s is more than offset by continued loss of inventory from structural heat release. The bundle inventory starts to level out at about 45 s but the PCT cell continues to drain at a rapid rate, leading to boiling transition and the start of the temperature excursion at 46 s. The PCT cell mixture density remains in the neighborhood of 60 kg/m³, corresponding to a void fraction of about 94%, until the activation of both the LPCS and LPCI systems provides sufficient vessel and bundle refill to reach the PCT cell and allow a liquid film to reform on the hot rod.

Figure 5.3-11 shows the more severe situation in ROSA without the benefit of early HPCS injection. The hot bundle continues to lose inventory until well after the start of the temperature excursion and the void fraction in the PCT cell increases to essentially 100%. The combined effect of LPCS flow and feedwater flashing at 70 s lead to increasing hot bundle inventory but it is not until well after the start of LPCI flow that the bundle refill finally reaches the PCT cell and stops the temperature increase.

For the BWR/6 (Figure 5.3-12), the HPCS provides sufficient liquid inflow to reverse the loss of hot bundle inventory in a relatively short time from the start of the temperature excursion. The restoration of bundle inventory is quite rapid, quickly reaching the PCT cell and turning the temperature over well before the actuation of the LPCS and LPCI systems.

In addition to the differences in the duration of the temperature excursions in FIST, ROSA and the BWR/6, it may be noted that there are differences in the average rate of temperature rise from the start of the temperature excursion to the time of PCT. These differences are caused by differences in the rated powers of the BWR/6 designs to which the test facilities were scaled, in the axial and radial peaking factors (RPFs) that relate the power at the PCT location to the average power per bundle, in the heat capacities of the electric heater rods and the BWR/6 fuel rod and in the rod radial temperature distributions. The radial temperature distribution is an example of a “bottom-up” scaling distortion in an electrically heated simulation of a nuclear fuel rod.

The above discussion of PCT in the FIST and ROSA test facilities and the BWR/6 can be summarized in terms of the following statements and conclusions:

1. The basic test facility scaling objective of obtaining rod surface convective heat fluxes comparable to the predicted convective heat flux in a BWR/6 during a LOCA was satisfactorily achieved.
2. The times at which the PCT temperature excursion initiates in the FIST and ROSA test facilities and the BWR/6 are bracketed between 38 and 55 s, indicating that the onset of boiling transition in the BWR/6 is adequately simulated in the test facilities.

3. Similar phenomena, albeit in varying degrees, govern the PCT behavior in the FIST and ROSA test facilities and the BWR/6. Calculations for all three show that a rod temperature excursion will begin when the local mixture density drops below about 100 kg/m^3 and will continue until ECCS injections raise the mixture density above that value.
4. The differences between the durations of the temperature excursions in the FIST and ROSA test facilities and in the BWR/6 result from a combination of differences in the availability of HPCS and liquid inventory boiloff from structural energy release. Availability of HPCS in combination with relatively low boiloff from structural energy release explains the lower PCT in BWR/6 relative to that in FIST and ROSA.
5. The differences in the temperature rise rates between the test facilities and the BWR/6 are the combined effect of differences in the scaled decay powers, the radial and axial peaking factors that relate the power at the PCT location to the bundle average power, the extent to which surface convection is suppressed during the temperature excursion.
6. The results of the PCT evaluation provide strong evidence of TRACG's ability to predict the PCT for a BWR LOCA because a) TRACG accurately predicts the PCT temperature excursion in the FIST and ROSA tests in terms of both PCT magnitude and temperature rise rate and b) the differences between the FIST and ROSA PCTs and the TRACG BWR/6 PCT prediction can be explained in terms of phenomena that are fully addressed by the TRACG thermohydraulic models.

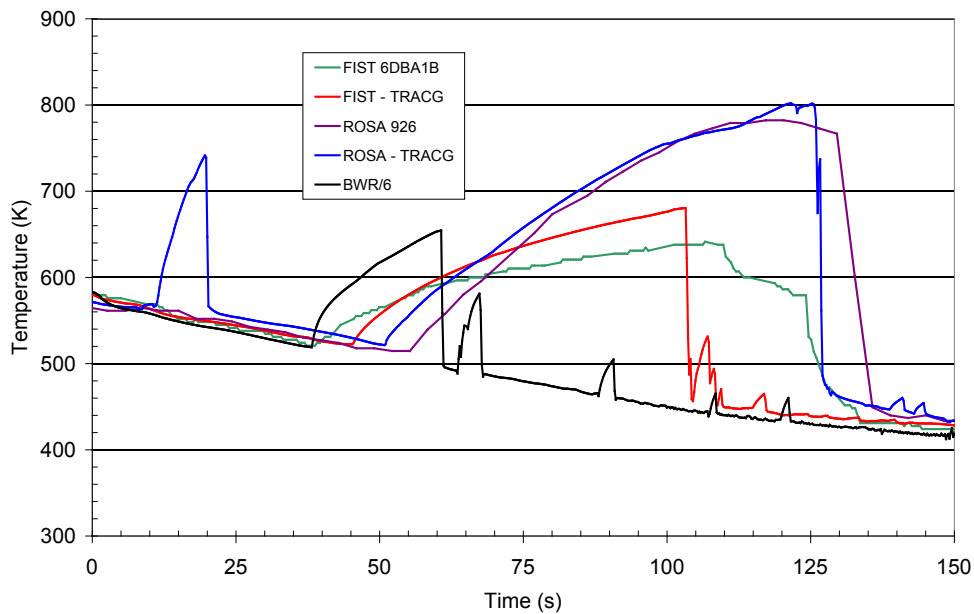


Figure 5.3-8 Peak Cladding Temperatures vs. Time

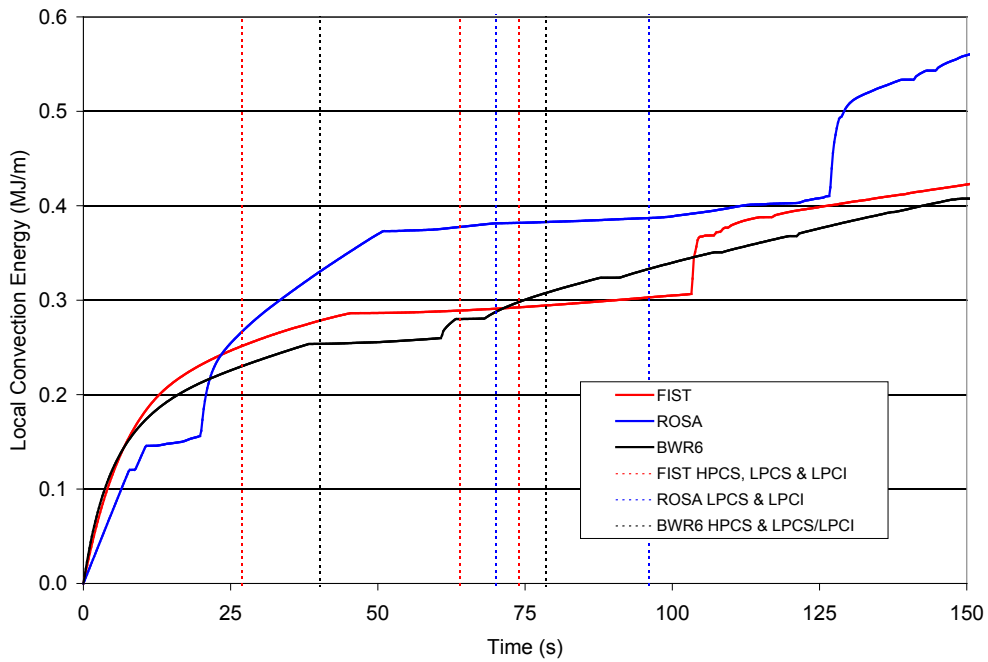


Figure 5.3-9 Local Convection Energy

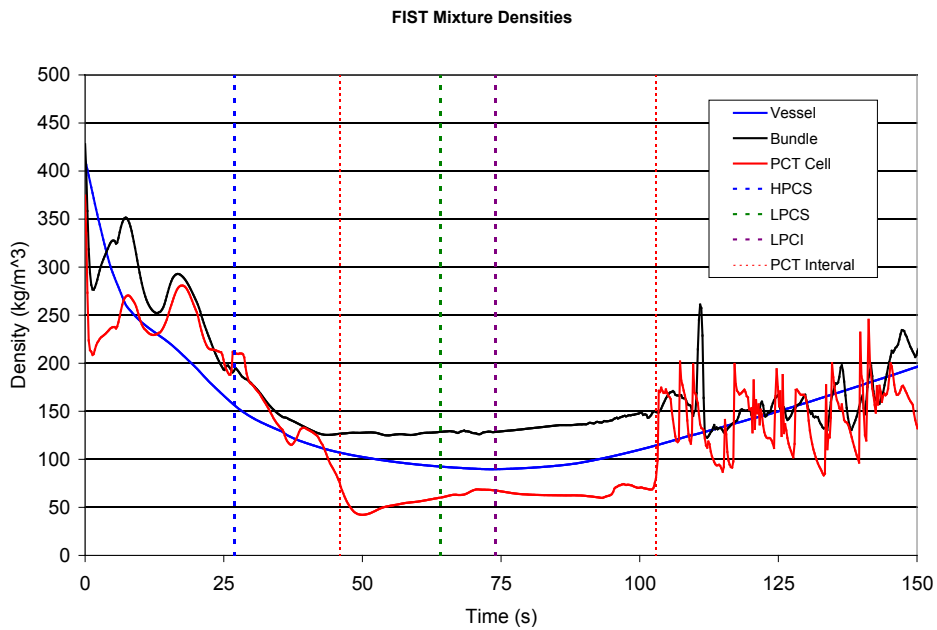


Figure 5.3-10 Mixture Densities for FIST

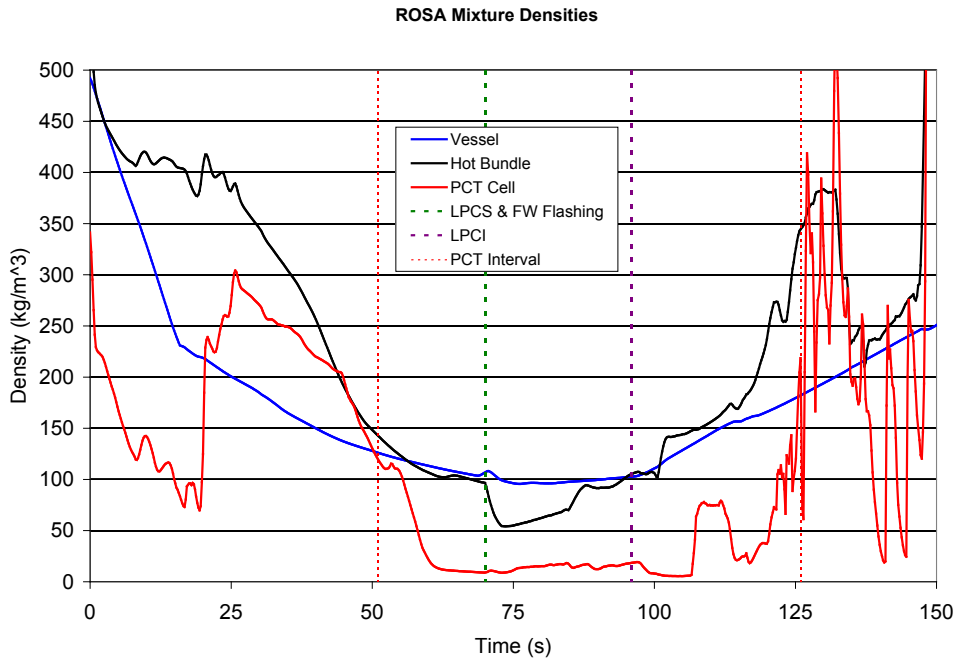


Figure 5.3-11 Mixture Densities for ROSA

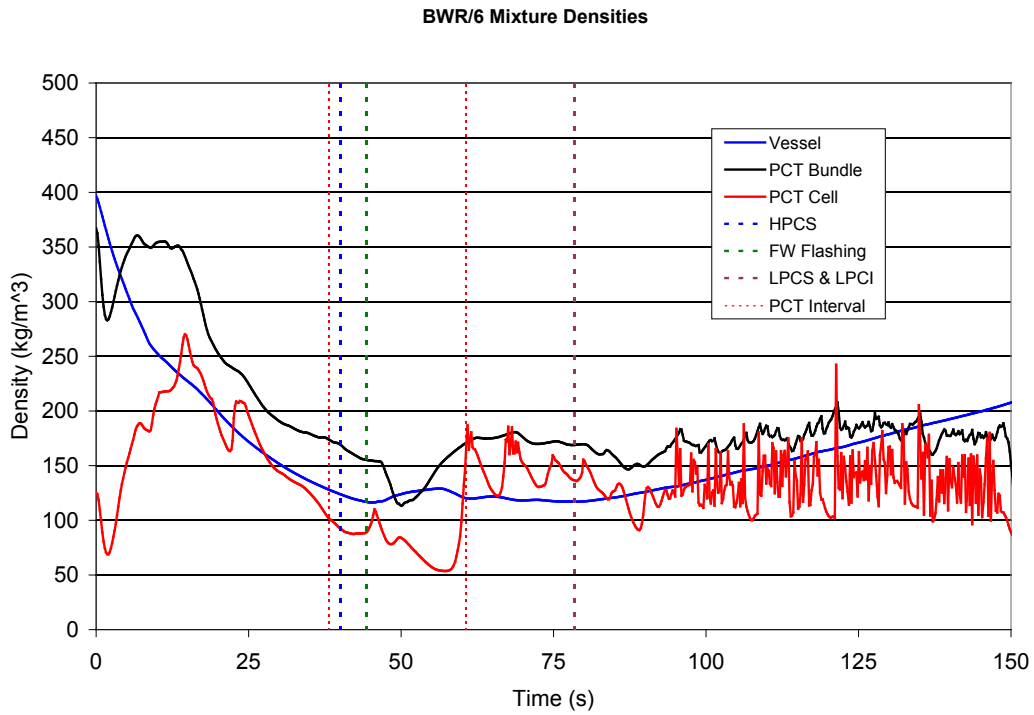


Figure 5.3-12 Mixture Densities for BWR/6

5.3.3 Scaled Integral LOCA Simulation Tests for Non-Jet Pump Plants

[[

]]

In summary, large-scale spray distribution data and full-scale bundle core spray heat transfer data provide adequate assurance that scale effects will not play a role in TRACG's capability to evaluate LOCA events in BWR/2 plants.

5.3.4 Summary – Effects of Scale

The results and discussion presented above justify the following conclusions:

- The TRACG models are applicable over the range of conditions expected in a BWR LOCA.
- TRACG is capable of simulating full-scale component, integral system (SSTF) and BWR plant tests.
- TRACG is capable of simulating full-scale heat transfer tests of BWR rod bundles under LOCA conditions.
- TRACG is capable of simulating scaled integral system LOCA tests over a range of scales.
- The integral system LOCA tests used for TRACG qualification were appropriately scaled for representation of the important phenomena associated with a BWR LOCA.

NEDO-33005-A Revision 1
Non-Proprietary Information – Class I (Public)

In summary, it has been demonstrated that there is no apparent effect of scale for LOCA calculations with TRACG and, consequently, that no scale-related bias needs to be applied to the results of TRACG plant LOCA evaluations.

6.0 APPLICATION UNCERTAINTIES AND BIASES

6.1 INPUT

Inputs for ECCS/LOCA calculations are specified by GEH internal procedures that are the primary means of control for the application of engineering computer programs. The input for a specific TRACG BWR LOCA analysis will be developed using this application LTR together with appropriate application specific procedures. The discussion in this section is focused on the manner in which the input is treated with respect to quantifying its effect on the calculated results. As such, it serves as a basis for the development of the application specific procedures.

The specification of code inputs can be divided into four broad categories: (1) geometry inputs; (2) model selection inputs; (3) initial condition inputs; and (4) plant parameters. If the calculated results are sensitive to the input value, then it is necessary to quantify the uncertainty in the input.

The geometry inputs specify lengths, areas and volumes and are the building blocks from which the spatial nodalization is constructed. Uncertainties in these quantities result from measurement uncertainties and manufacturing tolerances. In general, these uncertainties have a much smaller effect on the results than uncertainties associated with model simplifications such as the representation of multiple physical components with a single code component. When this is not the case, the geometric uncertainties can usually be quantified in a straightforward manner. For example, the uncertainty in the volume of the feedwater line up to the isolation valve is assigned a value of [[

]] Even though the feedwater inventory is considered to be of *medium importance*, the effect associated with the uncertainty in this parameter is small. A comprehensive assessment of sensitivities to spatial nodalization and model simplification (e.g., the combining of several similar fuel channels as one fuel channel group) is included in the *TRACG Qualification* [2].

Model selection inputs are used to select the features of the model that apply for the intended application. Once established, these inputs are fully specified in the procedure for the application and will not be changed.

A distinction is made in this document between *initial conditions* and *plant parameters*. The initial rated conditions for a nuclear power plant, specified in absolute units, are considered as plant parameters in certain contexts. In this document, however, those key plant inputs that determine the overall steady-state nuclear and hydraulic conditions prior to the transient are considered to be *initial conditions*. Initial conditions and the uncertainties associated with them are addressed in Section 6.2.

The term *plant parameter* is reserved for quantities such as protection system setpoints, valve capacities and stroke times, and scram characteristics that influence the characteristics of the transient response but do not have an effect on steady-state operation. Plant parameters, and the uncertainties associated with them, are addressed in Section 6.3.

6.2 INITIAL CONDITIONS

Initial conditions are those conditions that define a steady-state operating condition. Initial conditions for a particular transient scenario are specified in the procedure for the application. For example, the procedure may specify that the calculation be performed at a specific fuel exposure at 100% of rated power and flow using a power and exposure distribution that has been obtained from a prescribed process. The absolute values of these inputs may vary from plant to plant and from cycle to cycle. For example, the rated power and flow values for the plant are usually fixed (unless the plant has been re-licensed to higher rated values), but the cycle specific parameters (e.g., core fuel composition, OLMCPR) will change with each cycle.

Initial conditions may vary due to the allowable operating range or due to uncertainty in the measurement at a given operating condition. The plant Technical Specifications and Operating Procedures provide the means by which controls are instituted and the allowable initial conditions are defined. While the Technical Specifications allow fuel bundles to operate at the peak linear heat generation rate (PLHGR) and minimum critical power ratio (MCPR) limits, in practice the cores are designed to operate with a design margin [[]] to the Technical Specification limits. Moreover, it is very unlikely for a bundle to be simultaneously at both limits. The range of expected MCPR and PLHGR and the associated core exposure and peaking are discussed in the next subsection. At a given operating condition, the plant measurement system has inaccuracies that also must be accounted for as an uncertainty. The key plant initial conditions are identified in Table 6.2-1. The ranges of operating conditions and uncertainty for each of these inputs are addressed. For most of the quantities, the total uncertainty has already been quantified and approved by the NRC [32].

The effect of the total uncertainty in initial conditions must be quantified for each of the critical safety parameters for ECCS performance analysis: peak clad temperature, local clad oxidation and core-wide oxidation. Part of the development of the application methodology is to determine how the uncertainties in the initial condition will be considered in the ECCS performance analysis (e.g., whether they will be included in a statistical analysis or whether bounding values will be used). A recommended approach is proposed in Section 9.0 based on the outcome of these evaluations.

The analyses performed must be consistent with the allowed domains of operation. The effects of the initial condition on the results are characterized in the following manner:

- The results are sensitive to the initial condition and a generic basis for the limiting initial condition cannot be established. Plant specific analyses will consider the full allowable range of the initial condition.
- The results are sensitive to the initial condition and a generic basis for the limiting initial condition can be established. Plant specific analyses will consider the parameter to be at its limiting initial condition.
- The results are not sensitive to the initial condition and a nominal initial condition will be assumed for the parameter.

Each initial condition is monitored through the use of plant sensors or simulated prediction. Because of instrument or simulation uncertainty, the plant condition may vary from the indicated value. The results are characterized in the following manner:

- The results are sensitive to the uncertainty in the initial condition and the uncertainty in the initial condition will be included in the statistical analysis.
- The results are not sensitive to the uncertainty in the initial condition and the uncertainty does not need to be accounted for.

6.2.1 Total Core Power and Flow

The range of analyzed initial power/flow conditions are chosen to bound the operating envelope, including the expanded operating domain conditions. A typical expanded power/flow map is shown in Figure 6.2-1. The power/flow combinations, which bound the operating envelope for LOCA analysis, will be analyzed to determine the most limiting condition for a range of break sizes. The effect of uncertainty in the total core power will be conservatively accounted for performing the analysis at 2% higher power level (consistent with Reference [18]). A less bounding value could be justified for TPO plants. The effect of uncertainty in the total core flow is considered for the limiting condition. Typical power/flow combinations as a percentage of the Original Licensed Thermal Power (OLTP) and rated core flow are:

- 100% Power / 100% Flow
- 120% Power / 100% Flow
- 120% Power / 80% Flow
- 100% Power / 55% Flow

6.2.2 Feedwater Temperature

The feedwater temperature is basically set by the steam flow rate, which is a function of the total reactor power and the feedwater heater line-up. Each plant has a characteristic feedwater temperature as a function of reactor power. Many plants allow operation with reduced feedwater temperature based on an alternate imposed or out-of-service heater line-up. The effect of the normal feedwater temperature as compared to reduced feedwater temperature is evaluated to determine which is limiting.

Feedwater temperature also has measurement uncertainty. The typical uncertainty in feedwater temperature measurement is around [[]]. The effect of the feedwater measurement uncertainty is considered for the limiting condition.

6.2.3 Steam Dome Pressure

Plant Technical Specifications restrict the maximum operating pressure. Because the maximum pressure is expected to be limiting, plants treat this as an Analytical Limit (AL). The minimum dome pressure is controlled through turbine operational control. The minimum pressure is

typically smaller than the nominal dome pressure. The range of variation of the steam dome pressure is approximately twice the difference between AL and nominal pressure.

The uncertainty in the pressure measurement is [[

]]

6.2.4 Downcomer Water Level

The downcomer water level variation is between the low level (L4) and high level (L7) alarm setpoints. The effect of operation within this range is evaluated.

The water level measurement uncertainty is [[

]]

6.2.5 Limiting Bundle Power Distribution

The limiting bundle LHGR and MCPR is of critical importance to the prediction of ECCS performance analysis critical safety parameters. The LHGR affects the stored energy in the fuel rod. The MCPR affects the proximity to boiling transition that is important in the early phase of many LOCA scenarios. The MCPR also influences the maximum bundle power because the MCPR limit constrains bundle power.

[[

]]

The term LOCA-limited in the following sections refers to plants with PCT values close to 1,478 K (2,200°F). These plants experience extended uncover and rely on spray entering into the top of the bundle. In this sense, BWR/2s are LOCA-limited. LOCA-limited plants are highly sensitive to thermal radiation effects; therefore position of the fuel rods with higher peaking factors within the bundle is very important. [[

]]

Most jet-pump BWRs are not constrained by LOCA-related thermal limits. Non-LOCA limited plants are typically dependent on uncover and recovery timing. PCTs are lower and results are less sensitive to radiation effects.

In the following sections, the process and basis for establishing target initial conditions for MCPR and LHGR (or MAPLHGR) is described. [[

]]

Three limits constrain the design and operation of fuel bundles: Thermal Mechanical Operating Limit (TMOL), which is the limiting Peak Linear Heat Generation Rate (PLHGR), MAPLHGR and Operating Limit Minimum Critical Power Ratio (OLMCPR). Generally, it is not likely for a

bundle to be at or near both the LHGR and MCPR limits. The limiting bundles are close to their maximum heat generation limits in early to mid-fuel cycle, when their axial power distribution is peaked near the bottom of the bundle. The limiting bundles are closest to the MCPR limit from the middle to the end of the fuel cycle, when their axial power distribution is mid or top-peaked.

Operating plant data from the core tracking files were reviewed to determine the operating history of the limiting bundles. Figure 6.2-2 summarizes the data for the bundles operating close to their LHGR limits. [[

]]

The limits basis is reviewed for each cycle of application and may be updated based on the process defined above.

6.2.6 Average Bundle Power Distribution

The core power distribution for average peripheral and average interior bundles can be standardized. The radial peaking factor for the peripheral bundles is typically about 0.4. Figure 6.2-2 through Figure 6.2-4 represents typical average bundle power shapes. Sensitivity studies using TRACG have shown that results are not particularly sensitive to the average interior bundle axial peaking. Studies with inlet peaked, cosine and outlet peaked shapes have shown little sensitivity. A cosine axial shape is adequate to characterize the average bundles in the core. A representative radial power distribution is assumed and a sensitivity study is required as part of the TRACG implementation process (See Section 9.0). Sensitivity results are shown in Section 8.1.4.2.

6.2.7 Fuel Rod Exposure

BWR cores have a target burn-up and will operate to get to this target value. For a GE14 core, typical burn-up is around 47,000 MWd/MTU and cycle exposure might be 18,000 to 19,000 MWd/MTU. Considering an equilibrium core with half new fuel, the core average exposure will vary between 23,500 MWd/MTU to 33,000 MWd/MTU.

Fuel rod power is restricted based on the fuel rod exposure (i.e., PLHGR limit). The thermal mechanical design envelope for allowable PLHGR versus exposure provides the limiting conditions for the rod exposure. The gap conductance and the fission gas release in the fuel rods are calculated for the specified PLHGR and exposure values. Fuel thermal conductivity also varies with exposure. These factors contribute to exposure dependent fuel stored energy.

A range of fuel rod exposures will be considered to determine the limiting condition. The fuel bundle will include a typical number of Gadolinia rods that will be placed at the same exposure levels as the UO₂ rods. [[

]]

6.2.8 PLHGR, MCPR and MAPLHGR Uncertainty

As described in Section 6.2.5, initial conditions for LOCA evaluations conservatively assume that the fuel bundle in question is operating at the LHGR or critical power (MCPR) limit.

The core process computer takes total power, flow, pressure, and nuclear instrument signals from the reactor core and evaluates a peak LHGR, a peak average planar linear heat generation rate (APLHGR) for each six-inch node, and a CPR for each bundle in the core. There are uncertainties associated with each physical input to the process computer as well as the model used to evaluate the LHGR, APLHGR and CPR. The total input and model uncertainties have been combined to yield an uncertainty associated with the CPR. The monitoring uncertainties are included in the MCPR limits in accordance with NEDC-32694P-A [32], and in the Thermal Mechanical Operating Limit (TMOL) LHGR limit in accordance with NEDC-33258P-A [76].

[[

]]

Table 6.2-1 Key Plant Initial Conditions

Quantity	Control of Initial Condition	Range of Conditions	Uncertainty Considerations
Total Core Power	Plant Technical Specifications restrict the maximum operating core thermal power. For a given core flow, the maximum and minimum core power are controlled through operation within the analysis basis power/flow map.	Initial power/flow conditions will be chosen to bound the operating envelope. The limiting conditions will be identified through calculations at the corners of the envelope and some intermediate points.	Conservatively, analyses will be performed at a bounding 102% power level consistent with Reference [18]. A less bounding value could be justified for TPO plants.
Total Core Flow	For a given core power, the maximum and minimum core flow are controlled through operation within the analysis basis power/flow map.	Partial power/flow conditions will also be analyzed.	Total $\sigma = 2.5\%$ (Reference [32])
Feedwater Temperature	Given feedwater temperature and core power, the feedwater flow and steam flow can be determined. Some plants have analyzed for additional operating flexibility (Final Feedwater Temperature Reduction or Feedwater Heater Out-of-Service).	The normal range of feedwater temperature, considering measurement uncertainty and FW heater performance variations, will be considered. The limiting combination of power/flow/FW temperature will be identified.	Total $\sigma = [[\quad]]$ (Reference [32])
Steam Dome Pressure	Plant Technical Specifications restrict the maximum operating dome pressure. The minimum dome pressure is controlled through turbine operational control.	The maximum operating dome pressure is expected to be limiting. Plants treat this LCO pressure as an AL and allow a margin for drift/calibration.	Total $\sigma = [[\quad]]$ (Reference [32])
Downcomer Water Level	Plant would operate between the L4 and L7 alarm setpoint.	Sensitivity to initial water level is expected to be small. If not, minimum operating downcomer water level (L4) will be used.	Total $\sigma = 2\%$ or 0.04 m for a 2 m instrument range (Typical)

Table 6.2-1 (cont'd) Key Plant Initial Conditions

Quantity	Control of Initial Condition	Range of Conditions	Uncertainty Considerations
Core Loading Pattern	A reference core loading pattern is defined for each reload cycle. Acceptable deviation from the reference core is defined in GESTAR Section 3.4.2 [20].	For LOCA analysis, the effects of core loading, cycle exposure and control rod pattern are reflected in the initial values of core axial, radial and rod peaking. These operating parameters are constrained by the technical specification limits of PLHGR (or MAPLHGR) and OLMCPR. A methodology has been developed to define axial shape, and bundle power within these constraints. Generally, it is not possible to put one bundle on both limits while maintaining realistic peaking factors. Separate LHGR-limited and MCPR bundles, corresponding to different exposure conditions, will be modeled, with the other parameter set at the PLHGR (or MAPLHGR) limit or OLMCPR.	Core loading pattern, rod pattern, and local peaking are bounded by applying a conservative assumptions for average and hot bundles (See Sections 6.2.5 and 6.2.6) Also see Section 6.2.8.
Axial Power Distribution	Plants are not restricted with respect to axial power distribution as long as thermal limits are met.		
Radial Power Distribution	Plants are not restricted with respect to radial power distribution as long as thermal limits are met.		
Local Peaking Distribution in High Power Bundles	Plants are not restricted with respect to local power distribution as long as thermal limits are met.		
Control Rod Pattern (control rod density)	Plants are not restricted with respect to control rod pattern as long as thermal limits are met.		
Fuel Rod Exposure	Fuel rod power is restricted as a function of fuel rod exposure. Maximum exposure is also restricted.	A range of fuel rod exposures will be considered to determine the limiting condition. [[]]	Fuel rod exposure effects are bounded by choosing conservative initial conditions. (See Sections 6.2.5 and 6.2.8)

Table 6.2-2 Summary of LHGR and MCPR Targets

[]

]]

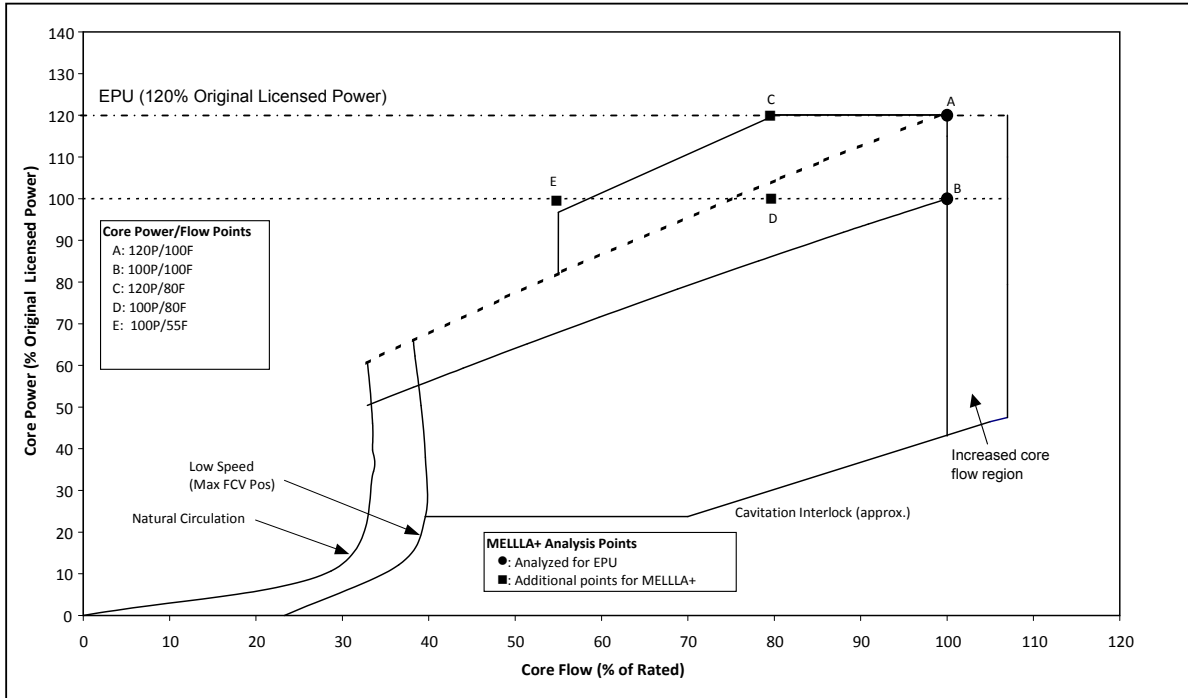


Figure 6.2-1 Typical MELLLA+ Power/Flow Map

[[

]]

Figure 6.2-2 Data for Bundles Close to LHGR Limits

[[

]]

Figure 6.2-3 Data for Bundles Close to MCPR Limits

[[

]]

Figure 6.2-4 Core Average Axial Shape

[[

]]

Figure 6.2-5 Maximum Nodal Peaking Channel Power Distribution

[[

]]

Figure 6.2-6 Maximum CPRRAT Channel Power Distribution

6.3 PLANT PARAMETERS

Plant parameters are plant-specific quantities such as protection system setpoints, ECCS pump capacities and diesel generator start times that influence the characteristics of the plant transient response. *Plant parameters* are distinguished from *initial conditions* by the fact that they have essentially no effect on steady-state operation. *Initial conditions* are the parameters that define steady-state operation.

To comply with Section 6.3 of the NRC standard review plan [19], the FSAR provides a list of significant inputs for LOCA analysis. GEH procedures provide for an update or re-confirmation of the values of these input parameters when significant changes are made to the LOCA analysis (e.g., for power uprate). Table 6.3-1 lists plant parameters that are unique to specific safety systems and Table 6.3-2 lists those that are common to multiple safety systems. The plant parameters identified in these tables are the same as those considered in the currently-approved process for LOCA analysis [25].

Most of the plant parameter values that are important for LOCA response are analytical limits related to processes that are controlled by the plant Technical Specifications. These processes may be periodically tested at the plants to assure compliance with the Technical Specifications. Performance and uncertainties for the processes that the Technical Specifications are designed to control are based on manufacturing specifications, performance data and required surveillances. A Technical Specification value will usually be a maximum or minimum acceptable value that bounds the entire population of values measured at the plant.

The technical specification allowable value (AV) or the limiting condition for operation (LCO) may be used to define a plant parameter AL for licensing analyses. The original ECCS licensing basis specified the AL for most of the plant parameters [23]. Use of these limits is one acceptable way in which conservatism can be added to a “best estimate” methodology. It is also possible to define a best-estimate distribution of a parameter around an AV or LCO. For example, the drift term used to relate the AV to the nominal trip setpoint (NTSP) can be used to determine a distribution of setpoints about the AV over the calibration interval. Similarly, the variation of equipment performance from the LCO, if known, can be used to specify a distribution of values for input to the LOCA analysis. Table 6.3-1 shows where the technical specification AV is used and for these parameters the AV value is determined at the LCO. The parameters marked as ‘nominal’ in Table 6.3-1 have been demonstrated to have no significant effect on the LOCA response so that use of a nominal value is justified. The LCO value either accounts for instrument accuracy in the governing surveillance acceptance criteria or, alternatively, in the specification of the value for use in the LOCA analysis. This procedure does not preclude the use of a more realistic distribution of values for these parameters if such is justified separately for plant-specific analysis.

Uncertainties in plant parameters are systematically combined with model and initial conditions uncertainties to establish a composite uncertainty for the application. The process used for this purpose is discussed in Section 7.0. The process is applied in the demonstration analyses described in Section 8.0.

6.3.1 Scram Time

BWR LOCA analyses assume a loss of all offsite power at the time of the break. A plant scram is initiated by low water level in the downcomer (Level 3) or by high drywell pressure followed by a time delay to process the signal (Table 6.3-2). TRACG mechanistically calculates the time to reach Level 3. The time taken to reach the high drywell pressure signal was correlated as a function of break size as described below.

Analyses for several Mark I, Mark II and Mark III containments were used to compile a matrix as a function of break area of the maximum times for drywell pressure to reach 2 or 2.5 psig depending on the plant-specific setpoint. All breaks considered were steam breaks because, for a fixed break size, a liquid break results in a shorter (less conservative) time to reach high drywell pressure due to its higher mass and energy outflow. The containment analyses accounted for heat sinks in the containment and assumed that all drywell coolers were available because this conservatively delays the timing of the scram signal initiated by high drywell pressure. In addition, a drywell to wetwell bypass flow area (as per the technical specifications) was modeled. The calculated conditions are plotted in Figure 6.3-1. The calculations for [[

]] Also shown on the plot is a TRACG curve that represents the average time for a typical BWR/4 plant to reach Level 3 as a function of break size. This curve crosses the curve showing time to reach a drywell pressure of 2 psig at a break area of approximately [[]. The time to reach Level 3 that is shown in Figure 6.3-1 is intended only for purposes of illustration [[]. For smaller break sizes, Level 3 will trigger the scram before the high drywell pressure signal. Thus, a range of break sizes from [[] is sufficient to derive a best fit to the drywell pressure data. The figure also shows a line that bounds the containment analysis results with a 95 % probability and 95% confidence. This curve, which will be adopted for ECCS LOCA analysis, can be represented by:

[[
]].

The demonstration analyses in Section 8.0 use a slightly different, but similarly conservative scram time in the calculations.

6.3.2 Scram Speed

The effect of scram speed on the LOCA PCT was investigated by considering the variation in scram insertion times for different plants. Figure 6.3-2 shows reactivity insertion as a function of the time after the rods start to move into the core. Four different scram insertion rates were evaluated: 67A (base scram curve for the BWR/2-5 product lines); Improved Technical Specifications for BWR/2-5; Option B scram for BWR/2-5; and Technical Specification scram for BWR/6. The corresponding reactivity insertion rates were calculated using the TRACG 3D kinetics model. For LOCA calculations, an additional time delay of [[] was incorporated for processing the scram signal before initiation of rod movement.

Figure 6.3-3 shows the reactor power transient following a DBA (guillotine break on the suction side of the recirculation line). The four curves represent the power transients corresponding to the four scram speeds referred to above. The PCT transients for the four cases are shown in Figure 6.3-4 for the LHGR limiting channel. This channel experiences an early boiling transition and heatup, which might be expected to show some sensitivity to the scram time. [[

]].

Figure 6.3-5 shows the reactor power transients following a small (0.01 m^2) break in the recirculation line. The early power reduction is due to the recirculation pump trip on loss of offsite power. The scram comes in at about [[]] for the case with the slowest scram. The power transients following the scram reflect the effect of the different scram speeds. The PCT transients for the different scram speeds are shown in Figure 6.3-6. The early portions of the transients are indistinguishable and it may be concluded that the variation in scram speed has no effect on the PCT transient following a small break.

[[

]]

Table 6.3-1 System Unique Plant Parameters

System Unique Parameters	Analysis Basis
Maximum delay time from diesel generator (DG) start signal until bus is at rated voltage	[[
Minimum detectable break size for Loop Selection Logic	
Leakage allowance for shroud access hole cover repairs or cracks	
Scram speed to 90% position	
Feedwater pump coastdown (from initial value to zero flow)	
Time constant for recirculation pump coastdown (intact loop and loop with break)	
ECCS makeup water temperature	
ADS Parameters Timer delay Bypass timer delay for sustained low water level ADS close on vessel pressure ADS reopen on vessel pressure ADS reclose on vessel pressure	
Pilot-Actuated Safety/Relief Valves (SRVs) Setpoints Pilot-actuated SRV Capacity at (100+ACC)% of Popping Pressure Closing pressure setpoint Time delay before opening Time constant of opening/closing	
Spring Safety Valves (SSVs) Opening setpoint Capacity of each at opening setpoint]]

Table 6.3-2 Parameters Common to Multiple Safety Systems

Parameter	Safety Systems									
	E D G	L P I	L P S	H P I	R C I	H P C	A D S	R P S	M S I V	
Initiating Signals										
Low-low-low water level (L1)	x	x	x				x		x	
Low-low water level (L2)				x	x	x				
Low level (L3)								x		
High drywell pressure	x	x	x	x	x	x	x	x		
Low vessel pressure		x	x							
Flows & Pressures										
Minimum flow delivered to vessel		x	x			x	x			
Pressure at above flow rate		x	x			x	x			
Maximum vessel pressure at which pumps can inject flow		x	x							
Vessel pressure at which flow rates are quoted		x								
Vessel pressure at shutoff head		x	x	x	x	x				
Minimum flow at 0 psid (vessel-to-drywell)		x	x			x				
Pressure at which injection valve may open or close		x	x							
In-vessel leakage flow rate		x	x							
Pressure at which leakage flow is defined		x	x							
Normal position of minimum flow valve at system startup		x	x			x				
System flow at which min. flow valve is signaled to close		x	x			x				
Minimum flow valve stroke time		x	x			x				
Minimum operating pressure				x	x					
Steam flow rates at maximum and minimum pressure				x	x					
Action Time										
Delay time to process initiation signal	x	x	x	x	x	x	x	x	x	
Timer delay for sustained low water level		x	x							
Maximum delay time from bus at rated voltage until power available for pump start		x	x			x				
Maximum delay time from pump start until pump is at rated speed		x	x							
Maximum allowed delay time from initiating signal to pump at rated flow speed and injection valve wide open and bypass valve closed				x	x	x				
Maximum allowed delay time from initiating signal to start of steam flow				x	x					
Maximum delay time from bus at rated voltage until power available at valve		x	x			x				
Maximum stroke time		x	x			x	x		x	

[[

]]

Figure 6.3-1 Time for Drywell Pressure to Reach High Drywell Pressure Following LOCA

[[

]]

Figure 6.3-2 Control Reactivity Insertion for Various Scram Speeds

[[

]]

Figure 6.3-3 Reactor Power Transient following DBA for Various Scram Speeds

[[

]]

Figure 6.3-4 Effect of Scram Speed on BWR/4 PCT (PLHGR Channel) for DBA

[[

]]
**Figure 6.3-5 Reactor Power Transient following Small Break for Various Scram
Speeds**

[[

]]
Figure 6.3-6 Effect of Scram Speed on BWR/4 PCT for Small Break

6.4 PCT ANALYSIS RESOLUTION

There exists an inherent uncertainty that is common to analyses using system codes, which is not separately identified by physical phenomena. Understanding this uncertainty and treating it as one of the uncertainty contributors is important. This uncertainty can be also characterized as the analysis resolution. Because this uncertainty exhibits itself as variability to small change in the input, it resembles, and sometimes is referred to as, computational “noise.” This section describes the process of quantifying the magnitude of this uncertainty, and explains the source of this variability in the computed results. No actual attempt is made here to individually quantify this uncertainty on PCT results. How this quantity is used and the evaluation process is described in Section 9.0.

The main reasons for computational uncertainty for the demonstration calculations presented in this report are numerical techniques and the parallel channel effect. The numerical techniques, including discretization errors and built-in empirical correlations describing the physical phenomena, have relatively less effect on the results. The studies for jet pump plants showed that the ‘parallel channel’ effect is a more dominant contributor of this uncertainty. The range of PCT results conservatively account for this uncertainty either by resulting in a larger standard deviation if normal distribution assumption can be supported, or by leading to a higher upper bound PCT when non-parametric order statistics is relied on for the licensing results.

[[

]] As a result of this experience, the concept of “noise” or *analysis*

resolution has been accepted as a fundamental element of LOCA calculations that must be considered when addressing the effects (on PCT) of uncertainties in model, input and plant parameters. The approach taken is to quantify the analysis resolution associated with a given LOCA simulation and use it to judge the significance of the individual parameter uncertainties.

Sections 5 and 6 have described and quantified the uncertainties associated with the model, input and plant parameters and have thereby provided the basis for the designation of a subset of these parameters to be addressed by statistical LOCA analysis. (See Section 7 for a detailed description of the procedure to be used for the statistical analysis.) The process to quantify the analysis resolution is by running a statistical analysis with the parameter uncertainties reduced by a factor of ten. [[

]] This approach was compared with two alternative evaluations based, respectively, on [[]] and [[]]. All three evaluations were shown to provide comparable results in terms of PCT range. Accordingly, the definition based on the statistical evaluation [[]] was adopted and will be used for evaluating the significance of the PCT sensitivity to the individual and collective parameter uncertainties in the calculations presented in subsequent sections of this report.

The demonstration cases for plant applications are presented in Section 8. Section 8.1 contains the BWR/4 LOCA analysis. The PCT analysis resolution for the BWR/4 limiting break is calculated by sampling the uncertainty parameters [[

]] indicated in Table 5.1-2. Figure 6.4-1 shows the range and the average of the PCT transient over the 59 trials along with the result of the nominal calculation in which all the random variables are set to their most probable values. Figure 6.4-2 shows the distribution of PCTs. The PCT analysis resolution for the demonstration plant corresponds to the calculated standard deviation of [[]]. The PCT traces with time for each of the individual trials are shown in Figure 6.4-3. The minimum to maximum range of PCT values is [[]]. Both the distribution plot (Figure 6.4-2) and the individual traces (Figure 6.4-3), indicate that [[

]] Figure 6.4-4 shows the hot channel PCT results where [[]] is more apparent. When compared to the PIRT parameters' contribution to the core PCT, [[]] in the top-peaked hot channel appear to be a major uncertainty contributor. Using a comparison of Spearman rank correlation, the dominant effect of [[]] becomes more evident. The comparison of Spearman rank correlation coefficients gives an indication of each parameter's contribution to the PCT variation. Figure 6.4-5 shows the Spearman's rho for the model PIRTs. Plant-specific PIRTs are shown in Figure 6.4-6. In both figures, the PIRT values used in the run matrix are sampled from their respective distributions [[]]. The parameter labeled as the [[]] is obtained from the inspection of the run results, and it is

not an uncertainty input. In this example, the cases [[]] are apparent from the inspection of the hot channel PCTs; they exhibit the early onset of heatup.

[[]] Figure 6.4-7 and Figure 6.4-8 show the hot channel PCTs for different set of cases where the uncertainty parameters are sampled from [[]], respectively. Compared to the perturbation applied in Figure 6.4-4, [[]] in Figure 6.4-7 which indicates [[]] in the PCT response. [[]]

[[]] Figure 6.4-9 shows the range of PCT and Figure 6.4-10 shows the PCT distribution for different set of cases where the uncertainty parameters are sampled using [[]] as shown in Figures 6.4-3, 6.4-4, 6.4-7 and 6.4-8 is [[]]

In conclusion, there are inherent uncertainties associated with the modeling. The uncertainty caused by [[]] appears to be a dominant contributor to the overall PCT uncertainty, which is minimized by using detailed core modeling. This uncertainty, together with the other computational contributors, can be quantified by [[]] As shown by this example in this section, the standard deviation of the PCT distribution from a statistical analysis [[]] is used to define and calculate the PCT analysis resolution.

[[

]]

Figure 6.4-1 PCT Range for BWR/4 Limiting Break

[[

]]

Figure 6.4-2 PCT Distribution for BWR/4 Limiting Break

[[

]]

Figure 6.4-3 Individual PCT Traces for BWR/4 Limiting Break

[[

]]

Figure 6.4-4 Hot Channel PCT Traces for BWR/4 Limiting Break

[[

]]

Figure 6.4-5 Model PIRTs Rank Correlations

[[

]]

Figure 6.4-6 Plant-Specific PIRTs Rank Correlations

[[

[[**Figure 6.4-7 Hot Channel PCT Traces for** [[]]
]]

[[**Figure 6.4-8 Hot Channel PCT Traces for** [[]]
]]

[[

Figure 6.4-9 PCT Range for BWR/4 0.67 ft² Break with [[
]]

[[

Figure 6.4-10 PCT Distribution for BWR/4 0.67 ft² Break with [[
]]

7.0 COMBINATION OF UNCERTAINTIES

A non-parametric statistical sampling technique is used to combine the individual biases and uncertainties specified for initial conditions, plant, and model parameters into an overall bias and uncertainty for the LOCA safety criteria. The statistical random sample is developed by performing random variations of the parameters over their individual uncertainty ranges. Using the histogram generated by the random sampling technique, a probability density function is generated for the calculated primary safety criteria parameters.

To determine the total uncertainty in computer code predictions, it is necessary to combine the effects of model uncertainties (CSAU Step 9), scaling uncertainties (CSAU Step 10) and plant condition or state uncertainties (CSAU Step 11). Various methods have been used to combine the effects of uncertainties in a safety analysis, which are discussed briefly in [3]. All these approaches are within the framework of the CSAU methodology. This section only describes the methods for combining uncertainties that are proposed to be used for the TRACG ECCS/LOCA application.

7.1 APPROACHES FOR COMBINING UNCERTAINTIES

Four approaches have been discussed and compared in [3] for combining uncertainties, which are: (1) Propagation of Errors; (2) Response Surface Technique; (3) Order Statistical (OS) Method, and (4) Normal Distribution One-Sided Tolerance Limit. Only the last two approaches will be briefly discussed in the following sections (Sections 7.1.1 and 7.1.2) since a multivariate version of order statistics is adapted for the TRACG ECCS/LOCA application and normal distribution assumption is used in some of the Chapter 8 demonstration calculations.

7.1.1 Order Statistics (OS) Method

The non-parametric sampling method that has been used in Germany by Gesellschaft für Anlagen- und Reaktorsicherheit (GRS) [28] and for the application of TRACG to AOOs by GEH [3] requires only a relatively small number of calculations and automatically includes the effects of interactions between perturbations to different parameters. In the OS method, randomly sampled trials are used to vary all uncertain model and plant parameters randomly and simultaneously, each according to its uncertainty and assumed PDF. A method based on the order statistics of the output values is then used to derive one-sided upper or lower tolerance limits (OSUTLs or OSLTLs). For ECCS/LOCA applications, OSUTLs are defined for primary safety parameters such as the PCT, maximum clad oxide thickness fraction, and maximum zirconium oxide volume fraction.

Random sampling of each model, plant and state parameter according to its assigned PDF yields the value of that parameter to be used for a particular trial. For example, a given trial could have the film boiling heat transfer coefficient set at its -1.5σ value and the interfacial shear set at its $+2.0\sigma$ value, each according to its own probability model. For each randomly sampled set of parameters, the calculation process determines the output parameters of interest. In this manner, the effects of interactions between parameters are captured in a single calculation. Once all of the

trials have been completed, the desired output parameter (e.g., PCT) is extracted from each of the trials and the set of all values of this parameter is used to construct its OSUTL. Figure 7.1-1 illustrates the process.

TRACG overlay files containing all the perturbed input parameter values are created for each trial. The overlay file is appended to the end of the base transient input file and the TRACG calculation is performed to determine the output parameter value (e.g., PCT) as a function of time for this particular set of inputs. Each repeat of the process defines a sample value of the output parameter of interest for the particular transient under consideration. Similar sample values for other output parameters (e.g., maximum cladding oxidation) can be generated at the same time without additional TRACG calculations.

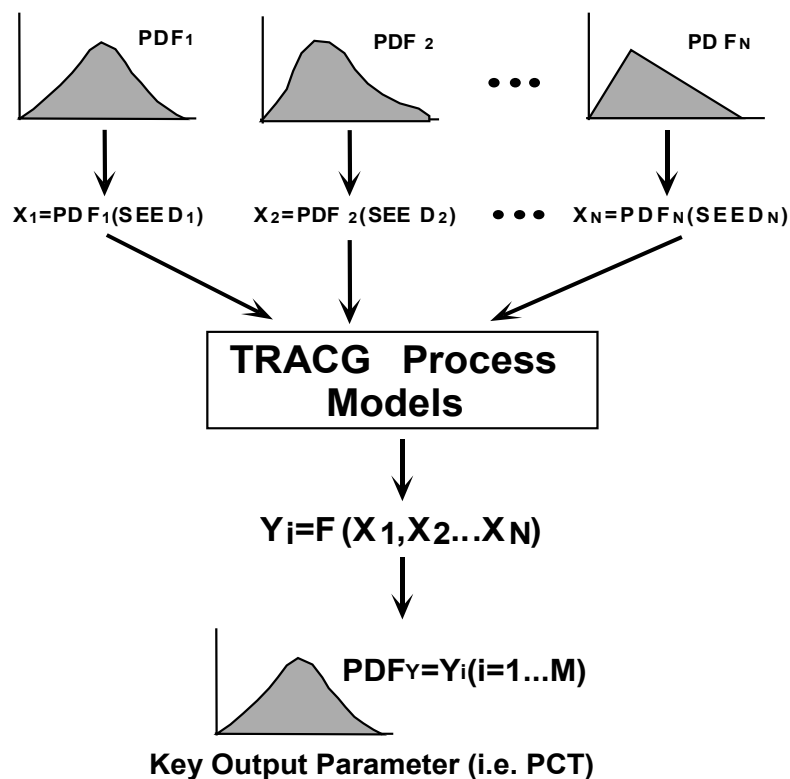


Figure 7.1-1 Schematic Process for Combining Uncertainties

The OSUTL of an output parameter, derived from the results of any given number of trials, is defined by two numbers, $0 < \alpha, \beta < 1$. Denoting the OSUTL by U , it can be stated that the percentage of future values of the output parameter (i.e., values determined from subsequent trials) that will be less than U is $100 \cdot \alpha\%$, with a confidence level of at least $100 \cdot \beta\%$. In formal practice, this is called an OSUTL with $100 \cdot \alpha\%$ content and (at least) $100 \cdot \beta\%$ confidence level. It has been shown [30] that, for prescribed values of α and β , the OSUTL can be defined for univariate case as the largest of the output parameter values if the sample size, n , satisfies $n \geq \log(1-\beta)/\log\alpha$. Thus

to claim the largest value of a set of trials is an OSUTL with 95%-content and 95% confidence level for a single parameter, the minimum sample size is $n = 59$.

In multivariate case, the minimum sample size for joint probability of three statistically dependant but not necessarily correlated parameters is 124. In other words, the highest value for each of the three critical safety parameters would provide the joint 95% tolerance limit 95% probability from a population of 124 cases.

The order statistics method is generally applicable without regard to the underlying probability distribution of the output parameter of interest. It requires only that the individual trials be independent realizations of a random variable from some single probability distribution. For a given number of trials, the upper bound value of the output parameter is itself a random quantity with a variability that depends on the sample size. The variability can be substantial and, on occasion, will yield an overly conservative bound.

To reduce this variability, a larger sample size can be used so that the 95%-content/95% confidence bound is given by the second or third largest observation. In a sample of 124, for example, the largest observation provides the desired bound for trivariate case. It is also possible to increase the sample size to 181 and sequentially eliminate 2 of the samples having the highest values from the population when determining the 95% tolerance limit with 95% confidence.

7.1.2 Normal Distribution One-Sided Upper Tolerance Limit

A special case of the order statistics method arises when the data that the tolerance bound will be derived from can reasonably be regarded as a sample from a normal probability distribution. In this case, it can be shown that the normal distribution one-sided upper tolerance limit (ND-OSUTL) is of the form

$$ND - OSUTL_{\alpha,\beta} \equiv \bar{y} + z_{\alpha,\beta} \cdot s \quad (7-1)$$

where \bar{y} is the average of the outcomes of the trials, s is their standard deviation and the factor $z_{\alpha,\beta}$ is chosen to guarantee $100\alpha\%$ -content with a $100\beta\%$ confidence level. The assumption of normality for the response data is typically justified via one or more goodness-of-fit tests (e.g., Ryan-Joiner, Shapiro-Wilk, or Anderson-Darling). The values of $z_{\alpha,\beta}$ are tabulated in many statistical textbooks (e.g., [31]) as *factors for one-sided normal tolerance limits*. For example, to establish a bound of 95% content with a 95% confidence level from a sample of 59 trials, $z_{95,95} = 2.024$. As the sample size increases, this factor approaches 1.645, the 95th percentile of the standard normal distribution. If the normality tests indicate that the data are unlikely to have originated from a normal population, the order statistics method should be used. [[

]]

7.2 PROCESS FOR COMBINING UNCERTAINTIES

The above description of the statistical basis for combining uncertainties indicates that a relatively small number of TRACG runs will suffice to determine 95th percentile with high probability OSUTLs for the output variables of interest using either the ND-OSUTL method or the order statistics method. The individual runs (trials) would be made with the statistically characterized model parameters and inputs selected randomly from populations governed by their respective probability density functions. The key advantages of using the proposed statistical method may be enumerated as follows:

- The required number of trials depends only on the desired content and confidence level of the bounding values to be derived from the results of the TRACG trials. In particular, the number of trials does not depend on the number of model and input parameters that are statistically characterized and randomly selected for each trial.
- It is not necessary to perform separate calculations to determine the sensitivity of the response variables to changes in the individual, statistically based model and input parameters. Furthermore, in contrast to the response surface method, it is not necessary to make assumptions regarding the effect on the response variables of interactions between the statistically based parameters.
- It is not necessary to perform the large number of calculations required to develop a separate response surface for each output parameter of interest. In addition, there is the advantage of having no restriction on the variety of PDFs (e.g., normal or uniform) that can be used for the statistical characterization of the model and input parameters.
- The OSUTL for each output parameter of interest can be defined over the entire duration of the transient as opposed to being limited to only the peak value or the value at a particular time.

Comparing the order statistics and ND-OSUTL methods, the advantage of the former is that the interpretation of the results does not depend on the underlying PDFs of the output variables. The disadvantage is that the OSUTLs, to the extent that they are order statistics, will vary from one set of TRACG trials to another. The differences may be substantial, especially for small trial sets, and particularly if the tolerance bound is the sample maximum. The ND-OSUTL method, in contrast, provides an OSUTL that is typically less sensitive to the particular set of TRACG trial values. Its application, however, depends on the output variable being normally distributed. [[

]]

7.3 IMPLEMENTATION OF STATISTICAL METHODOLOGY

The purpose of this section is to describe the process by which the statistical results derived from TRACG calculations will be used to: (1) determine the PCT, maximum local oxidation, and core-wide oxidation; and (2) establish that these safety parameters have acceptable margins to design limits prescribed by 10 CFR 50.46.

[[

]]

The intention of the implementation procedure described and demonstrated herein is that for fuel cycles subsequent to the initial TRACG ECCS/LOCA application for a specific plant, [[
]] Either of the following two circumstances would, however, require the detailed statistical analysis to be repeated for a subsequent fuel cycle:

- [[

]]

This aspect of the application procedure is justified on the basis that the uncertainties in the statistically characterized model parameters are not expected to change for subsequent cycles unless [[

]]

7.3.1 Conformance with Design Limits

The fundamental steps in the application of the method described in Section 7.2 are as follows:

- Identify all model and input parameters that are statistically characterized for inclusion in the uncertainty evaluation of the LOCA scenario to be analyzed.
- [[

-

]]

- Confirm that the OSUTLs for PCT, peak local oxidation and corewide oxidation are within their respective limits.

7.4 STATISTICAL ANALYSIS FOR QUALIFICATION EVENTS

In this section, statistical analyses are performed on a selected set of ECCS/LOCA qualification tests utilizing the model uncertainties developed in Section 5. Statistical analyses of the integral system tests validate the values used for the model uncertainties by showing that the test data fall within the resulting uncertainty band of the calculations. The integral tests selected for this evaluation are the large and small breaks from the FIST test series (Tests 6DBA1B and 6SB2C), which are included in the TRACG qualification suite [2]. Statistical analyses were also performed for the core spray heat transfer tests analyzed as part of the TRACG LOCA qualification. The approach is identical to that used for the BWR/4, BWR/6 and BWR/2 LOCA uncertainty analyses described in Section 8. The model PIRTs for these calculations use the same uncertainties and biases and are sampled from the same probability distribution function as those applied for the plant calculations. The calculations in this section are carried out using a sample size of 59, since the rod temperatures are considered as the main critical outcome of the simulations and there is no joint probability consideration for oxidation and combustible gas generation in the experimental facilities. The size of the random sampling is considered adequate for the statistical analyses of the qualification events.

7.4.1 FIST Large Break LOCA

Predictions of several of the FIST integral systems tests are part of the TRACG LOCA qualification. A description of the FIST facility, the tests performed, and TRACG model and nodalization can be found in the TRACG Qualification Report [2]. Two of these tests, the large break (Test 6DBA1B) and the small break (Test 6SB2C), were selected to demonstrate the effect of model uncertainties on the TRACG predictions. As noted above, the PIRT inputs used to examine the effects of model uncertainties for these calculations were the same as those used for the BWR/2, BWR/4 and BWR/6 LOCA uncertainty studies (Section 8). With these inputs, 59 calculations were made for each of the two FIST LOCA tests. The results for the large break case are summarized in this section and those for the small break are summarized in the next section.

The FIST large break test simulated a double-ended break in one recirculation loop of a BWR/6-218 Standard Plant. The break simulation included failure of two of the three LPCI pumps. The system response evolved as a rapid depressurization, followed by activation of the emergency core cooling safety systems. The heated rod bundle in the FIST facility simulated the heat-up and cooling of the hot fuel bundle in the BWR core. [[

]]

7.4.2 FIST Small Break Test 6SB2C

The FIST small break test simulated a 0.0046 m² break on the suction side of one recirculation loop of a BWR/6-218 Standard Plant with the HPCS unavailable. For the small break, the system pressure is maintained until activation of the ADS when the downcomer water level reaches Level 1. Vessel refill begins when the system pressure falls below the pump shutoff head of the low-pressure safety systems. The simulated fuel bundle in the facility simulates the heat-up and cooling of the hot bundle in the BWR core as the bundle is uncovered and the vessel is refilled. [[

]]

7.4.3 Conclusions from the FIST Test Simulations

[[

]]

7.4.4 SSTF Test EA3-1

The SSTF Test Facility simulated the refill-reflood phase of a BWR LOCA transient. The safety systems in the facility could be configured to model either a BWR/6 or BWR/4 refill-reflood transient and test data from both BWR/6 and BWR/4 simulations were used for TRACG

qualification [2]. Test EA3-1, a BWR/4 refill-reflood simulation, was selected for the statistical analysis presented here.

In this test, the lower plenum fill time controls the core reflood. The major purpose of the statistical analysis is to show that the measured lower plenum fill-time is bounded by the TRACG analysis when model uncertainties are taken into account. The liquid mass held up in the bypass region and upper plenum has an important effect on the LOCA analysis. The bypass and upper plenum fill time predictions are compared to the test results. It should be noted that the accuracy of the lower plenum fill time also depends on the amount of liquid held up above the core plate, and therefore the lower plenum fill time predictions depend on the bypass and upper plenum liquid fractions being predicted reasonably well. Several of the qualification test data vs. analysis comparisons are repeated as part of the uncertainty analysis.

The results of the statistical analysis of SSTF Test EA3-1 are compared with the test data in Figure 7.4-10 through Figure 7.4-17. The TRACG results include the nominal calculation, the band subtended by the 59 trials and the average of the 59 trials. Figure 7.4-10 compares measured and calculated system pressures. [[

]]

TRACG's prediction of temperature variations in the lower plenum is shown in Figure 7.4-11 through Figure 7.4-13. These figures show temperatures measured at the lower plenum periphery near the bottom, at mid-submergence and near the surface. The data for the bottom and mid-plane show the same trend until approximately 80 seconds, after which there are fluctuations of high magnitude at the mid-level and of lower magnitude at the bottom level. Since the lower section of the lower plenum is divided into bays, and the temperature is measured in the bay where the jet pump discharges into, the lower plenum temperature measured at the bottom of the lower plenum is expected to be close to the jet pump discharge temperature. There are occasional fluctuations in the test data after the lower plenum is filled as shown in Figure 7.4-11. [[

]]

Of particular interest in Test EA3-1 is the lower plenum refill time. The available test data show the refill time expressed as lower plenum mass fraction. [[

]]

Comparisons to the bypass and upper plenum fill fractions in Figures 7.4-16 and 7.4-17 provide a measure of the effects of CCFL correlations. [[

]]

These comparisons show that the TRACG predictions represent the ECCS mixing phenomena reasonably well in the upper plenum and lower plenum regions, CCFL behavior and the timing of reflood.

The uncertainty evaluation of the TRACG predictions of the SSTF test was extended to consider the potential range of the test conditions along with the model parameters in the Monte Carlo calculation. Uncertainties in the test conditions include the flow rates and temperatures of the ECC systems, the temperatures and flow rates of the steam injections that simulate vapor generation and the initial liquid masses in the various regions of the test facility. [[

]] The test conditions that were varied together in this manner are noted in Table 7.4-1.

Figure 7.4-18 and Figure 7.4-19 show the predictions for the pool temperature at the periphery near the bottom and for the lower plenum mass fraction when both the model parameters and test

conditions are varied. [[

]]

In summary, the statistical analysis of SSTF Test EA3-1, a BWR/4 refill-reflood simulation, [[

]]

7.4.5 Core Spray Heat Transfer Tests

A statistical analysis was performed for two of the Core Spray Heat Transfer (CSHT) tests described in Section 3.2.2 of the TRACG Qualification Report [2]. CSHT Tests 111 and 112 were chosen for this purpose because [[

]]

TRACG predictions of the peak rod temperature for both Test 111 and Test 112 with the TRACG LOCA model uncertainties established in the LTR provide the representative bound for the rod temperatures from the tests. It is also observed that [[

]]

It is acknowledged that [[

]]

As previously noted, [[

]]

In summary, TRACG predictions of the peak rod temperatures for [[

]]

Table 7.4-1 Test Parameters Varied for Monte Carlo Simulation of SSTF Test EA3-1

Test Parameter	Nominal Input	Variation Range
Low Pressure Core Spray (LPCS)	33.5 kg/s	[[
Low Pressure Core Injection (LPCI)	75 kg/s	
Fuel Bundle Steam Injection	9.7 kg/s	
Guide Tube Steam Injection	6.39 kg/s	
Lower Plenum Steam Injection	5.73 kg/s	
LPCS & LPCI Temperature (1)	Measures Temp	
Bundle, GT & LP Steam Injection Temp (2)	Sat Temp @ Press	
Upper Plenum Initial Mass	0 kg (empty)	
Fuel Bundle Initial Mass	380 kg	
Bypass Initial Mass	306 kg	
Guide Tube Initial Mass	693 kg (full)	
Lower Plenum Initial Mass	1969 kg	
Annulus Initial Mass	320 kg]]

Notes:

- (1) ECC flows are from common source; flows controlled separately; temperatures varied together.
- (2) Steam injection flows are from common source; flows controlled separately; steam superheat varied together.
- (3) The masses of test facility regions that were initially full or empty were not varied as part of the test parameter variation.

[[

]]

Figure 7.4-1 Comparison of System Pressure for FIST Test 6DBA1B

[[

]]

Figure 7.4-2 Comparison of Rod Temperatures (Elevation 1.96 m) for FIST Test 6DBA1B

[[

]]

Figure 7.4-3 Comparison of Rod Temperatures (Elevation 1.22 m) for FIST Test 6DBA1B

[[

]]

Figure 7.4-4 Correlation of Rod Temperatures (Elevation 1.96 m) with PIRTs for FIST Test 6DBA1B

[[

]]

Figure 7.4-5 Comparison of System Pressure for FIST Test 6SB2C

[[

]]

Figure 7.4-6 Comparison of Rod Temperatures (Elevation 2.97 m) for FIST Test 6SB2C

[[

]]

Figure 7.4-7 Comparison of Rod Temperatures (Elevation 1.96 m) for FIST Test 6SB2

[[

]]

Figure 7.4-8 Comparison of Rod Temperatures (Elevation 1.22 m) for FIST Test 6SB2C

[[

]]

Figure 7.4-9 Correlation of Rod Temperatures (Elevation 1.96 m) with PIRTs for FIST Test 6SB2C

[[

Figure 7.4-10 Comparison of System Pressure for SSTF Test EA3-1

]]

[[

]]

Figure 7.4-11 Comparison of Temperature at Pool Periphery at the Bottom for SSTF Test EA3-1

[[

]]

Figure 7.4-12 Comparison of Temperature at Pool Periphery at Mid-Depth for SSTF Test EA3-1

[[

]]

Figure 7.4-13 Comparison of Temperature at Pool Periphery at the Surface for SSTF Test EA3-1

[[

Figure 7.4-14 Comparison of Lower Plenum Fill Fraction for SSTF Test EA3-1

]]

[[

]]

Figure 7.4-15 Correlation of Lower Plenum Refill Time with PIRTs for SSTF Test EA3-1

[[

Figure 7.4-16 Comparison of Bypass Fill Fraction for SSTF Test EA3-1

]]

[[

Figure 7.4-17 Comparison of Upper Plenum Fill Fraction for SSTF Test EA3-1

]]

[[

]]

Figure 7.4-18 Comparison of Temperature at Bottom of Pool Periphery Including Variations in Test Conditions for SSTF Test EA3-1

[[

]]

Figure 7.4-19 Comparison of Lower Plenum Fill Fraction Including Variations in Test Conditions for SSTF Test EA3-1

[[

]]

Figure 7.4-20 Results of Monte Carlo Analysis vs. Test Data for Rod Group 2

[[

]]

Figure 7.4-21 Results of Monte Carlo Analysis vs. Test Data for Rod Group 3

[[

]]

Figure 7.4-22 Results of Monte Carlo Analysis vs. Test Data for Rod Group 4

[[

]]

Figure 7.4-23 Results of Monte Carlo Analysis vs. Test Data for Rod Group 6

[[

]]

Figure 7.4-24 Results of Monte Carlo Analysis vs. Test Data for Rod Group 9

[[

]]

Figure 7.4-25 Results of Monte Carlo Analysis vs. Test Data for Rod Group 2

[[

]]

Figure 7.4-26 Results of Monte Carlo Analysis vs. Test Data for Rod Group 3

[[

]]

Figure 7.4-27 Results of Monte Carlo Analysis vs. Test Data for Rod Group 4

[[

]]

Figure 7.4-28 Results of Monte Carlo Analysis vs. Test Data for Rod Group 6

[[

]]

Figure 7.4-29 Results of Monte Carlo Analysis vs. Test Data for Rod Group 2

[[

]]

Figure 7.4-30 Results of Monte Carlo Analysis vs. Test Data for Rod Group 3

[[

]]

Figure 7.4-31 Results of Monte Carlo Analysis vs. Test Data for Rod Group 4

[[

]]

Figure 7.4-32 Results of Monte Carlo Analysis vs. Test Data for Rod Group 6

8.0 DEMONSTRATION ANALYSIS

The analyses provided in this section demonstrate the TRACG ECCS/LOCA application process for typical BWR plants. [[

]]

The implementation of TRACG for a specific plant requires a nominal analysis of the break spectrum and identification of the *limiting conditions*. Statistical analysis will be performed at the *limiting conditions* with the applicable fuel at the time TRACG is first implemented for ECCS/LOCA analysis for the plant.

The demonstration analyses described in this section include:

1. TRACG analyses for representative plant types performed with an analysis procedure equivalent to that applied in plant USAR evaluations;
2. Demonstration of the sensitivity of the LOCA transient analysis to initial conditions and plant parameters; and
3. Statistical analysis in accordance with the process defined in Section 7.3.

The overall statistical application of TRACG for ECCS/LOCA analysis was validated in Section 7.4 where it was shown that the statistical tolerance bands on the predictions of integral-systems tests applicable to ECCS/LOCA encompass the test measurements.

The statistical analyses in this section are provided as a demonstration of the statistical process. This evaluation satisfies the requirements of Steps 13 and 14 in the CSAU process related to combination of uncertainties and biases, and the determination of a total uncertainty. Statistical analyses have been performed for each of the three product lines (BWR/2, 4 and 6). The statistical process to be followed conforms to Section 7.0. The uncertainties in the High and Medium ranked model parameters (Section 5.1) and the important plant initial conditions and

plant parameters (Sections 6.2, 6.3) are combined through a Monte Carlo process involving random draws from the individual probability distributions. A TRACG calculation of the PCT with a set of these randomly drawn values of the model and plant parameters represents one “trial” in the statistical process. A number of trials are made to derive the necessary statistical conclusions about the PCT distribution.

8.1 TRACG LOCA ANALYSIS AND SENSITIVITY STUDIES FOR A TYPICAL BWR/4 PLANT

The sections below describe a set of baseline ECCS/LOCA TRACG analyses performed for a typical BWR/4 plant. The presentation includes the representative TRACG nodalization of the plant, nominal results for both the DBA and small breaks, break spectrum analysis, sensitivities to the model parameters and sensitivities to the variability and uncertainty in the initial conditions, and the uncertainty analysis. Consistent with the discussion in the introduction to Section 6.3, all plant parameters were set at their analytic limits throughout this evaluation. Any exceptions are demonstrated to have no effect on the LOCA response.

8.1.1 TRACG Nodalization for ECCS/LOCA Calculations for a BWR/4 Plant

A typical BWR/4 plant forms the basis for these analyses. The plant has 560 bundles and an Original Licensed Thermal Power (OLTP) of 2436 MWth. The plant is assumed to be loaded with a mixture of fresh and exposed GE14 10x10 fuel. The TRACG vessel modeling is illustrated in Figure 8.1-1. Figure 8.1-2 illustrates the overall plant model consisting of [[

]] components. As shown in Figure 8.1-3, the BREK components are isolated from the piping in the steady state model. Breaks are initiated by opening communication with one or two BREK components depending on whether a split or double-ended break is being simulated.

Table 8.1-1 shows the channel grouping used for the calculations. [[

[[

]]

Figure 8.1-1 TRACG Vessel Nodalization for Typical BWR/4 Model

[[

]]

Figure 8.1-2 TRACG Component Nodalization for Typical BWR/4 Model

[[

]]

Figure 8.1-3 TRACG Modeling of Guillotine and Split Breaks

8.1.2 Nominal ECCS/LOCA Results for Large and Small Breaks for BWR/4

This section presents baseline TRACG results for a double-ended guillotine break (Design Basis Accident) and a small break in the recirculation line piping on the suction side of the pump. The

graphical presentation is limited to the RPV pressure, the ECCS flows and the PCTs for the three hot channels and one of the average channels. These results demonstrate the major features of the LOCA transient and are sufficient for the subsequent discussion of the sensitivity of the PCT to variations in the model parameters, plant parameters and initial conditions. Finally, they provide the necessary basis for the statistical evaluation that represents the major focus of the demonstration analysis.

8.1.2.1 Suction DBA Results

Table 8.1-2 shows the initial conditions and the key transient parameters for the double-ended guillotine break LOCA analysis case. The plant is operating at 120% OLTP and 80% of rated flow. As stated in Table 8.1-4, [[

]] A double-ended break of the recirculation line is assumed at time zero concurrently with a trip of the recirculation pumps on the assumed loss of offsite power. A reactor scram is initiated on High Drywell Pressure. MSIV closure occurs when the downcomer level reaches Level 1. As a result of the assumed battery failure, high pressure core injection (HPCI) and one diesel generator are not available. The available ECCS consists of one LPCS, two LPCI (one in each loop) and seven ADS valves. Table 8.1-2 shows the time delays and pressure permissives for the ECC systems.

Figure 8.1-4 shows the system pressure response and the ECC flows for the suction DBA. The RPV depressurizes from the break flow. The depressurization rate increases after the inlet to the recirculation line suction is uncovered. The depressurization causes the initially subcooled liquid in the lower plenum to flash. The ECC systems are activated as the pressure falls below the ECC pressure permissives. The LPCS starts injecting coolant into the upper plenum at 39 s and the LPCI through the recirculation lines and jet pumps at 68 s. Figure 8.1-5 shows the calculated peak temperatures in the hot bundles and an average bundle in Ring 2. The hot bundles go through an early boiling transition because of the power/flow mismatch where the channel flow rapidly drops while the power is still relatively high in the bundle. These temperature excursions are rapidly quenched by the lower plenum flashing. A sustained dryout and heatup in the core begins in the 20 to 25 s time period as the inventory in the core is depleted. The heatup is terminated following the refill of the lower plenum and core by the ECC systems. [[

]] A PCT of 863 K was calculated at about 128 s from the start of the event.

Table 8.1-2 BWR/4 Suction DBA Key Transient Parameters

Time Summary (s)	
Break	0
Scram	0.9
Recirculation Pump Trip on loss of offsite power	0
MSIV Closure initiated	5.9
LPCS diesel generator startup delay	27
LPCS initiation delay following pressure permissive of 28.59 bar	15
LPCI diesel generator startup delay	37
LPCI initiation delay following pressure permissive of 20.66 bar	37
Initial Conditions	
Initial core power (% OLTP)	120
Initial core flow (%)	80
Initial dome pressure (Pa)	7.29E6
Initial FW temperature (K)	495
Initial NR water level (m)	14.10
[[
]]
Key Transient Parameters	
Single Failure	Battery
ECC Systems available	1 LPCS, 2 LPCI (one in each loop), 7 ADS valves
LPCS initiated (s)	39
LPCI initiated (s)	68
Peak Cladding Temperatures	
[[
]]

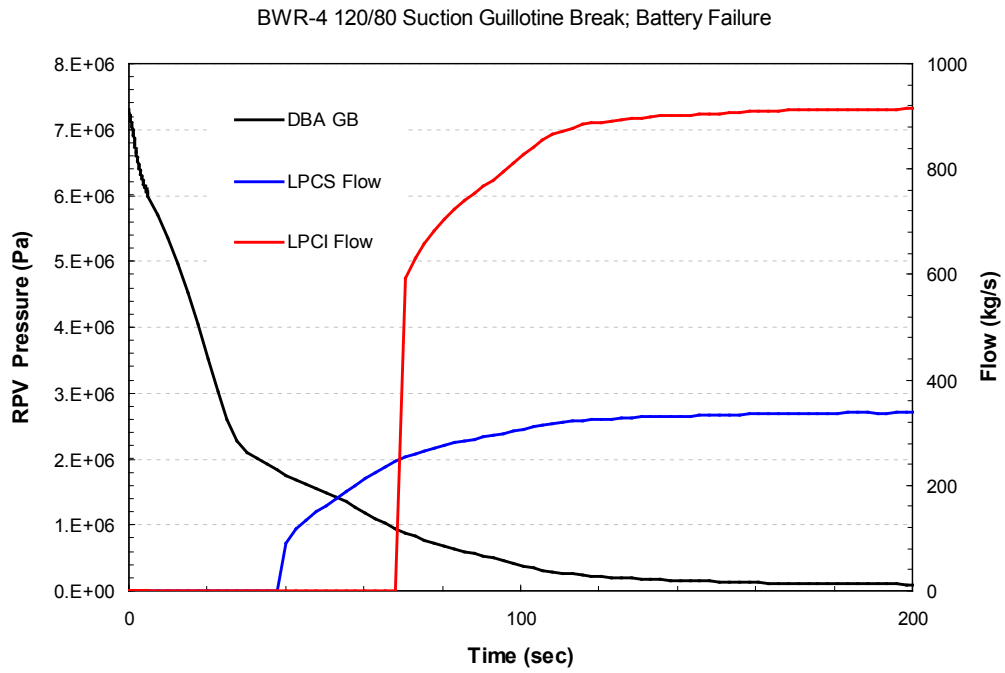


Figure 8.1-4 System Pressure and ECC Flows for BWR/4 Suction DBA

[[

Figure 8.1-5 PCT for Various Channels for BWR/4 Suction DBA

]]

8.1.2.2 Small Break Results

Table 8.1-3 shows the initial conditions and the key transient parameters for the small break case. The plant is operating at 120% OLTP and 80% of rated flow. A 0.0093 m² break in the recirculation line is assumed at time zero concurrently with a trip of the recirculation pumps. A reactor scram occurs at 5.9 s on Level 3 and the MSIVs start to close at 60 s on Level 1. As a result of the assumed battery failure, HPCI and one diesel generator are not available. The available ECCS consists of one LPCS, two LPCI (one in each loop) and seven ADS valves. Table 8.1-3 shows the time delays and pressure permissives for the ECC systems.

Figure 8.1-6 shows the system pressure response and the ECC flows for the small break. The RPV pressurizes after closure of the MSIVs. The energy lost through the break flow is less than the energy added through the decay heat. Opening of the SRVs maintains the pressure around 8 MPa. The ADS is tripped with a delay of 120 s when the downcomer level drops to Level 1. The ADS valves open at approximately 180 s and the RPV begins to depressurize. The ECC systems are activated when the pressure falls below the ECC pressure permissives. The LPCS starts injecting coolant into the upper plenum at approximately 300 s and the LPCI through the recirculation lines and jet pumps at 340 s. Figure 8.1-7 shows the calculated peak temperatures in the hot and average bundles. The hot bundles do not go through an early boiling transition because, in contrast to the DBA, the flow does not drop rapidly as the pumps coast down. Heatup occurs in the upper portion of the core due to loss of inventory at about 148 s from the start of the accident. A temperature increase is seen in both the CPR-limited and average bundles, which are peaked near the top and in the middle, respectively.

Activation of the ADS results in flashing of the inventory in the lower plenum. The resulting flow surge quenches the core and the heatup is terminated. As the effects of the flashing diminish, core inventory again drains and a sustained heatup results, beginning at about 230 s for the top peaked bundles without core spray and a little later for the others. The heatup is usually terminated following the refill of the lower plenum and core by the ECC systems. [[

]]

It was found for small breaks that there was a stronger PCT sensitivity to small perturbations in some of the TRACG model parameters than might be expected a priori. Detailed investigation identified the physical mechanism causing this behavior. When the core begins to drain after the effects of the depressurization have abated and the core pressure drop is low, some of the channels assume a cocurrent upflow mode while others assume a countercurrent flow mode. This behavior is consistent with experimental observations of both these flow modes in the SSTF facility [2].

Table 8.1-3 BWR/4 0.0093 m² Suction Break Key Transient Parameters

Time Summary (s)	
Break	0
Scram	5.6
Recirculation Pump Trip on loss of offsite power	0
MSIV Closure initiated	60
LPCS diesel generator startup delay	27
LPCS initiation delay following pressure permissive of 28.59 bar	15
LPCI diesel generator startup delay	37
LPCI initiation delay following pressure permissive of 20.66 bar	37
ADS trip delay following downcomer Level 1	120
Initial Conditions	
Initial core power (% OLTP)	120
Initial core flow (%)	80
Initial dome pressure (Pa)	7.29E6
Initial FW temperature (K)	495
Initial NR water level (m)	14.10
[[
]]
Key Transient Parameters	
Single Failure	Battery
ECC Systems available	1 LPCS, 2 LPCI (one in each loop), 7 ADS valves
LPCS initiated (s)	262
LPCI initiated (s)	316
Peak Cladding Temperatures	
[[
]]

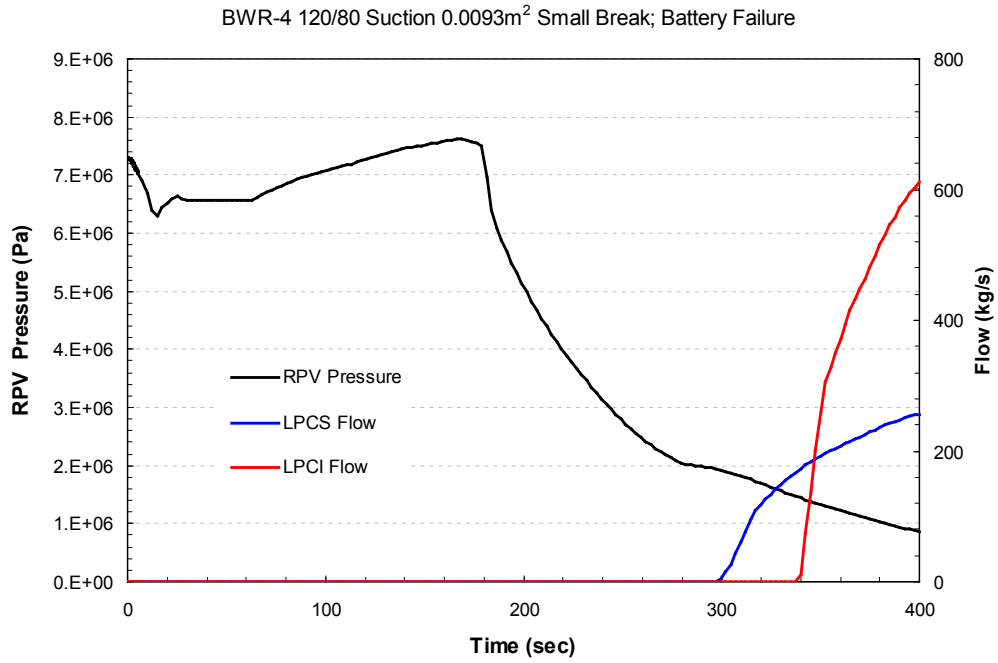


Figure 8.1-6 System Pressure and ECC Flows for BWR/4 Small Break

[[

]]

Figure 8.1-7 PCT for Various Channels for BWR/4 Small Break

8.1.3 Sensitivity to Model (PIRT) Parameters for BWR/4

A DBA LOCA and a representative small break (0.0093 m²) on the suction side of the recirculation line were evaluated with [[

]]

Figure 8.1-8 presents the sensitivity of the BWR/4 DBA LOCA PCT to individual PIRT parameter uncertainties. Figure 8.1-9 presents the sensitivity of the BWR/4 0.0093 m² suction line break PCT to individual parameter uncertainties. The discussion of the results focuses on the parameters that have a relatively large effect on PCT. On the basis of the numerical results, [[

]] (Note the different temperature scales on the DBA and small break plots.)

[[

]]

[[

]]

Figure 8.1-8 BWR/4 DBA PCT Sensitivity to PIRT Uncertainties

[[

]]

Figure 8.1-8 (cont'd) BWR/4 DBA PCT Sensitivity to PIRT Uncertainties

[[

Figure 8.1-9 BWR/4 0.1 ft² LOCA PCT Sensitivity to PIRT Uncertainties

]]

[[

]]

Figure 8.1-9 (cont'd) BWR/4 0.1 ft² LOCA PCT Sensitivity to PIRT Uncertainties

8.1.4 Sensitivity to Initial Conditions and Plant Parameters for BWR/4

8.1.4.1 Initial Conditions and Allowable Operating Range

As described in Section 6.2, the individual effects of the initial conditions on the results of a TRACG LOCA calculation are categorized in the following manner:

- A. The results are sensitive to the initial condition and a basis for the limiting initial condition can not be established. Plant analyses will consider the full allowable range of the initial condition.
- B. The results are sensitive to the initial condition and a basis for the limiting initial condition can be established. Plant analyses will specify the parameter at its limiting initial condition.
- C. The results are not sensitive to the initial condition and a nominal initial condition will be specified for the parameter.

Large and small break LOCA calculations were used to categorize the initial conditions as described above. The categorization analysis bases are described in Table 8.1-4. [[

]] The results of the sensitivity studies are discussed in the next section.

Table 8.1-4 Allowable Operating Range Specification Basis for BWR/4 LOCA

Quantity	Control Basis	Range	Analysis Basis
Total Core Power	Plant Technical Specifications restrict the maximum operating core thermal power. For a given core flow, the maximum and minimum core power are controlled through operation within the analysis basis power/flow map.	Initial power/flow conditions will be chosen to bound the operating envelope. This includes extended power uprate and MELLLA+. The limiting conditions will be identified through calculations at corners of the envelope. Partial power/flow conditions will also be analyzed with consideration of the application of power and flow dependent thermal limits.	Calculations will be made over the MELLLA+ operating map (Figure 6.2-1) at 100% OLTP/100% flow; 120/100; 120/80; and 100/55.
Total Core Flow	For a given core power, the maximum and minimum core flow are controlled through operation within the analysis basis power/flow map.		
Feedwater Temperature	The feedwater temperature and core power determine the feedwater flow and steam flow. Some plants have analyzed for additional operating flexibility (Final Feedwater Temperature Reduction or Feedwater Heater Out-of-Service).	[[
Steam Dome Pressure	Plant Technical Specifications restrict the maximum operating dome pressure. The minimum dome pressure is governed by turbine operational control.		
Downcomer Water Level	Plant operates between the L4 and L7 alarm setpoints.]]

Table 8.1-4 (cont'd) Allowable Operating Range Specification Basis for BWR/4 LOCA

Quantity	Control Basis	Range	Analysis Basis
Core Loading Pattern and Total Core Exposure	A reference core loading pattern is defined for each reload cycle. Acceptable deviation from the reference core is defined in GESTAR Section 3.4.2 [20].	[[
Axial Power Distribution	There is no restriction on axial power distribution as long as plant thermal limits are met.		
Radial Power Distribution	There is no restriction on radial power distribution as long as plant thermal limits are met.		
Local Peaking Distribution in High Power Bundles	There is no restriction on local peaking distribution as long as plant thermal limits are met.		
Control Rod Pattern (control rod density)	There is no restriction on control rod pattern as long as plant thermal limits are met.		
Bundle Exposure	There is no restriction on bundle exposure distribution as long as thermal limits are met.]]

Table 8.1-4 (cont'd) Allowable Operating Range Specification Basis for BWR/4 LOCA

Quantity	Control Basis	Range	Analysis Basis
Pellet Exposure	Peak pellet power is restricted as a function of pellet exposure.	[[
Steam Flow	Derived from core thermal power and feedwater temperature.]]

8.1.4.2 Allowable Operating Range Results

Axial Power Shape

A top peaked axial power shape is expected to be limiting because the top of the core uncovers first during a LOCA. To confirm this, [[

]] Figure 8.1-10 shows the axial profiles used in the study for the full-length rods. Because of part-length rods in the GE14 bundle, the corresponding channel average axial shapes differ from those of the full-length rods as shown in Figure 8.1-11. [[

]]

Operating Conditions on Power/Flow Map

A large guillotine break (DBA) and a small (0.0093 m^2) break in the recirculation line on the suction side of the recirculation pump were analyzed at four points on the power/flow map. In performing these calculations, [[

Table 8.1-6. [[

]] The results are shown in

]]

Core Average Exposure

From the standpoint of the limiting conditions for a LOCA, the core average exposure determines the core average gap conductance, which is directly related to stored fuel energy, and decay heat. [[

]]

Pellet Exposure

The peak pellet power (PLHGR) is constrained as a function of pellet exposure by the thermal mechanical design envelope. [[

]] (Section 6.2.5).

Sensitivity studies were performed by [[

]]

Radial Power Distribution

The radial peaking between the bundles in [[
]] Table 8.1-7 shows the cases studied. For each case, [[

]]

The results of the LOCA calculations, [[

]]

Steam Dome Pressure

Steam dome pressure [[

]]

Feedwater Temperature

Feedwater temperature [[

]]

Initial Downcomer Level

The initial downcomer level [[

]]

Table 8.1-8 summarizes the results of the studies to characterize the plant initial conditions and operating ranges.

Table 8.1-5 BWR/4 Sensitivity to Location of Axial Peak

Case	Small Break Δ PCT (K)	Limiting Break Δ PCT (K)	DBA Δ PCT (K)
[[
]]

Table 8.1-8 Allowable Operating Range Categorization for BWR/4 LOCA

Quantity	Category	Analysis Basis
Total Core Power	The results are sensitive to the initial conditions and a basis for the limiting initial condition can be established.	[[]]
Total Core Flow		
Feedwater Temperature	[[
Steam Dome Pressure		
Downcomer Water Level		
Core Loading Pattern and Total Core Exposure		
Axial Power Distribution		
Radial Power Distribution		
Pellet Exposure]]

[[

]]

Figure 8.1-10 Rod Axial Peaking Variations

[[

]]

Figure 8.1-11 Channel Average Axial Peaking Variations

8.1.4.3 Initial Conditions Uncertainty

As described in Section 6.2, the initial state of the plant is monitored through the use of plant sensors or on-line calculations based on plant sensors. Because of instrument or simulation uncertainty, the actual plant conditions may vary somewhat from the measured/calculated values. The results may be characterized in the following manner:

- A. The results are sensitive to the uncertainty in the initial condition and the uncertainty in the initial condition will be included in the statistical analysis.
- B. The results are not sensitive to the uncertainty in the initial condition and the uncertainty does not need to be taken into account.

The uncertainties in the initial conditions were evaluated and characterized for each baseline event. The characterization analysis bases are described in Table 8.1-9.

**Table 8.1-9 Bases for Initial Conditions Uncertainty Characterizations for BWR/4
 LOCA**

Quantity	Uncertainty Basis	Analysis Basis
Total Core Power	In demonstration calculations, a 2% uncertainty is assumed.	[[
Total Core Flow	Total $\sigma = 2.5\%$ per Reference [32]	
Feedwater Temperature	Total [[]] per Reference [32]	
Steam Dome Pressure	Total [[]] per Reference [32]	
Downcomer Narrow Range Water Level	Total [[]] of a 2 meter instrument range (typical).	
Bundle Power	Total [[]] per Reference [32]	
Nodal Power	[[]] per Reference [32]]]

8.1.4.4 Initial Condition Uncertainty Results

With the exception of MCPR and PLHGR, the results from the allowable operating range evaluations, documented in Section 8.1.4.2, [[

]] The
 characterization of these results is presented in Table 8.1-11.

Table 8.1-10 BWR/4 LOCA MCPR and PLHGR Initial Condition Uncertainty Results

Case	Δ PCT (K)	
	DBA	Small Break
[[
]]

**Table 8.1-11 Results of Initial Condition Uncertainty Characterizations for BWR/4
 LOCA**

Quantity	Characterization	Characterization/Analysis Basis
Total Core Power	[[
Total Core Flow		
Feedwater Temperature		
Steam Dome Pressure		
Downcomer Water Level		
[[
]]]]

8.1.4.5 Plant Parameters

As described in Section 6.3, critical plant parameters will be [[]]

This process is described in the procedure that defines the critical Operating Parameters for Licensing (OPL) for ECCS/LOCA analysis. It does not preclude the future use of statistically based plant parameters or setpoints, which would require the determination of nominal values, accounting of instrument drift and uncertainties and incorporation of these uncertainties into the application methodology.

Section 6.3.2 describes a study to determine the effect of scram speed on LOCA response. [[]]

]] (Section 6.3.1).

Drywell pressure and ECC temperature (i.e., suppression pool temperature) are treated as plant parameters or boundary conditions for ECCS/LOCA analysis because they involve interactions with the containment. It was shown in Section 5.1 that [[]]

]] The results

(Table 8.1-12) show that [[]]

]]

Table 8.1-12 BWR/4 Sensitivity to Containment Boundary Conditions

Parameter	Value	Δ PCT (K) DBA
[[]]		
]]

8.1.4.6 Summary of Initial Conditions and Plant Parameters

The following conclusions, based on the initial condition and plant parameter sensitivity analysis results, form the basis of the plant-specific analysis process.

- [[

]]

8.1.5 Break Spectrum Results for BWR/4

A recirculation line break spectrum analysis, consisting of a set of LOCA calculations for a range of break sizes up to and including the double-ended guillotine break (DBA), was performed for a BWR/4. Additional analyses were performed for double-ended breaks in a main steam line, Feedwater line, LPCS line and LPCI line. [[

]] The key transient parameters (Table 8.1-2) corresponded to the characterization basis discussed in Section 8.1.4.1. The model parameters were set to their nominal values (PIRT multipliers at 1.0) except [[

]]

Loss of offsite power, causing a trip of the recirculation pumps, was assumed at time zero. The scram time is obtained from the earlier of the High Drywell Pressure or L3 downcomer level signals as discussed in Section 6.3.1. MSIV closure was initiated on L1.

Figure 8.1-12 shows a schematic of the ECCS configuration for the BWR/4 plant. Two single-failure cases were considered: failure of the DC power source (battery); and failure to open of one of the two LPCI injection valves. The failed and available systems for each of these cases are shown in Table 8.1-13. Experience has shown that the battery failure is the most limiting single failure because it results in the loss of the larger number of ECC systems. The plant parameters (e.g., setpoints, ECC flow capacity) were set at their analytic limits. [[

]]

8.1.5.1 Recirculation Line Breaks on Suction Side of the Recirculation Pump

The scram time following a recirculation line break on the suction side of the recirculation pump is shown in Figure 8.1-13 as a function of break size. For break sizes larger than approximately 0.02 m^2 , the High Drywell Pressure signal occurs before the downcomer narrow range level drops to Level 3. For breaks smaller than 0.02 m^2 , the scram is caused by the Level 3 trip. Figure 8.1-14 through Figure 8.1-21 show the plant transient response for different break sizes in the suction side of the recirculation line ranging from 0.002 m^2 to a double-ended guillotine break (0.32 m^2 on each side). As stated above, battery failure is assumed for these analyses. All breaks smaller than the DBA are modeled as split breaks and, as with the DBA, flow from both sides of the break contributes to the total break flow.

Figure 8.1-14 shows the reactor vessel pressure response for small breaks ranging from 0.002 to 0.009 m^2 . Following the MSIV closure on Level 1, the pressure increases for these breaks until the ADS valves open. The ADS actuation is also on Level 1 with a timer delay of 120 s. Figure 8.1-15 shows the PCT response for the small breaks. For the smallest break, there is no heatup in the core until the flashing associated with ADS actuation subsides. As the break size increases, an earlier heatup is seen as the core inventory begins to deplete before the start of the depressurization. This early heatup is quenched by core flow induced by lower plenum flashing. A second period of cladding heatup begins after the ADS depressurization rate subsides. This later heatup determines the PCT for the transient.

Figure 8.1-16 shows the reactor vessel pressure response for intermediate breaks ranging in area from 0.019 to 0.037 m^2 . The 0.009 m^2 small break from Figure 8.1-14 is shown for reference. For the intermediate break sizes, the pressure remains close to the initial pressure following MSIV closure. The downcomer level drops to the elevation of the recirculation line suction before the ADS valves open. The uncovering of the recirculation line suction leads to vapor discharge from the reactor vessel and an increased depressurization rate. The depressurization rate increases further when the ADS valves open but ADS actuation is of lesser importance for the intermediate breaks (as compared with the small breaks) because of the early depressurization by the break flow. Figure 8.1-17 shows the PCT response for the intermediate size breaks. For break sizes of 0.019 and 0.028 m^2 , the PCT is similar to that for the 0.009 m^2 break. For the 0.019 m^2 break, the earlier depressurization reduces the core inventory loss prior to ADS actuation and the earlier actuation of the LPCS lowers the PCT after the ADS flow subsides. The early temperature rise is greater for the 0.028 m^2 break than for the 0.009 m^2 break but the PCT, which occurs after the ADS flow subsides, is lowered by the earlier actuation of the LPCS. As the break size increases to 0.037 m^2 , a more severe PCT scenario emerges. The early heatup from inventory depletion occurs sooner and is not quenched by lower plenum flashing. The heatup continues through the end of ADS flow up to the point where the LPCS is able to turn the temperature over. As seen in Figure 8.1-17 and in the following discussion, this effect gets progressively more severe with increasing break size up to 0.062 m^2 .

Figure 8.1-18 shows the pressure response for three intermediate to large breaks in the range 0.062 to 0.186 m^2 . The 0.037 m^2 break from the intermediate break set is shown for reference.

In this range of break sizes, the effect of the ADS continues to diminish and vessel depressurization is controlled by the loss of fluid through the break. Figure 8.1-19 shows the corresponding PCT responses. As stated above, the 0.062 m² break led to the highest PCT (1,038 K). As the break size increases further, the effect of earlier activation of the LPCS strengthens and the peak temperatures are reduced.

Figure 8.1-20 shows the pressure responses for the large break end of the break spectrum, ranging from 0.186 m² to the DBA. The reactor vessel depressurizes rapidly with no need for ADS actuation to supplement the blowdown. Figure 8.1-21 shows the PCT responses. For the large breaks, the large loss of inventory and early core heatup dominates the temperature rise. The effect of earlier activation of the LPCS is not sufficient to offset the early heatup and, consequently, the PCT increases with break size in this range. For the large breaks, a “first-peak” PCT occurs in the first few seconds of the transient because of the early mismatch between the power and the core flow. This first-peak PCT is not limiting and is quenched by the lower plenum flashing that follows the uncovering of the recirculation line suction.

The interplay between the timing of the depressurization, heatup, ADS actuation and ECCS actuation is displayed in Figure 8.1-22. It is seen that for break sizes smaller than approximately 0.025 m², the heatup leading to the PCT starts after the ADS flow subsides. For larger break sizes, an earlier dryout from inventory depletion becomes dominant. Figure 8.1-22 also shows the important relationship between the start of heatup and the activation of LPCS. The break spectrum results for the BWR/4 recirculation line suction break are summarized in Figure 8.1-23

]] Intermediate break sizes near 0.062 m² lead to the highest PCTs. At these break sizes, the early heatup is not terminated by the ADS induced flashing and is made more severe by further loss of inventory from the core as the flashing subsides. It is noted that the PCTs for the break size of 0.0557 m² (or 0.60 ft²) in Figure 8.1-23 show a temperature reduction of approximately 100 K, compared to the PCTs for 0.0567 m² size break. Further investigation of the flow conditions in the limiting channels was performed for this break size and its neighbors and the limiting break (0.062 m²). It was found that higher void fraction, gas and liquid phase velocities were observed at the bottom of the limiting channel for 0.0557 m² break than those for the limiting break. The liquid and gas are found to be nearly “stagnant” for the limiting size break. The channel seems to be “plugged” with water at its bottom, which reduces the channel cooling, resulting in channel early heatup, and finally higher PCT. On the contrary, the cooling provided by the two-phase flow inside the channel at the break size of 0.0557 m² postpones the channel heatup, resulting in the lower PCT.

8.1.5.2 Breaks on the Discharge Side of the Recirculation Pump

Two break spectrum analyses, similar to that described above for the recirculation line suction break, were performed for a range of break sizes on the discharge side of the recirculation piping. The first analysis postulated a battery failure and the second analysis postulated the failure of an LPCI injection valve (LPCIIV) to open. A significant feature of the discharge breaks is that

some part of the LPCI flow injecting into the broken loop is lost through the break. The fraction of LPCI flow lost depends on the break size. The pressure and PCT transients for the battery failure case are similar to those for breaks on the suction side. The break spectrum results (PCT vs. break area) are summarized in Figure 8.1-24. [[

]] The highest PCT (1027 K) corresponded to a break size of 0.062 m² and is slightly lower than the PCT for the limiting break on the suction side.

The recirculation line discharge break spectrum was also analyzed with the failure of one LPCI injection valve (LPCIIV) to open. The ECC systems available for this scenario include HPCI and two LPCS. Two LPCI pumps will be available but could discharge to the broken recirculation loop with a significant loss of ECCS flow through the break. Cases with the LPCI discharging into the intact and broken loops were analyzed. The PCT was not affected by the LPCI injection location because the temperature was turned over by the two LPCS discharging into the upper plenum. Figure 8.1-25 shows the break spectrum (PCT vs. break size) calculated with the LPCI discharging to the broken loop. The temperature rise is lower for the LPCIIV failure than for the battery failure case. [[

]] The highest PCT (937 K) corresponded to a break area of 0.062 m².

8.1.5.3 Non-Recirculation Line Breaks

Non-recirculation line breaks are not expected to be limiting compared to recirculation line breaks, either because they would be bounded by recirculation line breaks or because they would turn into high energy, low inventory loss breaks shortly after the onset of the transient due to their higher break elevation relative to the top of the core. Breaks in other lines were analyzed to confirm this expectation. These non-recirculation line breaks included breaks of a main steam line, a feedwater line, an LPCS line and an LPCI line. For these cases, a battery failure was assumed as for the recirculation line breaks because it would result in least amount of ECCS components available.

Figure 8.1-26 shows the pressure responses for the four non-recirculation cases. The steam line break depressurizes the vessel very rapidly because it is a vapor break with correspondingly large volumetric and enthalpy outflows. The ADS is inconsequential for the steam line break. The feedwater line break in the vessel downcomer starts out as a liquid break but the break flow quickly changes to two-phase as the downcomer level drops to the feedwater line elevation. The two-phase level remains near the break elevation because of the interaction between break uncover, depressurization rate, level swell in the downcomer and break flow. These interactions result in a depressurization rate that is slower than for a large break in the recirculation or steam lines. The guillotine break of the LPCI line (0.2356 m²) is similar to a discharge side recirculation break of the same area. For the smaller LPCS break (0.0255 m²), the break flow is initially two-phase, and the vessel does not depressurize significantly for about 80 s following MSIV closure. At this time, the level in the upper plenum uncovers the LPCS sparger

and the break flow becomes essentially single phase vapor. The vapor flow begins to depressurize the vessel and the depressurization rate is subsequently increased by the opening of the ADS valves at about 170 s.

The PCT response for the non-recirculation line break cases is shown in Figure 8.1-27. For the steam line break, the peak cladding temperature does not exceed the initial operating temperatures as the level in the shroud swells up and prevents core uncover. The PCT does not exceed the initial operating cladding temperature. As stated above, the LPCI line break is equivalent to a discharge break of the same size because the LPCI line is connected to the discharge side of the recirculation piping. The PCT for the LPCI line break (861 K) is comparable to the PCT for a similar size discharge break in the recirculation line. The LPCS line break is located above the elevation of the core so its effect on core heatup is milder than a comparably sized recirculation line break. Core uncover is delayed to about 240 s and is limited to the top of the core. There was only a small temperature rise and the PCT for the transient was the initial cladding temperature.

Table 8.1-14 summarizes the BWR/4 PCTs obtained for the various cases discussed in this section. For breaks in the recirculation line, the maximum PCT and the corresponding break size have been tabulated. The results include those for battery and LPCIIV failures. Results for the non-limiting break locations are listed for breaks in the steam, feedwater, LPCI, and LPCS lines. This set of analyses, except the feedwater line break, was performed with an earlier code version and the results are not updated because the PCTs are low and results are not expected to change.

The feedwater line break is further studied to investigate the flashing effect of the heated inventory in the line on the system depressurization, thus on ECCS actuation and resulting PCT. For this study, the feedwater lines are modeled individually instead of being lumped together. To correctly capture the effects of flashing, the liquid inventories in the lines are included up to the first set of heaters. Figure 8.1-28 summarizes the feedwater break spectrum PCTs for the hot channels. Because the core uncover is from the top, no heatup is observed at the peak location for the bottom peaked rods. [[

]] This is mainly associated with the timing of break uncover for system venting and overall depressurization rate for ECCS actuation. This break is further studied in a statistical manner in the uncertainty analysis section.

Table 8.1-13 BWR/4 Single Failures and Available ECCS

Failure	ECC Systems Not Available	ECC Systems Available
Battery	HPCI, 1 LPCS, 2LPCI (1 in each recirculation line)	1 LPCS, 2 LPCI (1 in each recirculation line), 7 ADS valves
LPCI Injection Valve	2 LPCI in one recirculation line	HPCI, 2LPCS, 2LPCI (in one recirculation line), 7 ADS valves

Table 8.1-14 BWR/4 PCT Summary

Break Location	Single Failure	ECCS Available¹	Break Area (m²)	PCT (K)
Recirculation Line Suction	Battery	1CS, 2LPCI (1+1) ²	0.0620	1,038
Recirculation Line Discharge	Battery	1CS, 2LPCI (1+1)	0.0620	[[
Recirculation Line Discharge	LPCI Injection Valve ³	2CS, 2LPCI HPCI	0.0620	
Steamline ⁴	Battery	1CS, 2LPCI (1+1)	0.2356	
LPCI Line ⁴	Battery	1CS, 1LPCI	0.2356	
LPCS Line ⁴	Battery	2LPCI (1+1)	0.0255	
Feedwater line	Battery	1CS, 2LPCI (1+1)	0.0659	
Feedwater line ⁵	Battery	1CS, 2LPCI (1+1)	0.0325]]

Notes:

- ¹ All cases include 7 ADS valves.
- ² (1+1) : one in each recirculation line.
- ³ Same PCT for LPCI injection into the broken loop or into the intact loop.
- ⁴ These cases were performed with an earlier version of the code and were not repeated because the results are not close to become limiting.
- ⁵ Case from additional modeling detail to characterize the FWLB spectrum.

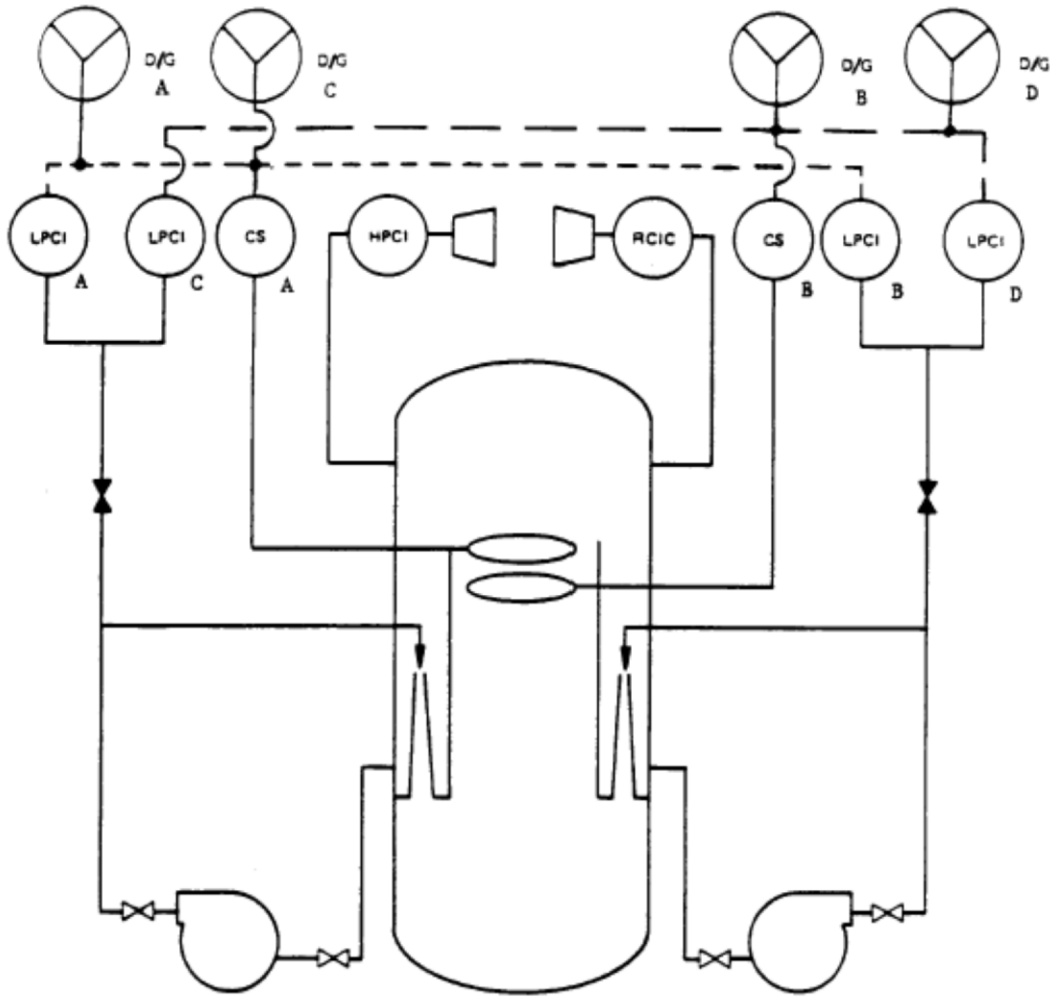


Figure 8.1-12 BWR/4 ECCS Configuration

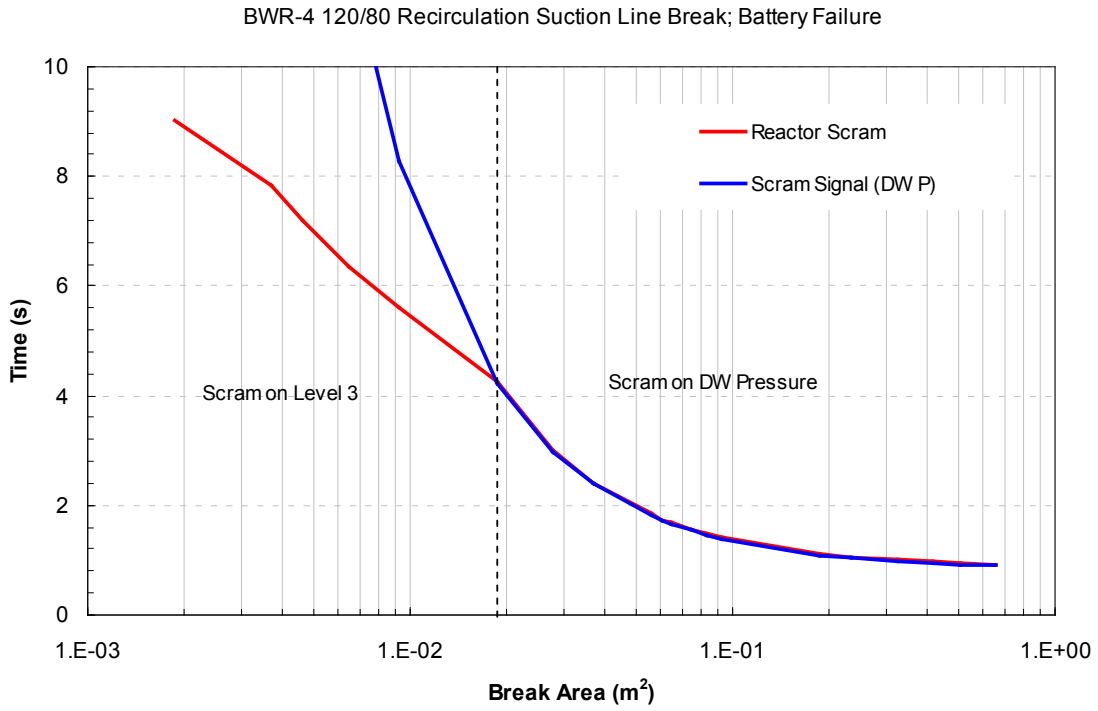


Figure 8.1-13 Scram Time vs. Break Size for BWR/4 Suction Breaks

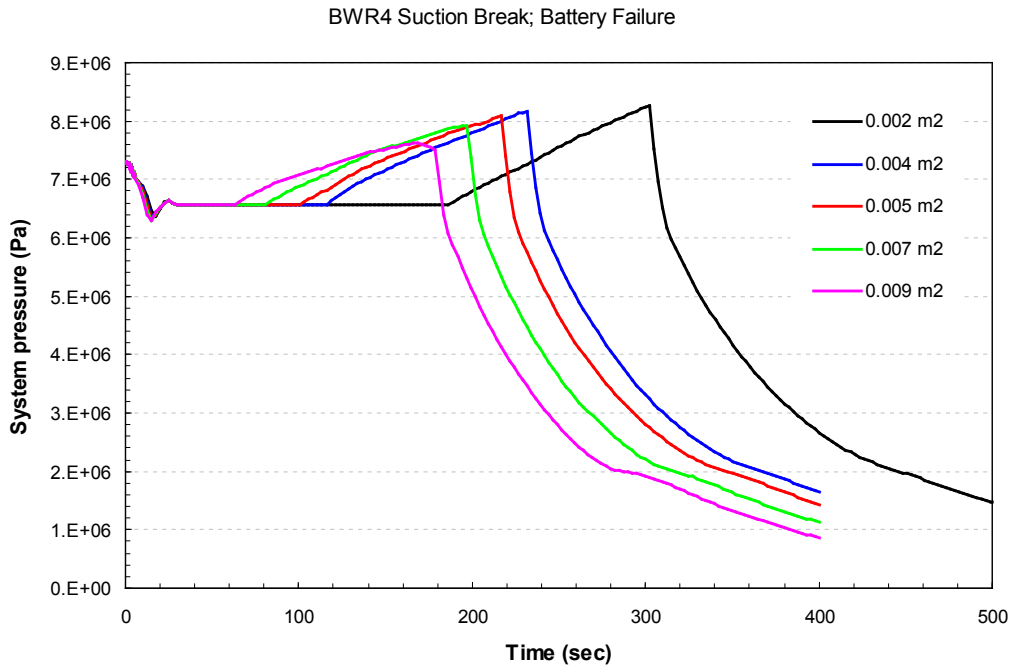


Figure 8.1-14 Pressure Response for BWR/4 Small Breaks

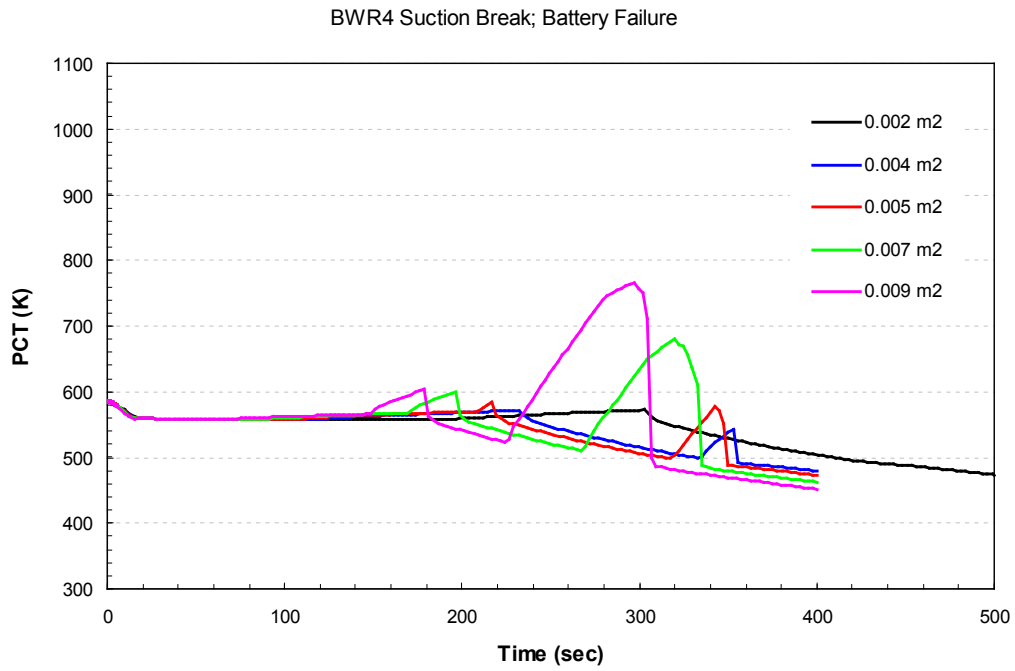


Figure 8.1-15 PCT Response for BWR/4 Small Breaks

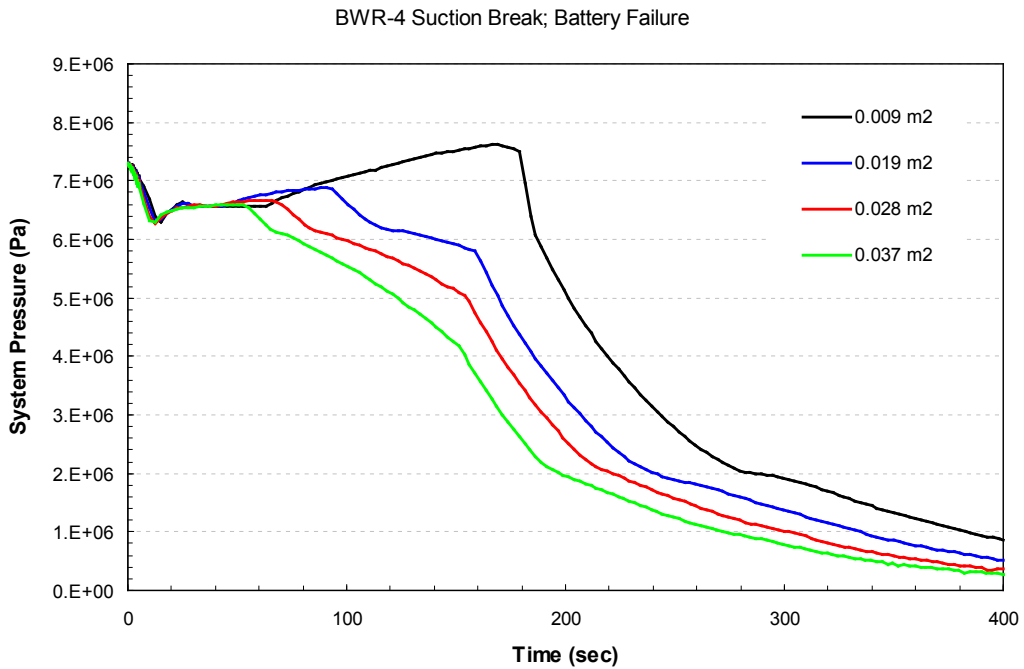


Figure 8.1-16 Pressure Response for BWR/4 Intermediate Breaks

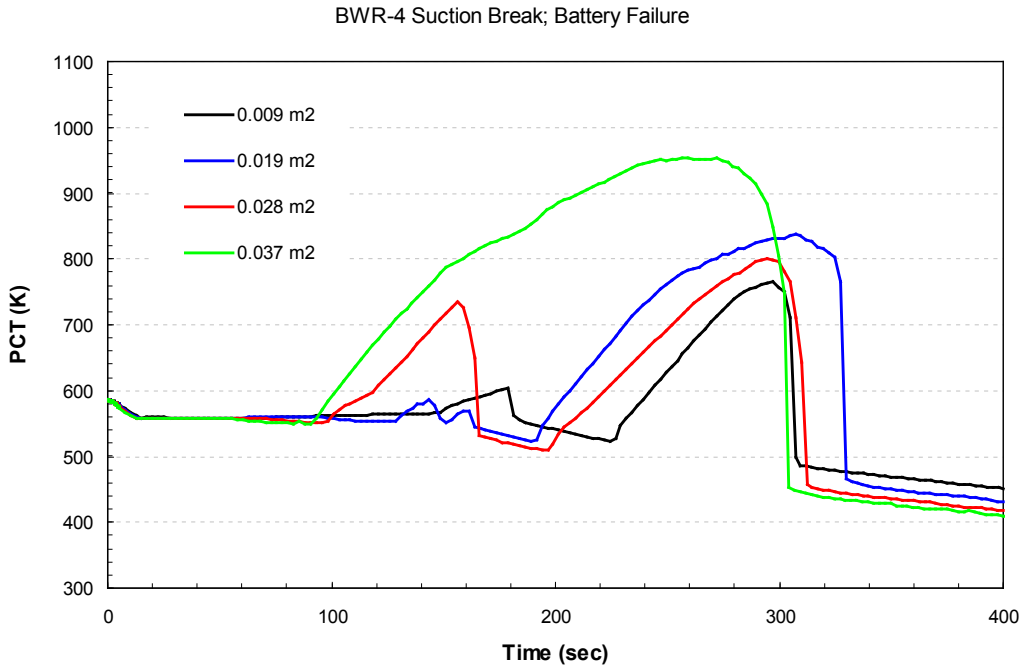


Figure 8.1-17 PCT Response for BWR/4 Intermediate Breaks

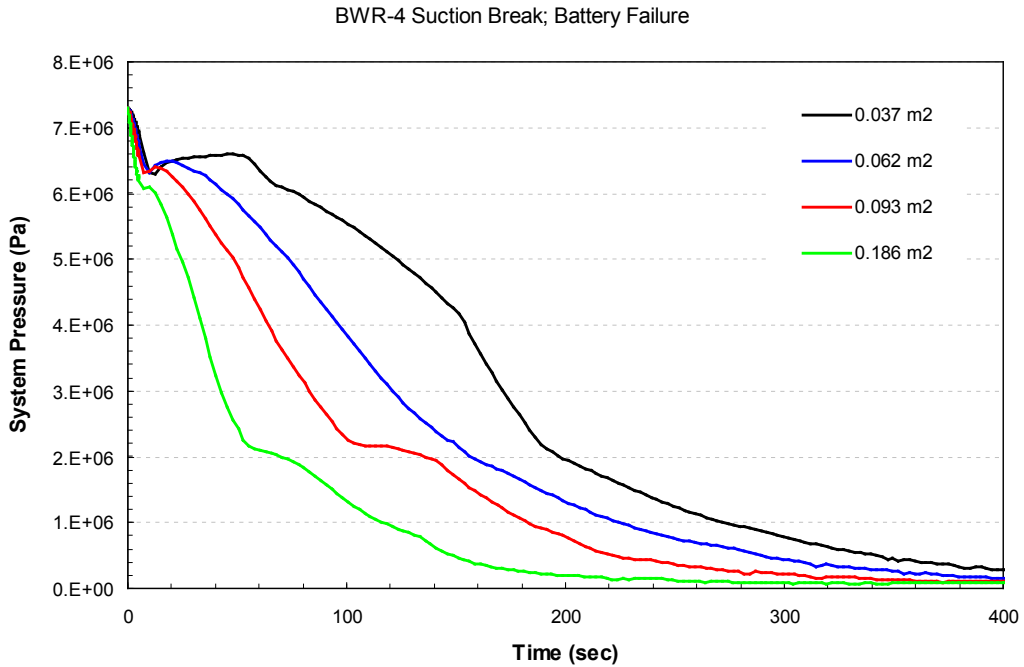


Figure 8.1-18 Pressure Response for BWR/4 Intermediate to Large Breaks

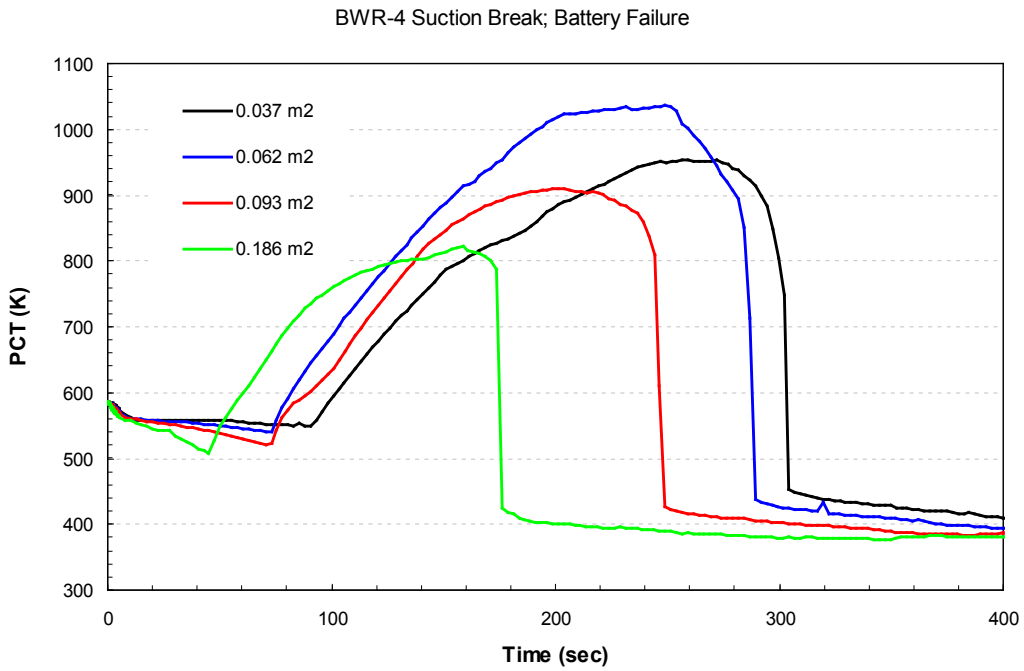


Figure 8.1-19 PCT Response for BWR/4 Intermediate to Large Breaks

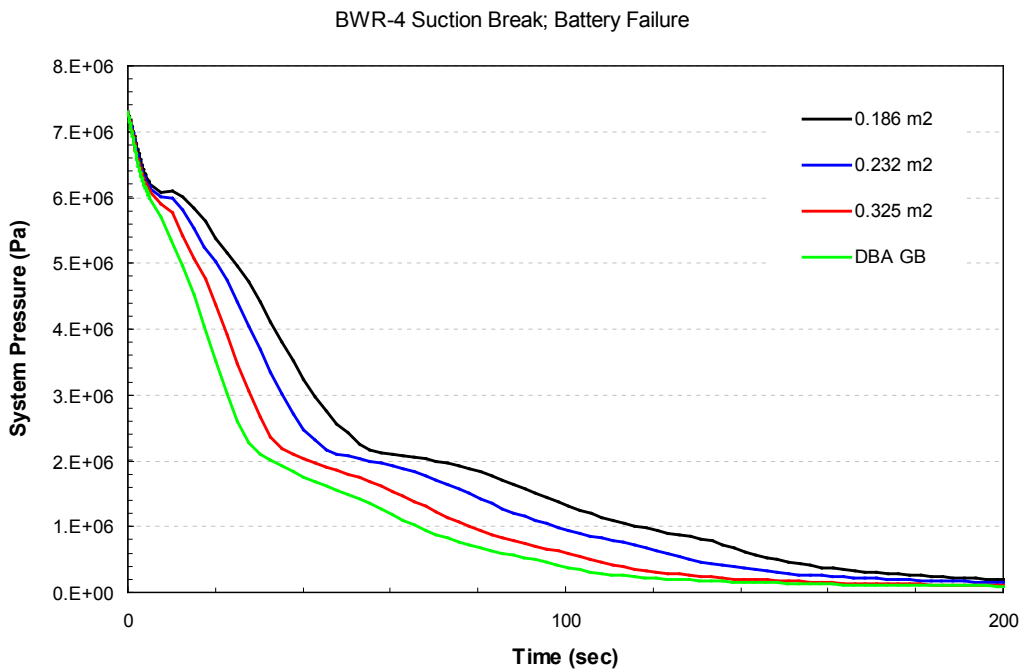


Figure 8.1-20 Pressure Response for BWR/4 Large Breaks

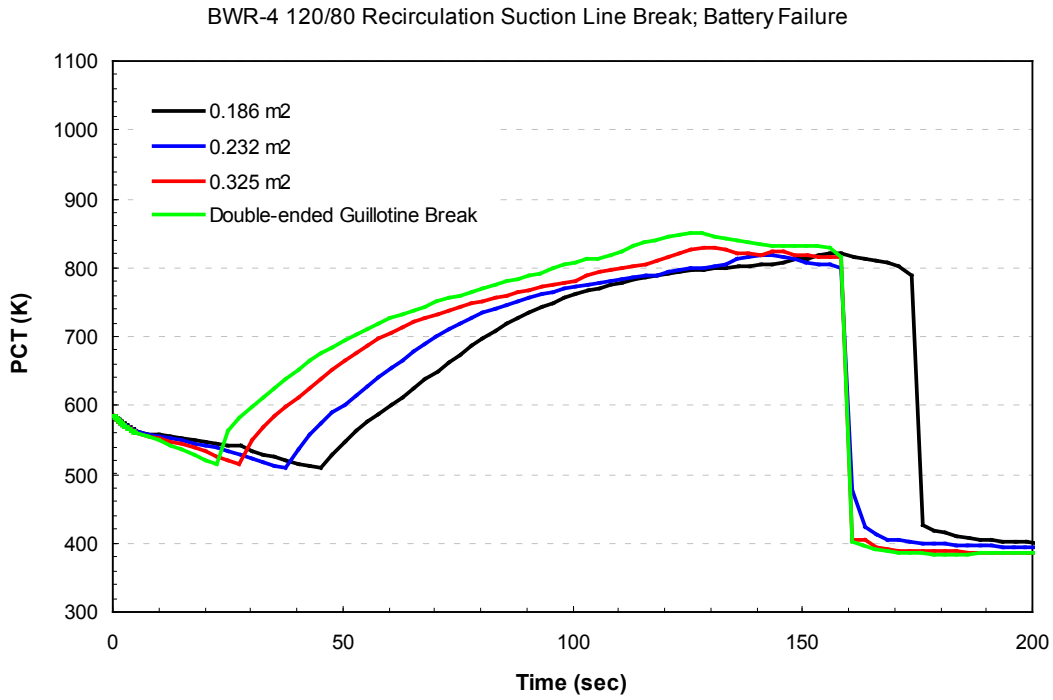


Figure 8.1-21 PCT Response for BWR/4 Large Breaks

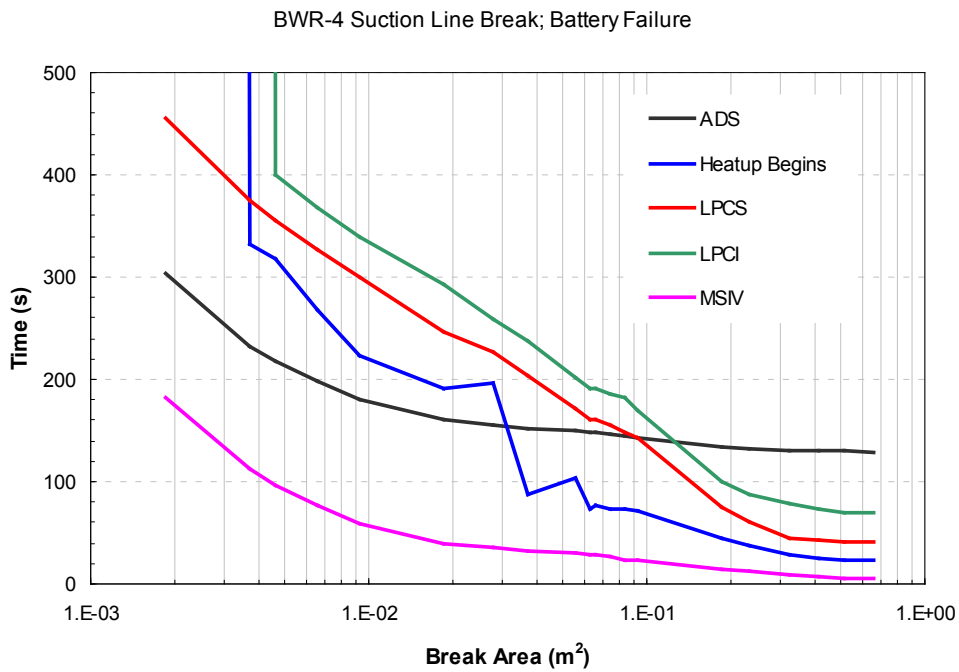


Figure 8.1-22 Start of BWR/4 Heatup Relative to ADS and ECCS Activation

[[

]]

Figure 8.1-23 BWR/4 Break Spectrum for Recirculation Line Suction Breaks with Battery Failure

[[

]]

Figure 8.1-24 BWR/4 Break Spectrum for Recirculation Line Discharge Breaks with Battery Failure

[[

]]

Figure 8.1-25 BWR/4 Break Spectrum for Recirculation Line Discharge Breaks with LPCI Injection Valve Failure

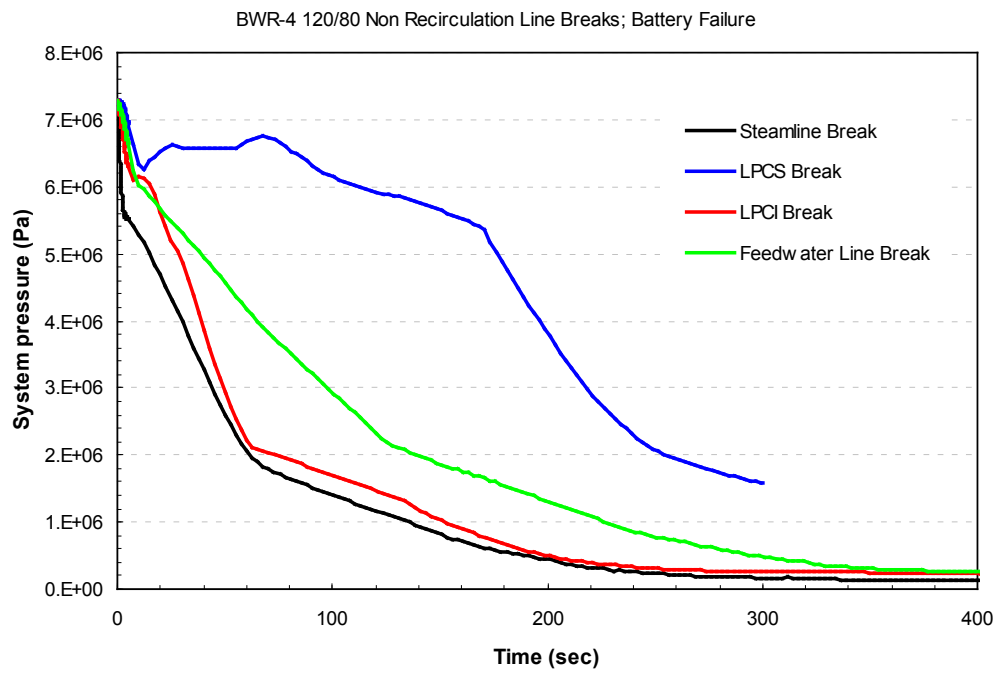


Figure 8.1-26 Pressure Response for BWR/4 Non-Recirculation Line Breaks

[[

]]

Figure 8.1-27 PCT Response for BWR/4 Non-Recirculation Line Breaks

[[

]]

Figure 8.1-28 BWR/4 Feedwater Line Break Spectrum for Hot Channels

8.1.6 Statistical Results for BWR/4 LOCA

The results of the uncertainty analysis for a BWR/4 LOCA are shown in this section. A statistical analysis for a number of breaks varying from 0.05 ft² (0.00465 m²) to double-ended guillotine break (0.65961 m²) is carried out by performing a set of 59 trials for each break size. The plant initial conditions were chosen on the basis of the discussion in Section 8.1 and are shown in Table 8.1-15. In each trial, random draws were made from the probability density functions for the set of previously identified model and plant parameters (Table 5.1-2 and Table 8.1-16). The PCT results from these runs are summarized in Table 8.1-17. Figure 8.1-29 provides a summary of the PCT results for nominal, trial minimum, maximum, and average with 2σ bands. In the nominal calculations, all the random variables used in statistical analysis are set to their most probable values, whereas, in the break spectrum calculations, no PIRT variables are applied. Therefore, the PCT results are slightly different between the two sets of calculations. The break spectrum calculation is a screening tool used for determining the vicinity of the limiting break and the PCTs from these runs do not directly enter to the downstream runs. In Section 8.1.5, the limiting break for a BWR/4 LOCA was identified as a recirculation line suction break of 0.67 ft² (0.0622 m²), which is presented as a demonstration case below, in Section 8.1.6.2. However, the highest PCT from the runs is obtained from 0.75 ft² (0.0697 m²) case. For the intermediate break size LOCA statistical runs, the PCT distribution does not appear to be Gaussian. Therefore, the PCT from this statistical analysis is 1076 K. The differences are within the statistical uncertainty because the PCT distributions in the vicinity of the limiting break size do overlap and the limiting PCT results are close to each other. For all the cases, the maximum local oxidation in terms of Equivalent Cladding Reacted (ECR) is less than 1%, resulting in insignificant amount of core-wide oxidation, hence hydrogen generation.

8.1.6.1 DBA/Large-Break LOCA Results

The results of the statistical analysis for the BWR/4 suction DBA are presented in Figure 8.1-30 through Figure 8.1-32. Figure 8.1-30 shows the range and the average of the DBA PCT transient over the 59 trials along with the result of the nominal calculation in which all the random variables are set to their most probable values. Figure 8.1-31 shows the distribution of PCTs. The corresponding individual deviations from the mean for each trial are shown in Figure 8.1-32. The mean and standard deviation values of the overall PCT for the 59 trials were 847.1 K and 35.47 K, respectively. The distribution of overall PCTs for the DBA satisfies the condition for normality. Based on a normal distribution of sample size 59, the 95th percentile with high probability value of PCT is estimated as:

$$\text{PCT}_{95/95} = \text{PCT}_{\text{Mean}} + 2.024 * \text{Std Deviation} = 919 \text{ K}$$

8.1.6.2 Intermediate Break LOCA Results

Figure 8.1-33 through Figure 8.1-35 show the results of the Monte Carlo analysis for the intermediate break in the recirculation line suction. The range and the average of the intermediate break PCT transient over the 59 trials are shown in Figure 8.1-33 along with the nominal result in which all the random variables are set to their most probable values. Figure

8.1-34 shows the distribution of the highest PCT. The corresponding individual deviations from the mean are shown in Figure 8.1-35. The mean PCT is 978.7 K with a standard deviation of 46.0 K. The p-value for the distribution of overall PCTs for the intermediate break does not meet the requirement for normality with 95% confidence. Therefore, the 95th percentile with high probability value of PCT for this case is based on the maximum of the trials and is estimated as 1060 K.

8.1.6.3 Small-Break LOCA Results

Figure 8.1-36 through Figure 8.1-38 show the results of the Monte Carlo analysis for the intermediate break in the recirculation line suction. The range and the average of the intermediate break PCT transient over the 59 trials are shown in Figure 8.1-36 along with the nominal result in which all the random variables are set to their most probable values. Figure 8.1-37 shows the distribution of the highest PCT. The corresponding individual deviations from the mean are shown in Figure 8.1-38. The mean and standard deviation values of the overall PCT for the 59 trials were 764.1 K and 44.8 K, respectively. The distribution of overall PCTs for the DBA satisfies the condition for normality. Based on a normal distribution of sample size 59, the 95th percentile with high probability value of PCT is estimated as:

$$PCT_{95/95} = PCT_{\text{Mean}} + 2.024 * \text{Std Deviation} = 855 \text{ K}$$

8.1.6.4 Feedwater Line Break LOCA Results

A statistical analysis over the feedwater line break spectrum was carried out by performing a set of 59 trials for different break sizes. As in the recirculation line break statistical analysis, the plant initial conditions were chosen on the basis of the discussion in Section 8.1 and are shown in Table 8.1-15. In each trial, random draws were made from the probability density functions for the set of previously identified model and plant parameters (Table 5.1-2 and Table 8.1-16). Figure 8.1-39 provides a summary of the PCT results from nominal, trial minimum, maximum, and average with 2σ bands. The limiting FWLB is a 0.35 ft² (0.0325 m²) break. Figure 8.1-40 shows the range and the average of the PCT transient over the 59 trials along with the nominal result for this break size. The maximum PCT from the statistical runs is 999.4 K. The mean and standard deviation values of the overall PCT for the 59 trials were 811.5 K and 79.8 K, respectively. Based on a normal distribution of sample size 59, the 95th percentile with high probability value of PCT is estimated as 973 K. This PCT is lower than the limiting recirculation line break results. Therefore, it is concluded that, for this demonstration, the feedwater line break is not limiting.

Table 8.1-15 Plant Initial Conditions for BWR/4 Monte Carlo Analysis

Parameter	Reference Value
Core Power/ Flow	120/80
Steam dome pressure	7.29 MPa
FW temperature	495 K
DC Level	14.07 m
[[
]]

Table 8.1-16 Plant Parameters varied in BWR/4 Monte Carlo Trials

Parameter	Gaussian Distribution as Analyzed		Region	Comment
	Mean	Standard Deviation		
Core Power	1.0	2%	Core	Parameter is the multiplier on the thermal power.
Core Flow	1.0	2.5%	Core	Parameter is the multiplier on the rated flow.
[[
]]

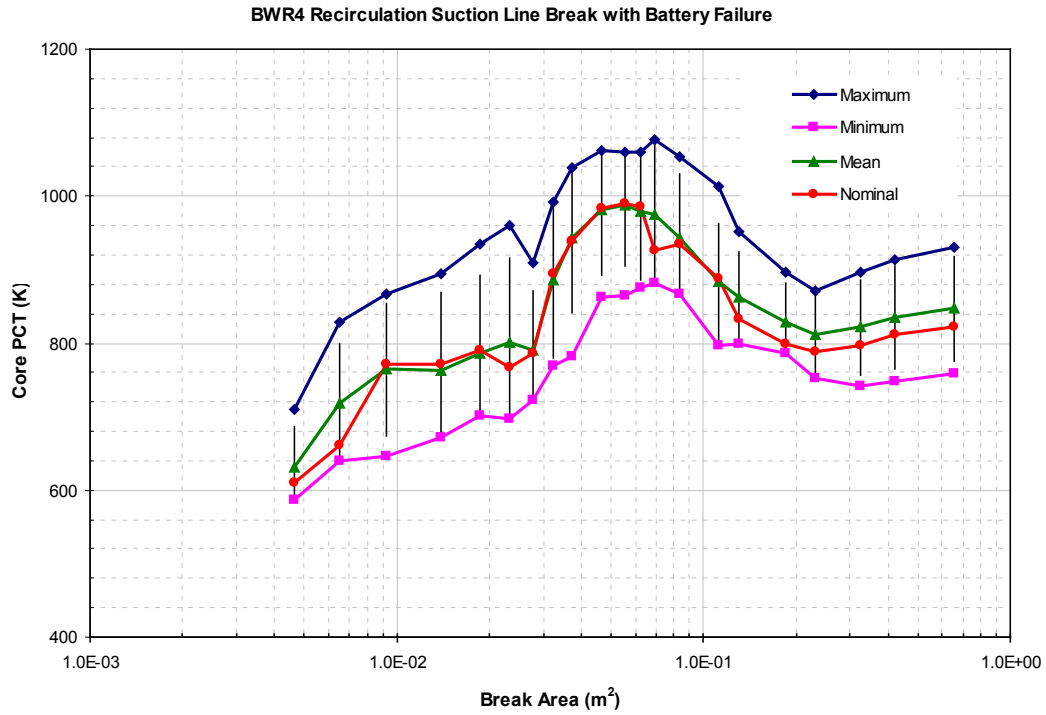


Figure 8.1-29 Summary of BWR/4 Statistical Analyses at Various Break Sizes

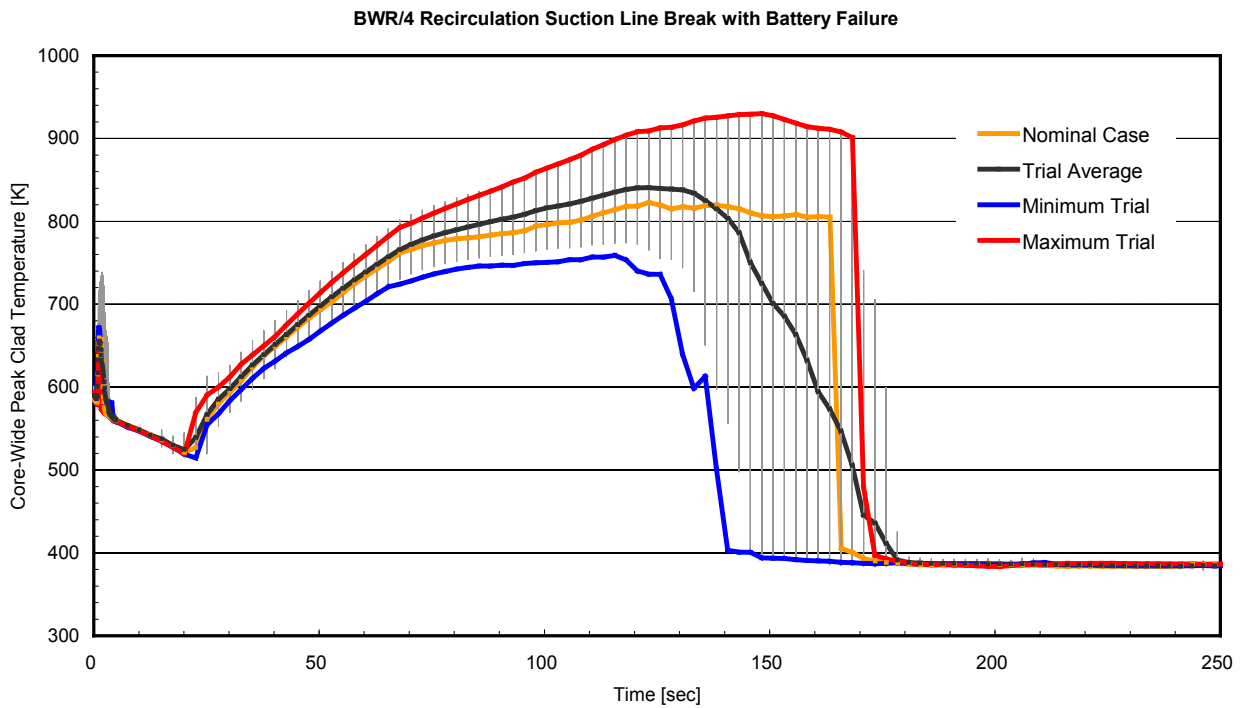


Figure 8.1-30 Range of Trials for PCT Transient for BWR/4 DBA

[[

]]

Figure 8.1-31 Overall PCT Distribution for BWR/4 Suction DBA

[[

]]

Figure 8.1-32 Overall PCT Trials for BWR/4 Suction DBA

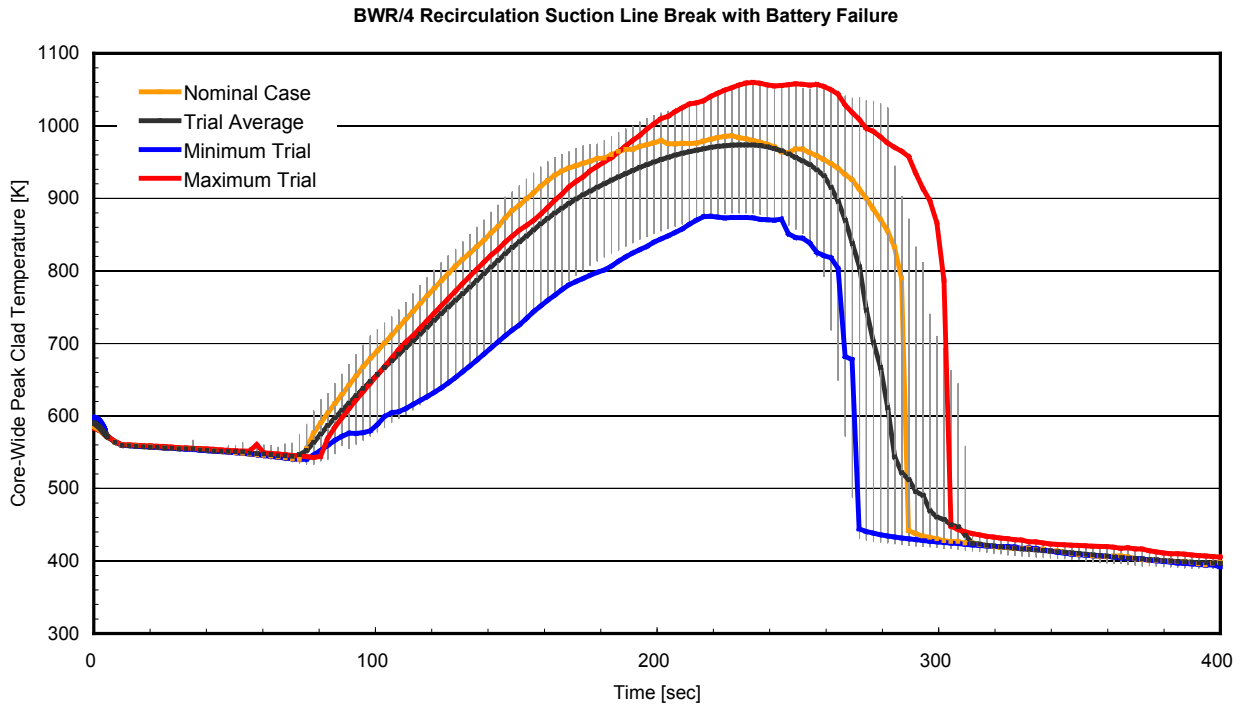


Figure 8.1-33 Range of Trials for PCT Transient for BWR/4 Intermediate Break

[[

]]

Figure 8.1-34 Overall PCT Distribution for BWR/4 Intermediate Break

[[

]]

Figure 8.1-35 Overall PCT Trials for BWR/4 Intermediate Break

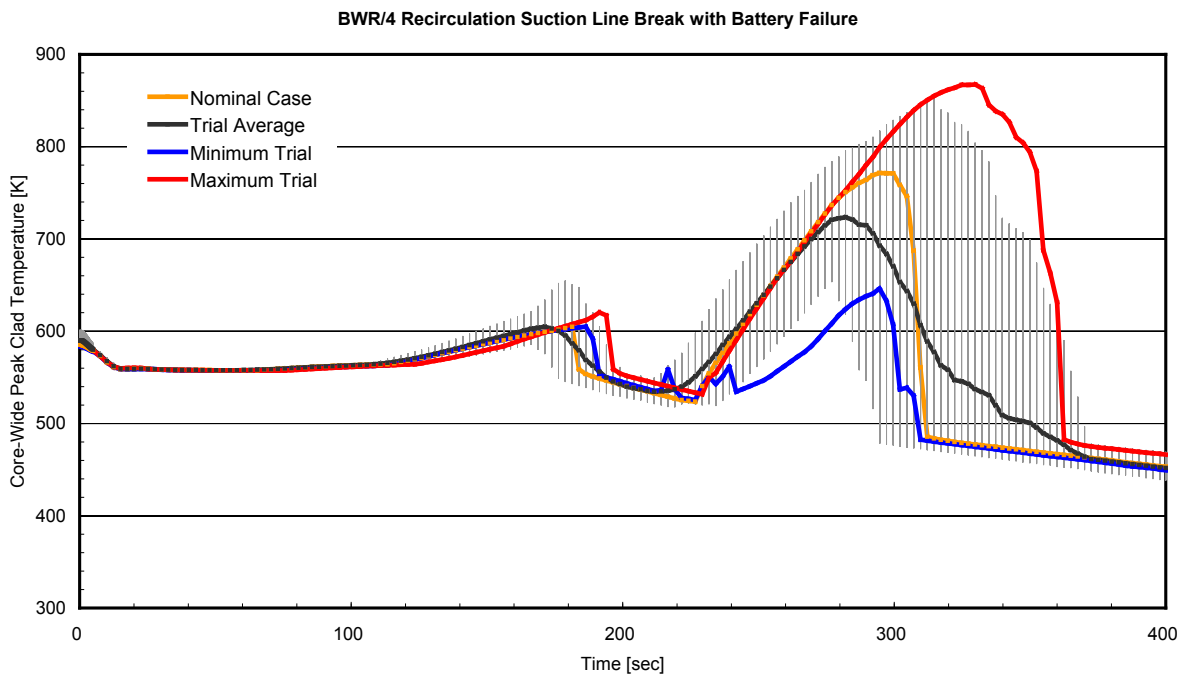


Figure 8.1-36 Range of Trials for PCT Transient for BWR/4 Small Break

[[

]]

Figure 8.1-37 Overall PCT Distribution for BWR/4 Small Break

[[

]]

Figure 8.1-38 Overall PCT Trials for BWR/4 Small Break

[[

]]

Figure 8.1-39 BWR/4 Feedwater Line Break Statistical Analysis Results

[[

]]

Figure 8.1-40 Range of Trials for PCT Transient for BWR/4 Limiting Feedwater Line Break

8.2 TRACG LOCA ANALYSIS RESULTS AND SENSITIVITY STUDIES FOR A TYPICAL BWR/6 PLANT

A baseline LOCA analysis was performed for a typical BWR/6 plant. The sections below discuss the representative TRACG nodalization and analysis procedure for a BWR/6 plant and the results for large and small breaks. Individual sensitivities to the model parameters were not examined for the BWR/6 plant. These sensitivities are expected to be similar to those for the BWR/4 plant from the standpoint of identifying the important parameters and, in any case, all the high and medium ranked phenomena will be accounted for in the BWR/6 Monte Carlo analysis. Plant parameters were set at their analytic limits for the BWR/6 analysis. Results for a complete BWR/6 break spectrum analysis are also presented.

8.2.1 TRACG Nodalization for ECCS/LOCA Calculations for a BWR/6 Plant

The representative BWR/6 type plant has 748 bundles and an Original Licensed Thermal Power (OLTP) of 3,579 MWth. The vessel modeling is illustrated in Figure 8.2-1. The plant is loaded with fresh and exposed GE14 10x10 fuel. Figure 8.2-2 illustrates the modeling of the steam lines and feedwater lines. The core spray and LPCI flows are modeled by FILL components with a prescribed flow rate vs. pressure. The recirculation lines are modeled (Figure 8.2-3) to allow for the simulation of pipe breaks on the suction and discharge sides of the recirculation pumps. Also simulated are the bottom drain lines that are attached to the recirculation line piping. Double-ended and split breaks can be simulated with this configuration of the recirculation piping and BREK components. As shown in the figure, the BREKs are isolated from the piping in the steady state model. Breaks are initiated by opening communication with one or two BREK components depending on whether a split or double-ended break is being simulated.

Table 8.2-1 shows the channel grouping used for the BWR/6 LOCA calculations. There are [[

]]

[[

]]

Figure 8.2-1 TRACG Vessel Nodalization for Typical BWR/6 Model

[[

]]

Figure 8.2-2 TRACG Nodalization of Feedwater and Steam Lines for Typical BWR/6

[[

]]

Figure 8.2-3 TRACG Nodalization of Recirculation Lines for Typical BWR/6 Model

8.2.2 Nominal ECCS/LOCA Results for Large and Small Breaks for BWR/6

This section presents baseline results for a double-ended guillotine break (DBA) and a small break in the recirculation line piping on the discharge side of the pump.

8.2.2.1 Discharge DBA Results

Table 8.2-2 shows the initial conditions and the key transient parameters for the BWR/6 DBA LOCA analysis. The plant is operating at 120% OLTP and 80% of rated flow. A double-ended break of the recirculation line is postulated at time zero. The recirculation pumps trip on the assumed loss of offsite power, a reactor scram is initiated on high drywell pressure and MSIV closure is triggered when the downcomer level reaches Level 1 at 10 s. Because of the assumed failure of the HPCS Diesel Generator (D/G), the available ECCS consists of the LPCS, three LPCI and seven ADS valves (one ADS valve assumed to be out of service). Table 8.2-2 shows the time delays and pressure permissives for the ECC systems.

Figure 8.2-4 shows the system pressure and the ECC flows for the discharge DBA. The break flow depressurizes the RPV with the depressurization rate increasing after the inlet to the recirculation line suction is uncovered. The rapid depressurization causes the initially subcooled liquid in the lower plenum to flash. The ECC systems are activated as the pressure falls below their respective pressure permissives. The LPCS starts injecting coolant into the upper plenum at 118 s and the LPCI starts injecting into the top of the bypass region at 135 s.

Figure 8.2-5 shows the calculated peak temperatures in the high power CPR-limited and PLHGR-limited bundles. At the beginning of the transient, the hot bundles go through an early boiling transition caused by the power/flow mismatch, which is quickly terminated by reduction in power. The subsequent early temperature excursions around 20 seconds into the transient are rapidly quenched by lower plenum flashing. A sustained dryout and heatup in the core begins between 55 and 80 s, depending on the bundle in question, as the core inventory is depleted. The heatup is terminated shortly after the ECC systems begin to add water to the upper plenum and bypass regions. In the final stage, the core is quenched from below by refill from the lower plenum. The top-peaked CPR-limited bundles heat up earlier and sustain the highest PCTs. A PCT of 807 K was calculated at about 164 s into the event. The LHGR-limited bundle exhibited a smaller heatup because the effect of its bottom-peaked power profile more than compensates for its higher linear heat generation rate.

8.2.2.2 Small Break Results

Table 8.2-2 shows the initial conditions and the key transient parameters for a BWR/6 small break case. The plant is operating at 120% OLTP and 80% of rated flow. A 0.0093 m² (0.10 ft²) break in the pump discharge side of the recirculation line is postulated at time zero. The recirculation pumps trip on the assumed loss of offsite power, the reactor scrams at 8.5 s on Level 3 and MSIV closure is initiated when the downcomer level reaches Level 1 at 35 s. Because of the assumed HPCS D/G failure, the available ECCS consists of the LPCS, three

LPCI and seven ADS valves (1 ADS valve assumed out of service). Table 8.2-2 shows the time delays and pressure permissives for the ECC systems.

Figure 8.2-6 shows the system pressure response and the ECC flows for the BWR/6 small break. The RPV depressurizes initially from the break flow but closure of the MSIVs - when the downcomer wide-range level measurement reaches Level 1 - reverses the pressure because the energy lost through the break alone is less than the energy added by decay heat. Level 1 also triggers the opening of the ADS valves with an assumed delay of 120 s. The ADS valves open at approximately 155 s and depressurization of the reactor vessel resumes. The ECC systems are activated when the pressure falls below their respective pressure permissives. The LPCS starts injecting coolant into the upper plenum at 263 s and the LPCI into the core bypass region at 293 s.

Figure 8.2-7 shows the calculated peak temperatures in the high power bundles. The high power bundles do not go through an early boiling transition because the core flow does not drop as rapidly as for the DBA. Heatup occurs in the upper portion of the core at about 130 to 150 s into the accident as the core inventory drains. [[

]] The activation of the ADS results in flashing of the lower plenum liquid and a resulting surge of flow through the core that is sufficient to quench the high power bundles and terminate the heatup. A more sustained heatup occurs following the abatement of the ADS-induced flashing. This heatup is terminated by the activation of the LPCI system, which refills the core bypass region, refloods the core and quenches the high power bundles. [[

]]

Table 8.2-2 BWR/6 Plant-specific Steady Operating and ECCS Parameters

Operating Parameters	Value
Core Power (MW thermal) / (% OLTP)	4295 / 120%
Core Flow (kg/s) / (%)	10484 / 80%
Dome Pressure (Pa)	7.183E+06
Feedwater Temperature (K)	500
Downcomer Narrow Range Water Level (m), relative to vessel bottom	14.32

ECCS Parameters	Value
Level 3 SCRAM setpoint (m) above vessel bottom	13.388
Level 3 SCRAM delay (s)	1.05
Drywell Pressure SCRAM time (s) for area in (ft ²), valid for MARK-III type containment systems	$0.5435 * A^{-1.1357}$
High Pressure Core Spray (HPCS) initiation delay time (s)	40.0
Low Pressure Core Spray (LPCS) initiation delay (s)	37.0
LPCS delay for diesel generator startup time (s)	52.0
LPCS pressure permissive (bar)	29.65
Low Pressure Core Injection (LPCI) initiation delay (s)	37.0
LPCI delay for diesel generator startup time (s)	52.0
LPCI pressure permissive (bar)	29.65
Level 1 (low-low-low level) setpoint (m) (MSIV closure actuation on L1)	9.245
Total number of HPCS / LPCS / LPCI systems	1 / 2 / 3
Number of available ADS valves / total number of ADS valves	7 / 8

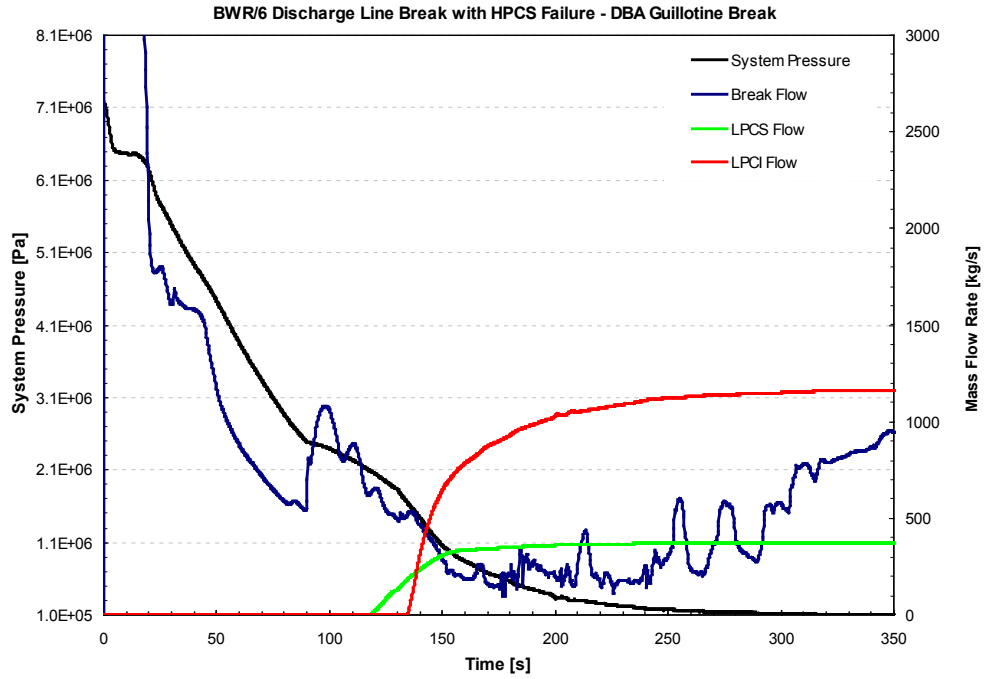


Figure 8.2-4 System Pressure and ECC Flows for BWR/6 Discharge DBA

[[

Figure 8.2-5 PCT for Various Channels for BWR/6 Discharge DBA

]]

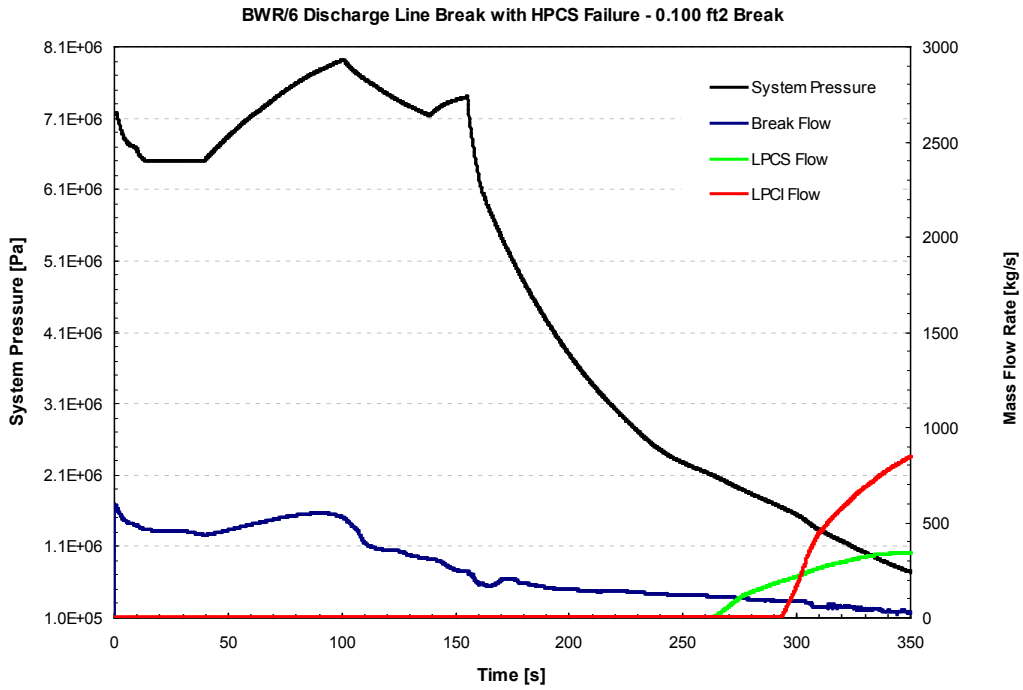


Figure 8.2-6 System Pressure and ECC Flows for BWR/6 Small Break

[[

]]

Figure 8.2-7 PCT for Various Channels for BWR/6 Small Break

8.2.3 Sensitivity to Initial Conditions and Plant Parameters for BWR/6

8.2.3.1 Initial Conditions and Allowable Operating Range

Initial condition sensitivity studies were performed for large and intermediate break LOCAs to characterize the initial conditions. As described in Section 6.2, the effect of an initial condition on the results of a LOCA analysis is characterized in the following manner:

- A. The results are sensitive to the initial condition and a basis for the limiting initial condition cannot be established. Future plant analyses (for example the reload licensing analyses) will consider the full allowable range of the initial condition.
- B. The results are sensitive to the initial condition and a basis for the limiting initial condition can be established. Future plant analyses (for example the reload licensing analyses) will consider the parameter at its limiting initial condition.
- C. The results are not sensitive to the initial condition and a nominal initial condition will be assumed for the parameter.

The characterization analysis bases are described in Table 8.2-3. [[

]] The results of the sensitivity studies are
discussed in the next section.

Table 8.2-3 Allowable Operating Range Specification Basis

Quantity	Control Basis	Range	Analysis Basis
Total Core Power	Plant Technical Specifications restrict the maximum operating core thermal power. For a given core flow, the maximum and minimum core power are controlled through operation within the analysis basis power/flow map.	Initial power/flow conditions will be chosen to bound the operating envelope. This includes extended power uprate and MELLLA+. The limiting conditions will be identified through calculations at the corners of the envelope and some intermediate points. Partial power/flow conditions will also be analyzed.	Calculations will be made over the MELLLA+ operating map (Figure 6.2-1) at 100% (OLTP)/ 100% flow; 120/100; 120/80; and 100/55.
Total Core Flow	For a given core power, the maximum and minimum core flow are controlled through operation within the analysis basis power/flow map.		
Feedwater Temperature	Given feedwater temperature and core power, the feedwater flow and steam flow can be determined. Some plants have analyzed for additional operating flexibility (Final Feedwater Temperature Reduction or Feedwater Heater Out-of-Service).	[[
Steam Dome Pressure	Plant Technical Specifications restrict the maximum operating dome pressure. The minimum dome pressure is controlled through turbine operational control.		
Downcomer Water Level	Plant would operate between the L4 and L7 alarm setpoint.]]

Table 8.2-3 (cont'd) Allowable Operating Range Specification Basis

Quantity	Control Basis	Range	Analysis Basis
Core Loading Pattern and Total Core Exposure	A reference core loading pattern is defined for each reload cycle. Acceptable deviation from the reference core is defined in GESTAR Section 3.4.2 [20].	[[
Axial Power Distribution	Plants are not restricted with regard to axial power distribution as long as thermal limits are met.		
Radial Power Distribution	Plants are not restricted with regard to radial power distribution as long as thermal limits are met.		
Local Peaking Distribution in High Power Bundles	Plants are not restricted with respect to local power distribution as long as thermal limits are met.		
Control Rod Pattern (control rod density)	Plants are not restricted with respect to control rod pattern as long as thermal limits are met.		
Peak Bundle Exposure	Plants are not restricted with respect to bundle exposure distribution as long as thermal limits are met.]]

Table 8.2-3 (cont'd) Allowable Operating Range Specification Basis

Quantity	Control Basis	Range	Analysis Basis
Pellet Exposure	Peak pellet power is restricted as a function of pellet exposure.	[[
Steam Flow	Derived from core thermal power and feedwater temperature.]]

8.2.3.2 Allowable Operating Range Results for BWR/6 Plant

Axial Peaking

A top peaked axial power shape is expected to be limiting because the top of the core uncovers first during a LOCA. [[

]]

Operating Conditions on Power/Flow Map

The LOCA calculations are not significantly sensitive for different power/flow conditions. The 120/80 power/flow combination will be used as the reference for subsequent calculations.

Core Average Exposure

From the standpoint of LOCA evaluations, the important effects of core average exposure are on core average gap conductance and decay heat. Stored energy, which is controlled by gap conductance, and decay energy both increase with increasing exposure. [[

]]

Pellet Exposure

The peak pellet power (PLHGR) as a function of pellet exposure is constrained to lie on the thermal mechanical design envelope. [[

]]

Radial Power Distribution

A sensitivity study was performed for BWR/4 large suction break in which [[

]]

Steam Dome Pressure

Sensitivity studies with respect to the steam dome pressure for the BWR/6 showed [[

]]

Feedwater Temperature

Sensitivity studies showed [[

]]

Initial Downcomer Level

Sensitivity studies showed [[

]]

The results of the characterization of the operating range are summarized in Table 8.2-4.

Table 8.2-4 Allowable Operating Range Characterization for BWR/6 LOCA

Quantity	Category	Analysis Basis
Total Core Power	The results are sensitive to the initial conditions and a basis for the limiting initial condition can be established.	[[
Total Core Flow		
Feedwater Temperature	[[
Steam Dome Pressure		
Downcomer Water Level		
Core Loading Pattern and Total Core Exposure		
Axial Power Distribution		
Radial Power Distribution		
Pellet Exposure]]]]

8.2.3.3 Initial Conditions Uncertainty

As described in Section 6.2, the plant initial conditions are monitored through the use of plant sensors or on-line calculations based on plant sensors. Because of instrument or simulation uncertainty, the plant condition may vary from the indicated or calculated value. The initial conditions uncertainties are characterized in the following manner:

- A. The results are sensitive to the uncertainty in the initial condition and the uncertainty in the initial condition will be included in the statistical analysis.
- B. The results are not sensitive to the uncertainty in the initial condition and the uncertainty does not need to be accounted for in the statistical analysis.

The uncertainties in initial conditions were evaluated and characterized. The characterization analysis bases are described in Table 8.2-5.

**Table 8.2-5 Bases for Initial Conditions Uncertainty Characterizations for BWR/6
 LOCA**

Quantity	Uncertainty Basis	Analysis Basis
Total Core Power	In demonstration calculations a 2% uncertainty is assumed.	
Total Core Flow	Total $\sigma = 2.5\%$ is specified by Reference [32].	
Feedwater Temperature	Total [] is specified by Reference [32].	
Steam Dome Pressure	Total [] is specified by Reference [32].	
Downcomer Narrow Range Water Level	Total [] of a 2 meter instrument range (typical).	
Bundle Power	Total [] is specified by Reference [32].	
Nodal Power	[] per Reference [32].]

8.2.3.4 Initial Condition Uncertainty Results

With the exception of initial MCPR and PLHGR, the results from the allowable operating range evaluations, documented in Section 8.2.3.1, [[

]] The results of the characterization study are summarized in Table 8.2-6.

Table 8.2-6 Initial Condition Uncertainty Characterizations for BWR/6 LOCA

Quantity	Characterization	Characterization/Analysis Basis
Total Core Power	[[
Total Core Flow		
Feedwater Temperature		
Steam Dome Pressure		
Downcomer Water Level		
[[]]]]

**Table 8.2-6 (cont'd) Results of Initial Condition Uncertainty Characterizations for
BWR/6 LOCA**

Quantity	Characterization	Characterization/Analysis Basis
[[
]]

8.2.3.5 Plant Parameters

As described in Section 6.3, critical plant parameters will be [[

]]

This process is described in the procedure that defines the critical OPL for ECCS/LOCA analysis. The bounding treatment of the plant parameters adopted for present purposes does not preclude the possible future use of statistically based plant parameters or setpoints. Inclusion in the statistical analysis would require determination of nominal values and consideration of instrument drift and recording uncertainties. Consideration of these uncertainties would then be incorporated in the application methodology.

Section 6.3.2 describes a study of the effect of scram speed on the LOCA response. [[

]]

Drywell pressure (and its gaseous environment) and ECC temperature (i.e., suppression pool temperature) are treated as plant parameters or boundary conditions for ECCS/LOCA analysis because they govern the interaction of the RPV with the containment. It was shown in Section 5.1 that [[

]]

8.2.3.6 Initial Conditions and Plant Parameters for BWR/6 LOCA Analyses

The conclusions from the initial conditions and plant parameter uncertainty characterizations form the basis of the plant specific analysis process as described below:

- [[

]]

8.2.4 Break Spectrum Results for BWR/6

A break spectrum analysis was performed for breaks in the recirculation line. Additionally, double-ended breaks in a main steam line, LPCS line and LPCI line were evaluated. [[

]] The initial conditions correspond to the results of the characterization basis discussed in Section 8.2.3 and shown in Table 8.2-4. The model parameters are set to their nominal values (PIRT multipliers set to 1) except [[

]] Loss-of-offsite power, causing a trip of the recirculation pumps, is assumed at time zero. The scram time is the earlier of the High Drywell Pressure or L3 signals as discussed in Section 6.3.1. MSIV closure was initiated on L1.

Figure 8.2-8 shows a schematic of the ECCS configuration for the plant. Three single-failure scenarios were considered: failure of the HPCS D/G; failure of the LPCI D/G; and failure of the LPCS D/G. The failed and available systems for each scenario are shown in Table 8.2-7. Prior experience has shown that the loss of the high pressure ECC system (HPCS D/G failure) is limiting. The plant parameters (e.g., setpoints, ECC flow capacity) were set at their analytic limits. [[

]]

8.2.4.1 Recirculation Line Breaks on Discharge Side of the Recirculation Pump

Figure 8.2-9 through Figure 8.2-14 show the transient response for break sizes ranging from 0.0037 m² to a double-ended guillotine break (0.238 m² on each side) on the discharge side of the recirculation line. All breaks smaller than the DBA are modeled as split breaks, with flow from both sides of the recirculation line feeding the break flow. For break sizes larger than 0.01 m², the High Drywell Pressure causes the scram. For breaks smaller than 0.01 m², the scram results from the Level 3 trip.

Figure 8.2-9 shows the reactor vessel pressure response for small breaks ranging from 0.0037 to 0.0093 m². Following the MSIV closure on Level 1, the pressure increases until the safety relief valves open. The actuation of the SRVs maintains the system pressure between the setpoints until the ADS actuation. The ADS actuation is also on Level 1 with a built-in delay of 120 s. Figure 8.2-10 shows the corresponding PCT response. For the smallest breaks, there is no significant heatup in the core until the flashing due to the ADS activation subsides. As the break size increases, the core inventory begins to deplete before the start of the depressurization and heatup occurs before the activation of the ADS. This early heatup is quenched by lower plenum flashing-induced flow through the core. A second cladding heatup begins after the ADS

depressurization rate subsides. This later heatup determines the PCT for the transient which turns around after the LPCI initiation.

Figure 8.2-11 shows the reactor vessel pressure response and the downcomer level relative to the bottom of the region for intermediate breaks ranging from 0.028 to 0.093 m². For these break sizes, the pressure does not increase markedly on the Level 1 MSIV closure. The ADS valves open after a delay of 120 s. The downcomer level drops to the elevation of the recirculation line suction before the ADS valves open. The uncovering of the recirculation line suction leads to vapor discharge from the reactor vessel and a faster depressurization rate. The opening of the ADS valves further increases the depressurization rate. The ADS activates earlier as the break size increases but its effect on the transient response is reduced in comparison to the early depressurization by the break flow. Figure 8.2-12 shows the PCT response for the intermediate size breaks. For break sizes of 0.028 and 0.046 m², the PCT occurs after the ADS subsides. As the break size increases to 0.065 m², the early heatup is not quenched by the ADS induced flashing. The heatup continues through the ADS blowdown period until the LPCI/LPCS turns the temperature downward. With increasing break size, the heatup starts earlier because of the larger break flow and the PCT gets progressively larger (Figure 8.2-12). The largest PCT (922 K) occurred at a break size of 0.093 m². Beyond 0.093 m², the trend is reversed as the heatup is attenuated by the earlier initiation of the ECC systems.

Figure 8.2-13 shows the reactor vessel pressure response for large breaks ranging from 0.186 m² to the DBA. The reactor vessel depressurizes rapidly and the ADS is not required to supplement the blowdown. The early loss of inventory is the dominant factor in the temperature rise. Figure 8.2-14 shows the PCT responses. The earlier activation of the ECCS causes the PCT to be lower than that for the intermediate size breaks. For break sizes greater than 0.279 m², the choking location shifts to the jet pump nozzles on the discharge side of the break and a further increase in break size has no effect. For large breaks, a first peak PCT occurs in the first few seconds of the transient because of the mismatch between the power and core flow. This first peak PCT is not limiting and is quenched by the lower plenum flashing that follows the uncovering of the suction line in the downcomer.

The interplay between the timing of the initial depressurization, ADS, core heatup and ECCS actuation is depicted in Figure 8.2-15. It is seen that for break sizes smaller than 0.050 m², the sustained heatup to the PCT starts after the ADS subsides because the earlier temperature rise is terminated by the ADS induced flashing. For break sizes of 0.050 m² and larger, earlier dryout from inventory depletion dominates. The figure also shows the relationship between start of heatup and the activation of ECCS. The longest lags between the start of heatup and the initiation of ECCS and the highest PCTs occur in the range from 0.06 to 0.09 m². The break spectrum results are summarized in Figure 8.2-16. [[

]] The intermediate break sizes (0.06 to 0.09 m²) lead to the highest PCTs. At these break sizes, the early heatup is not terminated by the ADS induced flashing and

is reinforced by loss of inventory as the flashing subsides and late ECCS initiation compared to the larger breaks.

8.2.4.2 Recirculation Line Breaks on the Suction Side of the Recirculation Pump

Analyses were performed for a range of break sizes on the suction side of the recirculation piping. A failure of the HPCS D/G was postulated for these calculations. The pressure and PCT transients are similar to those for breaks on the discharge side. The break spectrum results for the suction line breaks are shown in Figure 8.2-17. [[

]] The PCTs for breaks on the suction side were bounded by the PCTs for the discharge side breaks. The highest PCT (923 K) was obtained for an intermediate break size of 0.074 m^2 and is lower than the PCT for the corresponding break size on the suction side.

8.2.4.3 Non-Recirculation Line Breaks

Non-recirculation line breaks are not expected to be limiting compared to the breaks in the recirculation line because of the smaller range of possible break sizes and higher break elevation relative to the top of the core. The non-recirculation line breaks for BWR/6 include guillotine breaks of a main steam line, LPCS line, LPCI line, and a feedwater line.

Among these breaks, the largest one is the main steam line break (MSLB). The large volumetric vapor and enthalpy flow for the steam line break would depressurize the vessel very rapidly rather than losing coolant inventory. The level swell inside the shroud would cover the core and the PCT would not significantly exceed the initial operating cladding temperature.

In the case of the feedwater line break, the discharge would transition quickly to single-phase vapor as the level in the downcomer falls below the elevation of the feedwater nozzle. [[

]]

In BWR/5 and/6 designs, the LPCI line is connected to the region inside the shroud. The LPCI break with a maximum break area of 0.048 m^2 would discharge flow from inside the core shroud region. The break flow would transition quickly to two-phase flow from the upper plenum and the transient would not exhibit significant temperature rise prior to ADS actuation. The PCT would not significantly exceed the initial cladding temperature of 585 K.

A break in the LPCS line has a small break area (0.026 m^2) and results in a discharge elevation above the core. Therefore, transient would behave similar to a small break in the steam line and the PCT is not expected to exceed the initial cladding temperature.

Table 8.2-7 Single Failures and Available ECCS for BWR/6

Failure	ECC Systems Available
HPCS D/G	LPCS, 3 LPCI, 7 ADS valves
LPCI D/G	HPCS, LPCS, 1 LPCI, 7 ADS valves
LPCS D/G	HPCS, 2 LPCI, 7 ADS valves

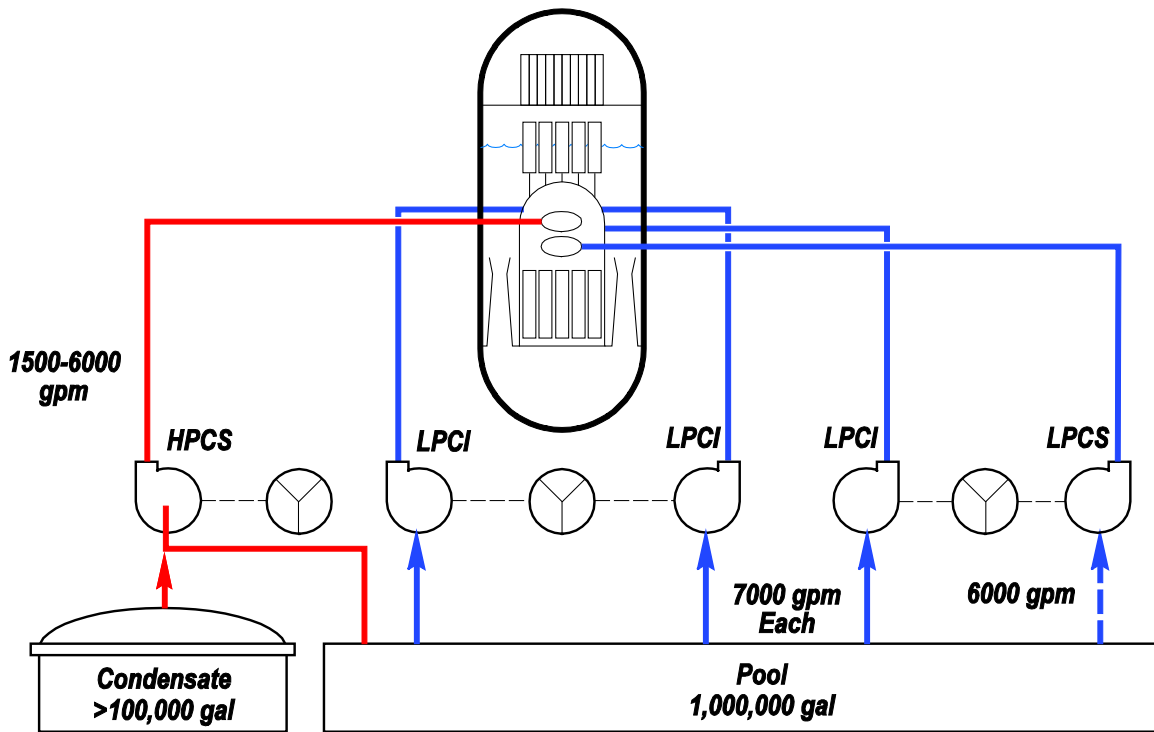


Figure 8.2-8 Typical BWR/6 ECCS Configuration

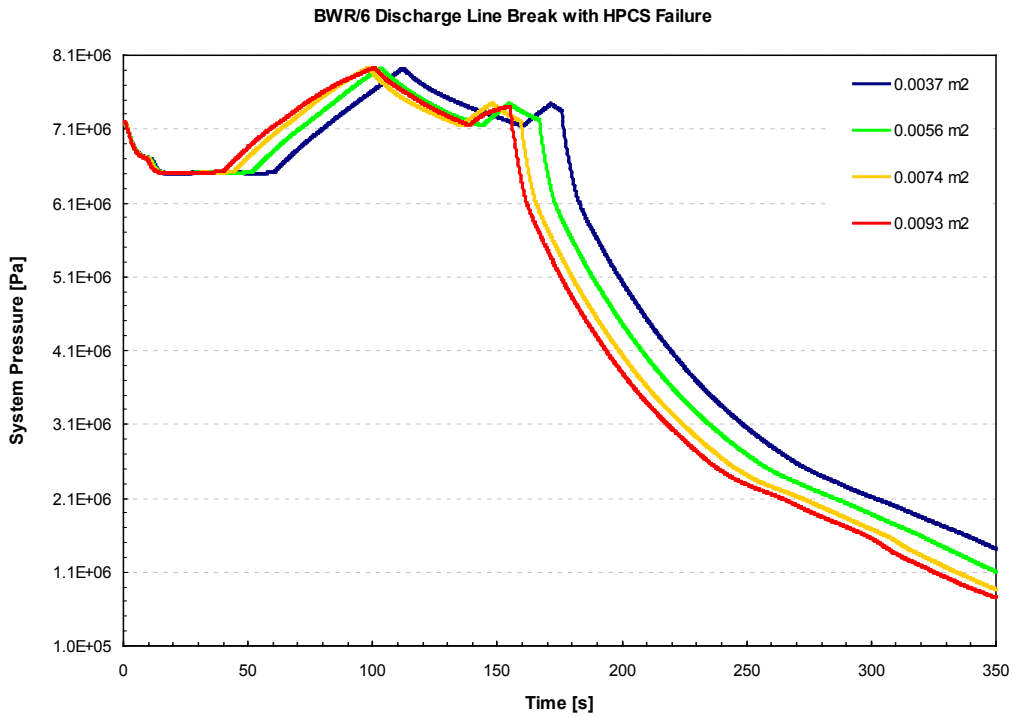


Figure 8.2-9 Pressure Response for BWR/6 Small Breaks

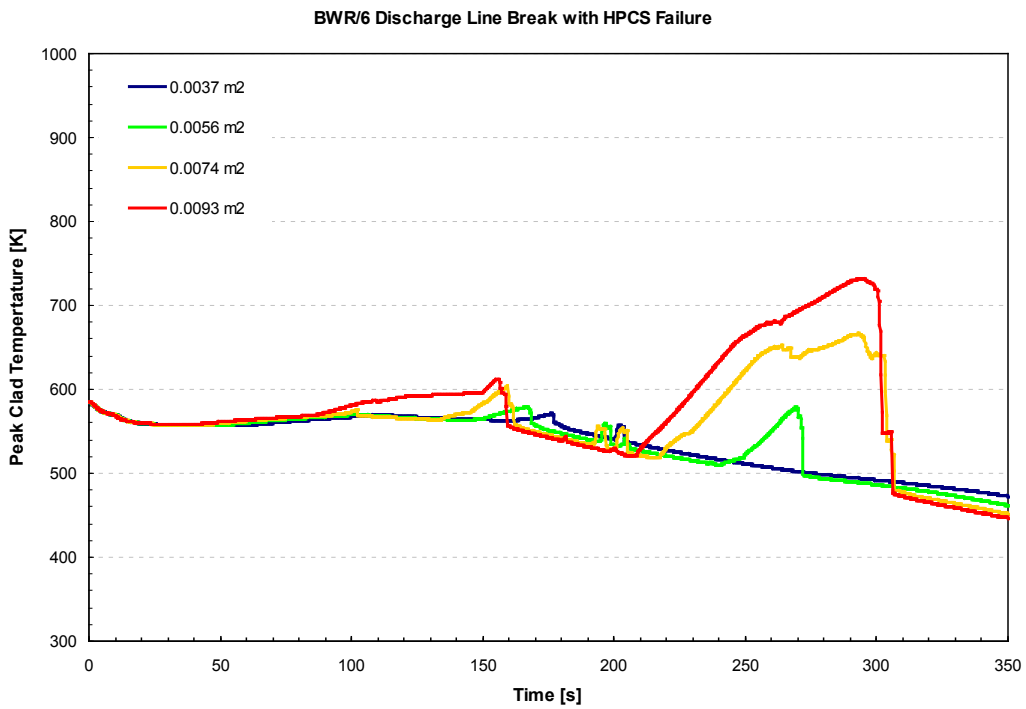


Figure 8.2-10 PCT Response for BWR/6 Small Breaks

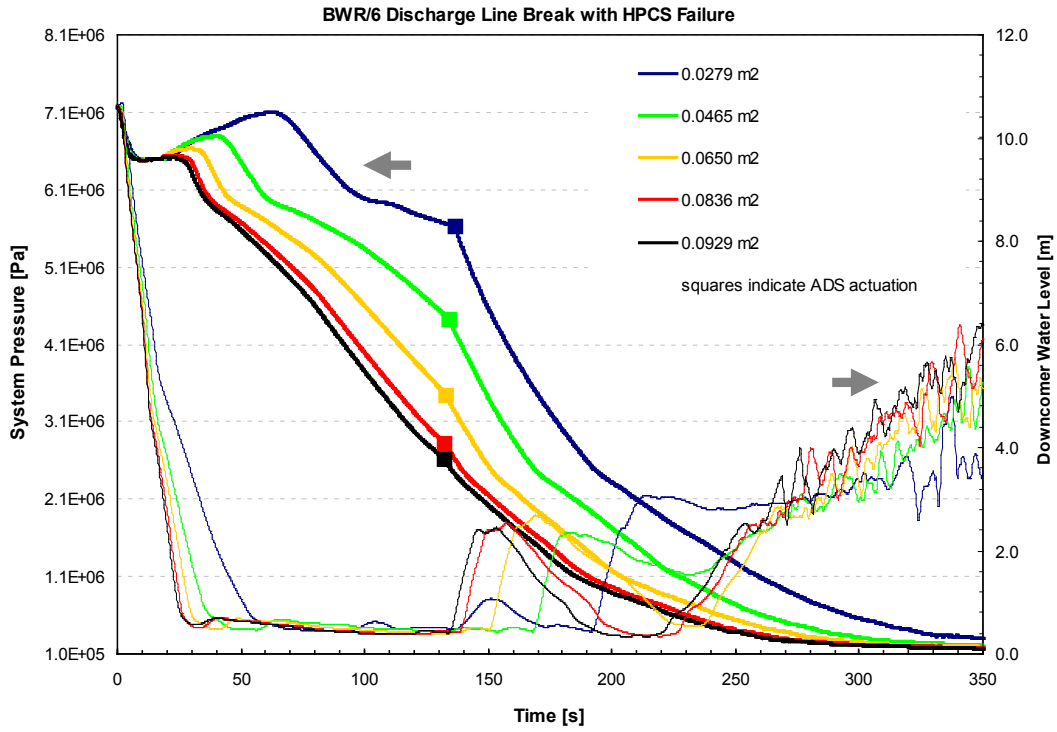


Figure 8.2-11 Pressure Response for BWR/6 Intermediate Breaks

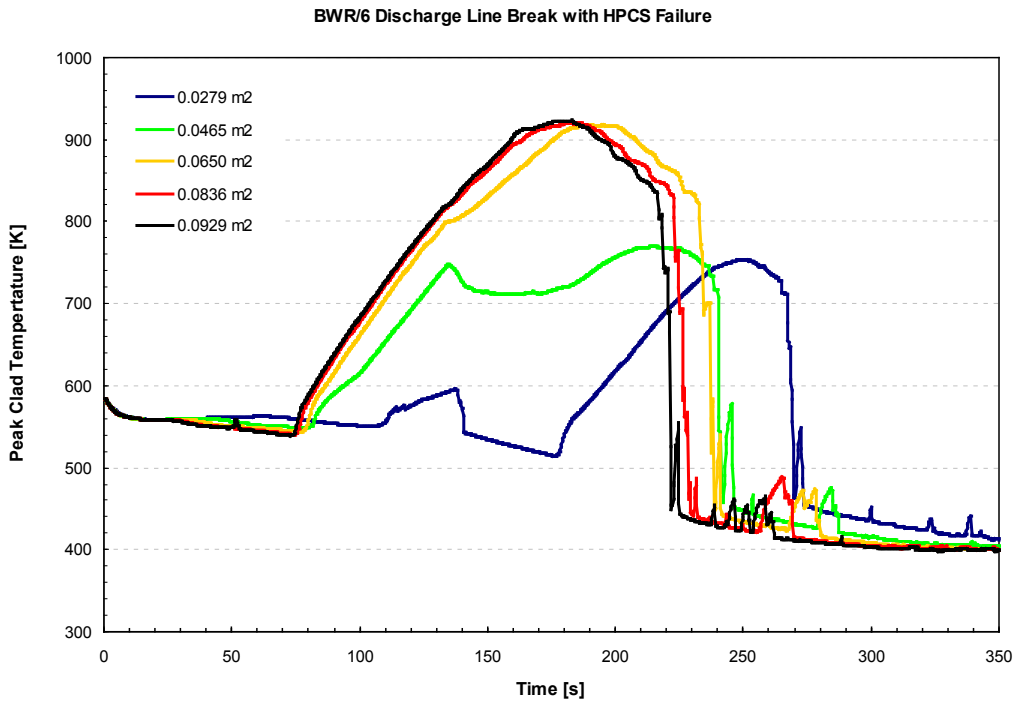


Figure 8.2-12 PCT Response for BWR/6 Intermediate Breaks

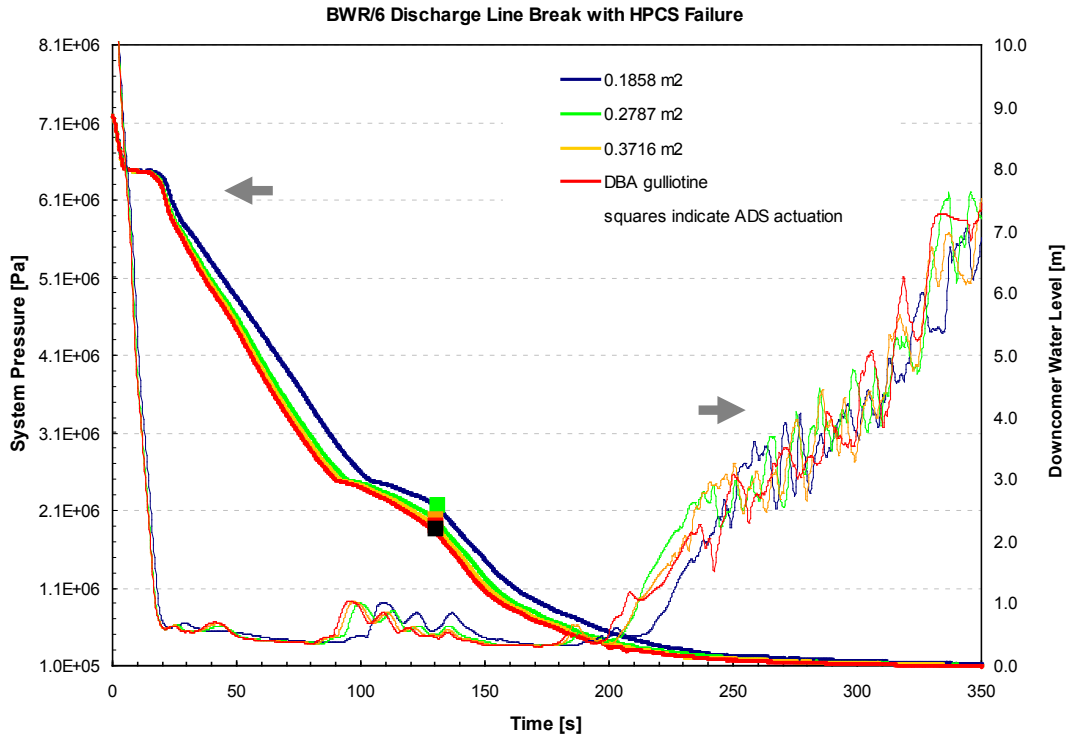


Figure 8.2-13 Pressure Response for BWR/6 Large Breaks

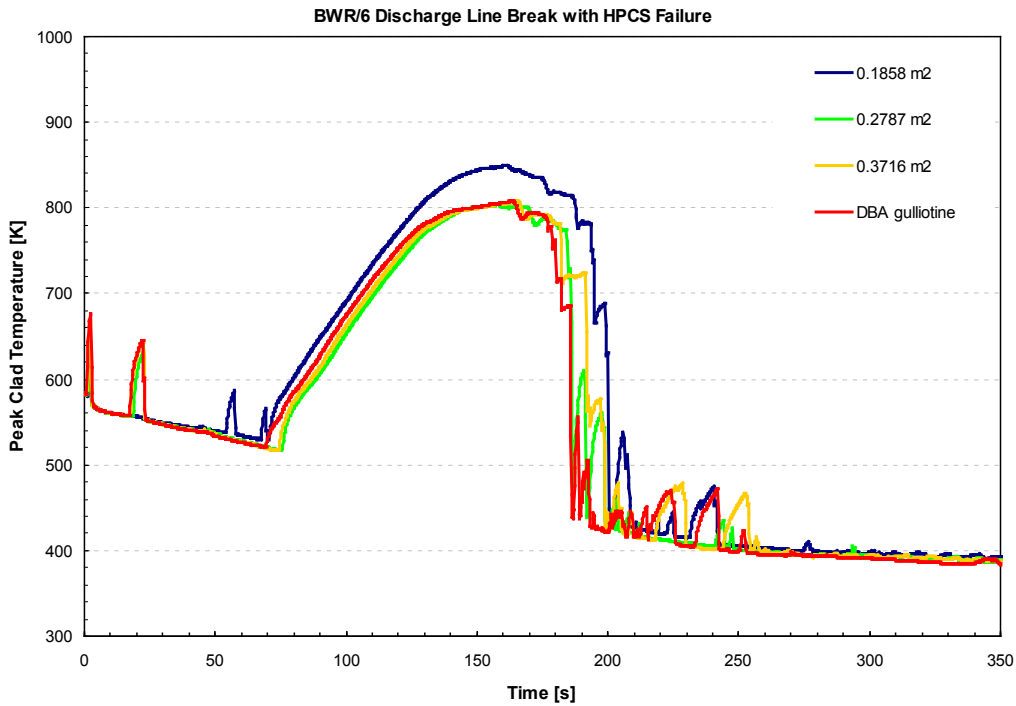


Figure 8.2-14 PCT Response for BWR/6 Large Breaks

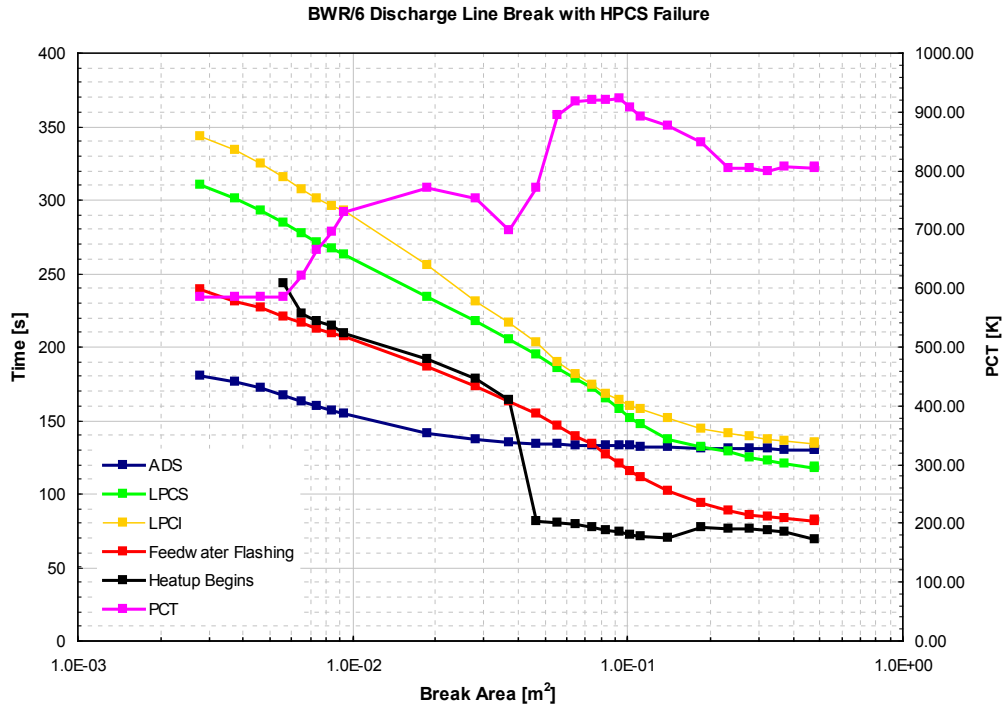


Figure 8.2-15 Start of BWR/6 Heatup Relative to ADS and ECCS Activation

[[

]]

Figure 8.2-16 Break Spectrum for BWR/6 Recirculation Line Discharge Breaks

[[

]]

Figure 8.2-17 Break Spectrum for BWR/6 Recirculation Line Suction Breaks

8.2.5 Statistical Results for BWR/6 LOCA

A statistical analysis for a number of breaks varying from 0.06 ft² (0.0056 m²) to double-ended guillotine break (0.477 m²) of the recirculation line on the discharge side of the pump was carried out by performing a set of 59 trials for each break size. In each trial, random draws were made from the probability density functions for the set of previously identified model and plant parameters (Table 5.1-2 and Table 8.2-8). The PCT results from these runs are summarized in Table 8.2-9. Figure 8.2-18 provides a summary of the PCT results from nominal, trial minimum, maximum, and average with 2σ bands. The highest PCT from the statistical study is obtained from 1.0 ft² (0.093 m²). In Section 8.2.4, the limiting break for a BWR/6 LOCA was identified as a recirculation line discharge break of 1.0 ft² (0.093 m²). As can be seen from these results, the break spectrum is relatively flat between 0.07 to 0.1 m², and the differences in OSUTL PCT for this range of breaks are within 1 K. For all the cases, the maximum local oxidation in terms of Equivalent Cladding Reacted (ECR) is less than 0.5%, resulting in insignificant amount of core-wide oxidation, hence hydrogen generation.

8.2.5.1 DBA/Large-Break LOCA Results

The results of the statistical analysis for the discharge DBA are presented in Figure 8.2-19 through Figure 8.2-21. Figure 8.2-19 shows the range and the average of the DBA PCT transient

over the 59 trials along with the result of the nominal calculation in which all the random variables are set to their most probable values. The initial heatup for the average of the transients is slightly sooner than for the nominal transient and, consequently, the average PCT is about 30 K higher than the nominal case. The difference is within one standard deviation. The gray shading in the figure shows the $\pm 2\sigma$ band limited at the extremes, indicating the range of expected results from the analysis. The corresponding individual deviations from the mean for each trial are shown in Figure 8.2-20. Figure 8.2-21 shows the distribution of PCTs. The overall PCT mean and standard deviation values were 813 K and 33 K. The p-value for the distribution of overall PCTs for the DBA does not meet the minimum requirement for normality. Therefore, the 95th percentile with high probability value of PCT for this case is based on the maximum of the trials and is estimated as 898 K.

8.2.5.2 Intermediate Break LOCA Results

Figure 8.2-22 through Figure 8.2-24 show the results of the Monte Carlo analysis for the intermediate break in the recirculation line discharge. The range and the average of the intermediate break PCT transient over the 59 trials are shown in Figure 8.2-22 along with the nominal result in which all the random variables are set to their most probable values. The corresponding individual deviations from the mean are shown in Figure 8.2-23. Figure 8.2-24 shows the distribution of the highest PCT regardless of the channel location. The mean and standard deviation values of the overall PCT were 925 K and 24 K. The p-value for the overall PCT distribution exceeds the minimum requirement for normality. Based on a normal distribution with a sample size of 59, the 95th percentile with high probability value of PCT is estimated as:

$$PCT_{95/95} = (925 \text{ K}) + 2.024*(24 \text{ K}) = 974 \text{ K}.$$

8.2.5.3 Small-Break LOCA Results

Figure 8.2-25 through Figure 8.2-27 show the results of the Monte Carlo analysis for the small break in the recirculation line discharge. The range and the average of the small break PCT transient over the 59 trials are shown in Figure 8.2-25 along with the nominal result in which all the random variables are set to their most probable values. The corresponding individual deviations from the mean are shown in Figure 8.2-26. Figure 8.2-27 shows the distribution of the highest PCT regardless of the channel location. The mean and standard deviation values of the overall PCT were 711 K and 73 K. The distribution is non-normal as indicated by a low p-value. Therefore, the 95th percentile with high probability value of PCT is estimated from the highest value of the 59 samples as 879 K.

Table 8.2-8 Plant Parameters varied in BWR/6 Monte Carlo Trials

Parameter	Gaussian Distribution as Analyzed		Region	Comment
	Mean	Standard Deviation		
Core Power	1.0	2%	Core	Parameter is the multiplier on the thermal power.
Core Flow	1.0	2.5%	Core	Parameter is the multiplier on the rated flow.
[[
]]

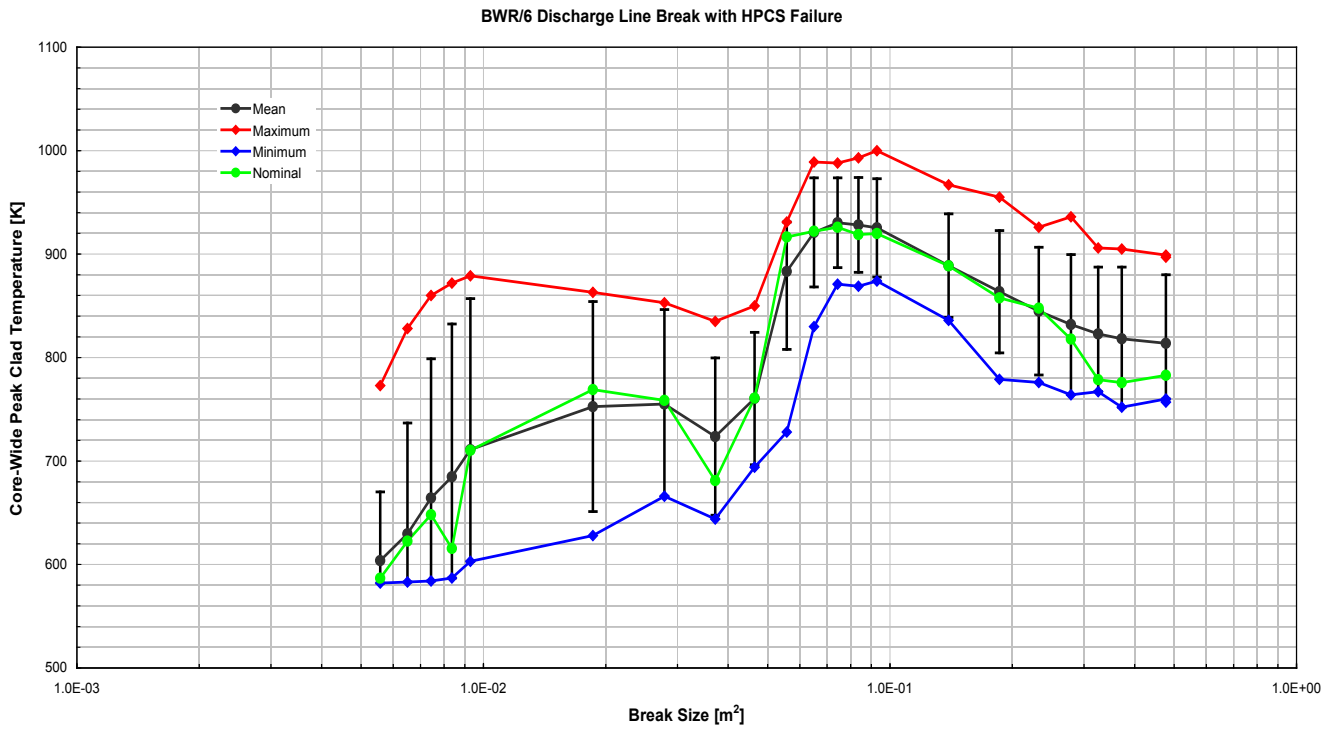


Figure 8.2-18 Summary of BWR/6 Statistical Analyses at Various Break Sizes

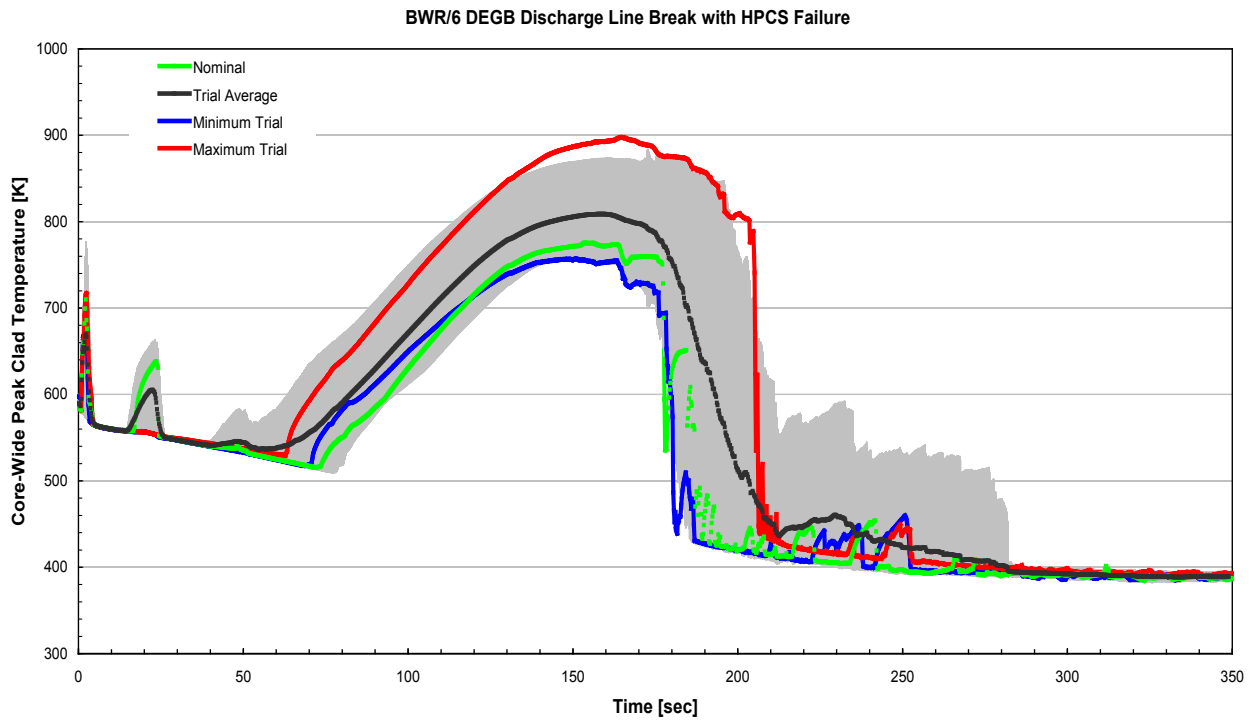


Figure 8.2-19 Range of Trials for PCT Transient for BWR/6 DBA

[[

Figure 8.2-20 Overall PCT Trials for BWR/6 Discharge DBA

]]

[[

Figure 8.2-21 Overall PCT Distribution for BWR/6 Discharge DBA

]]

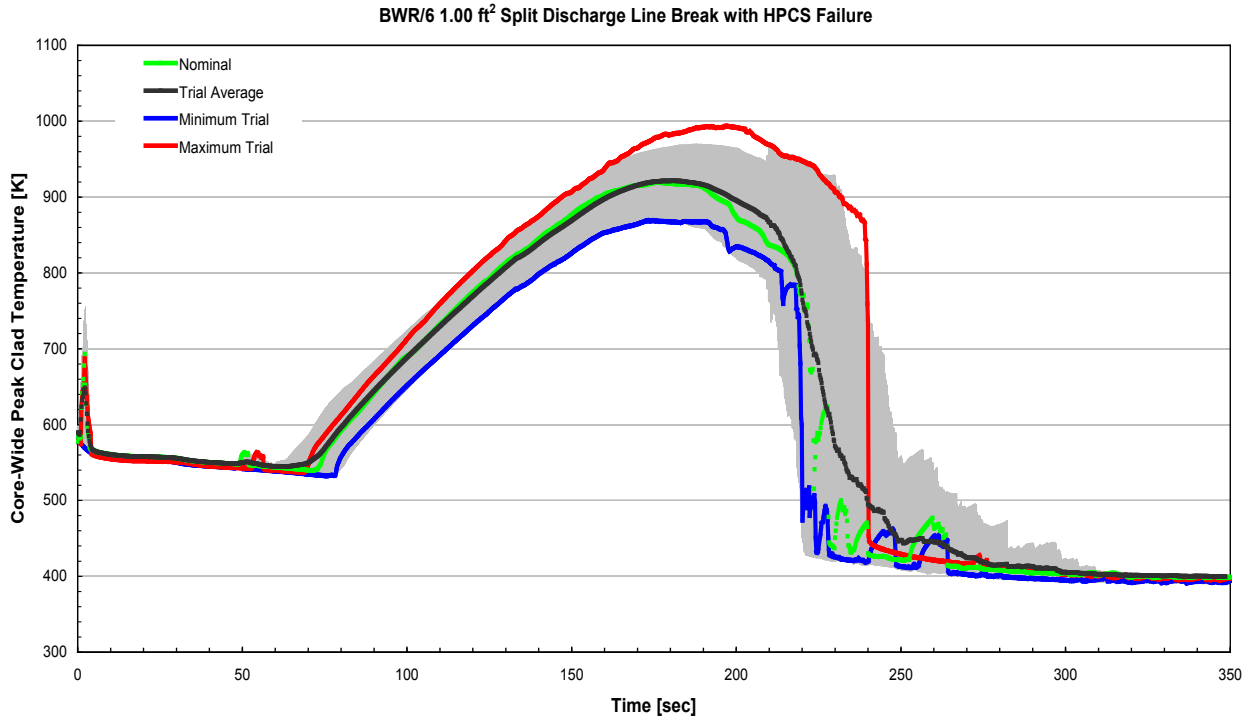


Figure 8.2-22 Range of Trials for PCT Transient for BWR/6 Intermediate Break

[[

]]

Figure 8.2-23 Overall PCT Trials for BWR/6 Intermediate Break

[[

]]

Figure 8.2-24 Overall PCT Distribution for BWR/6 Intermediate Break

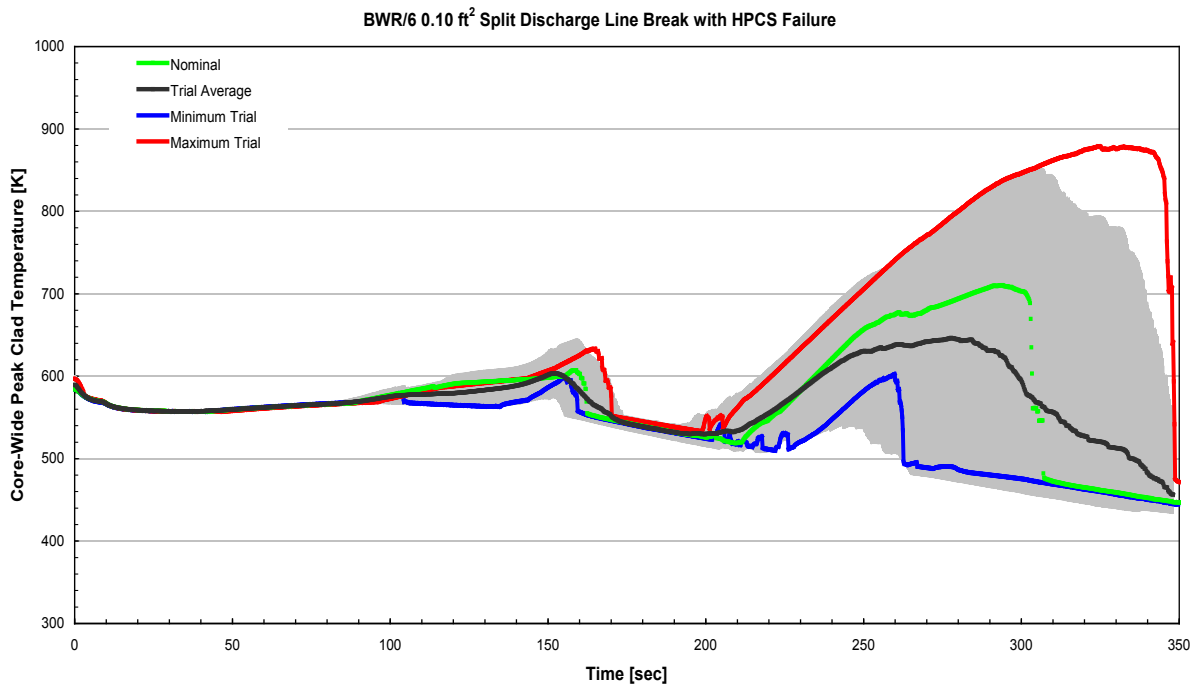


Figure 8.2-25 Range of Trials for PCT Transient for BWR/6 Small Break

[[

]]

Figure 8.2-26 Overall PCT Trials for BWR/6 Small Break

[[

]]

Figure 8.2-27 Overall PCT Distribution for BWR/6 Small Break

8.3 TRACG LOCA ANALYSIS RESULTS AND SENSITIVITY STUDIES FOR A TYPICAL BWR/2 (NON-JET PUMP) PLANT

A baseline analysis was performed for a typical BWR/2 plant. The sections below discuss the representative TRACG nodalization of the plant, nominal results for large and small breaks, sensitivities to the model parameters, range of initial conditions and uncertainties in the initial conditions. Plant parameters have all been set at their analytic limits for this analysis. Results for a complete break spectrum are presented.

8.3.1 TRACG Nodalization for ECCS/LOCA Calculations for a BWR/2 Plant

A typical BWR/2 type plant forms the basis for these analyses. The plant has 532 bundles and an Original Licensed Thermal Power (OLTP) of 1,850 MWth. The plant is loaded with fresh and exposed GE14 10x10 fuel. The TRACG vessel modeling is illustrated in Figure 8.3-1. Figure 8.3-2 illustrates the modeling of the components that represent the steam lines, recirculation lines and feedwater lines. The core spray system is modeled by FILL components with a prescribed flow rate vs. pressure. The recirculation lines are modeled to allow for the simulation of pipe breaks on the suction and discharge sides of the recirculation pumps. Double-ended and split breaks can be simulated with this configuration of the recirculation piping and appropriate use of BREK components set to the ambient drywell pressure. As shown in the figure, the BREK components are isolated from the piping in the steady state model. Breaks are initiated by opening communication with one or two BREK components depending on whether a split or double-ended break is being simulated.

Table 8.3-1 shows the channel grouping used for the calculations. [[

]]

Table 8.3-1 TRACG Channel Grouping for Typical BWR/2 Model

[[.....					
]]

[[

]]

Figure 8.3-1 TRACG Vessel Nodalization for Typical BWR/2 Model

[[

Figure 8.3-2 TRACG Component Nodalization for Typical BWR/2

]]

8.3.2 Nominal ECCS/LOCA Results for Large and Small Breaks for BWR/2

This section presents baseline TRACG results for a double-ended guillotine break (Design Basis Accident) and a small break in the recirculation line piping on the discharge side of the pump.

8.3.2.1 Discharge DBA Results

Table 8.3-2 shows the initial conditions and the key transient parameters for the double-ended guillotine break LOCA analysis case. The plant is at 100% OLTP and 100% of rated flow. A double-ended break of the recirculation line is assumed at time zero concurrently with a trip of the recirculation pumps on the assumed loss of offsite power. A reactor scram is initiated on High Drywell Pressure. MSIV closure occurs when the downcomer level reaches L1. A single failure resulting in the loss of the Isolation Condenser¹ is postulated. Furthermore, the remaining isolation condenser is not credited. Therefore no isolation condensers are modeled for the demonstration analyses. The available ECCS consists of two CS (which are single failure proof) and three ADS valves. Table 8.3-2 shows the time delays and pressure permissives for the ECC systems.

Figure 8.3-3 shows the system pressure response and the core void fraction for the discharge DBA. The RPV depressurizes to containment pressure in about 100 s because of the large break postulated on the discharge side of the recirculation pump. The downcomer is rapidly drained (Figure 8.3-21) and the depressurization leads to high void fractions in the core. Core flow reversal and the onset of the CS temporarily decrease the void fraction, but in the longer term, the void fraction remains in the vicinity of 0.7. When the pressure falls below the ECCS pressure permissives, the CS is activated and it starts injecting coolant into the upper plenum at 44 s. The break and core spray flows are shown in Figure 8.3-4. Figure 8.3-5 shows the position of the two-phase level in the lower plenum. The lower plenum is drained early in the transient. Subsequently, following CS actuation, water drains into the lower plenum through the core and fills it to the elevation of the discharge line so that, after about 250 s, the break flow nearly balances the injected CS flow.

Figure 8.3-6 shows the calculated peak cladding temperatures in the high power and average bundles. All of the bundles experience an early dryout as a result of the rapid depressurization. The temperature excursions are partially quenched by lower plenum flashing. Core heatup resumes when lower plenum flashing subsides and the inventory in the core is further depleted. The channel walls quench as liquid films form at the top unheated surfaces and move downward along the channel wall. The quenched channel provides a sink for radiative heat transfer from the peripheral rods in the fuel bundle. The rods attain a peak temperature governed by equilibrium between decay heat generation and core spray heat transfer. Heat transfer is split in roughly equal amounts between convection to the superheated steam and radiation to cooler surfaces. Starting at around 1000 s, the rods begin to quench, except the rods modeled with

¹ Also referred as “Emergency Condenser,” terms used interchangeably.

limited amount of spray into the hot channel available. Peripheral rods quench first as they radiate to the cooler channel wall. These are followed by the interior rods, which have a smaller view factor for radiation to cooler surfaces. [[

]]

8.3.2.2 Small Break Results

Table 8.3-3 shows the initial conditions and the key transient parameters for the BWR/2 small break case. The plant is operating at 100% power and rated flow. A 0.0186 m² break on the discharge side of the recirculation line is postulated concurrently with a trip of the recirculation pumps at time zero. A reactor scram occurs at 3.5 s on L3 and MSIV closure initiates at 15.5 s on L1. As for the DBA, a loss of the Emergency Condenser is postulated and the available ECCS consists of two CS and three ADS valves. Table 8.3-3 shows the time delays and pressure permissives for the ECC systems.

Figure 8.3-7 shows the system pressure response and the core void fraction (level 7, ring 1) for the small break. The small break size and closure of the MSIVs limit the initial depressurization rate. The core void fraction begins to increase at about 100 s as the depressurization rate increases. The core void fraction is subsequently reduced as the core is refilled by the CS. Figure 8.3-8 shows the break and CS flow transients. When the downcomer level reaches Level 1, the ADS is tripped with a delay of 120 s. The opening of the ADS valves at approximately 150 s is reflected in the depressurization rate (Figure 8.3-7). The emergency core cooling systems are activated when the pressure falls below the ECC pressure permissives. The CS starts injecting coolant into the upper plenum at 300 s. The two-phase levels in the bypass and lower plenum are shown in Figure 8.3-18 and Figure 8.3-9, respectively. The bypass and lower plenum drain through the discharge line connection. When the CS flow exceeds the break

flow (Figure 8.3-8), the lower plenum slowly begins to refill. Vapor generation in the lower plenum holds up inventory in the core and bypass as the recirculation discharge is covered.

Figure 8.3-10 shows the calculated peak cladding temperatures in the hot and average bundles. The hot bundles do not go through an early boiling transition because the flow does not drop rapidly as the recirculation pumps coast down. As the inventory drains, heatup occurs in the upper portion of the core at about 60 s into the accident. The heatup is terminated following the activation of the CS at 300 s. The bundles are quenched at about 450 s as the core refills. [[

]]

Table 8.3-2 BWR/2 Discharge DBA Key Transient Parameters

Time Summary (s)	
Break	0
Scram	0.16
Recirculation pump trip on loss of offsite power	0
MSIV closure initiated	2.4
CS diesel generator startup delay	35
CS initiation delay following pressure permissive of 25.09 bar	23
Initial Conditions	
Initial core power (% OLTP)	100
Initial core flow (%)	100
Initial dome pressure (Pa)	7.19E6
Initial FW temperature (K)	455.6
Initial NR water level (m)	12.92
[[
]]
Key Transient Parameters	
Single Failure	EC Failure
ECC Systems available	2 CS, 3 ADS
CS initiated (sec)	44
Peak Cladding Temperatures	
[[
]]

Table 8.3-3 BWR/2 0.0186 m² Discharge Break Key Transient Parameters

Trip Time Summary (s)	
Break	0
Scram	3.5
Recirculation pump trip on loss of offsite power	0
MSIV closure initiated	15.5
CS diesel generator startup delay	35
CS initiation delay following pressure permissive of 25.09 bar	23
Initial Conditions	
Initial core power (% OLTP)	100
Initial core flow (%)	100
Initial dome pressure (Pa)	7.19E6
Initial FW temperature (K)	455.6
Initial NR water level (m)	12.92
[[
]]
Key Transient Parameters	
Single Failure	EC Failure
ECC Systems available	2 CS, Three ADS
CS initiated (sec)	300
Peak Cladding Temperatures	
[[
]]

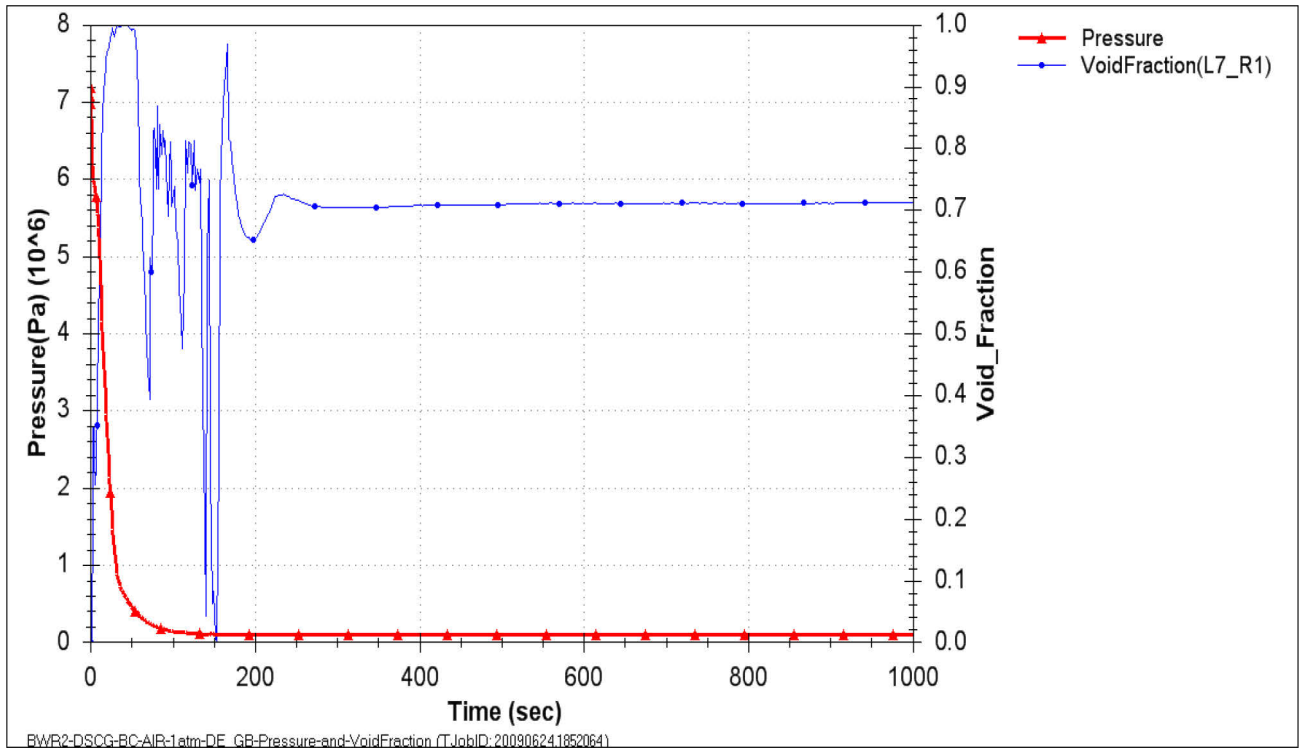


Figure 8.3-3 System Pressure and Void Fraction in Central Cell of Core for Discharge DBA

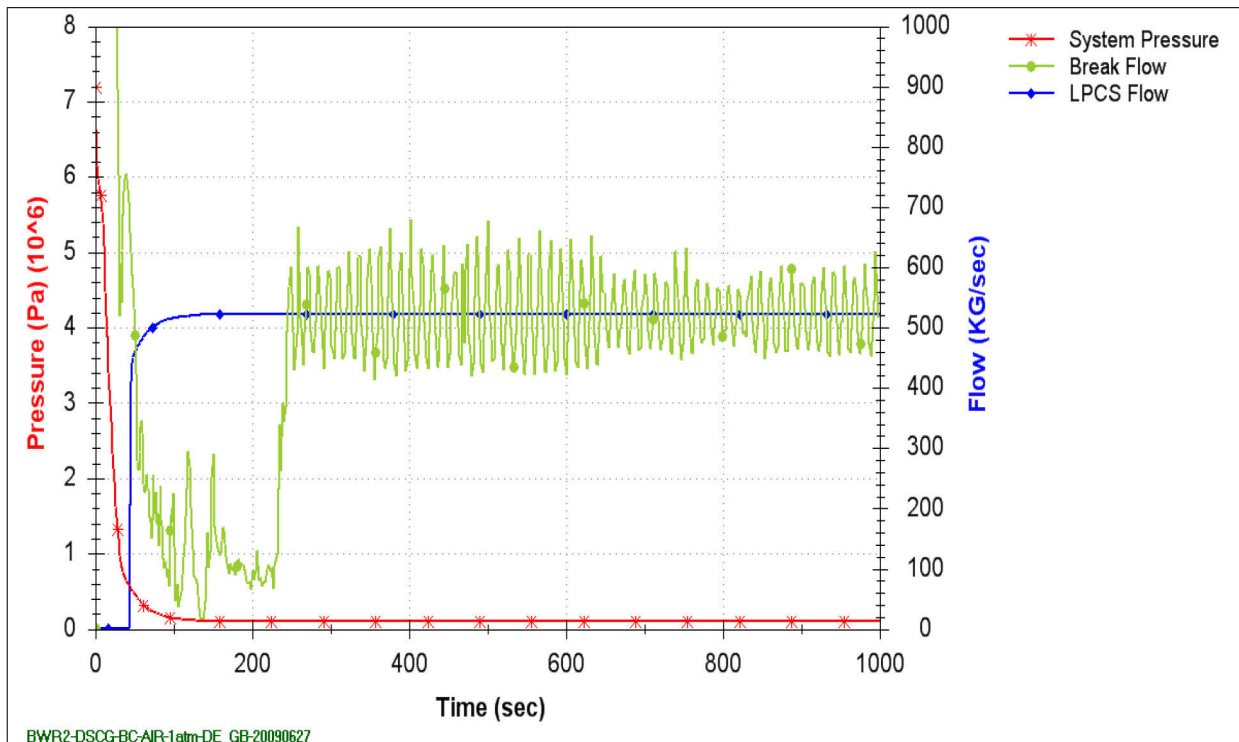


Figure 8.3-4 Break Flow and CS Flow for BWR/2 Discharge DBA

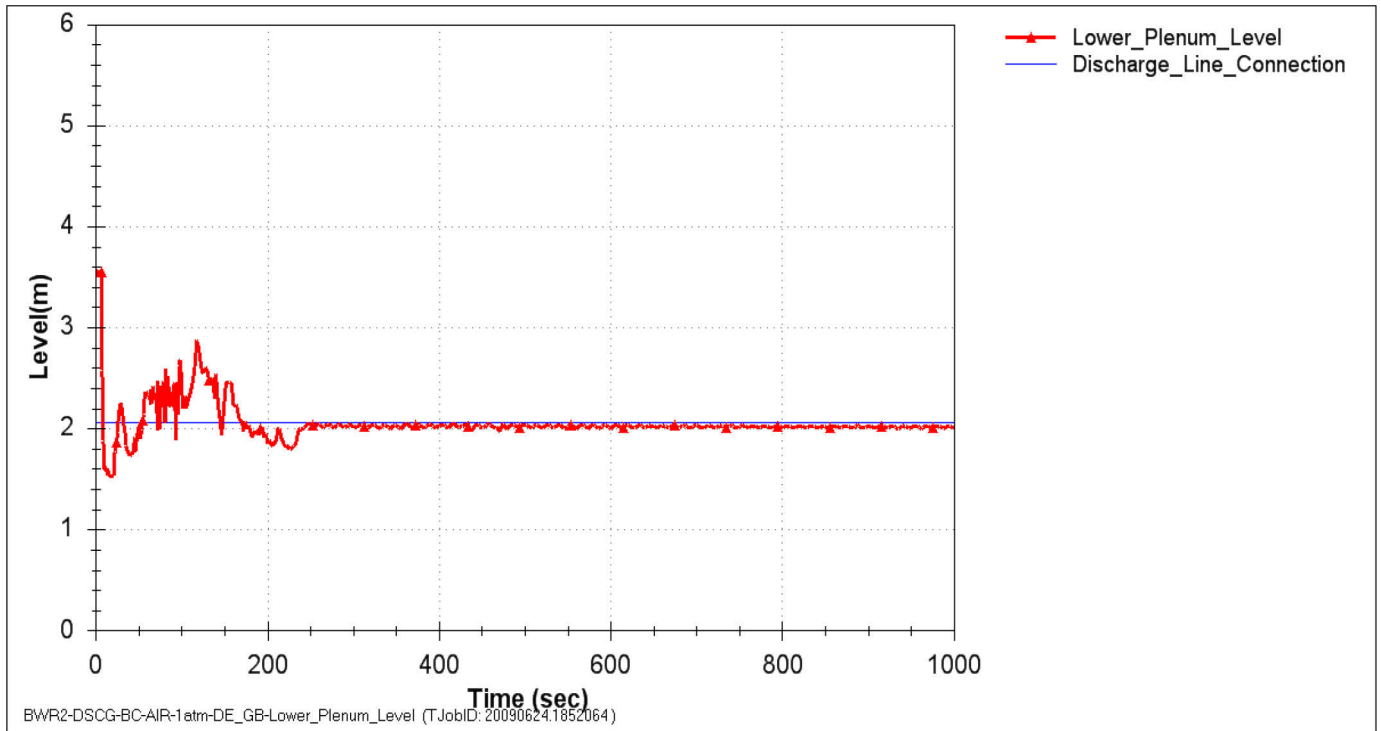


Figure 8.3-5 Lower Plenum Level for BWR/2 Discharge DBA

[[

Figure 8.3-6 PCT for Various Channels for BWR/2 Discharge DBA

]]

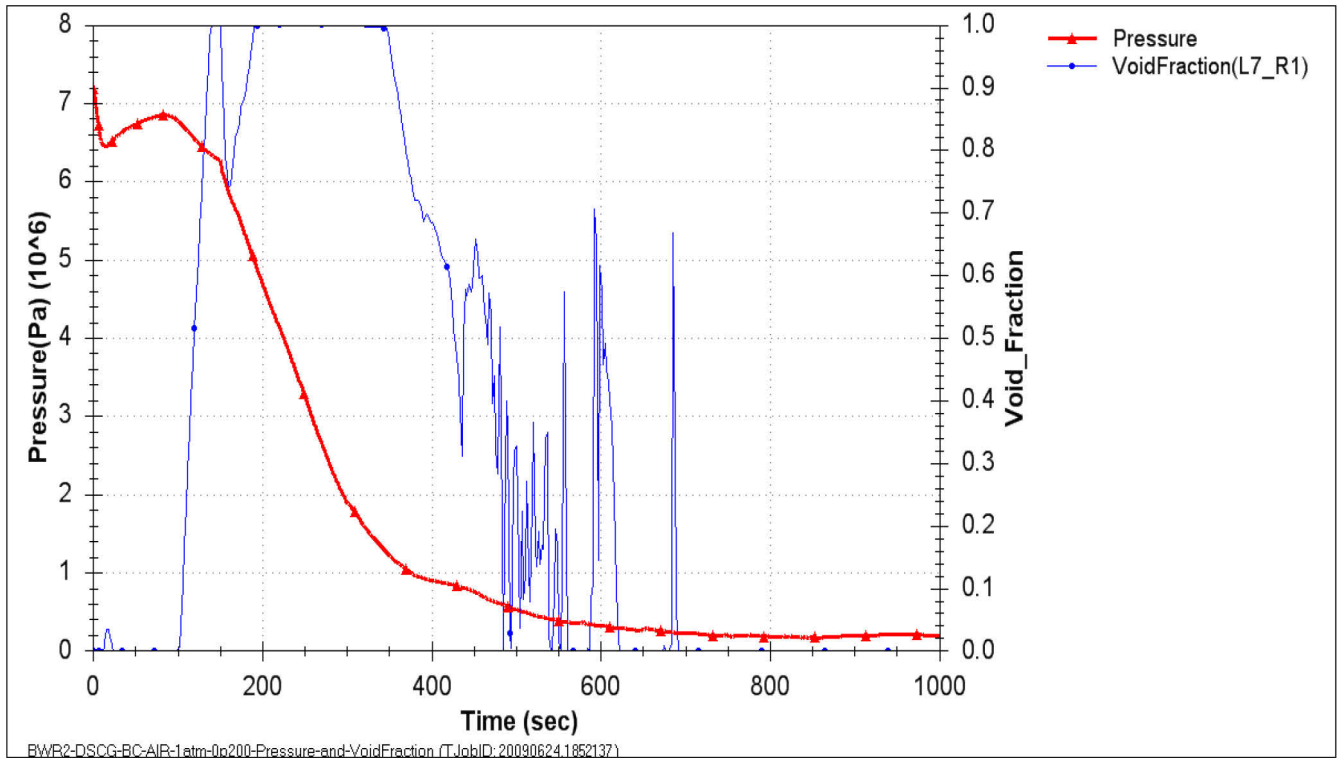


Figure 8.3-7 Pressure and Void Fraction in Central Cell for BWR/2 Small Break

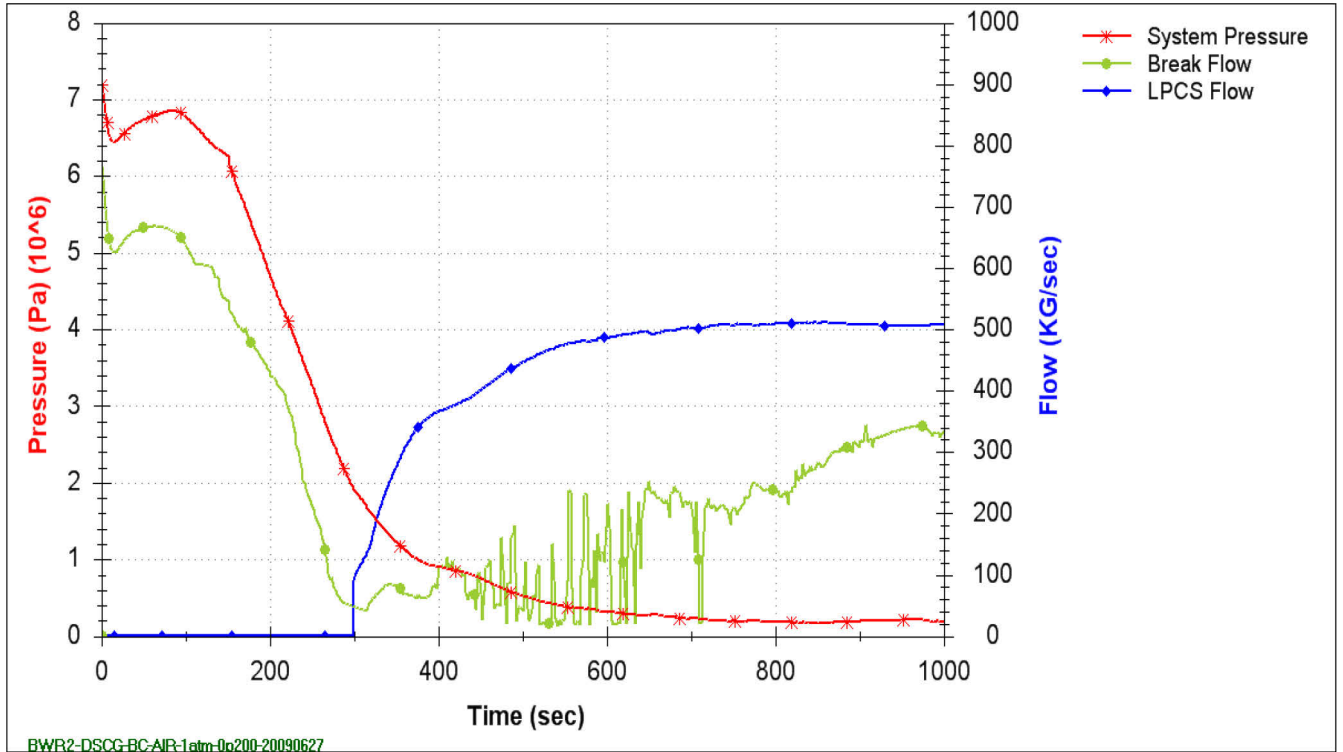


Figure 8.3-8 Break Flow and CS Flow for BWR/2 Small Break

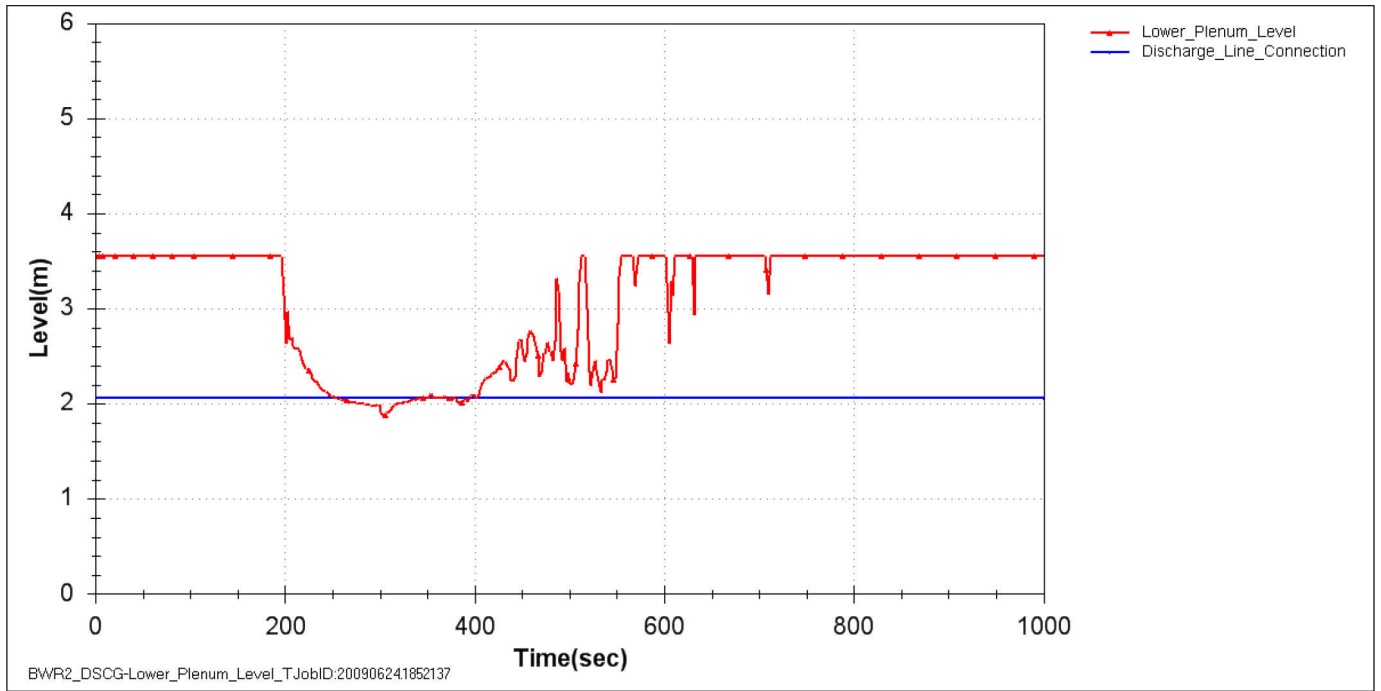


Figure 8.3-9 Lower Plenum Level for BWR/2 Small Break

[[

Figure 8.3-10 PCT for Various Channels for BWR/2 Small Break

]]

8.3.3 Sensitivity to Model (PIRT) Parameters for BWR/2

Representative cases for small, intermediate, and large break LOCA on the discharge side of the recirculation was evaluated with [[

]]

[[

]]

Figure 8.3-11 BWR/2 Small Break PCT Sensitivity to Individual Uncertainties

[[

]]

Figure 8.3-11 (cont'd) BWR/2 Small Break PCT Sensitivity to Individual Uncertainties

[[

]]

Figure 8.3-12 BWR/2 Intermediate Break PCT Sensitivity to Individual Uncertainties

[[

]]

Figure 8.3-12 (cont'd) BWR/2 Intermediate Break PCT Sensitivity

[[

]]

Figure 8.3-13 BWR/2 Large Break PCT Sensitivity to Individual Uncertainties

[[

]]

Figure 8.3-13 (cont'd) BWR/2 Large Break PCT Sensitivity to Individual Uncertainties

8.3.4 Sensitivity to Initial Conditions and Plant Parameters for BWR/2

8.3.4.1 Initial Conditions and Allowable Operating Range

As described in Section 6.2, the effect of the initial condition on the results of a TRACG LOCA calculation are characterized in the following manner:

- A. The results are sensitive to the initial condition and a basis for the limiting initial condition cannot be established. Future plant analyses (for example the reload licensing analyses) will consider the full allowable range of the initial condition.
- B. The results are sensitive to the initial condition and a basis for the limiting initial condition can be established. Future plant analyses (for example the reload licensing analyses) will consider the parameter at its limiting initial condition.
- C. The results are not sensitive to the initial condition and a nominal initial condition will be assumed for the parameter.

Large and small break LOCA calculations were used to categorize the initial conditions as described above. The characterization analysis bases are described in Table 8.3-4. [[
]] The results of the sensitivity studies are discussed in the next section.

Table 8.3-4 Allowable Operating Range Specification Basis for BWR/2 LOCA

Quantity	Control Basis	Range	Analysis Basis
Total Core Power	Plant Technical Specifications restrict the maximum operating core thermal power. For a given core flow, the maximum and minimum core power are controlled through operation within the analysis basis power/flow map.	Initial power/flow conditions will be chosen to bound the operating envelope.	Calculations will be for the rated power and flow conditions.
Total Core Flow	For a given core power, the maximum and minimum core flow are controlled through operation within the analysis basis power/flow map.		
Feedwater Temperature	The feedwater temperature and core power determine the feedwater and steam flows. Some plants have analyzed for additional operating flexibility (Final Feedwater Temperature Reduction or Feedwater Heater Out-of-Service).	[[
Steam Dome Pressure	Plant Technical Specifications restrict the maximum operating dome pressure. The minimum dome pressure is governed by turbine operational control.		
Downcomer Water Level	Plant operates between the L4 and L7 alarm setpoints.]]

Table 8.3-4 (cont'd) Allowable Operating Range Specification Basis for BWR/2 LOCA

Quantity	Control Basis	Range	Analysis Basis
Core Loading Pattern and Total Core Exposure	A reference core loading pattern is defined for each reload cycle. Acceptable deviation from the reference core is defined in GESTAR Section 3.4.2 [20].	[[
Axial Power Distribution	There is no restriction on axial power distribution as long as plant thermal limits are met.		
Radial Power Distribution	There is no restriction on radial power distribution as long as plant thermal limits are met.		
Local Peaking Distribution in High Power Bundles	There is no restriction on local peaking distribution as long as plant thermal limits are met.		
Control Rod Pattern (control rod density)	There is no restriction on control rod pattern as long as plant thermal limits are met.		
Peak Bundle Exposure	There is no restriction on bundle exposure distribution as long as plant thermal limits are met.]]

Table 8.3-4 (cont'd) Allowable Operating Range Specification Basis for BWR/2 LOCA

Quantity	Control Basis	Range	Analysis Basis
Pellet Exposure	Peak pellet power is restricted as a function of pellet exposure.	[[
Steam Flow	Derived from core thermal power and feedwater temperature.]]

8.3.4.2 Allowable Operating Range Results

Axial Power Shape

A bottom peaked axial power shape is expected to be limiting for a DBA because the quenching of the rods proceeds downwards from the top. [[

]]

Operating Conditions on the Power/Flow Map

DBA and small break LOCA calculations were performed at the rated conditions on the power/flow map. [[

]]

Core Average Exposure

From a LOCA perspective, the core average exposure determines the core average gap conductance (stored energy) and decay heat. [[

]]

Peak Pellet Exposure

Based on sensitivity studies performed for BWR/4 plants, [[

]]

Radial Power Distribution

The radial power distribution [[
]]

Steam Dome Pressure

[[
]]

Feedwater Temperature

[[
]]

Initial Downcomer Level

The initial downcomer level [[
]]

Table 8.3-5 summarizes the results of the characterization of the plant initial conditions and operating ranges.

Table 8.3-5 Allowable Operating Range Characterization for BWR/2 LOCA

Quantity	Category	Analysis Basis
Total Core Power	The results are sensitive to the initial conditions and a basis for the limiting initial condition can be established.	[[
Total Core Flow		
Feedwater Temperature	[[
Steam Dome Pressure		
Downcomer Water Level		
Core Loading Pattern and Total Core Exposure		
Axial Power Distribution		
Radial Power Distribution		
Pellet Exposure]]]]

8.3.4.3 Initial Conditions Uncertainty

As described in Section 6.2, the initial state of the plant is monitored through the use of plant sensors or on-line calculations based on plant sensors. Because of instrument or simulation uncertainty, the actual plant conditions may vary from the indicated values. The LOCA results are characterized in the following manner:

- A. The results are sensitive to the uncertainty in the initial condition and the uncertainty in the initial condition will be included in the statistical analysis.
- B. The results are not sensitive to the uncertainty in the initial condition and the uncertainty does not need to be taken into account.

The uncertainties in the initial condition were evaluated and characterized for each baseline event. The characterization analysis bases are described in Table 8.3-6.

**Table 8.3-6 Basis for Initial Condition Uncertainty Characterizations for BWR/2
 LOCA**

Quantity	Uncertainty Basis	Analysis Basis
Total Core Power	In demonstration calculations, a 2% uncertainty is assumed.	[[
Total Core Flow	Total $\sigma=2.5\%$ per Reference [32].	
Feedwater Temperature	Total [[]] per Reference [32].	
Steam Dome Pressure	Total [[]] per Reference [32]	
Downcomer Narrow Range Water Level	Total [[]] of a 2 meter instrument range (typical).	
Bundle Power	Total [[]] per Reference [32]	
Nodal Power	[[]] per Reference [32]]].

8.3.4.4 Initial Condition Uncertainty Results

[[

]] The

characterization of the initial condition uncertainties for purposes of the present analysis is given in Table 8.3-7.

Table 8.3-7 Initial Condition Uncertainty Characterizations for BWR/2 LOCA

Quantity	Category	Characterization/Analysis Basis	
Total Core Power	[[
Total Core Flow			
Feedwater Temperature			
Steam Dome Pressure			
Downcomer Water Level			
[[
]]]]	

8.3.4.5 Plant Parameters

As described in Section 6.3, critical plant parameters will be [[]] This process is described in the procedure that defines the critical OPL for the ECCS/LOCA analysis. This assumption does not preclude the future use of statistically based plant parameters or setpoints. It will require the determination of nominal values, accounting for instrument drift and uncertainties and the incorporation of these uncertainties within the application methodology.

Section 6.3.2 describes a study on the effect of scram speed on the LOCA response. [[]]

]]

Drywell pressure and ECC temperature (suppression pool temperature) are treated as plant parameters or boundary conditions for ECCS/LOCA analysis because they involve interactions with the containment. It was shown in Section 5.1 that [[]]

]]

8.3.4.6 Summary of Initial Conditions and Plant Parameters

The results from the initial conditions and plant parameter sensitivity evaluations described above form the basis of the plant specific analysis process. The following analysis procedures have been adopted on the basis of these results:

- [[]]

]]

[[

]]

Figure 8.3-14 Effect of BWR/2 Containment Boundary Conditions

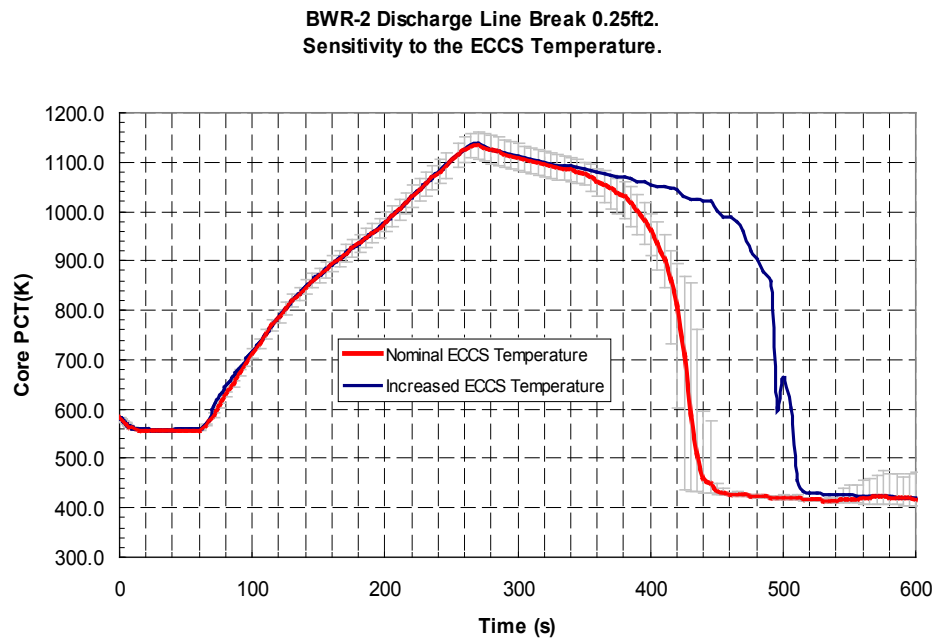


Figure 8.3-15 Effect of BWR/2 ECCS Temperature

8.3.5 Break Spectrum Results for BWR/2

A recirculation line break spectrum analysis, consisting of a set of LOCA calculations for a range of break sizes up to and including the double-ended guillotine break (DBA), was performed for a BWR/2. Additional analyses were performed for double-ended breaks in a main steam line, CS line and a feedwater line. [[

]] The initial conditions correspond to the results of the characterization basis discussed in Section 8.3.4 and shown in Table 8.3-2. The model parameters are set to their nominal values (PIRT multipliers set to 1) except [[

]] Loss-of-offsite power, causing a trip of the recirculation pumps, was assumed at time zero. The scram time is obtained from the earlier of the High Drywell Pressure or L3 signals as discussed in Section 6.3.1. MSIV closure was initiated on L1.

In BWR/2s, the primary ECCS component used to mitigate a large-break LOCA is CS. The CS system is single-failure proof. One Emergency Condenser is attached to the broken loop. Conservatively, both emergency condensers are assumed to be unavailable. Three of the six ADS valves are assumed to be available. The failed and available systems are shown in Table 8.3-8. The plant parameters (e.g., setpoints, ECC flow capacity) were set at their analytic limits. [[

]]

8.3.5.1 Recirculation Line Breaks on Discharge Side of the Recirculation Pump

The scram time following a recirculation line break is shown as a function of break size in Figure 8.3-16. For break sizes larger than approximately 0.01 m^2 , the High Drywell Pressure signal occurs before the downcomer narrow range level drops to Level 3. For breaks smaller than 0.01 m^2 , the scram is caused by the Level 3 trip. Figure 8.3-17 through Figure 8.3-22 show the plant transient response for different break sizes in the discharge side of the recirculation line ranging from 0.0046 m^2 to a double-ended guillotine break (0.33 m^2 on each side). All breaks smaller than the DBA are modeled as split breaks, with flow from both sides of the recirculation line feeding the break flow.

Figure 8.3-17 shows the reactor vessel pressure response for small-to-intermediate breaks ranging from 0.0046 to 0.037 m^2 . Following the MSIV closure on Level 1, the pressure increases for smaller breaks until the ADS valves open. The ADS actuation is also on Level 1 with a timer delay of 120 s. Figure 8.3-18 shows the corresponding PCT response for the small breaks. For the smallest break, there is relatively less significant heatup in the core until the flashing due to the ADS subsides. As the break size increases, an earlier heatup is seen as the core inventory begins to deplete before the start of the depressurization. This early heatup is quenched by the lower plenum flashing-induced core flow. A second period of cladding heatup

begins after the ADS depressurization rate subsides. This later heatup determines the PCT for the transient.

Figure 8.3-19 shows the reactor vessel pressure response for intermediate-to-large breaks ranging in break area from 0.037 to 0.185 m². The 0.185 m² break is shown for reference to the next figure. For these break sizes, the pressure remains close to turbine-controlled pressure following MSIV closure. The downcomer level drops to the elevation of the suction of the recirculation line before the ADS valves open. The uncovering of the recirculation line suction leads to vapor discharge from the reactor vessel and a faster depressurization rate. The depressurization rate increases further as the ADS valves open. The timing of the ADS is earlier as the break size increases but ADS actuation is of less importance for the intermediate breaks (as compared with the small breaks) because of the early depressurization following the break uncovering. Figure 8.3-20 shows the PCT response for the intermediate-to-large size breaks. The earlier depressurization for the larger breaks mitigates the core inventory loss before ADS activation and earlier activation of the CS limits the core heatup.

As the break size increases beyond 0.185 m², the effect of the ADS diminishes. Figure 8.3-21 shows the pressure response for large breaks in the range 0.185 m² to the DBA. For large breaks the reactor vessel depressurizes rapidly without a need for the ADS valves to supplement the blowdown. The reactor vessel depressurizes early because of the loss of fluid through the break. Figure 8.3-22 shows the PCT responses. Up to a point, the PCT continues to decrease as the break size increases because the earlier activation of the CS is more important than the increased rate of inventory loss. For the larger breaks, however, the CS flow addition cannot compensate for the increased break flow and a late heatup occurs. The large loss of inventory dominates the temperature rise. Slightly earlier activation of the CS is not sufficient to offset the early heatup and the PCT increases with break size. For the large breaks, a first peak PCT also occurs early in the transient because of the mismatch between the power and core flow. The first peak PCT is not limiting and is partially quenched by the lower plenum flashing that follows the uncovering of the break.

The break spectrum results for discharge breaks are summarized in Figure 8.3-23. Results are shown [[

]]

8.3.5.2 Recirculation Line Breaks on Suction Side of the Recirculation Pump

A break spectrum analysis was also performed for breaks on the suction side of the recirculation pump. For small-to-intermediate break sizes, discharge breaks resulted in higher PCT than suction breaks of the same size. For larger break sizes, the suction breaks are higher than the corresponding discharge breaks. For the DBA, discharge DBA resulted significantly higher than the suction DBA. Figure 8.3-23 compares the suction break spectrum with the discharge break spectrum.

8.3.5.3 Non-Recirculation Line Breaks

Breaks in the recirculation line are limiting for BWRs because of the range of sizes and low location relative to the top of the core. Breaks in other lines were also examined to confirm this expectation. These included guillotine breaks of a main steam line, a CS line and a feedwater line. All cases assumed an Emergency Condenser failure. Figure 8.3-24 shows the pressure response for the three cases. The steam line break with its large volumetric and enthalpy flow depressurizes the vessel very rapidly. The ADS is inconsequential for the steam line break. The feedwater line break is also a large break that rapidly transitions to a steam break. The CS break is smaller (0.0251 m²) with a break flow that is initially two-phase. The vessel does not depressurize significantly for about 30 s following MSIV closure. At this time, the level in the upper plenum uncovers the CS sparger and the break flow becomes essentially single phase vapor. The vapor flow begins to depressurize the vessel and depressurization is aided by the opening of the ADS valves at about 250 s.

The PCT responses for the non-recirculation line breaks are shown in Figure 8.3-25. The steam line break is benign as the level in the shroud swells up and keeps the core covered. The PCT does not exceed the initial operating cladding temperature. The feedwater line break has a similar response. The CS line break is located above the elevation of the core so its effect is milder than a comparably sized recirculation line break. Uncovery of the core is precluded and the PCT is limited to the initial cladding temperature. Table 8.3-9 summarizes the PCTs obtained for the BWR/2 for the various cases discussed in this section. For break locations in the recirculation line, the maximum PCT and the corresponding break size have been tabulated.

8.3.5.4 Peak Local Oxidation and Core Average Oxidation

LOCAs in BWR/2 plants result in higher PCTs than for jet pump plants and, for large breaks, the core is not reflooded and the heatup persists for a longer period. Consequently, cladding oxidation due to metal-water reaction becomes a design consideration. Two parameters are calculated for comparison to licensing limits: the peak local oxidation as a fraction of the original cladding thickness; and the core average oxidation volume as a fraction of original cladding volume. Figure 8.3-26 shows the calculated values of these parameters for the BWR/2 DBA. The oxidation parameters are well below the licensing limits of 17% for local oxidation and 1% for core average oxidation.

Table 8.3-8 BWR/2 Single Failures and Available ECCS

Failure	ECC Systems Available
Emergency Condenser	2 CS; 3 ADS valves

Table 8.3-9 BWR/2 PCT Summary

Break Location	Single Failure	Limiting Break Area (m ²)	PCT (K)
Recirculation Line Suction	EC	0.669	1,218
Recirculation Line Discharge	EC	DBA	1,311
Steamline ⁽¹⁾	EC	0.2356	[[
CS Line ⁽¹⁾	EC	0.0251	
Feedwater Line ⁽¹⁾	EC	0.0673]]

Notes:

- ⁽¹⁾ These cases were performed with an earlier version of the code and were not repeated because the results are not close to become limiting.

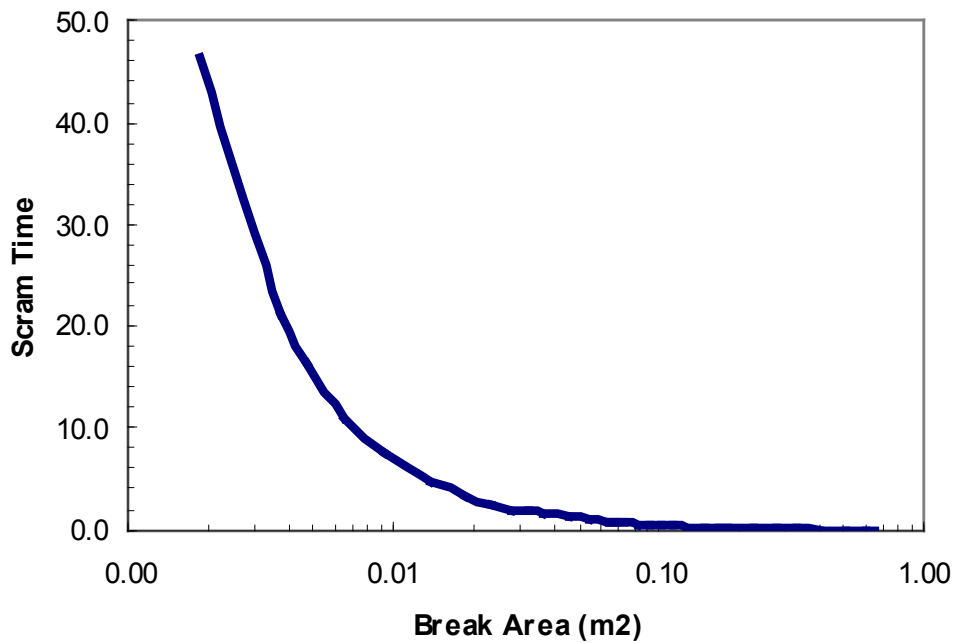


Figure 8.3-16 BWR/2 Scram Time vs. Break Size

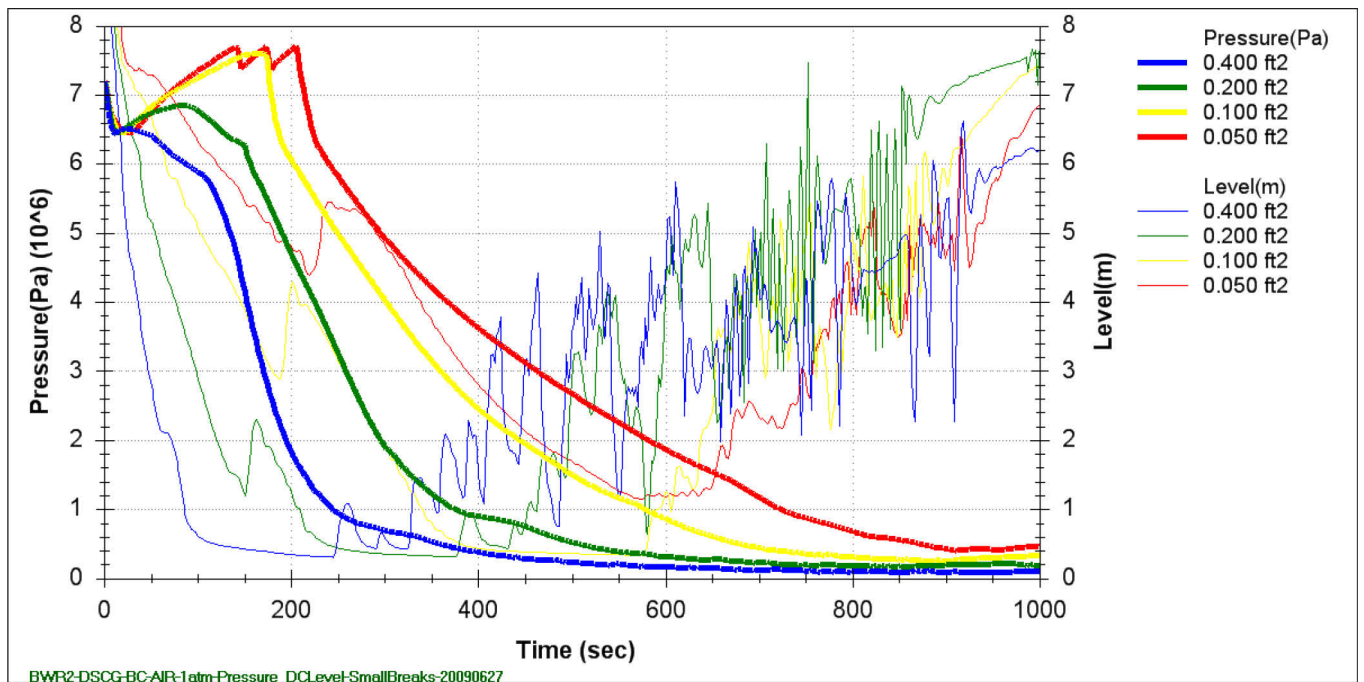


Figure 8.3-17 Pressure and DC Level Response for BWR/2 Small Breaks

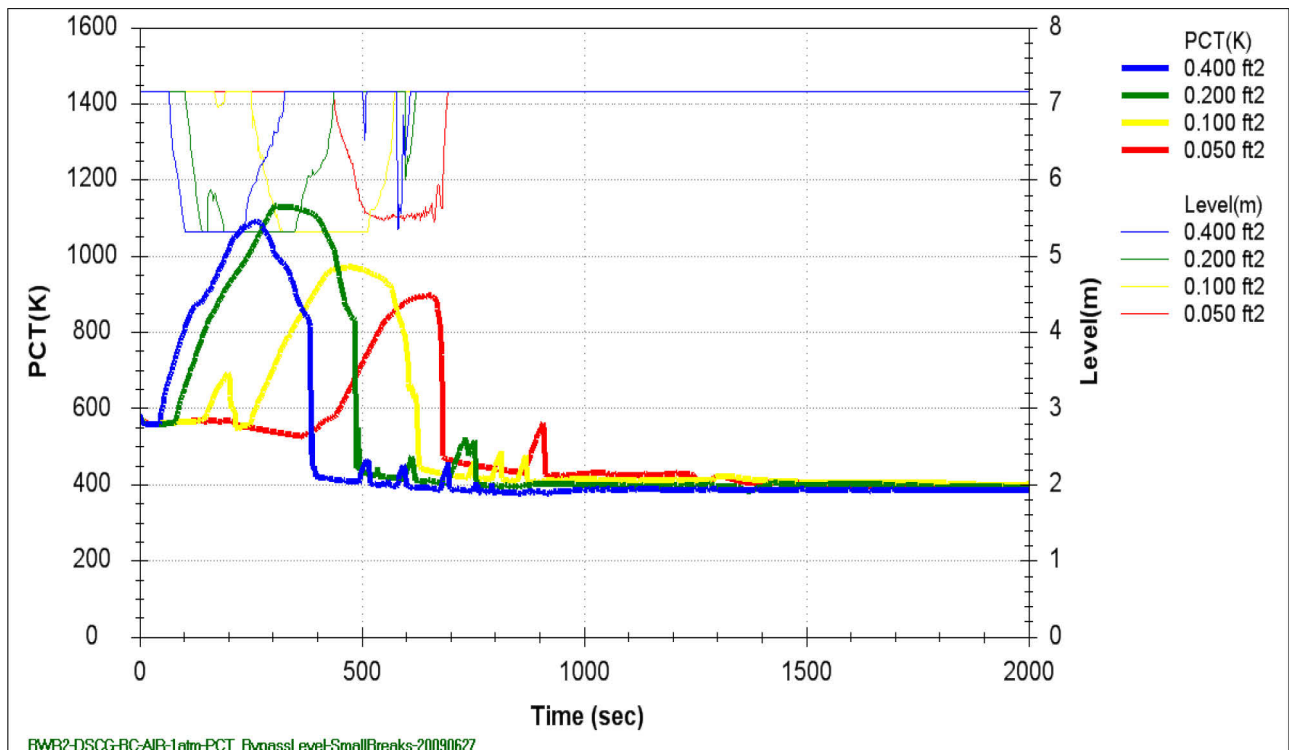


Figure 8.3-18 PCT and Bypass Level Response for BWR/2 Small Breaks

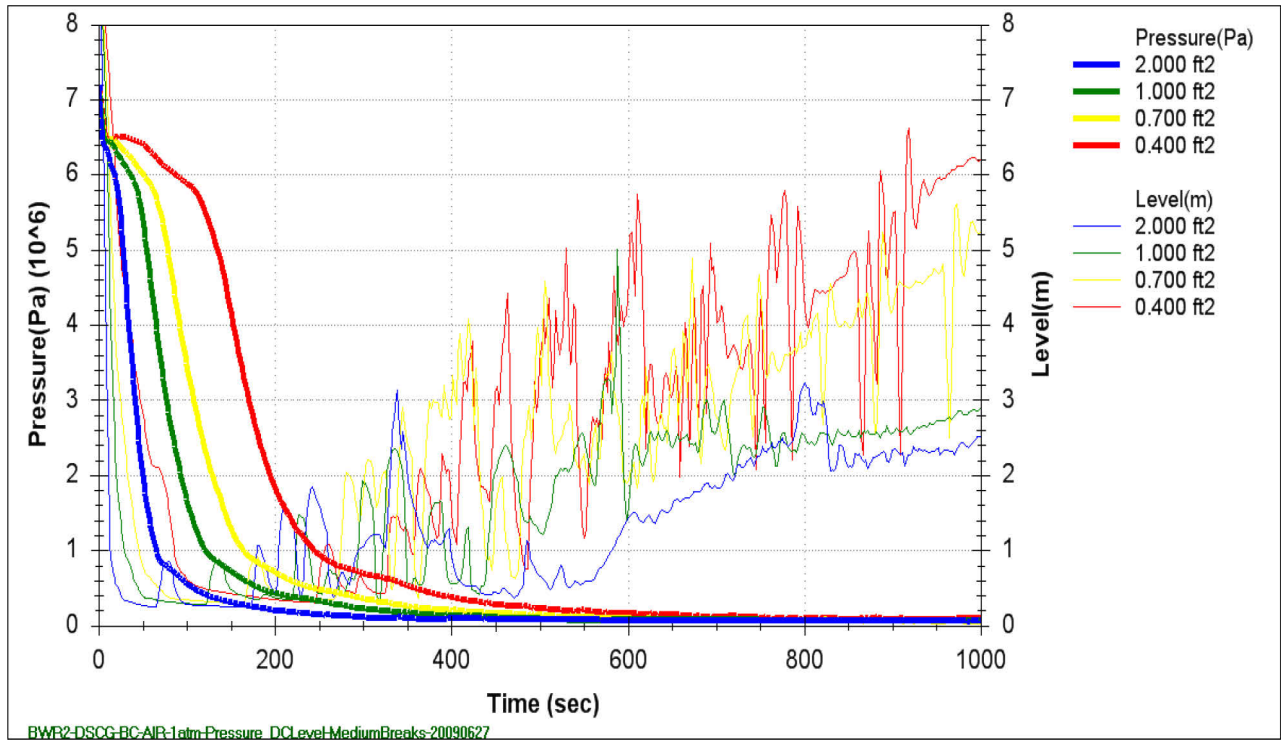


Figure 8.3-19 Pressure and DC Level Response for BWR/2 Intermediate Breaks

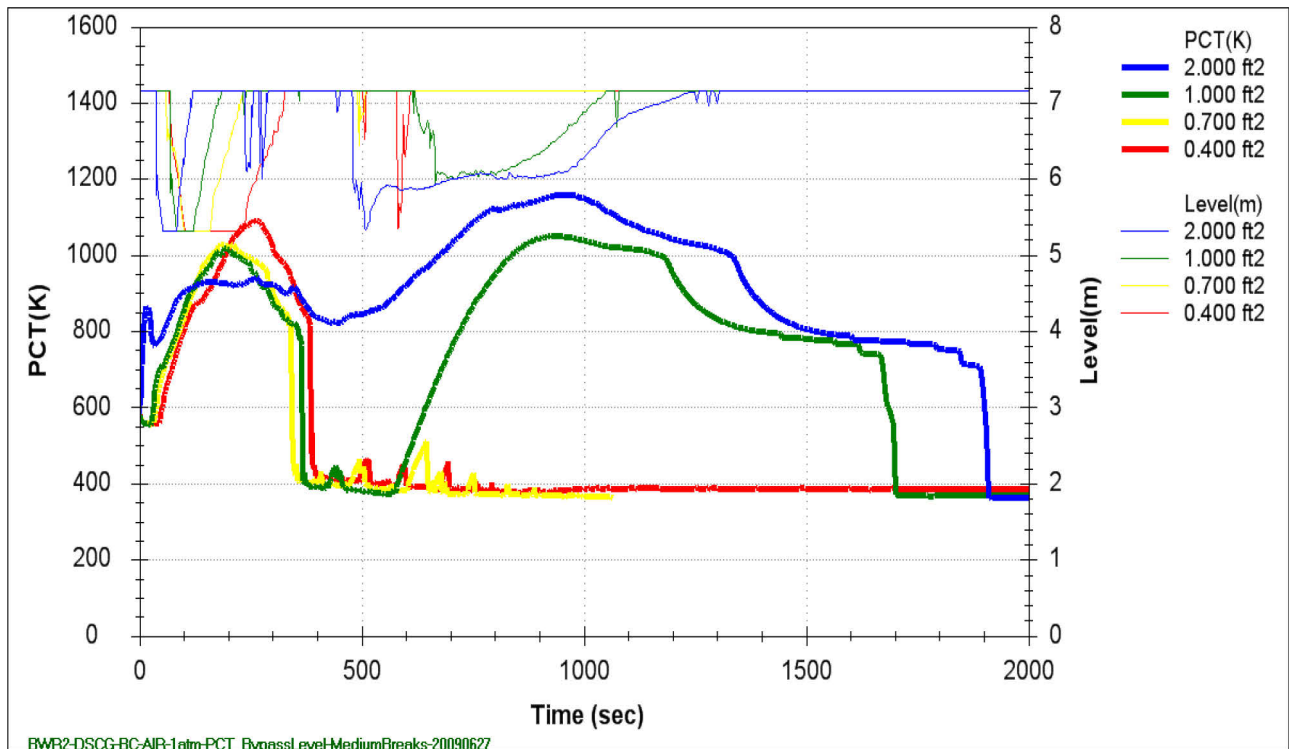


Figure 8.3-20 PCT and Bypass Level Response for BWR/2 Intermediate Breaks

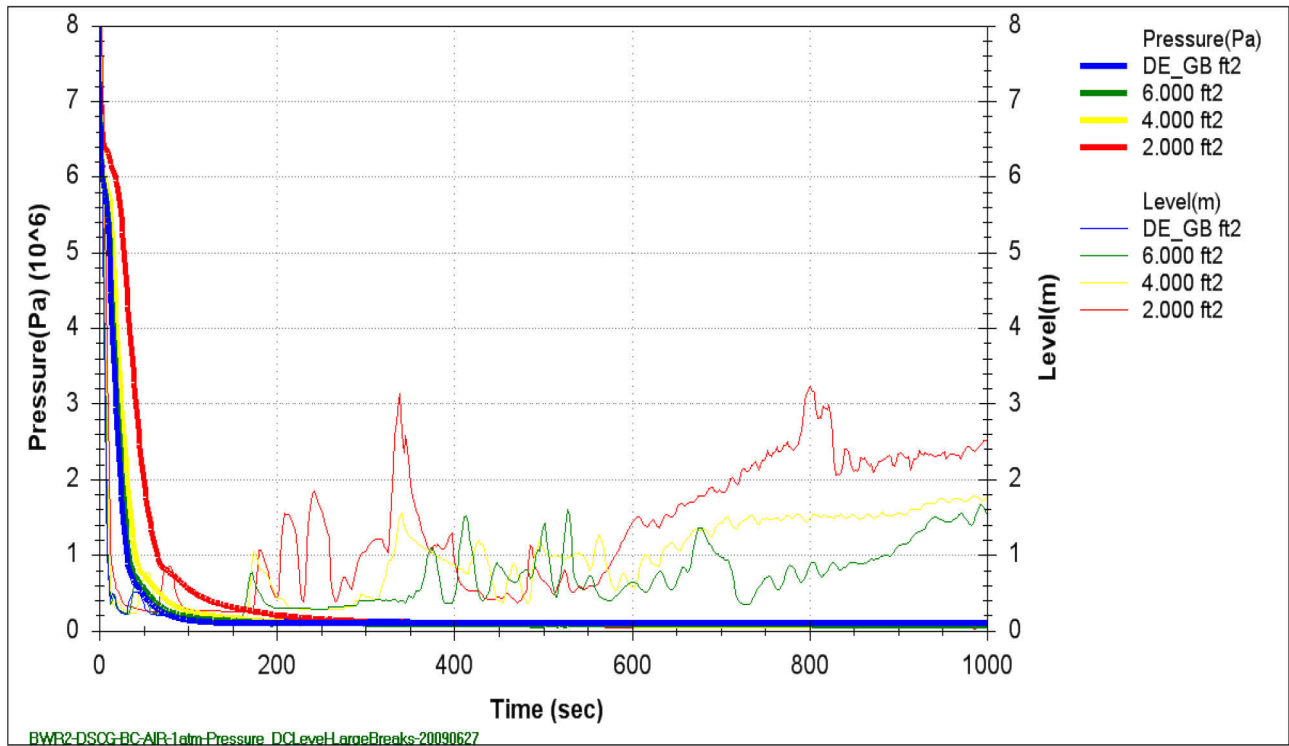


Figure 8.3-21 Pressure and DC Level Response for BWR/2 Large Breaks

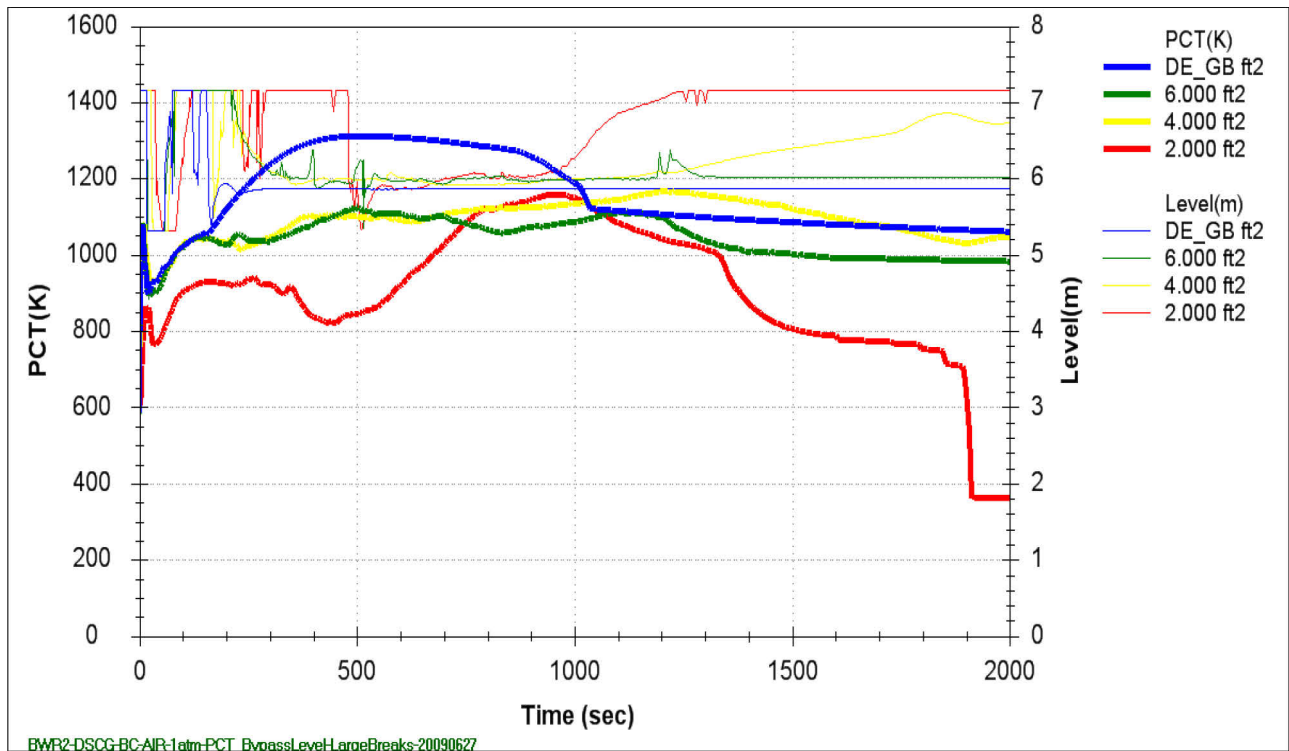


Figure 8.3-22 PCT and Bypass Level Response for BWR/2 Large Breaks

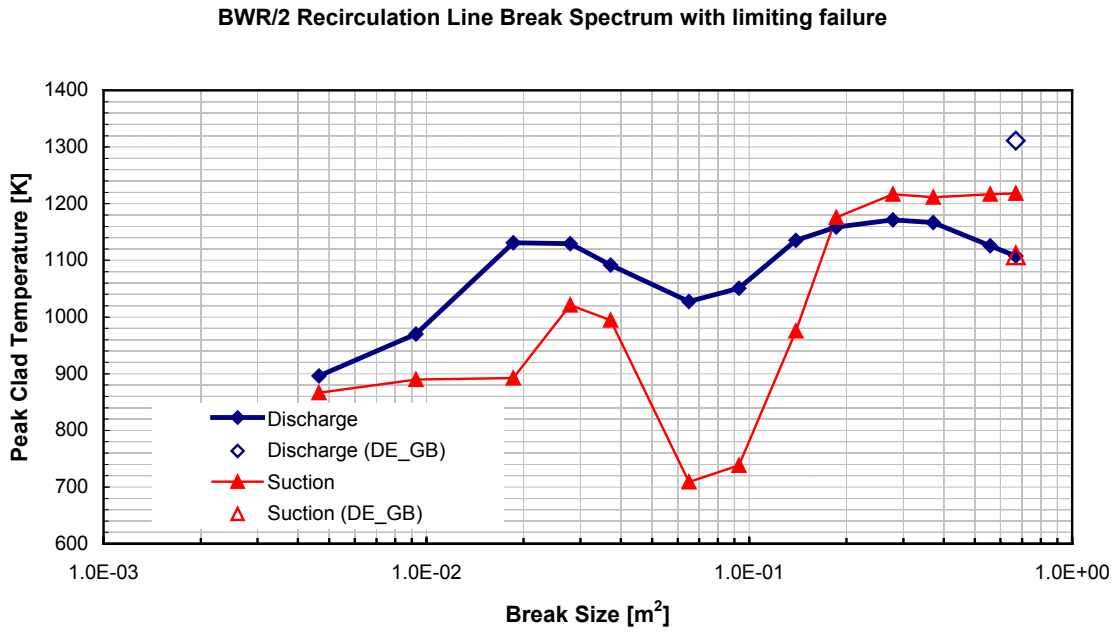


Figure 8.3-23 Break Spectrum for BWR/2 Discharge and Suction Side Breaks

[[

]]

Figure 8.3-24 Pressure Response for BWR/2 Non-Recirculation Line Breaks

[[

]]

Figure 8.3-25 PCT Response for BWR/2 Non-Recirculation Line Breaks

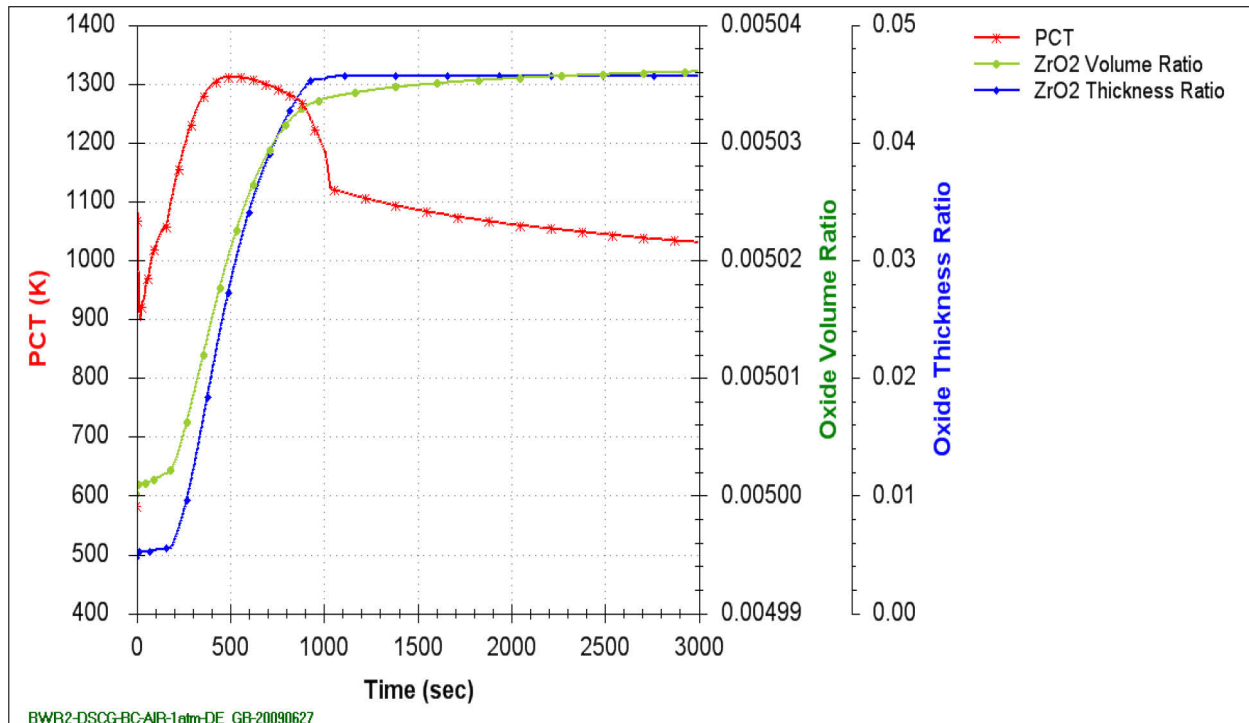


Figure 8.3-26 Oxidation for BWR/2 Limiting LOCA (DBA)

8.3.6 Statistical Results for BWR/2 LOCA

A statistical analysis for a number of breaks varying from small-break to double-ended guillotine break on the discharge side of the pump is carried out by performing a set of 59 trials. In each trial, random draws were made from the probability density functions for the set of previously identified model and plant parameters (Table 5.1-2 and Table 8.3-10).

8.3.6.1 DBA/Large-Break LOCA Results

Figure 8.3-27 through Figure 8.3-34 show the results of the Monte Carlo analysis for a DBA on the discharge side of the pump. 59 LOCA trials were made for this break size. The distribution of PCT for the 59 trials is plotted in Figure 8.3-27. The mean value of the PCT was 1310 K with a standard deviation of 63 K. The individual trials for PCT (in multiples of the standard deviation) are shown in Figure 8.3-28. The distribution of overall PCTs for the large break satisfies the condition for normality. Based on a normal distribution with a sample size of 59, the 95th percentile with high probability value of PCT is estimated as:

$$PCT_{95/95} = PCT_{Mean} + 2.024 * \text{Std Deviation} = 1438 \text{ K.}$$

The First Order Statistic for the distribution (highest trial) was 1448 K.

The distribution of peak oxidation thickness for the 59 trials is plotted in Figure 8.3-29. This distribution satisfies the requirements for normality. The mean value of the peak oxidation thickness was 0.045 with a standard deviation of 0.018. The individual trials for peak cladding oxidation thickness (in multiples of the standard deviation) are shown in Figure 8.3-30. As the distribution is normal, the peak oxidation fraction with 95% content and at 95% confidence is calculated as:

$$MLO_{95/95} = MLO_{Mean} + 2.024 * \text{Std Deviation} = 0.0814 = 8.14\%.$$

This First Order Statistic for the maximum local oxidation is 0.101 (10.1%). The calculated value for $MLO_{95/95}$ of 8.14% is below the licensing limit of 17%.

The distribution of core average oxidation volume fraction for the 59 trials is plotted in Figure 8.3-31. As for the oxidation thickness, the distribution is skewed and does not satisfy the requirements for normality. The mean value of the oxidation volume fraction is 5.03E-5 with a standard deviation of 2.44E-5. The individual trials for oxidation volume fraction (in multiples of the standard deviation) are shown in Figure 8.3-32. As the distribution is not normal, the First Order Statistic is used to bound the oxidation volume fraction with 95% content and at 95% confidence. This yields a value of 5.12E-3, well below the licensing limit of 0.01.

The range of the PCT transient was also plotted for the trials. Figure 8.3-33 shows a composite plot with the range of variations in the temperature transients. Also plotted are the “Nominal” calculation with all the variables set to their expected values, and an “Average” calculation. The latter is obtained by averaging the results of the 59 trials through the transient. The Nominal and Average temperatures are relatively close. The averaging process takes out some of the oscillations seen in the Nominal transient.

The range of the peak oxidation transient for the 59 trials is plotted in Figure 8.3-40. The non-linearities associated with metal-water reaction and the enhancement due to perforations at the more severe conditions result in a skewed distribution. The Average value of the oxidation fraction is therefore slightly higher than the Nominal value.

8.3.6.2 Small-Break LOCA Results

Figure 8.3-35 through Figure 8.3-40 show the results of the Monte Carlo analysis for the small break on the discharge side of the pump. 59 LOCA trials were made for this break size. Figure 8.3-35 shows the distribution of overall PCTs in the core. The mean value of the PCT for the 59 trials is 1161 K, with a standard deviation of 22 K. Results for the individual trials for the overall PCT are shown in Figure 8.3-36. The results are presented as deviations from the mean value in terms of the number of standard deviations. The distribution of overall PCTs for the small break satisfies the condition for normality. Based on a normal distribution with a sample size of 59, the 95th percentile with high probability value of PCT is estimated as:

$$PCT_{95/95} = PCT_{Mean} + 2.024 * Std Deviation = 1206 K.$$

The First Order Statistic for the distribution (highest trial) was 1202 K.

The distribution of peak cladding oxidation fraction for the 59 trials is plotted in Figure 8.3-37. This distribution is skewed even though the minimum requirement for normality is satisfied. The mean value of the peak oxidation fraction was 1.13E-02 with a standard deviation of 1.80E-03. The individual trials for peak cladding oxidation fraction are shown in Figure 8.3-38. These values are plotted as multiples of the standard deviation. Using the properties of a normal distribution,

$$Peak\ local\ oxidation_{95/95} = Peak\ local\ oxidation_{Mean} + 2.024 * Std\ Deviation = 1.50E-02$$

The First Order Statistic can also be used to bound the peak oxidation fraction with 95% content and at 95% confidence. This yields a value of 1.70E-02.

These values are negligible relative to the licensing limit of 0.17.

The core average volumetric oxidation fraction was also evaluated in the Monte Carlo trials. These values were miniscule and will not be discussed in detail. For small breaks, the rapid quenching of the core by reflooding eliminates oxidation as a concern.

As for the DBA, the range of the PCT transient was also plotted for the trials. Figure 8.3-39 shows a composite plot with the range of variations in the temperature transients. Also plotted are the “Nominal” calculation with all the variables set to their expected values, and an “Average” calculation. The latter is obtained by averaging the results of the 59 trials through the transient. During the heatup phase, the Nominal calculation and the Average are very close. Differences in quenching between the various trials lead to some deviation in the latter part of the transient.

The range of the maximum local oxidation (MLO) results for the 59 trials is plotted in Figure 8.3-40. These values of the oxidation fraction are very small. The small break transient is much

less severe than the DBA because of the early quenching of the core. The Average value of the oxidation fraction is only slightly higher than the Nominal value.

Figure 8.3-41 and Figure 8.3-42 summarizes the PCT and MLO results for various break sizes. DBA cases are limiting for both PCT and MLO results.

Table 8.3-10 Plant Parameters varied in BWR/2 Monte Carlo Trials

Parameter	Gaussian Distribution as Analyzed		Region	Comment
	Mean	Standard Deviation		
Core Power	1.0	2%	Core	Parameter is the multiplier on the thermal power.
Core Flow	1.0	2.5%	Core	Parameter is the multiplier on the rated flow.
[[
]]

[[

]]

Figure 8.3-27 PCT Distribution for BWR/2 Discharge DBA

[[

]]

Figure 8.3-28 Individual PCT Trials for BWR/2 Discharge DBA

[[

]]

Figure 8.3-29 Peak Oxidation Thickness Distribution for BWR/2 Discharge DBA

[[

]]

Figure 8.3-30 Peak Oxidation Thickness Trials for BWR/2 Discharge DBA

[[

]]

Figure 8.3-31 Core Average Oxidation Volume Distribution for BWR/2 Discharge DBA

[[

]]

Figure 8.3-32 Core Average Oxidation Volume Trials for BWR/2 Discharge DBA

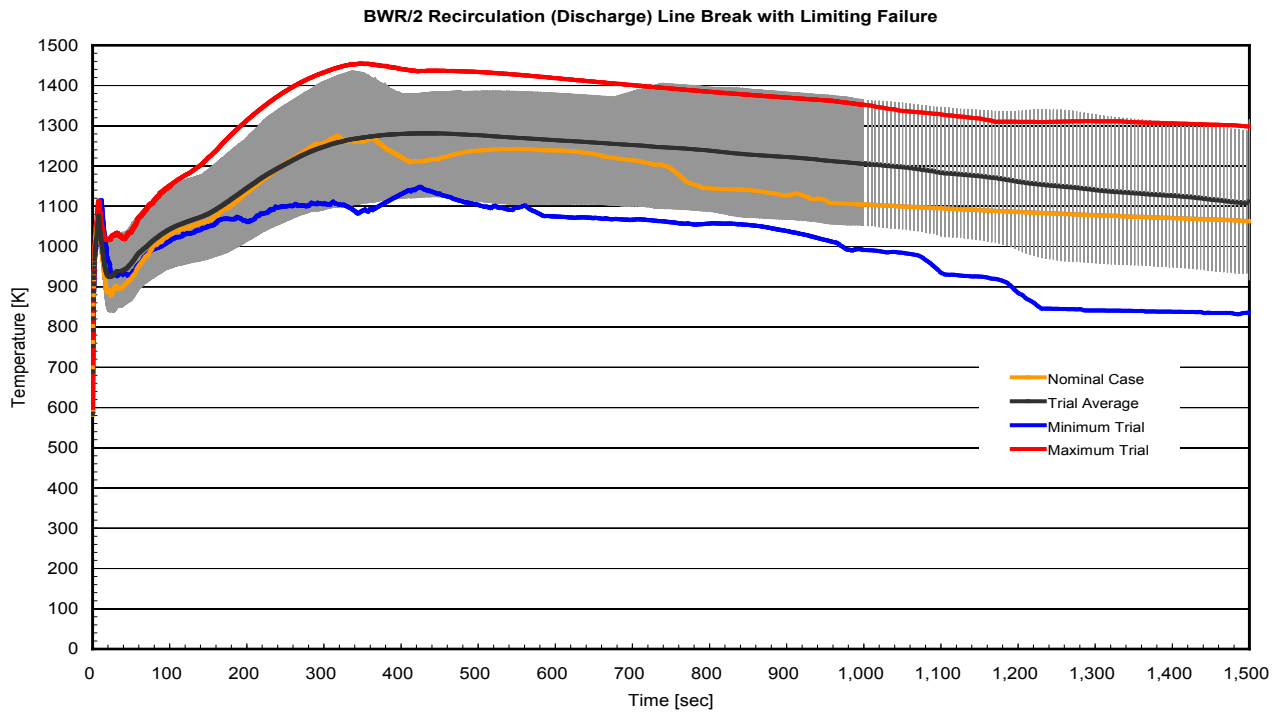


Figure 8.3-33 Range of Trials for PCT Transient for BWR/2 Discharge DBA

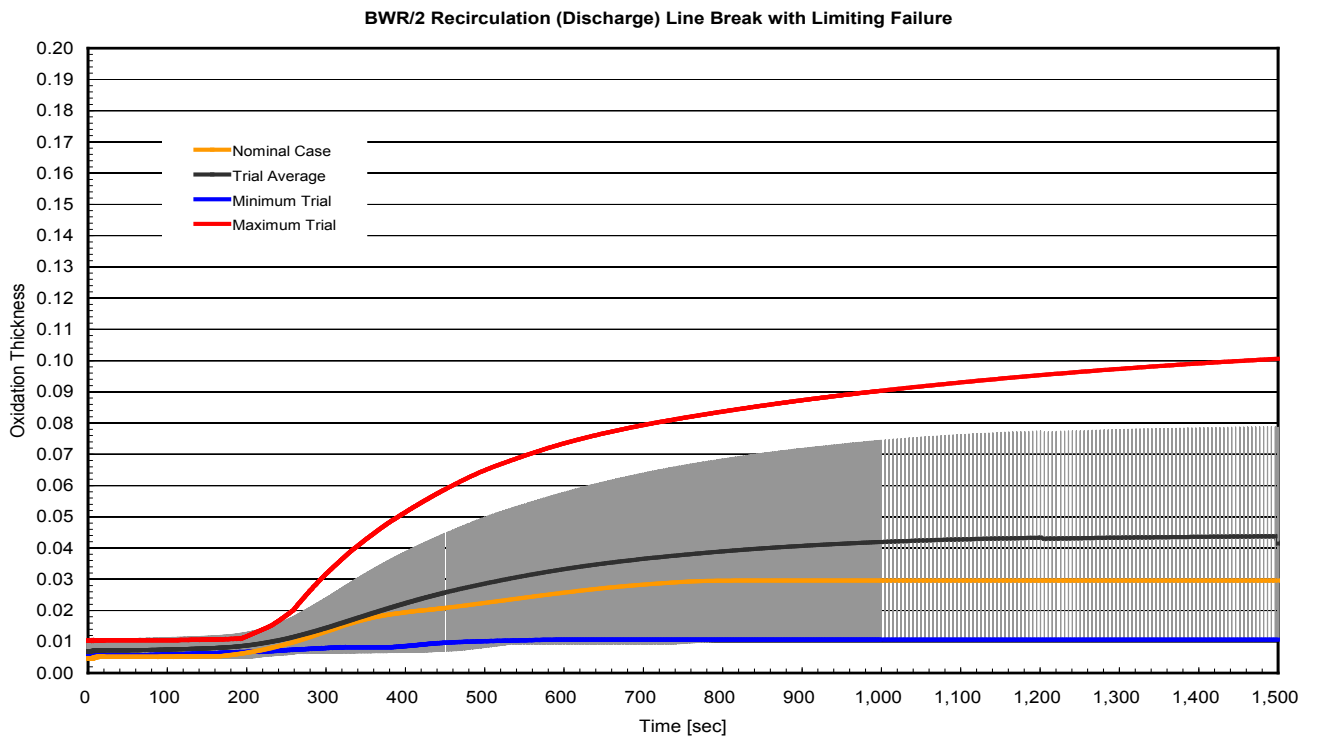


Figure 8.3-34 Range of Trials for Peak Oxidation Thickness Transient for BWR/2 Discharge DBA

[[

]]

Figure 8.3-35 PCT Distribution for BWR/2 Discharge Small Break

[[

]]

Figure 8.3-36 Individual PCT Trials for BWR/2 Small Break

[[

]]

Figure 8.3-37 Peak Oxide Thickness Distribution for BWR/2 Small Break

[[

]]

Figure 8.3-38 Individual Peak Oxide Thickness Trials for BWR/2 Small Break

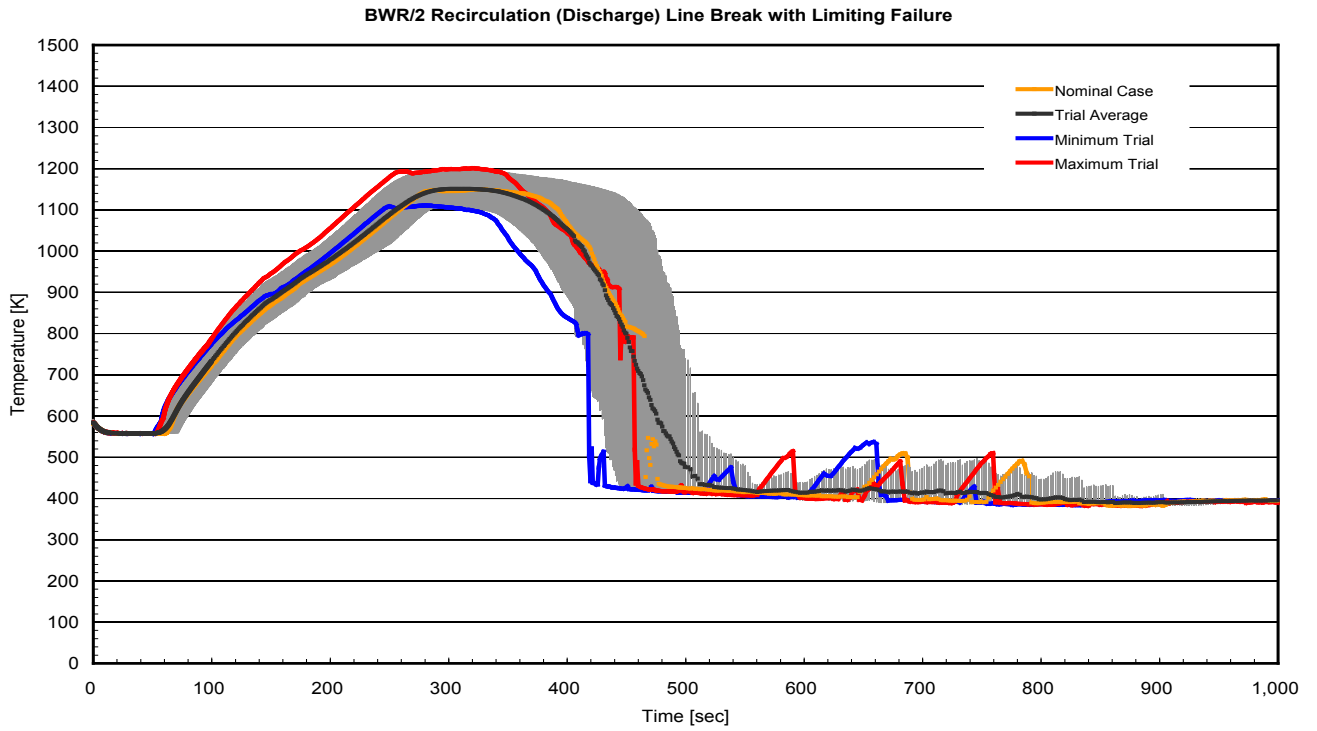


Figure 8.3-39 Range of Trials for PCT Transient for BWR/2 Small Break

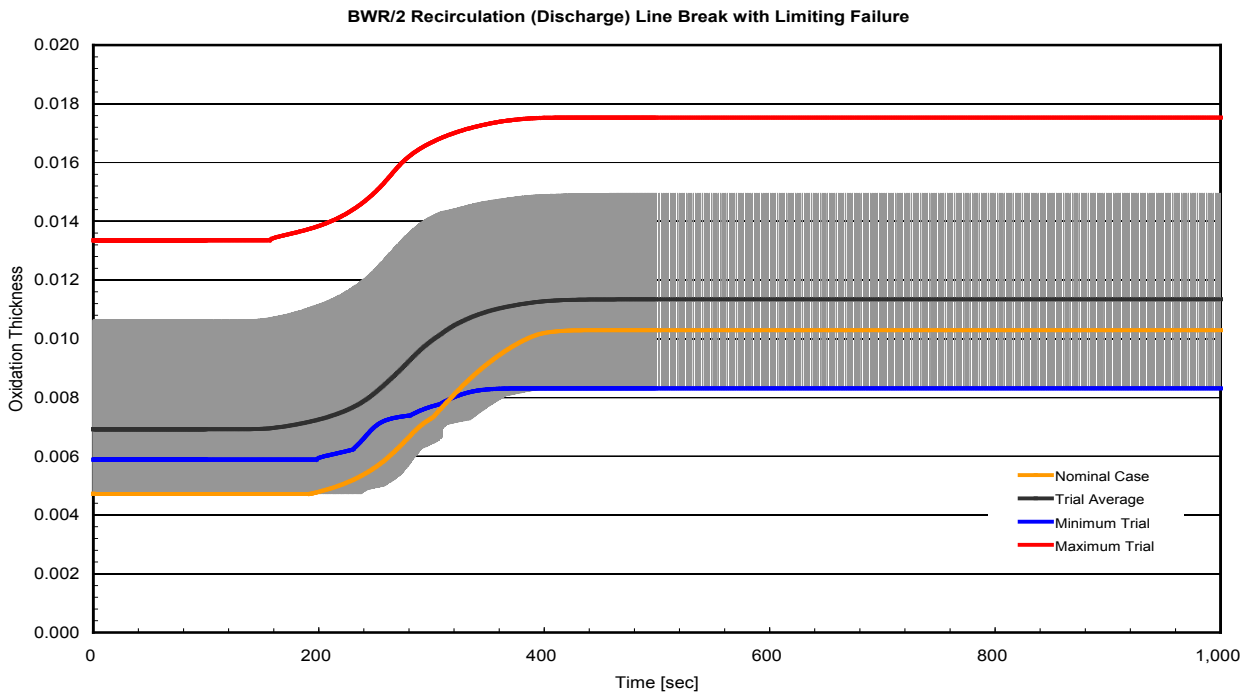


Figure 8.3-40 Range of Trials for Peak Oxide Thickness Transient for BWR/2 Small Break

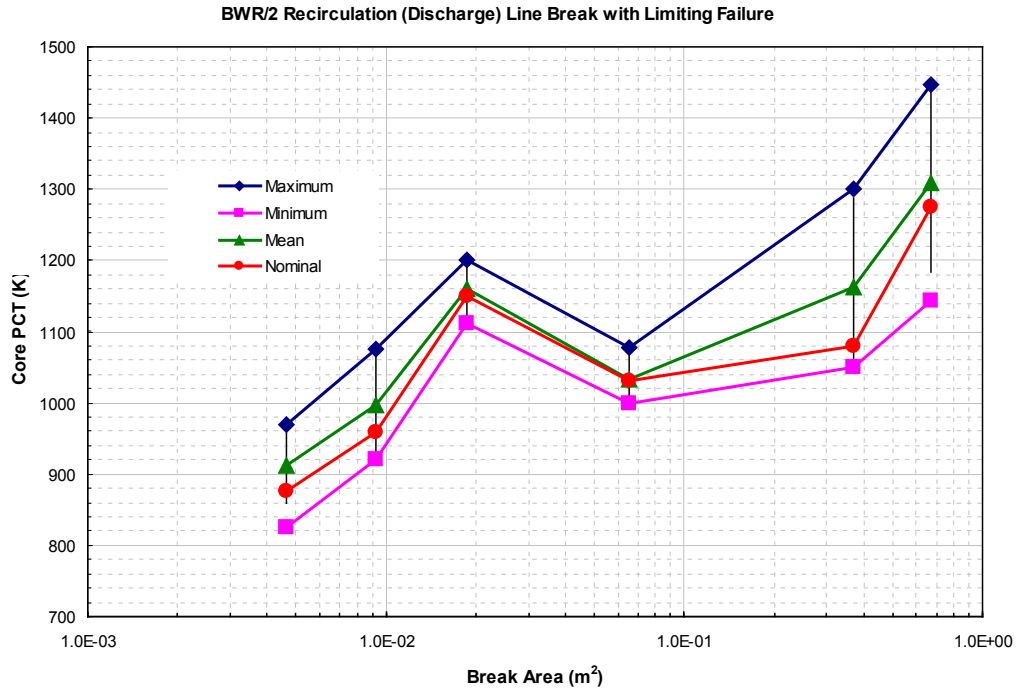


Figure 8.3-41 BWR/2 Break Spectrum with Uncertainties – PCT Results

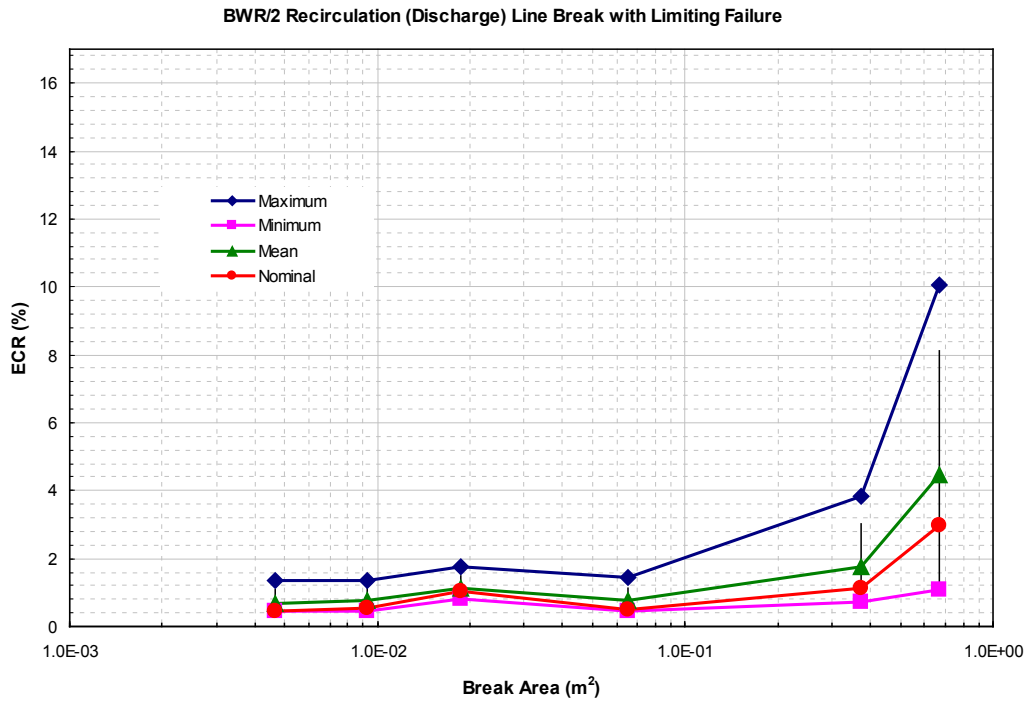


Figure 8.3-42 BWR/2 Break Spectrum with Uncertainties – MLO Results

9.0 METHODOLOGY APPLICATION

This section provides additional discussion on some of the methodology application aspects. These discussions are to clarify the intended use of the evaluation methodology in analyses.

9.1 ANALYSIS PROCESS SUMMARY

In this report, demonstration analyses are presented along with additional sensitivity studies that helped in making the methodology decisions. The demonstration cases are illustrative and do not represent any particular plant. Actual analysis of a given plant will employ plant-specific input modeling and plant-specific break spectrum calculation. The uncertainty analysis and post-processing of results are built on break spectrum studies. The overall analysis process can be depicted by the flowchart given in Figure 9.1-1.

The process begins with preparation of the plant-specific basedeck. Major inputs to this step are plant geometry data from the qualified database, plant licensing operating parameters for LOCA/ECCS performance evaluation, analysis initial conditions, fuel-specific TRACG channel model, and fuel performance data.

The next major step in the analysis process is the break spectrum studies. The primary goal of this step is to determine the limiting break for further uncertainty analysis. The break spectrum studies are primarily centered on the recirculation line breaks for external pump and jet pump type plants. The appropriate single failure assumption depending on the break analyzed is applied. Additional studies are carried out, if needed, to verify that no other single failure, break location and size, and combination of uncertainty contributors will result in a higher PCT than the limiting break case.

The purpose of the uncertainty analysis, the following step, is to quantify the uncertainties associated with the analysis. For jet pump plant LOCA analysis, [[

]] For the external pump
plant LOCA analysis, [[

]] The break spectrum studies
combined with sensitivities to the uncertainty contributors presented in this LTR indicate that intermediate breaks are more limiting for jet pump design, whereas the double-ended guillotine is the limiting case for external pump design plants. Although the limiting break size is expected to differ on a plant-specific basis, the overall trends in break spectrum are expected to be similar for the similar designs. Each LOCA analysis will include plant-specific break spectrum calculations.

The statistical analysis of uncertainty quantification relies on well-established techniques. [[

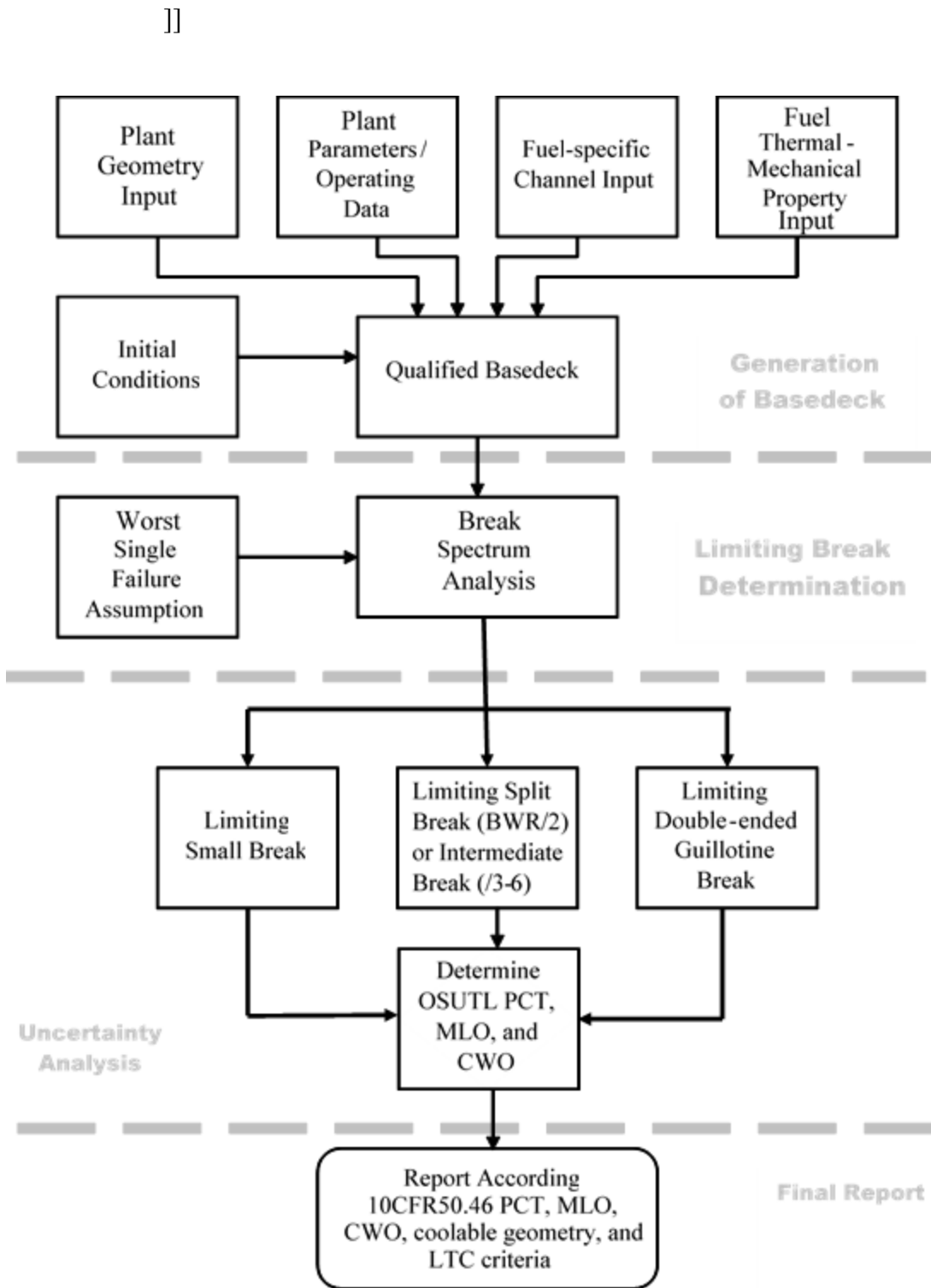


Figure 9.1-1 LOCA Analysis Process Flowchart

9.2 APPLICABILITY OF STATISTICAL ANALYSIS

The applicability of the statistical analysis covers a wide range of conditions; therefore, small variations in these conditions would not invalidate the overall trends and the combined effects of individual uncertainty contributors. A small change in the input and analysis conditions would typically have negligible effect in the results of the statistical analysis. This section explains the process of evaluating the changes and how the effect of a change can be quantified when there is an uncertainty associated with the analysis results.

The process flowchart to determine the applicability of the uncertainty analysis is depicted in Figure 9.2-1. The types of changes that can potentially introduce effects into the analysis are of three types: (1) an error or a change in the methodology; (2) a change in the plant configuration; or (3) new fuel introduction (NFI). For an error or a change in the methodology, the effect is assessed against the analysis uncertainty. According to the studies presented in Section 6.4, the analysis uncertainty, or the PCT resolution, is [[

]]

To quantify the effect of a change, [[

]]

If a change in the plant configuration affects the ECCS performance, such as a change in delay times, coolant delivery capacities, or available systems, an evaluation must be made to confirm validity of the break spectrum. This evaluation is necessary to confirm that the limiting break has not changed with different ECCS performance, and it can be carried out by running break sizes in the vicinity of the limiting break in the spectrum. After confirming or modifying the limiting break, uncertainty analysis will be performed by factoring in the change.

NEDO-33005-A Revision 1
Non-Proprietary Information – Class I (Public)

The break spectrum is predominantly a function of the ECCS and the overall system responses. For fuel designs changes that can potentially affect LOCA response, a subset of the break spectrum may be used to confirm validity. For the new fuel, a new uncertainty analysis will be performed.

The process path applied and the justification will be documented along with the results of the evaluation of the effects per the reporting rules of 10 CFR 50.46.

[[

]]

Figure 9.2-1 Analysis Change Evaluation Process Flowchart

9.3 BREAK SPECTRUM

The break spectrum profile for a particular plant is mainly dependent on the ECC system. Among the major parameters affecting the limiting break size are available systems per single failure assumption, amount of available coolant delivered based on ECCS performance, and system setpoints. Because many of these parameters differ from plant to plant, a plant-specific break spectrum is necessary for the first application of this methodology to a plant. The demonstration cases presented in this LTR are for illustration purposes and they are not generically applicable to individual plants.

The MSLB case is analyzed only for complete severance of the largest steam pipe. Smaller steam breaks, including LPCS or HPCS line breaks, do not result in higher PCTs than the 100% MSLB case. From a LOCA PCT perspective, steam breaks do not become more limiting than recirculation line because the fast depressurization is not coupled with large inventory loss. Therefore, the transient would turn around without reliance on ADS.

As discussed in Section 8.0, the PCT from the most limiting feedwater line break can get close to recirculation line break results. Additional sensitivities will be carried out on a plant-specific basis to confirm that they do not become more limiting than the limiting recirculation line break.

9.4 RELOADS

The way the LOCA analysis is set up and executed typically includes sufficient conservatism in core design parameters that vary from cycle to cycle. [[

described in Section 6.2.]]

As part of the reload evaluation, critical LOCA parameters will be examined to ensure validity of the original analysis. This evaluation process includes confirmation of

(1) [[

]]

Any of these parameters exceeding the analysis basis will be assessed, and if needed, their effect on the limiting case will be reevaluated.

9.5 MIXED CORES, VARIATIONS IN BATCH SIZES

The effect of mixed core and/or different batch sizes are almost negligible for reasons explained above in Section 9.4. This assumption is justified because: (1) bundles are thermal-hydraulically

compatible; and (2) thermal-hydraulic differences are less significant at the low core flow rates during post-blowdown conditions of LOCA.

In the methodology, the LOCA analysis is performed [[

]] Then, the LOCA analysis will be based on the most limiting results of different fuel types without requiring a reevaluation or separate analysis.

9.6 LOCA ANALYSIS OF NON-GNF FUEL

Non-GNF fuel will require a thermal hydraulic and fuel rod thermal mechanical model. [[

]]

9.7 EQUIPMENT OUT OF SERVICE FLEXIBILITY OPTIONS

In addition to licensing basis LOCA analysis for 10 CFR 50.46 compliance, the methodology can be used to evaluate various operating domain options and equipment out-of-service (EOOS) conditions. The process to evaluate the flexibility options is the same as the one discussed in Section 9.2 and will be dependent on the type of EOOS conditions. For example, ADS valve out-of-service would require a break spectrum evaluation because it can have an effect on limiting break size.

9.8 OPERATING DOMAIN

TRACG04P and associated uncertainties are applicable to all possible Power/Flow combinations shown in Figure 6.2-1. Therefore, there is no restriction on applicability of the methodology to various operating domains, such as EPU or MELLLA+. To evaluate a change in the operating domain, a TRACG LOCA analysis will be expanded by performing plant-specific sensitivities to provide sufficient information to demonstrate compliance.

9.9 COMPLIANCE WITH THE REQUIREMENTS OF METHODS LTR NEDC-33173P-A AND MELLLA+ LTR NEDC-33006P-A

Plants which include NEDC-33173P-A, Applicability of GE Methods to Expanded Operating Domains [78], as part of their licensing basis must meet the limitations and conditions specified in the associated SE. For plants licensed for the MELLLA+ operating domain,

NEDC-33006P-A, Maximum Extended Load Line Limit Analysis Plus [79] also has limitations and conditions relating to ECCS-LOCA analysis. Table 9.9-1 and Table 9.9-2 contain a discussion of the relevant limitations for both of these LTRs. Some of the limitations are, in effect, applicable only to the SAFER methodology, and by virtue of the approaches defined herein are rendered not applicable to the TRACG methodology; however, the dispositions of the underlying issues are described.

Table 9.9-1 Compliance with Methods LTR NEDC-33173P-A Limitations

Limitation	GEH Process
<p>Limitation 9.7: ECCS-LOCA 1 (Section 3.2.5.1.1):</p> <p>For applications requesting implementation of EPU or expanded operating domains, including MELLLA+, the small and large break ECCS-LOCA analyses will include top-peaked and mid-peaked power shape in establishing the MAPLHGR and determining the PCT. This limitation is applicable to both the licensing bases PCT and the upper bound PCT. The plant-specific applications will report the limiting small and large break licensing basis and upper bound PCTs.</p>	<p>SAFER traditionally used a mid-peaked axial power shape. This limitation imposes the requirement that a top-peaked power shape be considered in addition to the mid-peaked axial power shape.</p> <p>The axial power shape used in the TRACG application methodology is described in Section 6.2.5. The axial power shape is based on analyses of operating plant data to determine the conditions where fuel bundles are constrained by the thermal limits. [[</p> <p style="text-align: center;">]]</p>
<p>Limitation 9.8: ECCS-LOCA 2 (Section 3.2.5.1.2):</p> <p>The ECCS-LOCA will be performed for all statepoints in the upper boundary of the expanded operating domain, including the minimum core flow statepoints, the transition statepoint, as defined in Reference [79] and the 55 percent core flow statepoint. The plant-specific application will report the limiting ECCS-LOCA results as well as the rated power and flow results. The SRLR will include both the limiting statepoint ECCS-LOCA results and the rated conditions ECCS-LOCA results.</p>	<p>The range of analyzed initial power/flow conditions is described in Section 6.2.1 and is chosen to bound the operating envelope, including the expanded operating domain. This range satisfies the requirements of this limitation.</p>

Table 9.9-2 Compliance with MELLLA+ NEDC-33006P-A Limitations

Limitation	GEH Process
<p>Limitation 12.10: ECCS-LOCA Off-Rated Multiplier (Section 4.3.1.3)</p> <p>a) The plant-specific application will provide the 10 CFR Part 50, Appendix K, and the nominal PCTs calculated at the rated EPU power/rated CF, rated EPU power/minimum CF, at the low-flow MELLLA+ boundary (Transition Statepoint). For the limiting statepoint, both the upper bound and the licensing PCT will be reported. The M+SAR will justify why the transition statepoint ECCS-LOCA response bounds the 55 percent CF statepoint. The M+SAR will provide discussion on what power/flow combination scoping calculations were performed to identify the limiting statepoints in terms of DBA LOCA PCT response for the operation within the MELLLA+ boundary. The M+SAR will justify that the upper bound and licensing basis PCT provided is in fact the limiting PCT considering uncertainty applications to the non-limiting statepoints.</p> <p>b) LOCA analysis is not performed on cycle-specific basis; therefore, the thermal limits applied in the M+SAR LOCA analysis for the 55 percent CF MELLLA+ statepoint and/or the transition statepoint must be either bounding or consistent with cycle-specific off-rated limits. The COLR and the SRLR will contain confirmation that the off-rated limits assumed in the ECCS-LOCA analyses bound the cycle-specific off-rated limits calculated for the MELLLA+ operation. Every future cycle reload shall confirm that the cycle-specific off-rated thermal limits applied at the 55 percent CF and/or the transition statepoints are consistent with those assumed in the plant-specific ECCS-LOCA analyses.</p> <p>c) Off-rated limits will not be applied to the minimum CF statepoint.</p> <p>d) If credit is taken for these off-rated limits, the plant will be required to apply these limits during core monitoring.</p>	<p>The range of analyzed initial power/flow conditions is described in Section 6.2.1 and is chosen to bound the operating envelope, including the expanded operating domain. This range satisfies the requirements of this limitation. The thermal limits used in the analyses are described in the response to Limitation 12.11. The confirmation of the thermal limits for reloads is described in Section 9.4.</p>

Table 9.9-2 (Con't) Compliance with MELLLA+ NEDC-33006P-A Limitations

Limitation	GEH Process
<p>Limitation 12.11: ECCS-LOCA Axial Power Distribution Evaluation (Section 4.3.1.4)</p> <p>For MELLLA+ applications, the small and large break ECCS-LOCA analyses will include top-peaked and mid-peaked power shape in establishing the MAPLHGR and determining the PCT. This limitation is applicable to both the licensing bases PCT and the upper bound PCT. The plant-specific applications will report the limiting small and large break licensing basis and upper bound PCTs.</p>	<p>SAFER traditionally used a mid-peaked axial power shape. This limitation imposes the requirement that a top-peaked power shape be considered in addition to the mid-peaked axial power shape.</p> <p>The axial power shape used in the TRACG application methodology is described in Section 6.2.5. The axial power shape is based on analyses of operating plant data to determine the conditions where bundles are on the LHGR limit and where they are on the CPR limit. [[</p> <p style="text-align: center;">]].</p>
<p>Limitation 12.12 ECCS-LOCA Reporting (Section 4.3.1.5)</p> <p>a) Both the nominal and Appendix K PCTs should be reported for all of the calculated statepoints, and</p> <p>b) The plant-variable and uncertainties currently applied will be used, unless the NRC staff specifically approves a different plant variable uncertainty method for application to the non-rated statepoints.</p>	<p>This limitation addresses the SAFER and SAFER/CORCL methodologies that follow the requirements of 10 CFR 50, Appendix K.</p> <p>The TRACG application methodology follows Regulatory Guide 1.157 [17], and the licensing basis PCT is based on the 95th percentile with high probability upper bound temperature. The requirement of this limitation will be satisfied by reporting both the nominal and the upper bound PCT. The plant variables and uncertainties used in the TRACG application methodology are described in Section 6.</p>
<p>Limitation 12.13 Small Break LOCA (Section 4.3.2.4)</p> <p>Small break LOCA analysis will be performed at the MELLLA+ minimum CF and the transition statepoints for those plants that: (1) are small break LOCA limited based on small break LOCA analysis performed at the rated EPU conditions; or (2) have margins of less than or equal to [[]] relative to the Appendix K or the licensing basis PCT.</p>	<p>The break spectrum used in the TRACG application methodology is summarized in Section 9.1 and, together with the operating domain as described in the response to Limitation 12.10, satisfy the requirements of this limitation.</p>

Table 9.9-2 (Con't) Compliance with MELLLA+ NEDC-33006P-A Limitations

Limitation	GEH Process
<p>Limitation 12.14 Break Spectrum (Section 4.3.3)</p> <p>The scope of small break LOCA analysis for MELLLA+ operation relies upon the EPU small break LOCA analysis results. Therefore, the NRC staff concludes that for plants that will implement MELLLA+, sufficient small break sizes should be analyzed at the rated EPU power level to ensure that the peak PCT break size is identified.</p>	<p>The break spectrum used in the TRACG application methodology is summarized in Section 9.1 and, together with the operating domain as described in the response to Limitation 12.10, satisfy the requirements of this limitation.</p>

9.10 EXPOSURE-DEPENDENT MAPLHGR LIMITS

The MAPLHGR limit ensures that, in case of a LOCA, the plant would remain within the licensing basis analysis and not exceed the criteria set by 10 CFR 50.46. For LOCA-limited plants, the MAPLHGR limits for the cycle are determined from the LOCA analysis. For non LOCA-limited plants, LHGR limits provide adequate protection and ensure compliance with 10 CFR 50.46 criteria.

10.0 SUMMARY

This report describes the methodology for the application of TRACG for ECCS/LOCA analysis. The scope of application was stated in Section 1. The applicable licensing requirements and regulatory guides were discussed in Section 2 and the proposed TRACG application was shown to be consistent with these requirements. The phenomena of importance for BWR LOCAs were ranked in Section 3. TRACG was shown to be applicable for BWR LOCA analysis in Section 4. Sections 5 and 6 quantified the biases and uncertainties in the modeling of the phenomena of importance, and the ranges and uncertainties to be considered for the plant initial conditions and plant parameters. The statistical methodology for combining the individual biases and uncertainties was described in Section 7. The validity of this methodology was demonstrated by its application to the analysis of a number of test facilities in Section 7.6. As a final step, demonstration calculations were made in Section 8 for representative BWR/2, BWR/4 and BWR/6 plants. Values of key safety parameters (PCT, local oxidation and core-wide oxidation) were calculated, as appropriate, for the three plant types and were shown to meet the applicable licensing limits. Additional discussions on some of the methodology application aspects including analysis process summary, applicability of statistical analysis, break spectrum, handling of reloads, mixed cores, variations in batch sizes, non-GNF fuel, and considerations for EOOS flexibility options and operating domain, as well as the exposure-dependent MAPLHGR limits were provided in Section 9. Following review and approval by the NRC, the methodology will be applicable for ECCS/LOCA analysis of BWR/2-6 plants.

11.0 REFERENCES

- [1] J. G. M. Andersen, et al., “TRACG Model Description,” NEDE-32176P, Revision 4, January 2008.
- [2] J. G. M. Andersen, et al., “TRACG Qualification,” NEDE-32177P, Revision 3, August 2007.
- [3] J. G. M. Andersen, et al., “TRACG Application for Anticipated Operational Occurrences Transient Analysis,” NEDE-32906P-A, Revision 3, September 2006.
- [4] “Migration to TRACG04 / PANAC11 from TRACG02 / PANAC10 for TRACG AOO and ATWS Overpressure Transients,” NEDE-32906P, Supplement 3-A, Revision 1, April 2010.
- [5] R. J. Pryor, et al., “TRAC-P1A, An Advanced Best Estimate Computer Program for PWR LOCA Analysis,” Los Alamos Scientific Laboratory, NUREG/CRA-0665, May 1979.
- [6] J. G. M. Andersen, et al., “TRACG Model Description,” NEDE-32176P, Revision 2, December 1999.
- [7] J. G. M. Andersen, K. H. Chu and J. C. Shaug, “BWR REFILL/REFLOOD Program Task 4.7 - Model Development, Basic Models for the BWR Version of TRAC,” GEAP-22051, NUREG/CR-2573, EPRI NP-2376, April 1983.
- [8] Y. K. Cheung, V. Parameswaran and J. C. Shaug, “BWR REFILL/REFLOOD Program Task 4.7 - TRAC BWR Component Models,” GEAP-22052, NUREG/CR-2574, EPRI NP-2377, April 1983.
- [9] Md. Alamgir, “BWR REFILL/REFLOOD Program Task 4.8 - TRAC-BWR Model Qualification for BWR Safety Analysis, Final Report,” GEAP-30157, NUREG/CR-2571, EPRI NP-2377, October 1983.
- [10] J. G. M. Andersen and C. L. Heck, “BWR Full Integral Simulation Test (FIST) Program, TRAC-BWR Model Development, Volume 1 - Numerical Methods,” GEAP-30875-1, NUREG/CR-4127-1, EPRI NP-3987-1, November 1985.
- [11] K. H. Chu, J. G. M. Andersen, Y. K. Cheung and J. C. Shaug, “BWR Full Integral Simulation Test (FIST) Program, TRAC-BWR Model Development, Volume 2 – Models,” GEAP-30875-2, NUREG/CR-4127-2, EPRI NP-3987-2, October 1985.
- [12] Y. K. Cheung, J. G. M. Andersen, K. H. Chu and J. C. Shaug, “BWR Full Integral Simulation Test (FIST) Program, TRAC-BWR Model Development, Volume 2 - Developmental Assessment for Plant Applications,” GEAP-30875-3, NUREG/CR-4127-3, EPRI NP-3987-3, October 1985.

NEDO-33005-A Revision 1
Non-Proprietary Information – Class I (Public)

- [13] W. A. Sutherland, Md. Alamgir, J. A. Findlay, and W. S. Hwang, “BWR Full Integral Simulation Test (FIST) Program, Phase II Test Results and TRAC-BWR Model Qualification,” GEAP-30876, NUREG/CR-4128, EPRI NP-3988, October 1985.
- [14] D. D. Taylor, et al., “TRAC-BD1/MOD1: An Advanced Best Estimate Program for Boiling Water Reactor Transient Analysis,” Volumes 1-4, NUREG/CR-3633, Idaho National Engineering Laboratory, April 1984.
- [15] J. A. Borkowski, et al., “TRAC-BF1/Mod1 Models and Correlations,” NUREG/CR-4391, Idaho National Engineering Laboratory, August 1992.
- [16] B. Boyack, et al., “Quantifying Reactor Safety Margins: Application of Code Scaling, Applicability, and Uncertainty Evaluation Methodology to a Large-Break, Loss-of-Coolant Accident,” NUREG/CR-5249, December 1989.
- [17] U.S. NRC, “Best-Estimate Calculations of Emergency Core Cooling System Performance,” Regulatory Guide 1.157, May 1989.
- [18] Code of Federal Regulations, Title 10 “Energy,” Part 50 “Domestic Licensing of Production and Utilization Facilities,” Section 50.46 “Acceptance Criteria for Emergency Core Cooling Systems for Light-Water Nuclear Power Reactors,” and Appendix K to Part 50 “ECCS Evaluation Models.”
- [19] U.S. NRC, “Standard Review Plan for the Review of Safety Analysis Reports for Nuclear Power Plants: LWR Edition,” NUREG-0800, March 2007.
- [20] “General Electric Standard Application for Reactor Fuel (GESTAR II),” NEDE-24011-P-A-17, September 2010.
- [21] B. S. Shiralkar, et al., “The GESTR-LOCA and SAFER Models for the Evaluation of the Loss-of-Coolant Accident, Volume III: SAFER/GESTR Application Methodology,” NEDE-23785-1-PA, Revision 1, October 1984.
- [22] J. A. Findlay, et al., “SAFER Model for Evaluation of Loss-of-Coolant Accidents for Jet Pump and Non-Jet Pump Plants Volume II: SAFER Application Methodology for Non-Jet Pump Plants,” NEDE-30996PA, October 1987.
- [23] J. Duncan and P. W. Marriott, “General Electric Company Analytical Model for Loss-of-Coolant Analysis in Accordance with 10 CFR 50 Appendix K,” NEDE-20566-P-A Volumes I, II and III, September 1986.
- [24] S.O. Akerlund, et al., “The GESTR-LOCA and SAFER Models for the Evaluation of the Loss-of-Coolant Accident,” Volume I, NEDO-23785-1-A, February 1985.
- [25] F. D. Shum, et al., “SAFER Model for Evaluation of Loss-of-Coolant Accidents for Jet Pump and Non-Jet Pump Plants, Volume I, SAFER – Long Term Inventory Model for BWR Loss-of-Coolant Analysis,” NEDE-30996P-A, October 1987.

NEDO-33005-A Revision 1
Non-Proprietary Information – Class I (Public)

- [26] B.L. Charboneau, “Overview of TRACBD1/Model Assessment Studies,” NUREG/CR-4428, EGG-2422, November 1985.
- [27] J. E. Leonard, J. D. Duncan, A. S. Rao and R. C. Cipolla, “Emergency Core Cooling Tests of an Internally Pressurized Zircaloy-Clad, 8x8 Simulated BWR Fuel Bundle,” NEDE-20231-P-A, April 1976.
- [28] H. Glaeser and E. Hofer (GRS-Germany), “Determination of Importance of Uncertain Parameters in Code Applications,” Transactions of the American Nuclear Society, Washington, D.C., November 13-17, 1994, p. 308-309.
- [29] C. L. Heck and D. T. Rock, “TRACG04P User’s Manual,” November 2008.
- [30] H. A. David, “Order Statistics,” 2nd edition, John Wiley and Sons, 1969.
- [31] D. C. Montgomery, “Introduction to Statistical Quality Control,” John Wiley and Sons, 1996.
- [32] “Power Distribution Uncertainties for Safety Limit MCPR Evaluations,” NEDC-32694P-A, August, 1999.
- [33] O. Nylund and R. Eklund, “OF-64 Results of Void Measurements,” FRIGG PM-69, September 1970.
- [34] J. R. Fitch, et al., “TRACG Qualification for SBWR (Licensing Topical Report),” NEDC-32725P, September, 1997.
- [35] V. P. Carey, “Liquid-Vapor-Phase-Change Phenomena,” Hemisphere Publishing, 1992.
- [36] D. R. Liles, et al., “TRAC-PF1/MOD1 Correlations and Models,” NUREG/CR-5069, LA-11208-MS, December 1988.
- [37] P. Saha and N. Zuber, “Point of Net Vapor Generation and Vapor Void Fraction in Subcooled Boiling,” Proceedings of the 5th International Heat Transfer Conference, Tokyo, 1974.
- [38] “American National Standard for Decay Heat Power in Light Water Reactors,” ANSI-ANS 5.1, 23A6938, Revision 1, April 1991.
- [39] B. S. Shiralkar and Y. K. Cheung, “TRACG Application for ESBWR,” NEDC-33083 P-A, Revision 1, September 2010.
- [40] G. G. Bartolomei, V. A. Suvorov and S. A. Tevlin, “Hydrodynamics of Steam Generation in a Two-Circuit Nuclear Power Plant,” Teploenergetika 10(1), 1963 (pp. 52-57).
- [41] M. Petrick and E. A. Spleha, “Thermal Hydraulic Performance Characteristics of EBWR,” ANL 6693, May 1963.

- [42] H. A. Hasanein, A. M. C. Chan, M. Kawaji and Y. Yoshioka, “Steam-Water Two-Phase Flow in Large Diameter Vertical Piping at High Pressures and Temperatures,” 4th JSME/ASME Joint International Conference on Nuclear Engineering, New Orleans, March 1996.
- [43] A. M. C. Chan, “Void Fraction Measurements in Large Diameter Pipes with Thick Metal Walls or Complex Internal Geometries,” Proceedings of the National Heat Transfer Conference, American Nuclear Society, 1992 (pp. 236-244).
- [44] A. M. C. Chan and D. Bzovey, “Measurements of Mass Flux in High Temperature High Pressure Steam-Water Two-Phase Flow Using a Combination of Pitot Tubes and a Gamma Densitometer,” Journal of Nuclear Engineering and Design, V. 122, 1990 (pp. 95-104).
- [45] J. F. Wilson, R. J. Grenda and J. F. Patterson, “Steam Volume Fraction in a Bubbling Two-Phase Mixture,” Transactions, American Nuclear Society 4(2), pp. 356-357, (1961).
- [46] H. Nagasaka, “New Japanese Correlations on Core Cooling and CCFL Characteristics During BWR LOCA,” Transactions of the Thirteenth Water Reactor Safety Research Information Meeting, Gaithersburg, MD, October 1985.
- [47] S. Morooka, T. Ishizuka, M. Iizuka and K. Yoshimura, “Experimental Study on Void Fraction in a Simulated BWR Assembly (Evaluation of Cross-Sectional Averaged Void Fraction),” Nuclear Engineering and Design, 114, pp. 91-98 (1989).
- [48] T. Mitsutake, S. Morooka, K. Suzuki, S. Tsonoyama and K. Yoshimura, “Void Fraction Estimation within Rod Bundles Based on Three-Fluid Model and Comparison with X-Ray CT Void Data,” Nuclear Engineering and Design, 120, pp. 203-212 (1990).
- [49] K. C. Chan, et al., “The GESTR-LOCA and SAFER Models for the Evaluation of the Loss-of-Coolant Accident V.II, SAFER-Long Term Inventory Model for BWR Loss-of-Coolant Analysis,” NEDE-23785-1-PA, Revision 1, October 1984.
- [50] J. E. Leonard, et al., “Calculation of Counter-Current Flow Limiting Conditions in BWR Geometry,” NEDE-13430, September 1975.
- [51] B. S. Shiralkar and J. R. Ireland, “Backflow Leakage from the Bypass Region for ECCS Calculations,” NEDE-23690, October 1977.
- [52] J. P. Walkush, “High Pressure Counterflow CHF,” MIT Report, September 1974.
- [53] R. E. Dimenna et al., “RELAP5/MOD2 Models and Correlations,” NUREG/CR-5194 (EGG-2531), August 1988.
- [54] D. C. Groeneveld, S. C. Cheng and T. Doan, “1986 AECL-UO Critical Heat Flux Lookup Table,” Heat Transfer Engineering 7, pp. 46-62, (1986).

NEDO-33005-A Revision 1
Non-Proprietary Information – Class I (Public)

- [55] J. E. Leonard, “General Electric Company Analytical Model for Loss-of-Coolant Analysis in Accordance with 10 CFR 50 Appendix K; Amendment No. 1 – Calculation of Low-Flow Film Boiling Heat Transfer for BWR LOCA Analysis,” NEDO-20566-1-A, Revision 1, 77NED304, October 1982.
- [56] P. Saha, “A Study of Heat Transfer to Superheated Steam in a 4x4 Rod Bundle,” NEDE-13462, June 1976.
- [57] A. W. Bennett et al., “The Wetting of Hot Surfaces by Water in a Steam Environment at High Pressure,” AERE-R5146, 1966.
- [58] R. B. Duffey and D. T. C. Porthouse, “Experiments on the Cooling of High-Temperature Surfaces by Water Jets and Drops,” Report No. RD/B/N2386, Berkeley Nuclear Laboratories, England, August 1972.
- [59] ANSI/ANS-5.1-1979, “American National Standard for Decay Heat Power in Light Water Reactors.”
- [60] J. V. Cathcart and R. E. Pawel, “Zirconium Metal-Water Oxidation Kinetics: IV. Reaction Rate Studies,” ORNL/NUREG-17, August 1977.
- [61] “Nine Mile Point Unit 1 SAFER/CORECOOL/GESTR-LOCA Loss-of-Coolant Accident Analysis,” EAS-52-0889, August 1989, and, S. A. Wilson, “Calculating the Nominal Core Spray Flow Rate to the Minimum Flow Channel During a LOCA for NMP-1,” April 1989.
- [62] E. L. Burley, “Performance of a 1967 Product Line Steam Dryer,” NEDE-13002, March 1969.
- [63] S. Wolf, “Performance of a Development Steam Dryer with Delta-P, Inc. Vanes and Three AS-2B Steam Separators Simulating BWR/6,” NEDE-13391, August 1974.
- [64] R. Burch, D.C. Pappone, W.M. Wong, P. Wu and A. I. Yang, “Nine Mile Point Unit 1: Supplemental Loss-of-Coolant Accident Analysis for Small Break and Revised DBA LOCA,” NEDC-31446P, Supplement 5, January 2001.
- [65] F. T. Bolger and M. A. Holmes, “TRACG Application for Anticipated Transient Without Scram Overpressure Transient Analysis,” NEDE-32906P Supplement 1-A, November 2003.
- [66] B. S. Shiralkar, et al., “TRACG Application for ESBWR Stability Analysis,” NEDE-33083P, Supplement 1-A, Revision 2, September 2010.
- [67] C. R. Lehmann, et al., “Reactor Stability Detect and Suppress Solutions Licensing Basis Methodology for Reload Applications,” NEDO-32465-A, August 1996.
- [68] “DSS-CD TRACG Application,” NEDE-33147P-A, Revision 2, November 2007.

NEDO-33005-A Revision 1
Non-Proprietary Information – Class I (Public)

- [69] N. Zuber, “Hierarchical, Two-Tiered Scaling Analysis Appendix D to An Integrated Structure and Scaling Methodology for Severe Accident Technical Issue Resolution,” NUREG/CR-5809, EGG-2659, November 1991.
- [70] A. G. Stephens, “BWR Full Integral Simulation Test (FIST) Program Facility Description Report,” GEAP-22054, NUREG/CR-2576, EPRI NP-2314, December 1982.
- [71] H. Nakamura, et al., “ROSA-III 200% Double-Ended Break Integral Test Run 926 (HPCS Failure),” JAERI-M 84-008, February 1984.
- [72] J. E. Barton, et al., “BWR Refill-Reflood Program Task 4.4 – 30° SSTF Description Document,” GEAP-24939, NUREG/CR-2133, EPRI NP-1584, June, 1981.
- [73] K. Tasaka, J. A. Findlay, et al., “ROSA-III and FIST BWR Simulation Tests: Loss of Coolant Accident Response Comparisons,” NEDC-30895, October 1984.
- [74] P. Saha, et al., “ESBWR Scaling Report,” NEDC-33082P, Revision 2, April 2008.
- [75] I. Catton, et al., “Application of Fractional Scaling Analysis (FSA) to Loss of Coolant Accidents (LOCA),” NURETH-11, October 2005.
- [76] “The PRIME Model for Analysis of Fuel Rod Thermal-Mechanical Performance,” Technical Bases – NEDC-33256P-A, Revision 1, Qualification – NEDC- 33257P-A, Revision 1, and Application Methodology – NEDC-33258P-A, Revision 1, September 2010.
- [77] U.S. NRC Regulatory Guide 1.203, “Transient and Accidents Analysis Methods,” December 2005.
- [78] GE Hitachi Nuclear Energy, "Applicability of GE Methods to Expanded Operating Domains," NEDC-33173P-A, Revision 1, September 2010.
- [79] GE Hitachi Nuclear Energy, "General Electric Boiling Water Reactor Maximum Extended Load Line Limit Analysis Plus," NEDC-33006P-A, Revision 3, June 2009.
- [80] Letter, J. F. Harrison (GEH) to U. S. Nuclear Regulatory Commission, “Use of the Shumway Tmin Correlation with Zircaloy for TRACG Analyses,” MFN 13-073, September 9, 2013.
- [81] Letter, Kevin Hsueh (NRC) to Jerlad G. Head (GEH), “Final Safety Evaluation for GE Hitachi Nuclear Energy – Americas, LLC Topical Report NEDE-33005P and NEDO-33005, Revision 0, “Licensing Topical Report TRACG Application for Emergency Core Cooling Systems / Loss-of-Coolant-Accident Analyses for BWR/2-6” (CAC No. ME5405),” February 14, 2017.

NEDO-33005-A Revision 1
Non-Proprietary Information – Class I (Public)

- [82] Letter, J. F. Harrison (GEH) to U. S. Nuclear Regulatory Commission, "Response to Request for Additional Information Re: GE-Hitachi Nuclear Energy Americas Topical Report (TR) NEDE-33005P, Revision 0, "TRACG Application for Emergency Core Cooling Systems / Loss-of-Coolant-Accident Analyses for BWR/2-6" (TAC No. ME5405)," MFN 14-064, October 7, 2014.
- [83] Letter, J. F. Harrison (GEH) to U. S. Nuclear Regulatory Commission, "Response to Request for Additional Information Regarding Review of Licensing Topical Reports NEDE-33005P and NEDO-33005, "Licensing Topical Report TRACG Application for Emergency Core Cooling Systems / Loss-of-Coolant-Accident Analyses for BWR/2-6" (TAC No. ME5405)," MFN 16-008, February 19, 2016.
- [84] Letter, J. F. Harrison (GEH) to U. S. Nuclear Regulatory Commission, "Response to Request for Additional Information Regarding Review of Licensing Topical Reports NEDE-33005P and NEDO-33005, "Licensing Topical Report TRACG Application for Emergency Core Cooling Systems / Loss-of-Coolant-Accident Analyses for BWR/2-6" (TAC No. ME5405)," MFN 16-020, June 13, 2016.
- [85] Letter, J. F. Harrison (GEH) to U. S. Nuclear Regulatory Commission, "Response to Requests for Additional Information 101 and 102 Regarding Review of Licensing Topical Reports NEDE-33005P and NEDO-33005, "Licensing Topical Report TRACG Application for Emergency Core Cooling Systems / Loss-of-Coolant-Accident Analyses for BWR/2-6" (TAC No. ME5405)," MFN 16-039, June 21, 2016.
- [86] Letter, J. F. Harrison (GEH) to U. S. Nuclear Regulatory Commission, "Response to Requests for Additional Information 103 and 104, 65 (Revised) and 33 (Revised), Regarding Review of Licensing Topical Reports NEDE-33005P and NEDO-33005, "Licensing Topical Report TRACG Application for Emergency Core Cooling Systems / Loss-of-Coolant-Accident Analyses for BWR/2-6" (TAC No. ME5405)," MFN 16-072, October 21, 2016.

**APPENDIX A GEH RESPONSES TO NRC RAIS ON
NEDE-33005P REVISION 0**

RAI-1

- 1) The NRC staff requests additional technical basis to justify the adequacy of statistical distributions presented in section 5.1 of the topical report (TR) that are used to determine 95/95 upper tolerance limits for comparison to the criteria of Title 10 of the *Code of Federal Regulations*(10 CFR) Part 50.46. Please address the following issues either generically and/or for specific phenomena and parameters, as necessary:
 - a. Due to the strong influence of the data selection process on the resulting statistical distributions, objective rationale should be provided for the selection of test data and, equivalently, the implicit rejection of other potentially applicable data. Although some datasets may be more relevant than others, excessive selectivity could lead to underestimation of the true uncertainty.
 - b. Some data populations used in the TR are of limited size, and it is not apparent whether sufficient statistical power exists to justify conclusions regarding normality and other distribution characteristics. Although the probability for Type I error is established by the confidence level, the probability for Type II error can grow quite large as the sample size is reduced.
 - c. Please provide additional technical basis to justify the adequacy of statistical uncertainty distributions that are dependent on the data used to develop closure relations in the code (e.g., phenomenon identification and ranking table (PIRT) items A1, C26, F3, etc.). In this case, how does GEH account for the fact that the statistical distribution does not include a bias and/or fully account for the standard deviation that realistically may exist (e.g., due to issues such as those discussed in parts d. and e. below).
 - d. Due to the potential for systematic error, the statement in section 5.0 of the TR that measurement error is implicitly included in comparisons of code predictions with test data appears correct based on the NRC staff's understanding only when data from multiple test programs is considered. In light of the discussion above, please clarify GEH's position on how systematic error is accounted for if data from diverse sources is not used in deriving uncertainty distributions.
 - e. To avoid underestimating the true uncertainty, what consideration did GEH give to the fact that test conditions are generally idealized, simplified, and well controlled relative to complex plant conditions under which derived correlations and models are applied? For example, simplified geometries and reduced scales may lead to underestimation of uncertainty, steady state uncertainty may be less than transient uncertainty, and the uncertainty may increase in an extrapolated transition region between the validation ranges of two correlations.

RAI-1 Response

- a. To the extent possible and practical, rationale for selection of certain test data and rejection of other data for determining the model uncertainties are explained in the LTR. Resulting model uncertainty depends on the underlying data; however, the selection

process is neutral and independent from final distributions. In general, principles like applicability, geometry similarities, as well as the data availability and reliability, are used.

- b. Although some data populations used in the development of uncertainty distributions are of limited size, use of limited dataset ultimately penalizes the methodology by imposing a relatively larger uncertainty. Regarding the Type II errors, knowing the exact shape of the probability distribution for a given uncertainty parameter is less important than whether the statistics (bias and standard deviation with an associated distribution) applied for that parameter adequately covers the observed model uncertainties, for the application methodology. Increasing the population size for the underlying data used in model uncertainty evaluation could ultimately reduce the overall phenomenological uncertainties; but, having a limited population does not per se invalidate the systematic approach that was employed in development of the probability density functions. The essential need being addressed by the methodology is that the modeled uncertainty distribution represents either realistically or conservatively the tail of the distribution that will contribute to the tolerance limit of the critical licensing parameters associated with PCT and oxidation.
- c. In the U.S., all the current state-of-the-art best-estimate methodologies are similar in this aspect: they all rely on, to a certain extent, the same data to determine the code bias and uncertainties as well as to qualify specific aspects of the models. This, however, is not a deficiency since the model formulations themselves are to the greatest extent possible based on physical models and/or scalable dimensionless parameters rather than a brute-force correlation of the raw data. One should expect that any purely empirical fit to a complete dataset would represent that dataset without any bias and should be applied cautiously or not at all outside the range spanned by the data. The GEH approach is whenever possible to select separate effect tests that isolate the phenomenon of interest and use data from these tests to quantify the uncertainty and bias associated with the modeling of that phenomenon. The approach is checked by applying all the relevant biases and uncertainties to the simulation of integral system tests and plant cases (where multiple phenomena are interacting) to confirm that coverage of the experimental data variability is achieved. The types of data for the integral tests and plant cases tend to be macroscopic quantities such as clad temperatures, pressures, flows, etc. that depend on many separate modeling phenomena in much the same way as the critical licensing parameters.
- d. The statement in Section 5.0 indicates that the measurement uncertainty in the data is intrinsically accounted for when code comparison to experimental results is made. No further attempt to minimize or eliminate any potential systematic error in the experimental data is being made. If a systematic error exists in the experimental data, and if, without consideration of data from multiple test programs, it propagates through the evaluation, it will ultimately add more uncertainty. By using bias and uncertainty with potential systematic error, the methodology could lack a further refinement, but will

still capture at a minimum the uncertainty associated with the phenomena. From the methodology development point of view, that kind of compromise is deemed acceptable by GEH.

- e. Whenever possible, the uncertainty for each phenomenon must be obtained from separate effects tests, not from integral effects tests, as explained in part (c) of the response. The GEH approach is consistent with this principle. How the biases and uncertainties from separate phenomena combine into composite biases and uncertainties of macroscopic quantities depends on the interactions of the phenomena and their relative importance to the macroscopic parameter. These relative importances change depending on the facility being modeled, the modeling scenario, and even change with time during the scenario. It is the interactions within the code simulation that determine how a certain bias and uncertainty for a specific phenomenon will be manifested in the output parameter. The main reason GEH has applied the TRACG LOCA methodology to integral tests as documented in Section 7 of the LTR is to illustrate how separate biases and uncertainties via complex interactions among competing processes manifest themselves as uncertainties and biases in the macroscopic output parameters. The statistical results from the transient integral test simulations compared to macroscopic data from these tests supports the conclusion that the predicted biases and uncertainties of the macroscopic parameters are not underestimated.

LTR Impact

No changes to the LTR are proposed as the result of this RAI response.

RAI-2

- 2) The NRC staff requests additional technical basis to justify the adequacy of neglecting statistical dependencies between random variable input parameters. The TR generally appears to treat statistical parameters independently, although some parameters would presumably be correlated. Neglect of statistical correlation between input parameters could lead to underestimation of 95/95 upper tolerance limits. Therefore, please describe the approach for identifying and accounting for statistical dependencies between input parameters and justify its adequacy, with emphasis on the issues below.
- a. In a number of cases, random variables used to generate uncertainty for a model or correlation that is used in multiple locations within the computational domain are assumed to be independent. Although part of the uncertainty associated with a correlation may be attributable to uncorrelated differences in local parameters (e.g., flow conditions), generally, GEH's technical basis for presuming that there is no linkage between predictions from the same model in different spatial components could not be discerned from the NRC staff's review of the TR, especially where similar flow regimes exist. The following examples (not all-inclusive) illustrate the issue:
 - i. The Lee-Ryley correlation is used to calculate interfacial heat transfer within a variety of spatial components in the computational model, with independent, identically distributed random variable multipliers selected to perturb the heat transfer in each component. However, a significant piece of the model uncertainty is presumably driven by limitations residing in the Lee-Ryley correlation itself (e.g., the assumption of spherical bubbles), which would seemingly distort predictions in multiple spatial locations similarly.
 - ii. Similar conclusions apply to statistical distributions for other models used in multiple regions of the computational domain, such as those for interfacial drag, interfacial shear and entrainment, heat transfer (Chen, Dittus-Boelter), etc.
 - iii. Internal rod pressures may be correlated within a given assembly or section of core with a higher peaking than predicted.
 - iv. The thickness of an oxide or crud layer on fuel rods may depend on conditions common to all rods, and may affect all correlations for heat transfer from the fuel.
 - b. Uncertainties associated with predicting some parameters, for example interfacial heat transfer and interfacial drag / shear, are presumably correlated with each other through one or more fundamental input random variables influencing both parameters (e.g., in this case, interfacial area concentration and relative phase velocity). Please clarify how independence is assured in the selection of random parameters, or explain how the potential for correlation between random parameters is accounted for in the methodology.

RAI-2 Response

From a statistical point of view, if two or more parameters are statistically correlated, assuming independent uncertainty distributions would not lead to underestimation of upper tolerance limits of the output parameters. This can be visualized, in simple terms, by an example of combining two distributions with different mean values. The combined distribution would have lower frequency for the mean value, but a larger spread, i.e. uncertainty. This, in turn, would yield a higher upper tolerance limit for the uncertainty contributor. In other words, chances of sampling more extreme values of the input in the statistical analysis. In the practical applications, however, if the parametric effects are counterbalanced, or in other words, they have cancelling effect, the concern as explained in the RAI cannot be ignored.

The TRACG LOCA methodology considers the dependencies of the model uncertainties, in the statistical sampling process. In the application process, there exist provisions for determining to be done either concurrently or independently. [[

]]

In summary, the TRACG LOCA methodology does not neglect the potential effects of dependencies between random variable input parameters. According to the physical phenomena they represent and consistent with observed or expected actual behavior from plant conditions, the uncertainty contributors are either sampled and applied concurrently or independently for different components in the input model, as explained above.

LTR Impact

No changes to the LTR are proposed as the result of this RAI response.

RAI-3

- 3) A number of nodalization variations presented in Table 5.2-1 of the TR result in predicted changes to the peak cladding temperature (PCT) for a BWR/4 that approach or exceed the significance threshold of 50°F in 10 CFR 50.46 for changes or errors to a methodology. Estimating the aggregate effect of nodalization variations based on the available data shows that the potential range of cumulative variation is large (i.e., sum of absolute values of Δ PCT values in Table 5.2-1), particularly for the potentially limiting intermediate break. Further, there appears to be potential for an increase in PCT that could be significant (e.g., sum of Δ PCT values in Table 5.2-1). As such, it is unclear that nodalization error is small relative to the uncertainties determined in the demonstration analysis in Chapter 8 of the TR or on par with time step variations of the magnitude shown in Figure 6.9-5 of NEDE-32177P, Revision 3. Therefore, please address the following requests:
- a. Either (1) reduce the uncertainty band associated with nodalization to a level that is small relative to other uncertainties that are explicitly accounted for by the methodology, (2) reasonably estimate the nodalization error and include an allowance for this error in the methodology (e.g., through the analysis resolution), or (3) adequately justify the current approach.
 - b. Please provide results of similar nodalization and time step studies that are applicable to the expected limiting break for the BWR/2 design and further address the request in Part a. (above) considering the potential for limited margins to regulatory criteria.

RAI-3 Response

Summing the absolute value of the variations indicated by the nodalization studies is not the correct process for comparison to the significance threshold of 50°F in 10 CFR 50.46. The 10 CFR 50.46 criteria apply to changes in the model from the approved baseline. A standard nodalization has been proposed for purposes of establishing the baseline modeling to be approved and it is differences caused by deviations from this approved nodalization that will be subject to the 50°F threshold.

- a. In response to other RAIs, RAI-6 and RAI-9 in particular, [[

]]

The first row in Table 5.2-1 provides baseline PCT values that are [[

]]

- b. The nodalization and time step studies applicable to the BWR/2 design have been performed as sensitivities to the BWR/2 limiting break scenario [[

]] Table R3-1

summarizes the results from these nodalization sensitivity studies.

The analysis results presented in Table R3-1 demonstrate that in each of the sensitivity cases, the effect on the PCT is relatively small compared to the overall uncertainty of the statistical runs [[

]] The study

results are summarized graphically in Figures R3-1 and R3-2. These results will also be incorporated into Section 5.2 of the LTR.

LTR Impact

The results of the BWR/2 nodalization sensitivity study will be incorporated into Section 5.2 of the LTR. Table R3-1 will be added to the LTR as Table 5.2-2, and the title of Table 5.2-1 will be revised to distinguish it from Table 5.2-2. Figures R3-1 and R3-2 will be added as Figures 5.2-10 and 5.2-11. This added information, like that previously presented for jet-pump BWRs in LTR Table 5.2-1, is [[

]] GEH has committed to perform all future plant evaluations and applications using the detailed core models.

**Table R3-1 Summary of Nodalization Sensitivity Studies for BWR/2
Using the Original LTR Core Model**

II		
]]

[[

]]

Figure R3-1 Vessel Axial Nodalization Sensitivity for BWR/2

[[

]]

Figure R3-2 Channel Axial Nodalization Sensitivity for BWR/2

RAI-4

4) In a number of places in the TR, the proposed disposition of certain evaluation model parameters (e.g., [[

]] (e.g., Table 5.2-1, section 8.1.3, section 8.1.4, Table 8.1-12, section 5.1.8.2). In light of the potential for random noise to cause significant variation in figures of merit in certain scenarios, please discuss to what extent single-simulation sensitivity studies genuinely reflect the expected influence of parameter perturbations in future statistical calculations for a similar reactor design, versus being attributable to random, noise-level perturbations. Please discuss measures taken to ensure that the results of sensitivity studies provide useful and representative data (e.g., sensitivity cases are performed with noise-driven phenomena such as the “parallel channel effect” held constant or from multiple simulations with varied noise-level inputs).

RAI-4 Response

[[

]] These results are presented as part of the response to RAI-6 and RAI-9. GEH believes that with this smaller variability that single-simulation sensitivity studies can now provide a reasonable means to screen potential effects. Single-simulation sensitivity studies are appropriate to support technical justification for particular applications provided the results are not contrary to experience and physical principles. If a decision is to be made based on the direction and/or magnitude of the conservatism which is not known, then averaging of additional cases to eliminate or reduce the impact of ‘random noise’ can be utilized to better quantify the conservatism. In summary, a small PCT analysis resolution, i.e. a small variability associated with non-phenomenological uncertainty, enhances the robustness of the methodology. The commitment to use the detailed core models for all plant applications is the main measure taken to ensure that future sensitivity studies will provide useful and representative results.

LTR Impact

No changes to the LTR are proposed as the result of this RAI response. GEH acknowledges that the nodalization sensitivity studies shown in the LTR Table 5.2-1 and new results produced for the BWR/2 in response to RAI-3 [[]]

GEH does not intend to update these studies in the LTR for the reasons indicated in the response to RAI-3.

RAI-5

- 5) The TR asserts in section 6.4 that the range of PCT results conservatively accounts for the “parallel channel effect” via either normal distribution statistics or order statistics. However, no evidence is presented that the parallel channel behavior predicted by the TRACG [GEH proprietary version of the Transient Reactor Analysis Code (TRAC)] evaluation model would accurately represent multi-channel behavior in a reactor core. For example, due in part to phenomenological uncertainties as well as the grouping of bundles in the TRACG evaluation model, it is not clear that the probability of the TRACG peak-PCT bundle not being “plugged” with liquid is equivalent to the probability of all bundles in a reactor core containing similarly hot rods being unplugged during a LOCA. Without evidence of equivalence in this and similar comparisons between the evaluation model and an actual reactor core, confidence cannot exist that the parallel channel effect is realistically accounted for through upper tolerance limits derived from either normal distribution statistics or order statistics. In light of the discussion above, please address the following points:
- a. Either revise the TRACG evaluation model to account for the uncertainties associated with the parallel channel effect conservatively or (if justifiable) realistically, or provide sufficient evidence to justify that the parallel channel effect is simulated by the existing TRACG evaluation model in a physically and statistically representative manner.
 - b. Clarify the reactor types, break size ranges, and break locations for which the parallel channel effect is expected to have a significant impact on statistical predictions of PCT.

RAI-5 Response

It is important to clarify that the sensitivity to [[

]]

The discussion in LTR Section 6.4 describes [[

]] In light of the preceding discussion, the points from the RAI are addressed as follows:

NEDO-33005-A Revision 1
Non-Proprietary Information – Class I (Public)

- a. To realistically account for [[]] The detailed core model is described and employed in the responses to RAI-6 and RAI-9. The detailed core model will be used in all plant LOCA calculations.
- b. [[]]

LTR Impact

No changes to the LTR are proposed as the result of this RAI response.

RAI-6

6) Please illustrate the impact of phenomenological uncertainties on the PCT range predicted by the TRACG evaluation model with the parallel channel effect isolated. Please provide a summary of descriptive statistics similar to Figure 6.4-2 for the same case (i.e., BWR/4 limiting break) but with the variability due to the parallel channel effect suppressed and the random variables for PIRT multipliers chosen according to baseline uncertainty distributions. Please further explain the technique used to bias toward prediction of hot channel plugging.

RAI-6 Response

This RAI response is related to the responses for RAI-7 and RAI-9.

During the investigation of this and other related responses, an error was discovered in the analyses presented in Section 6.4. The error was a result of the decay heat range in the [[

]] The conclusions with respect to the [[
]] drawn from the Section 6.4 study, however, remain unchanged. The correction is implemented in the calculations presented in this response.

The original calculations were repeated to establish the correct basis for comparison. Both the [[

]] Figures R6-1 through R6-4 summarize the corrected results.

To illustrate the impact of phenomenological uncertainties on the PCT range predicted by the TRACG evaluation model with the parallel channel effect isolated, two additional sets of analyses were performed. One set of calculations [[

]] These methods are presented here to demonstrate that the large PCT variations shown in Figures R6-1 through R6-4 can be considerably reduced.

In Figures R6-5 through R6-8, the results from the cases with [[
]] are presented. These figures illustrate the phenomenological uncertainty [[

]] for BWR/4 model is shown in Table R6-1, which can be compared to the LTR channel modeling as shown in LTR Table 8.1-1. As shown in Table R6-1, the changes are [[

]] These results are shown in Figures R6-9 through R6-12. In future applications, GEH plans to utilize the detailed core modeling [[
]] for TRACG LOCA applications.

[[

Figure R6-1 PCT Range for BWR/4 0.67 ft² Break [[

]]
]]

[[

Figure R6-2 PCT Distribution for BWR/4 0.67 ft² Break [[

]]
]]

[[

]]

Figure R6-3 PCT Range for BWR/4 0.67 ft² Break [[

]]

[[

]]

Figure R6-4 PCT Distribution for BWR/4 0.67 ft² Break [[

]]

[[

Figure R6-5 PCT Ranges for BWR/4 with SEO [[

]]
]]

[[

Figure R6-6 PCT Distribution with SEO [[

]]
]]

[[

]]

Figure R6-7 PCT Range with SEO [[

]]

[[

]]

Figure R6-8 PCT Distribution with SEO [[

]]

[[

]]

Figure R6-9 PCT Ranges for BWR/4 0.67 ft² Break with [[
]]

[[

]]

Figure R6-10 PCT Distribution for BWR/4 0.67 ft² Break with [[
]]

[[

]]

Figure R6-11 PCT Range for BWR/4 0.67 ft² Break with [[
]]

[[

]]

Figure R6-12 PCT Distribution for BWR/4 0.67 ft² Break with [[
]]

LTR Impact

The following in LTR Section 6.4 (last two paragraphs) will be modified in response to this RAI.

Original

[[

]]

In conclusion, there are inherent uncertainties associated with the modeling. The uncertainty caused by [[] appears to be a dominant contributor to the overall PCT uncertainty. This uncertainty, together with the other computational contributors, can be quantified by [[]]

For example, it is known that [[

]] As shown by this example, the standard deviation of the PCT distribution from a statistical analysis [[] is used to define and calculate the PCT analysis resolution.

Revised

[[

]] Figure 6.4-9 shows the range of PCT and Figure 6.4-10 shows the PCT distribution for different set of cases where the uncertainty parameters are sampled using [[

]] as shown in Figures 6.4-3, 6.4-4, 6.4-7 and 6.4-8 is [[]]

In conclusion, there are inherent uncertainties associated with the modeling. The uncertainty caused by [[] appears to be a dominant contributor to the overall PCT uncertainty, which is minimized by using detailed core modeling. This uncertainty, together with the other computational contributors, can be quantified by [[

]] As shown by this example in this section and in the RAI-9 response , the standard deviation of the PCT distribution from a statistical analysis [[] is used to define and calculate the PCT analysis resolution.

[[

]]

**Figure 6.4-9 PCT Range for BWR/4 0.67 ft² Break with [[
]]**

[[

]]

**Figure 6.4-10 PCT Distribution for BWR/4 0.67 ft² Break with [[
]]**

RAI-7

7) Please address the following issues associated with the concept of analysis resolution that is outlined in section 6.4 of the TR:

a. The concept of analysis resolution is meaningful when used in the sense of practical limitations in the capability of an evaluation model to simulate known physical processes in a reactor to an arbitrary degree of precision. However, the linkage in section 6.4 between the analysis resolution and the parallel channel effect does not fully conform to this definition because the probability of bundles containing hot rods in the reactor being plugged with liquid appears to be a significant uncertainty that is fundamentally associated with a limitation in physical knowledge rather than the practical capability of an evaluation model. Therefore, please either redefine the analysis resolution in light of the discussion above, or provide adequate justification for the current approach.

b. The general method for determining the analysis resolution elaborated in section 6.4 of the TR appears to be predicated on the presumption that, for all potentially limiting LOCA scenarios for operating BWRs, variation in the figures of merit due to [[
]] that presumably influence the analysis resolution (e.g., nodalization error, time step error, model simplification error). If, however, the limiting LOCA scenario for a given BWR is not [[

]] Please either generalize the proposed method for determining the analysis resolution, or provide adequate justification for the general applicability of the current approach to all potentially limiting LOCA scenarios for operating BWR designs.

c. The NRC staff requests additional technical basis to justify the adequacy of a [[

]] Please use an alternate [[

]]

d. Once an appropriate analysis resolution is defined that ensures external factors are bounded, please clarify whether it would be justified to accept a lesser total uncertainty for determining upper tolerance limits (e.g., the standard deviation associated with calculation results). For example, [[

]]

RAI-7 Response

This RAI response is related to the responses to RAI-6 and RAI-9.

- a. GEH agrees with this assessment and has significantly reduced this ‘unwanted’ uncertainty. The responses to RAI-6 and RAI-9 document that excess non-phenomenological uncertainty can be effectively minimized without artificially biasing the PCT results. In the light of this discussion, the analysis resolution definition is unchanged but now has a much lower value that is easier for the methodology to address.
- b. Section 6.4 of the LTR was intended to accomplish two things: (1) introduce the concept that the methodology should address how it treats some level of “noise” that cannot be resolved; (2) identify [[
]] as an example of “noise” that needed to be addressed by the methodology. As explained in part (a) of this response, the amount of noise has been greatly reduced. As a result, it is now possible to determine contributions to the PCT sensitivity that previously were covered by [[
]] was being applied. LTR Figures 6.4-7 and 6.4-8 illustrate this point even for [[
]] Additional discussion of the [[
]] is provided in part (c) below.
- c. The process for determining the analysis resolution has been revised. The [[

]] Figure R6-11 in the response to RAI-6 and Figure R9-3 in the response to RAI-9 demonstrate the effective convergence of all the PCT traces to the reduced noise level [[

]]

- d. GEH agrees with the implication in part (d) of the request that accepting a total uncertainty for the tolerance limit that is less than the analysis resolution cannot be justified. As explained in the RAI-6 response, an error in the input uncertainty distribution caused a full range sampling of the decay heat in the [[
]] As shown in RAI-6 and RAI-9 responses, the PCT analysis resolution is now significantly reduced and is now much less than the total uncertainty used in determining the upper tolerance limits.

LTR Impact

No changes to the LTR are proposed as the result of this RAI response. See RAI 6 for the LTR impact of the change in [[]].

RAI-8

8) Please provide clarification regarding the process discussed in section 9.2 for determining whether it is necessary to perform a revised statistical analysis in response to a change or error in the evaluation model. The TR states that a [[

]] Please clarify the following points:

a. What is the [[

]]

b. The TR appears to be inconsistent with 10 CFR 50.46, which mandates use of a fixed difference in PCT (50°F) as the criterion for determining whether a cumulation of changes and errors is significant. Given that the 95/95 upper tolerance limit is the regulatory figure of merit, please clarify how the proposed approach complies with 10 CFR 50.46, or revise the approach to ensure compliance.

RAI-8 Response

It is important to understand that 10 CFR 50.46 does not mandate a reanalysis when a change or error in the evaluation methodology is discovered. Instead, an estimate is provided. In most of the cases, the nature of the change would not cause any significant difference in the underlying assumptions and the biases and the uncertainties associated with the methodology. Therefore, the impact can be estimated by various means. Among them, estimation from first principles or known sensitivities, as well as engineering judgment or actual calculations are all valid and allowable methods.

When the impact is estimated using a code calculation, it is also important to recognize that any result within the PCT analysis resolution has equal validity. By comparing the mean values from two sets of PCT resolution analysis [[], the nominal effect of the change or the error can be quantified. If this ΔPCT is within the original PCT analysis resolution (i.e., \leq the standard deviation of PCT from [[])) computed for the given plant/scenario, then the effect of the change/error would be concluded to be small and not to have significant impact on the validity of the plant calculations done as part of the original analysis. In that case, the ΔPCT would be the quantity used as the estimate reported per 10 CFR 50.46. If the ΔPCT exceeds the analysis resolution, then it would be prudent to evaluate the effect on the upper tolerance PCT. This evaluation would be performed on the limiting break by exercising the full range sampling of the uncertainty contributors to obtain a new upper tolerance PCT. The difference between the newly calculated upper tolerance PCT having the change or correction and the original PCT would be the ΔPCT reported as the estimate of the effect per 10 CFR 50.46. For more significant effects, the latter provides the means of fulfilling the reporting requirements.

NEDO-33005-A Revision 1
Non-Proprietary Information – Class I (Public)

This threshold of repeating the full range statistical evaluation is different than the 50°F threshold stipulated in 10 CFR 50.46 for significance. Regardless of the magnitude of the analysis uncertainty, Δ PCT impact arising from a change or an error would be reported according to 10 CFR 50.46 rules, as also indicated in Figure 9.2-1 of the LTR. The concept explained in Section 9.2 of the LTR clarifies how this Δ PCT would be obtained.

In this context,

- a. The “statistical analysis” (used in 3rd paragraph of Section 9.2) refers to the PCT resolution analysis [[
The “full statistical analysis” (used in 4th paragraph of Section 9.2) refers to the case where all the uncertainty parameters are sampled from the full range of their associated distributions. This clarification is added to Revision 1 of the LTR to avoid future confusions.
- b. LTR is not inconsistent with the regulation on this aspect of 10 CFR 50.46, since it explains the ways of obtaining the estimate. In the regulation, the fixed 50°F threshold for significance is for 30-day reporting. This threshold is set for either a single change/error effect or the sum of absolute values of the PCT estimates from multiple changes (and/or errors). The regulation requires the licensee to submit the plan for reanalysis in that 30-day reporting. The LTR does not introduce any different notion that is in conflict with these aspects of the regulation. Instead, Section 9.4 provides clarification on how the reportable Δ PCT can be obtained if computer code calculations are used for estimating the impact. This method provides a logical and robust way of determining the effect of a change or an error when there is an inherent computational uncertainty in the calculations, assuring the validity of existing analysis.

LTR Impact

Section 9.2 will be edited as noted in the response above.

RAI-9

9) Please illustrate whether [[

]] the BWR/4 demonstration case. Although general discussion of the topic is provided in section 8.3.2.1 of the TR, based on the information provided in this discussion, the NRC staff could not discern [[

]]

RAI-9 Response

This RAI response is related to the responses for RAI-6 and RAI-7.

The BWR/2 results presented in the LTR are [[

]] Figures R9-1 and

R9-2 show the results from such a study.

As indicated in LTR Section 6.4, [[

]] In the actual applications of the methodology, GEH plans to use this improved modeling [[

]]

To demonstrate this point, the BWR/2 core was modeled with additional details. The detailed channel grouping for the BWR/2 model is shown in Table R9-1, which is compared to the LTR channel modeling as shown in LTR Table 8.3-1. As shown in Table R9-1, [[

]] The results are presented in Figures R9-3 and R9-4.

The improved model was also exercised for the full-range uncertainty analysis. These results are summarized in Figures R9-5 and R9-6.

In summary, the BWR/2 results shown in the LTR [[

]]

LTR Impact

No changes to the LTR are proposed as the result of this RAI response.

[[

Figure R9-1 PCT Range for BWR/2 Discharge DBA [[

]]
]]

[[

Figure R9-2 PCT Distribution for BWR/2 Discharge DBA [[

]]
]]

[[

]]

Figure R9-3 PCT Distribution for BWR/2 Discharge DBA [[
]]

[[

]]

Figure R9-4 [[

]]

[[

]]

Figure R9-5 [[

]]

[[

]]

Figure R9-6 [[

]]

RAI-10

10) Please provide information similar to that provided in Figure 6.9-5 of NEDE-32177P, Revision 3, for the BWR/4 intermediate and small break time step sensitivity cases presented in Table 5.2-1 of the TR (NEDE-33005P). Please also provide similar information for the BWR/2 discharge Design Basis Accident discussed in section 8.3.2.1 of the TR.

RAI-10 Response

Figure R10-1 shows the time step sensitivity results for the DBA suction break for a BWR/4 with the updated basedeck and latest TRACG code version. This provides a re-baselining as it is a reproduction of the same case shown in Figure 6.9-5 of NEDE-32177P, Rev. 3.

As with the original figure the plot shows [[

]]

[[

]]

Figure R10-1 Time Step Sensitivity for BWR/4 Suction DBA

Figure R10-2 shows the time step sensitivity study performed for an intermediate size suction break (0.67 ft²). This is the limiting break for the BWR/4 model presented in the LTR. In this break [[

]]

[[

]]

Figure R10-2 Time Step Sensitivity for BWR/4 Intermediate Break

The time step sensitivity results for a representative small break are presented in Figure R10-3. The small break is similar to the intermediate break [[

]] calculated for the intermediate and DBA break sizes.

[[

]]

Figure R10-3 Time Step Sensitivity for BWR/4 Small Break

Figures R10-4 through R10-6 show the timestep sensitivity for the same three break sizes using the detailed average core model (see the description of the BWR/4 detailed core modeling in the response to RAI-6). The time step sensitivity results show no meaningful differences between the detailed and original core model.

[[

]]

Figure R10-4 Time Step Sensitivity for BWR/4 Suction DBA (Detailed Core)

[[

]]

Figure R10-5 Time Step Sensitivity for BWR/4 Intermediate Break (Detailed Core)

[[

]]

Figure R10-6 Time Step Sensitivity for BWR/4 Small Break (Detailed Core)

Similar time step sensitivities were carried out for the BWR/2. Figure R10-7 shows the individual hot channel PCTs in a BWR/2 for the limiting DBA discharge recirculation line break. In the BWR/2 DBA break case the [[

]]

Figure R10-7 also shows that [[

]]

[[

]]

Figure R10-7 Time Step Sensitivity for BWR/2 Discharge DBA

[[

]]

Figure R10-8 Core PCT for BWR/2 Discharge DBA

Reduced sensitivity to changing the maximum time step size is observed [[
]] (See the description of the BWR/2 detailed core modeling in the response to RAI-9.) Figure R10-9 shows the hot channel PCTs as a function of the maximum timestep [[
]] for the BWR/2.

The timestep sensitivity performed using [[

]]

[[

]]

Figure R10-9 Timestep Sensitivity for BWR/2 Detailed Core Model

[[

]]

Figure R10-10 Core PCT for BWR/2 Detailed Core Model

LTR Impact

No changes to the LTR are proposed as the result of this RAI response.

RAI-11

11) Please provide an overview of typical results for the calculated PCT and cladding oxidation from the proposed TRACG evaluation model demonstration analysis as compared to those using the current SAFER evaluation model best-estimate and licensing results for analogous initial conditions.

RAI-11 Response

In this response, the results from SAFER and SAFER/CORCL analyses of similar plants with total core thermal power and ECCS capacities that match the ones used in the LTR demonstration calculations are chosen. Note that the TRACG results show the larger uncertainty band associated with the calculations originally presented in the LTR rather than those calculated later using the more detailed core model as described in the responses to RAI-6 and RAI-9.

It is important to note that the SAFER methodology is not part of the LTR scope and the review and approval of the current LTR is not based on SAFER. Because of these points, no attempt is made to render the analyses more comparable by precisely matching the initial and boundary conditions to the ones used in TRACG calculations. Some noteworthy differences that were not resolved are: (1) different peak linear heat generation rates (PLHGR) used for the TRACG calculations compared to SAFER; (2) GE14 fuel for the TRACG calculations compared to GNF2 for the SAFER calculations for BWR/2 plant type; (3) different small break areas. Because of these differences, the comparisons presented here cannot completely isolate methodology differences. These comparisons are presented for information only and cannot be the basis for determining a degree of conservatism in either method.

Figure R11-1 through R11-4 show the comparisons of PCTs predicted using the SAFER and the TRACG methodologies for similar BWR/4 plant types. Tables R11-1 and R11-2 show the comparisons of the PLHGRs, PCTs and oxidations from these two methods.

The comparisons between SAFER/CORCL and TRACG results for a BWR/2 type plant are also provided. The results are shown in Figure R11-5 and 11-6 and in Table R11-3. Note that the TRACG calculations used a higher PLHGR than the SAFER/CORCL calculation yet the PCT predicted by TRACG was lower than SAFER/CORCL.

LTR Impact

No changes to the LTR are proposed as the result of this RAI response.

Table R11-1 PCT and Oxidation Results Comparison

BWR/4 Large-Break	SAFER	TRACG
Fuel Type	GE14	GE14
PLHGR ⁽¹⁾	[[
PCT		
ECR		
Break]]

Note: (1) For SAFER, this value is for Appendix K assumption; for TRACG the nominal value is listed. Those two values do not contain the adders used in the analyses.

Table R11-2 PCT and Oxidation Results Comparison

BWR/4 Small-Break	SAFER	TRACG
Fuel Type	GE14	GE14
PLHGR ⁽¹⁾	[[
PCT		
ECR		
Break Area (ft ²) ⁽²⁾]]

Note: (1) For SAFER, this value is for Appendix K assumption; for TRACG the nominal value is listed. Those two values do not contain the adders used in the analyses.

(2) Small break is for break area ≤ 0.1 ft². Reported value is small break area with the highest PCT.

Table R11-3 PCT and Oxidation Results Comparison

BWR/2 Large-Break	SAFER-CORCL	TRACG
Fuel Type	GNF2	GE14
PLHGR	[[
MAPLHGR		
PCT		
ECR		
Break]]

[[

]]

**Figure R11-1 PCT Results for BWR/4 Large-Break LOCA
Using SAFER with App. K Assumptions**

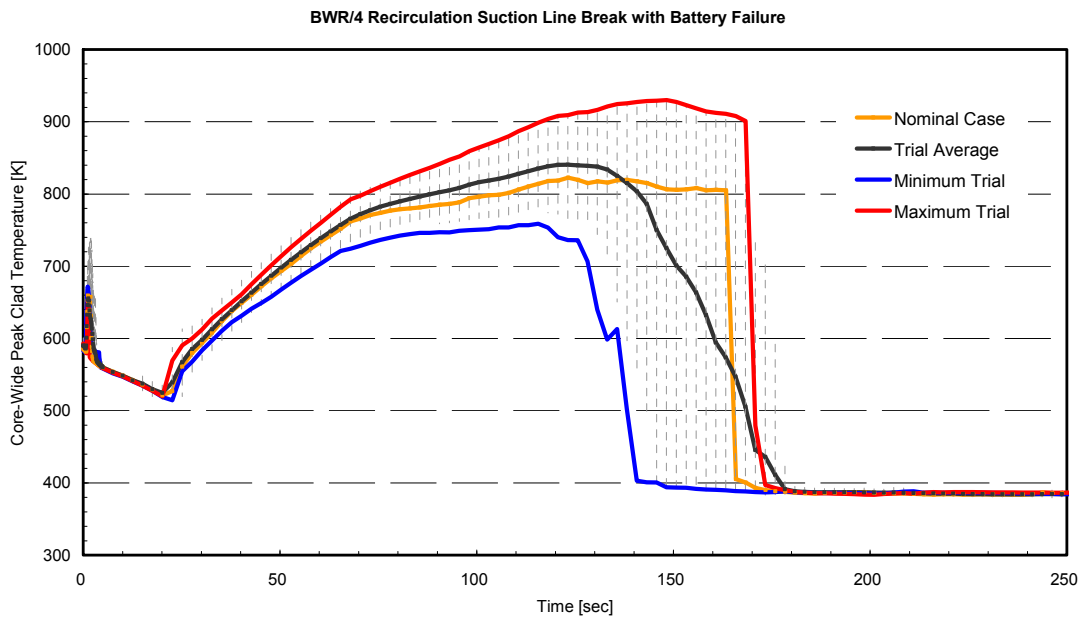


Figure R11-2 PCT Results for BWR/4 Large-Break LOCA Using TRACG

[[

]]

**Figure R11-3 PCT Results for BWR/4 Small-Break LOCA
Using SAFER with App. K Assumptions.**

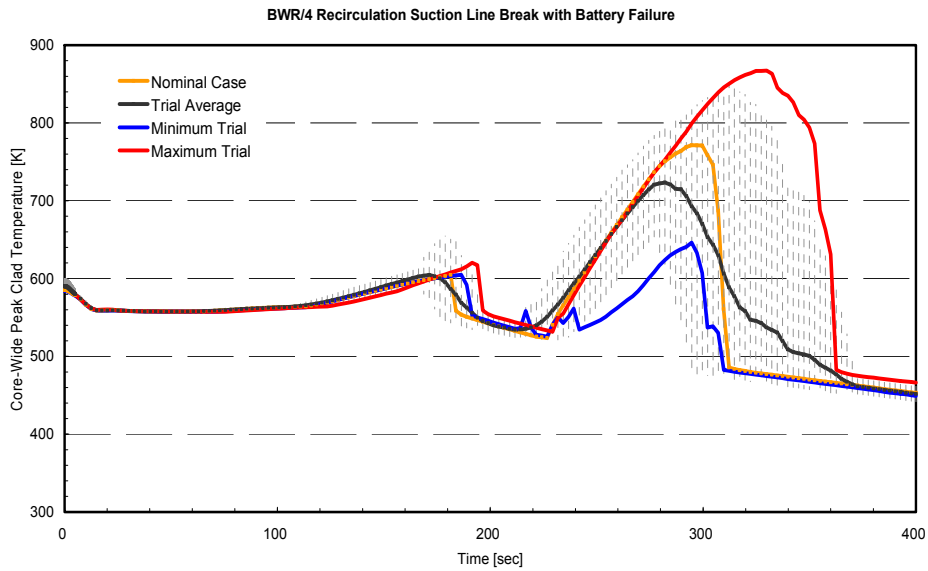


Figure R11-4 PCT Results for BWR/4 Small-Break LOCA Using TRACG.

[[

]]

**Figure R11-5 PCT Results for BWR/2 Large-Break LOCA
Using SAFER with App. K Assumptions.**

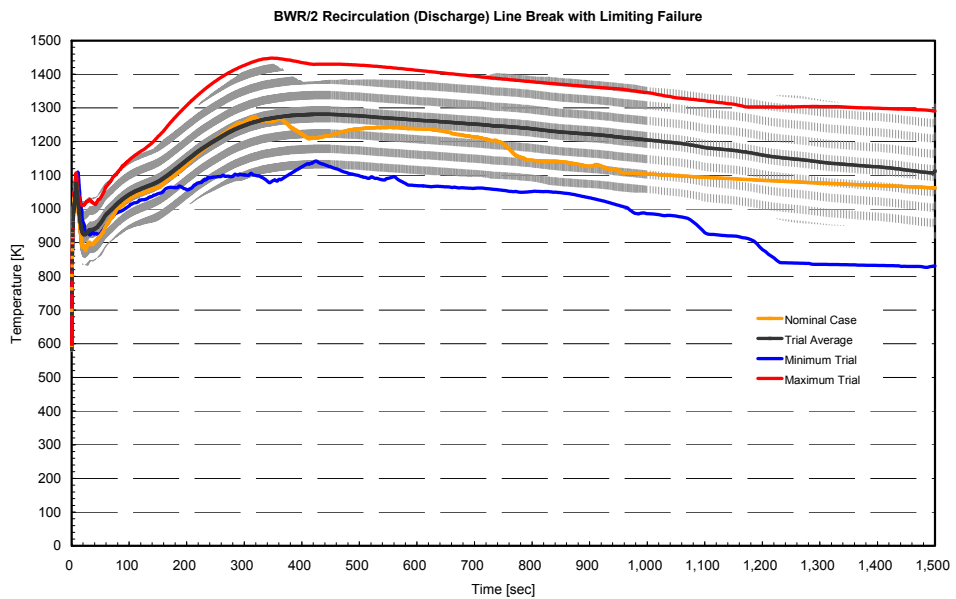


Figure R11-6 PCT Results for BWR/2 Large-Break LOCA Using TRACG

RAI-12

12) Please clarify what assumptions are made concerning offsite power and the availability of nonsafety systems in the demonstration cases and, likewise, how nonsafety systems would be treated for future plant-specific analysis. For example, the small liquid break scenario in Figure 3.2-1 of the TR suggests that reactor pressure is maintained at a control setpoint prior to main steam isolation valve closure, rather than being controlled through the cycling of safety relief valves (SRVs), as indicated in the text of section 3.2.3. An analogous observation is made regarding Figure 8.1-6 and section 8.1.2.2, both of which cases are contrasted with Figure 8.3-17, where SRVs appear to cycle. Please discuss how the availability of offsite power affects the figures of merit for compliance with 10 CFR 50.46 and justify that the assumptions made with respect to offsite power and nonsafety systems are consistent with analyzing the most limiting conditions. Please clarify whether these limiting conditions change as a function of break size.

RAI-12 Response

In the TRACG LOCA application methodology, there is no consideration of any credit gained from non-safety grade systems. This process is unchanged from the current approved LOCA methodology.

[[

]]

In the demonstration cases presented in the LTR, there are some deliberately conservative assumptions regarding Loss of Offsite Power (LOOP) or Offsite Power Available (OPA) conditions. Irrespective of offsite power availability, the SRV operation would have sufficient battery power for the solenoid and/or accumulator gas for the pilot valve to actuate during a small-break LOCA scenario. In safety mode, valve opening and closure does not rely on a power source, unlike in the relief mode.

[[

]]

For small to intermediate break sizes, a LOOP assumption consistent with the plant configuration would provide scram, feedwater trip, and MSIV closure signals concurrently at the beginning of the event. Similarly, OPA assumption consistent with plant configuration would not trip the reactor, feedwater, and MSIVs. The reactor scram would then take place on earlier of L3 or high drywell pressure signals. MSIVs will be signaled to close on L1 or low main steam line (MSL) pressure. When power is available, the feedwater (FW) pumps continue to operate. In this case, the level is maintained for an extended period of time, providing sufficient cooling mitigating any adverse effect of LOCA and practically rendering the small-break event insignificant. The signals for OPA and LOOP assumptions are summarized in Table R12.1. The table also contrasts the assumptions used in the calculations shown in Section 8.

Table R12-1 Assumptions for OPA and LOOP

	OPA Assumption	LOOP Assumption	Demo Calculations
Scram	L3 or High DW Press.	with LOOP (0 sec)	[[
FW trip	No FW trip	with LOOP (0 sec)	
MSIV trip	L1 or MSL Pressure	with LOOP (~5 sec stroke time to close)	
Recirculation pump trip	L2	with LOOP (conservative time constant for coastdown)	
ADS timer initiation	L1	L1]]

[[

]]

Table R12-2 Summaries of PCT's for BWR/4 LOCA Runs with current LTR assumptions and with LOOP assumptions

Break Sizes	PCT (K) (From LTR)	PCT (K) From the LTR cases re-run with the Detailed Core Model	PCT (K) From the cases with LOOP run with the Detailed Core Model
[[
]]

Figure R12-1 shows one example of the reactor pressure vessel (RPV) pressure responses between the LTR case and the LOOP case (both using detailed core model), which is for the 0.1ft² small liquid line break. [[

]]

[[

]]
Figure R12-1 RPV responses for LTR Figure 8.1-6 case (Current) and the case with LOOP (LOOP), both with Detailed Core Model.

LTR Impact

No changes to the LTR are proposed as the result of this RAI response.

RAI-13

13)[[

]] addressing the following points:

a. [[

]]

RAI-13 Response

The difference in BWR/2 discharge break PCT's between the double-ended guillotine break (DEGB) and the same area split break as shown in Figure 8.3-14 of TRACG LOCA licensing topical report (LTR) is attributed to [[

]]

The PCT time histories for those two cases (called DEGB and Split hereafter) are shown in Figure R13-1. It is observed that the PCT's for both breaks
[[

]]

In summary, the PCT differences for DEGB and the same area split break as shown in LTR
Figure 8.3-14 for BWR/2 discharge break

[[

]]

[[

Figure R13-1 PCTs for BWR/2 Discharge Split break and DE GB

]]

[[

Figure R13-2 Air Pressure in the RPV Upper Plenum for BWR/2 Split break and DE-GB

]]

[[

Figure R13-3 PCT for BWR/2 discharge original DE GB and Split break with vent at 160 seconds.]]

- a. Like BWR/2 discharge break, the difference in BWR/2 suction break PCT's

[[

]]

The PCT time histories for those two suction break cases (also called DEGB and Split) are shown in Figure R13-4. It is observed that

[[

]]

[[

]]

Figure R13-4 Core PCTs for BWR/2 Suction DE GB and the same break area Split break

[[

]]

Figure R13-5 Total Air mass inside the RPV for BWR/2 DE GB and the same area split break

[[

]]

Figure R13-6 RPV downcomer water levels (Above Vessel Zero) for BWR/2 Suction DE Gb and the same area split break

[[

]]

Figure R13-7 PCTs for BWR/2 suction original DE GB and Split break with vent at 125 seconds.

- b. For the BWR/2 discharge break, the limiting break is the DEGB, with a core PCT [[

]]

These results together with the sensitivity studies described in part (a) of the response show that [[

]]

- c. As discussed in the response to this RAI, [[

]]

The responses above were discussed in a meeting on July 1, 2013. The additional information provided below is in response to questions asked by the NRC staff at the July 1, 2013 meeting.

Regarding BWR/2 Break Locations

[[

]]

Regarding the BWR/2 Detailed Core Modeling (discussed in RAI-9)

The TRACG runs performed above for this RAI response are based on the same TRACG model as presented in the LTR. [[

]]

Regarding Intermediate Break

[[

]]

LTR Impact

No changes to the LTR are proposed as the result of this RAI response.

RAI-14

- 14) The TR indicates in section 3.4 that medium-ranked parameters have a small effect on primary safety parameters and may be excluded in the overall uncertainty evaluation. This definition and treatment is not consistent with the typical characterization of medium-ranked parameters as those having a moderate effect on figures of merit (i.e., neither dominant nor negligible). The NRC staff further noted that the demonstration analyses presented in section 8.1.3 appear to include several medium-ranked parameters among the most influential for determining PCT.
- a. Please confirm whether medium ranked parameters will be included in statistical analysis and revise the TR (e.g., section 3.4) as necessary to be consistent with the positions taken in this RAI response.
 - b. Please confirm whether future plant-specific analyses will be based on the use of the highest overall rank for a given PIRT phenomenon versus design-specific / scenario-specific PIRT rankings. This distinction is important because, while the NRC staff agrees that the design- and scenario-specific PIRT rankings in the TR are largely representative of typical BWRs of a given product line, it is not clear that they fully capture design variations among individual plants (e.g., certain BWR/3s and /4s with elevated PCTs).

RAI-14 Response

There are no medium-ranked phenomena that were excluded in the overall uncertainty evaluation. All high and medium ranked parameters are included consistent with all previously approved TRACG application methodologies.

- a. This response to the RAI formally confirms that the medium-ranked parameters are and will be included in statistical analysis along with the highly ranked parameters. In Revision 1 of NEDO-33005P, Section 3.4 is revised accordingly.
- b. This response to the RAI also confirms that plant-specific analyses will be based on the use of the highest overall rank for a given PIRT phenomenon versus design-specific (i.e., BWR/2, BWR/3-4, or BWR/5-6) and scenario-specific (small- or large-break LOCA) PIRT rankings. However, this confirmation does not constitute a new commitment to performing a PIRT evaluation in future applications. The Phenomena Identification and Ranking Table (PIRT) presented in Section 3 extensively covers all design- and scenario-specific rankings for all BWR types having either external recirculation pumps or jet pumps. The design variations among individual plants do not surmount to differences that depart from one particular product line, and hence, do not necessitate generation of plant-specific PIRT. The PIRT process is presented generically as part of the methodology review.

LTR Impact

LTR Section 3.4 will be revised to state that all high and medium ranked parameters are included.

RAI-15

15) The technical basis for the uncertainty distribution and justification GEH proposed for PIRT item M9 (LPCI/Break Flow Interaction) was not apparent to the NRC staff. In particular, the discussion in section 5.1.12.5 proposes that [[

]] However, other factors would apparently influence this phenomenon, such as local flow conditions, the assumed break orientation and geometry, and nodalization. Therefore, please provide adequate justification to support credit taken for LPCI flow from the broken loop to the core across the spectrum of breaks for which this flow would be split between the break and the vessel. To the extent possible, please include reference to experimental data that can be used to validate the flow splits predicted by the TRACG evaluation model.

RAI-15 Response

The sentence in Section 5.1.12.5 stating “The interaction between LPCI and break flow is controlled by the liquid-side interfacial heat transfer.” will be replaced with the sentence “Interfacial heat transfer of cooler LPCI water injected into the recirculation line with steam in the line influences the calculated pressure gradient in the line which in turn influences the break flow.” With respect to what fraction of the LPCI flow gets into the vessel versus flowing out the break, there are several other more important considerations that are discussed in this response. First an explanation is provided for how LPCI interaction with the break location is modeled so that LPCI fluid into the vessel from the broken loop will not be overestimated. Then, the role played by interfacial heat transfer is described in its proper context.

The concern in the RAI is limited to BWR/3s and some BWR/4s where LPCI is injecting into the recirculation loop. External pump plants (BWR/2s) do not employ LPCI. For the newer BWR/4s and all BWR/5s and BWR/6s, LPCI is directly injecting to the core bypass region inside the core shroud. For larger breaks in those plants that could be affected, all LPCI sweeps out from the break and is discharged out of the system before reaching the vessel. Therefore, the issue as described is only of concern for small break scenarios in some of the plants.

No undue credit is gained from the LPCI for the affected plants. The pump discharge break location for plant designs with LPCI injection into the recirculation line is modeled between the LPCI connection point and the reactor vessel so that the flow of LPCI water out the break is favored. In the case of pump suction break, LPCI flow toward the vessel is retarded because the pressure gradient is directed away from the vessel back toward the break. How much LPCI water makes it into the reactor vessel is determined by this pressure gradient which depends on the assumed size of the break.

There is no stratification in the recirculation line because the model for the line is one-dimensional; break orientation, shape and geometry of the break have no meaning in such a model. Sampling of the break flow uncertainty addresses any relatively small effects of shape and orientation over the break geometry. Any larger effects are covered by analysis of different break sizes.

The only potential interaction in the modeling is related to the mixing of the two flows: break flow from the vessel side and the colder coolant from the injection. [[

]] This is also demonstrated in the response to RAI-34. The sensitivity runs performed as part of RAI-34 response indicate that LPCI mixing impact is not significant in LOCA analysis.

LTR Impact

LTR Section 5.1.12.5 will be revised as indicated above.

RAI-16

16) Please clarify whether TR reference [46] is consistent with the assertions in section 5.1.2.4 that [[

[[]]. Because of the significant difference in
[[]]
is unclear.

RAI-16 Response

[[

]]

The sample calculations are performed for a BWR/4 intermediate break (0.67ft²). [[

]] These comparisons show that the choice of guide tube-bypass CCFL inputs given in the LTR for TRACG LOCA application is reasonable.

LTR Impact

No changes to the LTR are made as the result of this RAI response.

Table R16-1 Statistical Core PCT Summary

[[
]]

[[

]]

Figure R16-1 Comparison of Guide-bypass CCFL Ranges

Note for Figure R16-1:

[[

]]

[[

]]

Figure R16-2 Core PCTs for ORIGINAL Runs [[

]]

[[

]]

Figure R16-3 Core PCTs for PIRT Runs (NEDE-30996P[[

]]

RAI-17

- 17) Please clarify the nomenclature regarding lognormal distributions that is used throughout the TR.
- a. Please confirm what is meant by mode and gain when referring to the lognormal distribution. For example, see Figure 5.1-10, where the reported mode does not appear to correspond to the peak of the probability distribution function.
 - b. Please confirm whether, in the discussion of PIRT item A1, it is correct that the quoted standard deviation of [] belongs to the associated normal distribution, rather than the lognormal distribution being discussed.

RAI-17 Response

The definitions of **gain** and **mode** for log-normal distributions are given below. The NRC expectation is that **mode** should correspond to the peak of the probability distribution is correct. Figure 5.1-10 in the LTR is incorrect and will be replaced as indicated in the response to RAI-40. The discussion of a standard deviation for PIRT item A1 in the LTR will be removed since it is extraneous. As shown below, the mode and gain fully specify the log-normal distribution and from this specification other statistics of the random variable X can be calculated.

A log-normal probability density function (PDF) is defined by

$$f(x) = \frac{1}{\sqrt{2\pi x} \sigma_{\ln x}} \exp \left[-\frac{1}{2\sigma_{\ln x}^2} [\ln(x) - \mu_{\ln x}]^2 \right], \text{ for } \{x, \sigma_{\ln x}\} \quad (\text{R17-1})$$

where

- x is the value of a positive random variable X with a log-normal distribution,
- $\mu_{\ln x}$ is the mean of the of the random variable X,
- $\sigma_{\ln x}$ is the standard deviation of the \log_e of the random variable X.

In the TRACG LOCA application, the working range for the PDF is selected to be a 3σ on either side of the x_m , which is the value of x where the frequency $f(x)$ is the maximum. The value for the mode x_m can be found by differentiating Eq. R17-1 and solving such that

$$f'(x_m) = 0 \quad (\text{R17-2})$$

It follows x_m , $\sigma_{\ln x}$ and $\mu_{\ln x}$ are related to each other by

$$\mu_{\ln x} = \sigma_{\ln x}^2 + \ln(x_m) \quad (\text{R17-3})$$

$$x_m = \exp(\mu_{\ln x} - \sigma_{\ln x}^2) \quad (\text{R17-4})$$

The mode x_m of the log-normal PDF is of interest because **the intended application is to simulate a log-normal PDF where the mode x_m is given. What is needed is a way to define either $\sigma_{\ln x}$ or $\mu_{\ln x}$ such that the specified value of x_m will be realized.** One way of doing this is to relate $\sigma_{\ln x}$ to the expected working range for the PDF. For 95% probability and 95% confidence in a two-sided normal distribution requires a working range of at least $\pm(1.960*1.217)\sigma$ on either side of the mean for sixty or more samples. In other words for a set of 60 values $\{y\}$ from a normal distribution, a working range of $[y_1, y_2]$ where

$$y_1 = \mu - 2.38532\sigma \quad (\text{R17-5})$$

$$y_2 = \mu + 2.38532\sigma \quad (\text{R17-6})$$

is sufficient to assure with 95% probability and 95% confidence that any other sample will be inside the range. Choosing a broader (more conservative) 6σ span for the working range $[y_1, y_2]$ leads to

$$y_1 = \mu - 3\sigma \quad (\text{R17-7})$$

$$y_2 = \mu + 3\sigma \quad (\text{R17-8})$$

and

$$\sigma = \frac{1}{6}(y_2 - y_1) \quad (\text{R17-9})$$

This larger range with a 6σ span provides approximately 97.5% probability and confidence for a sample size of sixty. To relate this working range $[y_1, y_2]$ for the normal distribution to the working range $[x_1, x_2]$ for the log-normal distribution apply the relationship

$$\{y\} = \ln(x) \quad (\text{R17-10})$$

to write

$$\sigma_{\ln x} = \frac{1}{6}(y_2 - y_1) = \frac{1}{6}[\ln(x_2) - \ln(x_1)] = \frac{1}{6}\left[\ln\left(\frac{x_2}{x_1}\right)\right] \quad (\text{R17-11})$$

At this point it is convenient to introduce the concept of a “gain”, \mathbf{g} . For convenience the gain is defined about the mode such that the working range for the underlying normal PDF has minimum and maximum values defined by

$$x_1 = \frac{x_m}{\mathbf{g}} \tag{R17-12}$$

$$x_2 = x_m \mathbf{g} \tag{R17-13}$$

It is obvious that $\mathbf{g} \neq 0$ and to make physical sense it is necessary that $\mathbf{g} \geq 1$. It is also apparent that for $\mathbf{g} = 1$ that $x_1 = x_m = x_2$ and that all three values must always be greater than zero. Another useful relationship that follows from Eqs (R17-12) and (R17-13) is

$$\mathbf{g} = \sqrt{\frac{x_2}{x_1}} \tag{R17-14}$$

When the relationship between \mathbf{g} and $\frac{x_2}{x_1}$ is applied to Eq. (R17-11) one gets

$$\sigma_{\ln x} = \frac{1}{6} \left[\ln \left(\frac{x_2}{x_1} \right) \right] = \frac{1}{6} [\ln(\mathbf{g}^2)] = \frac{1}{3} \ln(\mathbf{g}) \tag{R17-15}$$

LTR Impact

Figure 5.1-10 will be revised.

LTR Section 5.1.1.1 will be revised as follows:

Flashing and the associated redistribution of liquid inventory in the lower plenum of the TRACG model are controlled by liquid-side interfacial heat transfer. The bubbly flow regime is the dominant flow regime for this behavior. TRACG uses the Lee-Ryley correlation in conjunction with a bubble diameter based on a critical Weber number for liquid-side heat transfer in the bubbly flow regime [1]. The Lee-Ryley correlation applies to heat transfer to spherical particles under forced circulation conditions. It predicts the water droplet evaporation data from which it was originally developed with an error less than 10%. Following the procedure previously adopted for the Anticipated Operational Occurrences (AOO) application [3], the uncertainty in the PIRT multiplier on the interfacial heat transfer at the bubble surface is specified as a [[

]]

RAI-18

18) Please address the following issues with the statistical distribution for PIRT item F1 by revising the statistical distribution or providing adequate justification for the current approach:

- a. Representation of the void deviation using $[[\quad \quad \quad]]$
- b. It is unclear that the distribution parameters and imposed cutoff capture data at both the upper and lower extremes of the distribution (Is the minimum of $[[\quad \quad \quad]]$ samples reasonably considered the minimum possible value of the distribution?).
- c. The selection of a $[[\quad \quad \quad]]$ inflate the expectation value of the multiplier.

RAI-18 Response

- (a) The $[[\quad \quad \quad]]$ associated with the void deviations for tests applicable to regions with large hydraulic diameter was only obtained from the Anderson-Darling normality test. Other statistical tests yield a $[[\quad \quad \quad]]$ indicating that it would not be unreasonable to assume $[[\quad \quad \quad]]$

$[[\quad \quad \quad]]$ was used for PIRT item F1.

The sentences of “ $[[\quad \quad \quad]]$ ” in $[[\quad \quad \quad]]$ in LTR Section 5.1.6.1 are deleted. See the discussion in the response to RAI-19.

- (b) The comparisons are directly obtained from TRACG calculations. The deviation of the predicted void fraction from measured data is well represented by the range of the data used in derivation of the uncertainty parameter. As indicated in Section 5.1.6.1 of the LTR, the individual deviations for the TRACG predictions of the data sets used to establish the void fraction uncertainty were in no case greater than $[[\quad \quad \quad]]$ and the maximum deviation between all predictions and the void data was $[[\quad \quad \quad]]$ indicating that no more extreme points would be anticipated. The current LTR PIRT F1 used $[[\quad \quad \quad]]$ data samples. In the response to RAI-19, more data samples have been used for this PIRT item. A refined PIRT F1 uncertainty is presented. The probability density function (PDF) is presented in RAI-19 response to bound all $[[\quad \quad \quad]]$
- (c) Application of the $[[\quad \quad \quad]]$ amplifies the impact on the expectation value of the multiplier, especially at the extremes. In contrast, $[[\quad \quad \quad]]$ this possible inflation, making it more in line with physical reality. This is further demonstrated in the response to RAI-19, in which the $[[\quad \quad \quad]]$

$[[\quad \quad \quad]]$ (See Response to RAI-17 Equation R17-12).

LTR Impact

The LTR change with this RAI is made in RAI-19.

RAI-19

19) Please explain and justify the criteria used for selecting test data for the uncertainty derivations for PIRT item A5 (lower plenum void distribution) and related PIRT item F1 (upper plenum void distribution). Different selections of data from some of the same test facilities (9 tests for A5 versus 28 tests for F1) were made to derive the respective uncertainty distributions.

RAI-19 Response

The discerning factors for limiting the experimental void fraction data for determining the lower plenum void distribution uncertainty (PIRT A5) only to the five Wilson data points and the four Bartolomei data points are: [[

]] (as seen from NEDE-32177P, R3 Section 3.1.3). The relevant discussion from Section 5.1.1.6 of the LOCA LTR is quoted below:

“[[

]]...”

Note that the label for Figure 5.1-2 is incorrect. The sensitivity study that is pictured was determined from the [[]] model and data.

For determining the void distribution and two-phase level uncertainty for the upper plenum (PIRT F1), [[

]]

LTR Impact

Figure 5.1-2 label will be corrected as

Sensitivity of TRACG Prediction of Average Void Fraction in Large Hydraulic Diameter Test Facilities to PIRT Multiplier

LTR Section 5.1.6.1 will be updated as follows.

5.1.6.1 F1 – Void Distribution/Two-Phase Level (H)

[[

]] These data are characterized by their applicability to the prediction of void fraction in regions with relatively large hydraulic diameter. Accordingly, selections from this data set, taking into consideration other aspects of the test conditions, will be used as the basis for defining the [[

]] A statistical summary of the comparisons of TRACG predictions with measurements from these four data sets, combined as a single set of deviations, is shown in Figure 5.1 20. The absolute mean bias is [[]] void and the absolute standard deviation is [[]] void.

[[

]] (A comparable evaluation for lower plenum is described under A5 in Section 5.1.1.6 and for the core and bypass is described below under C2AX in Section 5.1.3.3.)

[[

]]

LTR Table 5.1-2 will be updated as follows and Figures 5.1-20 and 5.1.22 will be updated with Figures R19-1 and R19-2.

[[

]]

Figure R19-1 Void Fraction Deviations for Tests Applicable to Regions with Large Hydraulic Diameter

[[

]]

Figure R19-2 Probability Distribution for Multiplier on Interfacial Drag Coefficient

RAI-20

20) In a number of demonstration cases in the TR, the PCT calculated for the limiting bundle [[

]] (e.g.,

Figures 8.1-5, 8.1-23, 8.1-24, and 8.1-25).

a. [[

]]

b. In cases where the maximum PCT occurs in a Ring 2 bundle, it does not appear to
[[as discussed in section 5.1.6.4,
[[Please
provide an alternate justification that the spray flow distribution uncertainty is bounded in
this case.

RAI-20 Response

This RAI response is related to the response for RAI-21.

a. During the post-blowdown phase of a large-break LOCA, the liquid that was present in the fuel channel would be almost entirely depleted either by flowing and draining out of the assembly or by flashing. As the rods dry out, the main heat transfer mechanism would be convection and radiation. Convective heat transfer by steam is the dominant cooling mechanism until sufficient amount of coolant penetrates the channel and the cladding surface temperature eventually drops down below the minimum stable film boiling temperature, allowing rewet. During this period, the magnitude of steam cooling is a strong function of the amount of steam available and its velocity. [[

]]

As the coolant forms a pool in the upper plenum, the amount of liquid that drains into the channel is governed by Counter Current Flow Limitation (CCFL) and can be further limited.

b. The uncertainty in the spray distribution, as discussed in Section 5.1.6.4 of the LTR is related to [[

]]

LTR Impact

No changes to the LTR are proposed as the result of this RAI response.

RAI-21

21) PIRT item F4 in section 5.1.6.4 discusses the spray distribution for an uncovered upper plenum.

a. Please clarify whether [[

]]

b. Please clarify GEH's position concerning whether the specific information contained in TR section 5.1.6.4 is applicable only to [[

]] or all BWR/2s.

c. Please provide TR references [64] and [61].

d. Please clarify whether spray degradation is primarily a function of reactor pressure or the differential pressure between the reactor vessel and wetwell. Please identify the wetwell pressure assumed in the calculation.

RAI-21 Response

This RAI response is related to the response for RAI-20.

a. [[

]]

b. As indicated Section 5.1.6.4, [[

]]

c. The requested references will be delivered to the staff.

d. Spray degradation is primarily a function of the differential pressure between the vessel and the wetwell. However, [[

]]

LTR Impact

No changes to the LTR are proposed as the result of this RAI response.

RAI-22

22) Please provide justification for ranking [[

]] The TR notes that choking may occur at the jet pump for large discharge breaks, and this behavior is exhibited in the demonstration calculations in Chapter 8. The demonstration calculations also indicate that discharge breaks may be limiting for some BWRs.

RAI-22 Response

In the PIRT process, the phenomena are ranked according to their relative influence on the LOCA critical parameters. [[

]] Although a relative ranking given to a particular physical aspect is somehow subjective and open to debate, the outcome does not change. It is also acknowledged that one particular PIRT item, [[]], might be more important than [[]]. However, the coarse assignment of rankings, such as H-M-L, does not permit discerning these differences.

Jet pump flow reversal and two-phase conditions in the jet pumps occur in early blowdown phase of a large-break LOCA. In smaller breaks, a milder initial flow transient would occur. As flow reversal in jet pumps on the broken loop side happens, choking at the jet pump nozzle will happen. These phenomena, including the expected behavior of jet pump flow, are modeled in the LOCA analyses as they are exhibited, and the biases and uncertainties associated with each of these phenomena are included in the calculations.

LTR Impact

No changes to the LTR are proposed as the result of this RAI response.

RAI-23

23) The NRC staff was unable to confirm the statistical distributions proposed for certain parameters from either Table 5.1-2 or the text of Chapter 5 (e.g., PIRT items A2, A3 (wall heat transfer), C20 (minimum stable film boiling temperature), Q5, C22, L3, M8, G3). Please explicitly identify the statistical distributions proposed for any parameters if not previously provided.

RAI-23 Response

The subsections in LTR Section 5.1 provide the uncertainty treatment for each phenomenon that is ranked high or medium. Either the distribution for the parameter that affects the uncertainty is provided or, if another parameter already covers the particular uncertainty or a different treatment is applied to address the uncertainty, an explanation is provided. Section 5.1 of the LTR provides complete accounting of model uncertainties that are considered in the TRACG LOCA methodology. All the uncertainty parameters listed in LTR Table 5.1-2 have normal distribution, unless noted otherwise in the comments column. The log-normal distributions are expressed with defining parameters given in parentheses. The LTR Table 5.1-2 will be updated to denote all normal distributions to eliminate ambiguity. Following items referred in the RAI, are listed with additional clarification:

A2 – heat slab stored energy release is controlled by wall heat transfer. A multiplier is applied to wall heat transfer coefficient. In the statistical analyses, the multiplier is [[
]], as stated in Section 5.1.1.2
and Table 5.1-2 of the LTR.

A3: The two-phase level and SEO uncovering timing are affected by [[

]].

C20: The uncertainty applied to the minimum stable film boiling temperature T_{min} is [[

]] See the response to the RAI-50 for updated discussion on C20.

Q5: The uncertainty of isolation condenser heat removal capacity was originally considered as a multiplier on the secondary side heat transfer with a large range around the nominal value. However, as indicated in Table 5.1-2, a bounding approach is taken in BWR/2 analyses and no IC is modelled. Therefore, there is no applicable uncertainty. As also committed in RAI-62 response, a heat transfer uncertainty model will be considered only if IC is modeled.

C22: Channel to bypass heat transfer uncertainty is treated by multipliers on the heat transfer coefficients of the channel inside and outside surfaces. The multiplier applied to inside channel wall heat transfer model [[

]] (LTR Section 5.1.3.28). The multiplier on the outside is same as A2 and it has an uncertainty [[]] (LTR Section 5.1.1.2). These parameters are listed in LTR Table 5.1-2.

L3: Although not a dominant factor in recirculation line breaks, the uncertainty of steam line pressure drop is applied as a multiplier on the local losses that is sampled from [[

]] (LTR Section 5.1.11.3 and Table 5.1-2). This uncertainty is the same value from the approved Anticipated Operational Occurrences (AOO) application (Reference R23-1).

M8: Similar to L3, the pressure drop in recirculation line has [[]] that was specified on the basis of comparisons between TRACG predictions and pressure drop data, as indicated in LTR Section 5.1.12.4 and Table 5.1-22.

G3: As explained in LTR Section 5.1.7.2 and given in Table 5.1-2, the reverse flow characteristics of a jet pump can be varied by [[

]]

Reference

R23-1 NEDE-32906P-A, “TRACG Application for Anticipated Operational Occurrences Transient Analyses,” Revision 3, September 2006.

LTR Impact

As indicated in the response, the LTR Table 5.1-2 will be updated to denote all normal distributions.

RAI-24

24) Please confirm that the TRACG LOCA evaluation model will require fuel parameter inputs from the PRIME code, and that code options associated with fuel thermal conductivity degradation will be implemented in a manner that addresses NRC staff concerns expressed in its letter dated March 23, 2012 (Agencywide Documents Access and Management System (ADAMS) Accession No. ML120680571). If approval for inputs from legacy fuel codes (e.g., GESTR is referred to in the TR) or legacy TRACG code options is requested, please provide justification.

RAI-24 Response

As noted in the NRC’s Safety Evaluation in Reference R24-1, “in accordance with IMLTR Limitation 12 and Supplement 3, GEH intends to use PRIME T-M methods for future applications”. GEH is not seeking approval for inputs from legacy fuel codes (e.g., GESTR) or legacy TRACG code options that invoke such models or inputs as part of the TRACG LOCA evaluation model. The TRACG LOCA application methodology uses only the PRIME-based thermal conductivity model together with fuel parameter inputs supplied by the PRIME code to address the NRC staff concerns associated with fuel thermal conductivity degradation.

Reference

R24-1 NEDC-33173P-A, Revision 4, “Applicability of GE Methods to Expanded Operating Domains,” November 2012.

LTR Impact

References to the GESTR thermal-mechanical model will be removed from LTR Table 2.5-1 so that PRIME is indicated as the only option.

RAI-25

25) Please clarify the behavior in Figure 8.1-5, wherein [[

]] as stated in section 8.1.2.1.

Nor does the difference appear to be primarily associated with the timing of reflood, since the divergence in temperature seems to originate approximately coincidentally with the start of low-pressure core spray (LPCS).

RAI-25 Response

The TRACG BWR/4 DBA run used to produce LTR Figure 8.1-5 was reviewed to determine the axial nodes where the channel PCT occurs. [[

]]

This DBA case was re-run with the graphical data saved in a much smaller time interval after the first 5 seconds of the transient (0.2s now versus 2.5s originally). Also, additional graphical information was obtained for the nodes where the channel PCTs were observed. The PCTs for those channels shown in LTR Figure 8.1-5 are presented in Figure R25-1. Note that the average channel results have been dropped from the figures in this RAI response since they are irrelevant. Comparisons between LTR Figure 8.1-5 and Figure R25-1 show that the overall behavior for each channel for the re-run is comparable to the original result.

Figures R25-2 and R25-3 show the void fraction and steam temperature at the PCT nodes for [[

]] as shown in Figure R25-1 and also with more detail in Figure 25-4. This divergence in heat up rates [[

]] as shown in Figures R25-2 and R25-3.

The NRC reviewer has correctly observed that

[[

]] as shown in Figure R25-

4. The sentence stating “The CPR-limited bundles, which are outlet peaked, heat up earlier and subject to the highest PCTs” in LTR Section 8.1.2.1 will be replaced with

“[[

]]”

LTR Impact

The sentence stating “The CPR-limited bundles, which are outlet peaked, heat up earlier and subject to the highest PCTs” in LTR Section 8.1.2.1 will be replaced with

“[[

]]”

[[

]]

Figure R25-1 PCT for Various Channels for BWR/4 Suction DBA

[[

]]

Figure R25-2 Void Fraction at PCT Nodes in Various Channels for BWR/4 Suction DBA

[[

]]
Figure R25-3 Vapor and Saturation Temperatures at PCT Nodes in Various Channels for BWR/4 Suction DBA. [[

]]

[[

]]
Figure R25-4 PCT for Various Channels for BWR/4 Suction DBA (Part of Figure R25-1)

RAI-26

26) Comparing Figures 8.1-6 and 8.1-7 (BWR/4 small-break LOCA), cladding temperatures appear to turn around rapidly following initiation of LPCS (even Ring 1 bundles), despite only faint quantities of core spray being injected prior to 300 seconds. Please explain this behavior and contrast it with the scenario analyzed in Figures 8.2-6 and 8.2-7 (BWR/6 small-break LOCA), where larger LPCS flows over approximately 30 seconds are unable to arrest the PCT transient.

RAI-26 Response

The BWR/4 small break (0.1 ft²) case presented in LTR Figures 8.1-6 and 8.1-7 has been reviewed, and it has been determined that [[

]]

This BWR/4 case from the LTR was re-run to obtain additional graphical results to facilitate better understanding of the results. Key results similar to those presented in LTR Figures 8.1-6 and 8.1-7 are shown in Figure R26-1.

[[]]

Figure R26-2 presents the results from a modified case for this break. All the inputs for this modified case are the same as the original case with only one change,

[[]]

The comparison of results shown in Figures 26-1 and 26-2 demonstrates that [[

]]

The following wording in the third paragraph of LTR Section 8.1.2.2:

“The heatup is terminated following the refill of the lower plenum and core by the ECC system. The outlet peaked CPR-limited bundles earlier than the LHGR-limited bundles and experiences the highest PCTs.”

will be revised to

“The heatup is **usually** terminated following the refill of the lower plenum and core by the ECC system.

[[

]]”

LTR Impact

The third paragraph in LTR Section 8.1.2.2 will be revised as discussed above.

[[

]]

Figure R26-1 PCTs for Various Channels for BWR/4 Small Break and CS, LPCI and Feedwater Flow. This is the re-run of LTR Figures 8.1-6 and 8.1-7 case with no changes.

[[

]]

Figure R26-2 PCTs for Various Channels for BWR/4 Small Break and CS, LPCI and Feedwater Flow. For this case [[
]], compared to the case in Figure R26-1.

[[

]]
Figure R26-3 PCTs for Various Channels for BWR/6 Small Break and CS, LPCI and Feedwater Flow. This is the re-run of LTR Figures 8.2-6 and 8.2-7 case with no changes.

[[

]]
Figure R26-4 PCTs for Various Channels for BWR/4 Small Break and CS, LPCI and Feedwater Flow. For this case [[
]] in Figure R26-1.

RAI-27

27) The demonstration cases in Chapter 8 refer to the MELLLA+ power-flow map to establish limiting conditions for the analysis basis of BWR/4 and BWR/6 reactors. For plants that do not use this map, please clarify how the limiting power and flow conditions will be determined.

RAI-27 Response

The demonstration cases presented in Chapter 8 are for illustrative purposes only. The power-flow map assumed in the demonstration cases is not presented as a generic map to be used to establish the limiting conditions for the analysis basis. Each application will use the plant-specific power-flow map and determine the power-flow condition that leads to the highest PCT.

LTR Impact

No changes to the LTR are proposed as the result of this RAI response.

RAI-28

28) Based on Figure 8.1-10 in the TR, the limiting condition for axial flux peaking appears to depend on fuel-specific factors, such as the extent to which partial-length rods are present. Please clarify whether differences in fuel and/or plant design would be accounted for in the determination of the limiting axial flux profile used for plant-specific LOCA applications, or whether GEH considers node [[]] to be generically limiting for axial flux peaking. The NRC staff notes that node [[]] was considered to be the limiting axial flux peaking location for all TR demonstration calculations, apparently based on the analysis in section 8.1.4.2.

RAI-28 Response

In the LTR demonstration cases, node [[]] is the node with highest LHGR for the top-peaked axial power shape bundles. Depending on the bundle design, the location of the peak yielding the highest PCT can vary. Among the factors affecting the limiting condition are partial rod configuration, enrichment and burnable absorber concentration in each rod, and bundle exposure. For a top peaked power shape, [[

]]

GEH will consider peak locations in the axial power shapes that are sufficiently bounding. The location of the peak used in the future applications will be consistent with the fuel design. For future fuel types, bundle design changes will be evaluated and power shape assumptions for bounding top and bottom peaks will be reevaluated.

LTR Impact

No changes to the LTR are made as the result of this RAI response.

RAI-29

29) Similar to what has been provided for the BWR/4 in Table 8.1-5, please present results for sensitivity studies for BWR/2 axial peaking for the PCT and maximum local oxidation to confirm that the limiting axial flux profile has been identified. For example, it is unclear to the NRC staff that a [[
]]

RAI-29 Response

The sensitivity of the transient behavior of the limiting BWR/2 break to axial power shapes was performed to evaluate the effect on peak cladding temperature (PCT) and equivalent cladding reacted (ECR). Such a sensitivity study follows a two-step process, wherein first the PCT and ECR are evaluated for the different hot channels in the core for the reference case, and second the elevation of the peak node in the limiting hot channel is varied in full-range CSAU analyses to identify the most limiting shape.

Table R29-1 shows the maximum PCT and ECR for the hot channels in the BWR/2 model with detailed average channel grouping (see response to RAI 9) for the limiting break scenario. [[

]]

With the [[
]] bundle identified as the appropriate limiting channel type, several sensitivities were performed which moved the peak axial power node position. The additional power shapes considered are summarized in Figure R29-1. Each power shape is evaluated [[
]].

The results in Tables R29-2 and R29-3 demonstrate that [[

]]

[[

]]

Table R29-1 BWR/2 DBA Discharge Break Scenario

[[
]]

Note [1]: The overall maximum values presented here are larger than all of the average values presented for individual channels. This is expected because the channel that sets the overall maximum can vary on a case-by-case basis.

[[

]]

Figure R29-1 BWR/2 Axial Power Shape Sensitivity

Table R29-2 BWR/2 PCT Sensitivity to Peak Node in [[
]]

[[°		°
]]

Table R29-3 BWR/2 ECR Sensitivity to Peak Node in [[
]]

[[^{0 0} ...]]		
]]

LTR IMPACT

No changes to the LTR are proposed as the result of this RAI response.

RAI-30

30) Please explain the [[

]] for the BWR/4 case shown in Table 8.1-12.

Further, although the upper bound ECCS coolant temperature considered seems relatively high, based on Figure 8.3-15, it is not clear that exceeding the nominal ECCS coolant temperature would not adversely impact cladding oxidation for a BWR/2. Please further discuss the influence of ECCS coolant temperature on oxidation for the BWR/2 (with emphasis on the limiting scenario) and adequately justify the choice of the limiting condition chosen.

RAI-30 Response

BWR/4

The results presented in Table 8.1-12 of the LTR originated from single-case sensitivity studies. An effect of using single-case studies is that the resulting sensitivity is a function not only of the parameter being varied, but also of the inherent code uncertainty, which can drive the PCT result upward or downward within the analysis resolution of the model. In the case of the LTR ECCS temperature sensitivity, the single-case comparison method [[

]].

This apparent trend is not characteristic of the actual sensitivity of the model. The true sensitivity of the limiting BWR/4 break model with detailed average channel grouping (see response to RAI 6) to bounding ECCS temperatures was assessed using [[

]], such as those presented in the response to RAI 29. Here, the ECCS temperature is set to the bounding high and low values used in the original demonstration presented in Table 8.1-12 of the LTR.

The results of the sensitivity calculation using the low and high pool temperatures are presented in Table R30-1. It is shown from these results that [[

]]. It is therefore concluded that [[]] is a defensible input for ECCS temperature for the BWR/4 model.

BWR/2

A single-case sensitivity of PCT history to ECCS temperature for a BWR/2 0.25 ft² small break scenario is presented in Figure 8.3-15 of the LTR. [[

]]

It is necessary, however, to assess the influence of ECCS temperature on the limiting BWR/2 break scenario, where the PCT is indeed high enough to warrant examination of the sensitivity of maximum oxidation thickness. This sensitivity is evaluated using [[

]] described above for BWR/4. [[

]]

The PCT sensitivity results presented in Table R30-2 show [[

R30-3 show [[]]. The maximum oxidation thickness results presented in Table R30-3 show [[

]]

Given the sensitivity described above, the nominal ECCS temperature of [[]] is a reasonable best-estimate condition for BWR/2 calculations.

Table R30-1 BWR/4 PCT Sensitivity to ECCS Temperature

[[°F]]	[[°F]]	[[°F]]
]]

Table R30-2 BWR/2 PCT Sensitivity to ECCS Temperature

[[°F]]	[[°F]]	[[°F]]
]]

Table R30-3 BWR/2 Oxidation Sensitivity to ECCS Temperature

[[°		
]]

LTR Impact

No changes to the LTR are proposed as the result of this RAI response.

RAI-31

31) Please explain further why it is not necessary or desirable to include biases in the break spectrum calculation (section 8.1.6). It is not clear that excluding biases would provide an acceptable method for identifying the limiting break location (discharge and suction breaks are observed to result in similar PCTs for both BWR/4 and BWR/6 demonstration cases) and size range that is potentially limiting for performing statistical calculations.

RAI-31 Response

The break spectrum analyses for LOCA application, such as presented in LTR Section 8.1.5 for BWR/4, are a screening tool used for determining the vicinity of the limiting break and the PCTs from these runs do not directly enter to the downstream runs. The break spectrum profile for a particular plant is mainly dependent on the ECC system. Among the major parameters affecting the limiting break size are available systems per single failure assumption, amount of available coolant delivered based on ECCS performance, and system setpoints. The model biases are not expected to change the limiting break size significantly. This can be demonstrated by comparing the curve labeled “Nominal” in LTR Figure 8.1-29 (with model biases removed) to the curves in LTR Figure 8.1-23 (with model biases included). From the determination of the limiting break size point of view, those curves are comparable, both of which effectively determine the vicinity of the limiting break for this plant type. This is also true for other BWR types, as shown in LTR.

The analyses support the conclusion that including or not including the model biases in the break spectrum analysis has insignificant impact in determining the limiting break scenario and size for each plant type. This conclusion is further confirmed by the analyses using the detailed core model (see the response to RAI-6 for the description of the detailed core model). Figure R31-1 shows the comparisons of the break spectrums obtained at different conditions for BWR/4 (As an example, only the break spectrum for suction break is shown here. Similar results are obtained for the discharge break). The curve labeled “LTR Core (Figure 8.1-23) – Biased” is the same curve from LTR Figure 8.1-23. For this curve, model biases are included. The other two break spectrum curves are both obtained with the detailed core model. The difference between these two curves is that one is obtained with model biases included (biased) and the other one with model biases removed (non-biased). [[

]] In the LTR, no particular position was declared for this aspect of the break spectrum as ‘not necessary’ or ‘desirable’.

For TRACG LOCA application, the overall analysis approach is further explained in Chapter 9. The break spectrum is traditionally determined from best-estimate nominal results. The limiting break size from the nominal break spectrum is analyzed by applying the uncertainty parameters to determine the upper tolerance results. In addition to the limiting break size identified in the nominal break spectrum, at least two other break sizes will be analyzed in the statistical evaluation to ensure that the uncertainties associated with the analysis are adequately quantified.

LTR Impact

No changes to the LTR are proposed as the result of this RAI response.

[[

]]

Figure R31-1 BWR/4 Break Spectrum for Recirculation Line Suction Breaks with Battery failure.

(DE GB: Double-Ended Guillotine Break; Biased: model biases included;

Non-biased: model biases removed)

RAI-32

32) The loss of an isolation condenser is taken as the limiting failure for the BWR/2 demonstration calculations in section 8.3.2.1. Given the marginal impact expected for the isolation condenser in mitigating a large-break LOCA, the basis for this choice is not clear. Although the TR states that the demonstration case core spray system is single-failure proof, these systems may experience failures (e.g., a booster pump or redundant pump) that degrade the system flow rate and/or discharge pressure. As such, it appears likely that the operational status of components within the core spray system may influence PCT and oxidation more than the isolation condensers. Please demonstrate the sensitivity of the BWR/2 to postulated single failures within the core spray system to identify whether these failures may be more limiting than the demonstration case. Based on the evaluation model proposed in the TR, the net influence of core spray system subcomponents is not clear due to the competing effects of increased spray cooling and the degradation of condensation heat transfer due to infiltration of noncondensable gases.

RAI-32 Response

It is necessary to correct a misunderstanding that was caused by the wording used in Section 8.3.2.1.

ECCS configuration for a typical BWR/2 is shown in Figure R32-1. In performing the ECCS performance analysis the postulated failure of a single active component will never result in less than certain minimum combinations of remaining operable systems.

For an assumed single failure of an Isolation Condenser (IC), it is conservatively assumed that the unfailed ICs are connected to the broken recirculation loop so that no ICs remain available. This single failure assumption is bounded by never crediting the ICs regardless of what other single failures are postulated. This approach supports the NRC premise that the ICs which have no ability to make up lost inventory have minimal impact in mitigating a large break LOCA.

For the scenario where the assumed single failure is one of the diesel generators, at least 2 Core Spray trains (2 sets of CS pump and booster pump) will remain available out of 4 CS trains shown in Figure R32-1. Any other single failure related to the CS pump, booster pump, CS lines, or sparger would still result in a minimum of two functional 2 CS trains (hence the analyzed minimum configuration crediting 2 CS trains is described as “single failure proof”). Assuming an additional booster pump failure (unless requested by customer for operational purposes) on top of the already assumed single failure makes the analyzed scenario beyond design basis because the scenario requires multiple failures. An example of a beyond-design-basis multiple failure scenario is DG failure (which takes 2 CS trains out) plus failure of a booster pump in one of the two remaining available CS trains.

The analyzed scenarios for the BWR/2 demonstration calculations adequately address the single failure requirements by crediting only the minimum configuration of two operational CS trains.

LTR Impact

No changes to the LTR are proposed as the result of this RAI response.

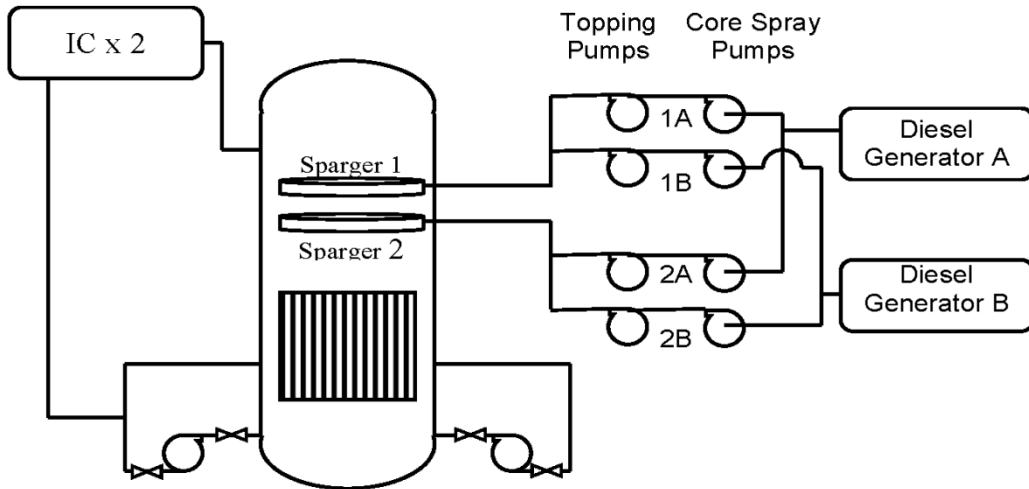


Figure R32-1 A Typical BWR/2 ECCS Configuration

RAI-33

33) Please provide the following information related to PIRT item C18 (cladding perforation):

- a. A summary of or reference for the tests that includes the number of tests, the type(s) of cladding tested, and the heatup rates used.
- b. The basis for applying the empirical data used to estimate clad rupture stresses to current-generation fuels.
- c. The basis for the assumption of normality for the upper and lower 95 percent groups used to determine the rupture stress.
- d. Explanation of the origin of and justification for the assumed uncertainty of the built-in fuel rod internal pressure curves and the normality of the multiplier on rod pressure.
- e. Relative to the high-temperature phase change of zirconium, please clarify the statement on page 2-11 of the TR that phase change of in-core materials is not modeled.

RAI-33 Response

- a. A summary of the cladding hoop stress versus perforation temperature testing used in defining the model and model uncertainty can be found in Reference R33-1. The figures in the referenced letter's enclosed report shows the comparison of high temperature test data to the rupture stress model. All of the tests presented are performed for heat-up rates [[
]]. The following symbol key gives the types of cladding tested, as presented in Figure 5.

[[

]]

- b. The clad rupture stress model is assessed using hoop stresses, as described by the method in Section 3.1 of Reference R33-2. By employing this method of converting differential pressure data to hoop stress data, design-specific dimensional effects are eliminated. This allows the clad rupture stress model to be extended beyond the 7x7 and 8x8 fuel from the test programs to current-generation fuel product lines. Additionally, the data in Reference R33-1 show that the differences between 7x7 and 8x8 fuel rods are insignificant compared to the scatter in the data, confirming that dimensional effects have been eliminated.
- c. The clad rupture stress uncertainty model was developed using temperature-dependent rupture stress data from GE material testing programs. The uncertainty model directly uses temperature-dependent summary data from these testing programs, including average rupture stress and the upper and lower bounds for 95% of the data. At each temperature, two half-normal distributions are used to construct a representation of the rupture stress distribution at that temperature. An example of this process is shown in Figure R33-1. In this application, the use of half-normal distributions is a simplification

to allow for the construction of temperature-dependent continuous probability distributions. While the half-normal distributions are used in the absence of normality tests of the model to data, they are preferred over uniform distributions, because normal distributions allow for the possibility of conservatively producing sampled values beyond the 95%-confidence interval.

- d. The LHGR- and exposure-dependent values of fuel rod internal pressure uncertainty used in TRACG LOCA analyses are calculated based on fission gas release using combination of uncertainties evaluations. These evaluations, performed at [[

]]

The actual uncertainty values for rod internal pressure applied in the LTR demonstration models are also presented in LTR Figure 5.1-16, where the model values are shown to [[
]] Treatment of the uncertainty multiplier on rod pressure as belonging to a normal population does not imply that the uncertainty population of this parameter is indeed normal. In this case, the normal distribution is a tool used to provide complete coverage of the possible values of rod internal pressure prior to the transient.

It is noted that the data presented in LTR Figure 5.1-16 represents rod internal pressure uncertainties from GESTR thermal-mechanical analyses. This calculation method has been qualified previously (Reference R33-3). The exposure-dependent uncertainties used in any TRACG LOCA plant application will be calculated using PRIME thermal-mechanical analyses (qualified in Reference R33-4) specific to the appropriate plant-type and fuel product line. It is largely understood, however, that the key driver of rod perforation is the temperature-dependent rupture stress. The rod internal pressure may alter slightly the timing of perforations but would ultimately have minimal effect on the amount of equivalent cladding reacted.

- e. On page 2-11 of the TR, GEH indicates the following:

TRACG does not model physical and chemical changes in in-core materials. These phenomena are not significant for BWR LOCA.

Rod internal pressure and the resulting hoop stress are modeled in TRACG for the purpose of tracking geometric changes due to rod perforation and to account for the resulting oxidation of the cladding. Additionally, material properties for the cladding and fuel take into account transient temperature effects. Physical and chemical changes resulting from cladding temperature transients, however, are not modeled. If the 10 CFR 50.46(b) acceptance criteria for ECCS systems are met, the effects of eutectic formation and phase change have no adverse impact on the fuel and can be ignored in cladding response calculations within the range of post-LOCA conditions.

[[

]]

Figure R33-1 Example of Half-Normal Distribution Generation Based on Experimental Data

References

- R33-1. Letter from R. W. Bucholz (GE) to C. S. Rubenstein (NRC), “General Electric Fuel Clad Swelling and Rupture Model,” May 15, 1981, MFN-097-81.
- R33-2. NUREG-0630 Cladding Swelling and Rupture Models for LOCA Analysis, April 1980.
- R33-3. B.S. Shiralkar, et al. “The GESTR-LOCA and SAFER Models for the Evaluation of the Loss-of-Coolant Accident, Volume I: GESTR-LOCA – A Model for the Prediction of Fuel Rod Thermal Performance,” NEDE-23785-1-PA, Revision 1, October 1984.
- R33-4. “The PRIME Model for Analysis of Fuel Rod Thermal-Mechanical Performance Part 3 – Application Methodology,” NEDC-33258P, Revision 1, September 2010.

LTR Impact

The following changes to LTR Section 5.1.3.24 will be made.

5.1.3.24 C18 – Fuel Cladding Strain /Perforation (H)

The TRACG parameters governing strain-induced fuel rod perforation are the clad rupture stress and the rod internal pressure. Based on material properties, the rupture stress and its associated uncertainty is modeled in TRACG as three curves corresponding to best-estimate, lower 95%, and upper 95% rupture stress curves as functions of cladding temperature (Figure 5.1 15). At each temperature, the upper and lower 95% bounds are used to define half-normal PDFs above and below the best-estimate rupture stress, respectively. This is done on the basis that the upper and lower 95% points are removed by 1.645σ from the best-estimate value.

The instantaneous clad hoop stress is directly related to the fuel rod internal pressure. The uncertainty in fuel rod internal pressure, which is dominated by the uncertainty in fission gas release, is expressed as a function of peak pellet exposure and linear heat generation rate (LHGR). The uncertainty in fission gas, and therefore fuel rod internal pressure, is calculated in a fuel-dependent analysis that combines the uncertainties in coolant pressure, pellet composition, and rod geometry. A qualified and approved model [24, 76] is used for performing such analyses. An example of the thermal-mechanical analysis results for the uncertainty in fuel rod internal pressure as used in the Chapter 8 demonstration analyses is shown in Figure 5.1-16. In support of a TRACG LOCA plant application, a fission gas uncertainty calculation specific to the appropriate plant-type and relevant fuel product line will be used to sample the rod internal pressure values. The open and closed symbols in Figure 5.1-16 denote, respectively, the pressure uncertainty for fuel with 7% gadolinium and fuel without gadolinium. The curves shown by solid lines have been built into TRACG to represent the uncertainties for both gadolinium and non-gadolinium fuel. The built-in curves are extrapolated back to a a_{min}

]]

RAI-34

34) From the discussion of PIRT entry B9 (three-dimensional effects of LPCI injection into the bypass region) in section 5.1.2.9, the basis for disposition of the issue appears to reference a nodalization sensitivity study performed for a BWR/4, for which the effect is presumably not relevant. Please provide adequate basis that increased azimuthal nodalization of the vessel is not necessary for modeling a BWR with LPCI injection into the bypass region, discussing any sensitivity studies that have been performed specifically for this case.

RAI-34 Response

This RAI is only applicable to the plants with LPCI injection to the core bypass region, such as BWR/5 and BWR/6. It is understood that the mixing of the LPCI with the bypass liquid may result in non-uniform liquid temperatures at the bottom of the bypass, and eventually at the bottom of the fuel bundles. As shown in the demonstration calculations in LTR Section 8.2, LPCS is more effective than the LPCI in preventing excessive cladding temperature heatup. Therefore it is expected the impact of non-uniformity of the LPCI mixing with the fluid in the bypass region on the peak cladding temperature is not significant, and the increased azimuthal nodalization of the vessel is not necessary.

To demonstrate that increased azimuthal nodalization of the vessel is not necessary for modeling a BWR with LPCI injection into the bypass region, sensitivity study was performed with the BWR/6 limiting break case (discharge break size of 0.093 m² with HPCSDG failure) using the same nodalization described in LTR Figure 8.2-1.

In this sensitivity study,

[[]] as shown

in Table R34-1. Changing the

[[

]]

Table R34-1 LPCI Parametric Study Cases

Case	LPCI Condition	Differences from Nominal (K)
1	[[
2		
3		
4		
5		
6		
7		
8		
9]]

The difference in PCT for the sensitivity cases are reported in Table R34-1 and it can be seen that [[

]]

The fuel cladding temperatures of the PCT bundle, in addition to the nominal LPCS and LPCI flow rates, are depicted in Figure R34-1. It shows that [[

]]

Based on the results of this BWR/6 LPCI sensitivity, it is concluded that increased azimuthal nodalization of the vessel is not necessary for modeling a BWR with LPCI injection into the bypass region.

LTR Impact

No changes to the LTR are proposed as the result of this RAI response.

[[

]]

Figure R34-1 BWR/6 LPCI Sensitivity Studies: Clad Temperatures and ECC Flow Rates

RAI-35

35) Unlike the other BWR demonstration calculations, the boiling transition peak for the BWR/2 case is not fully quenched for the limiting channel/rod. Thus, the temperature increase associated with boiling transition contributes to the eventual PCT. As such, please provide further justification that parameters affecting the boiling transition temperature increase (e.g., void coefficient, Doppler coefficient) do not appreciably influence the ultimate PCT.

RAI-35 Response

For LOCA applications, the flow component of the power/flow mismatch drives the early boiling transition (BT). In large break LOCAs, voiding in the core due to rapid pressure reduction is sufficient to reduce fission power to almost zero even before the scram becomes effective. Small variations in fission power are not important because the heatup is mainly caused by lack of coolant. During a LOCA transient, the core power drops down to decay heat levels within seconds following the scram. Only for small breaks where the scram may be delayed is the void coefficient and its uncertainty of minor importance. See LTR Sections 5.1.3.1 and 5.1.3.2 for a description of the void coefficient modeling and its impact on fission power. In general, fission power is a very small fraction of the time-integrated total power and any uncertainty in void or temperature reactivity coefficients has an insignificant effect on the thermal response of the fuel. The most important uncertainties with respect to determining the PCT are those associated with decay heat, stored energy in the fuel, and post-BT heat transfer.

LTR Impact

No changes to the LTR are proposed as the result of this RAI response.

RAI-36

36) PIRT item C3 includes phenomena associated with dynamic gap conductance and gap size, mainly focusing on post-scrum pellet contraction. Please clarify whether the impact of clad ballooning on gap size is captured in this or another PIRT item, and explain how the assigned uncertainty derived from pellet conductivity applies to or bounds the effect of clad ballooning. Please further characterize the approximate lower temperature threshold at which GEH considers ballooning important and identify whether the BWR/2 small-break LOCA, for which PIRT item C3 is ranked low, could reach this range.

RAI-36 Response

PIRT C3 is only one of the parameters that is relevant to ballooning. Uncertainty in the pressure of gases in the gap addressed by C18 is actually more relevant to ballooning. See also the discussion for PIRT C18 in the LTR (NEDE-33005P) and the response to RAI-33.

The dynamic gap model is described in Section 7.5.2 of LTR reference [1] (TRACG Model Description, NEDE-32176P, Revision 4). The discussion for C3 in the LOCA Application LTR (NEDE-33005P) pertains primarily to gap conductance which deals with both the size of the gap and the conductivity of gases in the gap. [[

]]

The uncertainties in gap conductance and gap size address only the phenomena for conditions when the gap is open or at least partially open. The discussion for PIRT item C3 focuses on the dynamic thermal contraction of the fuel pellet following the scram because the conditions where the fuel pellet has contracted away from the cladding inner surface result in a lower effective heat transfer coefficient between pellet and cladding than the case where the gap is closed. This lower overall heat transfer coefficient has a minor impact on the stored energy retained in the fuel pellet during the early stages of a LOCA. Whether the gap is open or closed, the dominant heat transfer resistance is the thermal conductivity of the fuel pellet which is why it is treated using C3BX. Note that the importance of both pellet thermal conductivity and gap conductance uncertainties decrease during the LOCA as the power drops to decay heat levels after the scram resulting in a greatly reduced heat flux from the fuel rod.

When the gap is completely closed, the pellet is in contact with the cladding and the primary stress associated with this condition is pellet and cladding contact pressure. [[

]]

Dynamic gap modeling applies to both opening and closing of the gap. When the gap is open the pellet retains more decay heat energy which causes the pellet to heat up and expand toward the gap. The contraction and expansion rates for the pellet and cladding are different which changes the gap size and feeds back into the pellet-cladding heat transfer. The strain rates for the pellet and cladding are also different and both depend on their respective temperatures. For higher temperatures and higher internal gas pressures, the clad can expand outward faster than the fuel pellet, thus resulting in ballooning. For this phenomenon [[

]]

For an open gap the primary radial stress is caused by the difference between the internal gas pressure and the fluid pressure outside the cladding. [[

]] Uncertainty for the internal gas pressure is accounted for by PIRT C18 [[]] as discussed further in the response to RAI-33. The gap size is an important feedback mechanism. The dynamics for how the pellet size changes depends on the fuel temperature and changes in the pellet size feeds back into the volume available for gases inside the cladding thus affecting the internal gas pressure. [[

]]

Clad ballooning and cladding perforation are closely related because both are determined by the relationship between cladding stress and strain. The fuel rod cladding perforation model is described in Section 7.5.3.3 of LTR reference [1]. [[

]] There are many uncertainties of high importance in the LTR that address the ability to calculate cladding temperatures. As described in Section 7.5.3.3 of LTR reference [1], [[

]]

Variable gap conductance (C3) is ranked [[

]] The critical parameter of interest is peak clad temperature (PCT). As explained above, C3 influences the initial conditions [[

]] For the BWR/2 in particular, the break size of most concern is the DBA large break because of the inability to refill the vessel and reflood the core which results in higher calculated peak clad temperatures (PCTs). In any event,

the highest importance ranking overall for C3 is [[
]]

The uncertainty attributed to lower fill gas pressures for BWR/2 fuel is addressed [[

]] For uncertainties affected by C18, the primary critical parameter of concern is oxidation because once the cladding perforates the inside of the cladding can start oxidizing and effectively double the local oxidation rate.

LTR Impact

No changes to the LTR are proposed as the result of this RAI response.

RAI-37

37) In Table 3.4-1, PIRT entry F3 indicates that the PCT transient is over before the vessel is depressurized to containment pressure. However, this does not appear consistent with Figures 3.2-6 (showing nearly complete depressurization by approximately 100 seconds) and 3.2-9, as well as independent calculations performed by the NRC staff. Therefore, please either clarify the technical basis or revise the statement.

RAI-37 Response

It is acknowledged that the sentences in Table 3.4-1 stating the “PCT transient is over before vessel is depressurized to containment pressure” are not completely true, especially for BWR/2 transients. Moreover, these sentences do not add any value for the discussion and have no impact on the demonstration calculations.

The sentences stating the “PCT transient is over before vessel is depressurized to containment pressure” will be deleted in the LTR revision of Table 3.4-1 for PIRT items F3 and M3.

LTR Impact

The sentence in Table 3.4-1 will be deleted in two places as discussed above.

RAI-38

38) PIRT item M3 is ranked medium, even for the BWR/2 case. However, based on the demonstration calculations, M3 appears to have a dominant impact on the PCT. Please clarify whether GEH considers the PIRT to be fundamentally correct (i.e., the influence of this factor in code simulations is primarily due to a conservative assumption regarding the containment boundary condition), or whether an increased ranking should be assigned for the BWR/2 case.

RAI-38 Response

The results in the LTR have shown that PIRT item M3 (or F3) [[

]]

LTR Impact

No changes to the LTR are proposed as the result of this RAI response.

RAI-39

39) Sections 4.3.3.2 and 4.3.3.1 referred to in the component performance qualification column of Table 4.2-1 do not appear to exist in NEDE-32177P, Revision 3. Please clarify whether these section numbers refer to NEDC-32725P, which addresses passive systems of the Simplified Boiling Water Reactor. Please explain the relevance of this testing to operating reactors or remove these references from NEDE-33005P.

RAI-39 Response

These section numbers were erroneously retained from an early draft of NEDE-33005P. The section references are to a planned revision of NEDE-32177P that was subsequently cancelled. Section 4.3.3.1 intended to refer to SSTF Upper Plenum testing, which is now Section 4.3 in Revision 3 of NEDE-32177P. Section 4.3.3.2 was intended to refer to SSTF Lower Plenum testing. SSTF Lower Plenum test is not explicitly discussed in Revision 3 of NEDE-32177P but some of the comparisons between the TRACG04 calculations and the lower plenum data are contained in Section 5.3 in Revision 3 of NEDE-32177P.

It should be noted that there are other references in Table 4.2-1 that are also not in Revision 3 of NEDE-32177P. In particular, 4.5, “PANTHERS”, is in NEDE-32725P Section 4.2. Section references to 4.1.4, “Two-Phase Jet Pump”, and 4.6, “Channel Leakage Flow” are not in either document.

LTR Table 4.2-1 will be revised to be consistent with Revision 3 of NEDE-32177P.

LTR Impact

Table 4.2-1 in the LTR will be revised as described above.

RAI-40

40) Regarding PIRT items C2AX, B2, and C23, please justify that random perturbations to the distribution parameter ($C_0 - 1$) and entrainment coefficient (η) are sufficient to provide the expected variation in void distribution, addressing the specific issues below:

a. Based on a comparison of Figures 5.1-8 and 5.1-9 to Figure 5.1-17, it is not clear that [[

]] Similar

limitations in reproducing the deviations in [[
]] as well.

b. Please justify that [[

]] in a simplified geometry for different flow regimes (i.e., bubbly/churn, transition, annular) may help to demonstrate adequacy.

c. Although GEH noted desirable properties of the [[

]] and justify that the distortion is either negligible or conservative.

d. Please compare the range of mass fluxes used in the Toshiba tests (section 5.1.3.3) with the mass fluxes expected for the hot bundles under limiting LOCA conditions and justify that the difference does not impact the assumed uncertainty distribution.

RAI-40 Response

This RAI has stimulated a reexamination of the process for covering the Toshiba void experimental data within the TRACG calculations. This response will first directly answer the questions listed above and will secondly describe the latest analysis basis that ultimately concludes [[

]].

a. There is merit to the observation that [[

]]

b. [[
issue with [[
]] is no longer an
]].

- c. As indicated in the response to part b., [[]]. The probability density function in Figure 5.1-10 is incorrect and will be replaced as the result of this RAI.
- d. The mass fluxes from the Toshiba test database are [[]]. These are similar to the observed mass fluxes in the hot channels of the demonstration BWR/4 model during the time of interest. Here, the time of interest is defined as the point in the transient where the system pressure reaches the low-pressure test condition from the Toshiba experiments. This time is approximately concurrent with the inventory recovery in the channel and the peak PCT. This confirms that the Toshiba database is appropriate to supplement the qualification of TRACG void calculations at low pressure conditions during the vessel blowdown.

As mentioned above, GEH has performed extensive design work to strengthen the basis for predicting void fraction in low-pressure conditions for LOCA calculations. These activities were manifold and included increasing the database of void fraction comparisons from additional Toshiba tests, [[]]

]]

The previous work included only [[]] tests from the available Toshiba void fraction data for TRACG comparisons. Of these, [[]] tests were conditions where high void fractions were predicted. To enhance the understanding of low-pressure void calculation resolution compared to experiment, an additional [[]] test points from the Toshiba data were modeled in TRACG, expanding the full database to [[]] tests, [[]]. The original [[]] tests were conducted with [[]]

]]. The full database is for the same pressure and flows, but also uses [[]]. TRACG predicted the expanded Toshiba data with a bias of [[]] and a standard deviation of [[]]. Figure R40-1 indicates that it is reasonable to assume that the void fraction deviations are normally distributed.

In an effort to justify [[]], each of the points in the expanded Toshiba database was studied using [[]]

]]

The statistical evaluations on the expanded Toshiba database also included [[]]

]]

The results from this study are presented in Table R40-1, where it is shown that the Toshiba data error has [[]]

]]. This uncertainty is [[]] when only the high void cases are considered, which is the region of interest for hot channel modeling in post-LOCA conditions.

[[

]] The expanded study discussed here proved [[

]]. Expanding the database from [[]] to [[]] samples in this study gave even higher confidence in that conclusion. Considering the lessons learned from these evaluations, [[

]].

Table R40-1 Numerical Summary of Toshiba Void Test Evaluations

[[.....
.....			
.....			
.....			
.....]]

[[

]]

Figure R40-1 Void Fraction Deviations for Expanded Database of Toshiba Tests

[[

]]

**Figure R40-2 Graphical Summary of Toshiba Void Test Evaluations with [[
]]**

LTR Impact

Section 5.1.3.3 will be rewritten as the result of this RAI response. Additionally, Figure 5.1-10 will be replaced by Figure R40-3.

[[

]]

Figure R40-3 Lognormal Probability Distribution for PIRT22

RAI-41

41) In section 5.1.1.9, the TR references NEDE-32177P, Revision 3, as containing a study of increasing the azimuthal sectors in the vessel from [[]] However, the NRC staff only located discussion of sensitivity studies that varied the number of azimuthal sectors from [[]] (Table 6.9-2 of NEDE-32177P, Revision 3, and Table 5.2-1 of NEDE-33005P). Please clarify whether additional sensitivity studies have been performed for azimuthal nodalization of the vessel and provide the results.

RAI-41 Response

A BWR/4 [[]] model was utilized in a 2002 nodalization sensitivity study for TRACG LOCA. The model consisted of [[

]]

This sensitivity study was not documented in the Qualification LTR. Thus, the TRACG LOCA LTR should not reference the Qualification LTR regarding the six-sector sensitivity study.

LTR Impact

Reference [2] will be removed from Section 5.1.1.9 of the LTR as shown below.

5.1.1.9 A11 – 3-D Effects (M)

Modeling of the lower plenum must also address possible azimuthal variations in the thermodynamic variables that may influence the plant response to a LOCA. A nodalization study was performed to ensure that the effects of azimuthal variations were adequately represented in the TRACG plant models. Increasing the number of azimuthal sectors from one (standard model) to [[]] for the BWR/4 design basis accident (DBA). The one-sector model can be used for the TRACG LOCA calculations because the modeling simplicity thereby realized [[]] that would result from the use of a more refined model.

RAI-42

42) Please clarify the basis for the [[
]] From the references cited in section 5.1.3.6, the justification for the individual uncertainties and their combination (i.e., presumably square root sum of squares) was not clear to the NRC staff.

RAI-42 Response

As discussed in the LTR, the TRACG fuel rod model based originally on the GESTR model has been updated to incorporate fuel thermal conductivity from PRIME (See the response to RAI-24). According to References [3] and [66] of the LTR, the overall uncertainty in pellet heat transfer is [[
]] and valid for PRIME (Reference [76] of LTR – NEDC-33258P-A, Revision 1).

For TRACG LOCA applications, two additional uncertainties in Reference [76] of the LTR are included to account for the transient variation. These two additional uncertainties are:

[[
]]

Therefore the total overall uncertainty [[
]], and is used for the LTR demonstration calculations.

LTR Impact

No changes to the LTR are proposed as the result of this RAI response.

RAI-43

43) Please clarify the statement in section 5.1.3.10 that an uncertainty of [[] is sufficient to bound the uncertainty in the side entry orifice (SEO) loss coefficient. Specifically, please identify the source of the available data and the extent to which it is applicable to two-phase flow conditions during a LOCA.

RAI-43 Response

Pressure drops at various locations, including SEO and Lower Tie Plate (LTP) for the 9x9 and 10x10 fuel bundles, were measured and the results can be found in Reference R43-1 and R43-2, respectively. The measurements were performed with single phase water inlet conditions. The uncertainty in pressure drop for the 9x9 and 10x10 SEO and LTP are documented in Table 5.1-1 of the TRACG Application for ESBWR Stability Analysis (Reference R43-3).

The two-phase pressure drop at the SEO is calculated in TRACG using the homogeneous two-phase multiplier. The uncertainty in the two-phase multiplier is estimated in Section 6.2.2.5 of NEDE-32176P, Rev. 4 to range from [[]]. For other TRACG applications (References R43-3 and R43-4), a [[]] uncertainty has been conservatively assumed in the SEO loss coefficient for single phase conditions. For LOCA application, a [[]] is applied to bound the RMS of the single-phase and two-phase uncertainty components. For two-phase conditions typical of a BWR LOCA, there are numerous comparisons against integral system data that confirm the accuracy of the modeling of the two-phase losses as indicated in Section 6.2.3 of NEDE-32176P, Rev. 4. Relevant comparisons between TRACG calculations and the test data are made for TLTA, FIST, GIST, and others in the TRACG Qualification LTR, NEDE-32177P, Rev. 3.

References

- R43-1 NEDC-31491P, “Retrofit Lattice Component Pressure Drop Tests for the STEP II Fuel Design Standardization Program,” November 1987.
- R43-2 NEDC-31998P, “STEP III Lower Tie Plate Pressure Drop Test with the BWR/2-5 Channel,” December 1991.
- R43-3 NEDE-33083 Supplement 1P, Revision 2, “TRACG Application for ESBWR Stability Analysis,” September 2010.
- R43-4 NEDE-33147P-A, Revision 4, “DSS-CD TRACG Application,” August 2013.

LTR Impact

No changes to the LTR are proposed as the result of this RAI response.

RAI-44

44) With reference to section 5.1.3.19, please clarify whether fuel-specific biases and uncertainties will be used in conjunction with the GEXL correlation, as in NEDE-32906P, unless acceptable statistical analysis demonstrates that data for different fuel types may be pooled.

RAI-44 Response

As explained in Section 5.1.3.19, either fuel-type specific values for the GEXL bias and uncertainty will be applied or a more conservative GEXL bias and bounding uncertainty that bounds all fuel types in the core will be applied. GEXL uncertainty and biases can be applied in the TRACG code on a CHAN group basis. A more conservative bounding approach will be applied for competitor fuel designs where determining the precise values is more difficult.

LTR Impact

No changes to the LTR are proposed as the result of this RAI response.

RAI-45

45) Please provide additional technical basis for the assumption that the uncertainty distribution for the Sun-Gonzalez-Tien correlation is [[
]]. Intuitively, the additional degree of freedom (i.e., droplets) implies the potential for greater uncertainty relative to a single-phase correlation. Please clarify whether adequate experimental data exists to estimate the uncertainty specific to the Sun-Gonzalez-Tien correlation. Please further justify the adequacy of the assumed uncertainty distributions in the large region ($0.1 < \alpha < 0.5$) in which the Sun-Gonzalez-Tien and Bromley correlations are interpolated.

RAI-45 Response

There are no known experimental data that could be used to estimate the uncertainty in the Sun-Gonzalez-Tien correlation. Consequently, the basis for the assumed uncertainties is engineering judgment. Note that perturbations are concurrently imposed that account for uncertainties in the void fraction. This will cause an additional perturbation in the applied heat transfer coefficients. The confirmation of the reasonableness of this choice is demonstrated by the statistical analyses for the integrated tests, especially the Core Spray Heat Transfer (CSHT), as presented in the LTR Section 7. With the proposed model uncertainties in LTR Section 5, the test data are well covered by the TRACG predictions.

For TRACG film boiling heat transfer calculations, it should be clarified that Sun-Gonzalez-Tien correlation is not used for the low void flow region (void fraction of 0.1 to 0.5 region); rather it is only used in high void fraction region (dispersed flow regime), and in the transition region from the inverted annular flow to the dispersed flow, where both Bromley and Sun-Gonzalez-Tien correlations are used with a weighting factor depending on the void fraction. See the discussion in Section 6.6.10.2 of NEDE-32176P, R4. For even lower void fractions, the modified Bromley correlation is used. See the discussion in Section 6.6.9.2 of NEDE-32176P, R4 for details on TRACG implementation.

LTR Impact

No changes to the LTR are proposed as the result of this RAI response.

RAI-46

46) Please confirm whether the data that is the basis for the uncertainty distribution for PIRT item C16 is the data shown in Figure 6-33 of NEDE-32176P, Revision 4. Please further justify the adequacy of the proposed uncertainty range given the limited size of the database.

RAI-46 Response

Data shown in Figure 6-33 of NEDE-32176P, Rev. 4 is the basis used to bound the uncertainty range of [[]] variation in thermal emissivity. For these steady-state tests, no liquid was injected at the top of the fuel bundle and the bundle contained only stagnant air. Under these conditions, the convective heat transfer is minimized and radiation heat transfer is the dominant mode. Core Spray Heat Transfer (CSHT) tests have been used for this qualification, as discussed in Section 6.6.10.3 of NEDE-32176P, Rev. 4. Note that [[

]] The limited amount of data to establish this component of the overall uncertainty in heat transfer is justified because for LOCA calculations the contribution due to thermal radiation is not dominant. The overall applicability and uncertainty associated with PCT calculations is justified by comparisons to data provided from the CSHT, THTF, TLTA, FIST, ROSA-III, FIX-II and GIST tests as documented in NEDE-32177P, Rev. 3.

LTR Impact

No changes to the LTR are proposed as the result of this RAI response.

RAI-47

47) Please address the following issues associated with the discussion in section 5.1.3.23:

- a. Heat transfer references indicate that the Dittus-Boelter correlation is appropriate for small to moderate temperature differences. The correlation tends to overpredict heat transfer at large temperature differences because it does not account for variations in physical properties due to the temperature gradient at a given cross section. The NRC staff understands that temperature differences of approximately 200-300K (jet-pump BWRs) and 400-600K (non-jet-pump BWRs) or higher can exist between fuel rods and steam during a LOCA. However, based on the results presented in NEDE-13462, the tests appear to be based on temperature differences of approximately [[]]. Please clarify whether allowance is made for the effect of the temperature difference in deriving the uncertainty distribution parameters and provide justification.
- b. Please justify that no significant scaling issues arise from applying biases and uncertainties associated with tests using a [[]] bundle to a full-sized bundle. For example, please explain why the [[]] bundle tested would not underpredict the temperature for the interior rods of a full-size bundle based on an underestimation of edge-to-center variation and an overestimation of mixing and heat transfer to peripheral rods and the channel wall. Has subchannel analysis been performed to validate that scaling effects are insignificant?
- c. The basis for the [[]] for internal rods appears to be derived from a deviation calculated from a bundle-averaged approach for the [[]] test bundle (i.e., including heat transfer from both interior and peripheral rods). Therefore, if a bias is applied only to heat transferred from interior rods, please clarify why the requisite bias would not need to be scaled up proportionally.

RAI-47 Response

- a. No allowance was made for the effect of the temperature difference in deriving the uncertainty distribution parameters in the LTR Section 5.1.3.23. The uncertainties in Section 5.1.3.23 are based on the test data in NEDE-13462, June 1976. However, the impact of the variations in fluid physical properties due to high temperature difference between the wall and vapor on the prediction of Dittus-Boelter correlation for vapor heat transfer is considered in TRACG code, as discussed in Section 6.6.5 of NEDE-32176P, R4, January 2008. The heat transfer coefficient for single phase steam flow is calculated using Dittus-Boelter correlation when the flow is in the turbulent regime. When wall temperature (T_w) is greater than the vapor temperature (T_v), the heat transfer coefficient predicted by Dittus-Boelter is multiplied by a factor $(T_v/T_w)^{0.5}$ to account for the increased vapor temperature.
- b. The current steam cooling uncertainty adopted in the LTR is derived based on the [[]]

]]This indirectly demonstrated that the scaling impact is not significant.

- c. As discussed in Section 5.1.3.23 of the LTR, the bias of [[]]] for the Dittus-Boelter heat transfer coefficient for internal rods are derived from two sources: [[

]] in NEDE-13462. The conversion factor is, however, based on 60 bundle internal rod measurement points presented in NEDE-13462.

For the demonstration calculations in the LTR, the bias developed for this PIRT is only applied to the internal rods in the bundles. However, it does not have to be scaled up. As discussed at the end of Section 5.1.3.23 and Figure 5.1-14 in the LTR, the bias from 60 internal rod measurement points presented in NEDE-13462 is estimated as [[]]] based on all measure points in NEDE-13462. This slightly smaller prediction bias for the internal rods was expected because the internal rods are impacted less by the channel wall boundary than the external rods.

LTR Impact

It is suggested that the following two sentences in Section 5.1.3.23 of the LTR

The data described in Reference [56] include 1935 measurement points. Of these, 60 points from four runs are shown graphically in the report along with the steam temperature calculated by both the bundle average and extended rod-centered subchannel approaches.

be followed immediately by the new sentence

It is worthwhile to note that those 60 points from four runs in Reference [56] are for internal rods only.

RAI-48

48) The TR indicates in section 5.1.3.25 that the uncertainty in spray cooling heat transfer is covered by uncertainties in other parameters. However, this conclusion is not sufficiently justified. In NEDE-32177P, Revision 3, [[

]] Please reconcile the apparent conflict or provide further justification for this conclusion.

RAI-48 Response

First of all it is worthwhile to note that there is not a separate ‘spray cooling heat transfer coefficient’ in TRACG methodology that is applied directly. The fuel spray cooling effects, as a result of the combinations of single or two phase flow (film boiling-dispersed flow, steam cooling), radiation heat transfer and heat conduction, are calculated by modeling the physical phenomena that take place such as single phase (steam cooling) and two-phase convection, droplet evaporation, radiation to cold surfaces including droplets, Counter Current Flow Limitation (CCFL), top-down quench, etc.

[[

]]

In summary, it is concluded that there is no conflict between the uncertainty reported in NEDE-32177P, R3 for CSHT) and the PCT uncertainty reported for the BWR/2 liming break.

LTR Impact

No changes to the LTR are proposed as the result of this RAI response.

RAI-49

49) Please clarify whether the uncertainty distribution discussed in section 5.1.3.27 applies to both rising and falling quench fronts. If the uncertainty distribution applies to both, please clarify whether the uncertainty distribution database includes data from rising quench fronts. If not, please clarify how the uncertainty for rising quench fronts is addressed.

RAI-49 Response

The uncertainty described in Section 5.1.3.27 of the LTR for PIRT item C21 is applied [[
]] The uncertainty perturbation is applied to the quench velocity as calculated from Equation (6.6-152) of LTR Reference 1 (TRACG Model Description, NEDE-32176P, Revision 4). [[

]] The uncertainty for C21 specified in Section 5.1.3.27 of the LTR was derived on the basis of the cited falling quench data which was used to develop the NRC-approved quench model in SAFER (LTR Reference 25). [[

]]

The functional form for the quench velocity correlation is the same for both rising and falling quench fronts. In the quench velocity correlation, the leading group of dimensional quantities is based on cladding thickness and material properties that do not depend on the direction that the front is moving because they are evaluated at the cladding temperatures behind the quench front where the cladding temperature is approximately the temperature of the water. All directional dependence enters the quench velocity correlation via the Biot number defined by Equation (6.6-154) of LTR Reference 1. [[

]] For a falling front a constant value for the heat transfer coefficient is used that was correlated from data and validated for core spray heat transfer data as described for SAFER in LTR Reference 25.

The quench model implemented in TRACG had been retained from TRAC-P1A and TRAC-BD1 and is based on the paper by Yu, Farmer and Coney identified in this response as Reference R49-1. The citation of WCAP-7435 (FLECHT) in Section 6.6.13 of LTR Reference 1 as the source of the heat transfer equation for reflood is not correct. Equation (6.6-158) of LTR Reference 1 for bottom flooding heat transfer coefficient is also incorrect. The correct expression for the bottom flooding heat transfer coefficient and a more detailed description of the TRACG quench model is available in Reference R49-2 listed below. The quench model in the TRACG code has been corrected and the corrected code will be used in all future TRACG LOCA applications. Qualification calculations related to the quench model have also been updated and the impact of the quench model on predicted PCTs have been evaluated as indicated in Reference R49-2.

Yu, Farmer and Coney (Reference R49-1) note in the introduction to their paper “that the bottom flooding correlations are consistent with the falling-film correlation for saturated flows, but that there are substantial differences where the water at the quench front is subcooled.” Later in the paper the authors note “the good agreement between bottom flooding and falling film rewetting

for saturated flows” and offer some possible explanations for why bottom flooding with subcooled water is different. It is important to stress that *agreement* is defined in Equation [9] of Reference R49-1 in terms of residual deviations between the measured wall temperature minus quench temperature compared to the correlation’s prediction. In terms of the quench velocity (actually inverse quench velocity), the correlation is a best fit value of the modified Biot number in order to minimize the disagreement in temperature differences as characterized by the authors in tabulated values of σ_{\min} . [[

]]

For each dataset considered in Reference R49-1, a different value of either T_0-T_s (saturated) or T_0-T_q (subcooled) was determined to minimize the variance in order to develop a best-estimate functional form of the correlation in terms of the modified Biot number. In applying the correlation a value for T_0-T_s is specified. For the 28 usable datasets from Reference R49-1 Table 5 for saturated data the values of T_0-T_s range from 17.5°C to 148.8°C with the weighted average calculated to be 74°C. [[

]] The authors of Reference R49-1 provide an average value of 67°C on page 432 of Reference R49-1 considering all saturated falling quench data from Tables 5 and 9. For all applications including saturated and subcooled fluid for falling and rising quenches the authors recommend a value of $T_0-T_s=80^\circ\text{C}$ since for $Bi \geq 5$ “the rewetting rate is very insensitive to this parameter and the variation caused by the uncertainty in (T_0-T_q) is often much less than the experimental scatter. This is demonstrated further in Figure 18” of Reference R49-1 using “extreme values for T_0-T_s of 20°C and 160°C”.

[[

]] The authors of Reference R49-1 believe that the larger uncertainty for bottom reflood (rising quench) is “entirely due to scatter in the data rather than to any inability of the theory”. [[

]]

The TRACG quench model has also been evaluated for the case of a rising quench front like that observed in a reflooding situation (see Reference R49-2). Use of the TRACG quench model is

shown to result in calculated cladding temperature responses that compare well to the measured temperature responses from LOCA integral system tests where reflood quenches were experienced. [[

]]

References

- R49-1 S. K. W. Yu, P. R. Farmer and M. W. Coney, *Methods and Correlations for the Prediction of Quenching Rates on Hot Surfaces*, International Journal of Multiphase Flow, 3, 1977, pp. 415-443.
- R49-2 Letter J. F. Harrison (GEH) to Document Control Desk (NRC), “Update TRACG Quench Front Model Description and Qualification,” MFN 13-085, October 15, 2013.

LTR Impact

No changes to the TRACG LOCA Application LTR (NEDE-33005P) are needed as the result of this RAI response. As indicated in Reference R49-2, GEH has committed to correct and enhance Section 6.6.13 of the TRACG Model Description (LTR reference [1]) and revise and augment the TRACG Qualification (LTR reference [2]) to reflect the comparisons to data obtained with the corrected quench model coding and add the new qualification cases for the Halden comparisons. All future TRACG LOCA applications will utilize the corrected code.

RAI-50

50) As shown in Figure 6-27 of NEDE-32176P, Revision 4, for post-LOCA pressures exceeding the range associated with a DEGB, the Iloeje correlation tends to predict values of the minimum stable film boiling temperature (T_{\min}) that exceed other available correlations. Break spectrum calculations performed with the TRACG evaluation model suggest the possibility that small or intermediate breaks, with pressures exceeding 0.5 megapascals (MPa) during the PCT transient, could represent a potential limiting condition for some BWRs. Given that the Iloeje correlation is based only on data taken at a pressure of 6.9 MPa, it is not clear that the pressure trend in the post-LOCA range of interest can be considered reliable. It is further unlikely that the pressure-dependent trend is linked primarily to pre-existing oxidation on fuel rod surfaces. Ultimately, it is not clear that the impact of the pressure-dependent trend of the Iloeje correlation can be adequately addressed by application of [] Furthermore, the NRC staff observed that the demonstration case input decks use the Shumway correlation, which is recommended in the TRACG04P User's Manual. Based on the discussion above, please revise the model used to predict rewet and/or its uncertainty distribution, or provide adequate justification for the current approach.

RAI-50 Response

Section 5.1.3.26 of the LTR is not correct and will be updated as indicated in this response. The Iloeje correlation was not used. The Shumway correlation was used for the current LTR demonstration calculations and will be used for predicting the minimum stable film boiling temperature (T_{\min}) for all future TRACG LOCA applications. Use of the Shumway T_{\min} correlation with zircaloy for TRACG analyses and its qualifications are discussed and justified in Reference R50-1 (sent to NRC through GEH MFN 13-073).

Reference

R50-1 Letter, J. F. Harrison (GEH) to U. S. Nuclear Regulatory Commission, "Use of the Shumway T_{\min} Correlation with Zircaloy for TRACG Analyses," MFN 13-073, September 9, 2013.

LTR Impact

Reference R50-1 listed above will be added as reference [80] in Section 11 of the LTR and LTR Section 5.1.3.26 for C20 will be replaced with the text provided below. Note that this replacement text has been aligned with the response to RAI-51 where clarification and additional details are provided regarding the constraint on equilibrium quality.

5.1.3.26 C20 – T_{\min} (Minimum Stable Film Boiling Temperature) (H)

TRACG calculates the minimum film boiling temperature (T_{\min}) using the Shumway correlation which is described mathematically by Equation (6.6-52) of Reference [1]. Comparisons of the Shumway correlation to data for a wide range of pressures are available in Section 6.6.7.3 of

Reference [1] and in Reference [80]. For the Shumway correlation, a [[
]] applied to the calculated difference between T_{\min} and the saturation
temperature (T_{sat}) sufficiently covers the correlation standard deviation of 55 K indicated in
Reference [80]. [[

]] Although the Shumway correlation was developed using stainless steel data, it
accounts for the material properties and is generally applicable for other materials (including
zircaloy) as is shown in Reference [80]. A key conclusion from Reference [80] is that the
Shumway correlation applied for zircaloy provides a value of T_{\min} that is lower than most of the
zircaloy data. Lower values of T_{\min} are more conservative because they delay the return to
nucleate boiling and thus result in higher and more conservative calculated values for the local
cladding surface temperatures (T_{clad}).

[[

]]

The reference to be added to Section 11 of the LTR:

- 80 Letter, J. F. Harrison (GEH) to U. S. Nuclear Regulatory Commission, “Use of the
Shumway T_{\min} Correlation with Zircaloy for TRACG Analyses,” MFN 13-073,
September 9, 2013.

RAI-51

51) As applicable to the TRACG LOCA evaluation model, please specify the circumstances under which rewetting is permitted without satisfying the requirement that the local equilibrium quality is below [[]] of the critical quality. In addition, please provide adequate basis for the [[]] The NRC staff could not locate adequate basis for these values in NEDE-32176P, Revision 4, and NEDE-32177P, Revision 3.

RAI-51 Response

In TRACG LOCA application, the local equilibrium quality below [[]] of the critical quality is a necessary condition for rewetting to occur. There is no circumstance under which rewetting is permitted without satisfying this local equilibrium quality requirement.

[[

]]

The uncertainties in critical quality should have no impact on non-jet pump plants (BWR/2) limiting large break scenario as the fuel bundle remains empty and the fuel rods are quenched by the falling film descending through the fuel bundles.

For jet pump plants, rewet occurs after reflood and the temperature has turned around and starts to come down. The uncertainty in the rewet has therefore no impact on the PCT. Likewise the impact on the fuel clad oxidization for jet pump plants is also minimal as the PCT is relatively low and the duration of refill/reflood phase is short.

LTR Impact

No changes to the LTR are proposed as the result of this RAI response.

RAI-52

52) In the discussion of PIRT item C22, the [[
]] Please clarify whether the intent of the discussion in section 5.1.3.28 is that heat from the channel wall may be transferred to fluid on either the inside or outside of the channel wall. It is the NRC staff's understanding that heat is transferred to fluid inside the bundle essentially only when liquid is in contact with the interior channel wall (i.e., [[
]]). Please revise the TR, as necessary. Please provide additional explanation and justification if the NRC staff has misunderstood the quoted statement.

RAI-52 Response

In TRACG LOCA LTR calculations, heat transfer at both sides of channel wall are considered and calculated separately. Under usual LOCA conditions, heat is transferred to/from the fluid inside the channel to the channel inside wall by convection and radiation heat transfer, then across the channel wall via heat conduction, and eventually to/from the bypass fluid through the convection heat transfer on the outside of the channel wall.

The heat transfer direction either from the fluid to the wall or from the wall to the fluid depends on the local fluid temperature conditions and the channel wall surface temperature.

According to TRACG model Description in NEDE-32176P Section 6.6 (LTR Reference 1), [[

]], whenever they are applicable for particular flow regime (s) as discussed in NEDE-32176P Section 6.6.

The wording in Section 5.1.3.28 is modified as follows:

The uncertainty in channel to bypass heat transfer is covered by an [[
]] which governs **heat transfer for sub-cooled and nucleate boiling** to the inside channel wall and a [[
]] uncertainty on wall heat transfer to the bypass which covers either nucleate boiling or single phase heat transfer.

LTR Impact

The LTR Section 5.1.3.28 will be revised as discussed above.

RAI-53

53) Please clarify the source of the data for PIRT item C24, which states that TRACG predicts the spacer component of the core pressure drop with [[
]] In contrast, Table 5-3 in NEDE-32906P, Revision 3, reports [[
]] Given the potential for increased uncertainty associated with two-phase flow throughout the bundle, please provide adequate justification for [[
]]

RAI-53 Response

The source of the data for C24 (spacer loss coefficient uncertainty) is Table 5-3 of NEDE-32906P, Revision 3 and the discussion cited therein. It is acknowledged that the sentence in the LTR [[
]] is misleading, and therefore will be revised in the LTR.

Considering that the pressure drop measurements used for deriving the spacer loss uncertainty are already for two-phase flow, there is no increased uncertainty unaccounted for in this regard. It is acknowledged, though, that the spacer loss uncertainty is fuel design dependent. The current proposed spacer loss uncertainty shall be compared against test data for a new fuel to determine the continuous applicability of the currently-applied spacer loss uncertainty for the new fuel. The update of the current proposed spacer loss uncertainty for a new fuel may be possible.

Based on the discussion for C24 in NEDE-32906P, R3 and the biases and uncertainties for SEO/LTP, spacer, and UTP, it can also be concluded that [[
]]

LTR Impact

The following paragraph in Section 5.1.3.30 is modified in the revised LTR.

Original

A detailed discussion of the uncertainty in the frictional components of the core pressure drop was provided in the Anticipated Operational Occurrences (AOO) application report [3]. The uncertainties in the core pressure drop include the uncertainties in SEO/LTP, spacers, and UTP. Data versus TRACG-predicted pressure drop analysis indicates a [[
]] the core pressure drop. For the LOCA application, the uncertainty in the SEO/LTR pressure drop is considered separately (see C5 in Section 5.1.3.10) and is bounded by an uncertainty of [[
]] It was shown that the uncertainty in all components of the core pressure drop could be bounded by imposing a [[
]] The LOCA application uses a [[
]]

Revised

A detailed discussion of the uncertainty in the frictional components of the core pressure drop was provided in the AOO application report [3]. The uncertainties in the core pressure drop include the uncertainties in SEO/LTP, spacers, and UTP, **which are presented in Tables 5-2, 5-3 and 5-4 of Reference [3].** ~~Data versus TRACG predicted pressure drop analysis indicates a~~ ~~the core pressure drop.~~ **The spacer frictional pressure drop is based on full-scale measurement for conditions covering the range of expected reactor conditions. The uncertainty in the pressure drop for the spacers is determined from full-scale ATLAS data and is presented in Table 5-3 of Reference 3 for different fuel types. It is concluded in [3] that**

[[]] **can be used for all bundle types.** For the LOCA application, the uncertainty in the SEO/~~LTR~~-LTP pressure drop is considered separately and is bounded by an uncertainty of **[[]]** (For additional discussion of the SEO/LTP pressure drop uncertainty see the response to RAI-43 and C5 in Section 5.1.3.10 of the LTR.) It was shown that the uncertainty in all components of the core pressure drop could be bounded by imposing a **[[]]**

]] The

LOCA application uses a **[[]]**

]]

RAI-54

54) The 1979 American Nuclear Society Standard 5.1 decay heat calculation for an exposure of 15 GWd/MTU with TRACG shown in Figure 5.1-18 appears to predict decay heat power fractions that are significantly less than predictions with the same model for an exposure of 10 GWd/MTU using SAFER in NEDO-23785, Volume 3, Appendix B, Figure 1. Please clarify the different input assumptions or other causes that lead to this difference.

RAI-54 Response

The curves from Reference 54-1 for SAFER include both fission power and decay power, whereas LTR Figure 5.1-18 represents only the decay power as needed by TRACG. Recall that TRACG uses a point kinetics model to account for the fission power in the earliest stages of the LOCA whereas SAFER does not. Regrettably, the decay heat curves generated for a 0 exposure condition were mislabeled and inadvertently used for Figure 5.1-18 of the LTR. This errant figure is being replaced in the LTR by a decay heat curve generated for 11 GWd/MTU.

A new decay heat fraction was generated for 11 GWd/MTU to better match the input assumptions for the cited SAFER figure from Reference 54-1. To facilitate comparison to the SAFER figure, a plot of the fraction of the initial total power fraction (fission plus decay powers) corresponding to the new decay heat fraction is given below.

[[

]]

Reference

R54-1 NEDE-23785-1-PA, Revision 1, “The GESTR-LOCA and SAFER Models for the Evaluation of the Loss-Of-Coolant Accident”, Volume 3, Appendix B, October 1984.

LTR Impact

Section 5.1.3.31 of the LTR will be revised in the following way:

- (1) 15 GWd/MTU will be revised to 11 GWd/MTU.
- (2) Figure 5.1-18 and its caption will be replaced with the following.

[[

]]

Figure 5.1-18 Decay Heat Uncertainty at a Bundle Average Exposure of 11 GWd/MTU

RAI-55

55) For some PIRT items, the uncertainty in future predictions of a regression model is assumed to be represented by the standard deviation associated with the data used to generate the regression model (e.g., [[]]). Please clarify why the uncertainty associated with future predictions (i.e., data not included in the regression model) need not be determined by the prediction interval for a new observation. See, for example, section 18.17 of NUREG-1475, Revision 1.

RAI-55 Response

As stated in Section 18.17 of NUREG-1475 (Revision 1) a regression equation provides only a prediction Y' for an expected value Y . It is understood that multiple samples from the same regression equation using the same inputs will always return the same prediction Y' . In a broader context a “regression model” is expected to behave in the same way. In the broadest context, a digital computer code also operates in this way by providing a set of predicted values that are determined once the set of inputs are specified. The term “regression model” used in RAI suggests a purely empirical fit of numbers that has been tuned to a small dataset and that the addition of data will require retuning. This characterization minimizes the importance of physical bases for the model functional form, the choice of dimensionless engineering parameters that represent fundamental processes, and even the type and range of allowed inputs. The key generic principle is that there exists a defined process that adequately transforms inputs into outputs whether that process is a simple regression equation, a regression model, or a computer code. Adequacy of the process and the outputs it produces are quantified together by defining tolerance limits for the critical outputs that reflect both the fidelity of the transformation process and the uncertainty of the inputs. Whenever possible, it is the calculated output that is compared to data and it is this comparison that determines whether the process and/or its inputs are in need of improvement. Rarely is it necessary to increase the uncertainty of the inputs to provide for a wider spread in the calculated outputs to adequately cover the data.

The RAI suggests using the prediction interval for the regression equation instead of the standard deviation to characterize the uncertainty of the prediction. This is not the correct application of the prediction interval. What is needed for application of Best Estimate Plus Uncertainty (BEPU) methodology is a way to model the variance of the sampled predicted values about the expected value. The appropriate statistical parameter that defines this variance is the standard deviation (σ), not the prediction interval. The prediction interval is defined from the standard deviation not vice versa. As the number of data points increases the standard deviation may tend to decrease slightly but more importantly the confidence increases which decreases the prediction interval. Thus modeling the variance of a population to be sampled based on a small number of data points tends to provide a conservatively larger variance in the model inputs. If new data becomes available then this data is evaluated to determine its impact on the biases and uncertainties used in the LOCA application methodology.

For BEPU the objective is to evaluate the uncertainty associated with complex interactions between many competing processes with many different inputs. In the BEPU methodology the ultimate concern is whether the final estimated uncertainty in the calculated critical output parameter is sufficient to cover the experimental data for the critical parameter. These types of coverage checks for the final outputs are more important than the span of particular inputs.

It is not clear from the RAI whether the concern is with *coverage* for the inputs or the outputs so both aspects are addressed. Begin with the more important aspect of uncertainty in the output critical parameters. The process is described in Section 7.1 of the LTR. A one-sided upper tolerance limit (OSUTL) is defined for each of the three critical parameters: (1) PCT, (2) maximum local oxidation, and (3) total core-wide oxidation. These three OSUTLs are defined independently for each set of 59 calculations using either a single bounding value based on order statistics (LTR Section 7.1.1) or a calculated OSUTL from a normal distribution (LTR Section 7.1.2). In either case the OSUTL is defined to provide at least 95% probability at 95% confidence that the OSUTL bounds the calculated population. The maximum OSUTL from all sets of calculations is compared to the appropriate 10 CFR 50.46 design limit independently for each of the three critical parameters as described in Section 7.4 of the LTR. This is done without any requirement or assumption regarding simultaneity of the maximums thus assuring that each maximum is less than 10 CFR 50.46 limit with a high degree of probability. The population of calculated outputs does not change unless new scenarios are required or new inputs are specified.

The statistical process used for BWR LOCA calculations has been applied to relevant integral system tests where generally the PCT and some other parameters of interest have been measured. Comparison of the calculated tolerance limits to the measured data demonstrates the adequacy of the BEPU approach. See Section 7.4 of the LTR for the specific results.

Next consider coverage for the inputs. For the cited examples of C21 and C26, models based on physical processes provide the expected values for the derived input quantities. These derived inputs are uncertain because the models used to obtain them are uncertain and even the inputs to these models that create other inputs are also uncertain. In accordance with the BEPU methodology, the sample for an input represents a best-estimate value distributed in some way about the mean (μ). The confidence interval for the mean is always much tighter than the individual samples. The concern with input *coverage* is addressed by considering over what range the sampled inputs are drawn. For GEH BEPU applications we typically use [[]] to assure adequate ranging of the uncertain inputs unless there is a physical constraint that limits the range to something smaller. The span for the inputs in GEH methodology is greater than the range needed to assure coverage of the inputs beyond the 95% confidence interval unless the input uncertainty was determined from a very small number of data points (less than 6). The next paragraph provides a specific example to illustrate why this process is adequate for purposes of providing input coverage.

Consider the particular example of C21 cited in the RAI. In Figure 5.1-17 of the LTR, the reported mean is [[]] with a 95% confidence interval on the mean of [[]]. The standard deviation is [[]] and the 95% confidence interval for the standard deviation is reported as [[]] data points. In GEH BEPU

modeling the sampling interval spans $[\pm 2\sigma]$ which for this example is $[\pm 1.96\sigma]$. By way of comparison, consider the prediction interval defined by Equation (18.60) of NUREG-1475 (Revision 1). If the regression equation is assumed to be linear to simplify the calculations then the mean value of the independent variable will produce the mean value of the dependent variable. At the mean of the independent variable where $x=\bar{x}$, the 95% confidence interval about the predicted mean value for the dependent value of y reaches a minimum span. The confidence interval expands slightly as the independent variable moves away from the mean but this expansion (which is greater when the database has fewer values) is negligible as illustrated in Figure 18.10 for $n=11$. For the C21 example where the database has $n=11$ a two-sided 95% confidence interval for a Student's t-distribution with $(n-2)$ degrees of freedom produces a 95% confidence interval span $\pm 2\sigma$ about the mean that covers $[\pm 1.96\sigma]$. GEH sampling has adequate coverage because it spans $[\pm 2\sigma]$ about the mean and covers $[\pm 1.96\sigma]$.

The BEPU statistical approach proposed and demonstrated in the LTR is justified because it provides a high probability that the 10 CFR 50.46 limits are not exceeded by: (1) adequately addressing the input biases and uncertainties, (2) accounting for the modeling biases and uncertainties, and (3) accounting for the uncertainty in the calculated outputs due to both input and modeling biases and uncertainties.

LTR Impact

No changes to the LTR are proposed as the result of this RAI response.

RAI-56

56) Based on the data plotted in Figure 5.1-19, it is not clear that a normal distribution explains the variation in predictions of the single-parameter model used for pre-accident oxidation. Please provide the Anderson-Darling normality test results for C26I (initial oxide thickness) and justify that the assumption of normality does not result in significant error relative to the criteria of 10 CFR 50.46.

RAI-56 Response

The variation in predictions of the exposure-dependent pre-transient oxidation (PTO) model are explained by the nominal and 95%-content tolerance limit curves presented in Figure 5.1-19 of the LTR. Using these curves, a statistical sampling model is generated where half-normal distributions between the nominal and $\pm 2\sigma$ tolerance limits are joined at each exposure. To show the comparison of the resulting model to metallographic data, each oxidation thickness t_i at exposure E_i is transformed to a z-value z_i using the exposure-dependent model values $t(E_i)$, $t_{LTL}(E_i)$, and $t_{UTL}(E_i)$ with the following relationship.

$$z_i = \begin{cases} 2 \left(\frac{t_i - t(E_i)}{t(E_i) - t_{LTL}(E_i)} \right), & t_i < t(E_i) \\ 2 \left(\frac{t_i - t(E_i)}{t_{UTL}(E_i) - t(E_i)} \right), & t_i \geq t(E_i) \end{cases}$$

A histogram of the z-values is presented in Figure R56-1. The transformed metallographic data are compared here to a standard normal distribution, although the data's Anderson-Darling p-value of 0.010 does not justify normality. It is shown, however, that the preponderance of the data is bounded by the standard normal distribution. This can be observed both in Figure R56-1 and in the cumulative distribution functions in Figure R56-2. In both figures, positive z-values indicate that the model PTO is greater than the observed data. A statistical calculation using this model therefore predicts a bounding distribution of pre-transient oxidation thickness values.

Furthermore, the oxidation thickness levels presented in Figure 5.1-19 of the LTR are on the order of 0.2-2% of GE14 fuel cladding thickness for the exposures of interest in LOCA analysis. The BWR/2 DBA demonstration results presented in Figure 8.3-29 of the LTR show an upper tolerance limit oxidation thickness on the order of 8%, with 9% margin to the 10 CFR 50.46 criteria. It is therefore justified that the assumptions surrounding PTO do not result in significant error relative to the margin to the oxidation limit.

LTR Impact

No changes to the LTR are proposed as the result of this RAI response.

[[

]]

Figure R56-1 Histogram of Pre-Transient Oxide Thickness Z-Values

[[

]]

Figure R56-2 Cumulative Distribution of Pre-Transient Oxide Thickness Z-Values

RAI-57

- 57) The basis for the adequacy of the database used to derive the uncertainty distribution for critical flow is not clear, and the uncertainty proposed by GEH appears substantially lower than other statistical studies. Please either revise the uncertainty distribution proposed in section 5.1.11.1 in response to the concerns below, or provide adequate justification that the proposed distribution remains appropriate in light of these concerns:
- a. A large body of critical flow data exists; however, only nine tests were used to derive the uncertainty parameters for the TRACG LOCA evaluation model. The limited dataset is particularly important because critical flow behavior and uncertainties vary significantly across various flow regimes (e.g., subcooled, saturated liquid, two-phase, steam). Because the chosen tests appear to have been selected to span these flow regimes, the proposed uncertainty distribution resembles an amalgamation of even smaller samples from several distinct populations, rather than a statistical treatment of a single population. (The dependence of uncertainty on the flow regime is alluded to in section 6.3.6 of NEDE-32176P, Revision 4, which references a slightly larger database of eleven tests.) As such, the amalgamated uncertainty distribution proposed by GEH includes single-phase data, which downwardly biases the uncertainty in the critical flow rate for the limiting recirculation breaks where larger two-phase uncertainties dominate.
 - b. The basis for the selection of the nine tests used to derive the proposed uncertainty distribution (or, equivalently, the rejection of other applicable tests) from the large body of existent critical flow data has not been justified. In particular, some of the test data chosen to derive the uncertainty distribution (e.g., the comparison with GIRAFFE break flow at twenty minutes) does not appear to be among the most applicable with regard to simulating the limiting LOCA scenarios expected for operating BWRs.
 - c. The basis for choosing specific datapoints from a given test for comparison, as well as the weighting of data during the statistical combination process is not clear. Uncertainty associated with times early in the blowdown (e.g., for a large break) can be higher and further is apparently more influential on PCT than uncertainty at later times.
 - d. As applicable, please discuss the selection of critical flow discharge coefficients for the statistical database used to derive the uncertainty distribution and to what extent latitude in making this choice influences the statistical results. Please further clarify how discharge coefficients will be chosen for plant-specific analysis.
 - e. Please clarify the significance of noncondensibles on critical flow and the consequent impact on figures of merit for the LOCA evaluation model. If significant, please further discuss the validation of the models used for noncondensibles and identify whether the influence of noncondensibles is included in any of the tests in the statistical database.

RAI-57 Response

GEH disagrees with the premise that the uncertainty for critical flow proposed by GEH is substantially lower than the uncertainties from other statistical studies, particularly when compared to other realistic LOCA methodologies approved in the U.S. See the discussion below in part (a).

- a) The TRACG critical flow model has been qualified, based on the test data discussed in the LTR. Those data points cover the whole spectrum of critical flow, spanning from liquid break to steam flow. The current TRACG critical flow uncertainty is then derived from those data. The maximum is used.

Although the assessment of the TRACG critical flow model uncertainty was limited to those representative test data considered to be the most appropriate, the model was developed using amalgamated data that spans the entire range of pressure and flow conditions. There is not a substantial difference in the uncertainty distribution of the critical flow discharge coefficient (CD) used in other approved realistic LOCA methodologies compared to the critical flow uncertainties used in the TRACG model. As discussed in LTR Section 5.1.11.1, the current GEH LOCA methodology [[

]] For comparison, based on the information obtained from References R57-1 and R57-2, the CD in one methodology ranges from 0.80 to 1.40, a spread of 0.60 between the min and max. Therefore, no substantial difference appears to exist in the applied uncertainties for the GEH methodology.

Similarly, another approved methodology appears to sample from -2-sigma to +2-sigma (or from the min to the max) for critical flow modeling, based on the information gathered from Reference R57-3. Further, the break critical flow uncertainty in this model seems to also be based on multiple data points from the 9 Marviken tests (See Table 3 and Figure 3 in Reference R57-3).

Significantly, the selection of various break sizes addresses any concern regarding the critical flow uncertainty when there is sufficient overlap between neighboring analysis points. The current TRACG LOCA methodology follows a procedure that would find the break type and location, which would result in the highest PCT.

When break flow is choked at the break location, the break flow uncertainty can be sufficiently compensated by varying the break sizes. Since the system response is primarily related to the total inventory loss through the break with other inputs unchanged, the same inventory loss through the break would result in similar system response (pressure, temperature and the PCT). Therefore, a break area increase while simultaneously reducing the break flow rate, or the break area decrease while simultaneously increasing the break flow rate, so that the total break flow rates are essentially the same would generate essentially the same LOCA response, and thus essentially the same PCT. The critical flow increase (or decrease) due to critical flow uncertainties is, therefore, equivalent to a break size increase

(or decrease) by an amount so that their product remains the same. The inconsequential effect of the critical flow uncertainties on limiting break size and PCT in break spectrum calculations can be demonstrated.

In the following sections, sensitivity studies are made regarding the above discussion and conclusion. In these sensitivity runs, the break critical flow is [[

]]

BWR/4

Using the detailed core channel model discussed in RAI-6, the BWR/4 recirculation suction line breaks are analyzed at 0.02, 0.07, 0.4, 0.67, 2.0 ft², and the maximum area split and DEGB (7.1 ft²). For each break, 11 TRACG runs are performed with different critical flow multipliers. The core PCTs for each break are presented in Figure R57-1. For each break size (A_{break}), the PCTs from all 11 runs with different critical flows are paired with the so-called equivalent break area, which is $CD * A_{break}$. The pairs of PCTs and the equivalent break areas are plotted in Figure R57-1. Included in this figure is the break spectrum, which is obtained with the nominal critical flow.

It can be observed from the results presented in Figure R57-1:

[[

]]

[[

]]

**Figure R57-1 BWR/4 Break Spectrum for Recirculation Line Suction Breaks
with Battery Failure**

BWR/2

Using the detailed core model discussed in RAI-9, the BWR/2 recirculation discharge line breaks are analyzed at 0.05, 0.3, 3.0 ft², and the maximum area split break and DEGB (7.2 ft²). The calculation and the process procedure for BWR/2 is the same as that for BWR/4 in the previous section. The pairs of the core PCTs and the equivalent break areas for BWR/2 discharge break are plotted in Figure R57-2. Included in this figure is the break spectrum, which is obtained with zero critical flow uncertainties.

It can be observed from the results presented in Figure R57-2:

[[

]]

[[

]]

Figure R57-2 BWR/2 Break Spectrum for Recirculation Line Discharge Breaks

In summary, the current critical flow uncertainties used for the TRACG LOCA methodology are comparable to the range adopted for other major US reactor vendors. Furthermore, the sensitivity studies have demonstrated that the selection of various break sizes addresses any concern regarding the critical flow uncertainty with sufficient overlap between neighboring analysis points. Extending the current critical uncertainties to a larger range has insignificant impact on the current method.

The current critical flow uncertainty distribution is therefore justified for the applications.

- b) The TRACG LOCA methodology is not sensitive to the critical flow uncertainty. See the discussion in Item a.
- c) The TRACG LOCA methodology is not sensitive to the critical flow uncertainty. See the discussion in Item a.
- d) Unlike other applications using discharge coefficients (CD), there is no tuning of CD to match results in the GEH TRACG LOCA methodology. Applications will calculate the

critical flow for the break area of interest and sample directly from the uncertainty distribution for the critical flow as given in the LTR.

- e) It has been found from the demonstration calculations in the LTR that the noncondensable gas does not infiltrate into the system for BWR/4 and BWR/6, and therefore, the current LOCA model is not impacted by the noncondensable gas from the outside. For BWR/2, ambient noncondensable gas has been found to have significant impact on the core channel LOCA responses (PCT and oxidation). However, by the time the ambient noncondensables are a significant portion of the vessel inventory by means of ingress through the break, the discharge is no longer choked. Therefore, the ambient noncondensables impact on critical flow is inconsequential. (This is unlike PWR LOCA scenarios where the accumulators discharge nitrogen into the RCS while the pressure is still high enough that the flow of nitrogen through the break can influence the critical flow.)

During normal operation, there would be some small amount of noncondensable gases in the system due to radiolysis. Those noncondensables will be primarily in the gas space. Their impact on the liquid breaks, which are the limiting breaks for all plant types, is inconsequential.

Another source of noncondensables inside the system is due to the metal water reaction. This reaction happens at high cladding temperatures and occurs usually at the later phase of the LOCA (Significant metal-water reaction is not expected for BWR/4 and BWR/6 LOCAs). Therefore, by the time the inside noncondensables are significant to the LOCA response, the discharge flow through the break is no longer choked. Therefore, the noncondensables generated during the LOCA do not impact the current critical flow and figures of merit for the LOCA evaluation model.

References

- R57-1. K. Takeuchi and M. E. Nissley, “Best Estimate Loss-of-Coolant Accident Licensing Methodology Based on WCOBRA/TRAC Code,” International Meeting on ‘Best-Estimate’ Methods in Nuclear Installation Safety Analysis, BE-2000, Washington DC, November 2000.
- R57-2. K. Takeuchi and M. E. Nissley, “Uncertainty Evaluation of Global Model Combined with Local Hot Spot Response Surface in the WCOBRA/TRAC BE Method,” International Meeting on ‘Best-Estimate’ Methods in Nuclear Installation Safety Analysis, BE-2000, Washington DC, November 2000.
- R57-3. R.P. Martin and L.D. O’Dell, “Development Considerations of AREVA NP Inc.’s Realistic LBLOCA Analysis Methodology,” Science and Technology of Nuclear Installations, Volume 2008.

LTR Impact

No changes to the LTR are proposed as the result of this RAI response.

RAI-58

58) The basis for the attribution in section 5.1.6.2 of all uncertainty associated with PIRT item F2 to the uncertainties associated with liquid side interfacial heat transfer and drag is unclear. For example, as discussed in section 7.8.2 and section 7.8.3 of NEDE-32176P, Revision 4, the modeling of injected spray and turbulent mixing both influence upper plenum mixing. Please justify the insignificance of these parameters or include them as factors in the uncertainty analysis for PIRT item F2.

RAI-58 Response

The premise of the question is that item F2 is important. This is not the case. The dominant impact of ECC interaction in the upper plenum is to change the upper plenum pressure and the temperature of the spray water. The ECC spray has a very large heat transfer surface area which over a short distance causes the sprayed water to increase in temperature to the saturation temperature. The speed at which this is done is dominated by the liquid side interfacial heat transfer. Interfacial drag is also important because it determines the ability of steam passing thru the upper plenum to carry spray drops upward and away from the core. These are the phenomena treated by F2.

Other important phenomena important to determining the LOCA licensing parameters are addressed in other ways. Ultimately, the key quantity that must be determined is how much of the water available in the upper plenum makes it down into the core. For this purpose the modeling of the spray distribution in the upper plenum (F4) is relevant for as long as the spray header is uncovered. A conservative approach based on experimental data was used in the LTR demonstration calculations. Spray distribution (F4) is the most important for BWR/2 calculations where the dominant flow path through the core is downward.

For jet pump plants, Counter Current Flow Limitation (CCFL) at locations near the top of the core (B5, C7) tends to hold up water in the upper plenum resulting in a pool that rises to cover the spray sparger. Once the spray sparger is approaching submergence the steam heating of the spray is diminished to the point that the upper plenum pool (if present) begins to subcool and CCFL breakdown (B5,C7) occurs allowing draining of water into the core first into the bypass then directly into the fuel bundles. The flow of water from the bypass into the fuel bundles is also important (B6, B9, C11).

The application of all these models is integrated with nodalization sensitivity studies and test results from integral facilities to provide a somewhat conservative evaluation of the fluid inventory in the fuel channels. What is actually conservative in terms of fluid inventory is complicated. It is one of the main reasons that it is necessary to perform a break spectrum analysis and quantify the uncertainty in PCT as a function of the break size.

LTR Impact

No changes to the LTR are proposed as the result of this RAI response.

RAI-59

59) Please provide Anderson-Darling normality test descriptive statistics for PIRT item F3. Please further clarify whether the correlation for turbulent films is of importance for the uncertainty analysis for a LOCA and whether this regime was covered by tests used to derive the uncertainty distribution or is otherwise accounted for by the TRACG evaluation model.

RAI-59 Response

The uncertainty associated with PIRT item F3, Noncondensable Return at Low Pressure, is assessed by estimating the uncertainty of the noncondensable degradation factor applied to the liquid-side interfacial heat transfer coefficient. The degradation factor is given in Eq. 6.5-28 of the TRACG Model Description report (LTR Reference [1]) and is reproduced here for convenience.

$$C_{ncg} = \min \left\{ 1.0, 0.168 \left(\frac{\alpha \rho_s^2}{(1-\alpha) \rho_a \rho_l} \right)^{0.1} \right\} \quad (\text{R59-1})$$

As noted in Section 5.1.6.3 of the LTR, the uncertainty of this degradation factor is estimated by examining the known uncertainty from a separate relationship involving condensation degradation, the Kuhn-Schrock-Peterson (K-S-P) correlation. The uncertainty of the noncondensable degradation factor is approximated by the uncertainty in the heat transfer coefficients from the K-S-P, because the degradation mechanism across the applications is essentially the same.

It is therefore not possible to provide descriptive statistics for PIRT item F3, as the uncertainty is estimated from another application, not from application-specific test data. For further information, the data that is used to derive the uncertainty of the K-S-P correlation is presented graphically in Figure 3.6-3 of Reference R59-1.

As demonstrated in Figures 8.3-11, 8.3-12, and 8.3-13 of the LTR, liquid-side heat transfer degradation due to noncondensables has a Spearman correlation factor with PCT of less than 0.4, and is therefore not a significant factor in PCT performance in BWR/2 accident scenarios.

Reference

R59-1 W.R. Usry, "Single Tube Condensation Test Program," NEDC-32301, GE Proprietary Report, March 1994.

LTR Impact

No changes to the LTR are proposed as the result of this RAI response.

RAI-60

60) Please clarify the pressure drop parameter that is varied for PIRT item H4 (pump pressure drop) in the LOCA evaluation model and specify the uncertainty distribution and parameters along with justification. Please further identify the number of tests that were considered in the derivation of the uncertainty assumptions, and summarize the test conditions and the basis for their applicability to LOCA conditions.

RAI-60 Response

The uncertainty in the recirculation pump pressure drop (PIRT item H4) was dispositioned by treating the modeled homologous pump curves as a plant parameter. In particular, the sensitivity of the limiting BWR/4 break scenario to the modeled pump curves has been evaluated. [[

]]

LTR Impact

No changes to the LTR are proposed as the result of this RAI response.

Table R60-1 Pump Curves Sensitivity Results for BWR/4 Limiting Break Scenario

Case	[[]]
Mean (K)		
Standard Deviation (K)		
Normal?		
Maximum (K)]]

[[

]]

Figure R60-1 Limiting BWR/4 Break PCT with [[
]]

[[

]]

Figure R60-2 Limiting BWR/4 Break PCT with [[
]]

RAI-61

61) For PIRT item M8, an effective reduction is proposed for its uncertainty relative to NEDE-32906P. However, under LOCA conditions, a greater uncertainty may actually be expected because (1) the peak mass flow rates during blowdown may exceed flows during normal operation (especially for the BWR/2 design) and (2) the flow is two-phase. Please clarify the extent to which these two factors are accounted for in the database used to derive the proposed uncertainty distribution, and if necessary revise the uncertainty distribution.

RAI-61 Response

Ranking of the phenomenon as high or medium is with respect to the expected impact on the critical safety parameters that are different for Anticipated Operational Occurrences (AOO) and LOCA applications. The distinction between a high and medium ranking is not relevant because for either high or medium rank the applied uncertainty is the same. The uncertainty in the correlations is determined from data that also cover the LOCA application range. Section 6.2 of TRACG Model LTR (NEDE-32176P, R4) shows that both wall friction and local form losses account for two-phase effects. The wall friction is also a function of Reynolds number. The [[]] is on the coefficient so that the absolute pressure drop uncertainty proportionally increases for higher flows expected for LOCA blowdown conditions. The amount of the applied uncertainty was confirmed by application to multiple integral tests including FIST and SSTF as discussed in Section 7 of the LTR. Therefore, there is no need to revise the uncertainty distribution.

LTR Impact

No changes to the LTR are proposed as the result of this RAI response.

RAI-62

62) The TR proposes in section 5.1.13.2 a range for isolation condenser heat transfer [[
]] If isolation condensers are credited for the limiting LOCA scenario for a given plant, please commit to validating that this distribution is appropriate on a plant-specific basis for future licensing calculations and revise the TR to state as such.

RAI-62 Response

As stated in Section 8.3.2.1 of the LTR, a single failure resulting in the loss of an isolation condenser is postulated (see the response to RAI-32 also). Furthermore, the remaining isolation condenser is not credited. Sections 5.1.13.2 and 8.3.2.1 and Table 5.1-2 of the LTR will be revised to reflect this statement. If the isolation condenser is to be credited, we commit to validate the distributions that are appropriate on a plant-specific basis.

LTR Impact

Sections 5.1.13.2 and 8.3.2.1 and Table 5.1-2 of the LTR will be revised as discussed in this response.

RAI-63

63) In May 2004, BWR/2 licensees submitted 10 CFR 50.46 notifications that refer to an exothermic hydrogen-oxygen recombination reaction having the potential to increase the calculated PCT and local oxidation. The phenomenon appears to have been dispositioned, in part, based on the conservatism inherent in the Appendix K evaluation model. Please discuss and provide justification if the hydrogen-oxygen recombination phenomenon is deemed insignificant for BWR/2s in the context of the best-estimate TRACG evaluation model.

RAI-63 Response

The issue that was first reported in May 2004 regarding the hydrogen recombination was based on an unrealistic conservative assumption that the hydrogen produced by the zirconium-steam reaction remains in close proximity with the cladding and reacts with oxygen from an unknown source of unlimited air without being displaced by that air or steam. Overly conservative and unrealistic assumptions of this type may be construed by some as being consistent with the philosophy of Appendix K evaluation models. Such an assumption is not appropriate for realistic best-estimate modeling. The scenario is not realistic because all U.S. BWR/2s have containment designs that are inerted with nitrogen and the amount of available oxygen is insufficient. Therefore, there is no credible mechanism to recreate a scenario as described for BWR/2s which have inerted Mark-I containments.

LTR Impact

No changes to the LTR are proposed as the result of this RAI response.

RAI-64

64) Please clarify the method used to derive the uncertainty bands for the CCFL constant, K, for PIRT items C6 and C7 and provide the following references:

- a. D.D. Jones, "Subcooled CCFL Characteristics of the Upper Region of a BWR Fuel Bundle," NEDG-23549, July 1977.
- b. D.D. Jones, S.S. Dua, "GE Analytical Model for LOCA Analysis in Accordance with 10CFR50 App. K; Amendment 4 – Saturated CCFL Characteristics of a BWR Upper Tieplate," NEDE-20566-4-P, July 1978.

RAI-64 Response

For the side entry orifice (SEO) Counter Current Flow Limitation (CCFL), item C6, the uncertainty is defined by the distribution of the difference between the value of CCFL constant used in the TRACG model, $K_T^{1/2}$, and the measured values from tests, $K_E^{1/2}$. In particular, the side entry orifice (SEO) CCFL test data is shown on Figure 13 of Reference R64-1. The default TRACG $K^{1/2}$ value for this location is [[]] For each test point, an experimental $K^{1/2}$ value is determined by adding the abscissa and ordinate values. The uncertainty reported in the LTR is then defined by the resulting distribution of $(K_T^{1/2} - K_E^{1/2})/K_T^{1/2}$ from these test points.

For the upper tieplate (UTP) CCFL uncertainty, item C7, the input constant is a function of fuel product line. The detailed discussion for UTP CCFL was presented in References R64-1 and R64-2. For the UTP uncertainty, [[]]

]]

Electronic versions of the documents referenced herein as well as the copies of the requested documents are provided.

References

- R64-1 NEDE-13430, "Calculation of Counter-Current Flow Limiting Conditions in BWR Geometry," September 1975.
- R64-2 NEDE-20566-4-P, "GE Analytical Model for LOCA Analysis in Accordance with 10CFR50, App. K; Amendment 4 – Saturated CCFL Characteristics of a BWR Upper Tieplate," July 1978.

LTR Impact

No changes to the LTR are proposed as the result of this RAI response.

RAI-65

65) Section 7.1.1 of the TR states that continuity in the probability density functions for figures of merit is a requirement for determining non-parametric tolerance limits according to Wilks' Theorem. However, it is not obvious that these probability density functions will, in general, be continuous. In fact, [[]] calls the TR's assumption of continuity into question. Therefore, please demonstrate that the requirement for continuous probability density functions will be satisfied in the application of the evaluation model described in the TR for quantifying a single probabilistic statement of safety for the complete spectrum of break locations and sizes, the complete spectrum of model parameters and their variation, and the nonlinear feedback introduced by the engineered safety features. In other words, please show that there are no disjoint density functions of the figures of merit, or they can be identified and taken into account in the application of Wilks' Theorem.

RAI-65 Response

Continuity of the probability density functions for figures of merit is not a requirement for determining the non-parametric tolerance limits. Although the original work by Wilks is based on continuity of the probability density function, Wald's work further extends the method to discrete distributions (Reference R65-1). As demonstrated in RAI-6 and RAI-9 responses, the bifurcated behavior is effectively eliminated from the computed results. The simulations performed to date support that the probability density functions for figures of merit are practically from continuous functions. The methodology does not depend on a continuity requirement. Therefore the sentence regarding this aspect being a requirement will be removed.

Reference

R65-1 A. Wald, "An Extension of Wilks' Method for Setting Tolerance Limits," *The Annals of Mathematical Statistics*, Volume 14, Issue 1, March 1943, 45-55.

LTR Impact:

Following sentence from Section 7.1.1 of the LTR will be removed:

"The only requirement for the validity of the OSUTL derived in this manner is continuity of the PDFs providing the samples for each trial."

RAI-66

66)

- (a) Please justify the conclusion made in the TR that 59 code simulations is sufficient to establish joint 95/95 upper tolerance limits for all pertinent criteria of 10 CFR 50.46 (i.e., PCT, local oxidation, and core-wide oxidation) using non-parametric order statistics. For background, please refer to the discussion provided in the NRC staff's review of a similar statistical approach (ADAMS Accession No. ML062150349).
- (b) Please justify the conclusion that assessing compliance with the criteria of 10 CFR 50.46 on an individual basis using a combination of parametric and non-parametric statistical approaches is capable of assuring that 95/95 limits are jointly satisfied. Please further justify that choosing between the parametric and non-parametric approaches *a posteriori* does not degrade the intended confidence level.

RAI-66 Response

The TRACG LOCA methodology conforms to 10 CFR 50.46(a)(1) which states:

“... Except as provided in paragraph (a)(1)(ii) of this section, the evaluation model must include sufficient supporting justification to show that the analytical technique realistically describes the behavior of the reactor system during a loss-of-coolant accident. Comparisons to applicable experimental data must be made and uncertainties in the analysis method and inputs must be identified and assessed so that the uncertainty in the calculated results can be estimated. This uncertainty must be accounted for, so that, when the calculated ECCS cooling performance is compared to the criteria set forth in paragraph (b) of this section, there is a high level of probability that the criteria would not be exceeded. ...”

Regulatory Guide 1.157 also states that a 95% probability level is considered acceptable for comparison of best-estimate predictions to the applicable limits. There is no defined requirement for the confidence interval associated with the upper one-sided probability limit. RG 1.157 states (highlighting added for emphasis):

“4.4 Statistical Treatment of Overall Computational Uncertainty

The methodology used to obtain an estimate of the overall calculational uncertainty at the 95% probability limit should be provided and justified. If linear independence is assumed, suitable justification should be provided. The influence of the individual parameters on code uncertainty should be examined by making comparisons to relevant experimental data. Justification should be provided for the assumed distribution of the parameter and the range considered.

In reality, the true statistical distribution for the key parameters (e.g., peak cladding temperature) is unknown. The choice of a statistical distribution should be verified using applicable engineering data and information. **The statistical parameters appropriate for that distribution should be estimated using**

available data and results of engineering analyses. Supporting documentation should be provided for this selection process. These estimated values are assumed to be the true values of the statistical parameters of the distribution. With these assumptions, an upper one-sided probability limit can be calculated at the 95% level. As the probability limit approaches 2200°F, more care must be taken in the selection and justification of the statistical distribution and in the estimation of its statistical parameters. **If a normal distribution is selected and justified, the probability limit can be conservatively calculated using two standard deviations.** The added conservatism of the two standard deviations compared to the 95th percentile is used to account for uncertainty in the probability distribution. Other techniques that account for the uncertainty in a more detailed manner may be used. **These techniques may require the use of confidence levels, which are not required by the above approach.**

The evaluation of the peak cladding temperature at the 95% probability level need only be performed for the worst-case break identified by the break spectrum analysis in order to demonstrate conformance with paragraph 50.46(b). However, in order to use this approach, justification must be provided that demonstrates that the overall calculational uncertainty for the worst case bounds the uncertainty for other breaks within the spectrum. It may be necessary to perform separate uncertainty evaluations for large- and small-break loss-of-coolant accidents because of the substantial difference in system thermal-hydraulic behavior.

The revised paragraph 50.46(a)(1)(i) requires that it be shown with a high probability that none of the criteria of paragraph 50.46(b) will be exceeded, and is not limited to the peak cladding temperature criterion. **However, since the other criteria are strongly dependent on peak cladding temperature, explicit consideration of the probability of exceeding the other criteria may not be required if it can be demonstrated that meeting the temperature criterion at the 95% probability level ensures with an equal or greater probability that the other criteria will not be exceeded.**”

- a. In the regulation, 10 CFR 50.46 and RG 1.157, there is no requirement for a “joint” 95/95 upper tolerance limits. Therefore, the expectation that peak cladding temperature, maximum local oxidation, and core-wide oxidation limits to be met jointly is in excess of current licensing requirements. Furthermore, GEH methodology already meets or exceeds the number of runs required for 95/95 upper tolerance limits as described in ML062150349. The similar statistical approach discussed in that reference utilizes break sizes sampling. When compared to the methodology and its statistical approach discussed in ML062150349 on an equal basis, GEH is running minimum of 177 (3 times 59) cases to obtain an equivalent PCT for the break sizes in consideration. This already exceeds the number of runs expected.

The process used by GEH is described in Section 7.1 of the LTR. A one-sided upper tolerance limit (OSUTL) is defined for each of the three critical 10 CFR 50.46 parameters: (1) PCT, (2) maximum local oxidation, and (3) total core-wide oxidation. These three OSUTLs are defined independently for each set of 59 calculations using either a single bounding value based on order statistics (LTR Section 7.1.1) or a calculated OSUTL from a normal distribution (LTR Section 7.1.2). In either case the OSUTL is defined to provide at least 95% probability at 95% confidence that the OSUTL bounds the calculated population for each critical parameter based on the specific scenario (break size/location and equipment). The maximum OSUTL from all sets of calculational scenarios is determined for each critical parameter and is compared to the appropriate 10 CFR 50.46 design limit independently for each of the three critical parameters as described in Section 7.4 of the LTR. This is done without any requirement or assumption regarding simultaneity of the maximums thus assuring that each maximum is always less than its specific 10 CFR 50.46 limit with a high degree of probability.

GEH further studied the impact of running 124 cases instead of 59 on the calculated one-sided upper tolerance limit (OSUTL). The BWR/4 simulations performed using the detailed core model described in the RAI-6 response are used as an example. A new random set of inputs were prepared and 124 simulations were carried out. Table R66-1 summarizes the figures of merit (FOMs) from that study. Consistent with the methodology, the OSUTL values in the table are either calculated using the mean and the standard deviation if the distribution is not non-normal, or set to be equal to the maximum value as in order statistics.

The study further demonstrates that 59-case statistical analysis is sufficient in determining 95th percentile PCT, Maximum Local Oxidation (MLO), and Core Wide Oxidation (CWO) with high probability and 124-case statistical analysis is not necessary to achieve similar outcome. Furthermore, by analyzing small, intermediate, and large breaks separately using a total of 177 runs, GEH methodology exceeds the expectation NRC imposed on other approved realistic LOCA methodologies.

**Table R66-1 Statistical Summary Comparison Between 59 and 124 Cases:
 BWR/4 0.67 ft² Break**

		59 cases	124 cases
Peak Cladding Temperature (K)	[[
Maximum Local Oxidation (ECR)			
Core-wide Oxidation			
]]

Notes: For normal distributions, OSUTL values are calculated using mean+(z-value)(std.dev); z-value for 59 cases is 2.024, and for 124 cases, it is 1.892. PCT values are rounded up to a whole number. For non-normal distributions, OSUTL is determined from the highest value for 59 cases, and the 3rd highest for the 124 cases.

- b. The statistical tests using limited quantity of random samples from an unknown distribution provide statistical information regarding true distribution with a certain level of confidence. When the random sampling takes place, there is no predetermined distribution function for the shape. If the distribution conforms with a normal distribution, then the upper tolerance limit is determined by parametric statistics. If the distribution does not conform to normality, then, the theory of order statistics provide the tolerance limits and the associated confidence level. A more descriptive characterization of this approach being *a posteriori* would be the fact that there is no *a priori* conclusion on what the distribution should look like, consistent with many applications of statistics. This approach is completely in-line with the regulatory guidance provided in RG 1.157 that states:

“If a normal distribution is selected and justified, the probability limit can be conservatively calculated using two standard deviations. The added conservatism of the two standard deviations compared to the 95th percentile is used to account for uncertainty in the probability distribution.”

NEDO-33005-A Revision 1
Non-Proprietary Information – Class I (Public)

TRACG methodology uses 2.024 times the standard deviation to account for uncertainty in the probability distribution due to number of sample calculations.

LTR Impact

GEH will reword LTR changing multiple references of “95/95” to read “95th percentile with high probability”.

SNPB RAI-67

Licensing Topical Report (LTR) Figure 5.2-8 appears to be an inadvertent repetition of Figure 5.2-5. Please provide the corrected figure.

RAI-67 Response

Figure 5.2-8 will be replaced with the correct one in the LTR. It was also noted that Figure 5.2-5 is missing the “Theta Nodalization” legend to denote the azimuthal nodalization sensitivity results so this missing legend will be added to Figure 5.2-5.

LTR Impact

The following figure is to replace LTR Figure 5.2-8:

[[

]]

NEDO-33005-A Revision 1
Non-Proprietary Information – Class I (Public)

The following figure is to replace LTR Figure 5.2-5:

[[

]]

SNPB RAI-68

Recent staff experience, in combination with the previous response to RAI 8 (regarding the treatment of evaluation model (EM) errors and changes) suggests that additional information is required concerning the treatment of input changes, plant modifications, and code changes. The treatment requires discussion both in the context of estimating the effect of an error or change, and in the context of performing a reanalysis, whether in fulfillment of a Title 10 of the *Code of Federal Regulations* (10 CFR) 50.46(a)(3)(ii) commitment or statement to “include with the report a proposed schedule for providing a reanalysis,” or simply for the purpose of developing a new baseline to eliminate an extensive error/change rackup list, or to analyze a major plant change like a fuel design change or operating domain extension. Discuss, or provide applicable procedures or modeling guidance that explains, how to discern between changes that may be estimated using engineering principles, using revision analysis (such as analyzing the effect of a change using the same population sample), or using more comprehensive techniques, such as generating a new sample or re-analyzing the break spectrum/operating domain.

RAI-68 Response

The reporting requirements mandated by 10 CFR 50.46 impose on the licensee for action. As the methodology owner, the fuel vendor supports the evaluations in case there are changes and/or errors in the evaluation model. The 10 CFR 50.46 reporting process is beyond the scope of approval this LTR is seeking. It would be expected that with an approved TRACG LOCA evaluation model, the resolution of changes and errors subsequently identified would follow a similar process as currently employed. The discussion below is provided as clarifying commentary.

According to 10 CFR 50.46(a)(3)(ii), reporting is required for a change in an evaluation model, a discovered error in an evaluation model, or an error in a plant-specific application of the evaluation model. This would not change for the TRACG LOCA methodology. Reporting for significance and compliance are checked for those changes or errors that affect the calculated peak cladding temperature (PCT). For these, the effect on the limiting emergency core cooling system (ECCS) analysis must be estimated.

In estimation of the PCT effect, engineering judgment is rarely used. Such approach would be only applicable if the effect of the change can be explicitly defined and the effect is conclusively confined. For example, in case of a discovered error, if the correction results in a negligible (less than 0.1%) change in critical parameters, then it would be possible to argue a negligible effect (i.e., 0°F). Also, some changes to the computer code, such as computing platform change or recompilation can be estimated as a 0°F effect using engineering judgment if the results after the change show no particular trend and one-to-one comparisons show fairly small difference in computed PCTs.

In some cases, it would be possible to use known sensitivities to estimate the effect. One example [[

]]

In some other cases, an estimate based on first principles can be made if the change or error correction provides a justifiable means for this approach. For example, if the heat transfer coefficient would be 10% lower when an error is corrected, it would be reasonable to estimate an increase in computed temperatures by about 10% of the temperature difference where the heat flows. In such instances, it would be prudent to take into account other non-linear effects. Such approximation would have limited applicability, in other words, would be acceptable if the resulting effect is relatively small.

The process employed by GE Hitachi Nuclear Energy (GEH) [[

]]

It would be expected that an accumulation of several changes or errors of small effect could be reported and monitored via the (annual) reporting cycle of the regulation as is done currently and not require specific re-analysis until the sum of the absolute values of these would reach the significance standard (50°F) of the regulation. Likewise, any error that resulted in a plant not conforming to acceptance criteria would require immediate remediating action to return to compliance along with subsequent re-analysis, those provisions of the regulation being operative with TRACG analyses in the same way as currently in force. Just as it is understood for the current process, an error found in the evaluation model is interpreted as a condition at variance with the evaluation model as approved by the Nuclear Regulatory Commission (NRC). Resolution of an error, with its resulting reporting of the effect will have the salutary effect of bringing the plant analysis back into conformance with the evaluation model of the LTR as intended to have been approved via the Safety Evaluation Report (SER).

As discussed in Chapter 9 of the LTR, there are some changes to the analyses that cannot be characterized as a 10 CFR 50.46 change. These include a new fuel introduction or a significant change in plant's ECCS configuration including flow capacities. In the case of a fuel type change, it would be reasonable to [[

]]

In any of the examples delineated above, [[

]]

Related to the 10 CFR 50.46 reporting topic, some changes in TRACG LOCA EM since it was submitted for review in 2011 (as of this writing more than 4 years ago) are acknowledged. Because there is no United States (US) plant that relies on TRACG LOCA methodology for 10 CFR 50.46 compliance, these changes need not be reported as part of a plant application. They will be resolved by the initial application analysis. Errors or changes to the EM discovered after it is approved by NRC will then be subject to reporting according to 10 CFR 50.46 requirements.

LTR Impact

No changes to the LTR are proposed as the result of this RAI response.

SNPB RAI-69

The uncertainty analysis appears to be based on correlations being used only within their applicable limits. Please explain what code features or processes ensure that correlations are used within applicable limits. For example: Does the code flag if correlations are used outside of their range of applicability? Are correlation ranges of applicability checked and validated by the analyst as part of the calculation process, or by a reviewer as part of the quality assurance process?

RAI-69 Response

Reference R69-1 provides the technical basis for the correlations used as auxiliary relations for closure of the basic mass, energy, and momentum conservation equations. The correlations are grouped into two broad categories: (1) those related to determination of the flow regime; and (2) those related to interfacial processes and wall heat transfer. Use of specific correlations within their applicable limits is largely achieved within TRACG by choosing correlations that have been demonstrated to be generically applicable over a wide application range for a particular flow regime or particular heat transfer mode and making a smooth transition to another correlation as the boundary for the range of application is approached. Details of how this process has been implemented in the code and qualified are provided in Section 5 and Section 6 of Reference R69-1. The remaining paragraphs of this response will highlight and summarize relevant key aspects of the code design, qualification of the models as coded against data, and describe the processes that regulate the use of the code so that the models are applied appropriately.

As noted in the introduction of Section 5 of Reference R69-1, the constitutive correlations expressing the rates of exchange of mass, momentum, and energy between each phase and their surroundings depend on the flow patterns. Thus the flow regime in each hydraulic cell is needed before proceeding with the solution of the flow equations for that cell. [[

]] The liquid-continuous regime applies to single-phase liquid flow, bubbly/churn flow, and inverted annular flow. The vapor-continuous regime applies to annular flow, dispersed droplet flow, and single-phase vapor flow. The correlations used to derive the expressions describing the relationship between the vapor and liquid velocities are specific and applicable to the specific regime where they are used as described in Section 5.1 of Reference R69-1. A transition regime between the liquid-continuous regime and the vapor-continuous regime is defined in terms of a transition void fraction that is calculated according to Equation (5.1-6) based on flow conditions and geometry. This process of a dynamic transition regime is what facilitates the use of the simple flow regime map, ensures appropriate application of correlations describing interfacial shear, and produces accurate predictions of void fractions over the entire range from 0.0 to 1.0. The

accuracy of the calculated void fractions is demonstrated by the separate-effects qualification cases documented in Section 3.1 of Reference R69-2.

Within the vapor-continuous regime annular flow may be accompanied by a varying amount of dispersed droplets as determined by the entrainment model described in Section 5.1.2 of Reference R69-1. The limited experimental range of pressures used for development of Ishii's correlation is addressed in part via the use of dimensionless correlation parameters that account for the relationships between fluid properties. For higher pressures approaching boiling water reactor (BWR) operating pressures, the entrainment correlation has been indirectly validated through comparisons to void fraction data that cover the needed application range as described in Section 6.1.8 of Reference R69-1. Specifically for LOCA applications, qualification of the entrainment and interfacial shear models at intermediate pressures has been added by comparisons to Toshiba void fraction data as indicated in Section 3.1.6 of Reference R69-2.

Section 6 of Reference R69-1 describes the constitutive correlations for interfacial shear and heat transfer, wall friction, and heat transfer for the individual flow patterns determined using the models from Section 5 that are summarized above. The models and correlations in Section 6 of Reference R69-1 are intended to cover the application range for a wide variety of BWR transients and LOCAs. The intended range of applicability for the various BWR regions in the reactor vessel is shown in Table 6-1 of Reference R69-1. Comparisons to the Table 6-1 intended application ranges are provided in the subsections of Section 6 for each of four model groups: (1) interfacial shear, (2) pressure drop, (3) interfacial heat transfer, and (4) wall shear. For each model group a table summarizes the suitability of the models in that group to predict the phenomena in the intended ranges given for each component in Table 6-1. Table 6-2 summarizes the applicability of the interfacial shear models for predicting the interfacial shear phenomena; Table 6-3 for pressure drop; Table 6-10 for interfacial heat transfer; and Table 6-18 for wall heat transfer. These four tables are supported by specific subsections within Section 6 of Reference R69-1 that address the applicability of specific correlations. Examples for each of the four model groups are provided below.

Interfacial shear models and correlations are described in Section 6.1 of Reference R69-1. Section 6.1.3.3 addresses the applicability for the correlations for the interfacial shear for bubbly flow; Section 6.1.4.3 for annular flow; Section 6.1.5.3 for droplet flow; Section 6.1.6.3 for annular/droplet flow; and Section 6.1.7.4 for counter-current flow. Ranges of application are specifically addressed. As described in the second paragraph of this response, use of the flow regime logic establishes where a specific correlation gets used to prevent for example use of a correlation for bubbly/churn flow in a flow regime where annular flow is indicated or vice versa. The models as coded are assessed by comparisons to data that are either presented in Reference R69-1 or referenced to Reference R69-2. The bulk of the data available for the evaluation of the interfacial shear and the wall friction are void fraction and pressure drop data as indicated in Section 6.1.1 of Reference R69-1. The quantification of model biases and uncertainties needed for statistical analyses for LOCA applications were provided in the LOCA Application LTR determined from comparisons to data. These are the assessments that support the overall assessment of the interfacial shear model summarized in Section 6.1.8 of Reference R69-1 and

the summary conclusions of Table 6-2 range-of-application coverage relative to the intended (or needed) ranges in Table 6-1.

Models and correlations for wall friction and form losses are described in Section 6.2 of Reference R69-1. The basic models and correlations used for wall friction in Section 6.2.1 are common ones that have been well established and extensively tested. Extensive comparison to rod bundle pressure drop data has been used to qualify modifications to the Chisholm correlation to achieve better two-phase performance in the fuel channel. Details for the code implementation are given in Section 6.2.1.4 and the applicability of the models and correlations to single-phase and two-phase conditions is assessed in Section 6.2.1.5.

Models and correlations for form losses are described in Section 6.2.2 of Reference R69-1. A local loss coefficient is input for each flow direction based on the geometry of the flow. User input errors are minimized by using standard templates and automation that calculates the inputs based on geometry recorded and verified in a database. The code also provides an input check that can be activated to assess the input local losses and print a warning for those that do not appear to be consistent with the geometry. Two-phase local loss values are internally calculated using a two-phase multiplier to the single-phase inputs as described in Section 6.2.2.3 of Reference R69-1. Applicability of the two-phase model is based on pressure drop data as described in Section 6.2.2.5 of Reference R69-1.

Overall assessment and applicability of the models for wall friction and form losses is documented in Section 6.2.3 of Reference R69-1. Citations are made to the qualification cases in Reference R69-2. [[]]

These are the assessments that support the summary conclusions of Table 6-3 of Reference R69-1 regarding the range-of-application coverage relative to the intended (or needed) ranges defined in Table 6-1 of Reference R69-1.

The critical flow model and correlations are described in Section 6.3 of Reference R69-1. As indicated in Table 6-7 of Reference R69-1, the code logic prescribes how the different models are integrated so that models specific to a particular range are not misapplied. Applicability of the models as coded is addressed in Sections 6.3.5 and 6.3.6 of Reference R69-1. Qualification using critical flow separate effects data is documented in Section 3.4 of Reference R69-2. There are also many break flow studies [[

]] that are summarized in Section 6.3.6 of Reference R69-1 and documented in detail in Section 5 of Reference R69-2.

Models and correlations for interfacial heat transfer are described in Section 6.5 of Reference R69-1. Determination of both the total heat exchange and mass transfer rates at the liquid-vapor interface require knowing the interfacial area per unit volume. This interfacial area is determined using the same flow regime map as used for the interfacial shear. Entrained drops in the vapor-continuous phase have a large effect on the interfacial area as do vapor bubbles in the liquid-continuous phase. In addition, the interfacial heat transfer coefficients themselves also depend on the characterization of the flow regime so that correlations are not applied outside the characterization for which they were designed and intended. These characterizations in

Reference R69-1 are organized in the following sections of this reference: 6.5.3 bubbly/churn flow; 6.5.4 annular flow; 6.5.5 droplet flow; 6.5.6 annular/droplet flow; and 6.5.7 transition to annular flow. Each characterization includes a discussion of the applicability of the model as-coded and/or correlation applicability.

As indicated in Section 6.5.11 of Reference R69-1, separate effects assessment of all the models and correlations integrated into the interfacial heat transfer model is not possible. Instead overall assessment is performed by selecting a set of steady state and transient qualification cases with a strong dependency on the interfacial heat transfer. These assessments include examples of sub-cooled boiling and film boiling where interfacial heat transfer effects are significant. The details in Section 6.5.11 of Reference R69-1 are quite lengthy and will not be repeated here. It is worth pointing out that based on combining the theoretical basis and applicability ranges of the individual models, Section 6.5.11 of Reference R69-1 defines for the most important bubbly/churn flow and annular flow regimes specific applicability ranges in terms of pressure, flow rate, dimension, and void fraction. Based on these, it is concluded as summarized in Table 6-10 of Reference R69-1 that the range-of-application coverage for the interfacial heat transfer models is sufficient as measured relative to the intended (or needed) ranges defined in Table 6-1 of Reference R69-1. These models are summarized here in Table R69-1 together with the application ranges.

Table R69-1 Summary of Wall Heat Transfer Models

Model LTR Section(s)	Heat Transfer Mode	Temperature and Fluid Conditions	[[]]]]
6.6.3	single phase liquid	[[
6.6.4	subcooled boiling $T_L < T_{sat}$					
	nucleate boiling					
]]

NEDO-33005-A Revision 1
 Non-Proprietary Information – Class I (Public)

Model LTR Section(s)	Heat Transfer Mode	Temperature and Fluid Conditions	[[]]
6.6.5	single phase vapor	[[
6.6.6	determination for onset of boiling transition (dryout)					
]]

NEDO-33005-A Revision 1
 Non-Proprietary Information – Class I (Public)

Model LTR Section(s)	Heat Transfer Mode	Temperature and Fluid Conditions	[[]]
6.6.7	determination of T _{min}	[[
6.6.8	Transition Boiling					
6.6.9	Film boiling - low voids					
6.6.10	Film boiling - high voids]]

NEDO-33005-A Revision 1
 Non-Proprietary Information – Class I (Public)

Model LTR Section(s)	Heat Transfer Mode	Temperature and Fluid Conditions	[[]]
6.6.11	Condensation (includes effects of NCGs)	[[
6.6.12	Thermal Radiation					
6.6.13	Quenching					
6.6.14	Metal-Water reaction]]

NEDO-33005-A Revision 1
Non-Proprietary Information – Class I (Public)

Symbols used in Table R69-1 above:

Symbol	Description	Symbol	Description
{..}	Abbreviation for another correlation in the table	h	Fluid enthalpy
[#]	Reference as cited in R69-1	G	Mass flux
T _w	Temperature at wall surface	P	Pressure of fluid (total)
T _L	Temperature of liquid	C _p	Specific heat at constant pressure
T _V	Temperature of vapor	Pr	Prandtl number
T _{sat}	Temperature of saturated water at the steam partial pressure	Re	Mixture Re number
T _{CHF}	Temperature at Critical Heat Flux	Re _L	Liquid Re number
T _{min}	Minimum Temperature for stable film boiling	x _e	Equilibrium quality of fluid
α	Void fraction of fluid	x _{crit}	GEXL critical quality
q	Heat flux	ρ	Density
β	Non-dimensional group defined by $\beta = \sqrt{(k\rho C_p)_c} / \sqrt{(k\rho C_p)_w}$	k	Thermal conductivity

The code selection logic is used to choose the heat transfer model appropriate for the wall surface temperature and the fluid and flow conditions. Special attention is given to ensure continuous transitions between models at the appropriate conditions. Consider for example the case of single phase liquid heat transfer. The transition between laminar and turbulent flow nominally occurs for $Re \sim 2300$ but this does not assure that the heat transfer correlations will provide exactly the same value for the heat transfer coefficient (HTC) at this flow condition. A similar issue exists for the transition between the forced and natural convection correlations. Because the application ranges for the correlations overlap, the code logic is to pick the largest heat transfer coefficients predicted by the turbulent, laminar and natural convection correlations. This approach takes advantage of knowledge about the flow dependency in the Dittus-Boelter correlation for turbulent flow that causes it to appropriately yield the highest HTC value of the three at the higher mass fluxes yet appropriately fall under the other two correlations for the lower mass fluxes corresponding to natural circulation and laminar flow. Figure R69-1 illustrates the selection of the highest HTC value from the relevant correlations for single-phase liquid evaluated for a specific fluid state that allows for comparison to the data presented in the cited figures from Reference R69-1. [[

]] Of course, the benefit of expressing the correlations in non-dimensional form is that the correlations scale for other fluid conditions. Note that the HTC as used by the code is determined from the maximum of the Nusselt numbers from the correlations as represented by the solid lines in Figure R69-1. It is evident from the figure that the modeled HTC value determined in this way either agrees well or is conservatively slightly under the data. Additional explanation and justification is provided in Section 6.6.3.3 of Reference R69-1.

As described above, TRACG code design specifically addresses how models and correlations are applied in order to preclude misapplications outside the qualified ranges of application. In some cases modifications have been made and/or additional qualification provided to extend the originally-designed ranges of application. Transition between different models and/or correlations has been designed into the code to address the limited application ranges for some specific models or correlations. Validation of this approach is supported by extensive qualification of the as-coded models to a wide range of test data.

Another code design feature is that TRACG provides checks to enforce the code limitations related to the domain covered by the properties for water, UO_2 , and Zr. These property ranges shown in Table R69-2 are quite wide to accommodate many uses of the code. An error message is triggered every time one of these limits is violated and must by procedure be adequately addressed by the responsible engineer to the satisfaction of the independent verifier and responsible manager. In many cases, a fatal abort is triggered for conditions where it is not prudent for the calculation to continue and the resulting message indicates the reason for the abort.

Due to other considerations, the application range for most problems is much more restrictive than the limits in Table R69-2. For example, although Zr properties extend to [[]], it is not credible that the fuel rod geometry in the core will be maintained above about 2500 K and for

LOCA licensing applications any evaluated Zr cladding temperature above 1477 K (2200°F) would not be acceptable. Limitations of this type are addressed administratively by the code Application Statement (contained in Reference R69-3) and are also factored into the controlled automation scripts that are developed for each approved licensing application. Usually technical design reviews are also extensively used to insure applicability of the code when developing a new application that challenges the code in ranges outside where it has been previously applied and proven.

[[

]]

Figure R69-1 Illustration of Selection of Highest HTC from Single-Phase Liquid Correlations

Table R69-2 TRACG Property Limitations

Minimum Value	Quantity [Symbol]	Maximum Value	Units
[[
]]

The TRACG code also provides for rigorous input checking that produces informative, warning, and fatal messages as describe in Reference R69-3. These checks enforce the code limitations for material properties, problem size, and also check for self-consistency in the geometric definitions of the problem and use of applicable correlations depending on the type of physical component that is being represented and simulated. A specific choice of correlation for cases where more than one choice is available is guided by recommendations in the User’s Manual and further enforced internally by the code via pre-selection of appropriate default inputs. Most applications employ automated scripts for defining inputs and running the code in order to minimize user errors. These automation scripts have been tested, verified, and are controlled in accordance with our quality assurance program.

The TRACG code provides extensive textual and graphical output. Information contained in the output allows users of the code to determine what models the code is applying as a function of time. Graphical output is especially useful for aligning trends and inflections in the transient responses to allow visualization of interactions between dynamic physical phenomena. Traditional time plots are often used together with animation to present information so that it can be understood and communicated. Users can compare to prior results from a similar problem and can also compare to the data provided in the extensive qualification bases. Both performers and reviewers use these tools and processes to evaluate the appropriateness of the calculated results before they are released as part of a quality record.

References

- R69-1 GE Hitachi Nuclear Energy, “TRACG Model Description,” NEDE-32176P, Revision 4, January 2008.
- R69-2 GE Hitachi Nuclear Energy, “TRACG Qualification,” NEDE-32177P, Revision 3, August 2007.
- R69-3 GE Hitachi Nuclear Energy, “TRACG04P User’s Manual,” December 2011.

LTR Impact

No changes to the LTR are proposed as the result of this RAI response.

SNPB RAI-70

Given the importance of the low pressure core spray (LPCS) system relative to the limiting peak cladding temperature (PCT) loss-of-coolant accident (LOCA) analyses, provide additional justification of the adequacy of the existing suite of LPCS benchmark tests included in the TRACG benchmark data in Table 4.4-1 of the Qualification Report, addressing the following specific topics:

- a. Explain how the database addresses system variability, such as varying nozzle designs.
- b. Is the channel power distribution in the testing bounding relative to the BWR/2 design?
- c. Explain how the uncertainty from 6x6 through 8x8 fuel data scales to modern 10x10 fuels.
- d. Explain how the uncertainty and model corrections discussed in the Qualification Report are applied in the emergency core cooling system (ECCS) EM.

RAI-70 Response

The General Electric (GE) core spray distribution methodology is described in Reference R70-1. The methodology was developed under the key assumption that the condensation (thermodynamic) effects in a steam environment can be handled independently from the hydrodynamic effects of multiple nozzle interactions. Under this assumption, the thermodynamic effects are evaluated from single nozzle spray distribution tests in a simulated reactor steam environment. The hydrodynamic effects of multiple nozzle interactions are determined from single nozzle and full-scale sparger spray distribution tests in an air environment using simulator nozzles. Simulator nozzles are specifically developed spray nozzles which produce spray patterns in an air environment similar to corresponding reactor nozzle spray patterns in a steam environment. Single nozzle tests in steam are performed at 29.5 psia where the steam density is approximately equal to the density of atmospheric air. This maintains dynamic similarity between performance in air and steam.

The GE Steam Sector Test Facility (SSTF) tests at Lynn, Massachusetts, utilizing the BWR/6¹ design (Reference R70-1), confirmed the capability of the methodology to predict spray distribution performance in a steam environment. The results substantiate the key assumption of separability of thermodynamic and hydrodynamic effects. The methodology was approved by the NRC in Reference R70-1.

It is important to note that the purpose of those core spray distribution tests in Reference R70-1 (also in References R70-3 and R70-4) was to determine core spray liquid available at each core location at zero or low steam updraft flow conditions. The core spray distribution generated using GE core spray distribution methodology, therefore, does not depend on specific bundle designs and bundle power.

For the demonstration calculations in the LTR for BWR/2 to 6, [[
]], as discussed in
Section 4.4.4 of Reference R70-2 and in the response to Item d below.

¹ Additional SSTF tests were performed utilizing the BWR/4 and 5 sparger design (Reference R70-3).

NEDO-33005-A Revision 1
Non-Proprietary Information – Class I (Public)

- a. The complete list of test matrix and test results is presented in NEDO-24712-A (Reference R70-1) Appendix C. Among all 37 tests in Reference R70-1, [[

]]

SSTF tests were initially performed for BWR/6-218, and later extended to BWR/4 and 5-218 by providing BWR/4 and 5 specific nozzle and sparger designs (Reference R70-1 and Reference R70-3). The GE core spray methodology was reviewed and approved by the NRC in Reference R70-1.

- b. The application of the GE core spray methodology to a BWR/2 plant (Nine Mile Point Unit 1 (NMP1) in this case) was made in Reference R70-4. This BWR/2 core spray design was compared to BWR/4 and 5 and BWR/6 core spray designs. It was found that the nozzle placement configuration of the BWR/4 and 5 designs is similar to the BWR/2 design, while the nozzle types of BWR/6 are similar to the BWR/2 nozzles (See Table A-1 in Reference R70-4). Core spray tests in both steam and air, according to the requirement of the GE core spray methodology in Reference R70-1, were made and the core spray distribution applicable to this specific BWR/2 were generated (See the results in Figures A-31 and A-32 in Reference R70-4). Section 3.2.4 of Reference R70-4 described how the GE core spray methodology in

NEDO-33005-A Revision 1
Non-Proprietary Information – Class I (Public)

Reference R70-1 was applied to NMP1. SSTF tests in steam environment were carried out to confirm the methodology (Reference R70-4 Section 3.2.5). The system pressure effect on the spray was considered (Section A.3). The dual sparger performance was also considered (Section A.6 of Reference R70-4), similar to the study for BWR/4&5 in Reference R70-3.

[[

]]

² This facility can also be used for single nozzle tests.

NEDO-33005-A Revision 1
Non-Proprietary Information – Class I (Public)

Although the above discussion is for a specific BWR/2, it is also applicable to other BWR types regarding core spray distribution tests (References R70-1 and R70-3).

c. []

]]

References

- R70-1 General Electric, “Core Spray Design Methodology Confirmation Tests,” NEDO-24712-A, March 1983.
- R70-2 GE Hitachi Nuclear Energy, “TRACG Qualification,” NEDE-32177P, Revision 3, August 2007.
- R70-3 NUREG/CR-1707, “BWR Refill-Reflood Program Task 4.2 – Core Spray Distribution Final Report,” September 1980.
- R70-4 General Electric, “Performance Evaluation of the Nine Mile Point Unit 1 Core Spray Sparger,” NEDE-30241, September 1983.

LTR Impact

No changes to the LTR are proposed as the result of this RAI response.

SNPB RAI-71

Please clarify the methodology for validating the acceptability of changes to the generic nodalization in the LTR for plant-specific calculations (as discussed in Section 5.2 of LTR), and justify its sensitivity for distinguishing the potential for nodalization changes to affect the determination of 95/95 upper tolerance limits for assessing compliance with the criteria of 10 CFR 50.46.

RAI-71 Response

The generic nodalization is representative and typical of the least-detailed nodalization that is considered acceptable for most applications. Additional details may be added or changed from the generic nodalization for specific applications provided the effect on modeling biases and uncertainties are assessed. Many plant basedecks may have more detail in the vessel component added to address specific needs for the AOO and stability applications. When available, these more-detailed base decks will be used to establish the baseline LOCA application for a particular plant. The methodology for validating the acceptability of changes to the baseline LOCA nodalization (once established for plant specific calculations) is discussed in Section 9.2 of the LTR.

As discussed in Section 9.2, [[

]] Once found to be acceptable, the results using the updated nodalization can be used for LOCA analyses.

[[

]] The updated nodalization strategy would then be validated similar to the validation of the generic nodalization (consistent with the TRACG Qualification Report (Reference R71-1). Once validated, the new nodalization can be used for LOCA analyses.

References

R71-1 GE Hitachi Nuclear Energy, “TRACG Qualification,” NEDE-32177P, Revision 3, August 2007.

LTR Impact

No changes to the LTR are proposed as the result of this RAI response.

SNPB RAI-72

The logic for selecting hot channels for TRACG simulations in the LTR prescribes [[
]]

However, particularly for BWRs with jet pumps, it is not clear that [[
]] Please justify
that the existing hot bundle selection logic in the LTR is adequate to determine the limiting
bundle for LOCA analysis or propose [[
]]

RAI-72 Response

Lower bundle MCPR increases the bundle power and higher LHGR increases the nodal power. Placing the bundle at these two target thermal limits assures that the PCT analysis includes the highest bundle and nodal powers.

The current TRACG LOCA experience shows that a higher bundle power for the top-peaked hot bundle is in general more limiting than a lower bundle power (higher axial peaking) if both bundles have the same LHGR at the peak power node. [[

]] Further implementation details are provided in the response to RAI-73.

As described in the RAI-73 response, the [[

]]

This change in the process will be applied to all plant types. Please also see the RAI-73 response.

LTR Impact

Section 6.2-5 of the LTR, including Table 6.2-2, is modified in the response to RAI-73 to include the requirement for the alternative top peaked bundle.

SNPB RAI-73

Please provide technical basis to support [[

]], addressing the following specifics:

- a. Please summarize the source of the data (e.g., size of database, number of plants, approximate time period represented, fuel types, etc.).
- b. Please clarify the expected differences in [[
]] Please address in particular why [[
]]
- c. Please clarify what verification would occur during the core design process and/or operating cycle to ensure that [[
]] is applicable to a given operating cycle for a particular plant and, [[
]]
- d. Regarding the limited data [[
]], please justify that the scarcity of limiting bundles is supported by sufficient measurements in these regimes.
- e. Given the [[
]]
- f. Please clarify the acceptable tolerance limit in the footnote to Table 6.2-2

RAI-73 Response

The responses are provided below to each part of this RAI. A revision is also made to the TRACG LOCA hot bundle selection criteria and the thermal limits applied to the hot bundles. Table R73-1 provided at the end of the responses replaces TRACG LTR Table 6.2-2.

- a. The data in Figures 6.2-2 and 6.2-3 of the LTR include [[

]]

- b. The process for selecting the hot bundle previously described in the LTR was [[
]] The revised process is summarized in Table R73-1 which replaces TRACG LTR Table 6.2-2. In general, a higher bundle power results in a higher PCT and/or oxidation given the same peak power node elevation and LHGR limit. [[

]]

The revised process is summarized in Table R73-1.

- c. The bundle operating parameters that may affect the PCT or oxidation calculations are,
- [[

]]

- f. Table 6.2-2 of the LTR is modified in Table R73-1 below. The table note that is the subject of this question no longer exists.

References

- R73-1 Letter, J. S. Charnley (GE) to M. W. Hodges (NRC), “Proposed Amendment 19 to GE LTR NEDE-24011-P-A (Power Distribution Limits),” MFN 031-87, April 7, 1987.

LTR Impact

LTR Sections 6.2.5 and 6.2.8 are updated (Attached at end of this RAI response).

Table R73-1. Modified Table 6.2-2 from the TRACG LOCA LTR

[[

]]

[[

]]

Figure R73-1 MAPRAT and Peak Power Node Number of Limiting Bottom Peaked Bundles

[[

]]

Figure R73-2 CRRAT and Peak Power Node Number of Limiting Bottom Peaked Bundles

[[

]]

Figure R73-3 MAPRAT and Peak Power Node Number of Limiting Top Peaked Bundles

[[

]]

Figure R73-4 CPRRAT and Peak Power Node Number of Limiting Top Peaked Bundles

LTR markups for LTR Section 6.2.5 and 6.2.8 due to the response to RAI-73 are attached below:

In addition, LPF, defined as Local Pin Power Peaking Factor, should be added to the “ACRONYMS AND ABBREVIATIONS” table in the LTR.

6.2.5 Limiting Bundle Power Distribution

The limiting bundle LHGR and MCPR is of critical importance to the prediction of ECCS performance analysis critical safety parameters. The LHGR affects the stored energy in the fuel rod. The MCPR affects the proximity to boiling transition that is important in the early phase of many LOCA scenarios. The MCPR also influences the maximum bundle power because the MCPR limit constrains bundle power.

[[

]]

The term LOCA-limited in the following sections refers to plants with PCT values close to 1,478 K (2,200°F). These plants experience extended uncover and rely on spray entering into the top of the bundle. In this sense, BWR/2s are LOCA-limited. LOCA-limited plants are highly sensitive to thermal radiation effects; therefore position of the fuel rods with higher peaking factors within the bundle is very important. [[

]]

Most jet-pump BWRs are not constrained by LOCA-related thermal limits. Non-LOCA limited plants are typically dependent on uncover and recovery timing. PCTs are lower and results are less sensitive to radiation effects.

In the following sections, the process and basis for establishing target initial conditions for MCPR and LHGR (or MAPLHGR) is described. [[]]

Three limits constrain the design and operation of fuel bundles: Thermal Mechanical Operating Limit (TMOL), which is the limiting Peak Linear Heat Generation Rate (PLHGR), MAPLHGR and Operating Limit Minimum Critical Power Ratio (OLMCPR). Generally, it is not likely for a bundle to be at or near both the LHGR and MCPR limits. The limiting bundles are close to their maximum heat generation limits in early to mid-fuel cycle, when their axial power distribution is peaked near the bottom of the bundle. The limiting bundles are closest to the MCPR limit from the middle to the end of the fuel cycle, when their axial power distribution is mid or top-peaked.

[[

]]

The limits basis is reviewed for each cycle of application and may be updated based on the process defined above.

6.2.8 PLHGR, MCPR and MAPLHGR Uncertainty

As described in Section 6.2.5, initial conditions for LOCA evaluations conservatively assume that the fuel bundle in question is operating at the LHGR or critical power (MCPR) limit.

The 3D MONICORE core process computer takes total power, flow, pressure, and nuclear instrument signals from the reactor core and evaluates a peak LHGR, a peak average planar linear heat generation rate (APLHGR) for each six-inch node, and a CPR for each bundle in the core. There are uncertainties associated with each physical input to the process computer as well as the model used to evaluate the LHGR, APLHGR and CPR. [[

]] The monitoring uncertainties are included in the MCPR limits in accordance with NEDC-32694P-A [32], and in the Thermal Mechanical Operating Limit (TMOL) LHGR limit in accordance with NEDC-33258P-A [76].

[[

]]

Table 6.2-2 Summary of LHGR and MCPR Targets

[[..... ----- ----- ----- -----

]]

SNPB RAI-74

Please define [[

]]. Please particularly address why [[

]] Please further clarify whether [[

]], or some other reference value, and additionally justify that a consistent reference is used relative to [[]].

RAI-74 Response

[[

]] Additional discussion can be found in the responses to RAI-72 and RAI-73. The following process is followed for the bundles that are being set to the MCPR target.

[[

]]

LTR Impact

No changes to the LTR are proposed as the result of this RAI response.

SNPB RAI-75

Please clarify whether scram times under realistic LOCA conditions may be affected by the interference of control blades with core structures due to seismic- or LOCA-induced motion, or due to operational effects such as shadow corrosion-induced channel bow. If so, please clarify why an appropriate delay due to these effects need not be included in a best-estimate analysis.

RAI-75 Response

The scram time used in the analysis is the Technical Specification (TS) allowable value which bounds the variations that may occur during normal operation while the plant is operating in accordance with the licensing requirements. The Limiting Condition for Operation (LCO) and the surveillance requirements for scram time in the TS (LCO 3.1.4 in the Standard Technical Specifications) assure that any deviations from the nominal geometry during normal operation do not interfere with the scram time requirements. The control rod motion is tested during each power ascension from shutdown and at specified intervals during normal operation thereafter in accordance with the surveillance requirements in the TS.

The fuel design accounts for the seismic and LOCA induced motion. The third fuel acceptance criterion for LOCA in the Standard Review Plan (NUREG-0800) Section 4.2 Appendix A requires that *“Loads from the worst-case LOCA that requires control rod insertion must be combined with the SSE loads, and control rod insertability must be demonstrated for that combined load.”* Compliance with this criterion is demonstrated in GESTAR II for GE and GNF fuels.

Therefore, no additional delay would need to be included in the scram time used in the analysis.

LTR Impact

No changes to the LTR are proposed as the result of this RAI response.

SNPB RAI-76

[Follow-on RAI-12] A passage in the response to RAI-12 discusses the difference between offsite power assumptions employed in the generic demonstration cases as compared to those that may be used in an actual application. Among the LTR demonstration calculations, the information contained in the RAI 12 response, and the information displayed in LTR Table 2.5-1 (bottom of Page 2-6), the LTR appears to lack a succinct description explaining GEH's proposed treatment of offsite power availability in plant-specific applications. Please include a brief passage in the LTR that describes how plant-specific applications will ensure that the offsite/onsite power availability requirements of GDC-35 are addressed.

RAI-76 Response

As required by General Design Criteria 35, for emergency core cooling systems, *“suitable redundancy in components and features, and suitable interconnections, leak detection, isolation, and containment capabilities shall be provided to assure that for onsite electric power system operation (assuming offsite power is not available) and for offsite electric power system operation (assuming onsite power is not available) the system safety function can be accomplished, assuming a single failure.”*

In the response to RAI-12, specifically in Table R12-1, system availability was presented for the offsite power available assumption (OPA) and loss-of-offsite power (LOOP) assumption. The conservative assumptions as shown in Table R12-1 were used for LTR demonstration calculations. For future plant applications, [[
]] will be used to show the compliance to the General Design Criteria 35 requirement regarding onsite and/or offsite power.

The GEH process regarding “Single failure and loss of onsite and offsite power” in LTR Section 2.5.1 (bottom of Page 2-6) is modified.

LTR Impact

The GEH process regarding “Single failure and loss of onsite and offsite power” in Regulatory Position 3, Section 3.1 of LTR Table 2.5-1 is modified as shown below.

Original

Single failure and loss of onsite and offsite power should be considered.	Loss of preferred power is assumed. Sensitivities to single failures are considered.	Process conforms to Regulatory Guide and Appendix A of 10 CFR 50.
---	--	---

Revised

Single failure and loss of onsite and offsite power should be considered.	<p>Consistent with the requirement of General Design Criteria 35, both loss of onsite power and loss of offsite power are assumed individually. System availability and system responses to loss of either onsite or offsite power is modeled [[</p> <p style="text-align: right;">]] Loss of preferred power is assumed.</p> <p>Sensitivities to single failures are considered.</p>	Process conforms to Regulatory Guide and Appendix A of 10 CFR 50.
---	--	---

SNPB RAI-77

Please discuss the steady-state initialization process and what parameters and criteria are used to determine that the steady-state calculation has adequately converged prior to performing transient calculations.

RAI-77 Response

The steady-state characterizes an idealized condition that is assumed to be most representative of the initial state of the reactor system for analysis purposes. In reality, small fluctuations in all physical and monitored system parameters are always present. Furthermore, experience in performing LOCA calculations using thermal-hydraulic system codes shows that the effects of reasonably small departures from the intended steady-state conditions on the computed results are insignificant and, to a large extent, akin to the perturbations introduced by small variations in uncertainty parameters. Therefore, they are typically bounded by the uncertainty in the analysis. Nevertheless, a converged steady-state at the onset of the transient calculations is part of the process of performing computations using thermal-hydraulic codes, at least for the purposes of repeatability.

TRACG steady state calculations are performed [[

]]

Given the above features, it is sufficient to check a limited set of heat balance parameters to assure that the convergence is achieved. These parameters checked and their tolerances are listed below.

- [[

]]

Because the tolerance in initial steady-state can be treated as an independent source of uncertainty in the initial conditions, the effect on the total uncertainty in the initial conditions can be estimated [[

]]

NEDO-33005-A Revision 1
Non-Proprietary Information – Class I (Public)

If a deviation becomes necessary from the tolerances specified above, the deviation is justified on a case-by-case basis and demonstrated to have no effect on the results in the non-conservative direction.

Steady state convergence to the specified targets is assured by [[

]]

LTR Impact

No changes to the LTR are proposed as the result of this RAI response.

SNPB RAI-78

How does TRACG-LOCA account for potential uncertainties in the flow regime? Explain the analytic treatment for uncertainties associated with the transitioning from one type of flow to another?

RAI-78 Response

[[
]] TRACG models of flow regimes and their transition from one regime to another are discussed in Section 5 of the TRACG Model Description LTR (Reference R78-1).
[[
]] It is important to note that the flow regime per se is not used by the TRACG field equations, but rather the values for the interfacial parameters. The main assessment of the flow regime map, therefore, should be done in connection with the interfacial shear model and based on the accuracy of the void fraction prediction. The flow regime potential uncertainties can then be represented in TRACG by how well TRACG predicts void fraction for BWR application and the uncertainties in flow regime predictions.

Interfacial shear modeling at different flow regimes are discussed in Section 6.1 of Reference R78-1. TRACG predictions of void fractions in varieties of test facilities can be found in the TRACG Qualification LTR (Reference R78-2). It has been shown in Reference R78-1 and Reference R78-2 that the void fraction is predicted by TRACG very accurately, [[
]]

The void fraction potential uncertainties have been considered in the TRACG LOCA application by including those PIRT parameters that affect void fraction predictions, as described in LTR Section 3 and 5.

[[
]]

References

- R78-1 GE Hitachi Nuclear Energy, “TRACG Model Description,” NEDE-32176P, Revision 4, January 2008.
- R78-2 GE Hitachi Nuclear Energy, “TRACG Qualification,” NEDE-32177P, Revision 3, August 2007.

LTR Impact

No changes to the LTR are proposed as the result of this RAI response.

SNPB RAI-79

Section 5.3.2 of the LTR states that feedwater flashing is a dominant phenomenon in the latter part of the blowdown phase of the integral LOCA tests, yet the phenomena identification and ranking table (PIRT) treatment of the feedwater system appears to assign a medium importance rank. Both the FIST and ROSA facilities included feedwater piping. Please provide additional detail concerning the TRACG modeling of these facilities, and the treatment of the feedwater system within the TRACG models. Provide additional discussion specifically characterizing the observed impacts of feedwater flashing, and discuss the results of the TRACG assessments with respect to this phenomenon. Explain what conclusions are drawn with regard to the validity of the TRACG-LOCA EM and its treatment of jet pump BWR feedwater piping.

RAI-79 Response

The PIRT (LTR Table 3.4-1) was developed early in the Code Scaling Applicability and Uncertainty (CSAU) process for the TRACG LOCA application. At the conclusion of CSAU Step 3, the highest importance rank assigned to Item R1 (feedwater flow dynamics) was medium with [[]]

as the critical parameter. It has been subsequently demonstrated [[]] (see the response to RAI-93 for further information [[]]) Note that the biases and uncertainties associated with all high and medium ranked phenomena are considered in LTR Section 5.1. Thus, the treatment of this item is the same as if it had originally been ranked as high importance.

Section 5.3.2 of the LTR indicates that feedwater flashing is one of the important phenomena to consider, for purposes of test facility scaling, for simulating large break LOCA blowdown transients. The conclusion of this section is that because the cited tests generally scale well to the postulated BWR/6 large break LOCA, conclusions regarding the ability of TRACG to model these tests translates to the ability of TRACG to model the corresponding plant LOCA. [[]]

It is true that both the FIST and ROSA facilities included feedwater piping. However, note that in Section 5.3.2, feedwater flashing is only mentioned for the ROSA facility. For the FIST facility, the hot feedwater control/isolation valve is just upstream of the feedwater mixer/vessel inlet nozzle. Consequently, there is a very small volume of feedwater piping modeled outside the vessel ([[]]). Thus, feedwater flashing is under-scaled for the FIST facility relative to the corresponding plant case.

The ROSA facility Test 926 TRACG model includes the [[]] feedwater piping [[]]

[[]] Because the vessel connection elevation is the high point of this pipe, feedwater delivery to the vessel will effectively cease once the feedwater is isolated,

until feedwater flashing begins. [[

]] The effect of feedwater flashing in this pipe is most readily observed by running the TRACG transient with and without the pipe, and comparing the system pressure response. Figure R79-1 provides this comparison, [[
]]

[[

]]

Figure R79-1 Impact of Feedwater Flashing on ROSA Test 926 TRACG Calculated Vessel Pressure

For a full-scale plant analysis with TRACG, it has been observed that feedwater flashing [[

]] Figure R79-2 is included to compare the TRACG calculated peak rod temperatures for the same three cases previously discussed. This figure is included for information [[

]]

As mentioned above, the FIST experiment did not include the feedwater flashing effect in any significant way. The feedwater flashing effect was included in the ROSA Test 926 experiment, but it was under-scaled relative to the corresponding plant case. However, the effect of this

phenomenon on pressure was observed in the TRACG simulation, as in the experiment measured pressure. Despite this under-scaling of feedwater flashing and over-scaling of the metal structure stored energy in the experiments, as LTR Section 5.3.2 indicates, the overall scaling parameters are reasonable for the corresponding plant LOCA analysis with TRACG. Finally, the ability of TRACG to calculate liquid flashing during depressurization has been shown by separate effects tests such as the PSTF level swell test (Section 3.1.5 in Reference R79-1) and various critical flow tests (Section 3.4 in Reference R79-1).

[[

]]

Figure R79-2 Effect of Feedwater Flashing on ROSA Test 926 TRACG Peak Rod Temperature

References

R79-1 GE Hitachi Nuclear Energy, "TRACG Qualification," NEDE-32177P, Revision 3, August 2007.

LTR Impact

No changes to the LTR are proposed as the result of this RAI response.

SNPB RAI-80

Please clarify the Steam Sector Test Facility test used in Figure 5.3-3.

RAI-80 Response

The test data for SSTF in LTR Figure 5.3-3 are from SSTF Test SRT-3 Run 26 for the bundle with counter-current flow, which can be found in Figure 3.4.4-22 (Reference R80-1). [[

]]

SSTF Test SRT-3 (Run 26) simulated the reflood phase of a large-break LOCA transient. The detailed discussion of this test and its comparisons with TRAC and TRACG can be found in References R80-1 and R80-2.

References

- R80-1 “BWR Refill-Reflood Program Task 4.8 – TRAC-BWR Model Qualification for BWR Safety Analysis Final Report,” GEAP-22049 (NUREG/CR-2571; EPRI NP-2377), July 1983.
- R80-2 GE Hitachi Nuclear Energy, “TRACG Qualification,” NEDE-32177P, Revision 3, August 2007.

LTR Impact

No changes to the LTR are proposed as the result of this RAI response.

SNPB RAI-81

Please explain the difference between the early boiling transition peak calculated in TRACG in Figure 5.3-8 for the ROSA test and the measurements that do not show a peak.

RAI-81 Response

The ROSA measurement shown in LTR Figure 5.3-8 is the ROSA data with 2nd peak from ROSA Test 926. The same data can be found in Figure 5.4-9 of Reference R81-1.

The early boiling transition PCT peak (called 1st peak) from ROSA test 926, as shown in Reference R81-1, is not included in LTR Figure 5.3-8 because the maximum PCT is the most important parameter for LOCA application. [[

]]

Reference

R81-1 GE Hitachi Nuclear Energy, “TRACG Qualification,” NEDE-32177P, Revision 3, August 2007.

LTR Impact

No changes to the LTR are proposed as the result of this RAI response.

SNPB RAI-82

Section 5.3.3 of the LTR discusses the scaled integral LOCA simulation tests for non-jet pump plants. This discussion is supplemented by Section 5.5 of NEDC-32177P, Revision 3. In particular, Section 5.5 of NEDE-32177P notes that neither of the two integral tests described therein involved ECCS actuation. It is not clear that the regulatory guidance is satisfied for this reactor design. In particular, Standard Review Plant (SRP) 15.0.2 notes that “Integral effects testing must be performed to demonstrate that the interactions between different physical phenomena and reactor coolant system components and subsystems are identified and predicted correctly.” As the LTR refers to a suite of integral effects tests as supplemented by additional separate effects tests, explain how the TRACG-LOCA EM is qualified in an integral sense. One important aspect, for example, is the behavior of non-condensibles in the vessel and primary system.

RAI-82 Response

The separate effects tests (SETs) and integral effects tests (IETs) play an important role in nuclear reactor thermal-hydraulics research. They are relied on developing the methodologies used in safety analyses. As stipulated in NUREG-0800 (Reference R82-1), the Standard Review Plan, and also exemplified in NUREG/CR-5249 (Reference R82-2), the CSAU Methodology, and subsequently in Regulatory Guide (RG) 1.157 (Reference R82-3), the IETs primary focus is on the interaction between parameters and processes by incorporating many or all of the important phenomena and components. In the art of computational thermal-hydraulics, there has been always a residual imperfection when it comes to integral tests. In some cases, this is caused by the scaling distortion, in some others mainly based on facility restrictions. Compared to an actual plant data, IETs cannot be considered ‘perfect’. Furthermore, it is not unusual to experimentally simulate portions of a LOCA event, rather than the entire transient in the integral effects testing. The referenced IET in Section 5.5 of Reference R82-6 is such an example that includes only the blowdown portion of the LOCA for a scaled external loop BWR prior to ECCS activation. During the blowdown the interactions between phenomena are complicated and that is why IETs are important during this stage. After blowdown the ECCS phenomena for a BWR/2 ECCS are limited to those represented by the core spray heat transfer SETs described in Section 3.2.2 of Reference R82-6. Although the entire system is not simulated, the key interactions related to spray distribution and heat transfer mechanisms within the fuel channel are captured. This is an example of the common practice of using SETs to address any gaps in the IET coverage.

One important distinction in use of IETs between the RG 1.157 guidance and the TRACG LOCA methodology is in how they contribute to quantification of code uncertainty. RG 1.157 states that the “*code uncertainty should be evaluated through direct data comparison with relevant integral systems and separate-effects experiments at different scales*”. The approach employed in the TRACG LOCA methodology primarily uses the SETs (rather than the IETs) to quantify the biases and uncertainties in specific modeling phenomenon. The primary role of IETs in the

TRACG LOCA methodology is to evaluate an overall quality of the predictions considering the interaction between the modeled phenomena. Similar points are also provided as part of the RAI-92 response.

In this context, it is also prudent to recognize that, in some cases, not all of the important phenomena were identified and factored in, a priori, when the integral tests were originally designed. The existence of some interactions or the effect of some phenomena that were not recognized as important during testing can be identified by the realistic simulations using capable prediction tools. A recent example in light water reactor (LWR) research and best-estimate LOCA field is the discovery of the importance of downcomer boiling in pressurized water reactors (PWRs). As indicated in Reference R82-4, downcomer boiling was not recognized as a process of high importance in the CSAU study, an aspect that was established before the experimental information from the two-dimensional (2D)/ three-dimensional (3D) test programs was available and well before realistic code simulations were performed and ultimately, causing experimental data from large scale test facilities ending up being limited.

Similarly, in the case of BWR/2 analyses, the importance of air ingress and behavior of non-condensable gas (NCG) in the vessel and the primary system is revealed by TRACG LOCA calculations rather than any particular IET (as documented in the response to RAI-13). Because the importance of such behavior was not highlighted when the IETs were designed, no particular accommodations were considered in the IETs. Therefore, the experimental data in the sense of integral testing is limited. To this extend, the observation offered in the RAI has merits. The TRACG LOCA methodology, similar to other state-of-the-art LOCA methodologies, relies on complementing information gaps that might exist from the IETs and plant data by SETs and component data. The identified gap of no NCGs in the IETs is not a critical issue for the methodology, because the non-condensable effects on physical phenomena such as condensation are well established by the TRACG LOCA methodology. Section 5.1.5.3 of the TRACG LOCA LTR describes how the uncertainty in the degradation in condensation due to the presence of NCGs was established from SETs. Section 6.6.11 of Reference R82-7 describes the model in detail and comparison of the model to other models and the data is documented in Section 6.6.11.3. As shown by this example, the quantification of bias and uncertainties on the key phenomenon of degradation of condensation heat transfer due to NCGs does not directly rely on IETs because this has been achieved using SET data instead.

The core spray test comparisons described in Section 7.4 of the TRACG LOCA LTR include the phenomenological interactions relevant for the ECCS portion of a LOCA in a non-jetpump BWR. Selected comparison of calculated and measured rod temperatures shown in the LOCA LTR demonstrate that the uncertainties considered are sufficient. Additional core spray results were provided in the response to RAI-92. Even more additional experimental data are evaluated here as part of this response. The additional data supplied in this response comes from the Studsvik core spray heat transfer tests (Reference R82-5). The facility could be configured in different ways. As shown in Figure R82-1, the setup for the core spray heat transfer tests allowed bottom venting. The vents were open to atmosphere. Although the tests were not aimed to study air effects, during the venting, it was possible for air to enter the test rig unrestricted.

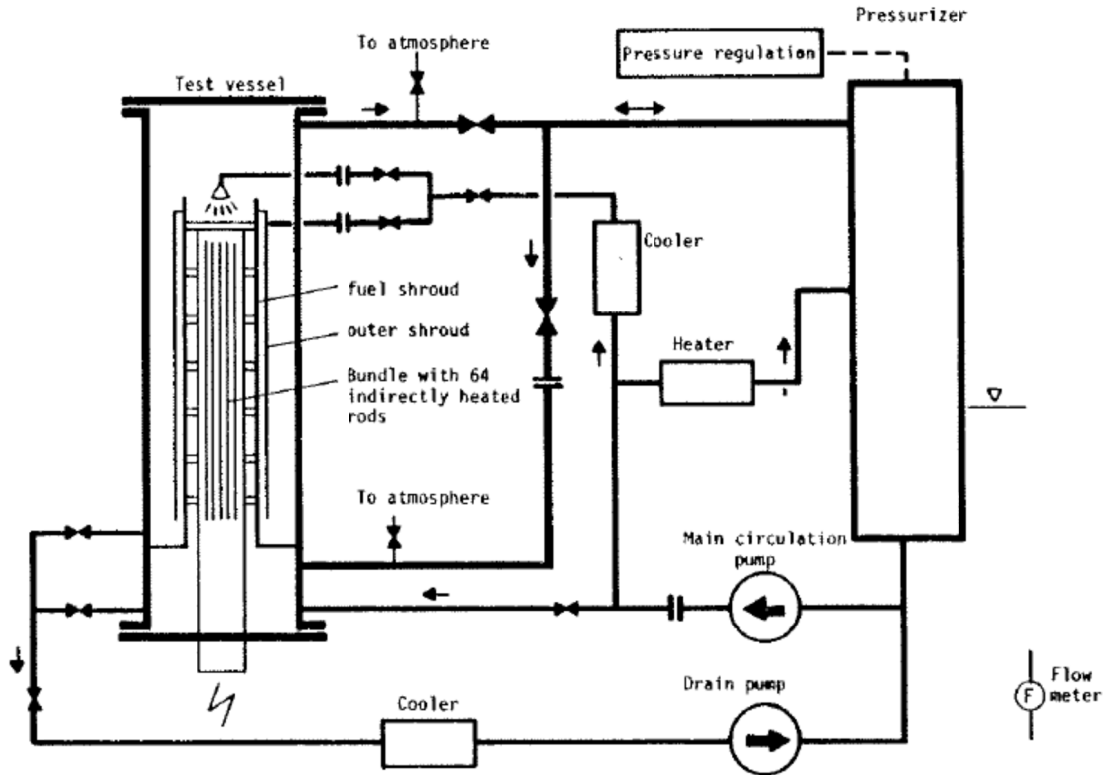


Figure R82-1 Spray Cooling Experiment Setup

A series of tests were conducted top and bottom venting configurations. The test run 123 was specifically designed as bottom vented. No measurements were made to determine how much air was ingested; however, the TRACG calculations for this test indicate [[

]] as shown in

Figure R82-2. Note that the calculational process to simulate conditions with and without possible air ingestion was achieved [[]] the same as used in the BWR plant simulations. The response to RAI-13 explained in detail the modeling approach used to ensure that effects of air ingestion would be reflected in the calculated PCT values used for the licensing basis.

[[

]]

Figure R82-2 Studsvik CSHT Test 123 – Cladding Temperatures

In this run, [[

]]

Additional core spray heat transfer tests were also evaluated by statistical treatment of uncertainties, sampling them from their respective distributions. Although these tests were designed as top venting, bottom venting was allowed in a controlled manner as the lower plenum was filled during the experiments. Three tests were selected because they had the highest peak temperatures. Figures R82-3, R82-4, and R82-5 show the comparisons for tests 111, 133, and 137, respectively.

[[

]]

Figure R82-3 Studsvik CSHT Test 111 – Cladding Temperatures

[[

]]

Figure R82-4 Studsvik CSHT Test 133 – Cladding Temperatures

[[

]]

Figure R82-5 Studsvik CSHT Test 137 – Cladding Temperatures

Combined with the statistical treatment, the TRACG results are [[

]] The conclusion is that the qualification basis is sufficient to support how the TRACG LOCA methodology is applied for non-jet pump plants.

References

- R82-1 U.S. NRC, “Standard Review Plan for the Review of Safety Analysis Reports for Nuclear Power Plants: LWR Edition,” NUREG-0800, March 2007.

NEDO-33005-A Revision 1
Non-Proprietary Information – Class I (Public)

- R82-2 B. Boyack, et al., “Quantifying Reactor Safety Margins: Application of Code Scaling, Applicability, and Uncertainty Evaluation Methodology to a Large-Break, Loss of Coolant Accident,” NUREG/CR-5249, December 1989.
- R82-3 U.S. NRC, “Best-Estimate Calculations of Emergency Core Cooling System Performance,” Regulatory Guide 1.157, May 1989.
- R82-4 NRC Memo S. Bajorek to J. E. Rosenthal, “Downcomer Boiling Technical Summary”, May 22, 2002 [ML021420196], and its attachment “Downcomer Boiling” [ML021420201].
- R82-5 Studsvik Report, “BWR Emergency Core Cooling Investigations – Spray Cooling Heat Transfer Experiment in a Full Scale BWR Bundle Mock-up,” STUDSVIK/E4-78/64, October 4, 1978.
- R82-6 GE Hitachi Nuclear Energy, “TRACG Qualification,” NEDE-32177P, Revision 3, August 2007.
- R82-7 GE Hitachi Nuclear Energy, “TRACG Model Description,” NEDE-32176P, Revision 4, January 2008.

LTR Impact

No changes to the LTR are proposed as the result of this RAI response.

SNPB RAI-83

Please clarify whether sensitivities associated with fuel channel grouping were performed for the LOCA event as indicated in Section 6.1 of the LTR and summarize the analysis and results, particularly as pertaining to [[]].

RAI-83 Response

The changes in [[]]

]] Results, summarized in Table R83-1, show that the effect on computed PCT is negligible with the average channel groups.

Table R83-1 PCT Comparison for Channel Grouping Sensitivity

	[[]]]]
BWR/4		
Double-Ended Guillotine Break	[[]]	
Intermediate Break (0.67 ft ²)		
Small Break (0.10 ft ²)]]
BWR/2		
Discharge DBA	[[]]]]

Based on the runs from this time step sensitivity study, the comparison of PCT results between the [[]]

]]

LTR Impact

No changes to the LTR are proposed as the result of this RAI response.

SNPB RAI-84

Please clarify whether analysis is required for the increased core flow region of the power/flow map. If not, explain why not.

RAI-84 Response

Consistent with the response to RAI-27, the increased core flow region will be evaluated to determine if the analysis is required for a specific application.

In general, [[

]]

LTR Impact

No changes to the LTR are proposed as the result of this RAI response.

SNPB RAI-85

Some LOCA-limited plants may not be BWR/2s; please ensure Table 6.2-2 reflects this consideration.

RAI-85 Response

[[
]]

Please note that Table 6.2-2 is updated in response to RAI-73.

LTR Impact

No changes to the LTR are proposed as the result of this RAI response.

SNPB RAI-86

Section 6.3 of the LTR indicates that more realistic distributions may be used for plant parameters than specified in Tables 6.3-1 and 6.3-2 if justified separately for plant-specific analysis. Please provide the following additional information regarding this topic:

- a. Please clarify whether all parameters in Table 6.3-1 and Table 6.3-2 may be substituted with more realistic distributions, or only a subset thereof, and justify that the data supporting more realistic distributions taken under normal conditions is relevant to performance during a LOCA (e.g., scram times, pump coastdown times, etc.).
- b. Please clarify the statistical requirements to support the use of more realistic distributions for plant parameters.

RAI-86 Response

- (a) A number of listed parameters in LTR Table 6.3-1 are physical parameters that define the plant configuration and are not changeable. Among these are total number of valves and grouping of these valves. As the table indicates, they are modeled based on the actual plant configuration. In the context of system performance and setpoint values, these parameters do not need to be listed and will be removed from the table.

Table 6.3-1 as modified by this response primarily relies on use of analytic limits (ALs) because the use of the established AL removes the need to establish and sample from a distribution. Using the established ALs ensures consistency between different functions when a trip is shared. Those parameters that currently use a basis other than the AL have already been justified in the LTR.

Consistent with the realistic modeling assumptions, other parameters given in the table that are currently set at the AL may have the AL replaced with a more realistic distributions based on the plant's approved instrument setpoint methodology. If the plant in question has not adopted an improved setpoint methodology program, then the justification of data for supporting more realistic distribution will be provided for approval.

- (b) The NRC-approved instrument setpoint methodology program provides the basis for developing realistic distributions for values of plant parameters (Reference R86-1). The nominal parameter values and distribution functions would cover at least 95% content with at least 95% confidence. A different method for generating more realistic distribution for LOCA use for any specific parameter currently using an AL will constitute a change in the application model and thus require that the change for that specific parameter to be submitted for approval.

Reference

- R86-1 GE Nuclear Energy, "General Electric Instrument Setpoint Methodology," NEDC-31336P-A, Revision 0, September 1996.

LTR Impact

Table 6.3-1 will be updated as marked below:

System Unique Parameters	Analysis Basis
Maximum delay time from diesel generator (DG) start signal until bus is at rated voltage	[[
Minimum detectable break size for Loop Selection Logic	
Leakage allowance for shroud access hole cover repairs or cracks	
Scram speed to 90% position	
Feedwater pump coastdown (from initial value to zero flow)	
Time constant for recirculation pump coastdown (intact loop and loop with break)	
ECCS makeup water temperature	
ADS Parameters Timer delay Bypass timer delay for sustained low water level Total number of relief valves with ADS function ADS close on vessel pressure ADS reopen on vessel pressure ADS reclose on vessel pressure	
Pilot-Actuated Safety/Relief Valves (SRVs) Number in each Setpoint Group Setpoints Low low set logic assumed in analysis for closing/opening pressure Pilot-actuated SRV Capacity at (100+ACC)% of Popping Pressure Closing pressure setpoint Time delay before opening Time constant of opening/closing	
Spring Safety Valves (SSVs) Number of groups Number of SSVs Opening setpoint Capacity of each at opening setpoint]]

SNPB RAI-87

Please clarify the code and LTR methodology (if applicable) used in the prediction of the containment pressure values used to characterize the drywell high pressure scram time, and contrast the results to times derived from existing licensing basis calculations. Please further clarify whether the hypothesis of normality was invoked in determining the 95/95 tolerance limit based on seven sample calculations performed at each break size.

RAI-87 Response

Drywell pressurization analysis was performed with the GE methodology used in sizing the vacuum breakers (VACBR code). [[

]] The results are compared in the table below. Because the initial containment pressure assumptions are also different in the licensing analyses, the comparisons are presented in terms of the time required to increase the drywell pressure by the same differential pressure. [[

]]

This simplified approach allows us to credit the delayed scram in the LOCA analysis in a conservative way without the complexity of coupled modeling of the containment.

NEDO-33005-A Revision 1
 Non-Proprietary Information – Class I (Public)

Break Size (ft ²)	Time to Increase DW Pressure by 2 psid			
	LTR Figure 6.3.1	Containment Licensing Method Results	Containment Licensing Method	LTR Correlation
[[
]]

[[

]]

LTR Impact

No changes to the LTR are made as the result of this RAI response.

SNPB RAI-88

Please clarify whether the entries in Table 6.3-1 for automatic depressurization system (ADS) close/reopen/reclose on vessel pressure refer to the relief valve mode of operation of the safety relief valves (SRVs) used by the ADS. If not, please explain the intent.

RAI-88 Response

The ADS close/reopen/reclose on vessel pressure entries in LTR Table 6.3-1 refer to the pressure at which the SRVs operated by the ADS in relief mode will either: close when the differential pressure between the vessel and the containment is not sufficient to keep the valves open (after depressurization) or open when the differential pressure becomes high enough to reopen the valves.

LTR Impact

No changes to the LTR are made as the result of this RAI response.

SNPB RAI-89

[Follow-on to RAI-31] In Section 7.3, please clarify why only the limiting nominal conditions (i.e., without consideration of uncertainty) are evaluated statistically. Because the uncertainty may vary substantially among different breaks, the limiting conditions with respect to the 95/95 tolerance limits used to assess compliance with the criteria of 10 CFR 50.46 may not necessarily correspond with the conditions that are nominally limiting. Further, the process used to obtain the biased results discussed in response to Set 1 RAI-31 is not clear. Finally, it would seem that a better way to address the concern would be to re-evaluate the demonstration analyses for several break sizes in close proximity to the nominally limiting break sizes to demonstrate the insignificance of identifying the limiting break size (and other properties) using a nominal analysis. Presently, LTR Figure 8.1-29 underscores the concern conveyed in this RAI question. Please base the justification provided in response to this RAI question on updated break spectrum analyses and explain whether the more detailed channel grouping has improved the TRACG-LOCA EM performance in this regard.

RAI-89 Response

The GEH approach is consistent with the requirements of Section 4.4 of RG 1.157, which requires that *“the evaluation of the peak cladding temperature at the 95% probability level need only be performed for the worst-case break identified by the break spectrum analysis in order to demonstrate conformance with paragraph 50.46(b)”*.

First, we discuss the process used to obtain the biased results in the response to Set 1 RAI-31. The biases referred in that response were obtained from the comparisons between TRACG predictions and test data, which were determined individually for each PIRT parameter and were discussed in details in Section 5 of the LTR (See a summary in Table 5.1-2 of the LTR). The biased results in the response to Set 1 RAI-31 refer to the TRACG calculation results in which those TRACG model biases determined in Section 5 of the LTR are not removed. On the contrary, the non-biased results in the response to Set 1 RAI-31 refers to the results in which the TRACG model biases are removed. The non-biased results are actually, more precisely, de-biased results, which will be called hereafter.

It is acknowledged that [[

]] (See the discussion in the response to RAI-6).

Regarding the results in LTR Figure 8.1-29, [[
]], as shown in the figure. LTR Section 7.3
provides the method for determining the One Sided Upper Tolerance Limit (OSUTL). Because
it is the OSUTLs that are compared to the acceptance criteria, the reasonable and appropriate
comparison between different breaks is for OSUTL values, not for maximum values. [[

]]

For a BWR/4, the PCT variability has been significantly reduced [[

]] Sensitivity studies are performed here to demonstrate that the PCT determined from
the limiting break determined from the nominal calculation is sufficient for TRACG application.
For this study, a BWR/4 is selected. As shown in the response to Set 1 RAI-31, [[

]] The results from all 10 sets of the analyses are summarized in Table R89-1.
As shown in Table R89-1, [[

]] (See Figure R31-1 in the response to Set 1
RAI-31).

It is found that [[
]] TRACG-LOCA EM performance
has been improved in predicting the OSUTL PCT in the close vicinity of the limiting break. This
further demonstrates that the statistical analysis at the limiting break sizes determined from
nominal conditions can sufficiently represent the results in the close proximity of the limiting
break.

LTR Impact

No changes to the LTR are proposed as the result of this RAI response.

Table R89-1 PCT Summary of Sensitivity Study for BWR/4 Suction Line Breaks

II						
						II

SNPB RAI-90

Section 7.3.1 states a minimum bound for the number of simulations that may be increased to raise the confidence level of the desired statistical bound. Please clarify whether GE Hitachi Nuclear Energy – Americas, LLC (GEH) will require that the number of simulations be set prior to performing analysis in order to prevent degradation of the statistical confidence level.

RAI-90 Response

The number of simulations that satisfy the 95th percentile with 95% confidence is set prior to performing the analysis. [[

]]

LTR Impact

No changes to the LTR are proposed as the result of this RAI response.

SNPB RAI-91

Please clarify the statement in Section 7.4.4 that TRACG underpredicts mixing in the VSSL component. It appears that the spread in lower plenum temperature predictions in the TRACG results are less than the data, and that the mean value of the lower plenum temperature is underpredicted by TRACG.

RAI-91 Response

The benchmarking to the SSTF had been updated using the current TRACG04 version and the updated PIRT table. The discussion in LTR Section 7.4.4 and Figures 7.4-10 through 7.4-17 are revised to include the updated results.

The lower plenum temperature distribution has an indirect effect on the LOCA response because the temperature of the water going into the core is nearly at saturation temperature. Stratification in the lower plenum may affect the LOCA response through the pressure and the amount of mass contained in the lower plenum. The revised LTR includes comparisons to the water mass in the lower plenum, core bypass region, upper plenum, system pressure and the temperature distribution. The statement that is the subject of this RAI is replaced by a more extensive discussion.

LTR Impact

LTR Section 7.4.4 (including figures) is updated by this RAI response as indicated in the following markups.

7.4.4 SSTF Test EA3-1

The SSTF Test Facility simulated the refill-reflood phase of a BWR LOCA transient. The safety systems in the facility could be configured to model either a BWR/6 or BWR/4 refill-reflood transient and test data from both BWR/6 and BWR/4 simulations were used for TRACG qualification [2]. Test EA3-1, a BWR/4 refill-reflood simulation, was selected for the statistical analysis presented here.

In this test, the lower plenum fill time controls the core reflood. The major purpose of the statistical analysis is to show that the measured lower plenum fill-time is bounded by the TRACG analysis when model uncertainties are taken into account. The liquid mass held up in the bypass region and upper plenum has an important effect on the LOCA analysis. The bypass and upper plenum fill time predictions are compared to the test results. It should be noted that the accuracy of the lower plenum fill time also depends on the amount of liquid held up above the core plate, and therefore the lower plenum fill time predictions depend on the bypass and upper plenum liquid fractions being predicted reasonably well. ~~A secondary purpose is to examine the effect of model uncertainties on the prediction of mixing of the cold ECCS injection in the lower plenum during refill.~~ Several of the qualification test data vs. analysis comparisons are repeated as part of the uncertainty analysis.

The results of the statistical analysis of SSTF Test EA3-1 are compared with the test data in Figure 7.4-10 through Figure 7.4-14~~17~~. The TRACG results include the nominal calculation, the band subtended by the 59 trials and the average of the 59 trials. Figure 7.4-10 compares measured and calculated system pressures. [[

]]

TRACG's prediction of ~~the mixing of the cold ECC water injected into~~ temperature variations in the lower plenum is shown in Figure 7.4-11 through Figure 7.4-13. These figures show temperatures measured at the lower plenum periphery near the bottom, at mid-submergence and near the surface. The data for the bottom and mid-plane show the same trend until approximately 80 seconds, after which there are fluctuations of high magnitude at the mid-level and of lower magnitude at the bottom level. ~~At the lower plenum bottom, where the injection takes place, TRACG predicts [[~~

Since the lower section of the lower plenum is divided into bays, and the temperature is measured in the bay where the jet pump discharges into, the lower plenum temperature measured at the bottom of the lower plenum is expected to be close to the jet pump discharge temperature. There are occasional fluctuations in the test data after the lower plenum is filled as shown in

Figure 7.4-11. [[

]]

Of particular interest in Test EA3-1 is the lower plenum refill time. The available test data show the refill time expressed as lower plenum mass fraction. ~~The TRACG lower plenum mass fraction was calculated from the cell mixture density.~~[[

]]

Comparisons to the bypass and upper plenum fill fractions in Figures 7.4-16 and 7.4-17 provide a measure of the effects of CCFL correlations. [[

]]

These comparisons show that the TRACG predictions represent the ECCS mixing phenomena reasonably well in the upper plenum and lower plenum regions, CCFL behavior and the timing of reflood.

The uncertainty evaluation of the TRACG predictions of the SSTF test was extended to consider the potential range of the test conditions along with the model parameters in the Monte Carlo calculation. Uncertainties in the test conditions include the flow rates and temperatures of the ECC systems, the temperatures and flow rates of the steam injections that simulate vapor generation and the initial liquid masses in the various regions of the test facility. [[

]] The test conditions that were varied together in this manner are noted in Table 7.4-1.

Figure 7.4-1618 and Figure 7.4-1719 show the predictions for the pool temperature at the periphery near the bottom and for the lower plenum mass fraction when both the model parameters and test conditions are varied. [[

]]

In summary, the statistical analysis of SSTF Test EA3-1, a BWR/4 refill-reflood simulation,
[[

]]

[[

]]

Figure 7.4-10 Comparison of System Pressure for SSTF Test EA3-1

[[

]]

**Figure 7.4-11 Comparison of Temperature at Pool Periphery at the Bottom for SSTF
Test EA3-1**

[[

]]

**Figure 7.4-12 Comparison of Temperature at Pool Periphery at Mid-Depth for SSTF
Test EA3-1**

[[

]]

**Figure 7.4-13 Comparison of Temperature at Pool Periphery at the Surface for SSTF
Test EA3-1**

[[

]]

Figure 7.4-14 Comparison of Lower Plenum Fill Fraction for SSTF Test EA3-1

[[

]]

Figure 7.4-15 Correlation of Lower Plenum Refill Time with PIRTs for SSTF Test EA3-1

[[

]]

Figure 7.4-16 Comparison of Bypass Fill Fraction for SSTF Test EA3-1

[[

]]

Figure 7.4-17 Comparison of Upper Plenum Fill Fraction for SSTF Test EA3-1

[[

]]

Figure 7.4-18 Comparison of Temperature at Bottom of Pool Periphery Including Variations in Test Conditions for SSTF Test EA3-1

[[

]]

Figure 7.4-19 Comparison of Lower Plenum Fill Fraction Including Variations in Test Conditions for SSTF Test EA3-1

SNPB RAI-92

In Section 7.4.5, Core Spray Heat Transfer (CSHT) Test 111 was chosen for comparison with TRACG results to justify the model parameter uncertainties and statistical combination process. Please address the following associated issues:

- a. Although most data for CSHT Test 111 is bounded by TRACG predictions, the peak temperatures for the hottest rods significantly exceed the mean of the TRACG predictions and in some cases even exceed the maximum value of the 59 TRACG predictions (e.g., Figure 7.4-18). Since it is the peak values that are of regulatory interest, please justify the LTR's conclusion that uncertainties proposed for modeling core spray are adequate.
- b. Please justify the selection of CSHT Test 111 for comparison and discuss whether the conclusions made in Section 7.4.5 of the LTR would hold if comparisons were instead made with additional CSHT tests such as Tests 112 and 121 (see Section 3.2.2 of the Qualification Report). Demonstrating that proposed uncertainty distributions provide a representative bound on tests such as CSHT is vital due to the lack of integral testing involving extended heatups characteristic of LOCA-limited BWRs.

RAI-92 Response

Before the justification and clarification is made for this RAI, it is worthwhile to emphasize the purpose of those statistical analyses presented in LTR Section 7.4. As discussed in the beginning of this section, *“in this section, statistical analyses are performed on a selected set of ECCS/LOCA qualification tests utilizing the model uncertainties developed in Section 5. Statistical analyses of the integral system tests validate the values used for the model uncertainties by showing that the test data fall within the resulting uncertainty band of the calculations.”* The statistical analyses in Section 7.4 are not used to justify the model parameters, which are determined individually using existing test data, as discussed in detail in LTR Section 5. To achieve this purpose, the same statistical process as that used for the Section 8 demonstration analyses is applied to those tests using the same model parameters and their uncertainties (determined in Section 5 of the LTR). The test-specific model parameter adjustments (biases) are not used.

It should be noted that the information presented in LTR Section 7.4 was from the draft LTR, and the updated information was not implemented in the submitted LTR. This has been captured in the GEH Condition Report process as CR 8235. The CSHT results presented in this RAI are updated with the current GEH Level 2 TRACG04P and updated PIRT table.

Response to Part a:

CSHT Test 111 was re-run with the current Level 2 TRACG04 and the updated TRACG LOCA PIRT table. The same process as described in Section 7.4.5 of the LTR is used. In addition to the TRACG model parameter uncertainties, the analysis also considers [[

]] The key outputs from the test are the temperature responses for various rods in the bundle at the peak power elevation.

Figure R92-1 through Figure R92-5 show the results of the analysis in terms of the temperature of five TRACG rod groups corresponding to the locations of the test measurements. [[

]] See further discussion in the Summary section of this RAI response.

Response to Part b:

There are total of six CSHT tests in Reference R92-1. As shown in Table 3.2-3 of Reference R92-1, Test 111 has the second highest initial rod PCT, and it has complete test data. In addition, [[]], as shown in Table 3.2-4 of Reference R92-1. Therefore Test 111 was selected in the original LTR for testing both rod PCTs and rod quenching characteristics.

CSHT Test 112 has the highest initial rod PCT, among all six tests (Table 3.2-3 of Reference R32-1), but this test only has test data up to 500 seconds. The comparison of this test for quenching with TRACG is not possible, and it was therefore not selected in the LTR.

Test 121 was not selected for the LTR due to the low initial rod PCTs. In addition, [[]] (see Table 3.2-4 of

Reference R32-1).

In response to this RAI, it was determined that the addition of TRACG [[

]]

CSHT Test 112 was run using the same process as that for Test 111. Figure R92-6 through Figure R92-8 show the results of the analysis in terms of the temperature of four TRACG rod groups corresponding to the locations of the test measurements. [[

]] The situation for

Test 112 is similar to Test 111 above.

Summary

TRACG predictions of the peak rod temperature for both Test 111 and Test 112 with the TRACG LOCA model uncertainties established in the LTR provide the representative bound for the rod temperatures from the tests. It is also observed that [[

]]

It is acknowledged that [[

]]

It is further noted that [[

]]

In summary, TRACG predictions of the peak rod temperatures for [[

]]

Reference

R92-1 GE Hitachi Nuclear Energy, “TRACG Qualification,” NEDE-32177P, Revision 3, August 2007.

LTR Impact

LTR Section 7.4.5 will be updated.

[[

]]

Figure R92-1 Results of Monte Carlo Analysis vs. Test Data for Rod Group 2

[[

]]

Figure R92-2 Results of Monte Carlo Analysis vs. Test Data for Rod Group 3

[[

]]

Figure R92-3 Results of Monte Carlo Analysis vs. Test Data for Rod Group 4

[[

]]

Figure R92-4 Results of Monte Carlo Analysis vs. Test Data for Rod Group 6

[[

]]

Figure R92-5 Results of Monte Carlo Analysis vs. Test Data for Rod Group 9

[[

]]

Figure R92-6 Results of Monte Carlo Analysis vs. Test Data for Rod Group 2

[[

]]

Figure R92-7 Results of Monte Carlo Analysis vs. Test Data for Rod Group 3

[[

]]

Figure R92-8 Results of Monte Carlo Analysis vs. Test Data for Rod Group 4

[[

]]

Figure R92-9 Results of Monte Carlo Analysis vs. Test Data for Rod Group 6

[[

]]

Figure R92-10 Results of Monte Carlo Analysis vs. Test Data for Rod Group 2

[[

]]

Figure R92-11 Results of Monte Carlo Analysis vs. Test Data for Rod Group 3

[[

]]

Figure R92-12 Results of Monte Carlo Analysis vs. Test Data for Rod Group 4

[[

]]

Figure R92-13 Results of Monte Carlo Analysis vs. Test Data for Rod Group 6

SNPB RAI-93

Regarding the statement in Section 8.1.1 that [[
]], please clarify the following:

- a. [[
]]
- b. Please provide the basis for terminating the model at this point (e.g., post-LOCA system isolation point, sensitivity calculations demonstrate no further impact from extending model, etc.).
- c. Please justify that the modeling of the feedwater system is either best-estimate or conservative.

RAI-93 Response

- a. The ‘first’ feedwater heater refers to [[
]]
- b. This is a convenient termination point because [[

]] The

results are summarized in the following table.

Table R93-1 Feedwater Additional Volume Sensitivity Results

[[
]]

[[

]]

c. Modeling of the feedwater piping [[

]]

LTR Impact

No changes to the LTR are proposed as the result of this RAI response.

SNPB RAI-94

[Follow-on to Set 1 RAI-20] The response to Set 1 RAI-20(a) states, in part, [[

]] Please clarify whether [[

]]

RAI-94 Response

Regarding the response to Set 1 RAI-20, it should be emphasized that the current core spray flow distribution presents an extreme or a limiting case that bounds any possible value. [[

]]

The expected insignificant effect on LOCA parameters has been demonstrated by sensitivity studies.

[[

]]

Reference

R94-1 General Electric, “Core Spray Design Methodology Confirmation Tests,”
NEDO-24712-A, March 1983.

LTR Impact

No changes to the LTR are proposed as the result of this RAI response.

**Table R94-1 PCT Summary of Sensitivity Study For BWR/4 Suction Line Breaks with
Different Spray Distributions in TRACG Ring 1 to 3
(0.5 ft² Recirculation Suction line break)**

[[
]]

SNPB RAI-95

Section 8.1.2.2 states that similar to results from the SSTF (e.g., as discussed in NUREG/CR-2566), it is possible for bundles in TRACG simulations to make a transition from the one mode [[]] to the other during the transient, and that the results confirm TRACG's capability to predict this behavior. Please clarify this statement relative to the results in Section 6.4 (particularly Figures 6.4-7 and 6.4-8), which appear to suggest very limited potential for transition between states beyond an initial bifurcation point.

RAI-95 Response

The discussion in the LTR Section 8.1.2.2 is for a small break. The sentence in this section that “*it is possible for bundles to make a transition from one mode to the other during the transient*” refers to the [[

]] The last paragraph of this section discussed the PCT bifurcation due to the [[]] phenomenon, which is more related to the discussion in Section 6.4, and should not have been in Section 8.1.2.2. This paragraph will be revised in the LTR.

As described in NUREG-CR-2566 (Reference R95-1), the “parallel channel effects” refers to the observations that all fuel channels in the core are not necessarily at the same flow mode following a jet-pump BWR LOCA. It is further indicated in NUREG-CR-2566 that “parallel channel effects” can only occur when there is a two-phase level in the lower plenum, which allows re-distribution of the low plenum steam to the channel inlet orifices. As discussed in Reference R95-1, especially in the Section 5 discussion, which is pertinent to a jet pump BWR LOCA, “parallel channel effects” are evidenced by three different channel flow modes that may occur simultaneously in the SSTF tests (SRT 3 Run 26), which are: (1) Counter-current flow, (2) Co-current upward flow, and (3) Co-current down flow. The capability of TRACG modeling the “parallel channel effects” from SSTF was demonstrated in TRACG qualification LTR Section 5.3.3 for SSTF Test SRT 3 Run 26.

In the following sections, first the “parallel channel effects” is discussed for a typical BWR/4 LOCA, then relationship between PCT bifurcation and “parallel channel effects” is investigated.

“Parallel Channel Effects” in a Typical BWR/4 LOCA

The similar “parallel channel effects” was also observed in the BWR/4 LOCA analysis, as described in LTR Section 6.4 in more detail and in Section 8.1.2.2. [[

]]

PCT Bifurcation

The illustrations for PCT bifurcations are shown initially in LTR Figure 6.4-7 and Figure 6.4-8, and recently in the response to RAI-6 in Reference R95-2 (Figure R6-3) for a BWR/4 LOCA. Further investigation of the RAI-6 response calculation in Figure R6-3 was made below, [[

]]

In response to Round 1 RAIs, RAI-6 in particular for BWR/4, GEH has effectively reduced the amount of variability [[

]]

In summary, [[

]]

References

- R95-1 NUREG/CR-2566, “BWR Refill-Reflood Program Task 4.4 – CCFL/Refill System Effects Tests (30 Sector) Evaluation of Parallel Channel Phenomena,” March 1982.
- R95-2 Letter, James F. Harrison (GEH) to NRC Document Control Desk, “Response to Request for Additional Information Re: GE-Hitachi Nuclear Energy Americas Topical Report (TR) NEDE-33005P, Revision 0, “TRACG Application for Emergency Core Cooling Systems / Loss-of-Coolant-Accident Analyses for BWR/2-6” (TAC No. ME5405),” MFN 14-064, October 7, 2014.

LTR Impact

The following in LTR Section 8.1.2.2 (the last paragraph) will be modified in response to this RAI.

Original

It was found for small breaks that there was a stronger PCT sensitivity to small perturbations in some of the TRACG model parameters than might be expected a priori. Detailed investigation identified the physical mechanism causing this behavior. When the core begins to drain after the effects of the depressurization have abated and the core pressure drop is low, some of the channels assume a cocurrent upflow mode while others assume a countercurrent flow mode. This behavior is consistent with experimental observations of both these flow modes in the SSTF facility [2]. As was also observed in the SSTF facility, it is possible for bundles to make a transition from one mode to the other during the transient. This behavior may be characterized as bi-stable. Small perturbations to the initial conditions can result in the hot channels changing mode. [[

]]

Revised

It was found for small breaks that there was a stronger PCT sensitivity to small perturbations in some of the TRACG model parameters than might be expected a priori. Detailed investigation identified the physical mechanism causing this behavior. When the core begins to drain after the effects of the depressurization have abated and the core pressure drop is low, some of the channels assume a cocurrent upflow mode while others assume a countercurrent flow mode. This behavior is consistent with experimental observations of both these flow modes in the SSTF facility [2]. ~~As was also observed in the SSTF facility, it is possible for bundles to make a transition from one mode to the other during the transient. This behavior may be characterized as bi-stable. Small perturbations to the initial conditions can result in the hot channels changing mode.~~ [[

]]

[[

]]

Figure R95-1 Liquid and Steam Velocities at Hot Channel SEO (Channel Inlet) for a Case in Figure R6-3 in Reference 2. BWR/4 Suction Line Break of 0.67 ft²

[[

]]

Figure R95-2 Hot Channel PCT Traces for Two Representative Cases from Reference R95-2 Figure R6-3 Run. BWR/4 Suction Line Break of 0.67 ft²

[[

]]

**Figure R95-5 Liquid and Steam Velocities at Hot Channel Node 19. BWR/4 Suction
Line Break of 0.67ft²**

[[

]]

**Figure R95-6 Void Fraction at Hot Channel Cell 19. BWR/4 Suction Line Break of
0.67 ft²**

SNPB RAI-96

According to Figure 8.3-35 of NEDE-33005P, [[
]] Please provide an evaluation of this result, considering whether the value of this standard deviation is an appropriate indicator of the total uncertainty associated with this result. Consider, in particular, that the standard deviations associated with other break sizes on the same spectrum are much greater.

RAI-96 Response

By reviewing the results of the BWR/2 break spectrum and statistical analyses and similar results for the BWR/4 and the BWR/6 in the LTR, it has been determined that the results for BWR/2 statistical analysis as shown in LTR Figure 8.3-35 for a small discharge break is reasonable.

The detailed discussion of the BWR/2 recirculation line break spectrum is presented in LTR Section 8.3.5.1. The break spectrum response as shown in Figure 8.3-23 for a BWR/2 is the result of [[

]] See LTR Section 8.1.5 for BWR/4 and Section 8.2.4 for BWR/6 for break spectrum discussions.

Because different break sizes affect the relative importance of different phenomena affecting PCT results, statistical results and hence standard deviations obtained from these analyses also vary for different break sizes. A summary of the statistical result for a representative BWR/2 is shown in Figure 8.3-41 of the LTR. As apparent from this plot, the standard deviations vary with different break sizes.

Similar results are also observed for a BWR/4 in Figure 8.1-29 and for a BWR/6 in Figure 8.2-18.

LTR Impact

No changes to the LTR are proposed as the result of this RAI response.

SNPB RAI-97

Based on the NRC staff review, NEDE-33005P appears to contain little, if any, discussion on changes in fuel pellet geometry, integrity, and location following fuel cladding ballooning and rupture. Please describe and justify the analytic treatment of these phenomena, with due consideration for available experimental data, and the specific results predicted using the TRACG-LOCA EM, such as fuel and cladding temperatures, fuel rod burnup, extent of cladding deformation, and time of rupture.

RAI-97 Response

The models addressing the effects of fuel pellet and cladding geometry changes are presented in the TRACG Model Description LTR (Reference R97-1) and are considered to be part of the methodology. Particularly, the models describing the effects of geometry changes on fuel pellet gap conductance, including the effects on gap gas conductance heat transfer, fuel-cladding contact heat transfer, gap size calculation, and fuel and cladding thermal expansion, are given in Section 7.5.2 of Reference R97-1.

Section 7.5.3 of Reference R97-1 presents the swelling and the cladding perforation model. The TRACG model is adapted from the previously approved LOCA evaluation model used in SAFER and presented in Reference R97-2. In the model, the fuel rod cladding hoop stress is calculated based on the pressure difference between the fuel rod internal gas pressure and the external coolant pressure during the transient. Initial values for the rod internal pressure and plenum volume, and fission gas parameters are calculated according to the PRIME fuel performance model (Reference R97-3). The effects of thermal conductivity degradation are accounted for in TRACG consistent with the approved PRIME model (Reference R97-3). The change in rod internal pressure during the transient is calculated [[

]]

The transient fuel rod cladding hoop stress is used with the perforation model to determine the onset of cladding plastic yielding and fuel rod perforation. [[

]]

This modeling of plastic strain is also the same as the SAFER model presented in Reference R97-2. In connection with the SAFER code, the NRC reviewed and found the model

acceptable as it does not underestimate the incidence of rupture based on applicable data including those data reported in NUREG 0630 (Reference R97-4).

If a fuel rod perforation occurs, the gap conductance is adjusted to reflect the presence of steam and hydrogen rather than fission gases inside the fuel rod. The oxidation and buildup of an oxide layer on the cladding inside surface is allowed after perforation occurs and also contributes to the heat source in the cladding.

[[

]]

Other effects of the cladding deformation include potential relocation of the fragmented fuel into the ballooned region of the rod. When typical operational bundle powers are considered, as the exposure increases, the reduction in LHGR has more influence than the increase in fuel rod pressure and, therefore, fewer fuel rod perforations are expected at very high exposures (Reference R97-9). However, realistic calculations performed at relatively higher LHGR would also indicate that it is possible to swell the rods at all exposures once the cladding has heated up beyond about 800°C. At the low exposures where higher cladding temperatures are expected, the fuel fragments are too coarse to be axially relocated inside the cladding. The concern with fuel relocation within the fuel rod primarily applies for higher exposures where the fuel fragments are smaller.

[[

]] This conclusion is consistent with earlier research results presented in Reference R97-10.

In summary, the calculated clad swelling combined with conservative fragment packing factor is not sufficiently large to pose a concern of added heat source when the fragmented fuel slumps into the ballooned region. This assertion is also valid for high burnup fuel, [[

]]

References

- R97-1 GE Hitachi Nuclear Energy, “TRACG Model Description,” NEDE-32176P, Revision 4, January 2008.
- R97-2 GE Nuclear Energy, “General Electric Company Analytical Model for Loss-of-Coolant Analysis in Accordance with 10 CFR 50 Appendix K,” NEDO-20566-P-A, September 1986.

NEDO-33005-A Revision 1
Non-Proprietary Information – Class I (Public)

- R97-3 Global Nuclear Fuel, “The PRIME Model for Analysis of Fuel Rod Thermal-Mechanical Performance,” Technical Bases – NEDC-33256P-A, Revision 1, Qualification – NEDC- 33257P-A, Revision 1, and Application Methodology – NEDC-33258P-A, Revision 1, September 2010.
- R97-4 Powers, D. A. and Meyer, R. O., “Cladding Swelling and Rupture Models for LOCA Analysis,” NUREG-0630, U.S. Nuclear Regulatory Commission, 1980.
- R97-5 Ihle, P. and Rust, L. “FEBA – Flooding Experiments with Blocked Arrays, Evaluation Report,” KfK-3657, 1984.
- R97-6 Erbacher, F. J., Neitzel, H. J., Wiehr, K., “Cladding Deformation and Emergency Core Cooling of a Pressurized Water Reactor in a LOCA – Summary Description of the REBEKA Program,” KfK-4781, August 1990.
- R97-7 Mohr, C. L. et al., “LOCA Simulation in National Research Universal Reactor Program, Data Report for the Third Materials Experiment (MT-3),” NUREG/CR-2528, PNL-4166, 1983.
- R97-8 Loftus, M. J. and Hochreiter, L. E. “Reflood Heat Transfer in the FLECHT-SEASET 163-Rod Bundle with Flow Blockage and Bypass,” ASME Paper 83-WA/HT-16, 1983.
- R97-9 Muftuoglu, K., et al., “Analytical Assessment of High-Exposure Fuel Dispersal Potential During Boiling Water Reactor Loss-of-Coolant Accident,” The 15th International Topical Meeting on Nuclear Reactor Thermal Hydraulics, NURETH15-696, 2013.
- R97-10 Siefken, L. J., “Axial Fuel Relocation in Ballooning Fuel Rods,” Transactions of the 7th International Conference on Structural Mechanics in Reactor Technology (SMiRT-7), August 1983. Available from:
<<http://www.iasmirt.org/transactions/07/C2-5.pdf>>

LTR Impact

No changes to the LTR are proposed as the result of this RAI response.

SNPB RAI-98

Provide additional information to describe the interrelationship among the interfacial shear, entrainment, and wall friction models in TRACG. Particularly, address the qualification of the code to predict two-phase flow and heat transfer behavior in fuel channels at high-void, low pressure conditions that would not otherwise be counter-current flow limited. Such conditions may exist in limiting channels at the point when the code predicts the termination of cladding heatup.

RAI-98 Response

As discussed in Reference R98-1 (Section 3.0), two-phase, two-fluid models are used in the TRACG code. To close the set of basic equations for two fluid models used in TRACG, a set of constitutive correlations describing interfacial shear and heat transfer, wall friction and heat transfer is needed. The response to RAI-69 addresses the application ranges for the models and correlations in each of these four model groups and also provides some details on how they are implemented in the code.

Calculation of interfacial shear and momentum exchange across the interface is a necessary part of the two-fluid equation system solution. In TRACG, the interfacial shear correlations are based on the set of drift flux correlations from void fraction data available in literature, and are provided for each different flow regime (See the discussion in Reference R98-1 Section 6.1.3 for bubbly/church flow, Section 6.1.4 for annular flow, 6.1.5 for droplet flow, and Section 6.1.6 for annular/droplet flow). The modifications to interfacial shear are also considered for subcooled boiling, counter-current flow limitations and virtual mass. For dispersed annular flow interfacial shear, the drift flux parameters are interpolated between the annular and the droplet drift flux parameters based on the entrainment fraction. The model for determining entrainment is discussed in Section 5.1.2.2 of Reference R98-1. How entrainment is used to interpolate the drift flux parameters is defined in Section 6.1.6 of Reference R98-1.

Like interfacial shear, the wall friction or wall shear is another parameter needed to close the set of basic equations for two fluid models in TRACG. The TRACG wall shear model is discussed in Section 6.2 of Reference R98-1. When in annular flow the wall shear is experienced only by the liquid film on the wall. This liquid film also experiences interfacial shear with the vapor phase and any liquid drops entrained within it. Because TRACG calculates only one liquid velocity, the liquid momentum equation contains both wall and interfacial shear force acting on the liquid.

The modified Ishii correlation is used for entrainment prediction in TRACG, as discussed in Reference R98-1 Section 5.1.2.2. The entrainment will affect the interfacial shear calculation in the annular/dispersed flow regime, and also affect the interfacial heat transfer in this regime by affecting the interfacial heat transfer area (See the discussion in Reference R98-1 Section 6.5 for interfacial heat transfer).

For two phase flow in a typical BWR, all those parameters (interfacial shear, wall shear, entrainment and interfacial heat transfer and wall heat transfer) are playing a role together in an entangled way in determining the important parameters for two phase flow, such as pressure drop, void fraction and heat transfer. Qualification of interfacial shear model in TRACG is assessed by examining the capability of TRACG to predict void fraction data, which is presented in Reference R98-2 Section 3.1. TRACG modeling of wall friction is assessed through pressure drop comparisons for the data from the ATLAS test facility in Reference R98-2 Section 3.5. TRACG capability of modeling natural circulation for test data from the FRIGG facility is discussed in Reference R98-2 Section 3.7.

TRACG qualifications are provided in Reference R98-2. Extensive TRACG prediction and test data comparisons have been made. Those comparisons cover the available data from varieties of tests, including separate effects tests, component performance tests, integral system effects tests and BWR plant tests.

The referred scenario in this RAI is observed in the late phase of a typical BWR LOCA, where the RPV has been depressurized, fuel heatup is close to the end and ECCS is cooling the bundle from the top of the bundle for non-jet pump plants (BWR/2s) or from both the top and the bottom of the bundle for jet pump BWRs (BWR/3-6s). Under this condition, [[

]] A summary of TRACG qualification of transition boiling heat transfer was transmitted to the NRC Staff in Reference R98-3 (Starting from Page 177). The most relevant TRACG qualifications to predict two-phase flow and heat transfer behavior in fuel channels at high-void, low pressure conditions [[

]] most closely related to the flow conditions in the RAI are briefly discussed. The detailed discussions of those test facilities and the test events and the results can be found in Reference R98-2. Additional information regarding CSHT and FIST can be found in the LTR and in the response to RAI-92.

- **Core Spray Heat Transfer (CSHT):** These tests were performed at ambient pressure. The bundle is only cooled from the liquid flowing down. This scenario represents the LOCA scenario in the RAI, and occurs in large break LOCA for non-jet pump plants. The detailed description of this test can be found in Reference R98-2 Section 3.2.2. [[

]] Additional

information for CSHT can be found in the response to RAI-92. The comparisons between the test and TRACG predictions showed that TRACG predictions are [[
]]

- **Full Integral Simulation Test (FIST):** The FIST facility was an integral single-bundle system scaled from a BWR/6-218 Standard Plant. It was capable of simulating full power steady-state operation and real time LOCA and operational transients. The detailed description for FIST can be found in Section 5.2 of Reference R98-2. [[

]]

- **Two-Loop Test Apparatus (TLTA):** TLTA large break test provided integral system LOCA response data in a scaled BWR facility. The detailed description of this TLTA event can be found in Section 5.1.2 of Reference R98-2, which is similar to the scenario referred in this RAI. The TRACG simulation of TLTA large break test shows [[

]]

- **ROSA-III Test Facility:** The ROSA-III test facility is a volumetrically scaled (1/424) BWR system with an electrically heated core simulator. It was designed to study the response of the primary system, core and ECCS during a postulated LOCA. The detailed description of the ROSA-III test facility can be found in Section 5.4 of Reference R98-2, which is similar to the scenario referred in this RAI. The comparisons between the ROSA-III test data and the TRACG predictions can be found in Reference R98-2 Section 5.4.

References

- R98-1 GE Hitachi Nuclear Energy, “TRACG Model Description,” NEDE-32176P, Revision 4, January 2008.
- R98-2 GE Hitachi Nuclear Energy, “TRACG Qualification,” NEDE-32177P, Revision 3, August 2007.
- R98-3 Letter, J. F. Harrison (GEH) to Document Control Desk (NRC), “Final Presentation for ACRS Thermal-Hydraulic Phenomena Subcommittee Meeting on September 21, 2015 and Final Presentation and Requested Information for NRC Audit Related to the Peach Bottom Units 2 and 3 License Amendment Request for MELLLA+, August 31, 2015 to September 2, 2015,” MFN 15-078, September 25, 2015.

LTR Impact

No changes to the LTR are proposed as the result of this RAI response.

SNPB RAI-33

Please provide the following information related to PIRT item C18 (cladding perforation):

- a. A summary of or reference for the tests that includes the number of tests, the type(s) of cladding tested, and the heatup rates used.
- b. The basis for applying the empirical data used to estimate clad rupture stresses to current-generation fuels.
- c. The basis for the assumption of normality for the upper and lower 95 percent groups used to determine the rupture stress.
- d. Explanation of the origin of and justification for the assumed uncertainty of the built-in fuel rod internal pressure curves and the normality of the multiplier on rod pressure.
- e. Relative to the high-temperature phase change of zirconium, please clarify the statement on page 2-11 of the TR that phase change of in-core materials is not modeled.

RAI-33 Response

- a. A summary of the cladding hoop stress versus perforation temperature testing used in defining the model and model uncertainty can be found in Reference R33-1. The figures in the Reference R33-1 enclosed report shows the comparison of high temperature test data to the rupture stress model. All of the tests presented are for heat-up rates [[

]]. In Reference R33-1, selected data from Reference R33-2 is compared with General Electric (GE) proprietary data for low heat-up rates. Note that ruptures occur at lower hoop stresses when the heat-up rates are lower so that is why the data for the higher heat-up rates in Reference R33-2 are not included. Figure 5 of Reference R33-1 aggregates data points from Figures 1, 2, and 4 of the same reference. Figure R33-1 has been reconstructed from the same data in order to provide a legend to indicate the origins of the data. The relevant NUREG-0630 (Reference R33-2) data that has heat rates of [[

]] are also depicted with open blue markers in Figure R33-1.

[[

]]

- b. The clad rupture stress model is assessed using hoop stresses, as described by the method in Section 3.1 of Reference R33-2. By employing this method of converting differential pressure data to hoop stress data, design-specific dimensional effects are eliminated. This allows the clad rupture stress model to be extended beyond the 7x7 and 8x8 fuel from the test programs to current-generation fuel product lines. Additionally, the data in Figure 1 of Reference R33-1 show that the differences between 7x7 and 8x8 fuel rod data extracted from NEDM-20350-3 (Reference R33-3) are insignificant compared to the scatter in the data, confirming that dimensional effects have been eliminated. This fact is also depicted by comparison of the red triangles (8x8) with the red squares (7x7) in Figure R33-1.

- c. The clad rupture stress uncertainty model was developed using temperature-dependent rupture stress data from GE material testing programs. Relevant low heat-up rate data from NUREG-0630 (Reference R33-2) has been shown for comparison. The uncertainty model [[

]]

- d. The Linear Heat Generation Rate (LHGR)- and exposure-dependent values of the nominal fuel rod internal pressure used in TRACG Loss-of-Coolant Accident (LOCA) analyses are calculated based on the Nuclear Regulatory Commission (NRC)-approved PRIME model [[
-]] The calculation method qualified previously for GESTR (Reference R33-4) has been replaced by PRIME thermal-mechanical analyses (References R33-5 and R33-6). [[

]] The key driver of rod perforation uncertainty is the uncertainty in the temperature-dependent rupture stress. The rod internal pressure is less important. PRIME nominal rod internal pressure as used in LOCA calculations is [[

]] shown in Figure 5.2 of Reference R33-6. Updated data provided in Figure 2-8 of Reference R33-7 is replicated here as Figure R33-3. [[

]]

- e. Clarifications to the entries in Columns 2 and 3 in Section 3.3.2 of Table 2.5-1 on page 2-11 of the LTR are proposed in view of the additional details and clarification provided below.

The entry in Column 2 labeled *GEH Process* will be modified to read:

Material properties for zircaloy account for the alpha and beta phases. The Zr-H₂O reaction to produce ZrO₂ is modeled. Melting of UO₂ is precluded by the GE SAFDL applied for AOO transients and this bounds all LOCA calculations provided the 2,200°F limit on PCT is satisfied. Eutectic formations are not significant provided the 2,200°F limit on PCT is satisfied.

The entry in Column 3 under *Evaluation* will be modified to read:

The phenomena necessary for BWR LOCA are modeled.

Cladding hoop stresses are modeled in TRACG for the purpose of tracking geometric changes due to rod perforation and to account for the resulting oxidation of the cladding. Additionally, material properties for the cladding and fuel take into account transient temperature effects. Specifically, the zircaloy cladding properties account for the physical differences associated with the alpha and beta phases of zircaloy. The contact pressure between the UO₂ pellet and cladding inside surface is specifically modeled and is strongly influenced by uncertainty in parameters that affect the temperature of the fuel pellet and its thermal expansion. If the 10 CFR 50.46(b) acceptance criteria for Emergency Core Cooling Systems (ECCS) are met, the chemical effects of eutectic formation will have no adverse effect on the fuel and can be ignored in cladding response calculations within the range of post-LOCA conditions. Proposed additional requirements from 10 CFR 50.46(c) related to post-quench ductility and break away oxidation are expected to be addressed by material testing that will be used to stipulate a time limit at a prescribed temperature that must not be exceeded in the LOCA calculations. Assessment relative to the new criteria is independent of the TRACG modeling and application methodology and can be achieved by comparing the calculated PCT trace to the required limit once the new rules are finalized.

[[

]]

Figure R33-1. Rupture Stress Model Compared to Data

[[

]]

Figure R33-2. Example of Half-Normal Distribution Generation Based on Experimental Data

[[

]]

Figure R33-3. PRIME Predicted versus Measured Fuel Rod Internal Pressure (Nominal)

References

- R33-1. Letter from R. H. Buchholz (GE) to L. S. Rubenstein (NRC), “General Electric Fuel Clad Swelling and Rupture Model,” MFN-097-81, May 15, 1981.
- R33-2. NUREG-0630, “Cladding Swelling and Rupture Models for LOCA Analysis,” April 1980.
- R33-3. General Electric Company, “Fuel Development Development Authorization Programs 1974 Third Quarterly Report,” NEDM-20350-3, December 1974.
- R33-4. General Electric Company, “The GESTR-LOCA and SAFER Models for the Evaluation of the Loss-of-Coolant Accident, Volume I: GESTR-LOCA – A Model for the Prediction of Fuel Rod Thermal Performance,” NEDE-23785-1-PA, Revision 1, October 1984.
- R33-5. Global Nuclear Fuel, “The PRIME Model for Analysis of Fuel Rod Thermal - Mechanical Performance Part 3 – Application Methodology,” NEDC-33258P-A, Revision 1, September 2010.

- R33-6. Global Nuclear Fuel, “The PRIME Model for Analysis of Fuel Rod Thermal - Mechanical Performance Part 2 – Qualification,” NEDC-33257P-A, Revision 1, September 2010.
- R33-7. Letter from Brian R. Moore (GNF) to Document Control Desk, “NEDC-33257P Supplement 1, ‘The PRIME Model for Analysis of Fuel Rod Thermal-Mechanical Performance 2015 5-Year Update,’” MFN 15-060, August 7, 2015.

LTR Impact

Entries in Columns 2 and 3 in Section 3.3.2 of Table 2.5-1 on page 2-11 of the LTR will be revised.

The entry in Column 2 labeled *GEH Process* will be modified to read:

Material properties for zircaloy account for the alpha and beta phases. The Zr-H₂O reaction to produce ZrO₂ is modeled. Melting of UO₂ is precluded by the GE SAFDL applied for AOO transients and this bounds all LOCA calculations provided the 2,200°F limit on PCT is satisfied. Eutectic formations are not significant provided the 2,200°F limit on PCT is satisfied.

The entry in Column 3 under *Evaluation* will be modified to read:

The phenomena necessary for BWR LOCA are modeled.

LTR Section 5.1.3.24 will be replaced to read as indicated below. In addition, Figure 5.1-16 will be deleted and its deletion indicated in the LIST OF FIGURES.

5.1.3.24 C18 – Fuel Cladding Strain /Perforation (H)

The key drivers governing strain-induced fuel rod perforation are the temperature-dependent clad rupture stress and the rod internal pressure. Based on material properties, the rupture stress and its associated uncertainty is modeled in TRACG as three curves corresponding to best-estimate, lower 95%, and upper 95% rupture stress curves as functions of cladding temperature (Figure 5.1-15). At each temperature, the upper and lower 95% bounds are used to define half-normal PDFs above and below the nominal rupture stress, respectively. This is done on the basis that the upper and lower 95% points are removed by 1.645σ from the nominal value.

The instantaneous clad hoop stress is directly related to the fuel rod internal pressure. Nominal fuel rod internal pressures are calculated in TRACG as described in Section 7.5.3.1 of Reference [1] using parameters calculated by PRIME [76] and passed to TRACG [[

]]

RAI-99 Statistical Meaning of Limiting Results (Follow-on to RAI 66)

In response to request for additional information (RAI) 66, General Electric-Hitachi (GEH, the vendor) reviewed the applicable regulations and regulatory guidance (Agencywide Documents Access and Management System (ADAMS) Accession No. ML14281A014). Following the review, GEH provided its rationale regarding the adequacy of both statistical approaches outlined in licensing topical report (LTR) NEDE-33005P, "TRACG Application for Emergency Core Cooling Systems/Loss-of-Coolant Accident Analyses for BWR/2-6," Section 7.1 (ADAMS Accession No. ML110280321). The following key concepts summarize the NRC staff understanding of the response:

- The applicable regulations do not include specific quantiles and confidence limits, and the available regulatory guidance specifies 95%-probability coverage.
- Consideration of joint statistical coverage is not required to demonstrate compliance with the applicable acceptance criteria.
- The normally distributed, one-sided upper tolerance limit (OSUTL) approach, as applied to 59 cases, is reasonably consistent with the approach delineated in Regulatory Position 4.4 of Regulatory Guide (RG) 1.157, "Best-Estimate Calculations of Emergency Core Cooling System Performance" (ADAMS Accession No. ML003739584).
- When considering the order statistic-based approach, GEH methodology exceeds the minimum required for tri-variate, joint 95% confidence.

Specific discussion is provided in the following sections; a request for additional information follows.

Application of a 95/95 Upper Tolerance Limit

Regarding an acceptable evaluation model, 10 CFR 50.46(a)(1)(i) states, in part:

This uncertainty must be accounted for, so that, when the calculated ECCS [emergency core cooling system] cooling performance is compared to the criteria set forth in paragraph (b) of this section, there is a high level of probability that the criteria would not be exceeded.

In accordance with various policy documents, the NRC position is established that results should be expressed "at the 95% probability limit," as stated in Regulatory Position 4.4, "Statistical Treatment of Overall Computational Uncertainty," of RG 1.157. The RG indicates that uncertainty may be estimated using normally distributed results and a 95% probability limit, or a conservative application of two standard deviations to the mean.¹ The RG also states that other techniques to quantify uncertainty "may require the use of confidence levels."

¹ The recommendation in RG 1.157 that the probability limit can be estimated using two standard deviations was likely based on consideration of the response surface technique discussed in NUREG/CR-5249, "Quantifying Reactor Safety Margins: Application of the Code Scaling, Applicability, and Uncertainty Evaluation Methodology to a Large-Break, Loss-of-Coolant Accident" (ADAMS Accession No. ML030380473). As documented, the technique relied on 50000 Monte Carlo trials, and practically, response surface and similar statistical methods employed thousands to tens of thousands of cases. At these high numbers of statistical trials, adding two standard deviations

Appendix A to SECY 83-472, “Emergency Core Cooling System Analysis Methods,” provides a brief discussion of the Commission’s philosophy in applying 95% probability level in licensing decisions regarding 10 CFR 50.46 compliance. The following passage is especially informative, regarding the origination and application of a 95% acceptance criterion to 10 CFR 50.46(b) acceptance criteria:

Ninety five percent was selected for a number of reasons. Primary was its historical significance in regulatory matters involving thermal-hydraulic performance. Many parameters, most notably the departure from nucleate boiling ratio (DNBR) were proposed by the industry and accepted by the NRC to be conservatively established at the 95 percent probability level.

The noted example is provided in Standard Review Plan (SRP) Chapter 4.4, “Thermal and Hydraulic Design” (ADAMS Accession No. ML070550060). In fuel system thermal-hydraulic review guidance, the NRC staff introduces the concept of acceptable confidence, stating, in part, that “One criterion provides assurance that there be at least a 95-percent probability at the 95-percent confidence level that the hot fuel rod in the core does not experience a DNB or transition condition during normal operation or AOOs [anticipated operational occurrences].”

In its reviews of Best-Estimate or Realistic ECCS evaluation models, the NRC staff has applied the same acceptance criterion. On the matter of statistical confidence in results, the 95% confidence level is considered acceptable. The accession number referenced in RAI 66 provides one example of NRC staff correspondence documenting this position; however, the practice is applied reasonably consistently in best-estimate ECCS evaluation model reviews (ADAMS Accession No. ML062150349).

Use of a Tolerance Interval

One statistical approach proposed by GEH identifies a normally distributed OSUTL. That is, the high probability statement leads to the conclusion that one is 95% confident that 95% of the actual population will fall below the specified value. This approach is in attempt to comply to rule language in 10 CFR 50.46(a)(1)(i), that includes the requirement that ECCS cooling performance “...must be calculated for a number of postulated loss-of-coolant accidents of different sizes, locations, and other properties sufficient to provide assurance that the most severe postulated loss-of-coolant accidents are calculated,” and that the results ensure “there is a high level of probability that the criteria [in 10 CFR 50.46(b)] would not be exceeded.”

Despite that GEH proposes to remove reference to a “95/95” limit, the selection of the z-value, according to Table R66-1 of the LTR, appears to relate to a 95% confidence limit for 95% coverage, given normally distributed parameters. Removal of the confidence limit renders the selection of a z-value arbitrary. If the sample size is always 59 cases, and the z-value remains greater than two, then the approach conforms to RG 1.157 because the upper tolerance limits exceeds two times the standard deviation of the sample. However, the use of a larger sample

to the mean is conservative relative to a statistically based, 95th percentile result with 95% confidence. It appears unlikely that the RG authors envisioned the comparatively low number of sample cases executed in concert with an order statistics-based method that subsequently became the state of the art.

without a specified confidence level could lead to the selection of a z-value less than two. The confidence associated with such a value would require justification.

Joint Coverage

The NRC staff acknowledges that the language in RG 1.157 states, in part, that “explicit consideration of the probability of exceeding the other criteria [aside from peak cladding temperature] may not be required if it can be demonstrated that meeting the temperature criterion at the 95% probability level ensures with an equal or greater probability that the other criteria will not be exceeded.” Generically, this demonstration is impractical because cladding oxidation and embrittlement are functions not only of the cladding temperature, but also the integral time at temperature. The results of the transient analyses are thus also important in ensuring that the cladding oxidation criteria are satisfied as well as the temperature criterion. For a longer transient, cladding oxidation could prove to be more limiting than the cladding temperature.

In the statistical combination of overall uncertainty, adherence to each of the criteria should be considered as separate events. The confidence in the results should be considered insofar as they provide simultaneous coverage of the population (i.e., $PCT < PCT^{95}$, $MLO < MLO^{95}$, and $CWO < CWO^{95}$). The specified confidence level should ensure that all three attributes are satisfied simultaneously. Thus, the NRC staff disagrees with GEH’s assertion that 10 CFR 50.46 and RG 1.157 contain no requirement for “joint” upper tolerance limits. This is because the regulation specifies that all criteria must be satisfied; exceeding any is not acceptable.

Order Statistics Based Approach

If results cannot be confirmed to be normally distributed, the sample size is selected as to provide high-confidence coverage that the sampled parameters can be rank ordered. Based on the sample size, a specifically ranked result can be used as an estimate of the upper tolerance limit. GEH contends that using the highest-ranked results from three samples consisting of 59 cases, each executed at a different limiting break size, provides higher-confidence assurance of statistical coverage than an approach based on a sample size adequate to provide 95% confidence for tri-variate, 95% coverage.

- A. For the normally distributed OSUTL approach, explain what measures will be taken to ensure that the specified confidence levels ensure coverage of each parameter simultaneously.
- B. For the order statistics approach, clarify whether GEH will generate independent samples for analysis of each break size.
- C. Explain whether the sample size is a fixed aspect of the methodology.

RAI-99 Response

- A. For the very same reasons the staff noted under the Joint Coverage section of the request for additional information (RAI), GEH concurs that simultaneous demonstration that equivalent cladding reacted (ECR) and peak cladding temperature (PCT) acceptance criteria are jointly satisfied with some probability and confidence level is “impractical because cladding oxidation and embrittlement are functions not only of the cladding temperature, but also the integral time at temperature.” Generically one should expect the PCT upper tolerance limit (UTL) to occur at a location and time that is different from the ECR UTL. For these same reasons, there should be no expectation that the distribution used to determine the ECR UTL be normal when the distribution used to determine the PCT UTL is normal or vice versa. This is the reason that the UTL values are determined independently for each parameter. GEH also agrees that all three criteria must be met so that for all cases and at all times the UTLs for PCT, maximum local oxidation (MLO) and core-wide oxidation (CWO) are always less than or equal to their respective Nuclear Regulatory Commission (NRC)-established limits as required by 10 CFR 50.46. It is in this way that the GEH methodology satisfies the requirement that all regulatory criteria are simultaneously met.

The GEH process does not directly sample PCT, local oxidation (MLO) and/or CWO from pre-generated response surfaces as noted in Footnote 1 of this RAI. Instead, a random sampling of the inputs, model parameters, and plant parameters from their respective uncertainty distributions is used for each trial to create multiple loss-of-coolant accident (LOCA) transient simulations. Each simulated LOCA transient trial yields a sample value for each of the three attributes PCT, MLO, and CWO that incorporates the combination of the input uncertainties. Upon completion of the N trials, the N values for each attribute are individually evaluated to determine the UTL for that attribute. This approach is consistent with the code scaling applicability and uncertainty (CSAU) process outlined in Regulatory Guide (RG) 1.157 (Reference R99-1) which provides very little guidance on how uncertainties are to be combined. RG 1.157 clearly pre-dates the wide-spread application of order statistics and thus could not have anticipated such a technique for combining a very large number of uncertain parameters that cannot be practically addressed using the response-surface approach. Prior to the use of order statistics, the approach was to generate multi-dimensional response surfaces and then create a very large number of samples from these response surfaces. The creation of a large number of samples does not imply increased analysis fidelity because statistics determined from these large sample sizes is limited by the fidelity of the response surfaces used to produce the samples, and these response surfaces, for practical reasons, are limited by the number of dimensions they can accommodate.

As indicated above, upon completion of the N trials, the N values for each attribute are individually evaluated to determine the one-sided upper tolerance limit (OSUTL) for that attribute. If the distribution of the N values for a particular attribute is determined to be appropriately modeled as a normal distribution, then the OSUTL is determined as the mean plus Z standard deviations where $Z=2.024$ corresponding to 95% probability at 95% confidence for the individual attribute for the case where $N=59$ trials. If the N trials for

NEDO-33005-A Revision 1
Non-Proprietary Information – Class I (Public)

the attribute are not normally distributed, then the highest rank is used to define the OSUTL for that attribute.

- B. In the response to RAI-66, GEH pointed out that, in comparison to the cited methodology in which the break size is sampled along with uncertainty parameters, in the proposed TRACG LOCA methodology, the equivalent number of runs that correspond to at least three different limiting break sizes would be 177 because each one of them is a set of 59. This assertion is not a way to sample the break size; it was only offered to point out the contrast. In light of further discussions with the staff, GEH has committed to [[

]]

Additionally, in concurrence with this commitment, it would be prudent to update the position given in Section 9.1 of the licensing topical report (LTR) where [[

]] is addressed.

- C. In Chapter 7 of the LTR, how a larger sample size could be utilized was explained. However, in practice, the methodology uses [[

]] The concern raised in the RAI is that the value for $Z=2.024$ corresponding to 95% probability and 95% confidence in an individual attribute that is normally distributed with $N=59$ trials could be reduced if N is increased. GEH understands and agrees with the recommendation in RG 1.157 regarding two standard deviations as an appropriate minimum. [[

]] In the RAI-66 response, the avoidance of particular reference to 95/95 was based on a different

understanding that was reached from discussions with the staff that pertains to joint probability and confidences not specification of OSUTL for individual attributes.

References

- R99-1. Regulatory Guide 1.157, “Best-Estimate Calculations of Emergency Core Cooling System Performance,” May 1989.

LTR Impact

Changes in Chapter 7 are as follows:

The heading of Section 7.2 will be changed to read: “Approach for Combining Uncertainties”

Bullet 2 in Section 7.3.1 will be changed as follows:

- Perform a set of [59](#) trials (TRACG calculations) in each of which the statistically characterized model and input parameters are randomly selected from their underlying PDFs. ~~The number of trials is at least 59 and can be increased to raise the confidence level of the desired statistical bound for the output quantities that are compared with design limits.~~

It should be noted that there are other corrections that were necessitated by an editorial mistake made in the compilation of Revision 0 of the LTR and other changes that emerged from the responses to RAIs 65, 91, and 92. These changes will be made as part of Revision 1 of the LTR.

Changes will be made to the 4th paragraph of Section 9.1:

The purpose of the uncertainty analysis, the following step, is to quantify the uncertainties associated with the analysis. For jet pump plant LOCA analysis, [[

]] For the external pump plant LOCA analysis, [[

]] The break spectrum studies combined with sensitivities to the uncertainty contributors presented in this LTR indicate that intermediate breaks are more limiting for jet pump design, whereas the double-ended guillotine is the limiting case for external pump design plants. Although the limiting break size is expected to differ on a plant-specific basis, the overall trends in break spectrum are expected to be similar for the similar designs. Each LOCA analysis will include plant-specific break spectrum calculations.

RAI 100 Limitation on Cathcart-Pawel Cladding Oxidation

Background

The requirements in 10 CFR 50.46(b) impose a limit on peak fuel cladding temperature of 2200 °F, and a limit on cladding oxidation of 0.17 times the total cladding thickness before oxidation. The oxidation limit is usually considered as a percentage, and more recently, has been expressed as equivalent cladding reacted (ECR) (i.e., 17% ECR). The Atomic Energy Commission's deliberation over the 17% ECR acceptance criterion is discussed in detail in the 1973 Opinion of the Commission regarding acceptance criteria for emergency core cooling systems (ECCS) for light-water-cooled nuclear power reactors (6 AEC 1085).

In its proceedings, the AEC noted that the "limits specified in these criteria will assure that some ductility would remain in the zircaloy cladding as it goes through the quenching process". The values were selected because experimental data indicated that cladding ductility is influenced not only by oxidation alone, but also by the temperature at which the oxidation occurs. The AEC received recommendations from fuel vendors, the AEC staff, and the public, regarding the selection of an appropriate oxidation limit. The AEC's consideration included not only the total oxidation, but also the thickness of brittle oxidation and zirconium layers in the cladding, and the ratio of the thickness of the brittle layers to the remaining ductile layers. Noting wide agreement on the value of 17%, ECR as a threshold above which cladding generally exhibited brittle behavior, the AEC settled in this value as the cladding oxidation limit.

The experimental studies supporting this limit evaluated cladding ductile performance and correlated it to the thicknesses of the differing layers (i.e., oxide, brittle zirconium, ductile zirconium), rather than to a measured ECR. The percentage values were calculated, based on the test conditions, using the Baker-Just correlation. Thus, the AEC also noted that "the Regulatory Staff in their concluding statement compared various measures of oxidation (page 90) and concluded that a 17% total oxidation limit is satisfactory, [emphasis added] *if calculated by the Baker-Just equation.*" (6 AEC 1097)

Realistic ECCS Research and Additional Cladding Oxidation Correlations

Upon revision in 1988 to 10 CFR 50.46 to allow more realistic emergency core cooling performance calculations, the state of the art for cladding oxidation calculations had evolved. In addition to Baker Just, Chapter 6.13 of NUREG-1230, "Compendium of ECCS Research for Realistic LOCA [loss-of-coolant accident] Analysis," reviews Cathcart-Pawel alongside two additional oxidation rate equations (ADAMS Accession No. ML053490333).

The NUREG, as well as RG 1.157 recommend the use of Cathcart-Pawel based on its superior accuracy when compared to Baker-Just. However, as noted in Research Information Letter (RIL) 02-02, Attachment 2, the original and confirmatory ring compression tests on which the 17% ECR criterion was based relied on an ECR value calculated using Baker-Just (ADAMS Accession No. ML021720709). As noted on Page 9 of RIL 02-02, Attachment 2, "had the Cathcart-Pawel correlation – which did not exist at that time – been used, the cladding oxidation limit would have been about 13%. Therefore, the Baker-Just correlation must be used when comparing results with the old 17% limit."

Safety Implication

The use of a 17% limit on ECR, when applied to cladding oxidation values calculated using the Cathcart-Pawel correlation, does not provide the same level of assurance of cladding ductility as the same limit, when applied to a result calculated using the Baker-Just correlation.

Implications of 10 CFR 50.46c Research

In 2008, the NRC published NUREG/CR-6967, "Cladding Embrittlement During Postulated Loss-of-Coolant Accidents" (ADAMS Accession No. ML082130389). The report identifies newly identified cladding embrittlement mechanisms, and provides a more detailed evaluation of expected post-LOCA cladding behavior. The NUREG also used more rigorous testing methods than the work that formed the basis for the original ECCS rule (e.g., Hobson and Rittenhouse). The NUREG documents, in part, is the basis for the draft performance-based rule at 10 CFR 50.46c. An accompanying RG, RG 1.224, "Establishing Analytical Limits for Zirconium-Alloy Cladding Material," provides an acceptable limit to ensure ductile cladding behavior for existing zirconium alloy cladding, and also provides methods acceptable to the NRC staff to establish new analytical limits for post-quench cladding ductility (ADAMS Accession No. ML15281A192). Most notably, the analytical limit for zirconium alloy fuels in RG 1.224 reduces the acceptable value of ECR calculated using the Cathcart-Pawel correlation as a function of hydrogen pickup, a phenomenon that occurs through the in-reactor design life of the fuel.

These documents, NUREG/CR-6967 and RG 1.224, can be used as a basis to apply new, performance-based limits for post-LOCA cladding ductility, once 10 CFR 50.46c is promulgated. However, for application within the existing prescriptive regulations and acceptance criteria at 10 CFR 50.46, it is more appropriate to apply the ECR value that is equivalent to 17% ECR, as stated in the 1973 Opinion of the Commission, "if calculated by the Baker-Just equation." This value, using the Cathcart-Pawel correlation, is roughly equivalent to 13%.

Request

In its present reviews of ECCS evaluation models, the NRC staff is imposing a review condition specifying that the ECR results calculated using the Cathcart-Pawel correlation will be considered acceptable in conformance with 10 CFR 50.46(b)(2), if the ECR value is less than 13%, which is equivalent to 17% ECR, if calculated using the Baker-Just equation. This condition will be considered temporary, and may be removed upon the NRC's adoption of a more performance-based regulatory framework with respect to ECCS performance.

In the unlikely event that the Commission chooses not to promulgate 10 CFR 50.46c, the NRC staff will consider further action to ensure that users of currently approved, realistic or best estimate ECCS evaluation models are using acceptance criteria that provide appropriate assurance of post-LOCA cladding ductility as set forth in 10 CFR 50.46(b)(2), in consideration of the Opinion of the Commission published in 1973.

In light of the staff's limitation, please provide the following information:

- A. Explain whether GEH will continue to calculate cladding oxidation as discussed in NEDE-33006P.
- B. If an alternative approach to calculate cladding oxidation is proposed, summarize that approach.
- C. Explain how TRACG-LOCA accounts for pre-transient cladding oxidation.

RAI-100 Response

- A. GEH expects to continue to calculate cladding oxidation using the Cathcart-Pawel correlation as discussed in NEDE-33005P and will apply the acceptance criterion that the Nuclear Regulatory Commission (NRC) staff stipulates (Approach 1). The choice of approach is up to the licensee for which the LOCA analyses are being performed. The TRACG LOCA methodology currently under review by the NRC staff is capable of and appropriate for demonstrating compliance with the equivalent cladding reacted (ECR) acceptance criterion specified for the oxidation rate correlation being applied to calculate local ECR.
- B. An alternate calculational approach (Approach 2) is to use the Baker-Just correlation together with its stipulated acceptance criterion. Another alternate approach (Approach 3) is to use the Cathcart-Pawel correlation consistent with the acceptance criteria associated with the proposed 10 CFR 50.46c performance-based limits (Reference R100-1). The licensing process needed for an early adoption of the third approach has not been completely defined by the NRC so some risk by the licensee is encountered should they choose this third option.
- C. Pre-transient oxide on the cladding exterior together with its uncertainty is calculated as described in Section 5.1.3.33 of the LTR (NEDE-33005P). Pre-transient oxide on the interior cladding surface is set to zero. In all modeling approaches, the initial oxide amount on the cladding surface(s) serves as the starting point for the metal-water reaction which adds to the oxide during the transient. In all modeling approaches, increased oxidation on the interior surface is modeled if rod perforation is predicted.

Reference

- R100-1 U.S. NRC 10 CFR Parts 50 and 52 Proposed Rule, "Performance-Based Emergency Core Cooling Systems Cladding Acceptance Criteria," RIN 3150-AH42, March 6, 2014. (ADAMS Accession No. ML12283A174).

LTR Impact

None.

RAI 101

In its review, the NRC staff has identified several issues with the description of the decay heat modeling approach provided in the TRACG-LOCA Licensing Topical Report (LTR). Please address the following:

- Describe the historical source of the decay heat model and explain how it has been adapted for use within TRACG-LOCA. Provide plots (or reference such plots within the LTR) comparing decay heat as a function of time between the current and prior models to illustrate the evolution.
- Explain how the decay heat is perturbed in the statistical analysis. Include examples reflective of production safety analysis, including a description of attributes important to characterizing the decay heat as applied to various limiting and average channel groupings.
- Correct in-text inconsistencies in the LTR, particularly on Pages 2-8 and 5-33.
- NEDE-30996P-A, as referenced in the LTR Table 2.5-1, has no Appendix B. Please explain.

RAI 101 Response

The reference to Appendix B of NEDE-30996P-A in LTR Table 2.5-1 is a typographical error. The correct reference is Appendix B of NEDE-23785-1-PA, Volume 3. This reference describes a generic decay heat curve based on the American Nuclear Society (ANS) 1979 standard for use with SAFER. In subsequent plots, this nominal decay heat curve is referred to as the “SAFER LTR” curve.

As discussed in Section 9.3 of NEDE-32176P, the 1979 and 1994 ANS standards are implemented in TRACG in a simplified manner. The source of these models in TRACG is the DECAY computer program (referred to as “DECAY01P” in subsequent plots). The DECAY program was developed in response to NRC Information Notice (IN) 96-39, which pointed out the inconsistent calculation of decay heat within the domestic nuclear power industry. Thus, the DECAY code was developed to faithfully replicate the ANS 1979 and 1994 decay heat standards. The simplifications employed relative to DECAY, for implementation in TRACG, are either of little consequence, or result in a conservatively high decay heat.

The major simplification to fit in the TRACG framework is that [[

]]. This is a noticeable conservatism for decay heat driven transients such as a Loss-of-Coolant Accident (LOCA). The conservatism is demonstrated by comparing the DECAY01P nominal, TRACG04P nominal, and SAFER LTR nominal ANS 1979 decay heat for a 10 GWD/ST exposure case. Note in Figure R101-1 and R101-2 that the TRACG04P nominal is increasingly greater than the DECAY01P nominal and SAFER LTR nominal after about [[]] seconds of shutdown time. To confirm that this simplification is the source of the conservatism, the DECAY01P nominal values are adjusted by [[

]] (“DECAY01P ADJUSTED”). The “DECAY01P ADJUSTED” points are visually identical to the TRACG04P nominal curve.

[[

]]

For the LOCA application, TRACG initializes the decay heat model [[

]]. For a constant irradiation time, the decay heat can be lower for a larger exposure, although the effect is very small for the first 20,000 seconds. However, since a [[

]].

For the LOCA application, the decay heat uncertainty is calculated as specified by the 1979 ANS standard. In particular, the standard specifies that uncertainties be determined for energy per fission, fission product decay power, and reactor power. Since the reactor power uncertainty is included in the initial total thermal power, it is not included in the decay heat uncertainty. The uncertainty in the energy per fission is 0.25%. The uncertainties in the fission product decay power are as specified by the ANS standard. For the same demonstration case, the TRACG04P +2 σ and DECAY01P +2 σ total shutdown power, as a fraction of initial, are compared in Figure R101-3.

For a given LOCA transient statistical trial, a particular decay heat uncertainty, in terms of number of standard deviations from the nominal is specified via input (the particular value is sampled from a specified probability distribution function). The same number of standard deviations is then applied [[]] in that trial. [[

]]

Table R101-1 indicates decay power fractions, as a function of exposure, for both the initial condition, and at 3,000 seconds after a large break LOCA. These values are for a typical nominal case (no decay heat uncertainty), and for a large positive and negative uncertainty relative to nominal. In general, the long term decay heat is higher for higher exposure.

Table R101-1 Typical [[]] Decay Power Fractions

[[.....]] Type	Exposure (GWD/MT)	Fraction of Initial Thermal Power due to Decay Heat At Time 0 / At 3,000 seconds		
		[[]]
[[
]]

[[

Figure R101-1 TRACG04P Decay Heat Comparison to DECAY01P and SAFER LTR (0 – 10,000 seconds)

]]

[[

Figure R101-2 TRACG04P Decay Heat Comparison to DECAY01P and SAFER LTR (0 – 1,000 seconds)

]]

[[

Figure R1 01-3 TR ACG04P Decay Heat Comparison to DECAY01P with + 2 Sigma Uncertainty (0 – 1,000 seconds)

]]

LTR Impact

Note: These changes are relative to the LTR version after implementing the changes for previous RAI responses. For example, the decay heat figure in the original LTR was Figure 5.1-18, corresponding to 15 GWD/MT. This figure was changed in the response to RAI-54 to correspond to 11 GWD/MT, and is now Figure 5.1-17, due to other changes.

1. Table 2.5-1; 3.2.2 Fission Heat, 3.2.3 Decay of Actinides, 3.2.4 Fission Product Decay Heat

a. Replace the third row, 2nd column (GEH Process) with:

The heat generation from radioactive decay of fission products is calculated in accordance with the 1979 ANS standard. [[

]]

b. Change the reference in the third row, 3rd column (Evaluation) from [25] to [21].

2. Replace the text of Section 5.1.3.31 C25 – Decay Heat (H) with:

TRACG calculates the decay heat as a function of time in a way that conservatively approximates the American National Standards Institute (ANSI)/ANS-5.1-1979 standard entitled “American National Standard for Decay Heat Power in Light Water Reactors” [59]. In this standard, values are provided for decay heat power from fissioning of the major fissionable nuclides present in light water reactors (LWRs) (i.e., U235 and Pu239 (thermal) and U238 (fast)) and methods are prescribed for evaluating the total fission product decay heat power from the data given for these specific fuel nuclides. By way of this methodology, the decay heat curve becomes a function of the fuel design, depletion environment and power history. Thus, in theory, each point in the reactor has a unique decay heat curve. Fortunately, the variations in decay heat due to the above effects are small and curves can be defined [[

]] with little

loss in accuracy. The details of the derivation as well as the calculation of the uncertainties are described in References [59] and [38]. TRACG implementation details are provided in Section 9.3 of Reference [1]. For the purpose of illustration, the nominal decay heat curve and the $\pm 1\sigma$ curves are shown in Figure 5.1-17 for an exposure of 11 GWd/MTU. [[

]], as determined from the uncertainty specified as part of the ANS decay heat standard.

3. Change the Figure 5.1-17 caption to: “Decay Heat Uncertainty at an Exposure of 11 GWD/MTU”.

RAI 102

During the course of the NRC staff review, GEH has revised its approach to addressing initial conditions, particularly the modeling of initial bundle power distribution. The relevant request for additional information responses and revised LTR text do not provide a sufficiently complete description as to enable the NRC staff to determine that the revised modeling approach (including adjustments to the level of detail of modeling for the core, to the approach for including a variety of limiting bundle characteristics, and to accounting for variability in the core spray distribution) provides an acceptable, best-estimate representation of “relevant factors such as the actual total power, actual peaking factors, and actual fuel conditions,” as recommended in Regulatory Position 3.1 of Regulatory Guide 1.157. Please provide a description of the minimum number of hot CHAN components required for use in production TRACG-LOCA safety analysis, and explain why additional hot CHAN components would be included. Provide examples and relevant core operating limit curves to illustrate the analytic method.

RAI 102 Response

The revision to Licensing Topical Report (LTR) Section 6.2.5 as part of the RAI-73 response was [[

]] This RAI response provides clarification of applied bundle power distributions and how they relate to Maximum Average Planar Linear Heat Generation Rate (MAPLHGR) limits that ensure that acceptance criteria are met.

In the response to RAI-73, GE Hitachi Nuclear Energy (GEH) provided the details of hot CHAN types modeled in the TRACG LOCA application. The summary table provided in the RAI-73 response for [[

[[]]

]]

**Figure R102-1 Minimum Hot Channel Modeling Approach for a Typical Jet Pump
Plant Application**

[[

]]

Figure R102-2 Minimum Hot Channel Modeling Approach for a Non-Jet Pump Plant Application

[[

]]

Figure R102-3 Typical Hot Channel Modeling Approach for a Non-Jet Pump Plant Application

LTR Impact

None.

RAI 33

Please provide the following information related to PIRT item C18 (cladding perforation):

- a. A summary of or reference for the tests that includes the number of tests, the type(s) of cladding tested, and the heatup rates used.
- b. The basis for applying the empirical data used to estimate clad rupture stresses to current-generation fuels.
- c. The basis for the assumption of normality for the upper and lower 95 percent groups used to determine the rupture stress.
- d. Explanation of the origin of and justification for the assumed uncertainty of the built-in fuel rod internal pressure curves and the normality of the multiplier on rod pressure.
- e. Relative to the high-temperature phase change of zirconium, please clarify the statement on page 2-11 of the TR that phase change of in-core materials is not modeled.

RAI 33 Response (Revised)

- a. A summary of the cladding hoop stress versus perforation temperature testing used in defining the model and model uncertainty can be found in Reference R33-1. The figures in the referenced letter's enclosed report show the comparison of high temperature test data to the rupture stress model. All of the tests presented are for heat-up rates [[

]]. In Reference R33-1 selected data from Reference R33-2 is compared with GE proprietary data for low heat-up rates. Note that ruptures occur at lower hoop stresses when the heat-up rates are lower so that is why the data for the higher heat-up rates in Reference R33-2 are not included. Figure 5 of Reference R33-1 aggregates data points from Figures 1, 2, and 4 of the same reference. Figure R33-1 of this response has been reconstructed from the same data in order to provide a legend to indicate the origins of the data. The relevant NUREG-0630 (Reference R33-2) data that has heat rates of [[

]] are also depicted with open blue markers in Figure R33-1. [[

]]

- b. The clad rupture stress model is assessed using hoop stresses, as described by the method in Section 3.1 of Reference R33-2. By employing this method of converting differential pressure data to hoop stress data, design-specific dimensional effects are eliminated. This allows the clad rupture stress model to be extended beyond the 7x7 and 8x8 fuel from the test programs to current-generation fuel product lines. Additionally, the data in Figure 1 of Reference R33-1 show that the differences between 7x7 and 8x8 fuel rod data extracted from NEDM-20350-3 are insignificant compared to the scatter in the data, confirming that

dimensional effects have been eliminated. This fact is also depicted by comparison of the red triangles (8x8) with the red squares (7x7) in Figure R33-1 of this response.

- c. The clad rupture stress uncertainty model was developed using temperature-dependent rupture stress data from GE material testing programs. Relevant low heat-up rate data from NUREG-0630 has been shown for comparison. The uncertainty model [[

]]

- d. The LHGR- and exposure-dependent values of the nominal fuel rod internal pressure used in TRACG LOCA analyses are calculated based on the NRC-approved PRIME model [[
-]] The calculation method qualified previously for GESTR (Reference R33-3) has been replaced by PRIME thermal-mechanical analyses (References R33-4 and R33-5). [[

]] The key driver of rod perforation uncertainty is the uncertainty in the temperature-dependent rupture stress. The rod internal pressure is less important. PRIME nominal rod internal pressure as used in LOCA calculations is [[

]] shown in Figure 5.2 of Reference R33-5. Updated data provided in Figure 2-8 of Reference R33-6 are replicated here as Figure R33-3. [[

]]

- e. Clarifications to the entries in Columns 2 and 3 in Section 3.3.2 of Table 2.5-1 on page 2-11 of the TR are proposed in view of the additional details and clarification provided below.

The entry in column 2 labeled *GEH Process* will be modified to read:

Material properties for Zircaloy account for the alpha and beta phases. The Zr-H₂O reaction to produce ZrO₂ is modeled. Melting of UO₂ is precluded by the GE SAFDL applied for AOO transients and this bounds all LOCA calculations provided the 2,200 °F limit on PCT is satisfied. Eutectic formations are not significant provided the 2,200 °F limit on PCT is satisfied.

The entry in column 3 under *Evaluation* will be modified to read:

The phenomena necessary for BWR LOCA are modeled.

Cladding hoop stresses are modeled in TRACG for the purpose of tracking geometric changes due to rod perforation and to account for the resulting oxidation of the cladding. Additionally, material properties for the cladding and fuel take into account transient temperature effects. Specifically, the Zircaloy cladding properties account for the physical differences associated with the alpha and beta phases of Zircaloy. The contact pressure between the UO₂ pellet and cladding inside surface is specifically modeled and is strongly influenced by uncertainty in parameters that impact the temperature of the fuel pellet and its thermal expansion. If the 10 CFR 50.46(b) acceptance criteria for ECCS systems are met, the chemical effects of eutectic formation will have no adverse impact on the fuel and can be ignored in cladding response calculations within the range of post-LOCA conditions. Proposed additional requirements from 10 CFR 50.46(c) related to post-quench ductility and break away oxidation are expected to be addressed by material testing that will be used to stipulate a time limit at a prescribed temperature that must not be exceeded in the LOCA calculations. Assessment relative to the new criteria is independent of the TRACG modeling and application methodology and can be achieved by comparing the calculated PCT trace to the required limit once the new rules are finalized.

[[

]]

Figure R33-1. Rupture Stress Model Compared to Data

[[

]]

Figure R33-2. Examples of Rupture Stress Uncertainty Modeling

[[

]]

Figure R33-3. PRIME Predicted versus Measured Fuel Rod Internal Pressure (Nominal)

References

- R33-1. Letter from R. W. Bucholz (GE) to C. S. Rubenstein (NRC), “General Electric Fuel Clad Swelling and Rupture Model,” MFN-097-81, May 15, 1981.
- R33-2. NUREG-0630, Cladding Swelling and Rupture Models for LOCA Analysis, April 1980.
- R33-3. B.S. Shiralkar, et al. “The GESTR-LOCA and SAFER Models for the Evaluation fo the Loss-of-Coolant Accident, Volume I: GESTR-LOCA – A Model for the Prediction of Fuel Rod Thermal Performance,” NEDE-23785-1-PA, Revision 1, October 1984.
- R33-4. “The PRIME Model for Analysis of Fuel Rod Thermal-Mechanical Performance Part 3 – Application Methodology,” NEDC-33258P-A, Revision 1, September 2010.
- R33-5. “The PRIME Model for Analysis of Fuel Rod Thermal-Mechanical Performance Part 2 – Qualification,” NEDC-33257P-A, Revision 1, September 2010.
- R33-6. “The PRIME Model for Analysis of Fuel Rod Thermal-Mechanical Performance 2015 5-Year Update”, NEDC-33257P Supplement 1, MFN 15-060, August 7, 2015.

LTR Impact

Entries in Columns 2 and 3 in Section 3.3.2 of Table 2.5-1 on page 2-11 of the TR will be revised.

The entry in Column 2 labeled *GEH Process* will be modified to read:

Material properties for Zircaloy account for the alpha and beta phases. The Zr-H₂O reaction to produce ZrO₂ is modeled. Melting of UO₂ is precluded by the GE SAFDL applied for AOO transients and this bounds all LOCA calculations provided the 2,200 °F limit on PCT is satisfied. Eutectic formations are not significant provided the 2,200 °F limit on PCT is satisfied.

The entry in Column 3 under *Evaluation* will be modified to read:

The phenomena necessary for BWR LOCA are modeled.

LTR Section 5.1.3.24 will be replaced to read as indicated below. The figure titled “Uncertainty in Fuel Rod Internal Pressure” in the LTR as originally submitted will be deleted. The figure titled “Clad Rupture Stress as a Function of Clad Temperature” in the LTR as originally submitted will be replaced using Figure R33-1 from this response.

5.1.3.24 C18 – Fuel Cladding Strain /Perforation (H)

The key drivers governing strain-induced fuel rod perforation are the temperature-dependent clad rupture stress and the rod internal pressure. Based on material properties, the rupture stress and its associated uncertainty is modeled in TRACG as three curves corresponding to nominal, lower bound, and upper bound rupture stress curves as functions of cladding temperature (Figure 5.1 15). At each temperature, the upper and lower bounds are used to define uniformly-distributed samples above and below the nominal rupture stress, respectively.

The instantaneous clad hoop stress is directly related to the fuel rod internal pressure. Nominal fuel rod internal pressures are calculated in TRACG as described in Section 7.5.3.1 of Reference [1] using parameters calculated by PRIME [76] and passed to TRACG [[

]]

RAI 65

Section 7.1.1 of the TR states that continuity in the probability density functions for figures of merit is a requirement for determining non-parametric tolerance limits according to Wilks' Theorem. However, it is not obvious that these probability density functions will, in general, be continuous. In fact, [[]] calls the TR's assumption of continuity into question. Therefore, please demonstrate that the requirement for continuous probability density functions will be satisfied in the application of the evaluation model described in the TR for quantifying a single probabilistic statement of safety for the complete spectrum of break locations and sizes, the complete spectrum of model parameters and their variation, and the nonlinear feedback introduced by the engineered safety features. In other words, please show that there are no disjoint density functions of the figures of merit, or they can be identified and taken into account in the application of Wilks' Theorem.

RAI 65 Response (Revised)

Continuity of the probability density functions for figures of merit is not a requirement for determining the non-parametric tolerance limits. Although the original work by Wilks is based on continuity of the probability density function, Wald's work further extends the method to multivariate applications (Reference R65-1), and Tukey's work extends the nonparametric estimation technique to discrete distributions (Reference R65-2). As demonstrated in RAI-6 and RAI-9 responses, the bifurcated behavior is effectively eliminated from the computed results. The simulations performed to date support that the probability density functions for figures of merit are practically from continuous functions. The methodology does not depend on a continuity requirement. Therefore, the sentence regarding this aspect being a requirement will be removed.

References

- R65-1 A. Wald, "An Extension of Wilks' Method for Setting Tolerance Limits," *The Annals of Mathematical Statistics*, Volume 14, Issue 1, March 1943, 45-55.
- R65-2 J. W. Tukey, "Nonparametric Estimation, III. Statistically Equivalent Blocks and Multivariate Tolerance Regions – The Discontinuous Case," *The Annals of Mathematical Statistics*, Volume 19 (1948), pp. 30-39.

LTR Impact:

Following sentence from Section 7.1.1 of the LTR will be removed:

"The only requirement for the validity of the OSUTL derived in this manner is continuity of the PDFs providing the samples for each trial."

RAI 103

In response to prior RAIs 66 and 89, GEH provided justification for its proposed approach of analyzing uncertainty using at least three statistical samples, each containing 59 cases. The NRC staff does not accept the GEH justification that this approach provides the high-probability results required 10 CFR 50.46. In particular, because the method is used to determine high-probability results for three different critical safety parameters, an approach based on order statistics should identify an upper quantile, but should do so with high confidence. The high confidence is required so that the variability associated with using quasi-random samples to infer upper quantiles is either minimized or conservatively taken into account. Thus, in identifying a basis for a specified sample size, consideration of tri-variate coverage and the use of tolerance intervals are considered by the NRC staff to be acceptable approaches. Provide a statistical sampling basis that estimates an upper tolerance limit and provides tri-variate coverage. If the approach is proposed to allow other than the first-ranked order statistic as the upper tolerance limit, please also clearly delineate the approach for setting the sample size and number of rejected order statistics, providing information to demonstrate that sample sizes are set prior to initiation of production statistical analysis.

RAI 103 Response

In RAI-66 response, the GEH position depended solely on the limited discussion provided in RG 1.157 regarding the acceptable ways of quantifying the uncertainty. This position partly stemmed from the following fact: For all fuel types and core designs in BWRs, when the maximum local oxidation (MLO) criterion is met, the hydrogen generation, also referred to as core-wide oxidation (CWO), is always limited to less than 1% of all cladding surrounding the fuel. Therefore, meeting the criterion is not a random outcome, but is a function of the MLO. The guidance provided by the regulatory guide did not place the MLO and CWO acceptance criteria at the same statistical treatment for uncertainty calculation compared to the peak cladding temperature (PCT) criterion. GEH understands that the staff's expectation has evolved, and now it demands the treatment of all three critical safety parameter with the same statistical rigor and reporting on their joint probability with a specified confidence as if they are from dependent distributions with no assumption on their correlation.¹ Since the approach using tri-variate coverage and tolerance intervals is considered acceptable by the NRC staff for quantifying the uncertainties to determine the three different critical safety parameters, GEH will comply with this expectation by adapting a sampling scheme that is purely based on order statistics.

To meet this expectation, it is necessary to adjust the minimum number of samples. The non-parametric statistical theory determines the sample size necessary to establish the statistical argument. In TRACG LOCA methodology, widely-accepted 95/95 criteria will be used. In other words, the joint probability on the reported 95th percentile values reported for the three

¹ As shown in Reference R103-1, if the parameters of interest have perfect correlation, the minimum number of samples reduces to the required number for single parameter. In this application, no assumption for the level of correlation will be made, but they are treated as statistically dependent.

critical safety parameter will be no less than 95%. The first multivariate generalization of Wilks' order statistics work [Reference R103-2] was made by Wald [Reference R103-3]. His method has been termed that of 'successive elimination.' The distribution of the coverage is shown by Wald to be the Beta distribution.

J. W. Tukey generalized the construction of distribution-free tolerance regions for any general shapes, such as rectangles, cubes, polygons, ellipsoids, or spheres, by introducing the concept of statistically equivalent blocks [Reference R103-4]. Using this concept, it is possible to construct a statistical sampling scheme that meets the aforementioned criteria.

Similar to the example given in References R103-1, for three critical safety parameters, or independent figures of merit (FOMs), evaluated at 95% coverage with 95% probability (95/95), the minimum number of cases without any rejection is 124. In other words, the highest ranked output parameters for each FOM, i.e. the maximum values from the 124 cases, will determine the 95/95 peak cladding temperature (PCT), maximum local oxidation (MLO), and core-wide oxidation (CWO). Using the same theory, the second highest value for only one of the critical parameter would be equal or greater than 95% of the true population with 95% confidence level when the sample size is 153. Similarly, with a sample size of 181, it is possible to have 2 samples with highest values for any of the critical safety parameters removed to form the tolerance limits and still satisfy the 95/95 requirement for each of them. Table R103-1 provides the sample size needed to ensure that 95th percentile of a given FOM would be exceeded with 95% probability for various degrees of freedom (DOFs).

Table R103-1 Minimum number of runs for different sampling schemes

	m (DOF-2)	n	# of allowed failures
Scheme A	3	124	0
	4	153	1
Scheme B	5	181	2
	6	208	3

Scheme A as noted in Table R103-1 meets the expectation of 95%/95% coverage for tri-variate sampling with no rejection. Scheme A will be used unless stated otherwise prior to the analyses.

Scheme B sampling provides for a more robust process that is less prone to added conservatism coming from statistical variation in the extreme values by allowing up to two failures from a larger sample size of 181 trials. In this context, the term failure is used for a trial with a FOM output that is beyond the 95% probability for 95% coverage. A trial value might be rejected for exceeding a preset limit such as a regulatory acceptance criterion; however, rejection of two samples with maximum values for any of the FOMs is allowed because two extreme values are beyond the needed 95% probability for 95% coverage when the sample size is 181. Scheme B allows a more accurate evaluation of the critical safety parameters. It will be employed for plant applications where there is a credible expectation that the regulatory limits would be challenged. For instance, BWR/2 applications would fall under this category.

The equivalency of Schemes A and B is demonstrated by the following examples. To simplify the subsequent discussions, the CWO dimension of the results is omitted in the following illustrations since the criterion is always met when the MLO critical safety parameter meets the acceptance criterion, eliminating the need to plot a third dimension in the figure. But, the same concept applies. The red circles and blue diamonds in Figure R103-1 show the MLO values versus PCT values for each of the trials from a 181-case and 124-case statistical analysis of BWR/2 large-break LOCA, respectively. Shown in the figure are the boxes that define the 95% coverage for the joint probability for three tri-variant critical parameters with 95% confidence level.

[[

]]

Figure R103-1 BWR/2 Large Break LOCA Results: MLO versus PCT

Figure R103-1 is constructed using two separate random sets, one with 124 cases (blue diamonds) and the other with 181 (red circles). As the number of samples increase, the distribution of the cases in the box would asymptotically converge to the exact 95%. Table R103-2 shows the numerical values for PCT and MLO. CWO is not shown because it is never limiting. The highest CWO value from all trials remaining after any trials are rejected based on PCT and/or MLO will be reported and checked to confirm it is under the regulatory limit.

Table R103-2 Highest calculated PCT and MLO values from 124- and 181-case exercises

.....		
.....		
.....		
.....]]

Furthermore, it is noted that when Scheme B is adapted using 181 samples, the boxes shown in Figure R103-2 are also statistically equivalent to describe the joint probability. Earlier work by Fraser (Reference R103-5) provides evidence that the method still remains valid if the function that determine the statistically equivalent blocks are chosen by a random process from a class of such functions. The point is true for any sequence and consequently is true when the sequence is chosen by a random process (Reference R103-5). Work by Kemperman (Reference R103-6) further generalized the method for constructing tolerance limits by allowing that each step of construction may not only depend on the blocks previously formed, but also on all the known boundary observations, replacing Tukey’s lexicographical ordering. Adaptation of generalized tolerance limits using sequentially determined statistically equivalent blocks implies that, when Scheme B is selected with 181 cases, eliminating (1) highest two PCT results, (2) highest two oxidation results, or (3) one of each would be statistically equivalent in evaluating the coverage. In Figure R103-2, both boxes define the 95% coverage with 95% confidence for the joint probability with the third dimension for CWO omitted from the figure as explained above.

[[

]]

Figure R103-2 Statistically Equivalent Blocks for BWR/2 Large Break LOCA Results

In accordance with the principles laid out in RAI-99, the sampling plan will be set at the onset of the analysis and there will be no modification of either the sampling scheme or the unique seed assigned to the analysis for a given plant. However, the commitment regarding the use of tri-variate order statistics overrides the position for analysis sample size given in the RAI-99 response. Similarly, the RAI-66 response is also superseded by the sample size scheme given in this response.

References

- R103-1 A. Guba, M. Makai, L. Pál, “Statistical aspects of best estimate method – I,” Reliability Engineering and System Safety, Volume 80, (2003) pp. 217–23.
- R103-2 S. S. Wilks, “Determination of sample sizes for setting tolerance limits,” The Annals of Mathematical Statistics, Volume 12 (1941), pp. 91-96.
- R103-3 A. Wald, “An Extension of Wilks` Method for Setting Tolerance Limits,” The Annals of Mathematical Statistics, Volume 14 (1943), pp. 45-55.

NEDO-33005-A Revision 1
Non-Proprietary Information – Class I (Public)

- R103-4 J. W. Tukey, “Nonparametric estimation II: Statistically equivalent blocks and tolerance regions – the continuous case,” *The Annals of Mathematical Statistics*, Volume 18 (1947), pp. 529-539.
- R103-5 D. A. S. Fraser, “Sequentially Determined Statistically Equivalent Blocks,” *The Annals of Mathematical Statistics*, Volume 22 (1951), pp. 372-381.
- R103-6 J. H. B. Kemperman, “Generalized Tolerance Limits,” *The Annals of Mathematical Statistics*, Volume 27 (1956), pp. 180-186.

LTR Impact

Pertinent parts of Chapter 7 and 9 will be updated. It will be noted in Revision 1, Chapter 8 runs will not be repeated with this change.

The affected Chapter 7 and 9 pages follow.

7.0 COMBINATION OF UNCERTAINTIES

A Monte Carlo technique is used to combine the individual biases and uncertainties specified for initial conditions, plant, and model parameters into an overall bias and uncertainty for the LOCA safety criteria. The Monte Carlo sample is developed by performing random perturbations of the parameters over their individual uncertainty ranges. Using the histogram generated by the Monte Carlo sampling technique, a probability density function is generated for the calculated primary safety criteria parameters.

To determine the total uncertainty in computer code predictions, it is necessary to combine the effects of model uncertainties (CSAU Step 9), scaling uncertainties (CSAU Step 10) and plant condition or state uncertainties (CSAU Step 11). Various methods have been used to combine the effects of uncertainties in a safety analysis, which are discussed briefly in [3]. All these approaches are within the framework of the CSAU methodology. This section only describes the methods for combining uncertainties that are proposed to be used for the TRACG ECCS/LOCA application. The method used for combining uncertainties in the application of TRACG to ECCS/LOCA analyses is the same as that used successfully and approved by the NRC for the analyses of AOO transient scenarios [3].

7.1 APPROACHES FOR COMBINING UNCERTAINTIES

Four approaches have been discussed and compared in [3] for combining uncertainties, which are: (1) Propagation of Errors; (2) Response Surface Technique; (3) Order Statistical (OS) Method, and (4) Normal Distribution One-Sided Tolerance Limit. Only the last two approaches will be briefly discussed in the following sections (Sections 7.1.1 and 7.1.2) since a multivariate version of order statistics is adapted for the TRACG ECCS/LOCA application and normal distribution assumption is used in some of the Chapter 8 demonstration calculations.

7.1.1 Order Statistics (OS) Method

In contrast to the Response Surface Technique, the non-parametric sampling method that has been used in Germany by Gesellschaft für Anlagen-und Reaktorsicherheit (GRS) [28] and for the application of TRACG to AOOs by GEH [3] requires only a relatively small number of calculations and automatically includes the effects of interactions between perturbations to different parameters. In the OS method, randomly sampled trials are used to vary all uncertain model and plant parameters randomly and simultaneously, each according to its uncertainty and assumed PDF. A method based on the order statistics of the output values is then used to derive one-sided upper or lower tolerance limits (OSUTLs or OSLTLs). For ECCS/LOCA applications, OSUTLs are defined for primary safety parameters such as the PCT, maximum clad oxide thickness fraction, and maximum zirconium oxide volume fraction.

Random sampling of each model, plant and state parameter according to its assigned PDF yields the value of that parameter to be used for a particular trial. For example, a given trial could have the film boiling heat transfer coefficient set at its -1.5σ value and the interfacial shear set at its $+2.0\sigma$ value, each according to its own probability model. For each randomly sampled set of

parameters, the calculation process determines the output parameters of interest. In this manner, the effects of interactions between parameters are captured in a single calculation. Once all of the trials have been completed, the desired output parameter (e.g., PCT) is extracted from each of the trials and the set of all values of this parameter is used to construct its OSUTL. Figure 7.1-1 illustrates the process.

TRACG overlay files containing all the perturbed input parameter values are created for each trial. The overlay file is appended to the end of the base transient input file and the TRACG calculation is performed to determine the output parameter value (e.g., PCT) as a function of time for this particular set of inputs. Each repeat of the process defines a sample value of the output parameter of interest for the particular transient under consideration. Similar sample values for other output parameters (e.g., maximum cladding oxidation) can be generated at the same time without additional TRACG calculations.

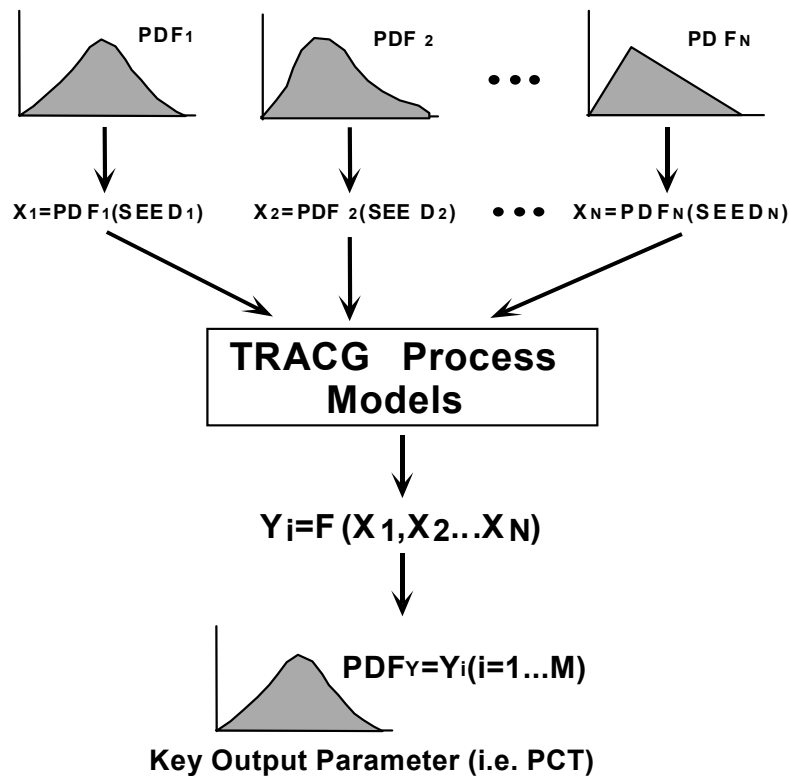


Figure 7.1-1 Schematic Process for Combining Uncertainties

The OSUTL of an output parameter, derived from the results of any given number of trials, is defined by two numbers, $0 < \alpha, \beta < 1$. Denoting the OSUTL by U , it can be stated that the percentage of future values of the output parameter (i.e., values determined from subsequent trials) that will be less than U is $100 \cdot \alpha\%$, with a confidence level of at least $100 \cdot \beta\%$. In formal practice, this is called an OSUTL with $100 \cdot \alpha\%$ content and (at least) $100 \cdot \beta\%$ confidence level. The only requirement for the validity of the OSUTL derived in this manner is continuity of the PDFs providing the input

samples for each trial. It has been shown [30] that, for prescribed values of α and β , the OSUTL can be defined for univariate case as the largest of the output parameter values if the sample size, n , satisfies $n \geq \log(1-\beta)/\log\alpha$. Thus to claim the largest value of a set of trials is an OSUTL with 95%-content and 95% confidence level for a single parameter, the minimum sample size is $n = 59$.

In multivariate case, the minimum sample size for joint probability of three statistically dependent but not necessarily correlated parameters is 124. In other words, the highest value for each of the three critical safety parameters would provide the joint 95% tolerance limit with 95% probability from a population of 124 cases.

The order statistics method is generally applicable without regard to the underlying probability distribution of the output parameter of interest. It requires only that the individual trials be independent realizations of a random variable from some single probability distribution. For a given number of trials, the upper bound value of the output parameter is itself a random quantity with a variability that depends on the sample size. The variability can be substantial and, on occasion, will yield an overly conservative bound.

To reduce this variability, a larger sample size can be used so that the 95%-content/95% confidence bound is given by the second or third largest observation. In a sample of 124, for example, the largest observation provides the desired bound for trivariate case. It is also possible to increase the sample size to 181 and sequentially eliminate 2 of the samples having the highest values from the population when determining the 95% tolerance limit with 95% confidence.

7.1.2 Normal Distribution One-Sided Upper Tolerance Limit

A special case of the order statistics method arises when the data that the tolerance bound will be derived from can reasonably be regarded as a sample from a normal probability distribution. In this case, it can be shown that the normal distribution one-sided upper tolerance limit (ND-OSUTL) is of the form

$$ND - OSUTL_{\alpha,\beta} \equiv \bar{y} + z_{\alpha,\beta} \cdot s \quad (7-1)$$

where \bar{y} is the average of the outcomes of the trials, s is their standard deviation and the factor $z_{\alpha,\beta}$ is chosen to guarantee 100 α %-content with a 100 β % confidence level. The assumption of normality for the response data is typically justified via one or more goodness-of-fit tests (e.g., Ryan-Joiner, Shapiro-Wilk, or Anderson-Darling). The values of $z_{\alpha,\beta}$ are tabulated in many statistical textbooks (e.g., [31]) as *factors for one-sided normal tolerance limits*. For example, to establish a bound of 95% content with a 95% confidence level from a sample of 59 trials, $z_{95,95} = 2.024$. As the sample size increases, this factor approaches 1.645, the 95th percentile of the standard normal distribution. If the normality tests indicate that the data are unlikely to have originated from a normal population, the order statistics method should be used. [[

]]

9.0 METHODOLOGY APPLICATION

This section provides additional discussion on some of the methodology application aspects. These discussions are to clarify the intended use of the evaluation methodology in analyses.

9.1 ANALYSIS PROCESS SUMMARY

In this report, demonstration analyses are presented along with additional sensitivity studies that helped in making the methodology decisions. The demonstration cases are illustrative and do not represent any particular plant. Actual analysis of a given plant will employ plant-specific input modeling and plant-specific break spectrum calculation. The uncertainty analysis and post-processing of results are built on break spectrum studies. The overall analysis process can be depicted by the flowchart given in Figure 9.1-1.

The process begins with preparation of the plant-specific basedeck. Major inputs to this step are plant geometry data from the qualified database, plant licensing operating parameters for LOCA/ECCS performance evaluation, analysis initial conditions, fuel-specific TRACG channel model, and fuel performance data.

The next major step in the analysis process is the break spectrum studies. The primary goal of this step is to determine the limiting break for further uncertainty analysis. The break spectrum studies are primarily centered on the recirculation line breaks for external pump and jet pump type plants. The appropriate single failure assumption depending on the break analyzed is applied. Additional studies are carried out, if needed, to verify that no other single failure, break location and size, and combination of uncertainty contributors will result in a higher PCT than the limiting break case.

The purpose of the uncertainty analysis, the following step, is to quantify the uncertainties associated with the analysis. For jet pump plant LOCA analysis, [[

]] For the external pump plant

LOCA analysis, [[

]] The break spectrum studies combined with sensitivities to the uncertainty contributors presented in this LTR indicate that intermediate breaks are more limiting for jet pump design, whereas the double-ended guillotine is the limiting case for external pump design plants. Although the limiting break size is expected to differ on a plant-specific basis, the overall trends in break spectrum are expected to be similar for the similar designs. Each LOCA analysis will include plant-specific break spectrum calculations.

The statistical analysis of uncertainty quantification relies on well-established techniques. [[

]]

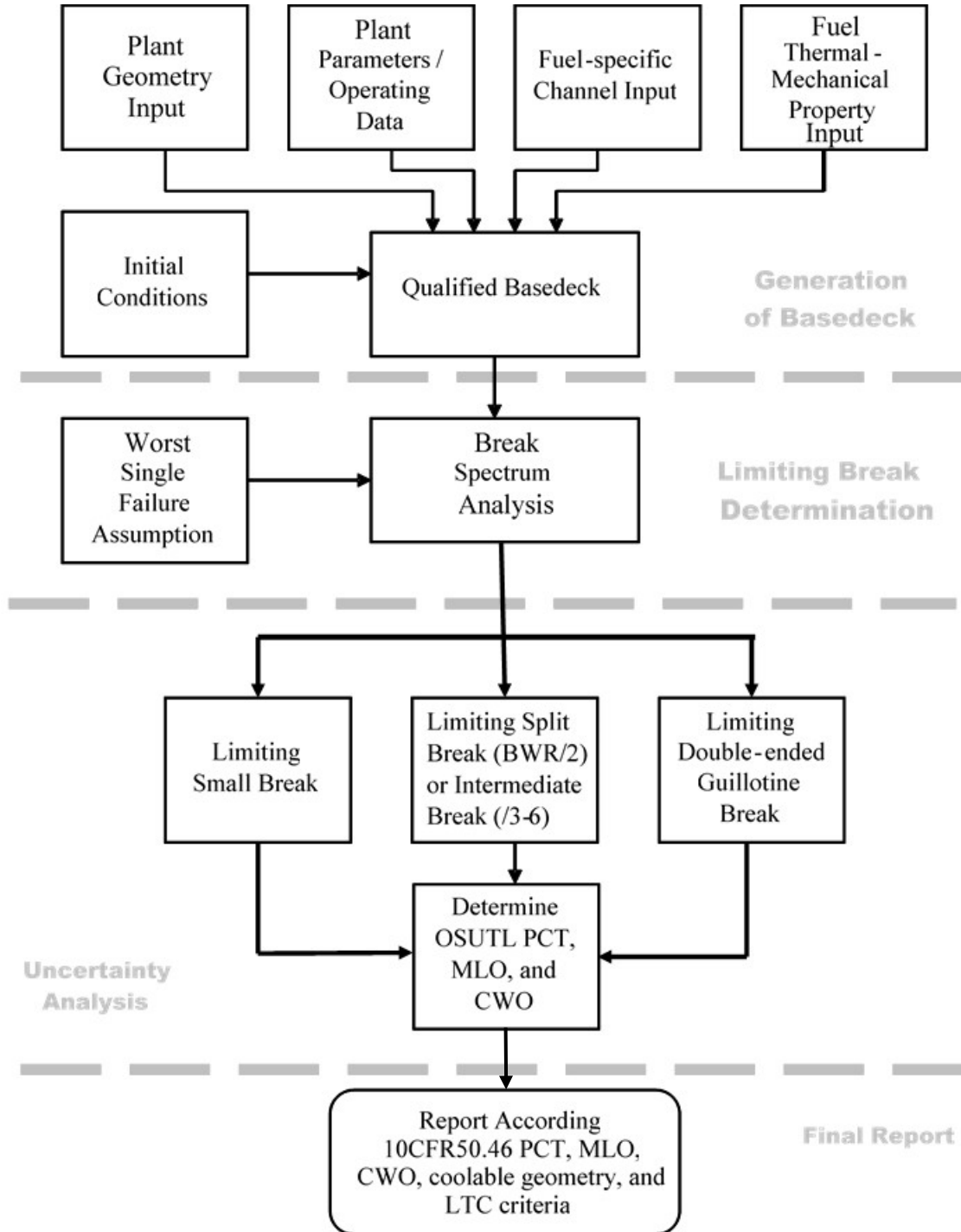


Figure 9.1-1 LOCA Analysis Process Flowchart

RAI 104

Provide additional information to justify the TRACG-LOCA modeling of rewet phenomena. In particular, show the sensitivity of the PCT and ECR to variations in the Shumway correlation-predicted rewet temperature and to variations in the uncertainty associated with the quench front model. Include discussion of limiting BWR transients as well as to appropriate integral effects test.

RAI 104 Response

Summary

Table R104-4 summarizes the additional sensitivity studies performed to assess the impact of the bias and uncertainty applied to the Shumway correlation treatment of minimum stable film boiling temperature (T_{min}) and the impact of the bias and uncertainty in the TRACG quench modeling. These sensitivities results provide context for the treatment of T_{min} and quench using the proposed best-estimate plus uncertainty (BEPU) approach and should not be viewed as suggesting an alternate analysis approach. The text that follows provides contextual and historical background as well the qualification basis for the T_{min} and quench models. Also there is a description of how the requested sensitivity studies were performed and how those results together with previously supplied information justify the TRACG proposed BEPU approach. Additional conservatism is not warranted because the BEPU modeling described in the TRACG LOCA LTR already accounts for bias and uncertainty in the modeling of T_{min} and quench in a way that satisfies the regulatory requirements and guidance.

Background

In the response to RAI-98, Reference R98-3 was a citation to MFN 15-078. For convenience Reference R98-3 is cited again here as Reference [R104- 1]. (Citations needed in this document are repeated so the reader is not inconvenienced with tracking down cascading references.) The enclosures to MFN 15-078 contain much information that is relevant to the TRACG models for T_{min} and quench. A roadmap to the contents of MFN 15-078 was provided informally to the NRC to facilitate their review and use of the supporting materials in MFN 15-078. Information from the roadmap to the MFN 15-078 enclosures will not be repeated here because information from those enclosures that are especially relevant for LOCA applications and qualification will be cited directly and specific elements will be gathered into this response for the convenience of the reader.

The TRACG implementation of the T_{min} correlation and the quench model have been extensively reviewed by the NRC staff and ACRS in association with TRACG ATWSI applications. NRC staff audits on the subject are indicated in Table R104-1 below. Interactions with the ACRS on these subjects are indicated in Table R104-2. The lists in Table R104-1 and Table R104-2 may not include all occurrences. The key point is that the NRC staff and the

ACRS have repeatedly requested and scrutinized information on the subjects of T_{min} and quench largely in connection with ATWSI applications where the importance of these model is greater than it is for LOCA applications.

Table R104-1 NRC Staff Audits Where TRACG T_{min} and Quench Models were Assessed

Audit Dates	Context of the Audit
October 24-25, 2012	NRC TRACG T _{min} and Quenching Methodology Audit MFN 13-073 and MFN 13-085 were produced following this audit so that they could be referenced for customer LARs requiring TRACG ATWSI application to support MELLLA+.
April 23-25, 2014	In connection with MELLLA+ LAR for Grand Gulf submitted by Entergy (see ADAMS Accession No. ML13269A140)
August 31, 2015	In connection with MELLLA+ LAR for Peach Bottom submitted by Exelon. MFN 15-078 was produced to provide documentation requested during this audit.

Table R104-2 ACRS Interactions Where TRACG T_{min} and Quench Models were Discussed

Date	Context of the Discussion
November 21, 2013	Presentation to the ACRS on TRACG modeling of T _{min} and quench.
March 17, 2015	In support of MELLLA+ for Grand Gulf
May 7, 2015	In support of MELLLA+ for Grand Gulf
July 8, 2015	In support of MELLLA+ for NMP2
September 21, 2015	Presented a simplified version of the materials contained in MFN 15-078.

With respect to TRACG LOCA applications, the biases and uncertainties for both the T_{min} and quench models are treated following the best-estimate plus uncertainty (BEPU) approach. The TRACG LOCA modeling conforms with the Code Scaling and Applicability, and Uncertainty (CSAU) methodology described in NUREG/CR-5249 and the guidance provided in Regulatory Guide 1.157. The modeling and bias for the Shumway T_{min} correlation are described in Section 5.1.3.26 of the LTR. For the quench model the basis for the bias and uncertainty are presented in Section 5.1.3.27 of the LTR. The descriptions in the LTR are augmented by responses to the RAIs as indicated in the following paragraph.

The responses to RAIs 23 and 50 provide additional information related to the modeling of T_{min}. The response to RAI 49 provides additional information related to the modeling of bias and uncertainty for the quench model. A distinction is made in the RAI 49 response regarding the low importance of quench modeling for jet pump BWRs/3-6 compared to the high importance of quench modeling for the BWR/2. As explained in the response to RAI-51: “For jet pump plants, rewet occurs after reflood and the temperature has turned around and starts to come down. The uncertainty in the rewet has therefore no impact on the PCT. Likewise the impact on the fuel clad oxidization for jet pump plants is also minimal as the PCT is relatively low and the duration of refill/reflood phase is short.” The Core Spray Heat Transfer (CSHT) tests provide the essential qualification for quenching due to a falling film like in a BWR/2.

That is the reason that Monte Carlo analyses of select CSHT tests were provided in Section 7.4.5 of the LTR. The text and figures in Section 7.4.5 have been updated and augmented in response to RAI 92.

To respond to the specific NRC request in this document, sensitivity studies have been performed to justify the current treatment of bias and uncertainty for both the Modified Shumway (MS) correlation for minimum stable film temperature (T_{min}) and the quench model. (“Modified Shumway” refers to the Shumway correlation with the elimination of the enhancement due to lower void fractions as explained later.) ALL sensitivity studies have been performed using 181 statistical trials and the limiting case for the NMP1 BWR/2 LOCA analysis. Use of the NMP1 BWR/2 calculations for the sensitivity studies is the most appropriate because the time in boiling transition for a BWR/2 is substantially longer than for BWRs/3-6 LOCA evaluations. For the limiting BWR/2 LOCA scenario only core spray is available to cool the core; consequently, rewetting occurs much later and the impact of any process that delays rewetting has the largest impact on oxide accumulation. By contrast, the cores in jet pump BWRs/3-6 can be re-flooded by the ECCS systems at least to the top of the jet pump diffusers within a comparatively shorter period of time so that total oxide accumulation remains much less than the imposed regulatory limit of 13% for cladding maximum local oxidation (MLO). It is also true that BWR/2 LOCA calculations tend to provide a higher calculated peak clad temperature (PCT) relative to BWRs/3-6 evaluated for the same or even higher linear heat generation rates (LHGRs).

For both the T_{min} and quench, the requested additional sensitivity studies are performed by setting the associated PIRT multiplier at its de-biased value minus two standard deviations (σ). The specific bias and uncertainty values are those indicated in the TRACG LOCA LTR and supported by responses to a number of different RAIs. Details that are presented below justify the proposed TRACG BEPU approach modeling of bias and uncertainty for the T_{min} and quench models for LOCA applications. To the greatest extent possible, the technically sound models implemented in TRACG are supported by comparing calculated results to relevant test data.

Justification of TRACG T_{min} Modeling

Detailed information on Shumway’s correlation for T_{min} is available in MFN 13-073 cited as Reference R50-1 in the response to RAI-50 and repeated in this document as [R104- 2]. Section 5.1.3.26 of the TRACG LOCA LTR has been modified as described in the RAI-50 response and the reference to MFN 13-073 added as Reference 80 in Section 11. The equation for the Shumway correlation is given in MFN 13-073 and also by Equation (6.6-52) of the TRACG Model LTR (cited as Reference 1 in the TRACG LOCA LTR and repeated here as [R104- 3]). The equation origin is Equation (19) in EGG-RST-6781 which is cited as Reference 3 in [R104- 2], Reference 23 in [R104- 3], and directly cited here as [R104- 4]. The primary purpose of MFN 13-073 was to justify using the Shumway correlation to calculate T_{min} for Zircaloy cladding. Key elements relevant to this justification are gathered from the sources listed above

and are assembled here. The specific focus here is on TRACG LOCA applications even though most of the justification is generic for any applications where T_{min} is important.

Shumway correlated the *quench temperature* (T_Q) and has done so with the intention that his correlation be implemented in the boiling water reactor (BWR) version of TRAC (TRAC-B). Shumway makes the point that a computer code like TRAC-B (also TRACG) does not need the so-called true T_{min} value corresponding to the location on the boiling curve where the heat flux is minimum (Q_{min}). Instead TRAC-B (and TRACG) need a higher T_{min} value consistent with how the heat flux for transition boiling is interpolated between a film boiling heat flux (Q_{FB}) and the critical heat flux (Q_{CHF}). All Shumway's statement for TRAC-B applied also to TRACG. As implemented in TRACG and explained in the response to RAI-069, the value for T_{min} is used as a logical check to prevent transition to nucleate boiling when the calculated cladding surface temperature is above T_{min} . The main point is that what the computer code needs is to define the temperature below which transition boiling can occur and the heat transfer coefficient will start increasing. Shumway defines the quench temperature (T_Q) to be the temperature of the surface at which significant deviations from film boiling are observed from a temperature versus time or distance curve. In other words, at T_Q there is an observable increase in the rate that the surface temperature is dropping that implies that the heat transfer coefficient is increasing. Carbajo (Reference 2 in [R104- 2]) equates the *quench temperature* with the *rewetting temperature* at which liquid can reestablish (and maintain) contact with the dry surface. By GEH's definition, this would be the *minimum stable film boiling temperature* (T_{min}) or the cladding surface temperature below which stable film boiling can no longer be maintained.

As Shumway states, the shape of the boiling curve is influenced by many phenomena which change in importance with the varying experimental conditions. The minimum heat flux (Q_{min}) and the temperature at which it occurs is not exclusively dependent on hydrodynamic or thermodynamic properties of the fluid. It varies with surface conditions such as roughness and surface thermodynamic properties. Factors such as velocity, pressure, subcooling, drop size, liquid contact angle, wetting agents, and even gravity influence the minimum heat flux. In fact, at higher mass fluxes the minimum conditions may not exist. The existence or nonexistence of a T_{min} point could be of little consequence provided the computer code implementation provides a reasonable heat transfer coefficient for modeling the transition between stable film boiling and nucleate boiling. In Shumway's words, " T_{min} is not a natural or physical property but is a consequence of many competing processes".

Shumway's correlation was established exclusively from stainless steel (SS) data over a relative wide range of pressures and flow rates as shown Figure R104-1. The GEH evaluation of the correlation compared to its own SS data is that on average it conservatively overestimates the 81 useable data points by 23 K with a standard deviation of 55 K when evaluated at $\alpha=1$. Most of the overestimation is at the higher pressures. For pressure at and below 0.7 MPa that are most relevant for LOCA applications, the bias is -1.2 K. As explained in RAI-50, a 20% uncertainty applied to the calculated difference ($T_{min}-T_{sat}$) sufficiently covers the 55 K standard deviation. In TRACG LOCA applications no credit is taken for the slight conservative bias at low pressure since this bias is not considered in the BEPU sampling. More important is the fact that the

Shumway evaluation of (Tmin-Tsat) as implemented in TRACG is even more conservatively biased for Zircaloy and this bias is not credited.

The Shumway correlation was developed using only SS data. Like many correlations for Tmin, the Shumway correlation accounts for the thermal properties of structure and fluid that impact quenching by using a nondimensional group denoted as β ; therefore, the correlation is generally expected to be applicable for a wide variety of metals and fluids as discussed more extensively in Reference [R104- 1]. Henry (Reference [R104- 5]) explains that β relates the invariant temperature that is achieved at the interface between two semi-infinite slabs of constant properties at different uniform temperatures when they are brought into intimate contact. The ability of β to account for material property differences was assessed by Henry in Figure 9 of his paper cited here as [R104- 5]. Figure 4 from [R104- 2] was created to be similar to Henry's Figure 9 with the addition of data from other authors as explained in the text of [R104- 2]. The augmented Figure 4 from [R104- 2] is replicated here as Figure R104-2. The solid symbols in Figure R104-2 were calculated from the Shumway correlation and follow the same color coding used for the other materials. Notice that Shumway's correlation predicts that the (Tmin-Tsat) values for SS304, SS316, and Inconel are very similar due to the fact that the thermal properties, and hence β , for these materials are very similar. As expected from the higher value for β , the Shumway (Tmin-Tsat) value for Zr is also higher. Notice how the Shumway prediction for these low pressures is in the middle of the Zr data from Peterson and Bajorek (Reference [R104- 6]). As shown in Figure R104-2, the Shumway correlation matches overall the trend in both the data and the correlation from Henry over a wide range of material thermal properties. In the range of most interest for SS, Inconel and Zr, the Shumway correlation agrees with both Henry's correlation and the low pressure data within the estimated scatter of the data. Thus the common practice accepted in the industry for over 30 years whereby β is used to account for differences in material properties is justified on a theoretical basis and more importantly supported by comparison with data.

For purposes of comparison, the Shumway correlation used in TRACG and the Groeneveld-Stewart (GS) correlation (Reference [R104- 7]) used in TRACE are shown together as a function of fluid pressure in Figure 5 of [R104- 2] which has been replicated here as Figure R104-3. The GS correlation (depicted by dashed green line) is a simple empirical fit versus only pressure that was developed using only Inconel data and does not include any effect due to different material properties. In the vicinity of the quench location TRACE uses the maximum of Tmin from the GS correlation and 725 K which is shown as dotted black line in Figure R104-3. The solid green curve in Figure R104-3 was obtained from Shumway's correlation using Inconel 600 material properties and the solid purple curve using SS316 material properties. Both evaluations of Shumway's correlation assume no credit for the void fraction term or the Reynolds term in the correlation. As expected, the Inconel and SS curves from Shumway are similar. The purple stars represent T_Q data for SS used by Shumway. The vertical scatter in the data reflects the range of Reynolds numbers for different flow rates as well as other factors such as differences in experimental techniques, geometry, and surface finish. All the open green symbols are for Inconel data extracted from Reference [R104- 8]. The solid green boxes with embedded purple

“+” signs were determined from measured T_Q values for SS data in Oak Ridge National Laboratory Thermal-Hydraulic Test Facility (THTF) and Inconel data in Two-Loop Test Apparatus (TLTA) and Rig of Safety Assessment (ROSA)-III Loss-of-Coolant Accident (LOCA) integral system tests that were simulated as part of the TRACG qualification^[R104- 9]. The data in Figure R104-3 is widely scattered but this scatter is accounted for in TRACG LOCA applications by consideration of a $\pm 60\%$ uncertainty span in $(T_{min}-T_{sat})$ that results from the $\pm 3\sigma$ sampling where $\sigma=20\%$.

In Figure 6 of Reference [R104- 2], the Shumway correlation was compared to an additional 894 Inconel data points from the Rod Bundle Heat Transfer (RBHT) tests^[R104- 10] as well as integral LOCA test data. Figure 6 of Reference [R104- 2] is replicated here as Figure R104-4. The RBHT and LOCA integral system tests evaluate quench temperature (T_Q) data consistent with the type of correlation that Shumway developed. To further support use of the Shumway correlation to Zircaloy where T_{min} is higher compared to Inconel because of the larger β term, the correlation using Zircaloy has been compared directly to Zircaloy data in Figure R104-4.

The solid red curve obtained from the Shumway correlation as implemented in TRACG using Zircaloy material properties is below the Zircaloy T_Q values extracted from References [R104- 11], [R104- 12], [R104- 13], and [R104- 14] and thus it is conservative for the intended LOCA applications of the TRACG code even without consideration of the uncertainties. There are several plausible explanations for why the Shumway correlation is conservatively low but the most important is that the correlation (solid red curve) was also evaluated assuming that $\alpha = 1$ so no credit would be realized from the term $\left[1+(1-\alpha)^2\right]$ in the correlation. This term has been judged to have inadequate experimental support because in Shumway’s words it is based on “a small amount of unpublished Semiscale void data” and the “accuracy of the void effect is untested”. Especially for the cases of the Hofmann and Halden data the quench occurs for a much lower void fraction than 1.0 just based on how the liquid water was forced into the test section. It is also likely that a credit for liquid subcooling is observed in the data that is not represented in the Shumway correlation. As an upper bound on the temperature prediction from the Shumway correlation, a value of $\alpha = 0$ was assumed to obtain the dashed red curve in Figure R104-4. The dashed curve is in reasonable agreement with the quench temperature data; however, in applications of the Shumway correlation in TRACG analyses the term $\left[1+(1-\alpha)^2\right]$ is replaced by 1.0 because of the inadequate experimental support for this term.

The Hofmann data contained different amounts of measured oxide although there is so much scatter in the data that the effect on the experimental quench temperatures cannot be discerned. The fuel rods from the GEAP-13112 tests also ended up with a maximum ZrO_2 thickness stated as 1.8 mils considering the measurement uncertainty but unfortunately the amount of oxide was not measured and reported for each TC location. There is no indication in the Halden reports how much oxide accumulated during the tests, but based on the high temperatures and the sustained time at these temperatures, it is likely to not have been negligible. The key point is that

the presence of zirconium oxide causes the quench temperatures to increase. Exactly how much the increase should be is debatable. As a basis for comparison, the Shumway prediction of the quench temperature for ZrO_2 is shown (without any credit due to void) by the solid black curve in Figure R104-4. This curve is also in reasonable agreement with the quench temperature data; nevertheless, TRACG analyses that utilize the Shumway correlation will conservatively not take credit for an increase in the predicted T_Q values due to ZrO_2 . In other words, the Shumway correlation will be conservatively evaluated using properties for unoxidized Zircaloy.

Based on the Zircaloy temperature data presented in Figure R104-4 one can conclude that using the Shumway correlation as implemented in TRACG to estimate T_{min} for Zircaloy is justified because it provides a value of T_{min} that is conservatively lower than most of the data even without consideration of the uncertainties as is done in the BEPU TRACG LOCA application. Lower values of T_{min} are more conservative because they delay the return to nucleate boiling and thus result in higher and more conservative calculated values for the cladding temperature.

An objection raised during NRC review of the TRACG LOCA methodology is that the sensitivity of the PCT and ECO results to modeling of uncertainty in T_{min} had not been demonstrated for LOCA applications as it was for ATWSI applications. The additional information provided in Table R104-4 of this response addresses that issue. For ATWSI applications of TRACG, sensitivity studies had previously been performed to cause the TRACG T_{min} value from the MS correlation to emulate the TRACE implementation of Groeneveld-Stewart (GS) correlation at the ATWSI pressure of 6.9 MPa. Document page 299 (PDF page 327) of the TRACE V5.0 Theory Manual (Reference [R104- 8]) indicates that Groeneveld-Stewart [GS] correlation is reset to the maximum of GS and 725 K within 15 cm of a quench front. In the most important vicinity of the quench front the GS correlation is never applied since 725 K is always higher than what the unaltered GS correlation predicts. Based on text from document page 298 (PDF sheet 326), the 725 K limit is applied to compensate for the fact that the GS correlation consistently under predicts the quench temperature.

The ATWSI sensitivity studies applied [[]] to obtain a T_{min} value of approximately 725 K (like TRACE) for the ATWSI conditions of pressure around 6.9 MPa and cladding temperatures associated with at power conditions. **For the BWR/2 LOCA conditions a lower pressure in the range of 0.10 to 0.14 MPa is appropriate.** [[

]]

Results from a preliminary sensitivity study performed for the limiting large break DBA for

NMP1 were shown to the NRC during a teleconference on August 16, 2016 and subsequently sent informally to the NRC as an attachment to an email on August 19th. In regard to Tmin sensitivity results, Table R104-4 presented here contains similar contents as presented previously in two tables in the email attachment. Results in Table R104-4 will be discussed in detail later in this document.

Justification of TRACG Quench Modeling

The quench model used in TRACG is essentially the same as the model used in the CORECOOL code currently used together with SAFER when analyzing BWR/2s. The quench modeling was previously reviewed and approved by the NRC as part of their review of NEDE-30996P-A. The relevant references in the TRACG LOCA LTR are [22] and [25]. NRC acceptance of the quench model is documented in the Safety Evaluation (SE) contained in [R104- 15] which is an attachment to the transmittal letter from NRC to GE cited here as [R104- 16].

The quench front model is well described in [R104- 18]. [[

]] These tendencies should be expected based on how the quench model is implemented. Refer to Equations (6), (7), and (8) in [R104- 18]. [[

[[

]]

]]

The quench model works together with the model for Tmin and other elements of the heat transfer package. [[

]]

The response to LOCA RAI-49 provides additional information related to how uncertainty for the quench model is addressed in TRACG. [[

]] The heat transfer coefficient for quenching due to bottom reflooding in TRACG had been retained from TRAC-P1A and TRAC-BD1 and is based on the paper by Yu, Farmer and Coney cited as reference R49-1 in the RAI-49 response and cited in this response as reference [R104- 17]. As explained in the response to RAI-49, the citation of WCAP-7435 (FLECHT) in Section 6.6.13 of the TRACG Model Description LTR [R104- 3] as the source of the heat transfer equation for reflood is not correct and Equation (6.6-158) of Reference [R104- 3] for bottom flooding heat transfer coefficient is also incorrect. The correct expression for the bottom flooding heat transfer coefficient and a more detailed description of the TRACG quench model is available in MFN 13-085 cited here as Reference [R104- 18] and previously provided together with the response to RAI-49. MFN 13-085 also describes the error that was corrected in the interpretation and TRACG coding of the heat transfer correlation for bottom up quenching. The falling film implementations in TRACG and CORECOOL were not affected since they rely on a different heat transfer correlation that was not related to the erroneous implementation of the heat transfer correlation for reflooding (bottom up). The quench model in the TRACG code has been corrected and the corrected code will be used in all future TRACG LOCA applications.

Summary of Qualification Relevant to BWRs/3-6 LOCA Evaluations

As part of the error assessment, qualification calculations related to the quench model for bottom reflooding were updated and the impact of the quench model on predicted PCTs quantified as indicated in the RAI-49 response for the case of a rising quench front like that observed in a reflooding situation. Use of the TRACG quench model was shown in MFN 13-085 (Reference [R104- 18]) to result in calculated cladding temperature responses that compare well to the measured temperature responses from LOCA Integral System Tests (IST) where reflood quenches were experienced. Key selected results from Reference [R104- 18] for LOCA scenarios are replicated in this document. The comparison to Halden tests that were added for ATWSI applications at high pressure are not included because for LOCA scenarios where fluid inventory and pressure are substantially lower, the comparisons with LOCA-like IST data are more relevant.

NEDO-33005-A Revision 1
Non-Proprietary Information – Class I (Public)

Cases were selected for tests performed at facilities that had previously been evaluated in the TRACG Qualification LTR (Reference [R104- 9]) except for THTF test 3.03.6AR which was specifically added at the request of the NRC because it had also been evaluated using TRACE. Selected cases are those where the test data temperature traces indicate a quench since these are the cases where the impact of the TRACG quench modeling are expected to be greatest. The tests evaluated in this response are: Thermal Hydraulic Test Facility (THTF) transient blow down tests 3.03.6AR, 3.06.6B, and 3.08.6C (References [R104- 19], [R104- 20]); Two-Loop Test Apparatus (TLTA) test 6423 (Reference [R104- 21]); ROSA-III test 912 (Reference [R104- 22]); and ROSA-III test 926 (Reference [R104- 23]). Relevant details for the re-evaluations presented here are summarized in Table R104-3. All the TRACG calculations were executed using the Shumway T_{min} correlation with the void term disabled and the cladding material appropriate for the test as indicated in Table R104-3.

The temperatures presented in Table R104-3 show that generally the maximum temperature calculated by TRACG [[

]] for these LOCA-like cases the maximum temperature is reached and begins to decrease based on precursory steam cooling that exists prior to when the quench occurs. The LOCA scenarios are unlike the ATWSi scenario because for LOCA the cladding has a longer heatup time at a much lower heat flux in a fluid environment where there is very little liquid water. The ATWSi scenario with power and flow oscillations near the operating reactor pressure is much better represented by the Halden test cases where the reactor remains at power, flow is reduced to produce the boiling transition and is later increased after the dryout to simulate the flow surge, which causes the return to nucleate boiling.

Table R104-3 : Test Data and TRACG Comparison Summary for LOCA-like Scenarios

Test	Clad Material	Maximum Temperature ¹ (K)				Quench Velocity ³ (m/s)		Estimated Pressure (MPa) at Time of Quench
		Test Data	TRACG		Elev-ation ² (m)	Avg. along rod	Last Second Before Quench	
			Quench Model OFF	Quench Model ON				
THTF 3.03.6AR	Stainless Steel	949	[[3.6	0.08	0.43	5.6
THTF 3.06.6B	Stainless Steel	1135			3.6	0.11	0.32	5.8
THTF 3.08.6C	Stainless Steel	1204			2.4	0.10	0.07	6.6
TLTA 6423	Inconel	802			2.0	0.01	0.05	0.60
ROSA-III 912	Inconel	839			0.94, 1.11	0.02	0.15	1.4
ROSA-III 926	Inconel	784]]	0.94	0.01	0.07	0.40

¹The *Maximum Temperature* corresponds to the peak value for the specific rod and location that is being compared.

NEDO-33005-A Revision 1
Non-Proprietary Information – Class I (Public)

²The elevation indicates where the maximum temperature was taken for the test data and TRACG. The maximum temperature from the node plotted for the respective test and elevation is used. For ROSA-III 912, the TRACG calculated temperature peak occurs for the node at 1.11m so it is the temperature trace at that elevation that is tabulated and plotted.

³The *Quench Velocity* was calculated by dividing the distance the quench front traveled by the elapsed time to travel that distance based on the TRACG indicated position of the quench front with time.

Table R104-3 shows that for THTF tests 3.03.6AR and 3.06.6B the calculated quench velocity over the last second before the quench at the thermocouple (T/C) elevations are respectively 0.43 and 0.32 m/s (16.9 and 12.6 inch/s). The ATWSi power/flow oscillations occur near the normal operating pressure of a BWR whereas for the LOCA-like test cases the quench occurs for a range of lower pressures as indicated in the rightmost column of Table R104-3.

Calculated TRACG temperature traces with time are compared to the test data in Figure R104-5 through Figure R104-10. The red curves labeled “TRACG Nominal” in these figures are from calculations where the quench model was turned OFF. The blue curves labeled “TRACG Quench” are with the quench model turned ON. The green and turquoise curves show the measured data. For these LOCA scenarios the quench front movement is limited by the rate of liquid water addition rather than the inability to return to nucleate boiling. Steam produced lower in the bundle serves to reduce measured temperatures at the higher elevations before the quench front propagates to the maximum measured temperature elevation. It is this precursory cooling process that is the reason both the measured and calculated temperature traces are trending downward even before quenching occurs. Quench is suggested at the *shoulder* in the measured temperature trace where the temperature suddenly drops.

It is not always possible from the measured temperature traces to distinguish a temperature drop due to quenching and a drop due to an improvement in the heat transfer mode that results when the surface temperature is reduced below the minimum stable film temperature (T_{min}). The need to make this distinction is not essential because the TRACG quench and T_{min} models work together. The T_{min} model defines the maximum surface temperature for which return to nucleate boiling can occur if there is sufficient liquid. When the surface temperature ahead of the quench front is above T_{min} , the quench model has a higher relative importance because it provides for heat removal via axial conduction to liquid near the saturation temperature that exists below the quench front. On the other hand, if the surface temperature decreases below T_{min} above the quench front then a higher heat transfer coefficient is calculated above the quench front and the axial temperature profile and thus the quench heat removal mechanism are decreased. The TRACG Quench calculations presented in Figure R104-5 through Figure R104-10 demonstrate that the TRACG quench and T_{min} models are working well together in matching the quench temperature data. For example, consider the results in Figure R104-6 for THTF test 3.06.6B. For pressures between 5 and 6 MPa the Shumway correlation predicts a T_{min} value of about 770 K for stainless steel for low flows and no void enhancement. Graphically it can be seen [[

]]

For comparison with the TRACG calculations and the test data, the TRACE calculated results are depicted by the purple curves in Figure R104-5, Figure R104-6, and Figure R104-7. As stated previously, the Groeneveld-Stewart T_{min} correlation (derived from Inconel data) is used in TRACE to predict a T_{min} value around 685 K at 5 MPa. This value is about 90 K lower than the Shumway prediction for stainless steel at 5 MPa. The impact of the lower value for T_{min} is most apparent in the purple curves on the left side of Figure R104-6 and the right side of Figure R104-7. Primarily because of the lower value for T_{min}, TRACE predicts a quench temperature that is lower than the data by at least 50 K.

In all cases of reflood quenching from below, both the measured and calculated results indicate quenching occurs after the temperature has peaked and has begun to decrease. In other words, the quenching phenomena for reflood scenarios with a rising quench front like those occurring in BWRs/3-6 is of “low” importance for determining the peak clad temperature (PCT) because precursory cooling has already caused the cladding temperature to start decreasing before the quench front rises to the PCT location. The differences in the calculated TRACG temperatures with the quench model off (red curve) and with the quench model on (blue) curve are insignificant as shown in Figure R104-5 through Figure R104-10. This is the main reason that C21 for quench is ranked as having “low” importance in LTR Table 4.2-1 for all phases of BWRs/3-6 LOCAs where the dominant quenching mechanism is due to bottom reflooding. As explained in the response to RAI-51: “For jet pump plants, rewet occurs after reflood and the temperature has turned around and starts to come down. The uncertainty in the rewet has therefore no impact on the PCT. Likewise the impact on the fuel clad oxidization for jet pump plants is also minimal as the PCT is relatively low and the duration of refill/reflood phase is short.”

Summary of Qualification Relevant to BWR/2 LOCA Evaluations

For larger breaks in a BWR/2, core reflooding is not possible, quenching as a result of core spray occurs from a falling quench front which does have an impact on the calculated PCT and ECO values. This is the reason that the bias and uncertainty for the quench front modeling were determined from falling quench front data as explained in the response to RAI-49. The relevant qualification of the model comes from the Core Spray Heat Transfer (CSHT) tests.

Uncertainty in the quench model is not modeled as part of the approved SAFER/CORECOOL application so in that sense the TRACG implementation is more rigorous. As indicated in Section 5.1.3.27 of the LTR and the response to RAI 49, the bias and uncertainty in the quench model are conservatively established as respectively, [[]]. In the proposed TRACG LOCA methodology the bias is removed and uncertainty is sampled as part of the

BEPU process. Accounting for the non-conservative bias and twice the uncertainty results in a PIRT83 value of [[]].

The modeling of quench bias and uncertainty for a falling film has been quantified by comparisons to CSHT data since for these tests quenching is due to a falling film like in a BWR/2. Monte Carlo analyses of select CSHT tests (using 59 statistical trials) were provided in Section 7.4.5 of the TRACG LOCA LTR to show how treatment of the uncertainties impacts the comparison with the data. The text and figures in Section 7.4.5 have been updated and augmented in the response to RAIs 82 and 92.

Studsvik Core Spray Heat Transfer Tests

Studsvik (Reference [R104- 24]) core spray heat transfer tests 111, 133, and 137 were analyzed in response to RAI-82. These three particular tests were selected because they had the highest measured temperatures. These evaluations augment CSHT tests previously evaluated in the TRACG LOCA LTR and in Section 3.2.2 of the TRACG Qualification LTR (Reference [R104- 9]). The maximum of the calculated temperatures from the locations where there were measurements is compared to the maximum of the measured Studsvik data for these locations in Figures R82-3, R82-4, and R82-5 of RAI-82. The comparisons show that on average TRACG tends to conservatively over predictive the measured data but still within the uncertainty band of the 59 Monte Carlo simulations. Data collection for Studsvik tests 111, 133, and 137 was terminated prior to quench.

Fortunately, data collection for Studsvik test 123 extended long enough to include the quench. TRACG evaluations were also performed for test 123 in response to RAI-82 even though test 123 produced a lower measured PCT than tests 111, 133, 137. Studsvik test 123 was specifically designed as a bottom-vented test so it is more representative for a large LOCA in a BWR/2. The TRACG simulations for this test were intended to show the negligible impact of noncondensable gases (NCG) but the results in Figure 82-2 of the RAI response also show that the maximum of the nominal calculated temperatures is conservatively high compared to the corresponding maximum of the measurements. TRACG also conservatively predicts a later quench than seen in the experimental data. For convenience, Figure 82-2 of the RAI response is replicated here as Figure R104-11.

GE Core Spray Heat Transfer (CSHT) Tests

The CSHT tests utilized a full-scale simulated 8x8 BWR bundle consisting of 63 electrically-heat *fuel* rods and one central un-heated water rod. The test facility, test descriptions, the TRACG modeling, and the comparison of calculated and measured results are all given in Section 3.2 2 of the TRACG Qualification LTR (Reference [R104- 9]). Essential elements are repeated here for convenience.

There are total of six transient CSHT tests documented in Section 3.2 2 of the TRACG Qualification LTR (Reference [R104- 9]). Figures 3.2-13 through 3.2-18 in Reference [R104- 9] show comparisons of the TRACG calculated temperatures from all rod groups (RGs) where test data was available for each of the six tests. All calculational setups used the rod grouping shown

in Figure 3.2-8 of Reference [R104- 9] together with the test-specific rod peaking factors shown in the table below the figure. For convenient referral during the discussion that follows, the figure and table are replicated here as Figure R104-12.

For three of the CSHT tests (111, 120, and 121) the data was recorded long enough to show the full quench. Test 111 has the highest measured initial PCT from tests 111, 120, and 121; therefore, test 111 was selected in the original TRACG LOCA LTR for assessing the calculated rod PCTs and rod quenching characteristics. Updated TRACG Monte Carlo calculations (using 59 trials) are presented in RAI-92 for CSHT tests 111, 112, and 110. Calculations for test 112 were also updated in RAI-92 because test 112 has the highest initial rod PCT, among all six tests (Reference [R104- 9] Table 3.2-3). Unfortunately, data collection for test 112 ended at 500 seconds (prior to the quench) so comparison of this test for quenching with TRACG is not possible.

The 59 Monte Carlo simulations for each of CSHT tests 110, 111, and 112 as documented in the RAI-92 response applied the same TRACG model uncertainties as established in the LTR for plant applications. Note that the statistical analyses for these CSHT tests only considered TRACG model parameter uncertainties and the uncertainties in the measured core spray flow to the bundle and in the spray liquid temperature. Other uncertainties associated with heater rod material properties, power distribution, initial conditions, and heat transfer due to spray on the outside of the channel were not considered. It is expected that consideration of these additional uncertainties and increasing the number of trials from 59 to at least 124 (as now required for plant calculations) would expand the span in calculated temperatures and cause them to cover all the measured values. As it was, a few of the measured temperature values for RGs 2 and 4 from tests 111 and 112 extend slightly outside the span of the Monte Carlo calculations. Calculated results for the hot rod group (RG=10) were not previously shown in the RAI-92 response but are included later in this discussion in Figure R104-18.

As noted in the RAI-92 response, TRACG calculated nominal peak temperatures on average are 13 K higher than the data when considering all six CSHT tests and all the rod groups identified in Table 3.2-4 of [R104- 9] where test data was available. Nominally considering these rod groups, the peak temperatures for tests 111 and 112 are slightly under predicted whereas the peak temperatures are over predicted for tests 113, 120, and 121.

For CSHT test 110 the nominal calculations for the peak temperatures for all rod groups are predicted well within the span of $\{-5.1, 15.0\}$ relative to the data. For purposes of demonstrating the coverage of the TRACG model uncertainties, CSHT test 110 is a good choice because any biases associated with modeling the power differences between rod groups appear to have been minimized. (Note that such biases are not relevant in the plant applications where the limiting LHGR values are prescribed to account for a conservative local peaking factor both radially and axially within the fuel bundles.) Calculated 59-trial Monte Carlo results for rod groups 2, 3, 4, 6 in CSHT test 110 are shown in the response for RAI-92. The measured temperature data shows a drop of about 50 K around 1000 seconds for rod groups 2 and 4 (see Figures R92-10 and R92-12 in RAI-92). A short time later the lower extremes of the TRACG Monte Carlo calculations

for these rod groups also show a drop which suggests that for some scenarios the quench has begun in the lower power rod groups. The recorded data was terminated before full quench was achieved; however, TRACG simulations that extend out to 3000 seconds for test 110 reveal that TRACG generally is predicting the quench slightly later than the data suggests so that TRACG results are conservative with respect to cladding temperature and accumulated oxidation.

Test 111 is the best CSHT test for assessing the timing of the quench predicted in the TRACG calculations because the test data extends past the time of full quench (defined as time when cladding temperature decreases within 10 K of the fluid temperature). Calculated results for rod groups 2, 3, 4, 6, and 9 are shown in Figures R92-1 through R92-5 in the response for RAI-92. These figures are replicated here as Figure R104-13 through Figure R104-17 for convenient referral during the discussion that follows. The calculated results for the hot rod group 10 are shown here in Figure R104-18 although they were not previously provided in the response to RAI-92.

Comparisons of the calculated temperature responses versus data for each rod group (RG) is informative because it demonstrates how the quench model has been implemented within the TRACG CHAN component. As explained in the description of the quench model, each surface is treated individually where a surface corresponds to a fuel rod group, water rod group, or channel box. The unpowered surfaces for channel box and water rod quench first generally followed by the powered corner rod then powered interior rods. Because of differences in radiative view factors, the expectation is that the powered RGs will quench in order starting from the corner and moving inward. The rod peaking factors play a role in determining the order of quenching but if they are reasonably close together the position of the rod within the bundle will be more important especially for higher temperatures where the radiative heat transfer component is more important. All rods within the one-dimensional CHAN component experience the same axial distribution of hydraulic conditions; however, the radiative view factors and rod heat conduction solution is performed individually for each RG. TRACG also applies a conservative bias for convective heat transfer to vapor for interior rods in a bundle.

For the surfaces where thermocouples (TCs) were present there are comparisons between the calculated and measured temperatures. The TC data for each RG that is plotted in the figures is taken as the maximum value from all TCs for rods assigned to that RG since this will present the greatest challenge for the uncertainty in modeling to cover. These data values for CSHT test 111 are indicated by the pink squares in Figure R104-13 through Figure R104-18.

Let us consider the comparisons between calculations and data for the RGs starting from the outside corner and working diagonally inward (see Figure R104-12) in what is the expected approximate order of quench; i.e., RGs 9, 6, 4, 3, 2, and 10.

[[

]]

[[

]] Overall, the TRACG quench model is conservatively providing a somewhat later quench than the data.

[[

]] Notice how this nominal slope from the calculation compares favorably with the slope in the data points. This excellent agreement suggests an accurate value for the overall heat transfer coefficient to vapor prior to quench.

Figure R104-18 shows calculations for RG 10 which has been designated in the TRACG input model as the “hot rod group” (HRG). These comparisons were not previously shown in response to RAI-92 although they probably should have been. [[

]]

As explained in Section 6.6.10 of Reference [R104- 3] on the film boiling heat transfer at high void fraction, [[

]]

Additional details for the hot rod model are provided in Section 7.5.7 of Reference [R104- 3]. Relevant portions have been summarized here. Experience from the qualification has shown that

NEDO-33005-A Revision 1
Non-Proprietary Information – Class I (Public)

TRACG calculates the average fuel rod temperatures very well based on the average hydraulic conditions. Cross-sectional variations in the hydraulic conditions, however, can lead to local variations in heat transfer and fuel temperatures that are different from the averages. This is particularly the case for high void fractions where the flow is in the annular flow regime and where the rods are in film boiling heat transfer. This is typically only important for the reflood phase of a LOCA prior to the quenching of the fuel rods. The hot rod model also accounts for this phenomenon. [[

]]

[[

]]

[[

]]

The appropriateness of the model parameter uncertainties associated with quench and the statistical process used to combine them has been demonstrated by applying the BEPU approach to Studsvik and GE CSHT integral system tests. [[

]] The calculations demonstrate that the quench model and hot rod model perform as designed. In general, the quench times predicted by the TRACG modeling is delayed relative to the CSHT data which means that TRACG will conservatively over estimate the amount of oxide that will accumulate prior to full quench when applied in plant LOCA applications.

Discussion of Table R104-4 Sensitivity Studies

To respond to the specific NRC request in this document, sensitivity studies have been performed to justify the current treatment of bias and uncertainty for both the Modified Shumway (MS) correlation for minimum stable film temperature (T_{min}) and the quench model. ALL sensitivity studies have been performed using 181 statistical trials and the limiting case for the NMP1 BWR/2 LOCA analysis. Use of the NMP1 BWR/2 calculations for the sensitivity studies is the most appropriate because the time in boiling transition for a BWR/2 is substantially longer than for BWRs/3-6 LOCA evaluations because for the limiting BWR/2 LOCA scenario only core spray is available to cool the core. Consequently, rewetting occurs much later and the impact of any process that delays rewetting has the largest impact on oxide accumulation. By comparison, the cores in jet pump BWRs/3-6 can be re-flooded by the ECCS systems at least to the top of the jet pump diffusers within a comparatively shorter period of time so that total oxide accumulation remains much less than the imposed regulatory limit of 13% for maximum local cladding oxidation (MLO). It is also true that BWR/2 LOCA calculations tend to provide a higher calculated peak clad temperature (PCT) relative to BWRs/3-6 evaluated for the same linear heat generation rate (LHGR).

During the teleconference on August 16, 2016 the NRC expressed concern that by biasing T_{min} the maximum local oxide from the highest rank trial could challenge the 13% acceptance criteria. To quantify the impact of adding an intentional bias on T_{min} , the MLO values for the highest rank were provided for 59 trials, 124 trials, and 181 trials as part of the follow-up email. It is not surprising that imposing additional conservative bias on T_{min} will increase the mean MLO and may also increase the highest rank values as well. It is not GEH's intention to suggest an alternative approach that biases T_{min} rather than de-biasing it and sampling since that would be a deviation from the BEPU approach that already appropriately accounts for bias and uncertainty in T_{min} .

Results presented in prior communications have been superseded. The design limitations for the NMP1 core have been re-specified to provide slightly more margin to the imposed 13% oxide limitation. Specifically, the LHGR curve used for LOCA analyses (hence core design) has been modified slightly as shown in Figure R104-19. [[

]] All values presented below in Table R104-4 reflect the revised LHGR design curve for NMP2. The effect of the slight change in LHGR curve is illustrated by noting that previously the highest rank MLO value out of 181 trials was reported as [[]] compared to the updated value of [[]] shown in cell [C11a] of Table R104-4.

Column and row numbers are used in Table R104-4 to facilitate discussion of the results. In this discussion particular cells are referenced as [a#] where “a” is the letter of the column and “#” is the row number in Table R104-4. Columns A and B in the table describe the quantities for which values are presented in columns C through F. The base values presented in column C are those for the BEPU sampling process described in the LTR. According to the TRACG LOCA methodology under review, the LOCA licensing basis would be defined from the values in column C. The other results in columns D through F are presented in response to this RAI request to show the sensitivity of the key results in response to the modeling of bias and uncertainty in Tmin and quench.

Table R104-4 also provides additional details for the specific trials that produce the three highest rank values for PCT and MLO. [[

]]

For the Tmin sensitivity results shown in column D [[

]]

For the T_{min} sensitivity results shown in column D, the impact on the mean of the maximum local oxide (MLO) is [[

]]

The results for the quench model sensitivity studies have not been previously presented. The quench study results like the results from the T_{min} studies are presented Table R104-4 and they also reflect the revised LHGR design curve for NMP2. Consequently, the base BEPU values in column C used as a reference for the T_{min} studies also are applicable as a basis for the quench studies. As explained previously, [[

]] This approach for assessing the quench model is parallel to the process used to assess the T_{min} model.

The sensitivity results for quench are shown in column E of Table R104-4. [[

]]

The mean MLO for the quench sensitivity [[

]]

There are some important observations regarding the quench sensitivity results in column E of Table R104-4. [[

]]

The PCT and MLO move in opposite directions when the quench rate is reduced (column E results). This is evidence that the presumed bi-variant relationship between PCT and MLO changes is complicated and likely to depend on the transient scenario. Repeatedly GEH has stated that the PCT and MLO values occur in different channels at different axial locations within the core. The maximum values of PCT and MLO also occur at different points in time and usually for a different trial as shown by the trial numbers that provided the max# value shown in Table R104-4 in the row below the max# value.

The proposed BEPU approach provides the best solution because it does not distort the transient scenario by increasing conservatism relative to one acceptance criterion at the expense of decreased conservatism for another acceptance criterion. Consider the base BEPU numbers in Column C of Table R104-4. [[

]]

Conclusions

The requested sensitivity studies are summarized in Table R104-4. The MLO values in the lower half of the table indicate the expected increases corresponding to imposition of additional conservatism in calculated MLO values associated with the modeling of T_{min} and quench. The PCT values in the upper half of the table generally indicate that imposing conservatism in modeling of T_{min} has only a small impact whereas imposing conservatism on the quench modeling reduces the mean and upper bound PCTs. The imposition of additional conservatism is not warranted because the BEPU modeling described in the TRACG LOCA LTR already accounts for bias and uncertainty in the modeling of T_{min} and quench in a way that satisfies the regulatory requirements and guidance. The current BEPU modeling of bias and uncertainty for T_{min} and quench are justified based on good comparisons between the relevant qualification calculations and the experimental data.

Table R104-4 Sensitivity Results for Tmin and Quench

[[

]]

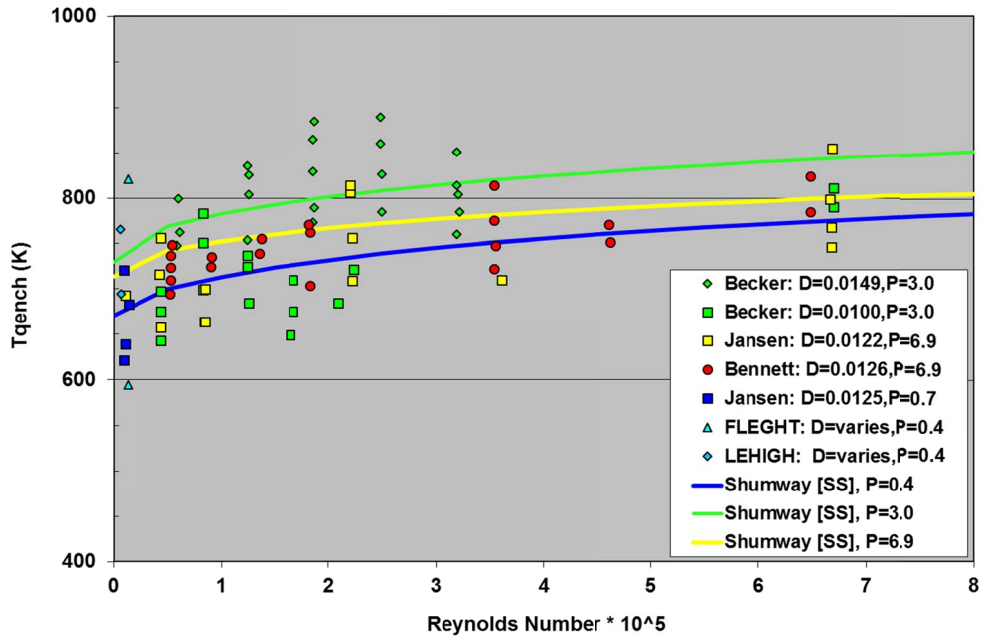


Figure R104-1 Shumway Correlation versus his Stainless Steel Data {Fig. 1 in [R104- 2]}

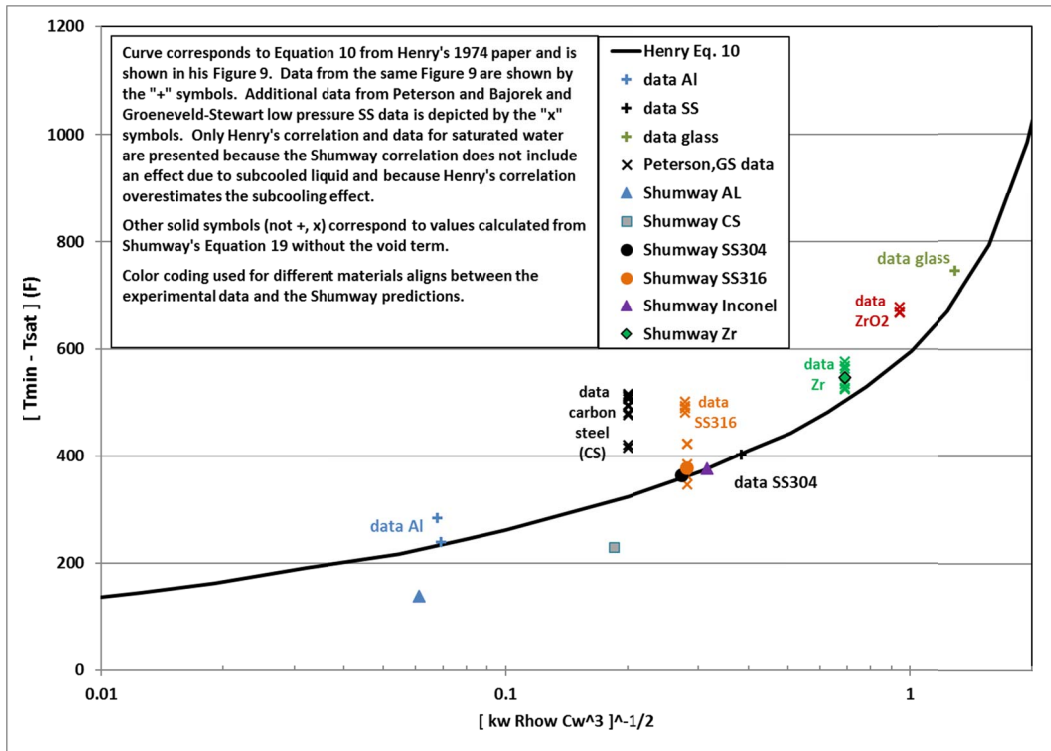


Figure R104-2 Shumway Correlation for Different Materials {Fig. 4 in [R104- 2]}

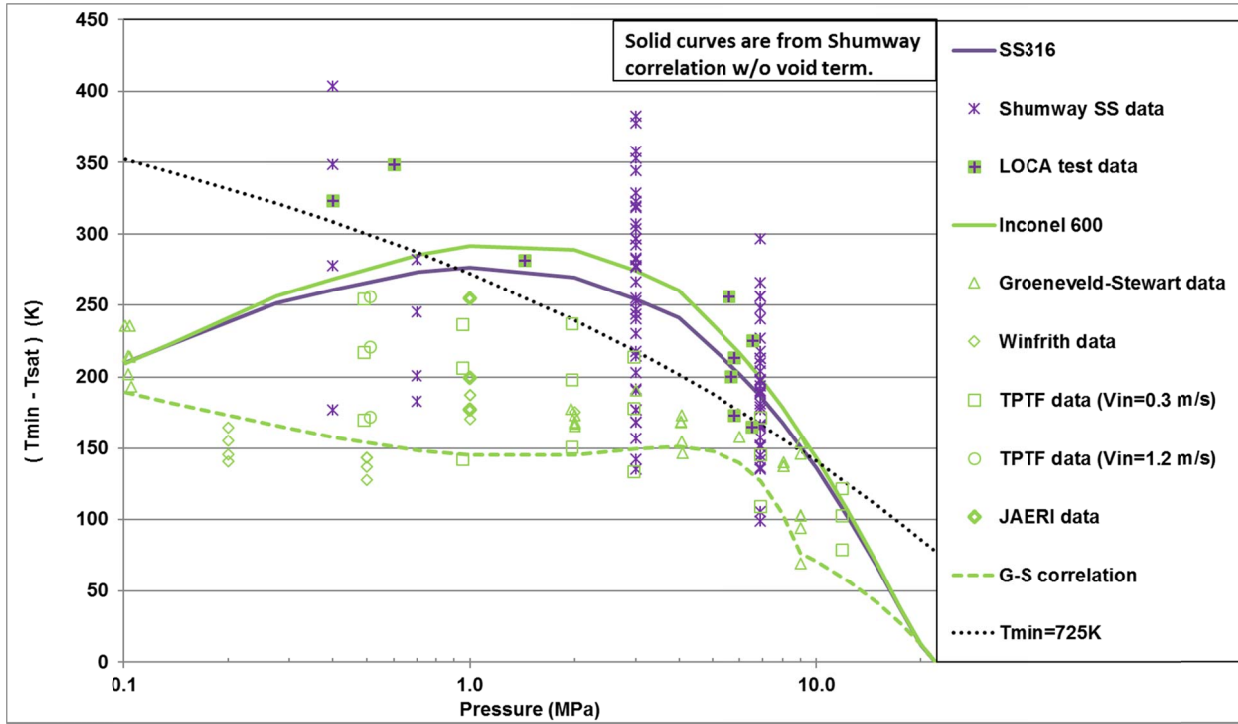


Figure R104-3 Shumway Compared to SS and Inconel Data {Fig. 5 in [R104- 2]}

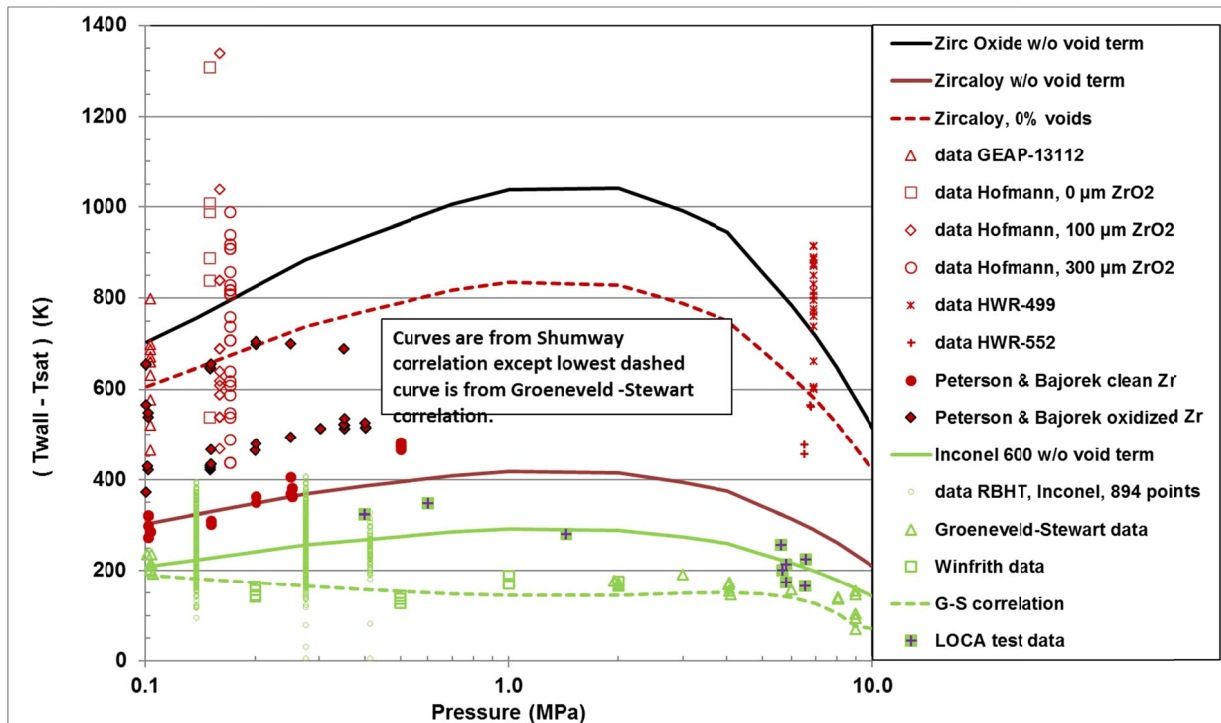


Figure R104-4 Shumway Compared to Inconel and Zircaloy Data {Fig. 6 in [R104- 2]}

[[

]]

Figure R104-5 Temperature Comparison for THTF Test 3.03.6AR {Fig. 8 in [R104- 18]}

[[

]]

Figure R104-6 Temperature Comparison for THT Test 3.06.6B {Fig. 9 in [R104- 18]}

[[

]]

Figure R104-7 Temperature Comparison for THT Test 3.08.6C {Fig. 10 in [R104- 18]}

[[

]]

Figure R104-8 Temperature Comparison for TLTA Test 6423 {Fig. 11 in [R104- 18]}

[[

Figure R104-9 Temperature Comparison for ROSA-III Test 912 {Fig. 12 in [R104- 18]}]]

[[

Figure R104-10 Temperature Comparison for ROSA-III Test 926 {Fig. 13 in [R104- 18]}]]

[[

]]

Figure R104-11 Studsvik CSHT Test 123 – Cladding Temperatures {Fig. R82-2}

[[

]]

Figure R104-12 Rod Grouping for CSHT Simulations {Fig. 3.2-8 of [R104- 9]}

[[

]]

Figure R104-13 CSHT Test 111, Rod Group 2 {Fig. R92-1}

[[

]]

Figure R104-14 CSHT Test 111, Rod Group 3 {Fig. R92-2}

[[

]]

Figure R104-15 CSHT Test 111, Rod Group 4 {Fig. R92-3}

[[

]]

Figure R104-16 CSHT Test 111, Rod Group 6 {Fig. R92-4}

[[

[[

Figure R104-17 CSHT Test 111, Rod Group 9 {Fig. R92-5}

]]

]]

Figure R104-18 CSHT Test 111, Rod Group 10 {not in R92}

[[

]]

Figure R104-19 Revised LHGR Design Curve for NMP1

REFERENCES

- [R104- 1] Letter, J. F. Harrison (GEH) to Document Control Desk (NRC), “Final Presentation for ACRS Thermal-Hydraulic Phenomena Subcommittee Meeting on September 21, 2015 and Final Presentation and Requested Information for NRC Audit Related to the Peach Bottom Units 2 and 3 License Amendment Request for MELLLA+, August 31, 2015 to September 2, 2015,” MFN 15-078, September 25, 2015.
- [R104- 2] Letter, J. F. Harrison (GEH) to U. S. Nuclear Regulatory Commission, “Use of the Shumway T_{min} Correlation with Zircaloy for TRACG Analyses,” MFN 13-073, September 9, 2013.
- [R104- 3] J. G. M. Andersen, et al., “TRACG Model Description,” NEDE-32176P, Revision 4, January 2008.
- [R104- 4] R.W. Shumway, “TRACG-BWR Heat Transfer: Assessment of T_{min}”, EGG-RST-6781, January 1985.
- [R104- 5] Henry, R.E., “A Correlation for the Minimum Film Boiling Temperature”, Heat Transfer Research and Design, AIChE Symposium, Series 70, No. 138, 1974, pp. 81-90.
- [R104- 6] Peterson, L.J. and S.M. Bajorek; *Experimental Investigation of Minimum Film Boiling Temperature for Vertical Cylinders at Elevated Pressure*; Proceedings of ICONE10 10th; Arlington, VA; April 14-18, 2002.
- [R104- 7] J.C. Stewart and D.C. Groeneveld, “Low-Quality and Subcooled Film Boiling of Water at Elevated Pressures,” *Nuclear Engineering Design*, 67, 1981, pp. 259-272.

NEDO-33005-A Revision 1
Non-Proprietary Information – Class I (Public)

- [R104- 8] *TRACE V5.0 Theory Manual: Field Equations, Solution Methods, and Physical Models*; citations used here is for version last updated 2012-05-07; following link may be more recent: <http://www.nrc.gov/docs/ML1200/ML120060218.pdf>
- [R104- 9] *TRACG Qualification*, NEDE-32177P, Revision 3, August 2007.
- [R104- 10] Hochreiter, L.E. et al., *RBHT Reflood Heat Transfer Experiments Data and Analysis*, NUREG/CR-6980, April 2012.
- [R104- 11] Duncan, J.D. and J.E. Leonard, *Thermal Response and Cladding Performance of an Internally Pressurized Zircaloy-Clad Simulated BWR Fuel Bundled Cooled by Spray Under Loss-of-Coolant Conditions*, GEAP-13112, April 1971.
- [R104- 12] Hofmann, P. et al., *Quench Behavior of Zircaloy Fuel Rod Cladding Tubes: Small-Scale Experiments and Modeling of the Quench Phenomena*, FZKA 6208, Forschungszentrum Karlsruhe, March 1999.
- [R104- 13] McGrath, M., *Minutes of the Fourth Workshop on Dry-out Fuel Behaviour Tests (IFA-613)*, HWR-499, OECD Halden Reactor Project, April 1997.
- [R104- 14] Ianiri, R., *The Third Dryout Fuel Behaviour Test Series in IFA-613*, HWR-552, OECD Halden Reactor Project, February 1998.
- [R104- 15] Safety Evaluation by the Office of Nuclear Reactor Regulation Relating to General Electric Company Licensing Topical Report NEDE-30996P Volume 1 “SAFER Model for Evaluation of Loss-Of-Coolant Accidents for Jet Pump and Non-Jet Pump Plants”.
- [R104- 16] Letter G.C. Lainas (NRC) to H.C. Pfefferlen (GE), “Review of NEDE-230996(P), ‘SAFER Models for Evaluation of Loss-of-Coolant Accident for Jet Pump and Non-Jet Pump Plants, Volumes I and II’,” HCP-017-087, February 19, 1987.
- [R104- 17] S.K.W. Yu, P.R. Farmer, and M.W. Coney, *Methods and Correlations for the Prediction of Quenching Rates on Hot Surfaces*, International Journal of Multiphase Flow, 3, 1977, pp. 415-443.
- [R104- 18] Letter J.F. Harrison (GEH) to Document Control Desk (NRC), “Update TRACG Quench Front Model Description and Qualification”, MFN 13-085, October 15, 2013.
- [R104- 19] *An Analysis of Transient Film Boiling of High-Pressure Water in a Rod Bundle*, NUREG/CR-2469, March 1982.
- [R104- 20] TRACE V5.0 Assessment Manual, Appendix B: Separate Effects Tests, <http://pbadupws.nrc.gov/docs/ML1200/ML120060191.pdf>
- [R104- 21] BWR Large Break Simulation Tests – BWR Blowdown/Emergency Core Cooling Program, GEAP-24962, NUREG/CR-2229, March 1981.
- [R104- 22] Experiment Data of ROSA-III Integral Test Run 912, JAERI-M 82-010, January 1982.
- [R104- 23] ROSA-III 200% Double-ended Break Integral Test RUN 926, JAERI-M 84-008, February 1984.
- [R104- 24] Studsvik Report, “BWR Emergency Core Cooling Investigations – Spray Cooling Heat Transfer Experiment in a Full Scale BWR Bund Mock-up”, STUDSVIK/E4-78/64, October 4, 1978.